AN INVESTIGATION OF WINDOW SYSTEMS
for
REDUCED ENERGY CONSUMPTION

Ramy El Diasty

A Thesis
in
The Centre for Building Studies
Faculty of Engineering

Presented in Partial Fulfillment of the Requirements
for the degree of Doctor of Philosophy

Concordia University
Montréal, Québec, Canada

August 1982

ABSTRACT

An Investigation of Window Systems
for
Reduced Energy Consumption

Ramy El Diasty, Ph.D.
Concordia University, 1982.

The use of mechanical cooling, heating, and electrical lighting to compensate for any inappropriate design of windows and external walls is no longer acceptable. In an effort to meet energy conservation demands two detailed models for thermal and daylight calculations for windows are presented.

In the transient, three-dimensional thermal model, heat transfer through windows and walls is calculated using a finite difference approximation. The model allows for variation of the external surface coefficient of heat transfer with wind speed and direction. The solar heat absorbed in the external layer of walls and in all the layers of windows is considered. An empirical formula for air infiltration heat loss as a function of wind speed is obtained. A correlation between the surface convection coefficient and wind speed for eight major directions was established.

The daylight model is a time dependent version of the Daylight Factor Method. Hourly daylight illumination and the energy saved when daylight is efficiently utilized are calculated. Both the C.I.E. luminance distributions for clear sky and overcast skies are used. A

first attempt is made to develop luminance distributions for partly cloudy skies. A parametric study for eight parameters affecting the daylight factor is performed. The variation with time was the most significant. Calculated illuminations agreed well with measured values.

An outdoor rotating test chamber was built and used in measuring energy gains and losses through external panels with 0.0, 25, 50, and 75% glazing. Each panel was tested for three main orientations and for three glazing types. Calculated temperatures and energy consumptions agreed well with the measurements.

The use of three-dimensional time-dependent analysis has confirmed that reduction or elimination of windows does not always lead to energy savings. When the storage of solar heat in multiple windows is considered, windows act, at times, as heat sources. Even in January, the internal surface of partly shaded triple windows can show two opposite directions of heat flow at the same time. The sideways heat exchange at the window opening and at the interface between wall panels was significant. The amount of window recess showed an effect on the net energy losses. Computer programs were developed and tested for both models. This study provides a reasonably realistic basis for the assessment of the energy effectiveness of windows for design purposes.

ACKNOWLEDGEMENTS

The author wishes to express his sincere gratitude to the individuals whose assistance and encouragement were instrumental in the realization of this thesis.

The author is grateful to his supervisor, Dr. Marvin Shapiro, and is greatly appreciative of his invaluable guidance and useful suggestions.

The author wishes to thank his co-supervisor, Dr. Paul Fazio, for his thoughtful suggestions, constructive guidance and his continuous encouragement throughout the course of this work.

The financial support of the National Science and Engineering Council of Canada and La Formation de Chercheurs et d'Action Concretée du Québec for this research is greatly appreciated.

The author also extends his thanks to Dr. Samir Mattar, Dr. Ted Stathopoulos, Dr. Helmi Attia, and Dr. Osama Moselhi for providing encouragement, inspiration, valuable criticism, and helpful advice throughout the course of this study.

The assistance of Joseph Zilkha, Alfred Clarke, Tony Sum, and Hans Obermeir in conducting the experiments and their continuous readiness to help are greatly appreciated.

Thanks are also due to: Lynnette Bauer, Dr. Mona Seddik and Itidal Sadek, for their valuable editorial assistance in the many drafts of

this thesis; Gloria Miller for her patience, reliability, and professional ability in typing this thesis so expertly; and Connie Anania for her continuous willingness to help and for typing the titles of the figures.

Last, but not least, the author would like to express his gratitude and special thanks to his wife, Maha, for her continuous support, encouragement, patience, and editorial assistance and to his daughter, Dina, for her patience and understanding.

TABLE OF CONTENTS

LIST OF FIGURES

LIST OF TABLES

NOTATION

A	Area, area ratio
a	Heat transfer coefficient, wind constant
B	Brightness factor
b	Coefficient of matrix [B], wind constant
C	Thermal capacity
DF	Daylight factor
d	Distance, thicknes
E	Energy, illumination
F	Infiltration coefficient, view factor
H	Inverse of the thermal resistance, height
h	Surface coefficient of heat transfer
I	Intensity of solar radiation
K	Extinction coefficient for glass
k	Thermal conductivity
$\bar{k}$	Effective conductivity
L	Glass thickness: surface luminance
n	Day of the year, total number of nodes glass refractive index
P	A reference point, a typical node
Pr	Prandtls number
q	Rate of heat flow
R	Thermal resistance
R_e	Reynold's number
RC	Reflected component of daylight
S	Surface slope from horizontal
SF	Sky factor
T	Temperature (present)
T'	Temperature (future)
t	Time
U	Area proportionality factor
v	Wind Speed
W	Width
w	window, wall
x,y,z	Cartesian Coordinates

Subscripts

b	Building surface containing the window
c	Clear sky, cloud cover
e	Sky element
f	Frame
g	Gain, ground
h	Horizontal
i	Sky ring, node, inside
ij	Sky element in the ith ring and jth subdivision
J	Subdivision
L	Heat loss
ℓ	ℓth node in the media surrounding the conducting body, light,
m	Total number of reflecting surfaces
o	Overcast sky, obstruction surface, opposite surface, outside
P	Reference point
r	Layer
s	Sun, solar, surface, series
v	Variable
w	Window, wall
x	x-direction
y	y-direction
z	z-direction, zenith
zc	Clear sky zenith
zo	Overcast sky zenith

Greek Symbols

α	Thermal diffusivity, solar altitude, absorptance, luminance factor
γ	Horizontal angle for the view factor
Δ	Time increment, distance increment
δ	Declination angle
ε	Relative emmissivity, solar heat generated in the node volume

η	Luminous efficiency, net heat input
θ	Altitude angle
λ	Wavelength
μ	Viscosity
ρ	Density, reflectance
Σ	Azimuth angle difference between solar beam and the normal to the surface
σ	Stefan-Boltzmann constant
τ	Cloud cover, glass transmittance
ϕ	Azimuth angle, profile angle
ω	Hour angle, angular distance

CHAPTER I

INTRODUCTION

1.1 Importance of Windows to the Built Environment:

Windows play a very important role in shaping the quality of the built environment. Being an element of the building enclosure, windows act as a sheath sheltering the indoor environment from the undesirable conditions outside. As the only transparent portion of the building enclosure, windows act as a link between indoor and outdoor environments.

As a sheath, windows resist heat losses during the cold season and heat gain during the hot season. Windows should also resist rain penetration, air leakage and withstand wind forces. In addition, windows are expected to reduce the intensity of the external noise to an acceptable level. As a link, windows permit visual contact with the outside, provide natural daylight, and admit solar heat gain.

Furthermore, windows may provide ventilation, air circulation, and access to emergency fire escapes. The psychological and physiological well being of the occupants and the quality of the indoor environment is enhanced by the presence of windows.

It is very difficult to make full use of all the benefits provided by windows. Some functions of the window are incompatible with others. Therefore a compromise between the conflicting functions is inevitable.

The most common incompatibilities are:

- Solar heat gain versus conductive, convective, and radiative heat losses.
- Reduction of electric lighting requirements versus conductive heat loss.
- Visual contact with the outside versus occupants' privacy.
- Ventilation versus reduction of external noise penetration.

In order to ensure an appropriate performance and to achieve the greatest possible benefits from windows, several trade-offs must be taken between various conflicting functions. It is important that the trade-offs should take place at an early stage of the design, to avoid costly change orders or a poor indoor environment.

1.2 The Energy Effectiveness of Windows

Buildings are considered the largest energy consumer after industry [1], 10% of the U.S. total national consumption of energy is lost through windows [2]. Until recently, little attention was accorded to the energy effectiveness of buildings in general and windows in particular . In common design practice mechanical heating, cooling, and electrical lighting were used to compensate for any inappropriate design of windows and external walls. The rapid escalation in energy prices has made such practices inappropriate for the community at large; though not yet for every builder. Accordingly the initial cost and aesthetics should no longer be the major design criteria. Energy effectiveness and operating cost criteria should also be taken into

account, and undoubtedly soon will be. Appropriate tools for this task were not available. In order to conduct a realistic assessment of the energy effectiveness of windows and walls there is a need for a reasonably accurate model to calculate the energy loss and gain associated with windows and walls. In the present study, a three-dimensional transient heat transfer model utilizing a realistic time varying sky luminance is used to calculate the effect of window-to-wall area ratio, orientation and number of glazing panes on the net winter energy consumption associated with windows and walls. The net energy consumption includes solar gains, conduction, convection and radiation losses, infiltration as a function of wind velocity, a benefit for electric lighting displaced by daylight, and a loss for the heating equivalent of the displaced electricity.

In this chapter, we present a literature review, the goals and objectives of the research, and an outline of the thesis. The literature is reviewed in four separate sections (sec. 1.3 to sec. 1.6). In section 1.3, the thermal aspects of windows and walls are reviewed. The literature related to daylighting is reviewed in section 1.4. The importance of windows to the quality of the indoor environment and to the psychological and physiological well-being of the occupants is the subject of the literature reviewed in section 1.5. In the literature, previous work fundamental to the present study requires special attention, given in section 1.6. Based on the literature review, conclusions that are directly related to the present study were drawn and are presented in section 1.7. The goals and objectives of

the present study are defined in the light of these conclusions in section 1.8. The outline of the thesis is presented in section 1.9.

1.3 A Review of Literature Related to the Thermal Aspects of Windows

The thermal aspects of windows have usually been investigated as a part of more general thermal studies. In this literature review, the papers are grouped as follows:

- thermal performance of windows
- optical and thermal characteristics of windows
- heat transfer through windows and walls
- air leakage around windows and through external walls
- the optimization of net energy consumption
- computer - oriented thermal modeling of buildings
- energy conservation in buildings
- previous net energy consumption calculations

1.3.1 Thermal Performance of Windows

Comprehensive performance requirements for windows were given by Paulsen [99]. A thorough evaluation of window performance was given by Wilson and Sasaki [3]. Design strategies for windows based on U.S. National Bureau of Standards studies with special emphasis on energy conservation, were developed by Hastings [4]. As part of the building enclosure, window performance was examined by Sasaki [5 & 6], Teitsma and Peavy [7], and Sabine and Lacher [8]. The thermal performance of wood framed windows was studied by Lowinski [9].

1.3.2 Optical and Thermal Characteristics of Windows

Data on optical and thermal characteristics of windows are available in several text books [10, 11, and 12]. The thermal properties of windows were examined experimentally by Agrawal and Verma [13] and by Lim and Conner [14]. The thermal transmission of double glazed windows was studied by Ambrose [15]. A computer program for the calculation of the solar absorption and transmission of single and double glazed windows was developed by Mitalas and Arseneault [16]. Isfält [17] provided a computer model for the calculation of the shading coefficients for various types of windows..

1.3.3 Heat Transfer Through Windows and Walls

A comprehensive literature review for heat transfer in buildings was given by Gupta [18]. A recent review of the fundamentals of heat transfer in buildings was presented by Kusuda [19]. Beijer [20] studied the thermal response of external walls to outdoor temperature variations. Mitalas [21] examined the relationship between the effective thermal resistance of walls and their heat storage capacity. The effect of external wall construction on indoor air temperature was investigated by Hassan and Hanna [22]. Air cavities effects on the heat transfer through external walls was studied by Bystrov and Galaktionov [23]. Personnel of the Building Research Station, in Garston, England standardized the heat transmission coefficients (U-values) for various categories of walls [24 and 25]. The effect of the thermal storage capacity of a building on indoor comfort conditions was

studied by Givoni [26].

Measurements of the thermal transmission of windows were done by Rennekamp [27] and by Lim and Conner [14]. Air leakage of windows was tested by Sasaki and Wilson [28]. The need for a comprehensive test program for windows and walls was emhpasized by Trechsel [29]. The portion of enclosure losses flowing through windows has been determined experimentally by Tamura and Wilson [30] and by Tamura [31].

One of the problems associated with windows in general and multiple pane windows in particular is breakage due to the thermally induced stresses. Sasaki [32 and 33], Sinha [34] and Solvason [35] have studied this problem in depth. With respect to the convective heat exchange at the external surface of a building, Cole and Sturrock [36] presented an extensive literature survey. The effect of inner surface air velocity and temperature on heat transfer through multiple glazing was studied by Pennington et al. [37] and Pennington and McDuffey [38]. Eckert and Carlson [39], and Railhby et al. [40] investigated the heat transfer by natural convection in an air layer enclosed between two vertical plates. Ozoe et al. [41] investigated this problem when the plates are inclined. Local heat transfer coefficients were determined in both cases.

Radiative heat transfer at internal and external surfaces of windows and walls is explained in several text books [11, 12, 42]. The radiant heat transfer for glass is reviewed by Garden [43].

Methods to predict the direct component of solar radiation were reviewed by Cole [45]. Kasten [46] surveyed the measurements and the

analysis of solar radiation data. Liu and Jordan [44] examined the interrelationship and the characteristic distribution of direct, diffuse, and total solar radiation using weather records. Cole [47] developed relationships to allow for the variation of atmospheric conditions in the calculation of solar radiation. Solar heat gain through windows is described by Stephenson [50]. Later he developed a simple procedure to estimate it with fair accuracy [48]. A tabulation of the solar heat gain factors for various latitudes are given in references [10 and 50]. Barakat [208] tabulated monthly total solar heat gain through single and multiple glazing for 13 cities in Canada. Nicol [52] examined the energy balance at an exterior window surface through experimental measurements of the radiative heat flux. A numerical simulation of the diffuse and direct solar energy striking a flat surface facing the sun was developed by Dave [53] using an isotropic distribution approximation for the diffuse radiation. Viskanta and Hirleman [54] studied the solar transmission and heat transfer through windows taking into account both the spectral and directional nature of solar and longwave radiation. Kiss and Benko [55] conducted an experimental study of the heat transfer through windows due to solar radiation. The effect of solar heat gain on indoor thermal conditions is described by both Stephenson [51] and in digest number 68 of the Building Research Station, Garston, England [56].

1.3.4 Air Leakage Around Windows and Through External Walls

Air leakage has a significant effect on the energy consumption in buildings. Sasaki and Wilson [57] reviewed the problems associated with window air leakage. They concluded that about 45% of the enclosure heat gain in summer and 60% of heat loss in winter leaks around windows when about 1/3 of the wall is glazed. In another study, Sasaki and Wilson [28] determined experimental air leakage values for different types of residential windows. The window portion of the overall air leakage was also investigated by Tamura [58 and 59], Tamura and Wilson [30], Tamura and Shaw [60], Shaw et al. [61], and Phillips et al. [62].

1.3.5 The Optimization of Net Energy Consumption

Several optimization techniques have been applied to different thermal design problems of buildings in an attempt to determine an optimum design for best thermal performance. Gupta [63 and 64] applied a systematic search technique changing components for buildings subjected to time-varying excitations, both climatic and operational. In another paper, Gupta used the simplex method to optimize building performance specifications [65]. The room/environment interaction was optimized using dynamic programming by Radford [66]. Bloomfield and Fisk [67] studied the optimization of intermittent heating, using optimal control theory. The optimization of the building shape to conserve energy was studied by Page [68]. Kimura [69] determined the optimum shape of external shade at specific angles to minimize annual

solar heat gain and to maximize the view. Arumi [70] optimized the energy performance of buildings taking into account daylighting as an energy-saving factor.

1.3.6 Computer-Oriented Thermal Modeling of Buildings:

Gupta et al. [71] reviewed the available literature on computer-oriented thermal models. Design considerations that should be taken into account in heat gain computer calculations were outlined by Norman and Mutka [72]. A computer simulation of air-conditioning systems using yearly weather data was developed by Magnussen [73]. Sheridan [74] applied thermal network analysis to the heat flow in buildings. Oegema and Euser [75] analyzed the transient thermal behaviour of office buildings numerically. A method to comptue the non-linear time dependent buoyant circulation of air in rooms was developed by Fromm [76].

ASHRAE [77] provided algorithms for building heat transfer sub-routines for computer-oriented energy calculations. Mitalas and Arseneault [78] used the Z-transfer function to calculate the transient heat transfer through building enclosures. Degelman [79] applied Monte-Carlo simulation to solar radiation and ambient temperature. Mitalas et. al. [16] modeled the absorption and transmission of thermal radiation by windows. A model for window shading coefficients was developed by Isfält [17].

1.3.7 Energy Conservation in Buildings

The ASHRAE Standard 90-75 [80] is intended to be a fundamental standard for energy efficient buildings. The energy savings possible through solar gains with various types of windows at various orientations were investigated by Berman and Silverstein [89]. The National Research Council of Canada has also brought out a standard for energy conservation in new buildings [81]. The estimation and prediction of building energy requirements were investigated by Ayres [82]. Dickens and Wilson [83] studied the relationship between building codes and energy conservation. Studies in the area of energy conservation in buildings were reviewed by Dubin [84]. Similarly, papers calculating ultimate potential savings were reviewed by Fantl [85]. Energy conservation utilizing the architectural aspects of the design were investigated by Ambrose [86]. Roudy and Duran [87] studied the effect of weather conditions and the building thermal parameters on energy consumption. Arens and Williams [88] studied the effect of wind on building energy consumption. Page [68] studied the relation between building shape and energy consumption.

The role of windows in energy conservation was investigated by Collins et al. [90]. Gujral [91] debated whether less glass would lead to more or less energy savings. Efficient utilization of solar energy through windows and its impact on building energy needs was studied by Silverstein [92]. Kusuda and Bean [93] estimated the energy conservation potential of ventilation control through weather data analysis.

Suggestions for improving the energy effectiveness of windows are given in two technical reports [2 and 94]. Energy consumption associated with windows can also be reduced by the use of shades and shutters [95]. Hagman [96] has shown that the use of insulated shutters leads to an improvement of the overall resistance of windows to both heat transfer and noise transmission. Rubin et al. demonstrated that shutters are means of energy conservation in their comprehensive study on blinds as a potential energy saver [97 and 98]. The potential of window management in energy conservation was investigated by Silverstein [100].

1.3.8 Previous Net Energy Consumption Calculations

Heating and cooling loads, associated with windows and walls, are usually calculated by means of a one-dimensional steady state analysis. Outside weather conditions are commonly represented by only two design days representing winter or summer conditions. This leads to an overestimate of energy requirements and thus to over design of the heating and cooling equipment. As a result, the equipment runs intermittently at reduced efficiency.

The calculation of heat transfer through a solid body such as a window or wall is described in heat transfer text books [101, 102, 103, 104, 105, and 112]. Heating degree days data published by the Meteorological Services are also used to proportion the monthly heating load.

In order to account for the radiative heat exchange at the wall

surface and the solar radiation incident on the wall in addition to the temperature difference across the wall, a single parameter known as the Sol-air Temperature was developed by MacKay and Wright.[106 and 111]. This concept was developed and enhanced by Parmalee and Aubele [107], Roux [108], and Hoglund et al. [109]. Recently, Kusuda [110] developed a similar concept, known as the "Sol-Air Temperature for Glass". Both of these concepts give a rapid estimate of heat transfer through windows and walls in the presence of solar radiation. Other simplified methods for heat transfer through windows were introduced by Viskanta and Hirleman [54], Kiss and Benko [55] and Alereza and Hossli [113].

In order to strive for an acceptable level of accuracy in the estimation of annual energy requirements for buildings, several hour-by-hour calculation procedures have been developed. The transfer function concept, which is recommended by ASHRAE, was first introduced by Mitalas and Stephenson [114] using thermal response factors. The transfer function concept was used in several studies [78, 115, 116, 117, and 118]. The transfer functions are filtered responses to excitation pulses caused by solar heat gain, conduction heat gain or loss, and heat gain from lighting, equipment, and occupants. Kusuda and Tsuchiya [119] introduced a similar technique called the equivalent thermal mass concept, which was further expanded by Kimura and Ishino [120]. Heating and cooling loads and indoor temperature were calculated after data had been fitted to a linear differential equation. Detailed calculations for a limited number of days are needed to derive accurate transfer functions based on the equivalent thermal mass of the

particular building under investigation. In order to reduce the computational effort for annual calculations, regression parameters were determined by fitting a simple algebraic equation to the transfer function parameters obtained from the results of a rigorous calculation for a limited period of the year.

1.4 A Review of Literature Related to the Daylighting Aspects of Windows

Daylight is considered one of the most important functions provided by windows, and it influences the overall quantitative and qualitative performance of the window. The spectral composition of daylight is unique. Throughout the ages, daylight has been utilized as the major source of illumination for interiors. The development of the fluorescent tube, forty years ago, marked a significant change away from reliance on daylight as the main source of lighting. Fluorescent tubes have offered an inexpensive, relatively efficient and reliable alternative for lighting. Artificial lighting in general has offered designers the possibility of control over the luminous environment. Gradually, the utilization of daylight decreased. Artifical lighting is convenient and dependable but is unable to provide people with the same visual, psychological and physiological stimulants as daylight. Recently, the realization of both the human need for daylight and the increasing cost of energy have encouraged the re-discovery of daylight as an essential source of illumination in buildings.

The literature review will be grouped as follows:

- luminance of the design sky
- daylight calculation techniques
- admission and control of sunlight
- daylight energy savings potential
- optimization studies in the area of lighting.

The available methods for handling both the quantitative and qualitative aspects of daylight are given in several text books [121, 122, 123, 124, 125, 126, 127, and 128]. Recommendations for the calculation of daylight are given both by the Illuminating Engineering Society, IES, [129 and 146] and the International Commission on Daylighting, CIE, [130]. A description of fifty-eight methods of daylight calculations that are in use world-wide are also given by the CIE [130]. The availability of daylight was investigated by Kingsbury et al. [131] and Boyd [132], and its relation to window design was investigated by Petherbridge [133] and Bryan [134].

1.4.1 Luminance of the Design Sky

Daylight design depends largely upon the assumed design sky. The most common choices are: the overcast sky, the standard uniform sky, and the clear cloudless sky. The overcast design sky was developed for locations where overcast conditions prevail. The luminance distributions of overcast skies, obtained from measurements in different parts of the world, were used by the CIE to develop a standard of relative

sky luminance under an overcast sky. This is known as the CIE standard overcast sky [135]. It varies with the altitude but not with the azimuth.

The standard uniform sky is characterized by a uniform luminance at each sky point sufficient to provide an illumination of 500 lumens/ft^2 on a horizontal plane when direct beam is ignored. This value is neither an average nor a minimum but is a representative value [136].

In contrast to the uniform and overcast skies, the clear cloudless sky luminance distribution is highly variable both in time and in space. The CIE [137] has adopted Kittler's formulation [138] as the standard luminance distribution for the clear cloudless sky. The measurements of sky luminance distribution are given in [139, 140, 141, and 142]. The techniques used for the determination of the sky luminance distribution are also available [143 and 144].

1.4.2 Daylight Calculation Techniques

Daylight design techniques can be classified into two groups. The first group comprises techniques requiring mathematical calculations. The other group consists of graphical techniques employing protractors, charts, diagrams, and nomograms. Hopkinson et al. [121] reviewed the various design sky conditions and calculation methods of both groups. Galbreath [67] summarized the common mathematical calculation techniques. The most widely-used methods of daylight calculation are the Daylight Factor Method [121] and the Lumen Method [123]. In the

daylight factor method, the illumination at a reference point is expressed as a ratio of the instantaneous illumination received on an unobstructed horizontal plane. This method was originally created for uniform and overcast sky conditions. Three components are calculated, the sky component, the externally reflected component, and the internally reflected component. The Lumen Method is used only for clear sky conditions. In this method the total light falling on a window due to direct sunlight, diffuse sky light, and reflected light from the ground and other exterior surfaces is calculated and then multiplied by a coefficient to account for the window transmission factor and internal reflections. The Lumen Method is described in several publications [123, 147 and 148].

For the calculation of daylight from clear skies, there are several alternative techniqes available in the literature. Krochman [149] developed a method to calculate the daylight factor under the CIE clear cloudless sky. Farrell [150] introduced a projection technique to calculate the direct illumination from a clear sky. Another projection technique was developed by Saxena and Bansal [151]. Narsimhan and Saxena [152] introduced an approach to calculate the sky component for a vertical rectangular aperture. In attempts to avoid the computation effort of daylight calculations from a clear sky Kpjic [153] introduced a graphic technique; Bryan [154] introduced a simplified procedure; and Farrel [155] proposed a perspective technique.

Other studies have focused on single aspects of the daylight calculation. Hopkinson et al. [156] developed an empirical formula for

the calculation of reflected light. Narsimhan et.al [157] developed a finite - difference approach for the calculation of the internally reflected component. Narsimhan [158] also studied the calculation of the reflected component for multiple-story buildings. Morris [159] studied the calculation of the internally reflected component for partially obstructed windows. Ground reflection was investigated by Griffith et al. [160] and Reed [161].

1.4.3 Admission and Control of Sunlight

One of the vital functions of the window is the admission of sunlight. Recommendations for the admission and control of daylight were given by Neéman et al. [162]. Neéman and Light [163] reviewed the availability of sunlight. In other publications by Neéman [164], and Hopkinson [165], sunlight requirements in buildings were reviewed. Implications for sunlight penetration in the design of windows were investigated by Smith [166]. Poorly controlled sunlight may cause visual as well as thermal discomfort to the occupants. As a result, solar control devices have become an essential feature in most buildings, particularly in dry climates where these problems are amplified. Some design methods for sun shading devices are shown in [167, 168 and 169].

Visual requirements for sunlight in buildings are well documented [170]. Dilaura [171] investigated the probability of visual discomfort with various geometries. The Illuminating Engineering Society, IES [129] recommended the Equivalent Sphere Illumination Concept, known as the ESI concept to calculate adequate visual performance. In this method, the visual performance in a real environment of known actual illumination is described as though the light came from a sphere of uniform luminance surrounding the reference plane. ESI is computed from the actual task illumination after allowing for ceiling reflection, disability glare effects, and the transient adaptive effect if required. The method for ESI computation is also given in [172].

1.4.4 Daylight Energy-Savings Potential

The use of daylight as a potential energy-saver has attracted the attention of many researchers. Hastings and Crenshaw [173] accounted for daylight as an essential factor in developing window design strategies to conserve energy. The daylight potential for conserving energy was also investigated by Dorsey [174] and Perry [175]. Other studies have dealt with conservation in electric lighting [176], with the control of lighting [177], and with energy management [181].

1.4.5 Optimization Studies for Lighting

The need for an optimum design of fenestration with respect to daylight was emphasized by Khan [178]. Kaufman [179] investigated the

optimum use of energy for lighting the buildings' interiors. Dorsey [180] applied cost benefit analysis to lighting, while Arumi [70] accounted for daylighting as a factor in optimizing the overall building performance. Hopkinson [182] and Kendrick [183] have investigated the integration of daylight and artificial light in the illumination of interiors, as a means to minimize the energy consumption associated with lighting.

1.5 A Review of Literature Related to the Comfort and Health of Occupants and the Quality of the Indoor Environment

The role of windows on the psychological and physiological well-being of the occupants and the overall quality of the indoor environment has been appreciated more in recent years. The lack of daylight in windowless buildings is believed to cause health disorders [184]. There are two types of health disorders: either somatic, (the upset of the regular bodily functions), or psychosomatic, (nervous disturbances of various kinds which could lead to physical illness). The physiological benefits of daylight for humans have not yet been studied in much detailed. Despite the difficulties of measuring the environmental aesthetics and qualities as indicated by Heath [185], several valuable studies have been conducted. The relations between windows and the environment were investigated by the Pilkington Environmental Advisory Board [186]. A recent review of the literature on the importance of windows to people is given by Collins [187]. In another study by

Collins [188] the human reaction and response to windows is investigated. The functions of windows were delineated by Markus [189] with emphasis on the quality of the indoor environment. The psychophysics of sunlight in buildings was studied by Hopkinson [190]. The problems associated with windowless environments were studied by Hollister [191], Brown et al. [192], Burts [193] and McDonald [194].

Windowless environments were developed as a means to eliminate some distractions for workers and to have full control over the indoor environment. The problems that are created associated with such environments have confirmed the human need for windows. Collins [187] provided an extensive review of literature related to windowless environments.

The relation between the size of the window and the quality of the indoor environment was investigated by Keighley [195], [196] and Neeman et al. [197]. Based on these studies and others, Collins [197] suggested that the area of windows should occupy at least 20% to 30% of the external wall area.

In order to achieve an energy-efficient window design without affecting the quality of the indoor environment, the well-being of the occupants must be considered as well as the energy related aspects. To recapitulate, the important aspects related to the quality of the indoor environment and the well-being of the occupants are:

i) provision of natural light and the admission of sunshine.

ii) visual contact and communication with the outside world with as large a depth of view as possible.

iii) relief from the monotony of most enclosed spaces.

1.6 Analysis of Previous Work Fundamental to the Present Study

Useful research areas can be deduced from a careful analysis of previous work in this field. In particular, the assumptions used in previous works and their effect on the final results require careful examination and understanding. Selection of the appropriate analytic approach for the analysis of the present study should be guided by the success and failures of the past. In the literature, there are two similar previous works, one by Arumi [70] and the other by Kusuda and Collins [198].

1.6.1 Analysis of Arumi's Work

In 1977, the first effort to integrate thermal and lighting calculations for the purpose of optimizing the overall energy consumption of buildings was made by Arumi [70]. He provided theoretical evidence to prove that proper window sizes, along with a proper selection of external wall surface to volume ratio can result in total energy savings for heating, cooling, and lighting in the peripheral zones of buildings.

This study was limited to Austin, Texas (31°N). The windows were assumed to have heat absorbing glass and fixed positions and were

shaded from direct sunlight from March to September. They were single glazed, faced due South and were assumed to be extended sources of diffuse radiation. Direct sunlight was considered only as it increased the luminance of internal surfaces by reflection. The intensity of the indoor illumination was calculated at nine points on the floor of the room. The rate of infiltration was assumed to be 2 air changes per hour and the surface to volume ratio varied from 0.5 m^{-1} to 0.3m^{-1}. The required level of lighting was assumed to be 322 lm/m^2. Artificial light fixtures were assumed to have a luminous efficiency of 20 lumens/watt, a maintainance factor of 0.8 and a utilization factor of 0.8. During unoccupied hours, the lighting was assumed to be off and the thermostat set back to 85°F for cooling and 55°F for heating. During occupied hours, the thermostat was set at 78°F for cooling and 68°F for heating.

Arumi's model consisted of two parts, a thermal part to calculate heating and cooling energy consumption, and a lighting part to calculate sky illumination. There was no description of the procedure used for energy calculations except that the calculations were based on hourly weather data averaged over nine years. Arumi used his sky illumination model to calculate the intensity of illumination as a function of the weather conditions and the orientation of the receptor relative to the sun. This model is based on an empirical formula fitted to solar radiation data (direct, diffuse and total solar radiation) measured on a horizontal surface. Although the data represented only the daily radiation averages, Arumi used them for hourly calculations.

He concluded that with the appropriate combination of window percentage and external wall surface to room volume ratio, a reduction as great as 50% can be achieved in the total energy consumption. He also reported some evidence pointing to the existance of an optimum window area that minimizes the total annual energy consumption for heating, cooling and lighting.

In his case study, Arumi found that for a surface-to-volume ratio of 0.1 m^{-1}, the optimum window area was about 25% of the external wall area. As the surface to volume ratio decreased, the dependence of the total energy consumption upon window-to-wall area ratio was reduced.

1.6.2 Analysis of Kusuda and Collins Works

One year later, another study was published by Kusuda and Collins [198] which focused on the analysis of annual heating, cooling, and lighting requirements associated with windows. The objective of their study was to illustrate ways in which natural light and the solar benefits of windows could partially or fully offset the cost of normal heat losses and also to calculate the energy consumption associated with windows as a percentage of the total energy consumption. Their study was limited to the Washington, D.C. area, and was carried out on two typical modules. One was a kitchen-living area in a residential building, the other was an office space for two people. In both cases, the module had only one wall exposed to the outside.

Single and double glazed fixed windows (assumed to be tightly fitted) were examined for the following window-to-wall area ratios;

0.0, 0.1, 0.25, 0.50, and .70. Walls were assumed to be well insulated in conformity with the U.S. energy conservation standards (U value = 2.84 $w/m^2.K$). Air leakage was assumed to be independant of wind speed at a constant rate of 0.25 air changes per hour.

Heat transfer across the external wall and window was assumed steady and uni-dimensional. Sol-air temperature for the wall and for the glass were used for the calculation of the net rate of heat flow. The calculations were carried out using monthly average values for the daily total radiation in the Washington area. The analysis performed by Kusuda and Collins took into account window size, heat transfer, solar shading, mode of operation, window orientation and window management. Different window shading devices were simulated by using several shading coefficients ranging from 1.0 to 2.0.

Dimmers were assumed so that artificial lighting only supplemented daylight whenever the latter fell below various minima. The fluorescent lighting required was assumed to 36.11 w/m^2 of floor area.

Daylight was calculated with the Daylight Factor Method. Direct beam illumination was taken into account only as it increased the luminance of external surfaces. The calculation of direct beam and diffuse illumination was based on two simple formulae which depend only on the solar altitude angle, α, viz:

i) direct beam illumination - a) for clear sky = $12847\ e^{\frac{[-.2259]}{\sin\alpha}}$

- b) for mean sky = half the value of clear sky

c) for overcast sky = 0.0

ii) diffuse illumination = a) for clear sky = 1500 sin α

b) for overcast sky = 2200 sin α

c) for mean sky = 53 α

The externally reflected component was obtained by multiplying the solar or sky intensity by the reflectance coefficient of the external obstruction, the view factor between the room reference point and the external obstruction viewed through the window.

The internally reflected component was calculated for all three different design skies (clear, overcast, and mean skies) using the "split flux" formula of the overcast sky.

Kusuda and Collins indicated that the use of daylight appeared to increase heating requirements over the reference value and to reduce cooling requirements. They also concluded that the use of double glazed windows instead of single glazed windows reduced the total annual heating requirement by half but hardly changed the cooling requirement. They also reported that the northern windows exhibited the greatest heating requirements and the least cooling requirements, and concluded that properly designed and operated windows could reduce operating costs below those of a solid wall. They found a range of window areas which maximize daylighting benefits and solar heat gain and minimize heat losses. Under their assumptions, this range appeared to be centered between 12% and 20% of the total wall area for the residential module and around 50% of the total wall area for the office

module, which had higher internal heat gains (lighting, people, and equipment).

1.7 Conclusions Drawn From the Literature Review

The following conclusions were drawn from the literature review:

i) The window-to-wall area ratio is an important factor in determining the energy consumption associated with windows.

ii) The major factors influencing the energy consumption associated with windows are heat transfer, air leakage, and daylighting.

iii) The dynamic nature of the heat transfer process across windows and walls and the heat storage capacity of most walls require the use of a transient heat transfer analysis to obtain reasonably accurate prediction of thermal losses on daily or seasonal basis.

iv) The heat exchange at the interface between the window and the wall and the resulting variation in temperature over the window surface have not been investigated previously. Thus there is a need for a three-dimensional analysis of the problem.

v) The thermal analysis should account for the hourly variation of direct and diffuse solar radiation absorbed by windows and walls on clear days.

vi) The utilization of daylight for lighting the interior will result in energy conservation for large buildings in most climates. Any realistic simulation of daylight inside buildings requires time-dependent model that would account for the variation of daylight intensity with time of day and year, in addition to the variation with sky conditions.

vii) The Daylight Factor Method has only been applied to overcast and uniform design sky situations, where the luminance can be assumed uniform and time-independent. There is a need to extend this method to various sky conditions and modify it for use with energy-oriented and time-dependent calculations.

viii) There is a need to investigate experimentally the relation between the window-to-wall area ratio and the net energy consumption for various types of glazing at various orientations.

1.8 Goals and Objectives of the Research

The goals of the present reasearch are:

i) To calculate the net energy consumption associated with windows and external walls with better accuracy than in previous reports.

ii) To develop an energy-oriented and time dependent daylight model to calculate the daylight illumination level at a

given reference point in the room. This will allow a reasonably accurate calculation of the electrical energy saved both in the lighting and in the cooling system when daylight is efficiently utilized.

iii) To identify, for different window orientations, the range of window-to-wall area ratios where the window energy benefits (solar heat gain plus energy replaced by daylight) exceed the total energy losses (heat conduction and air leakage).

In order to achieve the three goals above, objectives can be enumerated:

i) To develop a three-dimensional time-dependant heat transfer model to calculate the temperature distribution in the various layers of windows and walls, the rate of heat transfer through windows and walls, the rate of heat loss due to air leakage, and finally the net energy gain or loss through windows and the walls.

ii) To modify the daylight factor method to be applicable to sky conditions other than complete overcast and to allow for hour by hour daylight variations for a good match to the accuracy of the thermal load calculations.

iii) To design and construct a test chamber to determine experimentally the energy consumption of an external wall having different window-to-wall area ratios, different types of glazing, and different compass orientations.

iv) To determine an empirical relation suitable for this test chamber between the energy consumption associated with air infiltration and wind speed, outdoor-indoor air temperature difference, and the length of the crack around the windows.

v) To determine experimentally the relation between the external surface convection coefficient and the wind speed for various wind directions.

vi) To confirm the validity of the thermal and daylight models by comparing the calculated results to the experimental results.

vii) To develop computer programs of sufficient accuracy for the thermal and daylighting calculations to enable us to carry out parametric studies and to calculate the energy gain and loss associated with windows and walls under simulated conditions.

1.9 Outline of the Thesis

The development of the thermal model is presented in Chapter II. The thermal model consists of two part. The first deals with the calculation of the incident solar radiation and its transmitted, absorbed and reflected components in order to calculate solar gains. The second part is a three-dimensional and time-dependent finite-difference model used to calculate, at each time increment, the temperature distribution in every layer of the wall or the window and the consequent rates of

heat transfer and heat storage.

In Chapter III, a time-dependent daylight model is presented. This model is used to calculate, at each time increment, the luminance distribution of the sky and the consequent luminances of external and internal surfaces. An attempt to rationalize the treatment of partly cloudy skies is also given.

A variable sky factor is used to calculate the direct component of the daylight on a horizontal plane at desk height inside the room. The variable reflected component is used to calculate the indirect component of the daylight. The sum of these two components is the variable daylight factor, which is used to determine the electric energy displaced by utilizing the available daylight.

In Chapter IV, the experimental work done to verify the models is presented. A description of the test chamber, test procedures, and the field measurements used to determine the impact of varying the window-to-wall area ratio on the overall energy consumption, is presented. In addition, the work done to determine an empirical relation between the rate of air infiltration and wind speed as well as the relation between the external surface convection coefficient, wind speed and wind directions is presented here.

In Chapter V, the theoretical and experimental results from this thesis are presented and discussed. The basis for determining an optimal window-to-wall area ratio for different types of glazing and different orientations is displayed. A comparison between calculated and measured temperatures and energy loss or gain is presented. The

effect of the window-to-wall area ratio on the energy conserved by utilization of daylight is examined and combined with the thermal loss or gain calculations to yield the net energy gain or loss for the two extreme cases: a completely clear and a completely overcast sky.

In Chapter VI, a summary, conclusions, and recommendations for future research are presented.

CHAPTER II

FINITE - DIFFERENCE CALCULATION OF HEAT TRANSFER THROUGH WINDOWS AND WALLS

2.1 INTRODUCTION:

Sometimes windows provide a thermal gain. At other times they provide a thermal loss. On the useful side, windows admit solar radiation in winter, release a portion of the internally generated heat to the exterior by conduction during most summer nights, and if daylight is utilized properly they reduce the cooling load generated from lamps. Solar heat gain through windows arises from the internal absorption of the visible radiation transmitted. The visible radiation is converted into heat and infrared radiation by molecular and atomic processes in the internal surfaces. The internal surfaces, in turn, emit some of the long-wave radiation, which is absorbed and partially re-emitted to the outside by the glass. The imbalance between the rate of entry and loss of radiation warms the room. This is commonly referred to as "the green house effect". On sunny winter days the daily total solar heat gain caused by southerly oriented windows often exceeds the conductive heat loss through the entire wall.

The major negative aspect of windows is their relatively low thermal resistance. The conductive and convective heat gains or losses through a unit area of window are several times greater than the heat gain or loss through a unit area of a typical external wall. Other negative thermal aspects include undesired solar heat gain on hot

summer days and the heat losses associated with air leakage through cracks and gaps around windows.

In current design practices, only the thermal losses through windows are normally considered in the calculation of winter heat loss. Benefits such as solar heat gain and the use of daylight to replace part of the artificial light are ignored. As a result, all four facades are usually glazed identically despite the large differences in winter solar gains.

Since current design practices are based on the steady state and unidimensional heat transfer formulation, the variations in solar radiation intensity, air-temperature, wind speed and direction are usually ignored. In most cases, monthly averages of weather data are used for the calculation of the heating and cooling loads. In recent years, the availability of powerful computers has made it possible to calculate hourly heating and cooling loads rapidly. Transient heat transfer calculation techniques have been developed for computers to take reasonable account of the hourly variations in the weather conditions outside, thermal conditions inside, and the thermal storage capacity of the building. The transient heat transfer calculation techniques require a somewhat more complex mathematical treatment than the steady state calculations. Due to the approximations used in the transient calculations there are some limitations on their applications. Section 2.2 of this chapter will be devoted to the evaluation of such methods and the selection of the most appropriate method for window thermal analysis. The solar heat input and the heat transfer at

the facade surfaces are investigated in section 2.3. In the fourth section of this chapter the development of our finite difference model is presented in seven subsections; the thermal network representations (2.4.1), the finite difference approximation (2.4.2), identification of the types and positions of nodes (2.4.3), the thermal conductance coefficients between nodes (2.4.4), the solar heat input (2.4.5), coefficients for the set of algebraic equations (2.4.6), and heat flow and energy calculation (2.4.7). Examination of the sideways heat exchange is given in section 2.4.8.

Using a three-dimensional finite difference time dependent model for thermal flows through windows and walls, the range of window-to-wall area ratio where energy benefits exceed energy losses for various facade compass orientations, types of glazing, and types of wall panel were calculated as a function of climatic factors (air temperature, solar radiation, wind speed and wind direction). As shown by comparison to the experiments in Section 5.3 this model provides a better estimate of the energy gains and losses associated with the windows and walls than the steady state model. In addition, the model allows, for the first time, a three-dimensional analysis of the transient heat transfer through windows which provides the temperature distribution over and between internal, median and external surfaces of single, double, and triple glazed windows in all directions.

2.2 Rationale For the Choice of the Thermal Model

In current practice, the calculation of heat transfer through windows and walls is commonly carried out assuming one-dimensional

steady state heat flow [10]. In the "Heating Degree Day" method [10, 217], thermal losses are calculated as proportional to the product of the inside to the outside air temperature difference times the number of hours when the outside air temperature is below 18°C.

The development of time dependent techniques has made computer simulation of the hourly variation, in both weather conditions and internal thermal loads (lighting, equipment, and people), possible and a better estimate of heating and cooling loads can be achieved. The most common computer-oriented method, known as the Transfer Function Concept, was developed by Mitalas and Stephenson [114]. In this method, three sets of numerical constants, called response factors, are used to represent the heating and cooling load arising from previous variations of solar heat gain, conduction, radiation, of convection heat gain or loss, and of heat gain from lighting, equipment, and people. A similar method called "The Equivalent Thermal Mass Concept" was later introduced by Kusuda and Tsuchiya [119] and expanded by Kimura and Ishino [120]. Several large computer programs are currently available for the calculation of heating and cooling loads, few of which are also able to calculate the total energy needed. Available programs are usually not well documented or supported, expensive to process and difficult to use [213]. They are unsuitable for the present study for six reasons.

i) Most of these programs provide only heating and cooling load calculations (not energy requirements).

ii) It is difficult to modify or manipulate the input for these programs to allow a prediction of the heating and cooling

loads and the consequent fuel demand for a single building component such as the window instead of the whole building.

iii) One-dimensional heat flows normal to the surfaces are assumed in all previous programs. In this study the sideways heat flow and the vertical as well as the horizontal temperature distributions in various layers of windows and the adjoining sills and wall panel are examined.

iv) The shading effect of recessing the window within the window opening as well as the effect of the window recess on the energy demand associated with the surrounding panel could not be investigated when previous programs were used.

v) No allowance was previously made for the variation of the surface coefficient of heat transfer due to wind speed and direction, or for the variation in the thermal load associated with window-wall air leakage.

vi) Even though previous programs would allow hourly rigorous calculations for the whole year, simple algebraic equations are normally fitted to the results of the rigorous calculations obtained for limited discrete periods of the year. The accuracy for annual heating and cooling loads is reduced considerably when such a simplification is made.

In order to develop a three-dimensional time dependent model for thermal flows through windows and walls, a choice must be made between two of the most powerful numerical techniques, the finite difference

and the finite element. Both methods can be used to approximate the governing differential equations for the temperature distribution in heat conducting systems. In the finite difference method, time derivatives are approximated using a central finite difference scheme. In the finite element method, variational calculus is employed. The calculus of variations shows that solving certain differential equations is equivalent to minimizing a related quantity called "the functional". This equivalence is known as a variational principle [212]. Neither method has been applied much to building heat transfer since in the era of cheap oil there was no apparent need for such sophisticated methods, and also computer facilities were required. Since each method has advantages and disadvantages, the choice between them is dependent upon the details of the particular problem. For example, when the arrangement of the nodes is irregular because of the system geometry, the finite element method is usually preferred because the finite difference method may lead to many terms for the heat balance equation at each node, requiring a lot of computer time. Non uniformity of temperature within each element can only be handled by the finite element method. In addition to the algebraic and conceptual complexity of the finite element method, the number of applications is limited, since the variational principle does not exist for all differential equations of interest [212]. In contrast, the finite difference method is simpler to program and to use. In the finite difference method, future temperature for a node can be obtained either explicitly (i.e. successively in terms of the present temperatures of surrounding nodes) or implicitly (with a simultaneous solution in terms

of the future temperature of the surrounding nodes). In the finite element method, the temperature of a node can only be obtained implicitly since a simultaneous solution is required.

In this study, the finite difference method was chosen because of the following reasons:

i) The geometry and node arrangement in the case of windows and walls are regular parallelepipeds, so excessive computer time is not required with the finite difference method.

ii) In the case of windows and walls, the temperature variation within each element can safely be ignored without using a large number of elements. Thus the major advantage of the finite element method does not apply here.

iii) The use of the finite element method in heat transfer in buildings is relatively recent. Few previous results are available, so all possible pitfalls may not have been exhibited.

iv) The finite difference method is simpler to formulate and to program and does not require as much background preparation as the finite element method.

After choosing the finite difference method, two further choices must be made. The first is between the explicit and the implicit formulations. In preliminary trials, the explicit formulation, though easier to use, led to impractically small maximum time increments (3.4 to 12 seconds depending on the examined case), beyond which instability

and oscillations of the solution occurred. Moreover, attempts to improve the accuracy of the calculation by reducing the truncation error led to the use of smaller spatial increments which resulted in a further reduction of the maximum allowable time increment. In the implicit formulation, no restrictions are imposed on the time increment by the choice of spatial increments, so we were able to obtain stable solutions with hourly time increments and thus reasonable computation time.

The second choice is whether to solve the resulting simultaneous algebraic equations by a direct or an indirect method. Direct methods such as Gauss elimination and matrix inversion are simple to use but require larger amounts of computer time and storage. Indirect methods, such as the Gauss Seidel (point by point) method and other similar methods [213], usually require less computer time and storage, particularly for systems having larger number of unknowns. When a large number of nodes are used, convergence may not occur due to inaccuracies in the intermediate stages of the calculation. To speed up the convergence, an over-relaxation technique is usually employed and the resulting scheme is known as the successive over relaxation method.

Despite the fact that the exact solution of most of the three-dimensional nonsteady state problems are either unknown or difficult to predict, the accuracy of the numerical approximate solutions can still be examined. A stable solution tends to converge as the number of nodes is increased. The number of nodes which is sufficient to provide reasonable convergence is problem dependent. In the present study, the

problem changes as the type of glazing or the type of wall is changed. In the trial studies, on the single, double, and triple glazings, and a multilayered wood frame wall, the sufficient number of nodes per layer was found to be 25 for windows and 36 for the wood frame wall.

2.3 Heat Exchange at the External Surface and the Solar Radiation Input

2.3.1 Convective and Radiative Heat Exchange

The thermal conductance between a solid surface and the surrounding air can be most conveniently expressed in terms of a surface coefficient, h, representing the combined effect of convective heat transfer to the air and radiative heat transfer to surrounding surfaces or the sky. The surface coefficient, h, is given by

$$h = h_r + h_c \tag{2.1}$$

where h_r and h_c are the radiation and convection coefficients. If we assume that all surrounding surfaces are at ambient temperature and that the air is humid, the radiant energy emitted from a unit area of the surface, q_r, can be approximated, for most building surfaces, by

$$q_r = h_r (T_s - T_{air}) \tag{2.2}$$

where T_s and T_{air} differ by a small fraction of their value on an absolute temperature scale. This is an approximation to the Stefan - Boltzmann law

$$\begin{aligned} q_r &= \sigma\varepsilon (T_s^4 - T_{air}^4) \\ &= \sigma\varepsilon [(T_s^2 + T_{air}^2)(T_s + T_{air})](T_s - T_{air}) \end{aligned} \tag{2.3}$$

Thus,

$$h_r \simeq \sigma\varepsilon [(T_s^2 + T_{air}^2)(T_s + T_{air})] \tag{2.4}$$

where the Stefan-Boltzmann constant $\sigma = 5.68 \times 10^{-8}$ w/m^{2}K^4 and ϵ is the relative emissivity between the emitting and receiving surfaces.

The convection coefficient, h_c, has been determined experimentally as a function of wind speed [52, 105, 201, 203]. Most of these studies have developed empirical formulae relating the convection coefficient to wind speed based on laboratory or wind tunnel testing on small plates. We therefore conducted experiments on a full scale model exposed to actual weather conditions to derive a relation which takes into account the wind direction as well as the wind speed. Here we review the results of the previous work and then compare them to the results obtained in this study. The effect of wind direction on the outside convection coefficient was investigated experimentally by Rowley and Eckley [200]. At low wind speed (7m/s), they found that the convection coefficient was substantially the same for wind directions ranging between 15° and 90° and was less than that for parallel flow. Above 7m/s wind speed, they found a slight reduction in the convection coefficient as the angle between the surface and the air stream was increased. They concluded that for practical purposes, the existing values for parallel flow are satisfactory for design purposes and the effect of wind direction can be ignored. In another study, Kind et al [201] reported a noticeable effect of wind direction on the convection coefficient except when the wind blew from behind the surface at directions ranging from 90° to 135° from the normal to the surface. Sriramulu's [202] experiments showed a third relation between the convection coefficient and the direction of the wind. From normal incidence to 45° it was almost constant and from 45° to grazing

incidence it increased linearly to 1.67 times the value at normal incidence.

The convection coefficient, h_c, tends to increase as one or more of the following three parameters is increased : i) temperature difference between the air and the surface, ii) the degree of surface roughness, and iii) wind speed. Rowley, Algren and Blackshaw [207] showed that the effect of varying the mean temperature of the air and the surface was measureable but insignificant. For constant wind speed, a higher mean temperature brought about a slightly higher convection coefficient. Also, they found that surface roughness affects the convection coefficient significantly. For example, the convection coefficient for a rough material (i.e. stucco) is almost twice as high as that for a smooth surface (i.e. glass) [10]. Wind speed affects the convention coefficient more than any other parameter. Sturrock [203] found the relation between the convection coefficient and wind speed to be linear and well represented by:

$$h_c = a + bv \qquad (w/m^2 .k) \qquad (2.5)$$

where a and b are experimental constants and v is the wind speed (m/s). Wind tunnel experiments gave a = 23 w/m^2 .k. Field measurements on actual building surfaces [203], [204] gave a = 11.4 w/m^2 .k for surfaces on the windward side and a = 0.0 for leeward surfaces. He found b = 5.7 w/m^2 .k in all experiments. Nicol [52] measured the variation of the window surface coefficient with wind speeds up to 5 m/s. The values of constants a and b were found to be 7.55 and 4.35 respectively. McAdams [105] relation has values of 5.7 and 3.8 for constants a and b respectively.

ASHRAE [10] provides two relations for forced convection at vertical surfaces the first is limited to wind speed ranges between 4.88 m/s (16 fps) and 30.48 m/s (100 fps) and is given by:

$$h_c = 7.34(v)^{0.8} \quad w/m^2.k° \tag{2.6}$$

and the second is given for wind velocity less than 4.88 m/s (16 fps) and is given by:

$$h_c = 5.62 + 3.91(v) \quad w/m^2.k° \tag{2.7}$$

Kind et al [201] showed that the linear relation given by McAdams did not fit their experimental measurements. For a parallel flow, which gives maximum convection coefficient, they found a equal to McAdams' 5.7 but b was about 1.2 instead of McAdams' 3.8.

Federov [205] developed a theoretical relation describing the convection coefficient in terms of the thermophysical properties of the surrounding fluid. The relation is given by:

$$h_c = 0.94\ (R_e)^{0.5}(P_r)^{0.333}(k/d) \quad W/m^2.K° \tag{2.8}$$

where R_e is Reynolds' number

$$R_e = \frac{\rho v L}{\mu} \tag{2.9}$$

and

Pr = Prandtl's number, dimensionless

k = thermal conductivity, w/m.K

d = characteristic dimension

ρ = density of the fluid, Kg/m^3

v = velocity, (m/s), (variable)

L = height of the surface, m

μ = viscosity of air, Kg/m.s

For external walls and windows, the surrounding fluid is air. Variations in the properties of air over the temperature range from 250 K° to 300 K° are very small. Consequently, it is quite reasonable to use here air properties evaluated at 275 K° (Pr = 0.715, k = 0.0243, d = 1.0, ρ = 1.295, L = 2.25, and $\mu = 1.667 \times 10^{-5}$). Substituting for air properties at 275 K° in Eq. (2.8) and then adding it to Eq. (2.4) yields:

$$h = 5.68 \left((LV)^{0.5} + 10^{-[illegible]} \varepsilon T_m\right) \quad w/m^2.K \qquad (2.10)$$

where

$$T_m = \left((T_s^2 + T_{air}^2)\ (T_s + T_{air})\right)$$

During the experimental field measurements that were conducted for the purpose of this study, the dependence of the surface convection coefficient on wind speed and wind direction was investigated. The technique that was used for estimating the surface convection coefficient differs from previous experimental studies. In addition, it was based on full-scale field measurements rather than laboratory testing. Despite the fact that the technique used is simple and based on several assumptions, the results were very encouraging. A comparison between previous studies and the present study has shown good agreement. A complete description of the experimental investigation is presented in Chapter IV. The surface convection coefficient varied linearly with the wind speed, as in Eq. (2.5)

$$h_c = a + bv \quad w/m^2 .K$$

where a and b are the experimental regression coefficients and v is the wind speed (m/s). From the experimental measurements of the present study, values of a and b obtained for five wind directions ranging from normal to 180° away from normal are shown in Table 2.1.

Wind Direction	a	b
0.0° (Normal)	7.77	2.90
45°	7.50	3.26
90° (Parallel)	7.52	4.10
135°	6.83	2.63
180°	6.27	2.65

Table 2.1 : Experimental values for the Regression Coefficients a and b

The thermal resistance of a surface is proportional to the inverse of the surface coefficient of heat transfer, h. The surface resistance of a window constitutes a relatively larger share of the window total thermal resistance than in the case for a typical external wall. Thus, the overall heat transmission coefficients (U-values) of windows vary more with wind speed than external walls. The effect of wind speed on the U-value of an external insulated wood wall and on the U-values of single, double, and triple glazed windows is shown in Fig. 2.1. It is apparent that the use of insulated windows instead of the single glazed windows reduces the dependency of the window total thermal resistance on wind speed.

2.3.2 The Solar Radiation Input

In this section, the beam, diffuse, and total solar radiation incident upon an external surface and the portion of the total solar radiation transmitted through window will be calculated. The intensity of the direct solar radiation, I, is given by [50]

$$I = A/e^{(B/\sin\alpha)} \tag{2.11}$$

for solar altitudes greater than 15°.

Here α is the solar altitude angle. Parameters A and B are functions of the time of the year and vary because of changes in the sun earth distance, and in the ozone and water vapour content of the atmosphere. Based on assumed average local atmospheric clearness at a value of 1.0, parameters A and B values at the twenty-first of each month are given in Table 2.2. The solar altitude, α, is related the latitude angle, ϕ, the hour angle, ω, and the declination angle, δ, by

$$\sin\alpha = \cos\phi \cos\delta \cos\omega + \sin\phi \sin\delta \tag{2.12}$$

The hour angle ω decreases 15° each hour with mornings positive and afternoons negative. The zero is at solar noon (i.e. due south). The declination angle, δ, describes the tilt of the earths' axis at solar noon from a plane perpendicular to the earth's orbit and tangent to the orbit at the sun's position. It is also the elevation of the sun at solar noon with respect to the plane of the equator (north positive), and it is given approximately by [209]

$$\delta = 23.45 \sin\left[360\left(\frac{284+n}{365}\right)\right] \qquad (2.13)$$

where n is the day of the year (i.e. $\delta = 0$ at the equinoxes). The intensity of beam radiation upon a given surface is related to the incident angle, θ, by

$$I_b = I \cdot \cos\theta \qquad (2.14)$$

where $\cos\theta$ is given by [50]

$$\cos\theta = \cos\alpha \cos\Sigma \sin S + \sin\alpha \cos S$$

where Σ is the difference between solar azimuth and the azimuth of a normal to the surface, and angle S denotes the surface slope from the horizontal.

The diffuse radiation intensity, I_d, that is incident upon a vertical surface from both sky and ground is given by [50]

$$I_d = I\,(c.y + .5\,\rho_g\,(c+\sin\alpha')) \qquad (2.15)$$

where c is a factor shown in Table 2.2 to account for the dust and ice content of the atmosphere and y is an empirical function of the $\cos\theta$ for beam radiation required because scattering causes bright spots in the sky which move as the sun moves. When $\cos\theta$ is -0.2 or less y is equal to 0.45. Otherwise y is given by [206]

$$Y = 0.55 + 0.437 \cos\theta + 0.313 \cos^2\theta \qquad (2.16)$$

The total solar radiation, I_t, for a given surface, is the sum of the beam and the diffuse components incident upon the surface.

In order to account for shadows on recessed or shaded windows, the shaded area of the window must be determined. The shaded area does not

receive direct solar radiation or the total diffuse radiation. The width of the direct beam shadow cast by a vertical rib projecting from the edge of the window is given by

$$W_{sh} = L \tan \eta \qquad (2.17)$$

where L is the perpendicular distance from the plane of the glass to the outermost edge of the projection and η is the difference between the wall azimuth angle and the solar azimuth angle and is given by [48]

$$\tan \eta = (1 - \cos^2 z - \cos^2 \theta)^{0.5} / \cos \theta$$

where z is the sun zenith angle.

Date	A	B	C
	(W/m^2)	Air mass^{-1}	Dimensionless
Jan. 21	1230	0.142	0.058
Feb. 21	1215	0.144	0.060
March 21	1186	0.156	0.071
April 21	1136	0.180	0.097
May 21	1104	0.196	0.121
June 21	1088	0.205	0.134
July 21	1085	0.207	0.136
Aug. 21	1107	0.201	0.122
Sept. 21	1151	0.177	0.092
Oct. 21	1192	0.160	0.073
Nov. 21	1221	0.149	0.063
Dec. 21	1233	0.142	0.057

Table 2.2: Data for calculation of Solar Radiation Intensity Ref. [50].

The length of the shadow cast by a horizontal rib projecting from the top of the window is expressed by

$$H_{s_H} = L \cdot \tan \varphi \tag{2.18}$$

where φ is the profile angle, given by:

$$\tan \varphi = \cos \gamma / \cos \theta$$

The area of the window that is exposed to both direct and diffuse radiation is then obtained from

$$A_{sun} = (H_w - H_{s_H})\ (W_w - W_{s_H}) \tag{2.19}$$

and consequently the area exposed only to part of the diffuse radiation

$$A_{s_H} = A_w - A_{sun} \tag{2.20}$$

Thus, the total radiation incident on the window, Q_s, is the sum of the incident diffuse radiation, Q_d, and the incident beam radiation, Q_b.

$$Q_s = Q_d + Q_b = A_{s_H}\ (I_d \cdot \ell) + A_{sun}\ (I_d + I_t) \tag{2.21}$$

where ℓ is a factor for the obstructed sky. It is equal to 0.5 if the shade is vertical. The total solar radiation transmitted through a clean window, Q_g, is given by

$$Q_g = Q_d\ \bar{\tau}_g + Q_b \cdot \bar{\tau} \tag{2.22}$$

where $\bar{\tau}_g$ is the average transmittance of the glass and $\bar{\tau}$ is the incident angle dependent transmittance for the glass. Based on Snell's and Stokes' equations given in reference [12], the angle dependent transmittance $\bar{\tau}$, along with the angle dependent reflectance $\bar{\rho}$ and absorptance $\bar{\alpha}$ were calculated as follows.

The effective reflectance, transmittance, and absorptance of a single, double, or triple glazing can be calculated, for a given angle of incidence, from two basic optical properties, the relative refractive index n_r between air and the particular glass and the extinction coefficient K for the absorption of the solar spectrum in glass. Snell's equation relates the angle of refraction θ_r, to the angle of incidence θ_i as follows

$$\text{Sin } \theta_i \, n_1 = \sin \theta_r \, n_2$$

where $n_2/n_1 = n_r$ and n_1 and n_2 are the refractive indices of the two mediums (i.e. air and glass pane). θ_i and θ_r are shown in Fig. 2.2a.

The reflectance ρ' has two components; one parallel (||), and one perpendicular ($\perp$) to the plane of incidence (the plane containing the incident ray and perpendicular to the surface) [12].

For normal incidence $\rho'_\perp = \rho'_{||} = (n_r-1)^2/(n_r+1)^2$ (2.23)

for grazing incidence $\rho'_\perp = \rho'_{||} = 1.0$ (2.24)

and for other angles of incidence

$$\rho'_\perp = \sin^2(\theta_i-\theta_r)/\sin^2(\theta_i+\theta_r) \quad (2.25)$$

$$\rho'_{||} = \tan^2(\theta_i-\theta_r)/\tan^2(\theta_i+\theta_r) \quad (2.26)$$

Even though incident direct beam solar radiation is unpolarized, both the reflected and transmitted beams may be partly polarized because of the difference between Eqs. (2.25) and (2.26).

Accounting for absorption only the transmittance τ' is given by

$$\tau' = e^{-kL}$$

where L and K are the thickness and extinction coefficient of the glass pane.

Reflectance transmittance, and absorption for single glazing with multiple reflectance (shown in Fig. 2.2.b) can be obtained using the following three equations by Stokes [12].

$$\rho_1 = \rho' [1+(\tau'^2(1-\rho')^2 / 1-\rho'^2\tau'^2)] \quad (2.28)$$

$$\tau_1 = \tau' [(1-\rho')^2 / 1-\rho'^2\tau'^2] \quad (2.29)$$

and

$$\alpha_1 = 1. - \tau_1 - \rho_1 \quad (2.30)$$

where α_1 is the absorptance of the single glazing and ρ' denotes either $\rho'_\perp$ or $\rho'_{\nu 1}$. For unpolarized direct beam incident radiation, the average reflectance $\bar{\rho}$ and the average transmittance $\bar{\tau}$ for both component rays can be obtained after two calculations, as

$$\bar{\rho} = 0.5 [\rho_1(\perp) + \rho_1(\parallel)] \quad (2.31)$$

$$\bar{\tau} = 0.5 [\tau_1(\perp) + \tau_1(\parallel)] \quad (2.32)$$

For the case of double identical glazings separated by air, with multiple reflections.

$$\rho_2 = \rho_1 + (\rho_1\tau_1^2 / 1 - \rho_1\rho_1) \quad (2.33)$$

$$\tau_2 = \tau_1\tau_1 /(1-\rho_1\rho_1) \quad (2.34)$$

for each component ray (11 or⊥).

For the case of triple identical glazings separated by air,

$$\rho_3 = \rho_2 + (\rho_2\tau_1^2 / 1-\rho_1\rho_2) \quad (2.35)$$

$$\tau_3 = \tau_2\tau_1 / 1- \rho_2\rho_1 \quad (2.36)$$

Average reflectances and transmittances for double and triple glazing were obtained as shown in Eqs. (2.31) and (2.32). Since the sum of reflectance, transmittance and absorptance is equal to unity, the

average absorptance for any of the three cases was obtained as a residual term. The absorptance of each glass pane was also calculated as a residual term using Eq. 2.30 (single glazing), Eqs. 230, 231, 232 (double glazing), and Eq. 230 to 236 (triple glazing). The variation of the average transmittance, reflectance, and absorptance with the angle of incidence is shown in Figs. 2.3, 2.4, and 2.5 for single, double and triple glazing with normal ¼ inch panes respectively.

2.4 Development of the Finite Difference Model

This model can be described as a numerical approximation to the partial differential equation for unsteady state heat conduction in three dimensions. We use the implicit formulation of the finite difference method to calculate the temperature distribution over the various layers of external walls and windows. The future temperature of a given node after a given time interval is determined implicitly along with the future temperatures of the surrounding nodes, from the present temperature of the nodes, the material properties and the boundary conditions. The number of nodes used was that number beyond which computation time became prohibitive while the accuracy improvement was insignificant (less than 1.0%).

2.4.1 Network Representation:

A conducting body such as a window or a wall is first divided into a given number of layers. Each layer in turn is divided into a number of sub-volumes called lumps. These lumps are centered on the nodal points shown in Fig. 2.6 and 2.7a with edges parallel to Cartesian axes, of length Δx, Δy, and Δz. We did not follow the usual customs of using cubic lumps with $\Delta x = \Delta y = \Delta z$ = a uniform separation between

adjacent nodes, because the horizontal depth, Δz of walls and windows is usually much smaller than the height or horizontal width. In the case of walls, the layer thickness, Δz was usually the actual thickness of a sublayer (insulation, gyproc, etc.). Therefore, Δz varied from one layer to another while Δx and Δy were kept constant in a square grid for all layers.

The thermal resistance for conduction between two nodes, R_{ij} can be expressed as

$$R_{ij} = \frac{d}{kA} \tag{2.37}$$

where d is the distance between the two nodes, k is the thermal conductivity and A is the area of interface between the two lumps. If the two nodes lie in the same layer, k is the conductivity of a single material, but if the two nodes lie in two different layers, the effective conductivity $\bar{k}$ is equal to

$$\bar{k} = k_1 k_2 \, (\Delta z_1 + \Delta z_2)/(k_1 \Delta z_2 + k_2 \, \Delta z_1) \tag{2.38}$$

where Δz_1 and Δz_2 are thicknesses of the two layers, and k_1 and k_2 are the conductivity of the two layers.

For exterior nodes which are placed at the surface (shown in Fig. 2.7b), the heat exchange with the surrounding air is by convection and radiation. Thus, the thermal resistance between a boundary node i and air is given by

$$R_{i\text{-air}} = \frac{1}{hA} \tag{2.39}$$

where h is the surface coefficient of heat transfer and A is the area of interface between the boundary lump and the surrounding air.

The thermal capacity C_i of node i is given by

$$C_i = V_i \rho_i c_{pi} \tag{2.40}$$

where V_i, ρ_i and c_{pi} denote the volume, the density and specific heat of lump i respectively.

2.4.2 The Finite Difference Approximation:

To derive the equations used to calculate the temperature distributions, we start with Fourier's equation [104] for the transient heat conduction through a unit volume containing no heat sources or sinks. In Cartesian coordinates,

$$k \left(\frac{\partial^2 T}{\partial x^2} + \frac{\partial^2 T}{\partial y^2} + \frac{\partial^2 T}{\partial z^2}\right) = \rho c_p \frac{\partial T}{\partial t} \tag{2.41}$$

where

k = thermal conductivity of the material

ρ = density of the material

c_p = specific heat of the material

T = temperature

t = time

In one-dimension, Eq. (2.41) is

$$\left(\frac{\partial^2 T}{\partial x^2}\right) = \frac{\rho cp}{k} \frac{\partial T}{\partial t} = \frac{1}{\alpha} \frac{\partial T}{\partial t} \tag{2.42}$$

where α is the thermal diffusivity of the material, $\alpha = \frac{k}{\rho cp}$

The solution is a one-dimensional time dependent function

$$T = T(x,t) \tag{2.43}$$

Forward Taylor's expansion [211] of this function at $|x + \Delta x|$ and $t = |t|$, in terms of its value at $x = |x|$ and $t = |t|$ is

$$T(x+\Delta x,t) = T(x,t) + \Delta x\left(\frac{\partial T}{\partial x}\right)_{x,t} + \frac{\Delta x^2}{2!}\left(\frac{\partial^2 T}{\partial x^2}\right)_{x,t} + \frac{\Delta x^3}{3!}\left(\frac{\partial^3 T}{\partial x^3}\right)_{x,t} + \sigma(\Delta x)^4 \qquad (2.44)$$

The notation $\sigma(\Delta x)^4$ indicates that the subsequent terms are of the order of $(\Delta x)^4$ and higher, and the reverse Taylor's expansion is

$$T(x-\Delta x,t) = T(x,t) - \Delta x\left(\frac{\partial T}{\partial x}\right)_{x,t} + \frac{\Delta x^2}{2!}\left(\frac{\partial^2 T}{\partial x^2}\right)_{x,t} - \frac{\Delta x^3}{3!}\left(\frac{\partial^3 T}{\partial x^3}\right)_{x,t} + \sigma(\Delta x)^4 \qquad (2.45)$$

By adding Eqs. (2.44) and (2.45), the central Taylor's expansion, which will be used in the derivation, is

$$T(x+\Delta x,t) + T(x-\Delta x,t) = 2T(x,t) + \Delta x^2\left(\frac{\partial^2 T}{\partial x^2}\right)_{x,t} + \sigma(\Delta x)^4 \qquad (2.46)$$

By neglecting the fourth order terms, the finite difference approximations to the first derivatives above can be obtained

$$\left(\frac{\partial T}{\partial x}\right)_{x,t}{}_{\text{forward}} \simeq \frac{1}{\Delta x}\left[T(x+\Delta x,t) - T(x,t)\right] \qquad (2.47)$$

and

$$\left(\frac{\partial T}{\partial x}\right)_{x,t}{}_{\text{backward}} \simeq \frac{1}{\Delta x}\left[T(x,t) - T(x-\Delta x,t)\right] \qquad (2.48)$$

and, to the same approximation, the central finite difference approximation to the second derivative becomes:

$$\left(\frac{\partial^2 T}{\partial x^2}\right)_{x,t}{}_{\text{cent.}} \simeq \frac{1}{\Delta x^2}\left[T(x+\Delta x,t) - 2T(x,t) + T(x-\Delta x,t)\right] \qquad (2.49)$$

At time $t = t+\Delta t$ Eq. 2.42 becomes:

$$\left(\frac{\partial^2 T}{\partial x^2}\right)_{x,t+\Delta t} \simeq \frac{1}{\Delta x^2}\left[T(x+\Delta x,t+\Delta t) - 2T(x,t+\Delta t) + T(x-\Delta x,t+\Delta t)\right] \qquad (2.50)$$

In the same way, we find finite difference approximations for the time variation as:

$$\left(\frac{\partial T}{\partial t}\right)_{x,t\ \text{forward}} \simeq \frac{1}{\Delta t}\left[T(x,t+\Delta T) - T(x,t)\right] \tag{2.51}$$

$$\left(\frac{\partial T}{\partial t}\right)_{x,t\ \text{backward}} \simeq \frac{1}{\Delta t}\left[T(x,t) - T(x,t-\Delta t)\right] \tag{2.52}$$

and

$$\left(\frac{\partial^2 T}{\partial t^2}\right)_{x,t\ \text{cent.}} \simeq \frac{1}{\Delta t^2}\left[T(x,t+\Delta t) - 2T(x,t) + T(x,t-\Delta t)\right] \tag{2.53}$$

Hence, the implicit representation of the unidimensional transient heat conduction per unit volume can be obtained by substituting Eq. (2.50) and Eq. (2.51) in Eq. (2.42).

$$\frac{k}{(\Delta x)^2}\left[T(x+\Delta x,t+\Delta t) - 2T(x,t+\Delta t) + T(x-\Delta x,t+\Delta t)\right] =$$

$$\frac{\rho c_p}{\Delta t}\left[T(x,t+\Delta t) - T(x,t)\right] \tag{2.54}$$

Using a for x, b for x+Δx, c for x-Δx, and T' for a future temperature at t+Δt and inserting the actual node volume AΔx, Eq. (2.54) becomes

$$\frac{A\Delta x k}{\Delta x^2}\left[T'_b - 2T'_a + T'_c\right] = \frac{A.\ \Delta x \rho_a C_p}{\Delta t}\left[T'_a - T_a\right] \tag{2.55}$$

where A is the area of interface between lumps in the direction normal to the heat flow and Δ x is the distance between nodes. Subsituting Eq. (2.37) and (2.40) in Eq. (2.55), we get

$$\frac{(T'_b - T'_a)}{R_{ab}} + \frac{(T'_c - T'_a)}{R_{ac}} = \frac{C_a}{\Delta t}(T'_a - T_a) \tag{2.56}$$

where R_{ab} and R_{ac} are the thermal resistances between node a and the neighbouring nodes b and c at x+Δx and x-Δx, and C_a is the thermal capacity of lump a.

For a cubic grid, if we add a heat source, the general three dimensional form of Eq. (2.56) is

$$\left(\sum_{j=1}^{n_k} \frac{T_j'-T_i'}{R_{ij}}\right)+\left(\sum_{\ell=1}^{n_R} \frac{T_\ell'-T_i'}{R_{i\ell}} + \varepsilon_g + \varepsilon_s\right)= \frac{C_i}{\Delta t}\ (T_i'-T_i) \qquad (2.57)$$

where ε_g is any internally generated heat, ε_s is any solar heat generated in the actual volume, n_k is the number of surrounding nodes in the same conducting body, and n_R is the number of surrounding nodes outside the conducting body (i.e. outdoor air, indoor air, and other media in contact with the conducting body). $n_k + n_R = 6$ in all cases. If the node of concern, i, is surrounded by nodes within the same conducting body $n_K = 6$ and $n_R = 0$.

In the present model, we have no interally generated heat, thus ε_g is zero here. If we call $\left(\varepsilon_s + \sum_{\ell=1}^{n_R} \frac{T_\ell'}{R_{i\ell}}\right) = n_i$, since in all cases we have measurements of T_ℓ' for the air and surrounding panels, the future temperature T_i' of node i can be expressed as

$$T_i'\left[\ 1 + \sum_{J=1}^{n_k} \frac{\Delta t}{C_i R_{ij}} + \sum_{\ell=1}^{n_R} \frac{\Delta t}{C_i R_{i\ell}}\ \right] = T_i + \frac{\Delta t}{C_i} \sum_{J=1}^{n_k} \frac{T_j'}{R_{ij}} + \frac{\Delta t}{C_i}\, n_i$$

$$\text{or} \quad T_i' = \frac{T_i + \frac{\Delta t}{C_i} \sum_{J=1}^{n_k} \frac{T_j'}{R_{ij}} + \frac{\Delta t}{C_i}\, n_i}{\left[1 + \sum_{j=1}^{n_k} \frac{\Delta t}{C_i R_{ij}} + \sum_{\ell=1}^{n_R} \frac{\Delta t}{C_i R_i}\right]} \qquad (2.58)$$

Replacing $(1/R_{ij}$ by H_{ij}, $(\Delta t/c_i)$ by N_i, and $[1+ \sum_{j=1}^{n_k} \frac{\Delta t}{c_i R_{ij}} + \sum_{\ell=1}^{n_R} \frac{\Delta t}{c_i R_{i\ell}}\ ]$ by L_i gives

$$T_i' = \frac{T_i}{L_i} + \left(\frac{N_i}{L_i} \sum_{j=1}^{n_k} T_j' \cdot H_{ij}\right) + \frac{N_i}{L_i}\, n_i \ ,$$

or

$$T_i' - \left(\frac{N_i}{L_i} \sum_{j=1}^{n_k} T_j' \cdot H_{ij}\right) = \left(\frac{T_i}{L_i} + \frac{N_i}{L_i}\, n_i\right)$$

$$\text{or} \quad T_i' + \left(\sum_{j=1}^{n_k} a_{ij} T_j' \right) = b_i \qquad (2.59)$$

where $a_{ij} = -\left(\frac{N_i}{L_i} \cdot H_{ij}\right)$ and $b_i = \left(\frac{T_i}{L_i} + \frac{N_i}{L_i} n_i\right)$

with all the components of b_i known at time t from the previous calculation at time $t - \Delta t$. For the first time interval, an assumption must be made for the present temperatures T_i. We took a uniform temperature in each layer distributed between the measured inside and outside temperature according to the interlayer resistances.

The indoor temperature was kept constant with a thermostatic control . For experiments with constant outdoor temperature, the solution reached its steady state 3-dimensional distribution during the second hour. All simulations were started at midnight, when the outdoor temperature is relatively constant and no oscillations of the computed temperature were observed after the proper grid size had been adopted. Applying Eq. (2.59) to each node of the system will result in a set of n algebraic equations in n unknown temperatures.

$$\begin{aligned}
&a_{11} T_1' + a_{12} T_2' + a_{13} T_3' + \ldots\ldots + \ldots\ldots + a_{1n} T_n' = b_1 \\
&a_{21} T_2' + a_{22} T_2' + a_{23} T_3' + \ldots\ldots + \ldots\ldots + a_{2n} T_n' = b_2 \\
&a_{31} T_1' + a_{32} T_2' + a_{33} T_3' + \ldots\ldots \\
&\ldots\ldots \quad \ldots\ldots \\
&\ldots\ldots \quad \ldots\ldots \\
&a_{n1} T_1' + a_{n2} T_2' + a_{n3} T_3' \ldots + \ldots + a_{nn} \quad T_n' = b_n
\end{aligned}$$

or in matrix form

$$[A]\,[T'] = [B] \qquad (2.60)$$

where matrices A, B, and T' represent the thermal coefficients a_{ij}, b_i, and the future node temperature T_i'. They are given by

$$[A] = \begin{bmatrix} a_{11} & a_{12} & a_{13} & \cdots & a_{1n} \\ a_{21} & a_{22} & a_{23} & \cdots & a_{2n} \\ a_{31} & a_{32} & a_{33} & \cdots & n_{3n} \\ a_{41} & a_{42} & - & - & - \\ - & - & - & - & - \\ - & - & - & - & - \\ - & - & - & - & - \\ a_{n1} & a_{n2} & a_{n3} & & a_{nn} \end{bmatrix}, \quad [T'] = \begin{bmatrix} T_1' \\ T_2' \\ T_3' \\ T_4' \\ \cdot\cdot \\ \cdot\cdot \\ \cdot\cdot \\ \cdot\cdot \\ \cdot\cdot \\ T_n' \end{bmatrix}, \text{ and } [B] = \begin{bmatrix} b_1 \\ b_2 \\ b_3 \\ b_4 \\ \cdot\cdot \\ \cdot\cdot \\ \cdot\cdot \\ \cdot\cdot \\ \cdot\cdot \\ b_n \end{bmatrix} \quad (2.61)$$

The solution for the future temperature [T'] was obtained by using Gauss elimination.

2:4.3 Classification of Nodes by Type and Position:

In this model there are two different procedures for the calculation. The first is used for windows or uniform wall panels. The second is used for wall panels with openings for windows. The nodal arrangements for both procedures are shown in Figs. (2.8) and (2.9). There are five types of nodes that are common to both procedures.

Type 1: Reference nodes

Type 2: Boundary nodes

Type 3: Corner nodes

In the case of symmetrical geometry with symmetrical boundary conditions in either procedure, we need only the temperature distribution for one-quarter of the system. The axes of thermal symmetry are adiabatic interfaces because heat flow through an axis or plane requires a temperature

difference across the axis or plane. They are shown for a uniform panel or window in Fig. (2.10a) and for a panel with opening for window in Fig. (2.10b). The adiabatic conditions at the axis of symmetry require two additional common types of nodes.

Type 4: Adiabatic reference nodes

Type 5: Adiabatic boundary nodes

The above 5 common types of nodes are shown in Figs. (2.8) and (2.9). Other types of nodes are used only in one of the two procedures. For windows and uniform panels (Fig. 2.8) the following type is needed.

Type 6: Adiabatic reference corner nodes

For panels with openings for windows (Fig. 2.9), the following three types of nodes are used to allow for different materials in the window frame.

Type 7: Frame boundary nodes (Frame reference nodes)

Type 8: Adiabatic frame boundary nodes

Type 9: Frame corner nodes.

The layers of rectangular windows or solid wall panels (Fig. 2.11) and the layers of wall panels with openings for windows (Fig. 2.12) are classified into three groups. The first group for the outside boundary layer, the second for median layers, and the third for the inside boundary layer. The nodes in the outside boundary layer are in contact with the outside air and can receive solar heat by absorption. These nodes exchange heat by radiation and convection to the outside air and by conduction to the surrounding nodes. The nodes in the median layers are connected thermally to the surrounding nodes only by conduction.

For windows, solar heat is partly absorbed in the median and the inside layers, as well. Nodes in the inside boundary layer exchange heat with room air by radiation and convection and with surrounding nodes by conduction.

The positions of the nodes were input to the computer with a three dimensional label, x, y, z for column, row and layer. For the solution of the future temperature equations, a single subscript i was derived, from

$$i = x + \ell_1(y-1) + \ell_2(z-1) \qquad (2.62)$$

where ℓ_1, and ℓ_2 denote the number of nodes per row and the number of nodes per layer (i.e. for a square panel $\ell_2 = \ell_1^2$, and for a rectangular panel $\ell_2 = \ell_1$ x the number of columns). Consequently, a typical node $P_{x,y,z}$ corresponds, to P_i and the six surrounding nodes $P_{x-1,y,z}$, $P_{x+1,y,z}$, $P_{x,y-1,z}$, $P_{x,y+1,z}$, $P_{x,y,z-1}$ and $P_{x,y,z+1}$ correspond to P_{i-1}, P_{i+1}, $P_{i-\ell_1}$, $P_{i+\ell_1}$, $P_{i-\ell_2}$, and $P_{i+\ell_2}$ respectively as shown in Fig.2.13. Thus, the thermal interaction between two nodes i and j is represented by the element a_{ij}. Each diagonal element a_{ij} has a value of 1.0. In each row, at most only six off diagonal coefficients centred on the diagonal have non zero values, since only a maximum of six surrounding nodes interact with the node i described thermally by row i. The column location of each of the six diagonal coefficients is conveniently described in terms of the particular row i of concern (i.e. the six non zero off diagonal elements in row i are:, $a_{i,i-1}$, $a_{i,i+1}$, $a_{i,i-\ell_1}$, $a_{i,i+\ell_1}$, $a_{i,i-\ell_2}$, and $a_{i,i+\ell_2}$).

2.4.4 Determination of the Heat Transfer Coefficients:

The heat transfer coefficient is the inverse of the thermal resistance (given by Eqs. (2.37) and (2.39)) between the node i of concern and a neighbouring node j. If the neighbouring node does not lie within the same conducting body it is called node . Thus the heat transfer coefficient is denoted by either H_{ij} for internal nodes or $H_{i\ell}$ for boundary nodes.

The coefficients a_{ij} of matrix [A] and n_i in matrix [B] were determined from the heat transfer coefficients H_{ij} and $H_{i\ell}$. Since the spacing between nodes in the x- and y- directions was taken equal ($\Delta x = \Delta y$), the heat transfer coefficient H_{ij} between any two adjacent nodes in the same layer, shown in Fig. (2.14.a), is

$$H_1 = k_r \frac{A}{\Delta x} = k_r \frac{\Delta y \Delta z}{\Delta x} \qquad (2.63)$$

$$= k_r \cdot \Delta z_r$$

with k_r being the thermal conductivity of the layer r in either the x or y direction. Δz_r is the thickness of layer r. For two adjacent nodes in two different layers (c.f. Fig. 2.14b), the heat transfer coefficient H_{ij} is given by

$$H2 = \overline{k}_r (\Delta X)^2 / ((\Delta Z_r + \Delta Z_{r+1})/2) \qquad (2.64)$$

where $\overline{k}_r$ is the equivalent thermal conductivity between the two interacting nodes in the two different layers, obtained from Eq. 2.38. For the two major boundary layers the heat transfer coefficient $H_{i\ell}$ is given by

$$H3 = h_o (\Delta X)^2 \quad \text{(outside boundary layer)} \tag{2.65}$$

and

$$H4 = h_i (\Delta X)^2 \quad \text{(inside boundary layer)} \tag{2.66}$$

where h_o and h_i are the outside and inside surface coefficients for convection and radiation. The value of h_o varies with wind speed, wind direction, and outdoor air temperature as discussed in section 2.3 and Chapter IV. h_i was assumed constant at 8.3 w/m^2. K° (still air) [10].

The heat transfer coefficients H_{ij} and $H_{i\ell}$ were evaluated as the inverse of the thermal resistance given by Eq. (2.37). The value of a heat transfer coefficient depends on the thermal conductivity of the material, k, between the two interacting nodes or the surface coefficient for convection and radiation h, the spatial distance between the two nodes, d, and the area of contact between the two lumps centred on these two nodes, A. Since d and k or h are independent of the node type, the thermal conductance coefficients differ from one type to another, within the same layer, only if there is difference in the area of contact, A. This difference is proportional to the area of contact.

The heat transfer coefficients H1, H2, H3, and H4 were calculated for the reference nodes of every layer (type 1). The heat transfer coefficients H1, H2, H3 and H4 for other types were expressed in terms of those of type 1 after being multiplied by a factor proportional to the ratio of the areas of contact, i.e. the area of contact (in the xy plane) for type 4 (adiabatic reference nodes) and type 6 (adiabatic reference corner nodes) is identical to type 1. Nodes of type 2

(boundary nodes) and type 5 (adiabatic boundary nodes) have a proportionality factor of ½, and type 3 (corner nodes) has a portionality factor of ¼.

Similarly, the frame boundary nodes (type 7) in every layer, were taken as a reference node for the other two node types of the frame (type 8, adiabatic frame boundary nodes and type 9; frame corner nodes). The heat transfer coefficients H_{ij} for two interacting frame nodes in the same layer is given by

$$H5 = K_f \Delta Z_r \Delta_f / \Delta X \qquad (2.67)$$

where K_f is the thermal conductivity of the frame material and Δ_f is the frame thickness in the x or y direction and is shown in Fig. (2.14a).

If the two nodes lie in the same layer but one is a frame node and the other is a panel node (as shown by H6 in Fig. 2.14 a) the heat transfer coefficient H_{ij} is given by

$$H6 = \overline{k} \ \Delta Z_r \Delta y / (\Delta_f + \tfrac{1}{2} \Delta X) \qquad (2.68)$$

where $\overline{k}$ is the series conductivity and is calculated as

$$\overline{k} = k_f k_r (\Delta f + \tfrac{1}{2} \Delta x) / (\tfrac{1}{2} k_f \Delta x + k_r \Delta f)$$

If the frame reference node (type 7) is in contact with air or window glass, we have

$$H7 = h_f \Delta y \Delta Z_r \qquad (2.69)$$

where h_f equals h_o if the layer is exposed to the outside air, and equals h_i if the layer is exposed to the inside air. For nodes of type 7 that are in contact with window glass, we used a constant $h_f = 10$

$w/m^2.K$ determined by matching calculated temperatures for both the window and frame nodes to experiments.

In the case where the two frame nodes lie in two consecutive median layers, the heat transfer coefficient H8 (shown in Fig. 2.14b) is given by

$$H8 = K_f \Delta_f \Delta X / ((\Delta Z_r + \Delta Z_{r+1})/2) \quad (2.70)$$

For the inside and outside frame layers in contact with air; H9 is given by

$$H9 = h_0 \Delta X \Delta_f \quad \text{(outside layer)} \quad (2.71)$$

and

$$H10 = h_i \Delta X \Delta_f \quad \text{(inside layer)} \quad (2.72)$$

Coefficients H5, H6, H7, H8, H9, and H10 were calculated for the frame boundary nodes (type 7). As before, coefficients for type 8 have an area of contact proportionality factor of 1.0. For frame corner nodes (type 9), the proportionality factor for H5 and H6 is also equal 1.0 but the proportionality factor for coefficient H7 becomes

$$U_1 = \frac{2(\Delta X - \Delta f)\, \Delta z}{\Delta Z\, \Delta X} \quad (2.73)$$

and for coefficients H8, H9, and H10, the propotionality factor for type 9 becomes

$$U_2 = ((2\Delta_f \Delta X - \Delta_f^2)) \,/\, (\Delta_f \Delta X) \quad (2.74)$$

Finally, we need a coefficient for boundary nodes at the panel or window outer edges, H11 (shown in Fig. 2.14a and b) that do not come into contact with the air.

$$H11 = h_c \Delta y \Delta z_r \quad (2.75)$$

with $h_c = 10\ w/m^2.K^\circ$

Wall panels were divided into five layers each of thickness ΔZ_r matching the actual five layers of the wall panel. The air gap after the insulation between the studs was considered as one layer. The thermal properties, dimensions, and geometry of each layer are described in Chapter IV. Glass panes were divided into two layers each to allow the calculation of a different temperature distribution on each surface and to allow a temperature gradient across their depth without too much computer time. The air layers in multiple windows were left undivided. Thus, a double glazed window has five layers and a triple glazed window has eight layers.

The eleven heat transfer coefficients were calculated for single, double, and triple windows, and for the particular wall panel used in the experiments (with and without window openings). The values of the eleven coefficients are shown in Table 2.3 for nodes interacting within the same layer and in Table 2.4 for nodes interacting in two consecutive layers. For nodes in contact with air, the values of the coefficients are given in Table 2.5.

Coefficients H1, H2, H5, H6, and H8 were used to evaluate the a_{ij} coefficients of matrix [A], while H3, H4, H7, H9, H10, and H11 were used to evaluate the n_i term.

The thermal storage capacity of a reference node (type 1) was calculated for each layer of the window and of the panel. For panels with window openings, the thermal storage capacity was also calculated for a frame boundary node (type 7). For types 2 to 6, thermal storage capacities were obtained according to their volume ratio with type 1.

Similarly, the thermal storage capacities for types 8 and 9 were obtained as a volume ratio to type 7. The thermal storage capacities of types 1 or 7 for each layer are shown in Table 2.6.

Layer number	WINDOW		WALL	FRAME		
	H1	H_{11}	H1	H5	H_6	H7
1	0.003192	0.00547	0.00286	0.00035	0.0046	0.0854
2	0.003192	0.00547	0.00142	0.00140	0.00276	0.3416
3	0.000328	0.02188	0.00142	0.000175	0.00230	0.0427
4	0.003192	0.00547	0.00414	0.00245	0.0073	0.68318
5	0.003192	0.00547	0.00296	0.00035	0.0046	0.0179
6	0.000328	0.02183				
7	0.003192	0.00547				
8	0.003192	0.00547				

Table 2.3: Heat transfer coefficients between nodes within the same layer (w/K)

Layer number	WINDOW	WALL	FRAME
	H2	H2	H8
1,2	10.350	0.04475	0.03125
2,3	0.5548	0.04680	0.04160
3,4	0.5548	0.04123	0.0250
4,5	10.350	0.03963	0.0208
5,6	0.5548		
6,7	0.5548		
7,8	10.350		

Table 2.4: Heat transfer coefficients H_{ij} between two nodes in two consecutive layers (w/K)

Layer Position	WINDOW		WALL		FRAME	
	H3 (outside)	H4 (inside)	H3 (outside)	H4 (inside)	H9 (outside)	H10 (inside)
First or Last layer	2.0875	0.51810	1.38596	0.34404	0.1708	0.0424

Table 2.5: Heat transfer coefficients $H_{i\ell}$ (w/K)

Layer number	WINDOW	WALL	FRAME
	C	C	C
1	403.36	35.624	4.354
2	403.36	22.447	17.416
3	0.9251	17.812	2.177
4	403.36	12.528	30.478
5	403.36	35.624	4.354
6	0.9251		
7	403.36		
8	403.36		

Table 2.6: Thermal storage capacity of reference lumps in each layer (J/K)

2.4.5 Heat Sources and Sinks in the Panels

The coefficients n_i were determined for every node in order to determine the elements b_i of matrix [B]. The term n_i accounts for the heat that is created by absorption of solar radiation in the external surfaces of opaque panels and in all layers of glazing. The solar radiation reflected back to the inside of the glazing was measured, and never exceeded 8% of the input solar radiation, so solar heating from reflected radiation was ignored for all compass orientations. Each

glazing layer absorbs a portion of the radiation transmitted through the layer preceeding it, so the numerical value of the solar heat absorbed changes layer by layer.

The term η_i was determined for three types of nodes (type 1,2, and 7) and is given in Table 2.7.

Layer	Node type		η_i at time t (watts)
Outside layer	Window or Wall	Type 1	$\eta_i = (A.\alpha_s .I(t) + H3 . To(t))$
		type 2	$\eta_i = .5(A\alpha_s . I(t) + H3. To(t))+H11. T_\ell (t)$
		type 7	$\eta_i = (A_f.\alpha_s. I(t)) + H9\ T_o(t) + H7.T_o (t)$
Median layers	Window	type 1	$\eta_i = (A. \alpha_s. \tau I(t))$
		type 2	$\eta_i = .5\ (A. \alpha_s.\tau I(t)) + H11. T_\ell(t)$
	Wall	type 1	$\eta_i = 0.0$
		type 2	$\eta_i = H11.T_\ell (t)$
		type 7	$\eta_i = H7. T_v(t)$
Inside layer	Window	type 1	$\eta_i = (A.\alpha_s. \tau I(t) + H4.T_i(t))$
		type 2	$\eta_i = .5(A.\alpha_s. \tau I(t)+H4.T_i(t)) + H11.T_\ell(t)$
	Wall	type 1	$\eta_i = H4. T_i(t)$
		type 2	$\eta_i = .5(H4. Ti(t)) + H11. T_\ell(t)$
		type 7	$\eta_i = H7. T_i(t) + H10. T_i (t)$

Table 2.7: Net rate of heat input for nodes type 1, 2, and 7.

Notation for Table 2.7

A = Surface area exposed to input for a reference lump (m^2)

A_f = Surface area exposed to input for a frame reference lump (m^2)

α_s = absorptance of the layer

τ = average transmittance of the preceeding layers

I_t = incident solar radiation intensity at time t (w/m^2)

$T_o(t)$ = outdoor air temperature at time t

$T_i(t)$ = inside air temperature at time t

$T_\ell(t)$ = temperature in the gap at the edges of a panel or window

$T_v(t)$ = air temperature of the medium surrounding a given layer of the frame ($T_v(t) = T_o(t)$, or $= T_i(t)$, or $= T_f(t)$ where T_f is frame-window air gap temperature).

2.4.6 Determination of Matrix [A] and [B] Coefficients

The energy balance of node i was given in Eq. (2.59) as

$$T_i' + \sum_{j=1}^{j=n_k} T_j' \cdot a_{ij} = b_i \qquad (2.76)$$

with

$$a_{ij} = -\frac{N_i}{L_i} H_{ij}$$

and

$$b_i = \frac{T_i}{L_i} + \frac{N_i}{L_i} \eta_i$$

where

T_i' = the future temperature of node i after a time interval (K)

T_i = the present temperature of node i, (K)

T_j' = the future temperature of one of the N_k surrounding nodes, (K)

$n_i = [\epsilon_s + \sum_{\ell=1}^{n_R} \frac{T_\ell'}{R_{i\ell}}]$ (given in Table 2.7)

$N_i = \Delta t/C_i$ (K /W), Δt = time interval(sec.), C_i = thermal storage capacity of the lump (j/K)

$$L_i = 1 + N_i[\sum_{j=1}^{n_k} H_{ij} + \sum_{\ell=1}^{n_R} H_{i\ell}]$$

where H_{ij} and $H_{i\ell}$, are heat transfer coefficient between node i and a surrounding node j and ℓ respectively.

In order to obtain the future temperature at all nodes, the terms N_i and L_i and the elements a_{ij} and b_i must be determined with respect to the various types of nodes.

For each layer, r, the term N_i can be determined for the main reference lump, N(r), and for the frame reference lump $N_f(r)$. The term N_i for lump i depends on the lump type. For type 1 to 6, N_i is given as a ratio of N(r) and for type 7 to 9, N_i is given as a ratio of $N_f(r)$ where

$$N(r) = \Delta t/C(r) \quad (K/w) \qquad (2.77)$$

and

$$N_f(r) = \Delta t/C_f(r) \quad (K/w) \qquad (2.78)$$

where Δt is the time interval in seconds, and C(r) and $C_f(r)$ are the thermal storage capacity for the main and frame reference lumps of layer r respectively. N_i for types 1 to 9 is given in Table 2.8.

The parameter L_i is determined for various types of nodes. For windows and solid wall panels, there is a maximum of six different types of nodes used (type 1 to 6). In the case of panels with window openings, an additional three node types are used to account for the frame of the window opening created in the panel. This results in a special situation for panels with window openings where nodes of type 1,2,4 or 5 may adjoin each other or nodes of type 7, 8 or 9 and parameter L_j must be determined twice for type 1,2,4 and 5, depending on the conductivity and size of the neighbouring nodes. The various formulae for the parameter L_i are shown in Table 2.8.

Having determined N_i and L_i, the a_{ij} and b_i can be evaluated. The a_{ij} are classified into two groups, group I comprises the coefficients between two interacting nodes that are in the same layer. Group II comprises the coefficients between two interacting nodes in two consecutive layers. Because of the different types of edge geometry, Group I is subdivided into 2 cases a, and b.

In group I., case I.a is limited to the cases where

$H_{ij} = H1$ (for types 1 to 6) and $H_{ij} = H5$ (for type 7 to 9)

Case I.b is limited to the situations where

$H_{ij} = 0.5\ H1$ (for types 1 to 6)

and

$H_{ij} = H6$ (for types 7 to 9)

Similarly group II is limited to the situations where

$H_{ij} = H8$ (for types 7 to 9).

Node Type	Parameter N_i	Parameter L_i (Typical cases)	Parameter L_i (Special Cases)***
Type 1	$N_i = N(r)$	$L_i = 1.0 + N_i[4H1 + H2 + H_v^*]$	$L_i = 1.0 + N_i[3H1 + H6 + H2 + H_v^*]$
Type 2	$N_i = 2\ N(r)$	$L_i = 1.0 + N_i[2H1 + .5H_2 + .5H_v + H11]$	$L_i = 1.0 + N_i[H1+H6+.5H2+.5H_v+H11]$
Type 3	$N_i = 4\ N(r)$	$L_i = 1.0 + N_i[H1 + .25H2 + .25H_v + H11]$	———
Type 4	$N_i = N(r)$	$L_i = 1.0 + N_i[3H1 + H2 + H_v]$	$L_i = 1.0 + N_i\ [2H1+H2+H_v+H6]$
Type 5	$N_i = 2N(r)$	$L_i = 1.0 + .5N_i[3H1 + H2 + H_v]$	$L_i = 1.0 + N_i\ [0.5H1+0.5H2+0.5H_v+H6]$
Type 6	$N_i = N(r)$	$L_i = 1.0 + N_i\ [2H1 + H2 + H_v]$	———
Type 7	$N_i = N_f(r)$	$L_i\ 1.0 + N_i\ [2H5 + H6 + H7 + H8 + H_f^{**}]$	———
Type 8	$N_i = N_f(r)$	$L_i = 1.0 + N_i[H5 + H6 + H7 + H8 + H_f]$	———
Type 9	$N_i = v_r^{****} N_f(r)$	$L_i = 1.0 + N_i[2H5+2H6+U_1H7+U_2H8+U_2H_f]$	———

* For median layers, $H_v = H_2$, for outside layer $H_v = H3$, and for inside layer $H_v = H4$.

** For median layers, $H_f = H8$, for outside layers $H_f = H9$, and for inside layer $H_f = H10$.

*** For nodes in contact with the frame.

**** v_r = type 7 to type 9 volume ratio.

Table 2.8 Parameters N_i and L_i for each node type.

Node Type	Coefficients a_{ij} for matrix [A]		
	CASE I.a	CASE I.b	CASE II
Type 1	$a_{ij} = \frac{-Ni}{L_i} \cdot H1$	———	$a_{ij} = \frac{-Ni}{L_i} \cdot H2$
Type 2	$a_{ij} = \frac{-Ni}{L_i} \cdot H1$	$a_{ij} = \frac{-0.5\ Ni}{L_i} \cdot H1$	$a_{ij} = \frac{-0.5Ni}{L_i} \cdot H2$
Type 3	———	$a_{ij} = \frac{-0.5\ Ni}{L_i} \cdot H1$	$a_{ij} = \frac{-.25Ni}{L_i} \cdot H2$
Type 4	$a_{ij} = \frac{-Ni}{L_i} \cdot H1$	———	$a_{ij} = \frac{-Hi}{L_i} \cdot H2$
Type 5	$a_{ij} = \frac{-Ni}{L_i} \cdot H1$	$a_{ij} = \frac{-0.5\ Ni}{L_i} \cdot H1$	$a_{ij} = \frac{0.5\ Ni}{L_i} \cdot H2$
Type 6	$a_{ij} = \frac{-Ni}{L_i} \cdot H1$	———	$a_{ij} = \frac{-Ni}{L_i} H2$
Type 7	$a_{ij} = \frac{-Ni}{L_i} \cdot H5$	$a_{ij} = \frac{-Ni}{L_i} \cdot H6$	$a_{ij} = \frac{-Ni}{L_i} H8$
Type 8	$a_{ij} = \frac{-Ni}{L_i} \cdot H5$	$a_{ij} = \frac{-Ni}{L_i} \cdot H6$	$a_{ij} = \frac{-Ni}{L_i} H8$
Type 9	$a_{ij} = \frac{-Ni}{L_i} \cdot H5$	$a_{ij} = \frac{-Ni}{Li} \cdot H6$	$a_{ij} = \frac{-U2\ Ni}{L_i} H8$

Table 2.9: Thermal Coefficient a_{ij} for each node type.

The coefficients a_{ij} for both groups are shown in Table 2.9.

The coefficients b_i of matrix [B] can be evaluated since N_i, L_i, and n_i were previously determined.

2.4.7 Net Energy Gain or Loss

Heat gain or loss for a window or a wall panel occurs at the boundary surfaces. The boundary surfaces are the external surface facing out, the internal surface facing in, and the side surfaces. A solid wall panel or a window has four side surfaces. In the case of panels with openings for windows, there are additional side surfaces to be considered at the window opening as shown in Fig. 2.15.

When the future temperature of the nodes after a time increment t' have been determined, the heat gain or loss is calculated from the heat flow equations for the boundary nodes. In this model the heat flow equation for boundary nodes on any single boundary surface was expressed as

$$q_i = H_{i\ell} \cdot \Delta\bar{T}_{i\ell} \qquad (2.79)$$

where

q_i = the average rate of heat flow for node i through that single surface during the time interval (w)

$H_{i\ell}$ = is the coefficient of heat transfer between node i and the adjacent air or panel at position ℓ opposite i (w/K)

$\Delta\bar{T}_{i\ell}$ = is the average temperature difference between node i and the adjacent air or panel at position ℓ given by

$$\Delta\bar{T}_{i\ell} = \tfrac{1}{2}[[T_\ell(t) + T_\ell(t+\Delta t)] - [T_i(t) + T_i(t+\Delta t)]]\,°K \qquad (2.80)$$

A negative heat flow rate indicates heat loss from the node. In order to check the heat balance calculated later, separate sums were done for heat gains and for heat losses at boundary surfaces.

Thus the average heat gain, $q_g\ (t+\frac{1}{2}\Delta t)$ and heat loss $q_L(t+\frac{1}{2}\Delta t)$ are expressed as

$$q_g(t+\tfrac{1}{2}\Delta t) = \sum_{\text{boundary nodes}} H_{i\ell}\ \Delta\bar{T}_{i\ell} \quad \text{for} \quad \Delta\bar{T}_{i\ell} > 0.0 \qquad (2.81)$$

and

$$q_L(t+\tfrac{1}{2}\ t) = \sum_{\text{boundary nodes}} H_{ij}\ \Delta\bar{T}_{j\ell} \quad \text{for} \quad \Delta\bar{T}_{i\ell} < 0.0 \qquad (2.82)$$

The corresponding energy gain, E_g, and energy loss, E_L, during the time interval were expressed as

$$E_g = 10^{-6}.\ \Delta t\ .\ q_g\ (t + \tfrac{1}{2}\ \Delta t) \quad \text{(MJ)} \qquad (2.83)$$

and

$$E_L = 10^{-6}.\ \Delta t\ .\ q_L\ (t + \tfrac{1}{2}\ \Delta t) \quad \text{(MJ)} \qquad (2.84)$$

The total energy stored in the system during the time interval is the sum of the energy stored in each node.

$$E_{st} = 10^{-6}.\ \sum_{i=1}^{n} c_i\ (T_i(t+\Delta t) - T_i\ (t)) \quad \text{(MJ)} \qquad (2.85)$$

We check the energy calculation for each time interval with

$$E_g + E_L + E_{st} = 0.0 \qquad (2.86)$$

Another source of heat loss or gain in buildings is that associated with infiltration through gaps and cracks around windows and external panels.

Energy loss or gain due to air infiltration is difficult to determine theoretically because the rate of air infiltration can be limited by the rate of exfiltration and depends more on workmanship,

(i.e. the width and length of cracks and gaps), than on the pressure difference across a particular wall. ASHRAE [110] gives infiltration rates for specific walls and window at only a few discrete pressure differences. More detailed information was required to evaluate the energy loss associated with air infiltration in this study. The results of an experimental investigation to relate the amount of air infiltration to the wind speed are presented in Chapter IV. An infiltration coefficient F, representing the rate of sensible heat loss or gain per degree temperature difference per meter length of crack, was found to be related to wind speed, v, by

$$F = .081 + .024\ v + .0096\ v^2 + .0053\ v^3 \qquad (2.87)$$

where F is in W/K. m when the wind speed is in m/sec. As shown later in Chapter IV, F represents the product of the density of the air, the specific heat of the air, and the volume of the air infiltrating per unit time per unit length of crack. This air volume depends on the pressure difference, and crack size.

2.4.8 Examination of Sideways Heat Exchange

In the case of normal concrete or brick external walls heat gain or loss takes place only at the external and internal surfaces. If these walls contain openings for windows, heat gain or loss takes place at the sides of these openings. For a panelized external wall, heat gain or loss also takes place at the air gaps between panels. In order to examine the significance of the sideways heat exchange at the interface between panels, the heat loss was calculated for two computer

simulated cases. In the first case with no air circulation in the gaps, adiabatic conditions were assumed. In the second case heat was exchanged between the panel and air circulating through the air gap between panels. In both cases the temperatures of room air and outdoor air were assumed constant at 20°C and -16°C respectively. In the second case the air temperature in the gap was assumed constant at -10°C. Outside and inside surface heat transfer coefficients were also assumed constant at 17.9 $w/m/^2.K$ and 8.3 $w/m^2.K$ respectively. In the gap the heat transfer coefficient was taken as 10 $w/m^2.K$ in the non-diabatic case. This value was chosen based on a best fit between calculated and measured temperature at the edge.

The rate of heat loss from the panel for the non-adiabatic case was 35% more than that for the adiabatic case. The dimensions of the simulated panels were 2.5 x 2.5 x 0.1625 meters. The edge area is 26% of the inside or the outside surface area. About ¼ of the extra heat loss arises because close to the gaps, the inside edges of the panels are cooled by the air circulation in the gaps. Thus a panelized external wall will often have a higher rate of heat loss than a normal wall with the same materials.

The thickness of an external wall is several times larger than the thickness of a window. How far the window is recessed influences the edge heat losses of the panel around the window opening. The sideways heat loss at the window opening was simulated for various window positions. The total sideways heat transfer of the wall panel at the window opening comprises three components. The first is the heat

transfer at the outer portion of the window opening. The second is the heat transfer at the inner portion and the third is the heat transfer to the window edges. The three portions of the side surfaces at the window opening are shown in Fig. 2.15.

The sideways heat transfer at the window opening was calculated using the same temperatures and surface coefficients as the adiabatic case discussed earlier. The results are shown in Fig. 2.16 along with front and back heat transfer. The index numbers shown indicate the number of the panel layer in contact with the window. The effect of window distance from the exterior surface of the panel on the heat loss is shown in Fig. 2.17. Minimum heat loss occurs with the window aligned with the insulation layer (layer 2). For other types of construction, the position of the window which gives minimum heat loss will depend on the thermophysical properties of the wall layers, their thicknesses, and their order.

2.5 SUMMARY

Chapter II was limited to the thermal aspects of the present study. The methods that are commonly used in the calculation of heat transfer through windows and walls were discussed. The advantages of the present thermal model were explained in sec. 2.2. The basis upon which the finite difference technique was preferred over the finite element technique was also discussed in sec. 2.2. Heat exchange at the external surface by convection and radiation was reviewed (sec. 2.3). The relations relating the convection coefficient at the external

surface to wind speed and wind direction were presented in sec. 2.3.3. The development of the finite difference model to approximate the partial differential equation for unsteady state heat conduction in three-dimensions was presented in sec. 2.4. The implicit formulation was used to calculate the temperature distribution over the various layers of external walls and windows. In this model, we also accounted for the solar heat generated in the volume of the external boundary nodes of walls and all nodes of windows excluding the shaded parts. The nodes were classified according to their type and position within the conducting body (sec. 2.4.3). This model is applicable to windows (single, double, or triple glazed) and wall panels (uniform or with openings for windows). In sec. 2.4.4., the heat transfer coefficients between any two interacting nodes were determined with respect to their relative positions, their types, and whether both nodes lie within the same conducting body or not. The coefficients of matrix [A] and [B] were developed along with the parameters L_i N_i needed for the calculation of the future temperatures of all nodes in sec. 2.4.6. The calculation of the net energy gain or loss during each time increment is described in sec. 2.4.7 along with the relation used to calculate the energy gain or loss associated with air infiltration as a function of wind speed. The sideways heat exchange at the panel to panel interface and at the window opening were examined in sec. 2.4.8 and the significance of the window recess on the heat loss was also examined.

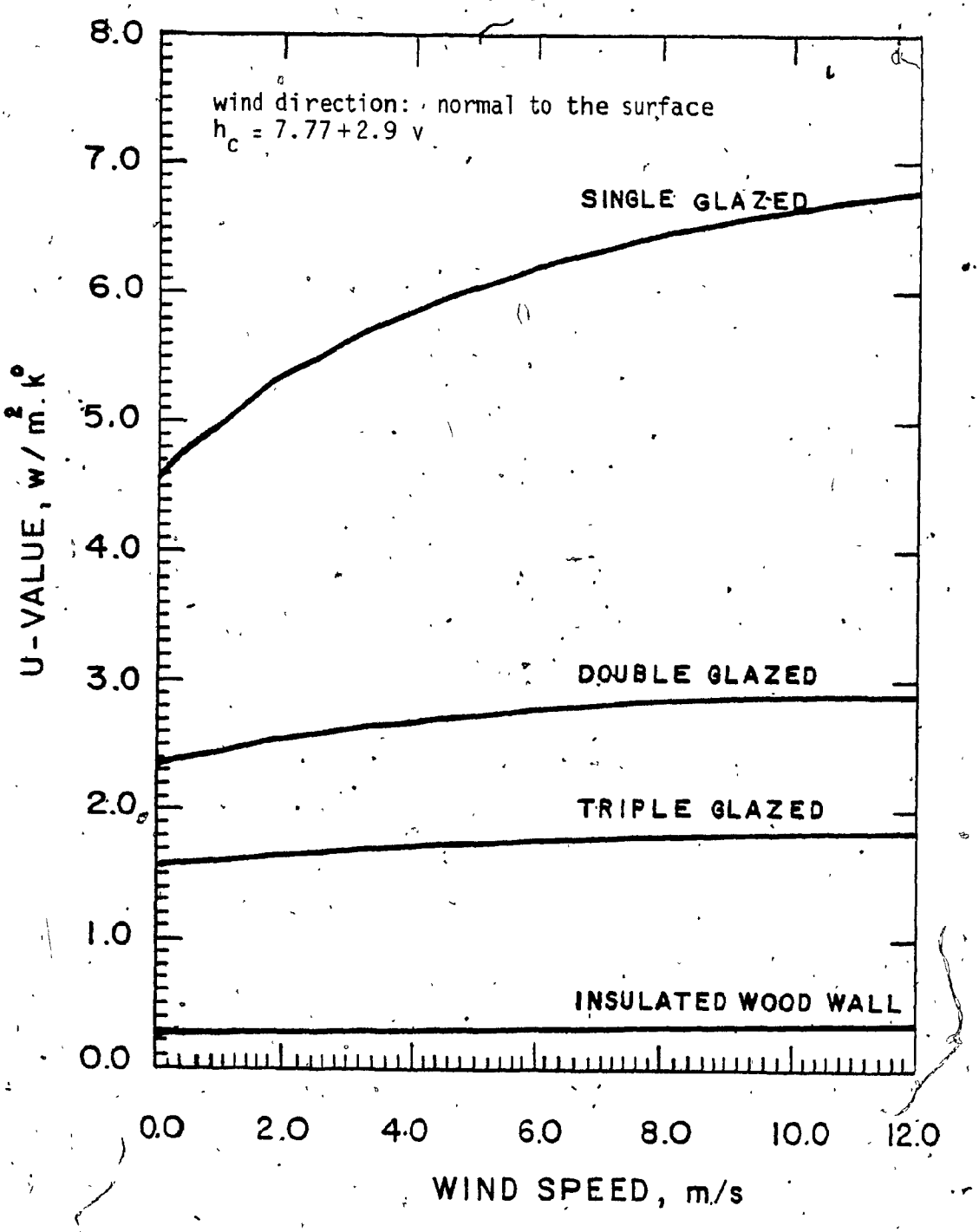

Fig. 2.1: Variation of the U-value of single, double and triple glazed windows with wind speed

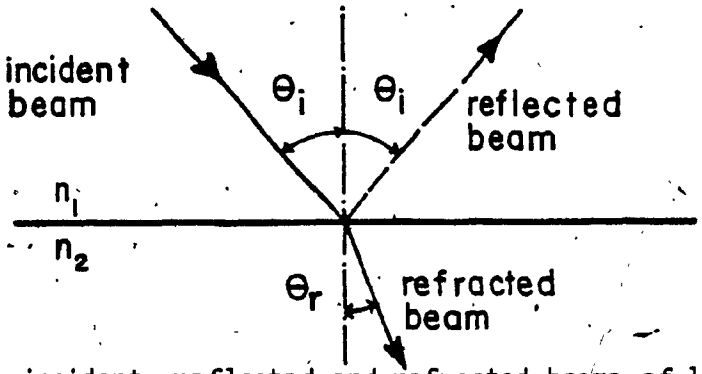

a) incident, reflected and refracted beams of light and incidence and refraction angles of a transparent medium

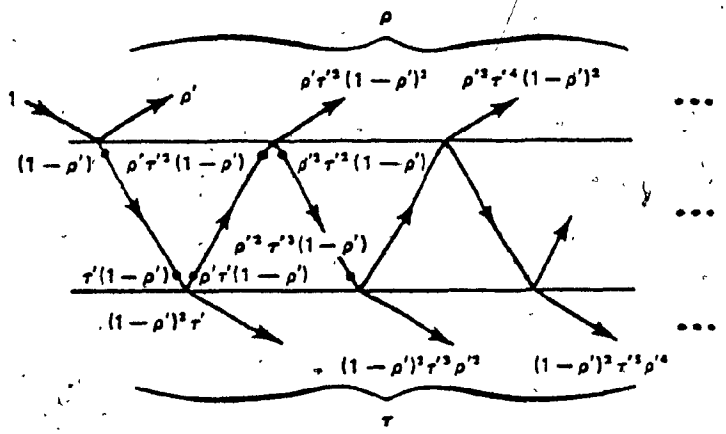

b) Ray trace diagram for a transparent medium showing the reflected and transmitted fractions accounting for multiple interreflection

Fig. 2.2: Transmission and reflection of light for a transparent medium (12).

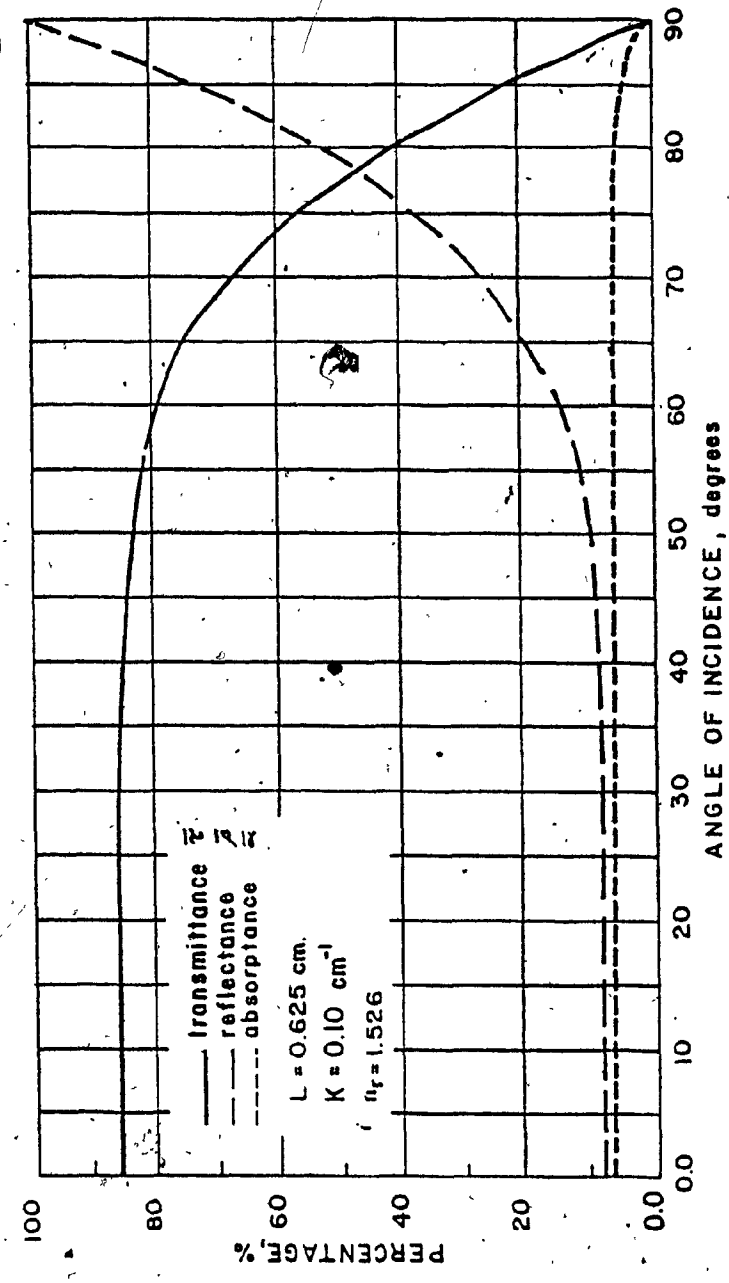

Fig. 2.3: Average transmittance, reflectance and absorption for single glazing

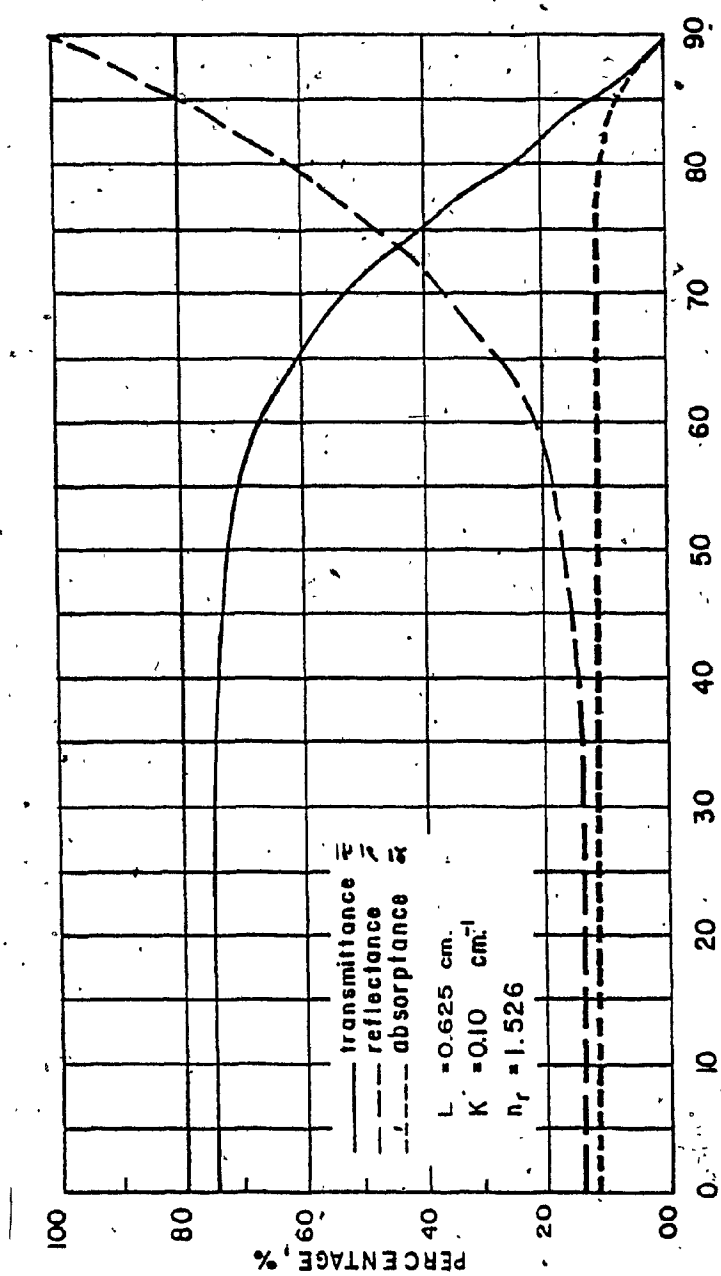

Fig. 2.4: Average transmittance, reflectance and absorption for double glazing

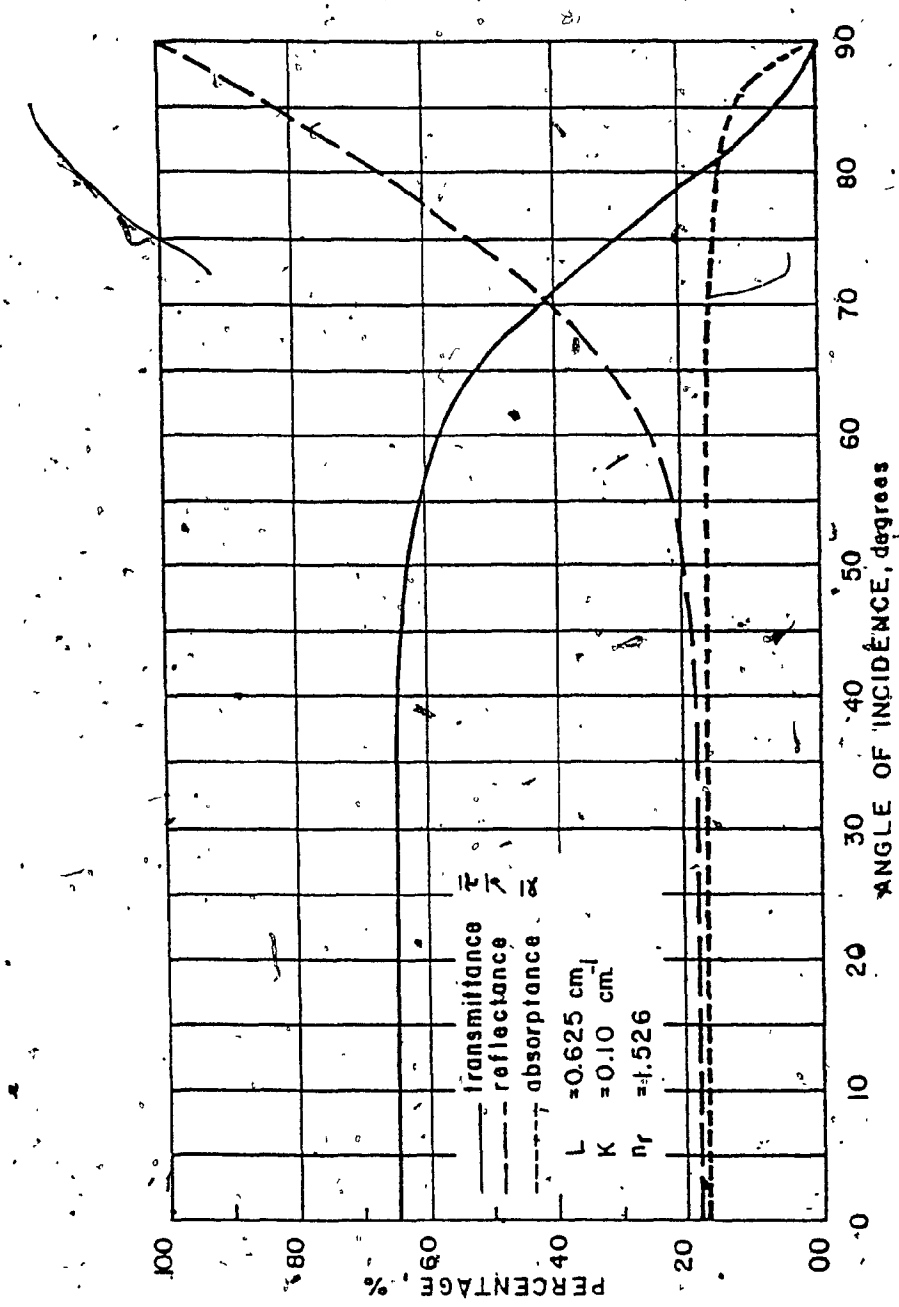

Fig. 2.5: Average transmittance, reflectance and absorption for triple glazing

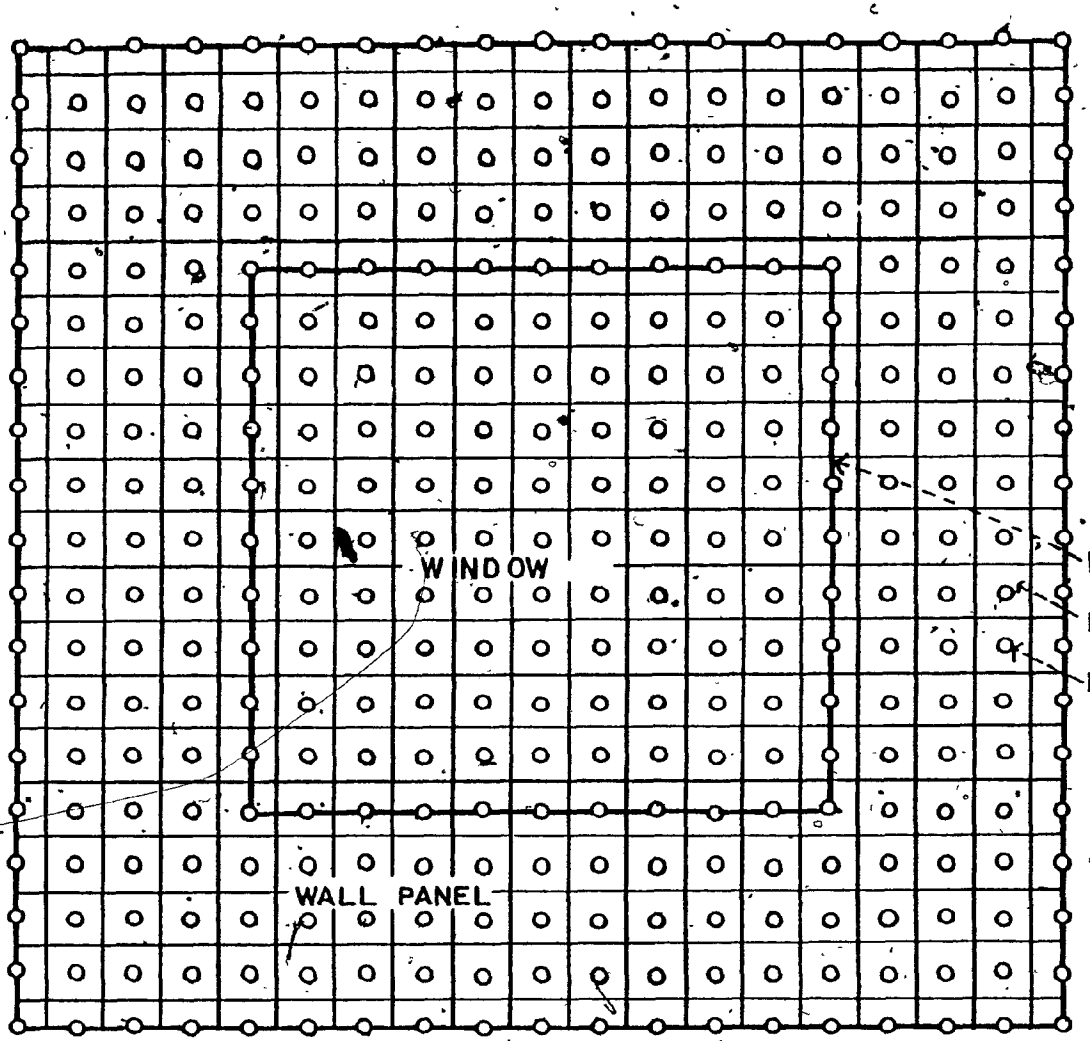

FIG. 2.6: Nodal network representation for a typical layer

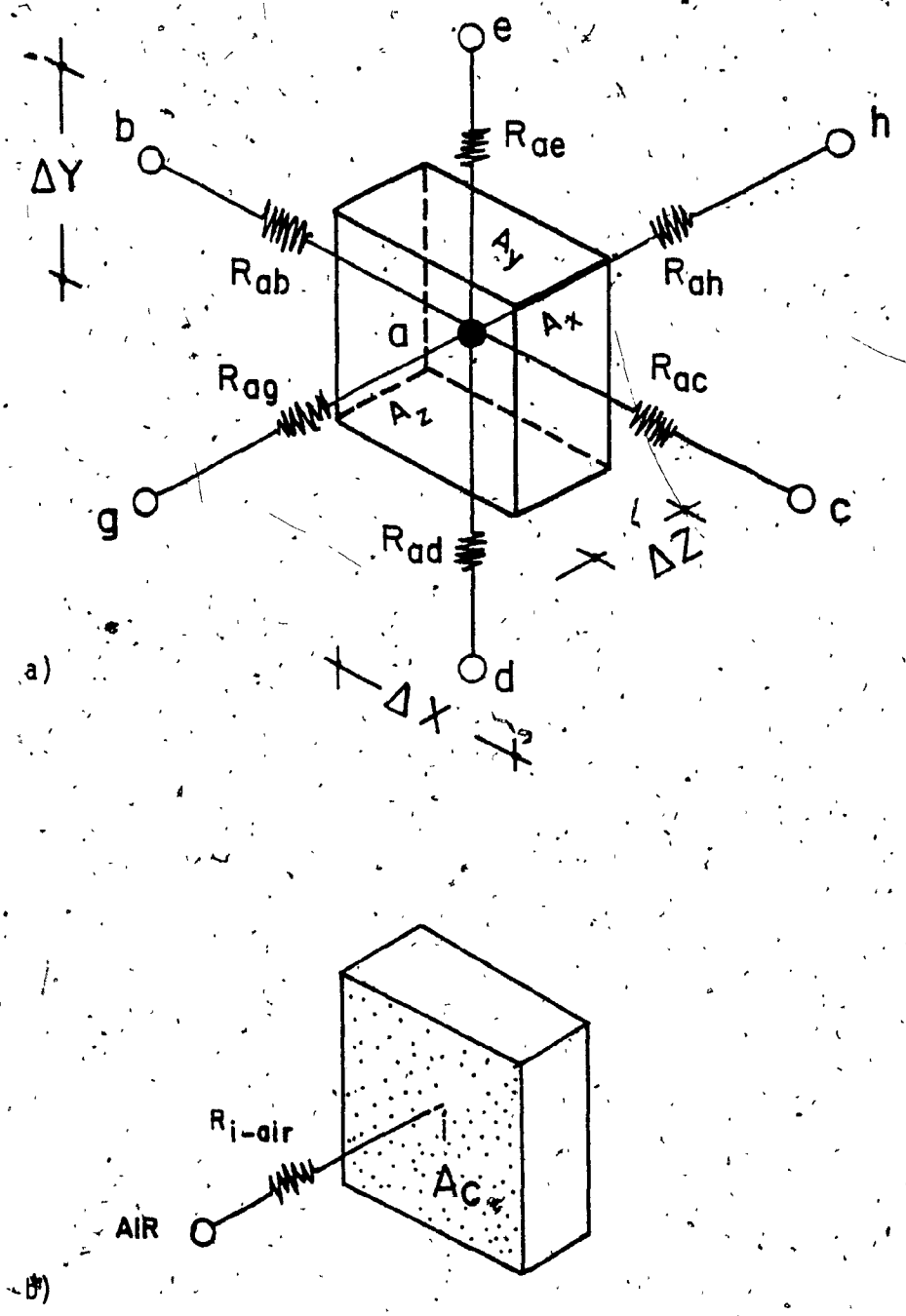

Fig. 2.7: Schematic representation of thermal resistances between nodes
a) thermal conduction resistances between an internal node and its surrounding nodes
b) thermal convection resistance between a boundary node and air.

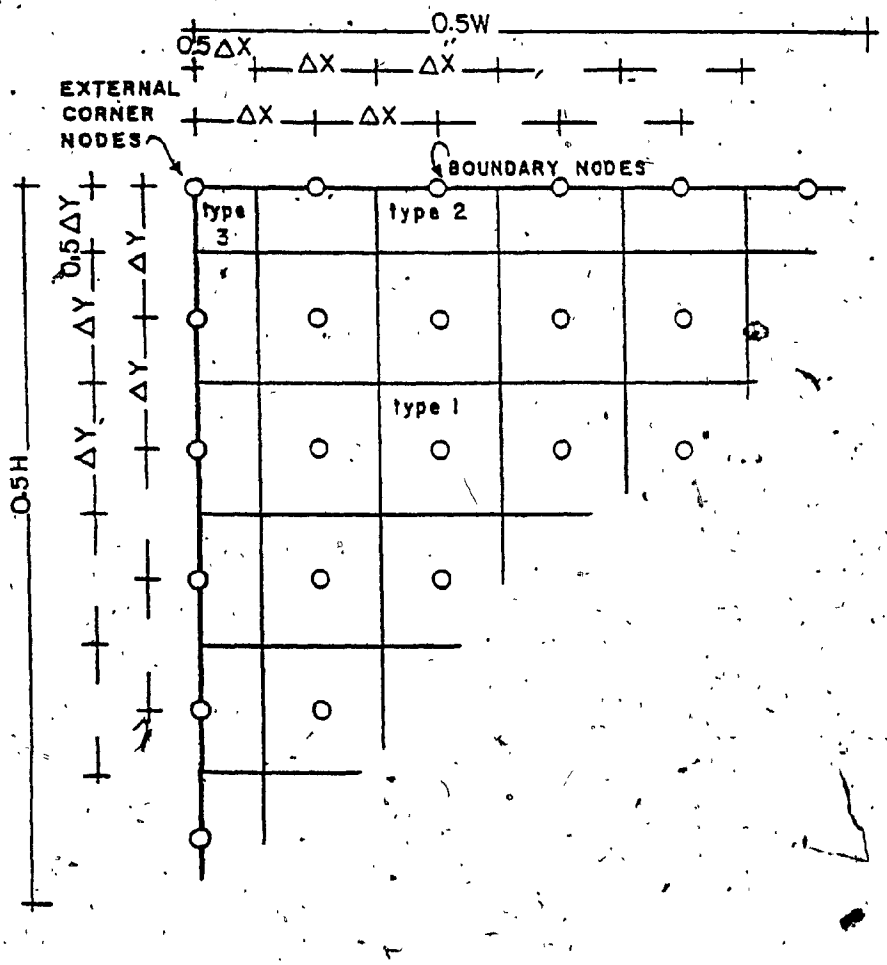

Fig. 2.8: Dimensions and nodes spatial distances for a typical layer of a window or a solid wall

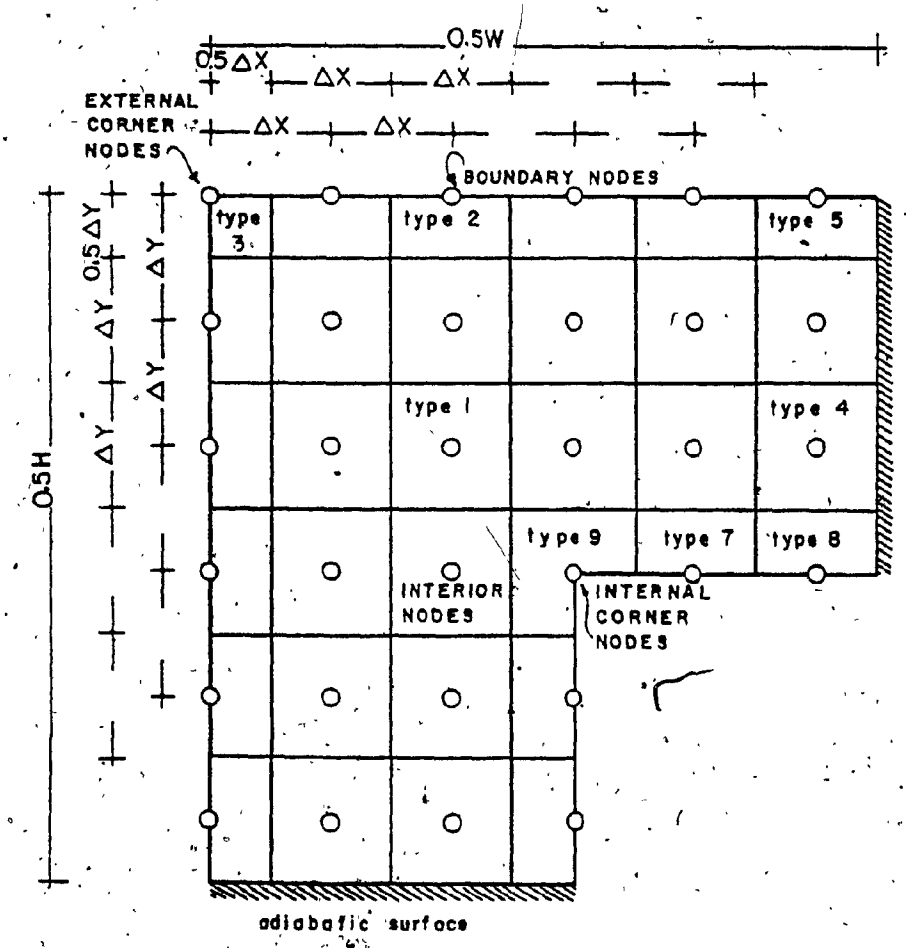

Fig. 2.9: Dimensions and nodes, spatial distances for a typical layer of a panel with opening for a window

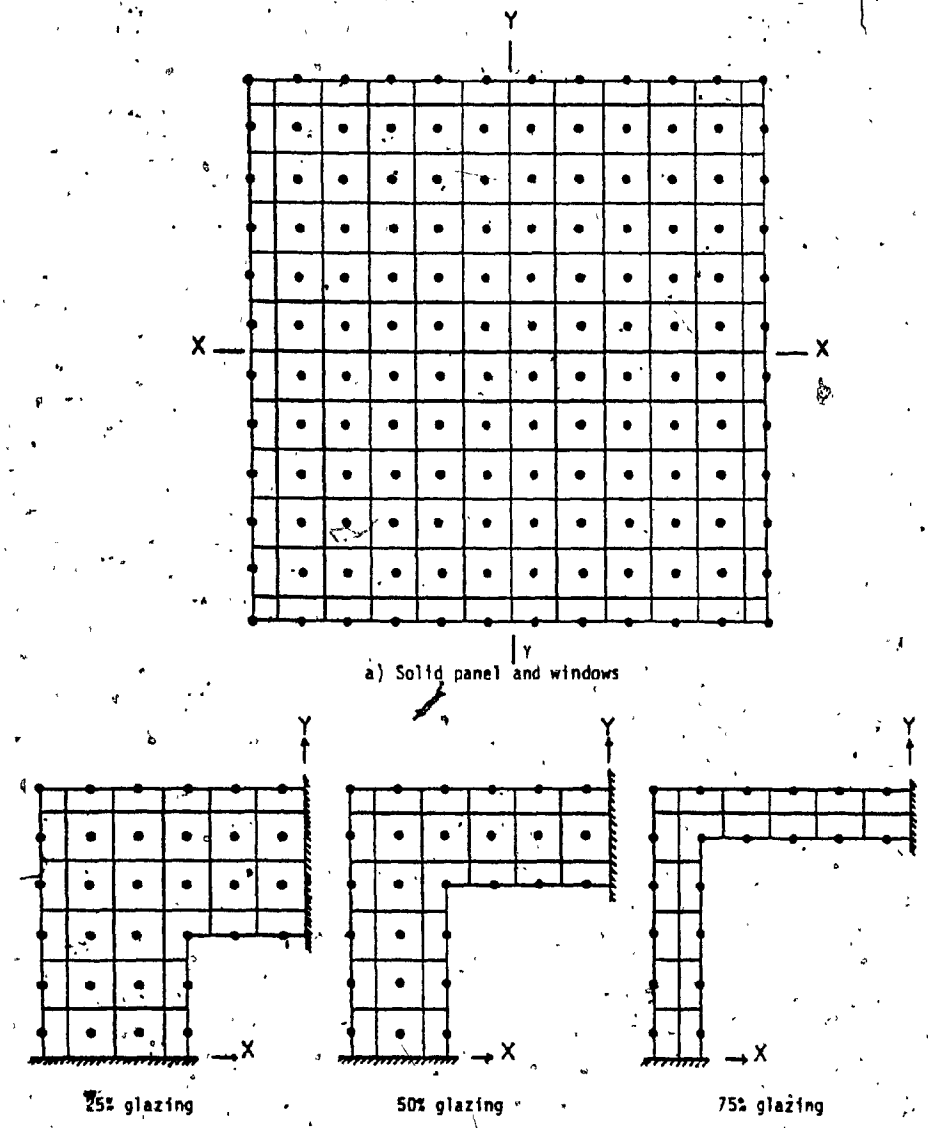

Fig. 2.10: Axes of symmetry (adiabatic interfaces) for: a) a solid panel and windows, b) for incomplete panels with 25%, 50% and 75% glazing

numbers indicate type of node

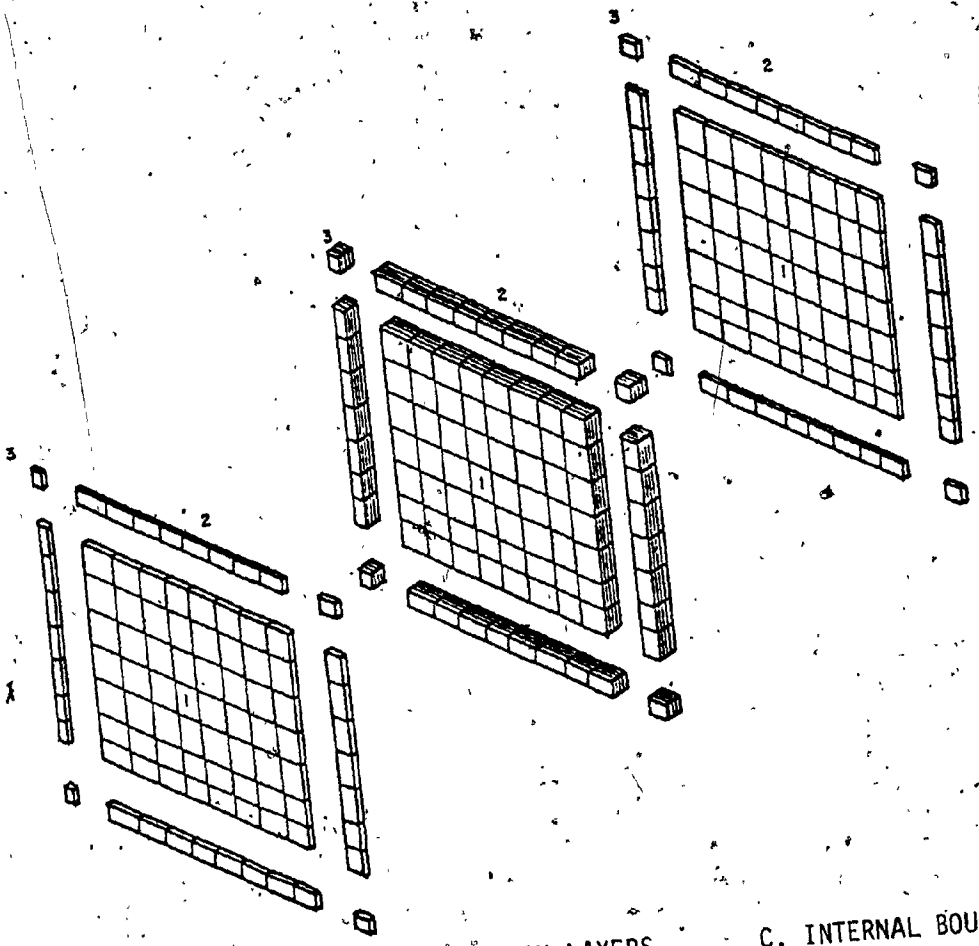

A. EXTERNAL BOUNDARY LAYER B. MEDIAN LAYERS C. INTERNAL BOUNDARY LAYER

FIG. 2.11: Isometric view showing the conducting lumps of the different layers

number indicates type of node

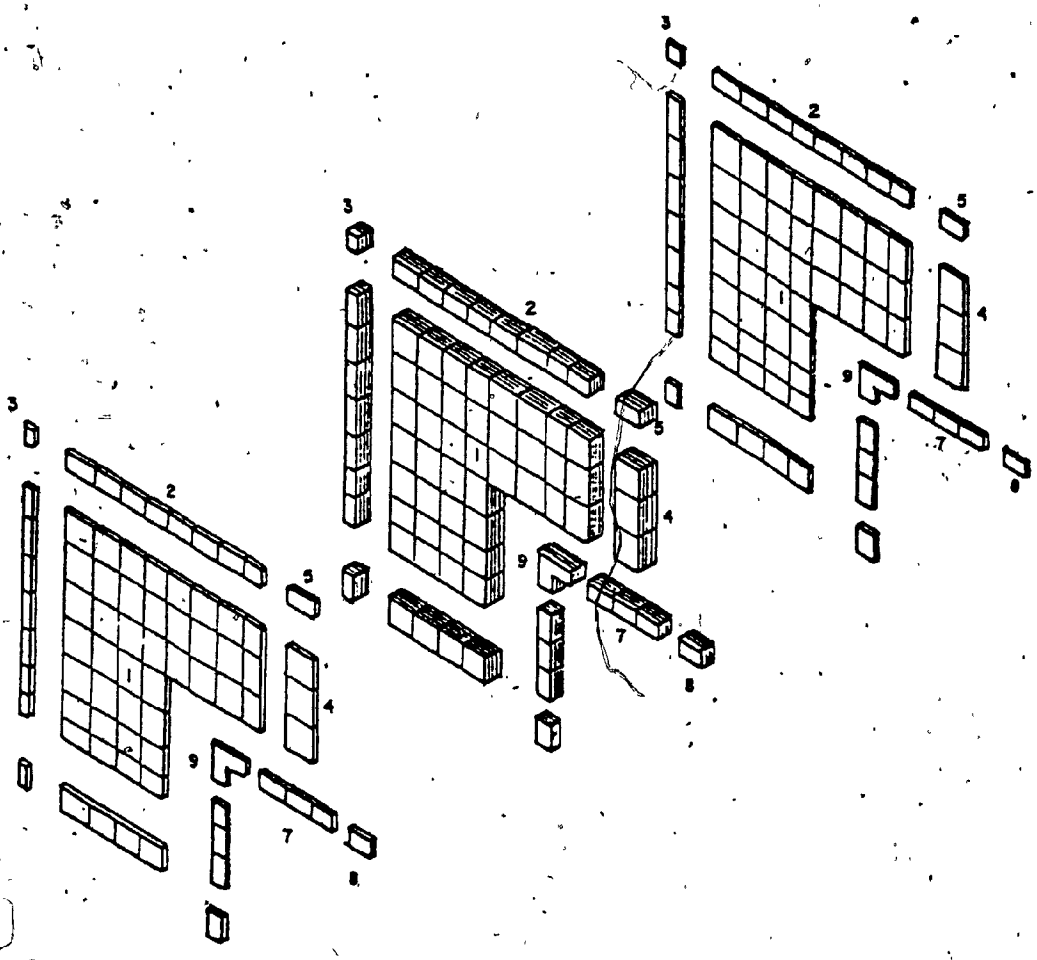

A. EXTERNAL BOUNDARY LAYER B. MEDIAN LAYERS C. INTERNAL BOUNDARY LAYER

Fig. 2.12: Isometric view showing the conducting lumps of the different layers in the case of incomplete panels

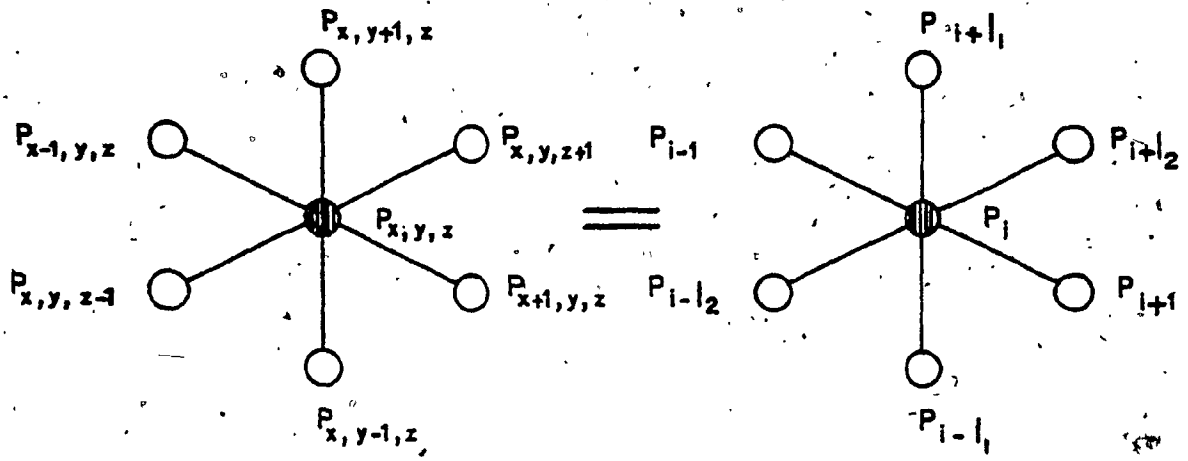

Positions of node $P_{x,y,z}$ and its surrounding nodes

Positions of node $P_{x,y,z}$ and its surrounding nodes after being expressed by the single subscript i

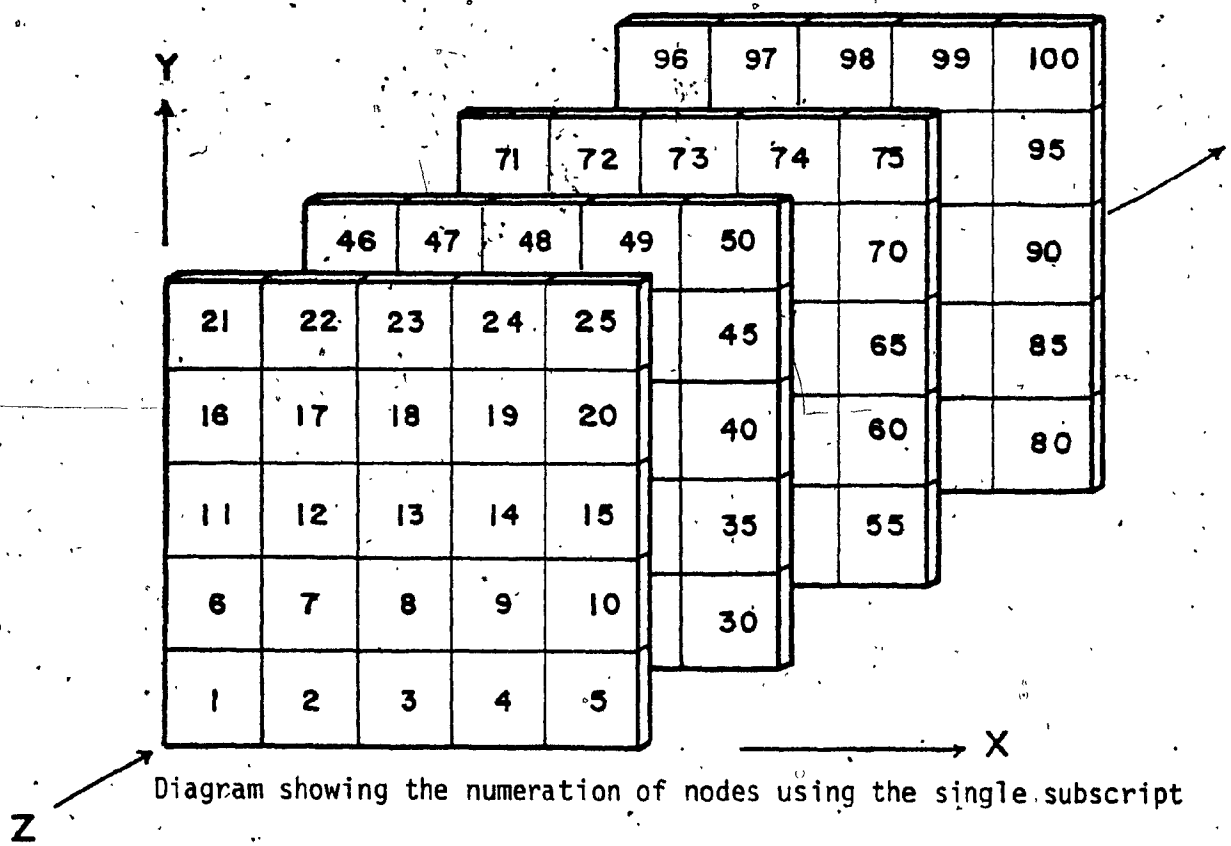

Diagram showing the numeration of nodes using the single subscript

Fig. 2.13: Position of nodes expressed by a single subscript

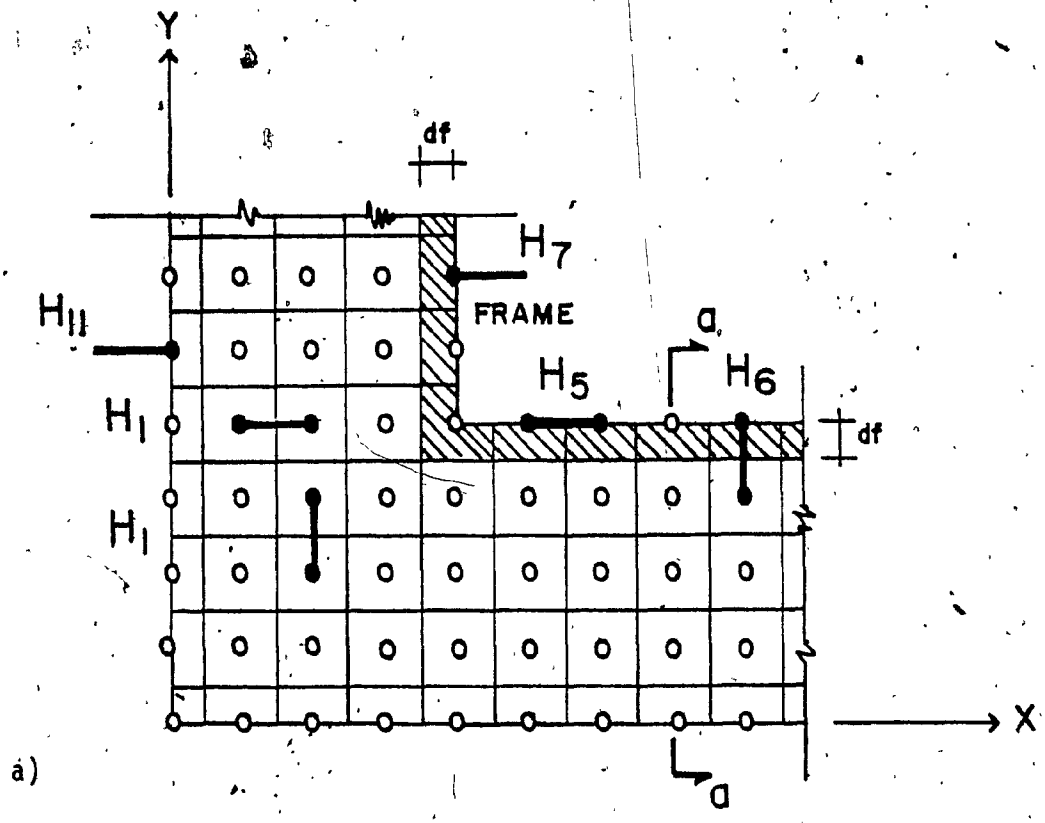

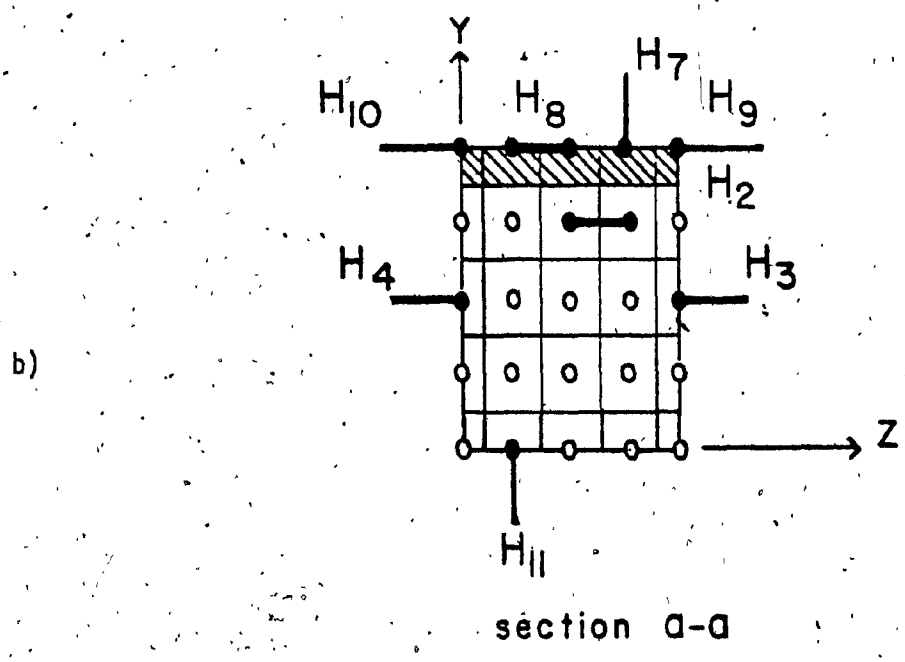

Fig. 2.14: Heat transfer coefficients between two neighbouring nodes:
a) within the same layers
b) in two consecutive layers

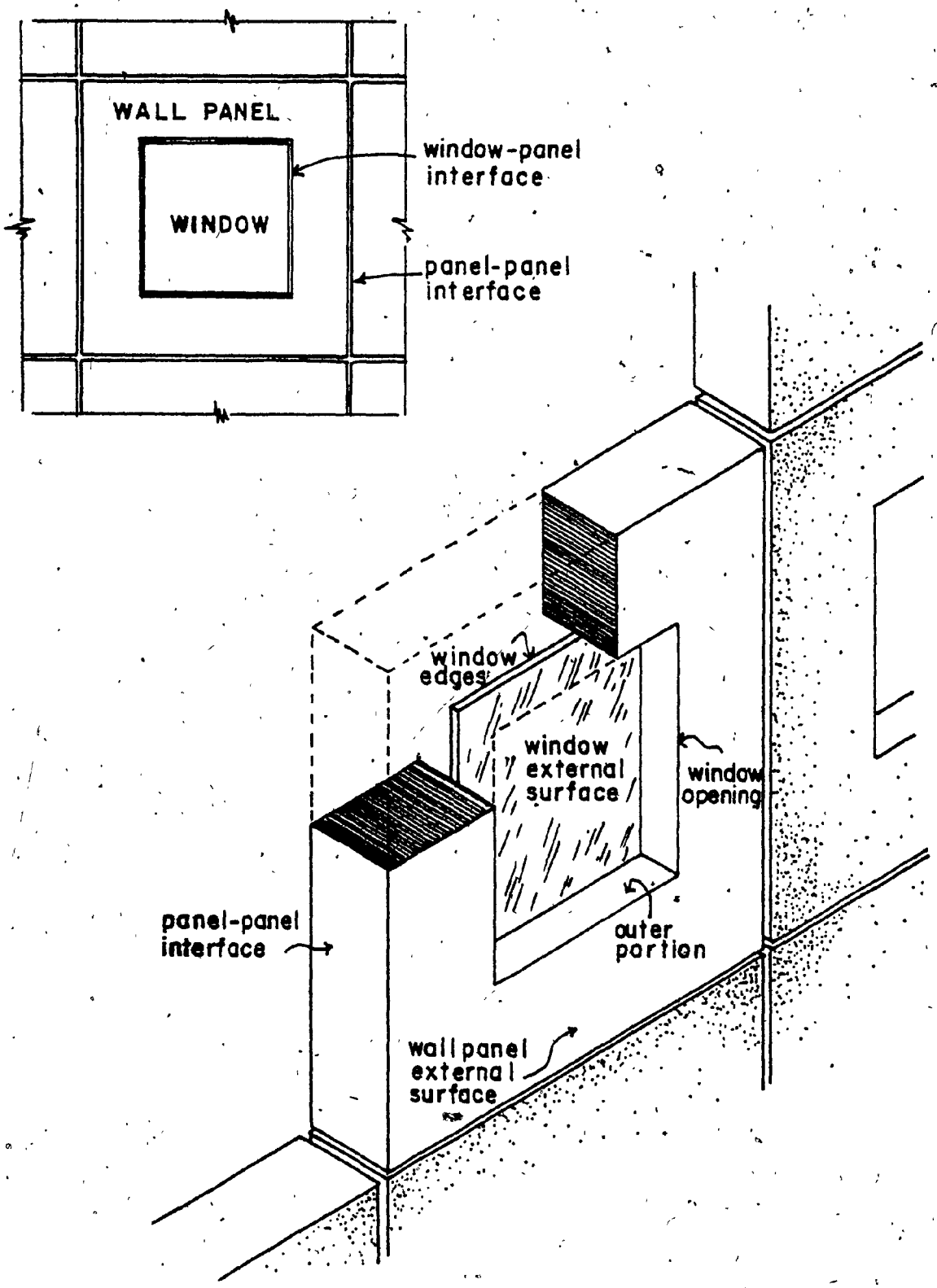

Fig. 2.15: Isometric showing exterior surfaces of a wall panel and a window

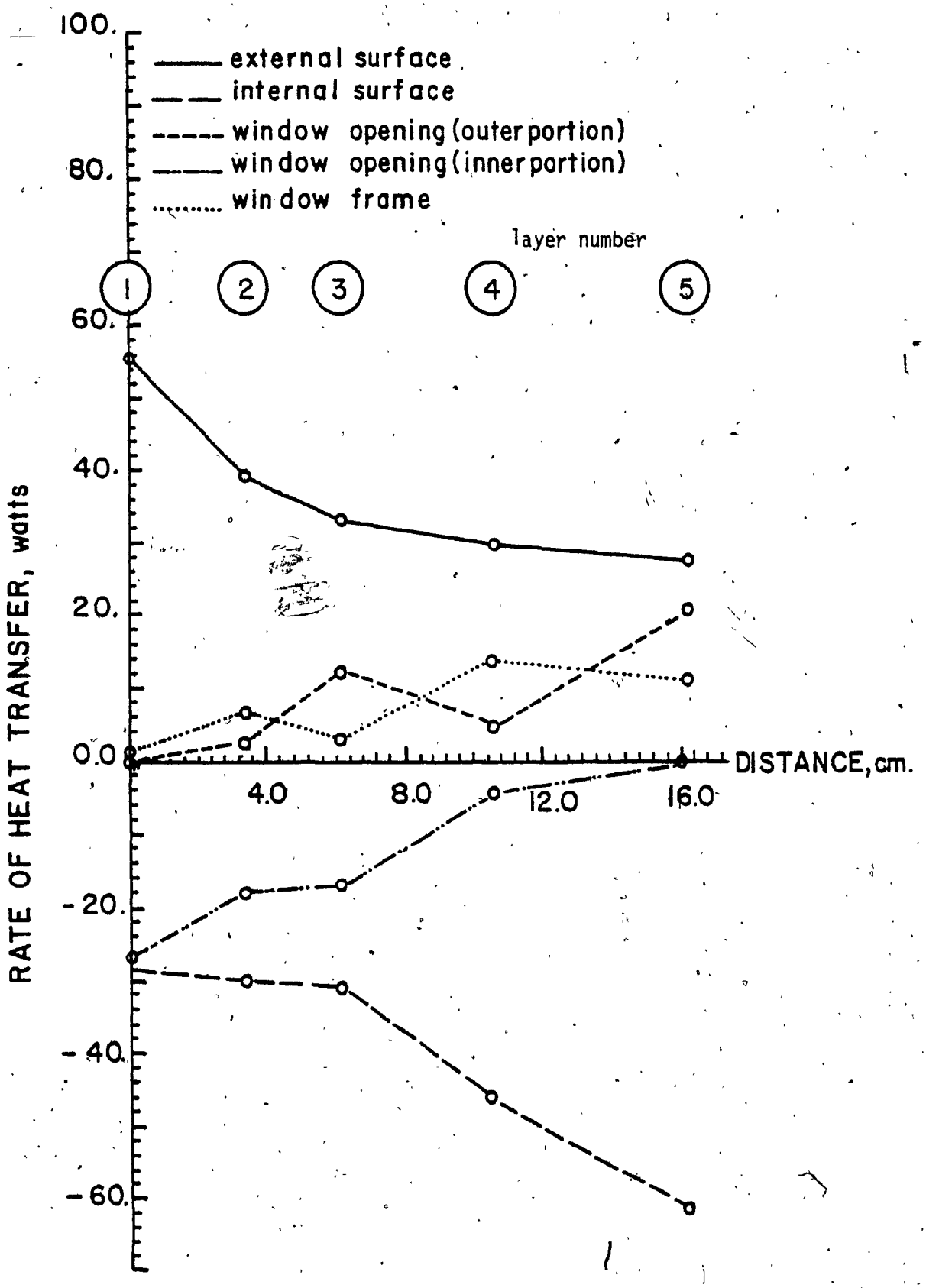

Fig. 2.16: Variation of the rates of heat transfer at the exterior surface with the window recess from the exterior edge

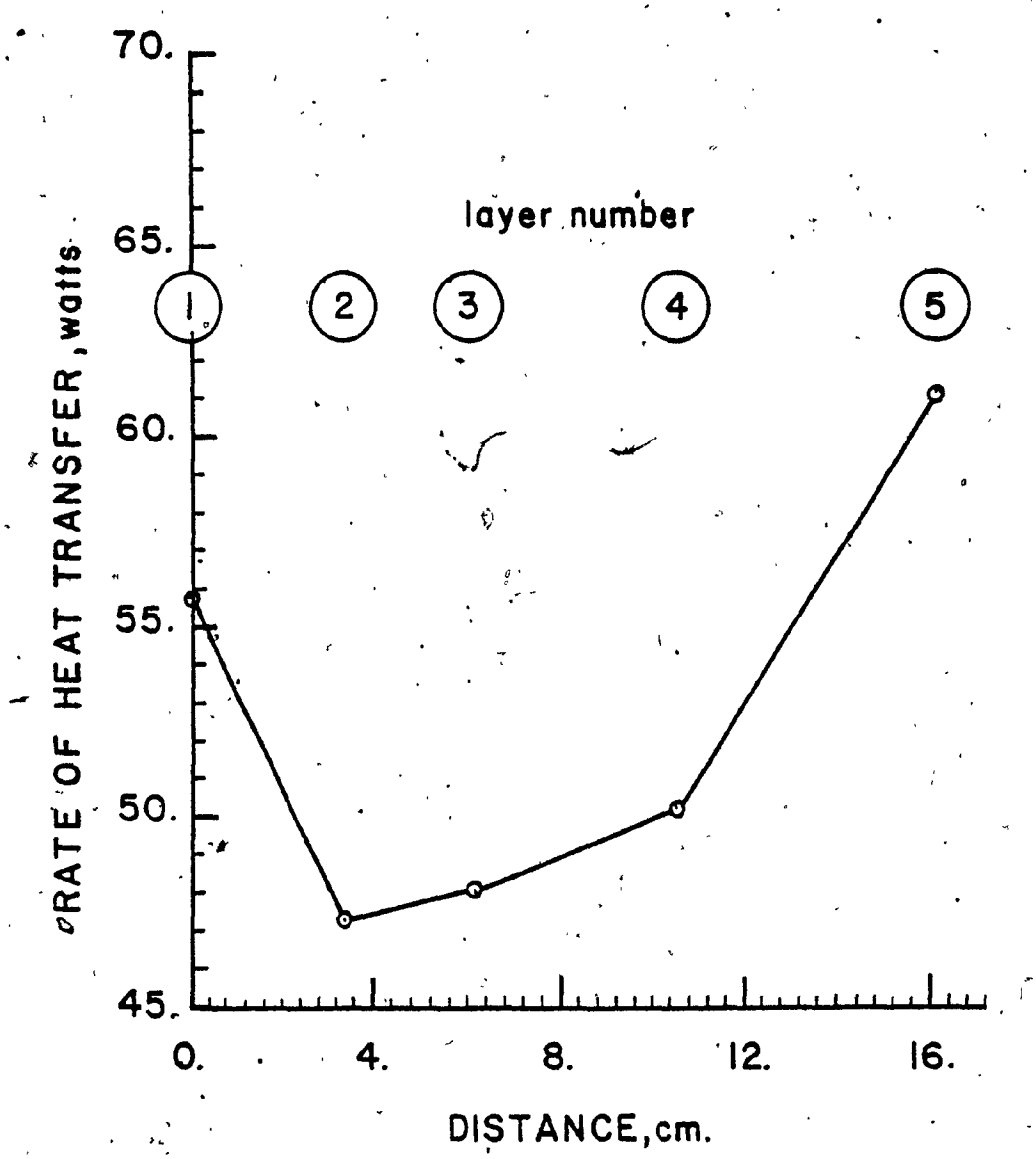

Fig. 2.17: Variation of the total rate of heat transfer through a wall panel with a window as the window distance from the exterior edge increases

CHAPTER III

CALCULATION OF NATURAL LIGHT ON A HORIZONTAL PLANE INSIDE A ROOM USING A TIME DEPENDENT DAYLIGHT FACTOR

3.1 INTRODUCTION:

Provision of natural daylight is one of the fundamental functions of windows. Daylight is psychologically and physiologically important to the well-being of the occupants. In buildings, electric lighting takes the second largest amount of energy after heating [1]. Thus, energy consumption can be reduced if daylight is efficiently utilized as a dominant lighting source for the interior, particularly at peripheral areas. Electric lighting can then be used as a supplemental source whenever daylight falls below the required level of illumination. The current daylight calculation methods were not devised for energy calculations. In the present study, we develop an energy oriented and time dependent version of the Daylight Factor Method, which is the one most commonly used. The present form of this method is limited to a time-independent design sky luminance and the calculation of the minimum level of daylight in a given room from a densely overcast sky to satisfy some architectural design purposes and the building codes. Our modified daylight factor method is extended to include daylight energy calculation due to time dependent sky luminance distributions, and the supplemental electric energy required when daylight is efficiently utilized.

The daylight factor, by definition, is the daylight illumination

at a reference point inside expressed as a percentage of the simultaneous illumination, from the whole sky, on an unobstructed horizontal plane. The daylight factor has two components, a sky component and a reflected component. The sky component is the product of a sky factor times the window glass transmittance.

The sky factor, by definition, is the diffuse sky illumination that would reach the reference point directly through an unglazed window opening expressed as a percentage of the simultaneous illumination from the whole sky that is received on an unobstructed horizontal plane outside. The reflected component is the reflected light received at the reference point from both external and internal reflecting surfaces. It is also expressed as a percentage of the illumination from the whole sky that is received on a horizontal unobstructed plane. In order to calculate the daylight factor, an appropriate sky luminance distribution must be assumed. There are three sky luminance distributions that are commonly used.

In the simplest distribution, the luminance of the sky is assumed to be that of a hemispherical perfect diffuser. This is known as the uniform sky luminance. Accordingly, the value of the sky factor depends only upon the area of the window and the distance of the reference point from the window. The second distribution is the C.I.E. overcast sky where the luminance of a point in the sky is independent of its azimuth angle but varies with the altitude angle. This distribution is characterized by the fact that the sky at the zenith is almost three times brighter than the sky at the horizon. The third

distribution is for a clear cloudless sky with no direct beam solar radiation (as though the sun is always obstructed by a small cloud). The sky factor under this distribution is not only a function of the window geometry but also the latitude angle, the window azimuth angle and the time of day and year. A sky factor generated from this distribution is time-dependent and therefore, it will be referred to as the variable sky factor, SF_V. The subscript v is used to distinguish the variable daylight factor and its components from the conventional ones. In a similar fashion, the reflected component and the daylight factor will be referred to as the variable reflected component RC_V and the variable daylight factor DF_V.

In order to ensure that the calculation of the reflected light will conform to a nonuniform time dependent sky luminance some of the assumptions in current use must be changed. The common assumptions used in the calculation of the externally and internally reflected light are a source of error when the time dependent concept is introduced. For instance, the luminance of a building opposite to the window of concern is commonly assumed to be 1/10 the average sky luminance and in the case where the reflectance of the opposite building is known, the calculation is based on illumination provided by the complete half sky facing it. This is unrealistic, since the building containing the window blocks a portion of the light flux to the opposite building. It is also common to calculate the ground luminance by assuming the ground to be an unobstructed surface, but this is untrue since both buildings obstruct the light flux from the lower portions of

the sky to the ground between them. The internally reflected light is usually calculated using the theory of the integrating sphere [121]. In this theory the true shape of the room is ignored and the user cannot account for the variation in reflectance from one internal surface to another, so the value of these reflectances are represented only by the average of their actual values. Also, a single total daylight flux entering the sphere at the window surface is utilized for each wall. This assumption is untrue for real geometries since the daylight flux varies from one internal surface to another. The B.R.S. Split Flux Method [121] is somewhat preferable since the total flux entering the sphere is split into two parts with two surface reflectances, one for the average reflectance of the upper part and one for the lower part of the room. The B.R.S. split flux method was originally developed to estimate the internally reflected daylight due to C.I.E. overcast sky conditions, but later Gupta [65] used it for clear sky conditions without any modification. Krochman [149] also used this method for clear sky conditions with modified coefficients to represent the flux entering the room. However, Krochman did not account for direct beam sunlight or time variations in the calculation of the luminance of external surfaces. His solutions for the sky factor were given, in the form of diagrams, only for a fixed solar altitude angle and for 10 degrees intervals of the altitude and azimuth angles of the visible patch of the sky.

In this chapter, a more precise time-dependent daylight model will be presented, in order to adopt the Daylight Factor Method for more

precise calculations of the annual energy needed to supplement the available daylight by electric lighting. Our variable daylight factor varies with respect to:

1. window compass orientation
2. time of day
3. time of year
4. latitude angle
5. window aspect ratio
6. distance of the reference point from the window
7. window-to-wall area ratio
8. height of the obstruction
9. height of the building containing the window
10. distance between building and obstruction
11. room geometry and height of the reference point
12. wall thickness
13. type of glazing
14. reflection coefficients of internal walls, ceiling, ground, building, and obstruction.

A parametric study with respect to the first eight parameters will be presented along with the luminance distribution of other sky conditions (i.e. overcast, and partly cloudly skies), and an experimental verification of the model.

3.2 Development of a Time-Dependent Daylight Factor

The variable daylight factor, DF_V has two components, a sky component SC_V, and a reflected component RG_V. Both components depend largely on the luminance distribution of the sky.

3.2.1 The Luminance Distribution of a Clear Cloudless Sky

A clear cloudless sky has a nonuniform and time-dependent luminance distribution. The scattering processes which cause a certain luminance distribution of the clear blue sky, were reviewed by Kittler [138]. He arrived at a formula, which was later adopted by the C.I.E, to describe the luminance of any point in a clear sky as a ratio of the zenith luminance [137].

$$L_e = \alpha_c L_{zc} \tag{3.1}$$

where,

L_e = luminance of a given element in a clear sky at time t.

L_{zc} = luminance of the zenith at time t (clear sky).

α_c = a factor representing the geometrical and intensity relationship between the sun, the sky element, and the zenith with a clear sky at time t.

The factor, α_c, is a function of the angular zenith distance of the sky element, ω_{ez}, the sun-zenith angular distance, ω_{sz}, and the angular distance of the sun from the sky element ω_{se} shown in Fig. 3.1. The factor α_c is given by:

$$\alpha_c = \frac{(1.0 - e^{-.32 \sec\omega_{ez}})\ (0.91 + 10e^{-3\ \omega_{se}} + 0.45\ \cos^2\omega_{se})}{0.27385\ (0.91 + 10e^{-3\omega_{se}} + 0.45\ \cos^2\omega_{sz})} \tag{3.2}$$

These three angles can be calculated from the altitude angle of the element θ_e, the solar altitude, θ_s, and the sun-element azimuth difference ω_{se}.

$$\omega_{sz} = (90 - \theta_s)$$

$$\omega_{ez} = (90 - \theta_e)$$

and

$$\omega_{se} = \cos^{-1}(\cos \omega_{sz} \cdot \cos \omega_{ez} + \sin \omega_{sz} \cdot \sin \omega_{ez} \cdot \cos \phi_{se})$$

For ease of computation, the luminance is calculated at a finite number of points each at the centre of a small sky element (Fig. 3.2a). The luminance is assumed to be uniform within each sky element.

The sky hemisphere was divided into 324 elements with 8 latitude circles and 35 longitude arcs. Thus the solid angle subtended by each element at the centre of the earth decreases from horizon to zenith. The area ratio of a given element A_i in the ith ring above the horizon is

$$A_i = \Delta\phi_i [\sin (\phi_i + 0.5\ \Delta\theta) - \sin (\theta_i - 0.5\Delta\theta)] \qquad (3.3)$$

where θ_i is the altitude of the centre of the element and $\Delta\theta$ and $\Delta\phi_i$ denote the angular increments in the altitude and azimuth directions respectively. $\Delta\theta$ is the same for every ring, but $\Delta\phi_i$ changes because there are 36 subdivisions around each ring. The total diffuse sky illumination on a horizontal unobstructed plane, E_h is then:

$$E_h = \sum_{i=1}^{9} \sum_{j=1}^{36} L_{ij} A_i \sin \theta_i \qquad (3.4)$$

where L_{ij} is the luminance of the element ij.

3.2.2. The Luminance Distribution for Overcast and Partly Cloudy Skies

The luminance distribution for a fully overcast sky is only

dependent upon the altitude angle of the sky element θ_e. The C.I.E. formula describing the luminance distribution for an overcast sky is given by [130]:

$$L_e = \alpha_o L_{zo} \quad cd/m^2 \tag{3.5.a}$$

or

$$L_e = \frac{9}{7} \alpha_o E_h \quad \ell m/m^2, \tag{3.5.b}$$

where α_o is given by

$$\alpha_o = (1.0 + 2 \sin \theta_e)/3.0$$

E_h is the illumination on the horizontal plane from an unobstructed overcast sky and L_{zo} is the zenith luminance of the overcast sky.

The luminance value of a given sky element can not be determined unless the luminance of the zenith for the design sky of concern is known. For a clear sky, the luminance of the zenith, L_{zc}, is dependent upon solar altitude angle and will be discussed in detail in sec. 3.3. For an overcast sky, the luminance of the zenith, L_{zo}, is commonly assumed to be independent of the solar altitude angle, even though Hopkinson [121] and the IES [123] have confirmed experimentally that the illumination on a horizontal plane from an overcast sky is dependent upon the solar altitude angle.

In this model, L_{zo} was assumed to be dependent upon the solar altitude angle. From Eqs. (3.5.a) and (3.5.b), one can deduce that the luminance of the zenith L_{zo} is related to the illumination on the horizontal plane from an unobstructed overcast sky by

$$L_{zo} = \frac{9}{7} \pi E_h$$

$$= 0.41 E_h \quad cd/m^2 \qquad (3.6)$$

where π was introduced to convert $\ell m/m^2$ to cd/m^2. This relation is needed to determine L_{zo} from the available relation [123] for the illumination on the horizontal plane, E_h, from an overcast sky (c.f. Fig. 3.3).

The luminance distribution of a partly cloudy sky is difficult to predict since it is dependent upon the height, depth, position, and motion of the clouds. In the literature this difficulty is ignored. For instance, Hopkinson et al. [121] assumed that the average illumination on a horizontal unobstructed plane from a partly cloudy sky, E_h, varied only with the solar altitude angle ($E_h = 538\,\theta_s$). In a similar study, Lynes [125] used $E_h = 570\,\theta_s$. In both studies, the average illumination was assumed to be independent of the amount and positions of the clouds. Lynes [125], Yager [214], and Budde [215] have all reported measured intensities under partly cloudy skies which exceed clear sky values.

To have a more realistic model here, partly cloudy skies were treated differently. We assume that the clouds are uniformly distributed and that the coverage of the sky dome ranges between the clear sky and the fully overcast sky. To account for the non linearity of the illumination of partly cloudy skies as a function of cloud cover, a brightness factor, B, that is a function of the cloud cover was used.

This factor represents the additional brightness caused by the white scattered clouds in the sky and their bright edges when the sun is not covered. This brightness factor is one both for clear and for overcast skies because completely overcast sky is grey and clear sky is cloudless.

The cloud cover for a given design sky is represented by a cloud coefficient, τ_c, equal to zero for a clear sky and equal to 1.0 for an overcast sky. Accordingly, a partly cloudy sky luminance distribution can be expressed in terms of the luminance distributions already assumed for clear and overcast skies plus the cloud coefficient τ_c. Thus, the luminance of a sky element L_{ij} for a partly cloudy sky becomes

$$L_{ij} = B\,[(1-\tau_c)\,L_{ij}\,(\text{clear}) + \tau_c\,L_{ij}\,(\text{overcast})]$$

$$= B[(1-\tau_c)\,L_{zc}\,\alpha(i,j) + \tau_c L_{zo}\,\alpha_o(i,j)] \qquad (3.7)$$

where the brightness factor B is greater than or equal to 1.0.

Illuminations measured on the horizontal, under different partly cloudy skies, were compared to illuminations calculated using the distribution given by Eq. (3.7) with B = 1.0 and appropriate values for τ_c. These calculated illumination values were found to be 88-95% of the measured values when the cloud cover τ_c ranged between 0.6 and 0.9 but only 70-85% when τ_c ranged between 0.1 and 0.5. The maximum measured values corresponded to τ_c between 0.1 and 0.3 and the minimum occurred at τ_c = 0.9.

As the extra brightness from white clouds is not encountered when the sky is clear (τ_c = 0.0) or overcast (τ_c = 1.0), the function, to be chosen for B, should have a value of 1.0 at τ_c = 1.0 and at τ_c = 0.0.

Otherwise, B should be greater than 1.0 and its value is governed by the cloud cover τ_c so that the difference between the calculated illumination with B = 1.0 and the measured illumination is minimal. A good fit to the observations taken with the shadow band for three different days in February 1980 on the horizontal plane shown in Fig. 3.4 was found with

$$B = 1.0 + [b((1-\tau_c)^m)^2 \sin(180\,(1-\tau_c))] \qquad (3.8)$$

where b is a factor to account for the color and depth of the clouds (i.e. b ranges from 0.12 for light white clouds, through 0.05 for average gray clouds, to 0.0 for a fully overcast sky). The value of b used for the curve shown in fig. 3.4 is 0.09. The curve was fitted above the experimental points to account for the difference caused by the shadow band ($\simeq$ 15%).

Under the assumption of a uniform cloud cover we can calculate the sky illumination on any plane by using the proper view factors and the visible part of the sky. As an example, we show the calculated illumination (with b=0.09) received on the horizontal and four vertical surfaces facing due south, east, west and north in Fig. 3.5 for January 21st at solar noon. The maxima of the curves are not at precisely the same τ_c value because of the relation's slight incompatability between using the C.I.E. clear sky formula containing a bright aura around the sun while assuming the clouds to be uniformly distributed. To the accuracy of this model the 15% shift in the curves peaks is not significant. All partly cloudy skies give more illumination than the overcast sky on all planes. Note that the C.I.E. overcast sky is brightest at

the horizon while the clear sky is brighter at the horizon than at the zenith only when the sun is low. So, the curves are not symmetric and the ratio of horizontal illumination to say illumination on the east wall varies with τ_c. The effect of the amount of cloud cover on the illumination reaching a reference point 2.5 m inside the room is shown in fig. 3.6. Note that there is little difference between the curves for northerly oriented windows since the visible patch of sky is far away from the bright aura around the sun and is near the horizon. However, for a reference point closer to the window east/west windows give higher illumination than anorth window.

3.2.3 The Variable Sky Component SC_V:

The variable sky component, SC_V, is the product of the glass transmittance factor times the variable sky factor, SF_V. To find SF_V, we need only to project the luminance of the appropriate patch of the sky on to the horizontal working plane. The patch of the sky that gives light at a reference point p, through the window aperture, depends on the window azimuth angle, window size and geometry, and the relative position of p with respect to the window. The reference point was assumed to lie on the perpendicular bisector of the window sill in the horizontal plane through the sill. The relevant patch of the sky can be expressed in terms of an altitude range (described by the lowest altitude, θ_g, and the highest altitude, θ_h which contribute light at p) and an azimuth range (described by the azimuth angle of elements at the extreme right-hand side of the window, ϕ_r, and the azimuth angle of

elements at the extreme left-hand side of the window, ϕ_ℓ): Angles θ_g, θ_h, ϕ_r, and ϕ_ℓ are shown in Fig. 3.7 and are expressed by:

altitude range

$$\theta_g = \tan^{-1} (H_o/(d_1+d_2)) \qquad (3.9)$$

$$\theta_h = \tan^{-1} (H_w/d_1)$$

azimuth range

$$\phi_r = \phi_w + \tan^{-1} (W_w/2d_1) \qquad (3.10)$$

$$\phi_\ell = \phi_w - \tan^{-1} (W_w/2d_1)$$

where H_o is the height of the opposite building (the obstruction surface) above the horizontal plane of p. H_w and W_w are the height and width of the window respectively. d_1 and d_2 are the distances from the window to point p and to the opposite building respectively. ϕ_w is the window azimuth angle. In the case of an unobstructed window, θ_g corresponds to the horizon ($\theta_g = o$).

The visible patch of the sky (defined by angles θ_g, θ_h, ϕ_r, and ϕ_ℓ) contains a number of fully visible elements at the patch core and partly visible elements at the patch boundary. The partly visible sky elements (at the boundary) appear only if the window outline does not coincide with the assumed grid of the sky ($\Delta\theta = \Delta\phi = 10°$) at one or more of the 4 sides of the window outline. The luminance of each fully visible element is evaluated at its centre. The centre point of a partly visible element may lie outside the sky patch. Therefore, a secondary grid was used with each boundary element to subdivide it equally into 100 subelements (Fig. 3.2b). The luminance at the boundary was calculated at the centre of each visible subelement.

From θ_g, the lowest visible sky ring, i_g can be determine ($i_g = 1$ if $0° < \theta_g < 10°$, $i_g = 2$ if $10° < \theta_g < 20°$, etc..). In a similar fashion, the highest visible sky ring i_h, and the extreme visible subdivisions within each ring at the left hand side j_ℓ and the right hand side J_r can be determined from angles θ_h, ϕ_ℓ, and ϕ_r respectively.

In the case where the patch of the sky of concern contains only fully visible sky elements, illumination at the reference point, E_p with no glazing can be expressed as

$$E_p = \sum_{i=ig}^{i_h} \sum_{j=\ell}^{j_r} L_{ij} A_i \sin \theta_i \qquad (3.11)$$

where θ_i is the altitude angle of the sky element centre. In the case where the patch of the sky contains fully visible sky elements at the core as well as partly visible sky elements at the four sides of the window outline, E_p is expressed as

$$E_p = E_p(\text{CORE}) + E_p \text{ (4 side strips)} \qquad (3.12)$$

and

$$E_p(\text{Core}) = \sum_{i=ig+1}^{i_h} \sum_{j=j_\ell+1}^{j_r} L_{ij} A_i \sin \theta_i$$

$$E_p(\text{lower strip}) = \sum_{j=j_\ell}^{j_r} \sum_{k=1}^{m} L_{ijk} A_{ik} \sin \theta_{ik}, \qquad i = ig$$

$$E_p(\text{upper strip}) = \sum_{j=j_\ell}^{j_r} \sum_{k=1}^{m} L_{ijk} A_{ik} \sin \theta_{ik}, \qquad i = i_h$$

$$E_p(\text{left strip}) = \sum_{i=ig+1}^{i_h-1} \sum_{k=1}^{m} L_{ijk} A_{ik} \sin \theta_{ik}, \qquad j = j_\ell$$

$$E_p(\text{right strip}) = \sum_{i=ig+1}^{i_h-1} \sum_{k=1}^{m} L_{ijk} A_{ik} \sin \theta_{ik}, \qquad j = j_r$$

where k is a variable representing the number of visible subelements within the boundary sky element of concern, The order of summation of

k is from the subelement at the lower left-side corner to the subelement at the upper right-side corner of the visible portion of the boundary sky element. A_{ik} is the area of the subelement k in the ith ring and equals 0.01 A_i. The variable sky factor at time t becomes

$$SF_v = \frac{E_p}{E_h} \times 100\ \% \qquad (3.13)$$

A block diagram showing the calculation sequence of the variable sky factor is shown in Fig. 3.8.

3.2.4 The Variable Reflected Component, RC_v

The variable reflected component is the ratio expressed as a percentage, between the summation of all reflected light, that is received at the reference point from both external and internal surfaces and the simultaneous diffuse sky illumination received on a horizontal plane from an unobstructed sky. Therefore, the luminance of all contributing external and internal surfaces, and the solid angles subtended by these surfaces must first be determined. A block diagram illustrating the calculation sequence of the RC_v is shown in Fig. 3.9.

i) Luminance of External Surfaces:

The luminance was calculated for three external surfaces; the building surface containing the window; the external obstruction surface facing the building surface; and the ground between the buildings. Both building surfaces were assumed to be vertical parallel, and infinite in length for ease of calculation since portions far from the window contribute negligible intensity.

Both the obstruction surface and the ground surface affect the daylight level inside the room directly. The building surface influences the daylight level inside the room indirectly through two mechanisms. Firstly, it may prevent direct beam sunlight and part of the sky light from reaching the ground and the obstruction surface. Secondly, it reflects light towards the ground surface and the obstruction surface which is re-directed to the window.

The total luminance of any of the three surfaces is the sum of three components, luminance due to incident direct beam light, L_{sun}, luminance due to diffuse skylight, L_{sky}, and luminance due to reflected light from the other two external surfaces, L_{ref}. The luminance due to direct beam light, L_{sun}, is expressed by

$$L_{sun} = \rho I \eta_{sun} \qquad (3.14)$$

where ρ is the average diffuse reflectance of the external surface (assumed to be independent of the directions of the incident radiation), I is the incident beam radiation upon the surface and is given by Eq (2.14), and η_{sun} is the annual average luminous efficiency of beam radiation with a value recommended by Hopkinson of 100 lumen per watt [121].

The Luminance due to diffuse skylight, L_{sky}, depends on the luminous flux, Y from the visible patch of the sky to which the surface is exposed (expressed as a ratio of the zenith luminance, L_z), and the average diffuse surface reflectance ρ. Thus, L_{sky} is expressed as:

$$L_{sky} = \rho L_z Y \qquad (3.15)$$

where Y for the building surface is given by

$$Y = \sum_{i=r_1}^{9} \sum_{J=S1}^{S1+17} L_{ij} A_i \cos\theta_i \cos(\phi_b - \phi_J)$$

and for the opposite building, Y is equal to

$$Y = \sum_{i=r_2}^{9} \sum_{J=S2}^{S2+17} L_{ij} A_i \cos\theta_i \cos(\phi_o - \phi_J)$$

and for the ground between them, Y becomes

$$Y = \sum_{i=r_3}^{9} \sum_{J=S_1}^{S1+17} L_{ij} A_i \sin\theta_i + \sum_{i=r_4}^{9} \sum_{J=S2}^{S2+17} L_{ij} A_i \sin\theta_i$$

where

r1 = The lowest sky ring seen above the obstruction surface from a given point on the building surface.

r2 = The lowest sky ring seen above the building surface from a given point on the opposite building surface.

r3 = The lowest sky ring seen above the obstruction surface from a given point on the ground.

r4 = The lowest ring seen above the building surface from a given point on the ground.

S1 = The first visible subdivision on the right-hand side of the building surface.

S2 = The first visible subdivsiion on the left-hand side of the obstruction surface.

ϕ_b, ϕ_o = The azimuth angle of the building surface and the obstruction surface respectively.

For unobstructed buildings, r1 and r3 correspond to the first ring above the horizon.

Having determined the luminance due to sunbeam light and diffuse sky light for each of the three external surfaces of concern, the luminance due to the doubly reflected light can be evaluated. Since none of these surfaces has a high reflectivity, and the reflected light is generally a small percentage of the total, triple reflections were ignored. Thus, the luminance due to reflection at a given point on an external surface from the other two surfaces can be expressed by

$$L_{ref} = \rho \sum_{k=1}^{2} F_k \cdot L_k \qquad (3.16)$$

where

F_k = view factor of surface K from a given point on the surface of concern (the calculation procedure is given in Appendix A.

Having determined L_{sun}, L_{sky}, and L_{ref} at several points on each external surface, the average total luminance of each surface can be obtained. In the present model, total luminance was evaluated at the centre of the upper, intermediate, and lower thirds of each surface. As an example, the luminance of the ground and the obstruction surface for June 21st at solar noon and their variation with the building azimuth angle are shown in Fig. 3.10.

ii) Luminance of Internal Surfaces

Multiple reflections inside the room were ignored in this model so no calculation of luminance is required for two of the internal surfaces. The first is the wall surface containing the window which is neither exposed to sky nor any of the external surfaces. The second is

the floor which reflects light only to the underside of the working plane. The other four internal surfaces; ceiling, backwall, and both side walls, all contribute to the illumination received at a given reference point on the working plane.

The luminance of a point on an internal surface is dependent upon three factors; firstly the solid angles subtended by the external surfaces and by the patch of sky illuminating the internal point, secondly, the luminance of the subtended external surfaces, and thirdly the internal surface reflectance. Since the first factor certainly varies from one point to another on the internal surface and the second and third factors may also vary, the luminance of an internal surface should be calculated at several points and averaged whenever a single luminance value is required.

The luminance of an internal surface, at a given point, due to diffuse skylight can be expressed as

$$L_{sky} = \rho \tau_g \; L_z \; E_p \qquad (3.17)$$

where

ρ = reflectance of the internal surface of concern

τ_g = average glass transmittance

L_z = luminance of the sky zenith

E_p = total diffuse sky illumination, expressed as a ratio to the luminance of the sky zenith, reaching a given reference point on the vertical internal surface of concern, and is calculated using Eq. 3.12.

The luminance of an internal surface, at a given reference point, due to reflected light from the obstruction surface and the ground is expressed by

$$L_{ref} = \rho\tau_g \, [F_o \, L_o + F_g \, L_g] \qquad (3.18)$$

where F is the view factor of the visible part of the external surface and it is calculated as shown in Appendix A. L is the luminance of the external surface of concern. Subscripts o and g denote the obstruction surface and the ground respectively.

Thus, the luminance of an internal surface is the sum of the luminances due to skylight and light reflected from external surfaces. The vertical walls and ceiling surfaces were each divided into three equal strips. The luminance of each strip was evaluated at its centre. The luminance of each internal surface was taken as the average value of three luminances.

After the luminance of the external and internal surfaces have been calculated, the variable reflected component of the daylight factor RC_v can be evaluated at the room reference point

$$RC_v = \left(\sum_{i=1}^{m} L_i \, F_i \right) / E_h \qquad \% \qquad (3.19)$$

where m is the total number of external and internal contributing surfaces. L_i and F_i are the luminance and the view factor of the contributing surface i respectively.

Summing the variable sky component and the variable reflected component given by Eq. 3.8 and 3.14 respectively yields the variable daylight factor

$$DF_V = SC_V + RC_V \quad \% \tag{3.20}$$

The daylight factor can now be calculated each hour to match the hourly calculations of heat losses and gains in buildings.

3.3 Examination of the Time Dependence of the Daylight Model:

The daylight model was subjected to two tests. In the first test, the agreement between our results and those obtained in a similar previous study was tested. In addition, the symmetry of the results obtained from the daylight model was checked against the solar motion with respect to both the time of day from solar noon and the time of year from the winter solstice. In the second test, the results generated by the model were compared to our experimental measurements.

3.3.1 Comparison Against the Results of a Previous Study

The effect of the solar altitude angle on the illumination ratios for the horizontal surface and the four vertical surfaces, having 0°, 90°, 180°, and 270° azimuth angle differences with the sun, was examined for solar altitude angles ranging from 0° to 60°. The calculated illumination ratios every 5° increment in the solar altitude were compared to similar calculations made by Krochman [149]. The illumination ratios calculated from our daylight model were so close to those of Krochmann that no difference was seen on the scale of Fig. 3.11.

The symmetry of the calculation was checked by calculating the illumination on vertical surfaces at equal time intervals before and after solar noon. The annual symmetry with respect to winter solstice

was also examined by comparing the illumination on various surfaces for 36 consecutive 5-day intervals both before and after winter solstice. No discrepancies were found. (Fig. 3.24).

3.3.2. Comparison with Experimental Measurements

The illumination calculated with the variable daylight model was compared to the illumination derived from the radiation measurements. The main advantage of deriving illumination from radiation measurements in this model is to allow the model to be useful in the absence of illumination data. In Canada, illumination is measured only in Toronto, and only few stations measure it in the United States. On the contrary, radiation measurements are recorded in almost all weather stations.

During the period from January to April 1980, total and diffuse solar radiation (with shadow band) were measured on clear cloudless days in Montreal (latitude 45.3°N). Dodge products solar sensors (type SS-100) were used to measure radiation on the horizontal surface, the vertical surface containing the window, and the internal surface of the window. The measurements were recorded every 3 seconds on 11.2 cm wide carbon loaded paper using Rustrack Model recorder. The measuring site on the roof of the Centre for Building Studies was partly obstructed by surrounding buildings, so measurements taken early in the morning and late in the afternoon were excluded from the comparison.

The illumination calculated with the variable daylight model was compared to the illumination derived from the radiation measurements for the horizontal and two vertical surfaces facing due west and due north.

Radiation measurements on a surface indicate the amount of the incident radiative energy. Illumination however, represents the luminous effect caused by this energy as sensed by the human eye. The sensitivity of the human eye at any given wavelength is always expressed as a ratio of the maximum luminous efficiency, which is taken as 680 lumens per watt at .555 μ m [123]. This ratio is called "the relative luminosity factor". The response of the human eye to the radiation at each wavelength is described by the luminosity function. The illumination, E, is derived from radiation distribution R_λ by the use of the luminosity function

$$E = K_m \int_{\lambda_1}^{\lambda_2} R_\lambda \, f_\lambda \, d\lambda \quad \text{lumens} \tag{3.21}$$

where

K_m = The maximum spectral luminous efficiency (lm/watt)

R_λ = The monochromatic radiant energy flux in the wave length interval $d\lambda$ at wavelength λ (watts)

f_λ = Relative luminosity factor at wavelength λ

λ_1 λ_2 = Lower and upper wavelength limits of the visible spectrum.

For wavelength insensitive detectors, good approximation to the illumination, E, can be derived from the radiation measurements by using a mean value for the luminous efficiency of the source (i.e. $E = K_m (R)_{ave} (\lambda_2 - \lambda_1)$). Natural sources of illumination such as sky and sun, show little variation in spectral energy distribution. The values used to represent the mean luminous efficiencies for the direct beam radiation, clear sky diffuse radiation, and the global radiation were 100,150, and 115 lumens per watt respectively [121].

In the present study, silicon solar detectors were used for radiation measurements. Illumination was derived from the measured radiation. In a silicon photocell, only radiation with wavelengths less than 1.12 μ m can generate a photovolatic current. Thus, to account for the whole solar radiation spectrum, the actual spectral response of a silicon photocell is amplified and corrected. In Fig. 3.12, the spectrum of the luminous response of the human eye (curve c) is shown in relation to a black body equivalent to the spectrum of the beam radiation (curve A), and both the actual and amplified spectral responses of a silicon photocell (curves B and b respectively). Curve B is adopted from a study by Wolf [210]. The product of curve A (solar black body source) and curve B (amplified silicon photocell) is nearly flat over the region where curve c (eye response) is non zero.

Thus, we need only scale the detected signal with the integrated relative luminosity factor to obtain the illumination, E. In order to compare the experimental measurements with the results generated by the model, the radiation measurements were expressed as a ratio of the zenith luminance. For clear skies, the luminance of the zenith has been investigated, in chronological order, by Drono, Dogniaux, Boldyrev and Fesenkova as reported in Ref. [138]. The curves they obtained for the zenith luminance as a function of the solar altitude are shown in Fig. 3.13. During the present study, a test for the zenith luminance was conducted in order to select the most suitable curve of the four which would best fit the sky conditions in Montreal. Fesenkova's curve, shown in full line in Fig. 3.13, was found to be the closest to our clear sky zenith luminance measurement for a single day (April 27,

1980). A Hagner Universal photometer was used for measurements. This instrument has a field of view of 1.94×10^{-4} steradians (contained in a circle whose diameter subtends 1°) and its accuracy is ± 5%. The Fesenkova's curve

$$L_{zc} = 55.943 \ \theta_s + 164 \ \text{cd/m}^2 \qquad (3.22)$$

was used in the calculation of the zenith luminance.

Knowing the mean luminous efficiency of the diffuse sky illumination and the zenith luminance, radiation measurements on an unobstructed surface can be used to obtain the diffuse sky illumination on a horizontal plane as a ratio of the zenith luminance, E_{sky}.

$$E_{sky}(\text{horiz.}) = I_{sky} \ \eta_{sky} / L_z \ (\text{Lux}/(\text{cd/m}^2)) \qquad (3.23)$$

where

I_{sky} = Measured intensity of sky diffuse radiation on the surface. (W/m^2).

η_{sky} = Mean luminous efficiency of the sky diffuse (ℓm/w)

L_z = Luminance of the zenith (cd/m^2).

To measure the diffuse sky radiation, I_{sky}, on the horizontal, a shadow band consisting of a semicircular strip, adjustable about horizontaland vertical axes was placed over the radiation sensor to obstruct the direct beam radiation. The shadow band is 40 mm wide with a radius of 200 mm in order to block off the 25 mm wide sensor. In its short dimension, the shadow band subtended an angle of 11.3° at the centre of the sensor. For the first 4 months of the year, the illumination derived from the measurements on the horizontal surface using Eq. (3.23) was plotted against the illumination obtained from the clear sky

model at two hours from solar noon (Fig. 3.14), at one hour from solar noon (Fig. 3.15), and at solar noon (Fig. 3.16). In these three figures, it is evident that the model represents the hourly and seasonal variations in the illumination satisfactorily. The experimental measurements were always below the illumination values predicted by the model. Two effects are likely to account for this discrepancy. First, the shadow band obstructs a portion of the bright aura around the sun. Second, the bright portion of the sky, near the horizon, is obstructed by remote buildings.

Unlike illumination on the horizontal, illumination on vertical surfaces is significantly affected by reflections from the roof and surrounding buildings. Therefore, illumination due to reflection must be subtracted from the total diffuse radiation measured on vertical surfaces in order to evaluate the sky illumination. Accordingly, the diffuse sky illumination on a vertical surface, E_{sky}, is expressed by

$$E_{sky}(\text{vert.}) = E_v - (E_g + E_o) \quad \text{lux}/(\text{cd}/\text{m}^2) \qquad (3.24)$$

$$= [\eta_v I_v - (\eta_g \rho_g F_g I_g + \eta_o \rho_o F_o I_o)]/L_z$$

where

E_v = total diffuse illumination on the vertical surface as a ratio of the zenith luminance (lux/(cd/m^2)).

E_g, E_o = reflected illumination on the vertical surface, as a ratio of the zenith luminance, from ground and the opposite buildings respectively (lux/(cd/m^2)).

η_v, η_g, η_o = luminous efficiency of the incident radiation on the surface of concern, on ground and on opposite surface respectively, (lumens/watt).

I_v = Total diffuse radiation measured on the vertical surface (w/m^2).

I_g, I_o = global radiation on the ground and opposite buildings respectively.

ρ_g, ρ_o = average reflectance of ground and opposite buildings respectively.

F_g, F_o = view factors of ground and opposite buildings as viewed from the measuring point on the vertical surface. (See Appendix A for the calculation procedure).

For the first 4 months of the year, clear sky diffuse illumination derived from the radiation measurements were compared to the illumination calculated by the model for a vertical surface facing due west (Figs. 3.17, 3.18, and 3.19) and for a vertical surface facing due north (Figs. 3.20, 3.21, and 3.22). For both vertical surfaces, good agreement was found between the illumination derived from the radiation measurements and the illumination calculated by the model.

The hourly variations are well represented by the model. No discrepancy with the seasonal variation was found, but more experimental points will be required to verify this aspect of the model completely.

3.4 Variation of the Daylight Factor with Various Parameters

The variability of the daylight factor is due to the direct (sky) component of daylight and to the indirect (reflected) component of daylight.

To further emphasize the inappropriateness of the original (single- valued) daylight factor the variation of the sky and reflected components of daylight, with eight particular parameters, was calculated. The first four parameters; compass orientation, time of day, time of year, and the latitude angle govern the relative position of the sun with respect to the window and consequently the luminance of the visible patch of the sky. The last four parameters define the geometrical configuration of the window with respect to the reference point and consequently control the size of the visible patch of the sky and the external obstruction surface.

3.4.1 Variation of the Sky Component

The variation of the sky component will be examined in terms of the variable sky factor SF_V.

Parameter i: Compass Orientation of the Surface

Illumination varies considerably with surface compass orientation. It is clear that a vertical surface having the same azimuth angle as the sun ($\phi_W = \phi_S$), shown in Fig. 3.23, has the highest illumination ratio as long as the solar altitude angle, θ_S is less than 45° (the entire winter season and summer mornings and afternoons). For solar altitudes greater than 45°, the horizontal surface has the highest

illumination ratio. The figure also shows that a vertical surface facing away from the sun ($\phi_w = \phi_s \pm 180°$) will always have the least illumination ratio regardless of the solar altitude angle. Due to the importance of this parameter, the effect of window or wall surface azimuth angle will be shown with the effect of the following parameters.

Parameter ii: The Time of Day

Due to symmetry with respect to solar noon, only half of the day need be examined. For January 21st, hourly curves of SF_v as a function of window azimuth angle were calculated (c.f. Fig. 3.23). As expected, maximum SF_v occurs when the solar azimuth is on the perpendicular to the window and minimum when it is in the plane of the window. The change in the illumination ratio from one hour to the next is large if the window faces the brighter half of the sky (270° to 90°). Illumination on a north window is relatively constant through the day. Previously, it was believed that due north windows receive the least illumination at all times.

Parameter iii : The Time of Year

The annual variation of illumination is symmetrical with respect to the solstices. The noon illumination on the horizontal and vertical surfaces, as a ratio of the zenith luminance, versus days from winter solstice is shown in Fig. (3.24). It can be seen that the maximum yearly illumination ratio for all 5 surfaces occurs on the winter solstice (December 21st), and the minimum on the summer solstice (June 21st. This is due to the fact that the zenith luminance is maximum on

the summer solstice where the solar altitude of the sun is at its peak. From September 21st to March 21st, a south vertical surface receives the maximum illumination ratio while a horizontal surface receives the maximum illumination ratio from March 21st to September 21st. the variation of the noon SF_v with window azimuth angle at the beginning of each season of the year is shown in Fig. (3.25). The maximum variations with the azimuth angle occur in the winter when the sun is low and the minimum in the summer when the sun is high.

Parameter iv: Latitude

Illumination ratios for latitudes ranging from 0.0°N to 60°N were calculated at the beginning of each season of the year as shown in Figs. (3.26) and (3.27). Except for the tropics in the summer, the lower the latitude the lower the illumination ratio. On June 21st, the sun is to the north of latitude 23.45°N, so south facing surfaces receive the least illumination in the tropics. The absolute minimum illumination ratio, on June 21st, corresponded to latitude 23.45°N. As shown in Fig. (3.28) for January 21st, at solar noon, the variation of the variable sky factor with respect to the window azimuth angle decreases as the latitude angle decrease.

Parameter v: Window Aspect Ratio

The window aspect ratio (width to height ratio) is one of the parameters that defines the patch of the sky to which the reference point will be exposed. Thus, windows having the same area are expected to have different SF_v (at the same distance from window), as long as they have different window aspect ratios. Three windows having the

same area (3.00 m^2) but each with a different aspect ratio (.333, 1.0, or 3.0) were chosen for comparison. On January 21st, the short wide window (Fig. 3.29 provided slightly higher SF_v than the square window (Fig. 3.30) at 1.0 m from the window and slightly lower SF_v at the deeper positions. Except for the deepest position, the tall narrow window (Fig. 3.31) provided lower SF_v values than the square window. Since the comparison was made on January 21st, the difference in SF_v between the tall narrow window and the square window is not very large because the brightest part of the sky (the aura around the sun) is low in winter and visible at the back of the room for both shapes.

Parameter vi: Distance of the Reference Point from Window

The variable sky factor decreases as the distance of the reference point from the window increases regardless of the window aspect ratio and the window azimuth angle. However, the rate of decrease of SF_v with distance from window depends both on the window aspect ratio and the window azimuth angle as shown in Fig. 3.32. Eight main window azimuth angles were examined for each of the three different window aspect ratios. At solar noon, the steepest SF_v gradient occurs for due south windows. At other times, they will occur for windows with the same azimuth angle as the sun.

Parameter vii: Window-to-Wall Area Ratio (WWAR)

For a square window, the effect of the window-to-wall area ratio on the noon SF_v at the beginning of the winter, spring/fall, and summer is shown in Figs. (3.33), (3.34), and (3.35) respectively. Throughout the year, WWAR has a significant effect on the SF_v for southerly

oriented windows, and a moderate, relatively constant, effect on the northerly oriented windows. On the winter solstice, the sun relatively is low and the WWAR has a significant effect on SF_V of the southerly oriented windows; while at the summer solstice, with a high sun this effect is reduced. These results are summerized for the eight major compass directions in Fig. (3.36).

3.4.2 Variation of the Reflected Component RC_V

The objective of this section is to investigate, under a clear sky, the dynamic nature of the variable reflected component, RC_V, at different times of day, times of year, latitude angles, window orientations, window-to-wall area ratios, and the height of the obstructing surface. Only one parameter was varied at a time. The remainder of the parameters were kept constant with values shown in Table 3.1. Thus, the sensitivity of the variable reflected component and consequently the variable daylight factor to the variation in each parameter can be examined. In the case of a fully obstructed window; the reflected light at the reference point is the only source of natural daylight; (i.e. the variable daylight factor DF_V = the variable reflected component RC_V).

Obviously, if the reflected component is ignored, one cannot hope for a realistic estimate for either the daylight factor or the electricity savings.

Parameter i: Compass Orientation

Due to its importance, the effect of the window azimuth angle will

Parameter	Assumed value
Sky condition	clear
Day of the year	June, 21
Hour of the day	Noon
Latitude of location	45°
Building height	7.m
Obstruction Height	7.m
Building-obstruction surface-to-surface distance	8.m
Room height	3.m
Room width	4.m
Room depth	4.m
Height of working plane and window sill from ground	.90m
Window height	1.2m
window width	2.0m
Window position in panel	centered
Distance of reference point from window	2.0m
Distance of reference point from side wall	2.0m
External wall thickness	.15m
Glass Transmittance	.85
Reflection of building surface	.30
Reflection of obstruction surface	.30
Reflection of ground	.20
Reflection of side walls	.60
Reflection of back wall	.60
Reflection of cieling	.60

TABLE 3.1: Assumed constant values for the remainder of the parameters.

be examined simultaneously with the following parameters.

Parameters ii and iii: Time of Day and Time of Year

The variable reflected component of a fully obstructed window (SC_V = 0.0), was calculated every hour during the first half of the 21st day of June as a function of the window azimuth angle Φ_W. The results are shown in Fig. 3.37. For a fully obstructed window, the variable reflected component is greatly influenced by the luminance of the obstruction surface which changes with the time of day (i.e. solar position). The obstruction surface was moved with the window azimuth, so it was always parallel to the window surface.

The variation of RC_V with window azimuth angle increases as the time difference from solar noon increases. At each hour, the maximum value of RC_V occurs for an obstruction surface perpendicular to the sun's azimuth at that hour. Thus, the maximum at solar noon occurs for a window facing due north and at five hours before noon by a window facing due west as shown in Fig. 3.37. When the variation of the obstruction surface luminance shown in Fig. 3.38 is compared to the variation of the variable reflected component shown in Fig. 3.39, it is evident that the obstruction surface luminance is the major influence on the variable reflected component.

An example of the variation of the noon time variable reflected component with the time of the year is shown in Fig. 3.40. The variation with the time of year is also dependent on the solar altitude angle. On the winter solstice, the solar altitude angle is at its lowest noon value, so RC_V is maximum for south facing obstruction and

minimum for north facing obstruction.

Parameter iv: Latitude

At the beginning of each season, RC_v was examined at solar noon for latitude angles ranging from 0° to 60°N. Fig. 3.41 shows the variation of noon RC_v with latitude angle on December 21st. For obstructions facing south, the value of RC_v increases with latitude and decreasing solar altitude until shading by the building containing the window sets in at 40°N latitude. For windows due east, due west, and with southerly orientations, RC_v decreases as the latitude angle increases. For these window orientations, the obstruction surface is in shade at solar noon and illuminated only by sky diffuse and ground reflected radiation. The latitude at which a sudden drop in the RC_v value occurs (i.e. northerly windows at noon) depends on the solar altitude and the heights of buildings.

The variation of RC_v with latitude angle at solar noon on March 21st (September 21st will be the same) is shown in Fig. 3.42. The solar altitude angle is large enough so that no shading of southerly oriented obstructions occurs at any of the latitudes examined. Thus, no sudden drop appeared. Again, the RC_v at solar noon increases with decreasing solar elevation for the northerly oriented windows while it decreases for the other window orientations. At noon, on the equinoxes, the sun is directly overhead at the equator, so all vertical surfaces are equally illuminated. A similar situation occurs at noon on the summer solstice over the tropic of cancer (c.f. Fig. 3.43). For latitudes greater than 23.45°N, the trend of noon RC_v with latitude is

similar to that for the other three seasons. For latitudes less than 23.45°N, the trend is reversed because the sun position is to the north at solar noon.

Parameter v: Window Aspect Ratio

Illumination from a tall narrow window with an aspect ratio of 3.0 was compared to illumination from a reference square window of the same area with an aspect ratio of 1.0. In each case, the illumination was calculated at several reference points along the perpendicular bisector of the window sill. On June 21st at solar noon, the long narrow window provides higher values of the variable daylight factor than the square window for energy orientations as shown in Fig. 3.44. The short wide window provided less illumination than the square window, as shown in Fig. 3.45. However, the short wide window will give more uniform illumination across the width of the room.

Parameter vi: Distance of the Reference Point from Window

For an unobstructed window, the intensity of daylight decreases exponentially with distance from the window. For a fully obstructed window, illumination decreases almost linearly with distance from the window. In the case of a partly obstructed window, the variation of illumination with distance from window in the perpendicular direction shows a combination of both trends. An example for solar noon on June 21st is shown in Fig. 3.46. Since the obstruction is from below, points close to the window are illuminated mostly by light from the clear sky and receive several times the illumination striking points near the back wall.

As shown in Fig. 3.47, when we move the reference point off the right bisector of the window sill, RC_v declines as distance from the centre of the sill increases. The largest variation occurs with a due south facing obstruction. For the other 3 main orientations, this effect was not significant because the luminance difference between the obstruction surface and the internal surface is relatively small.

Parameter vii: Window-to-Wall area ratio

As this ratio increases with constant wall area, the illumination on the reference plane and on the internal surfaces from skylight and from externally reflected light increases as the subtended solid angle increases. The variable reflected component of a fully obstructed window on June 21st at solar noon was calculated for window-to-wall area ratio increments of 0.10 as shown in Fig. 3.48. Between 90° and 270° window azimuth, the obstruction surface is illuminated by direct beam radiation and the June 21st noon RC_v varies strongly with azimuth. The variable daylight factor, DF_v, was calculated for windows oriented towards the four main compass points, once assuming no obstruction (Fig. 3.49) and once assuming the window to be fully obstructed (Fig. 3.50). The northerly oriented window (ϕ_w = 180°) received more illumination when it was obstructed because the luminance of the obstruction with ρ = 0.3, is higher than the luminance of the clear sky. For the other three orientations (ϕ_w = 90°, 270°, or 360°) windows received more illumination when they were unobstructed. The variation with window-to-wall area in the case of obstructed windows was small.

Parameter viii: The Height of the Obstruction

The patch of sky illuminating a reference point inside a room can vary with the height of the obstruction surface facing the window and its distance from the building surface. As a result, the diffuse skylight received at the reference point decreases with the height of the obstruction as shown in Fig. 3.51. The reflected light from the obstruction surface increases with the obstruction height up to a maximum which corresponds to the height that would fully obstruct the sky at the reference point (an obstruction height of 7 meters for the dimensions of Table 3.1). Fig. 3.52 shows the effect of obstruction height (up to 7.0 meters) on the sky diffuse illumination (direct component), the reflected component and the total illumination for due north and due south windows. The values of illumination were calculated for a reference point 2.5 meters away from the window.

3.5 Daylight Potential as an Energy Saver

While energy was cheap, designers ignored the available daylight and relied completely on electric lighting. The rapidly increasing cost of energy in recent years has encouraged designers to consider daylight as the primary source of light for peripheral zones. Designers have also realized that electrical lighting has a very low luminous efficiency when compared to daylight. The use of daylight will also reduce the cooling load associated with the heat generated from electric lighting and can reduce demand load charges for all of the electricity used in a building. Since the energy consumed for

lighting is the third largest portion of the energy consumed in air-conditioned buildings after heating and cooling, daylight utilization can have a significant impact on the national energy consumption.

As the window area increases, the admitted daylight and the solar heat gains increase. In order to determine whether or not the energy savings from the utilization of extra daylight and solar heat gain can exceed the increased energy losses through the window, the energy savings potential for both daylight and solar heat gain must be determined. In Chapter II, the utilization of solar heat gain was assessed. In this section, the energy saved by utilizing daylight will be examined.

3.5.1 Estimation of the Annual Energy Consumption caused by Electric Lighting, Q_{AN}:

Q_{AN} has two components; the energy consumed to operate the lights, Q_ℓ , and the cooling energy consumed to offset the heat generated from the lighting system, Q_C. Dividing the required light flux (lumens), by the luminous efficiency of the particular lamps and fixtures used (lumens/watt), the total wattage required, W, for the given space can be determined and Q_ℓ can thus be obtained

$$Q_\ell = .0036\ n.\ W \quad MJ \tag{3.25}$$

where n is the total number of hours per year during which the light is switched on and a conversion factor of 0.0036 is used to convert watts to megajoule.

The instantaneous energy required to offset the heat generated from lamps, $Q_c(t)$, depends on the time lag between the time when the heat and light are radiated from the lamps and the time when the heat is received by the room air. Therefore, the cooling load for the lamps at time t is partly due to the electricity used at time $(t - \Delta t)$.

The total annual energy required to offset the heat generated from lamps, Q_c, depends on the total wattage, the type of light fixture, the ventilation rate, the arrangement of air supply and return, the heat storage capacities of walls, ceiling, floor, and furniture, and the thermal conductance of the room surfaces. Mitalas [215] described the relation between a step change in power input to lights and the corresponding cooling load component by an exponential expression with two independent coefficients; a_1 and b and one dependent coefficient, a_2 Coefficient a_1 is the ratio of the cooling load one hour after the lights are switched on. The coefficient a_1 depends largely on the short term thermal storage characteristics of the room. These short term characteristics depend, in turn, on, (i) the proportions of the light power that is dissipated by radiation to that dissipated by convection, (ii) the geometry of the light fixtures, (iii) the rate of ventilation, (iv) the arrangement of air supply and air return, (v) the type of ceiling and, (vi) the thermal conductance of the various surrounding surfaces. The other independent coefficient, b, which defines the rate of cooling load, increases or decreases after the lights are switched on and is mainly dependent on, (i) the rate of ventilation, (ii) type of light fixtures, (iii) arrangement of air

supply and air exhaust and, (iv) thermal properties of the room.

Assuming that the cooling load and the power input to the lights eventually become equal, the dependent coefficient a_2 is expressed by

$$a_2 = 1.0 - (a_1 + b)$$

Thus, using Mitalas' relation between the power input to lights and the corresponding cooling load, $Q_c(t)$ at time t can be expressed by

$$Q_c(t) = a_1 W(t-\Delta t) + a_2 W(t-2\Delta t) + b\, Q_c(t-\Delta t) \text{ watts} \quad (3.26)$$

The annual energy required for the cooling load caused by electric lighting is

$$Q_c = (.0036/COP) \sum_{t=1}^{n} Q_c(t) \quad MJ \quad (3.27)$$

Adding Eq. 3.25 and Eq. 3.27 yields the annual energy consumption caused by electric lighting Q_{an}.

3.5.2 Estimation of the Annual Energy Saved by Daylighting and the Residual Demand for Artificial Lighting:

The development of a time-dependent daylight model allows the calculation of the daylight energy savings and of the residual energy required for artificial lighting. For a particular hour, i of any particular day, j, the room average daylight illumination, E(i,j), received at a given reference point in the room is:

$$E(i,j) = DF(i,j) \cdot E_h(i,j) \quad (3.28)$$

where DF(i,j) and E_h(i,j) are the variable daylight factor and the total diffuse sky illumination on an unobstructed horizontal plane at the hour i of the day j respectively. E_h(i,j) and DF(i,j) were calculated as in Eq. 3.4 and Eq. 3.20 respectively. Thus annual energy

saved by daylighting, Q_S becomes

$$Q_S = .0036\ (1.0+q_C)\ .\ (A_r/\eta_\ell) \sum_{i=1}^{m1} \sum_{j=1}^{m2} E(i,j)\ \ MJ \qquad (3.29)$$

where m_1 is the number of hours during daytime when the lights could be turned off and m2 is the number of days per year when lights are on during the day. A_r is the room area and η_ℓ is the luminous efficiency of the lamps installed. q_C is the specific cooling load per each watt of electric light saved and is given by

$$q_C = Q_C/W \qquad (3.30)$$

In the calculation of the annual energy saved by daylight, Q_S, two main assumptions were made. First, the variation in the illumination level within the time interval is negligible. This assumption is only violated when large changes in sky conditions occur as a weather front moves by (i.e. for a few hours per week). Second, the calculations were made for a single reference point, assuming that illumination at this point represents the room average illumination. This assumption is valid for rooms having a small depth (i.e. less than 1.5 the height) if the reference point is carefully chosen.

The annual demand for artificial lighting can also be estimated by subtracting the annual energy saved Q_S from the annual energy consumption Q_{an} caused by electric lighting when daylight is not utilized. A case study is shown in Chapter VI.

The dollar savings are not simply proportional to the energy savings because there is a savings in demand load charges for all consumption as well as in the cost of maintenance and operation of the

lights. The demand load savings gives a powerful multiplication factor (between 2 and 3) to the dollar savings for daylighting and consequently allows a faster rate of return for capital expenditures on light level sensitive controls.

3.6 Summary

A time-dependent version of the daylight factor method was developed. Unlike the conventional daylight factor, the variable daylight factor can be used for clear, cloudy, and overcast skies. Based on the C.I.E. luminance distributions for clear and overcast skies, a luminance distribution for partly cloudy sky was developed.

The value of the variable daylight factor depends on the time of day and year, the sky conditions, the compass orientation of the window, the latitude, the window-to-wall area ratio, the window aspect ratio, the distance of the reference point from the window, height and distance of the obstruction from window, and the reflectance of the internal and external surfaces which contribute to the illumination at the reference point.

A parametric study was conducted, for a simple geometry and the dependence of both the sky and reflected components of the variable daylight factor on each parameter was presented.

Results from the variable daylight model calculation agreed well with measured hourly variations during 30 days and with the seasonal variation from January 1st to April 27 1980.

In this model direct beam light was taken into account after being reflected by external surfaces. Reflected light from internal surfaces is calculated separately for each internal surface, so changing the reflectance of each internal surface can be investigated. The time dependent version of the daylight factor allows a reasonable calculation of the annual energy required to power and to cool artificial lights.

We now have a procedure for daylight energy calculations compatible with hourly calculations of the heat gains and losses from buildings. Consequently, the daylighting calculation can become an integral part of comprehensive building energy analysis and design programs.

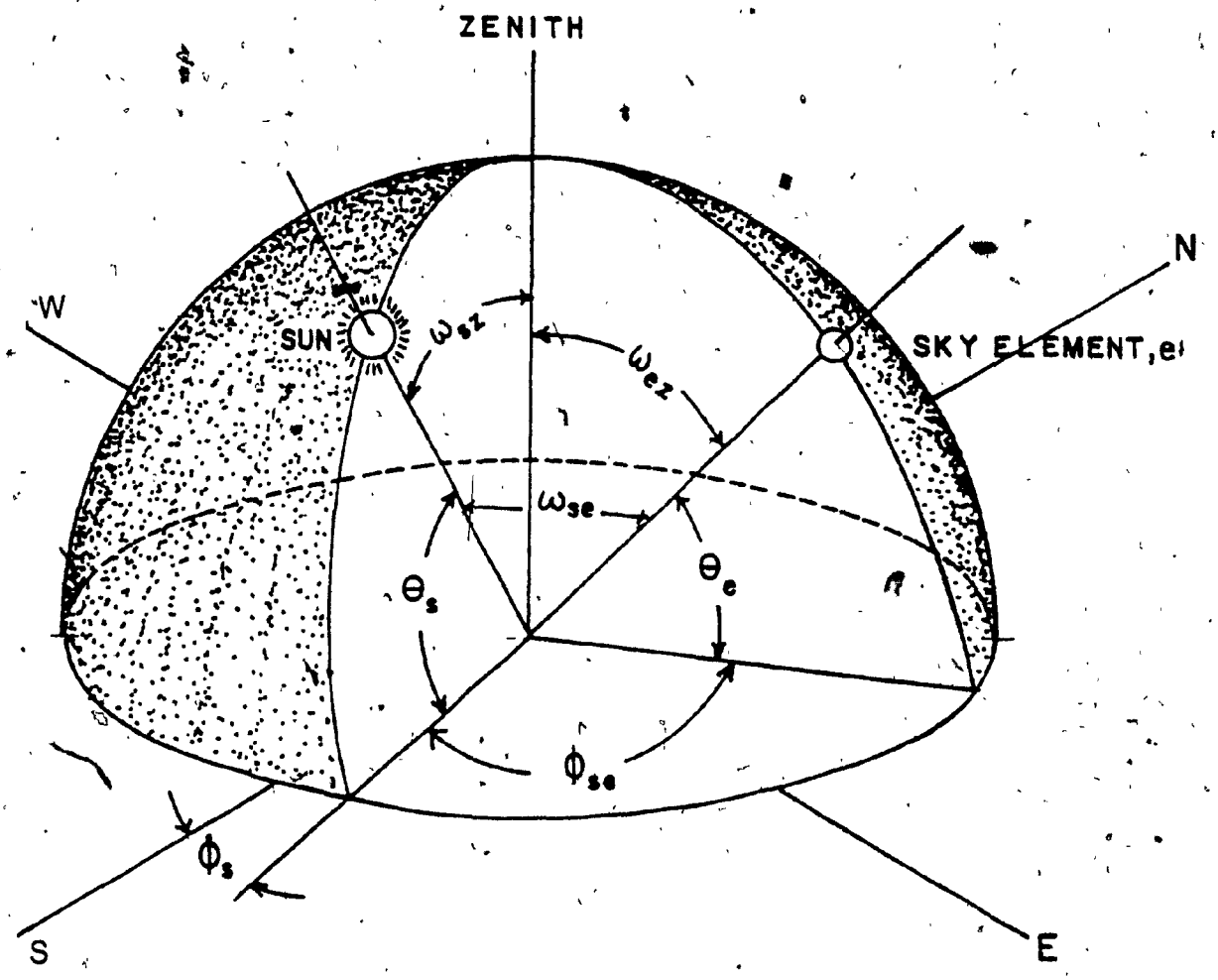

Fig. 3.1 : Angular distances ω_{sz}, ω_{ez}, and ω_{se} representing the geometrical relationship between the sun, zenith, and the sky element.

(A)

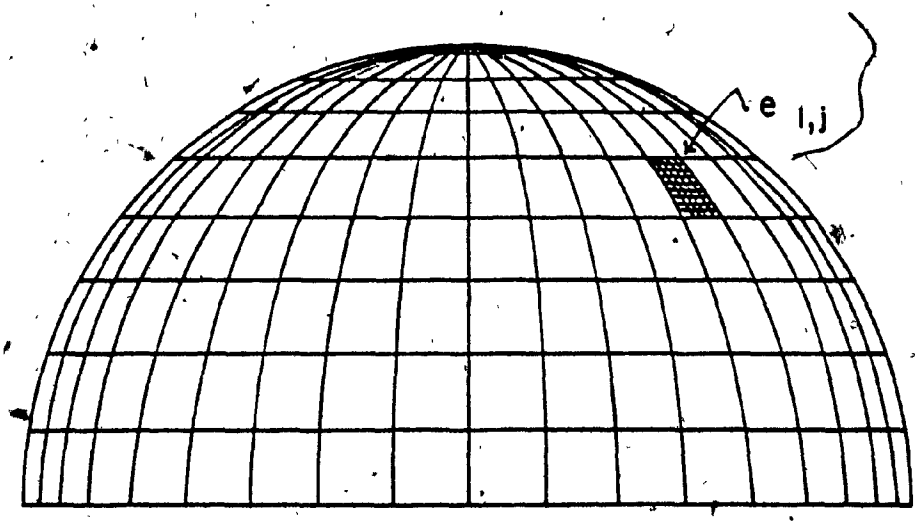

(B)

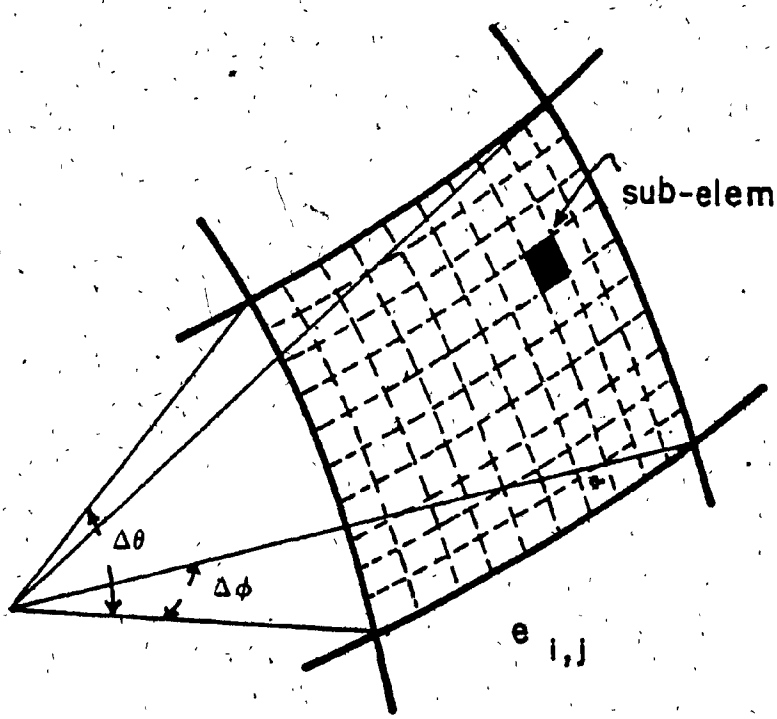

Fig. 3.2 : Elements of the sky dome and subelements within each sky element.
(A) The sky dome after division into a finite number of sky elements.
(B) A sky element divided into a finite number of subelements.

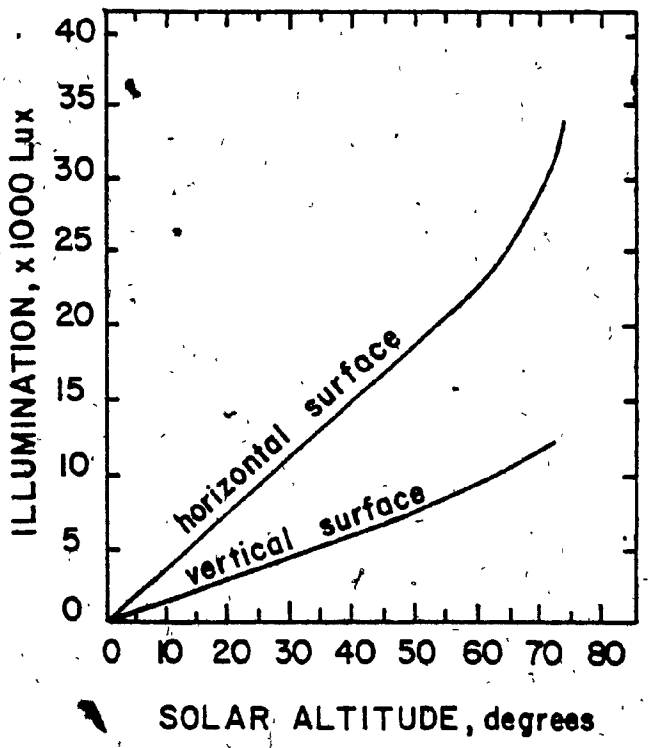

Fig. 3.3 : Variation of illumination on horizontal and vertical surfaces with the solar altitude under an overcast sky [123]

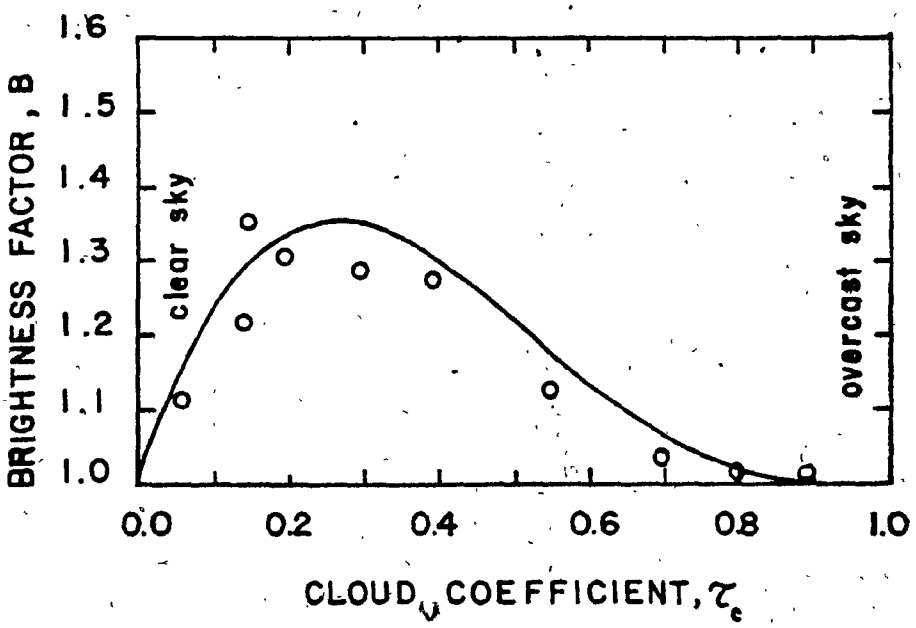

Fig. 3.4 : Observations of the additional brightness caused by clouds in relation to the proposed function of Factor B.

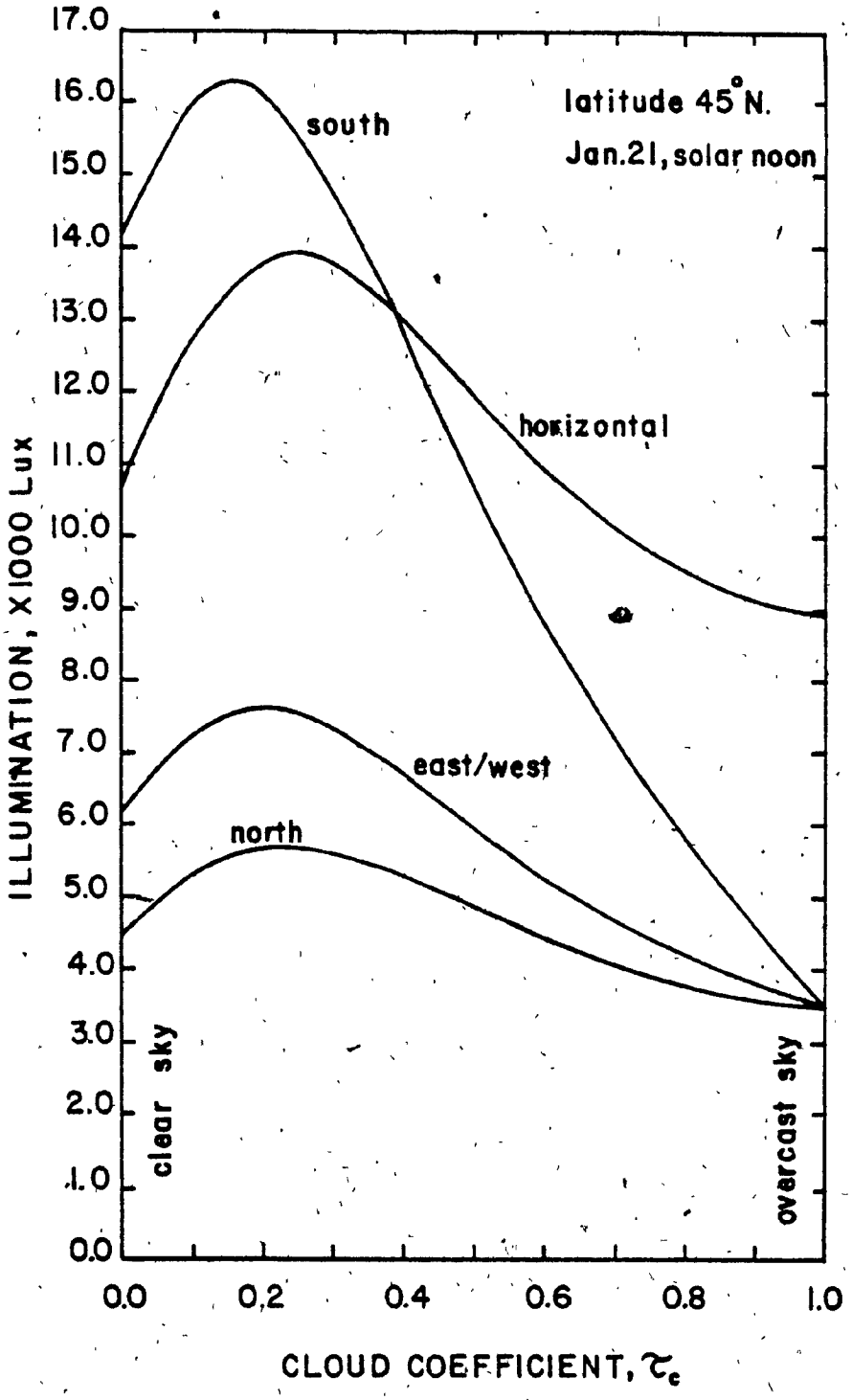

Fig. 3.5 : Illumination on horizontal and four main vertical surfaces as a function of the cloud coefficient.

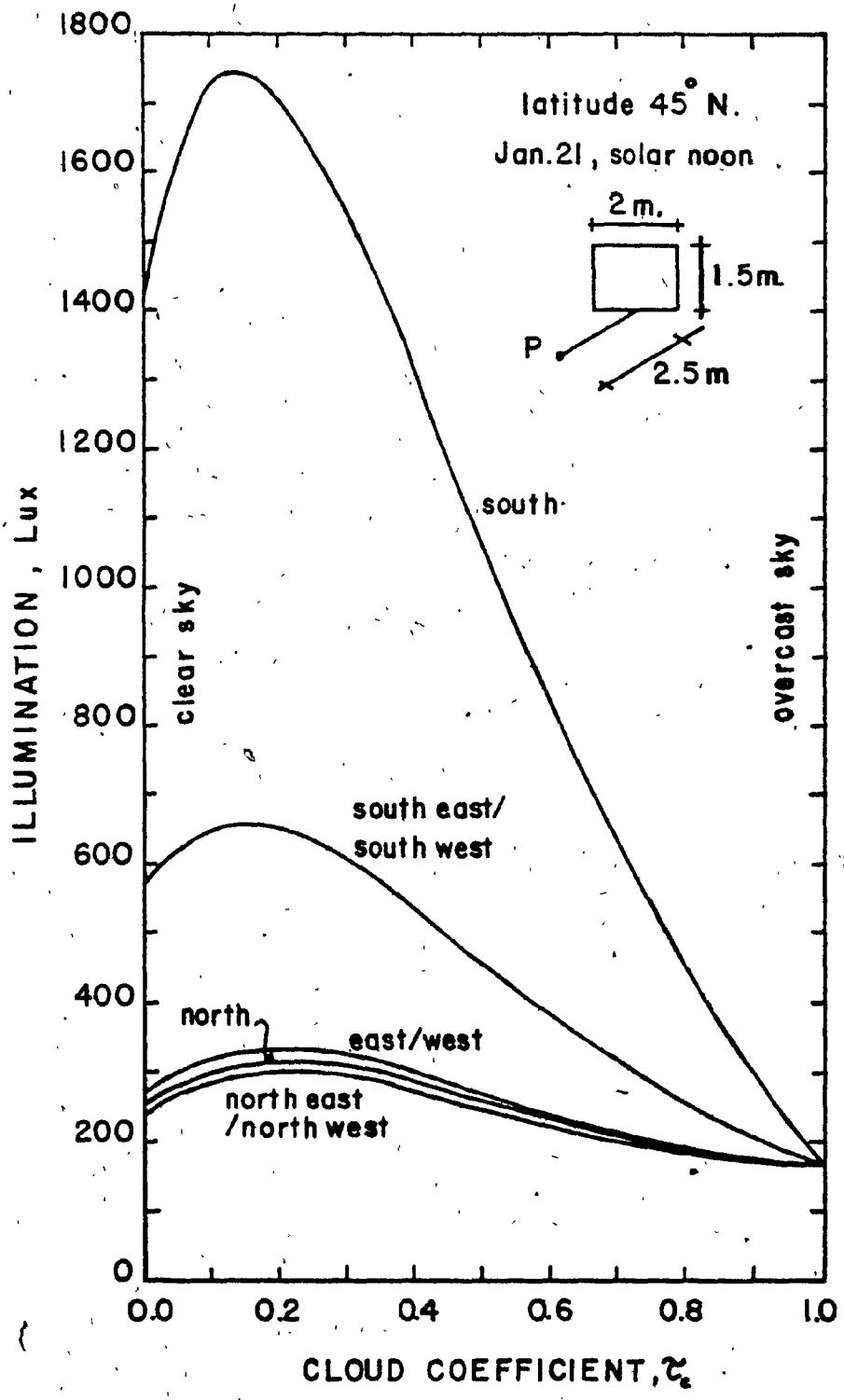

Fig. 3.6 : Illumination at an internal reference point as a function of the cloud coefficient for the main eight orientations.

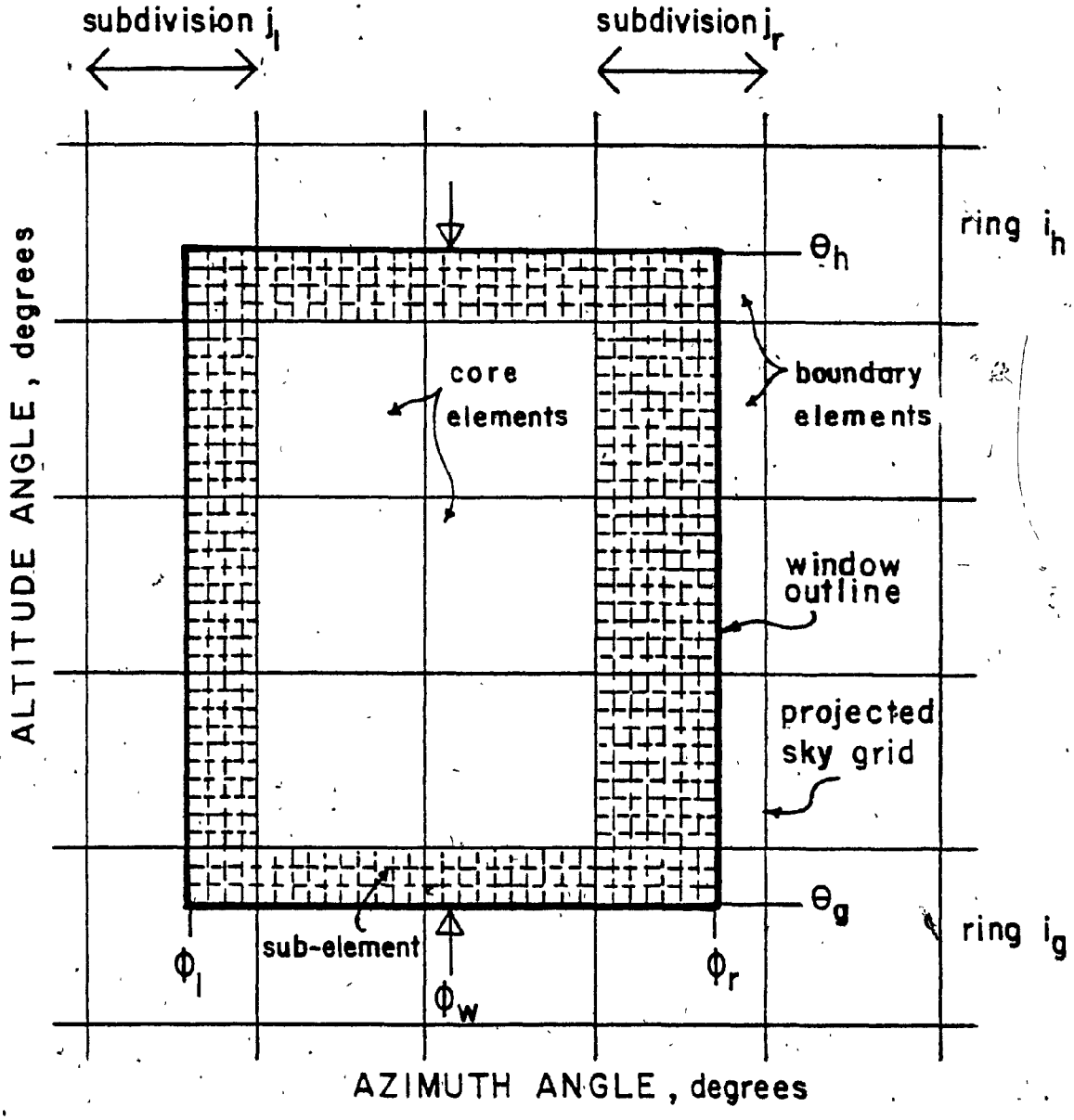

Fig. 3.7 : An orthogonal projection of the visible patch of the sky seen through the window showing core elements, boundary elements, the altitude range, and the azimuth range of the visible patch of the sky.

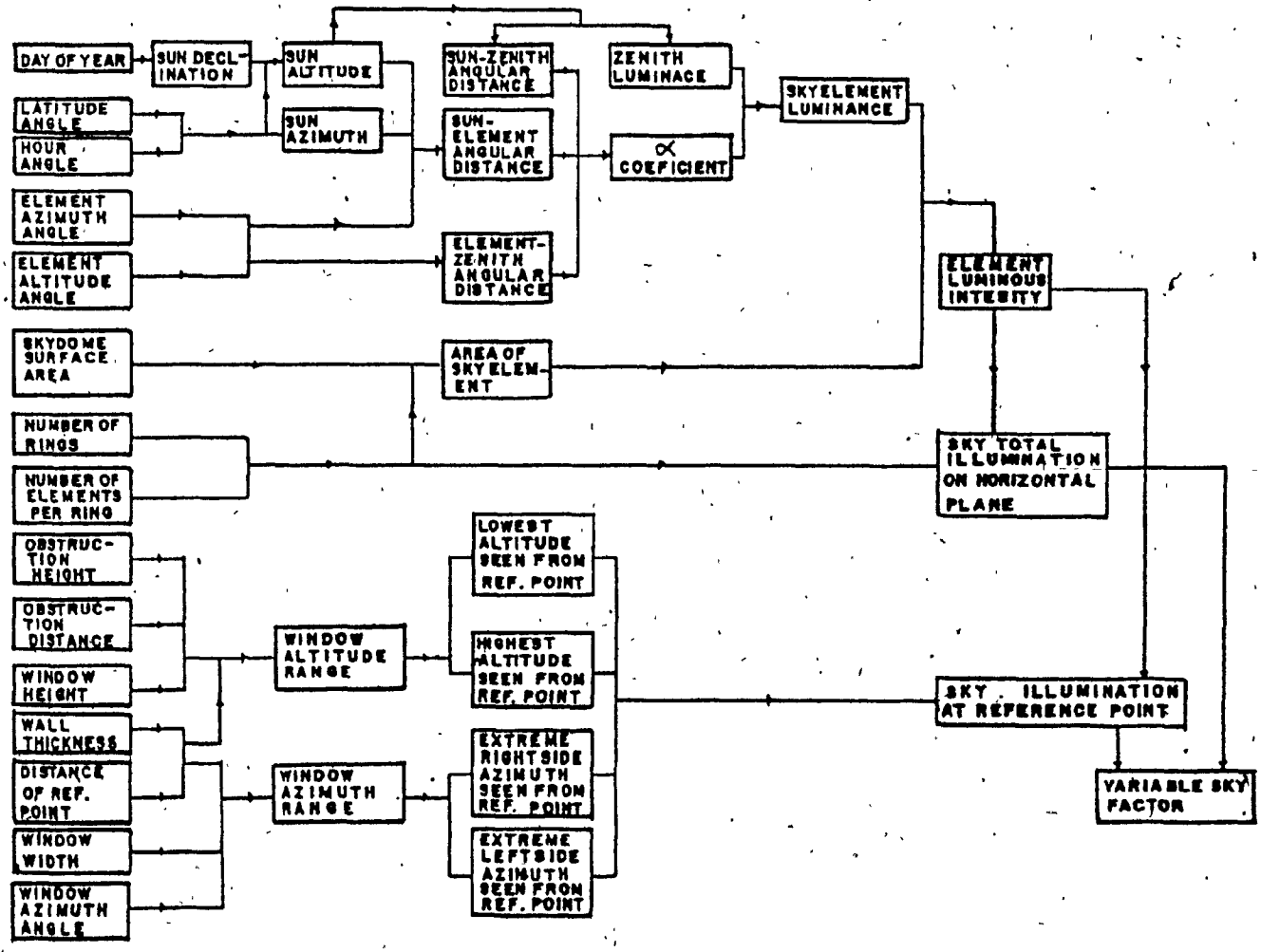

Fig. 3.8 : Block diagram for the calculation of the variable sky factor.

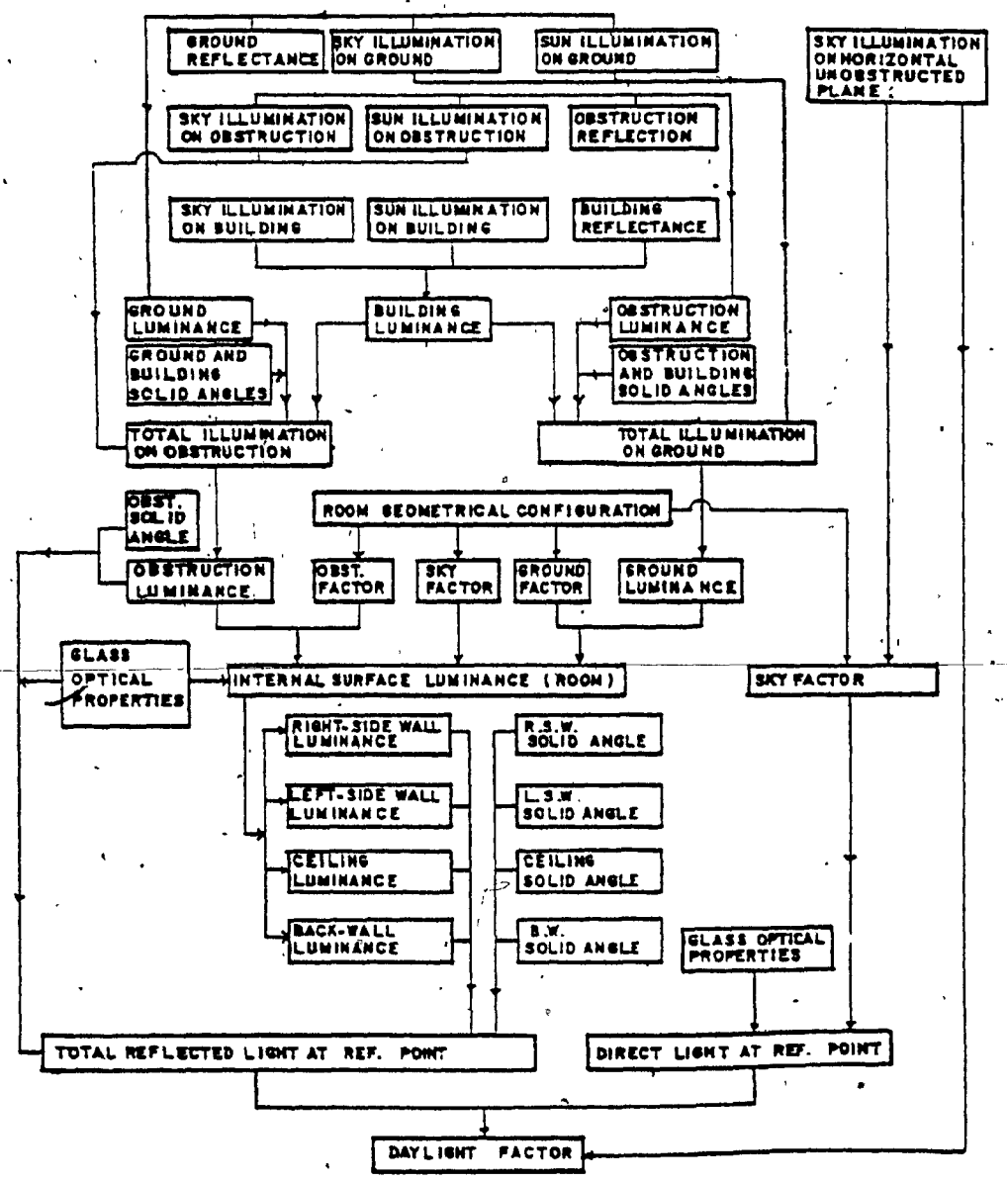

Fig. 3.9 : Block diagram for the calculation of the variable reflected component and the variable daylight factor.

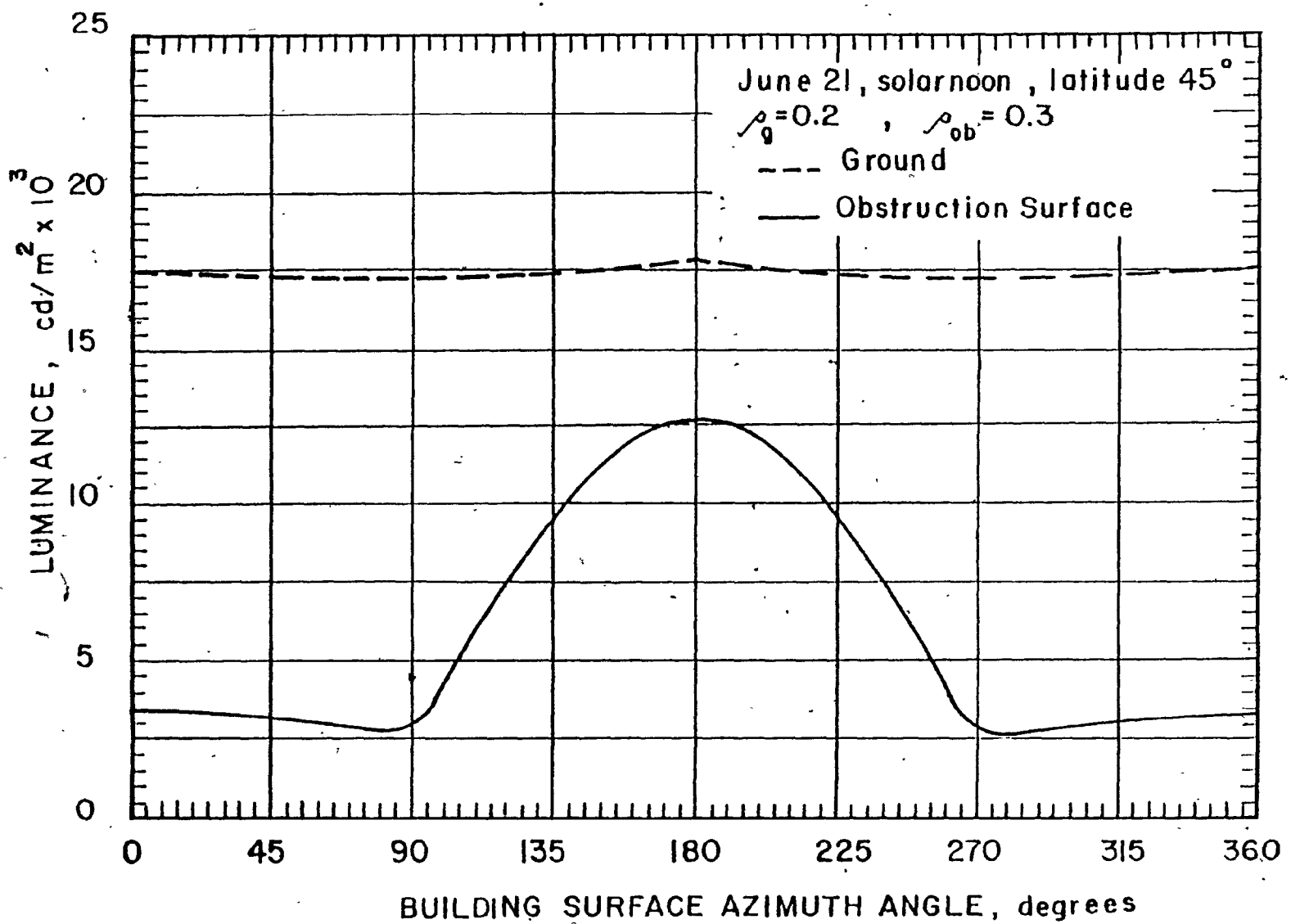

Fig. 3.10 : Variation of ground and obstruction luminances with building azimuth angle.

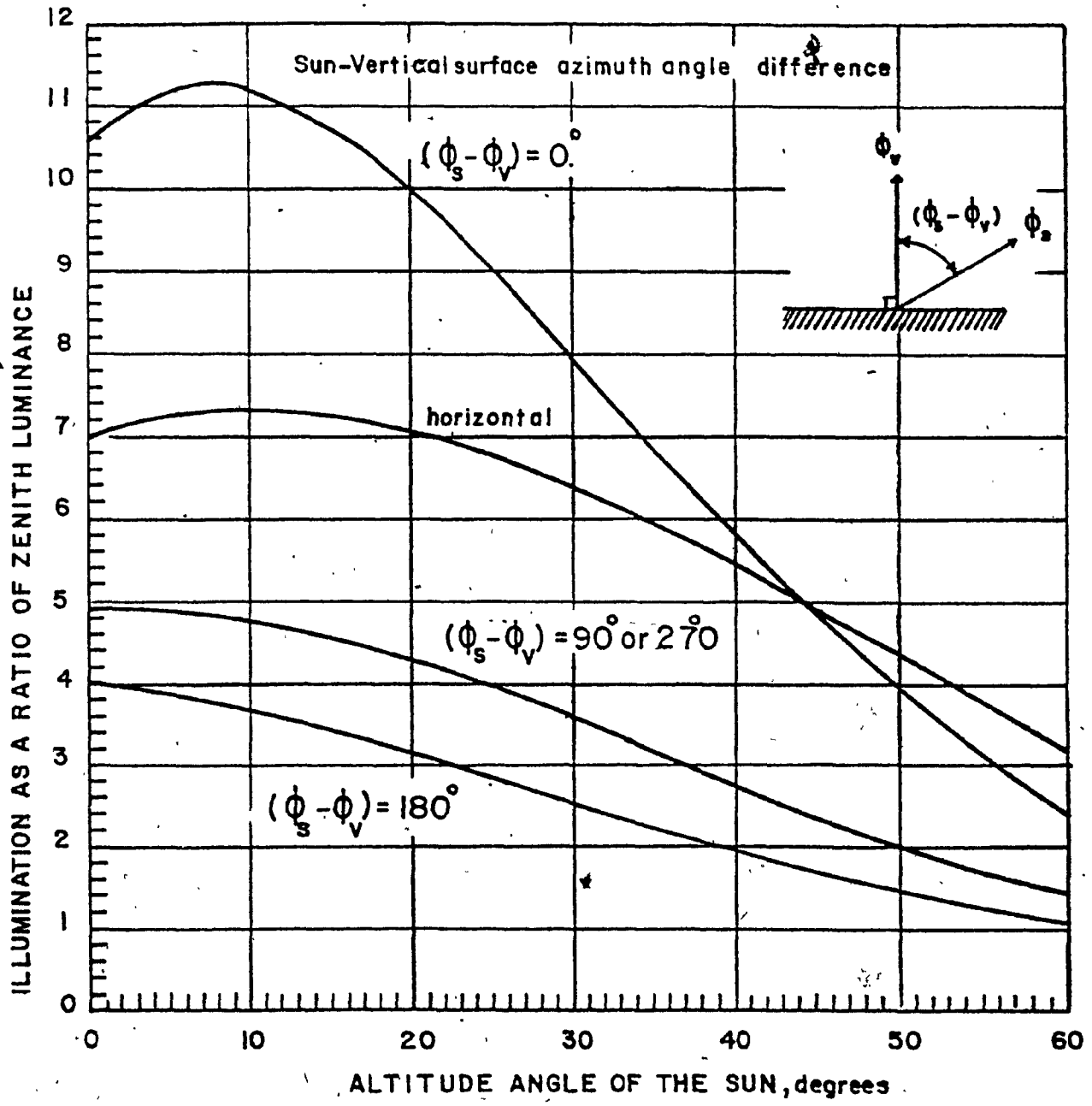

Fig. 3.11 : Variation of illumination with respect to the altitude angle of the sun for a horizontal surface and for vertical surfaces having 0°, $90^\circ/270^\circ$, and 180° azimuth angle differences with the sun.

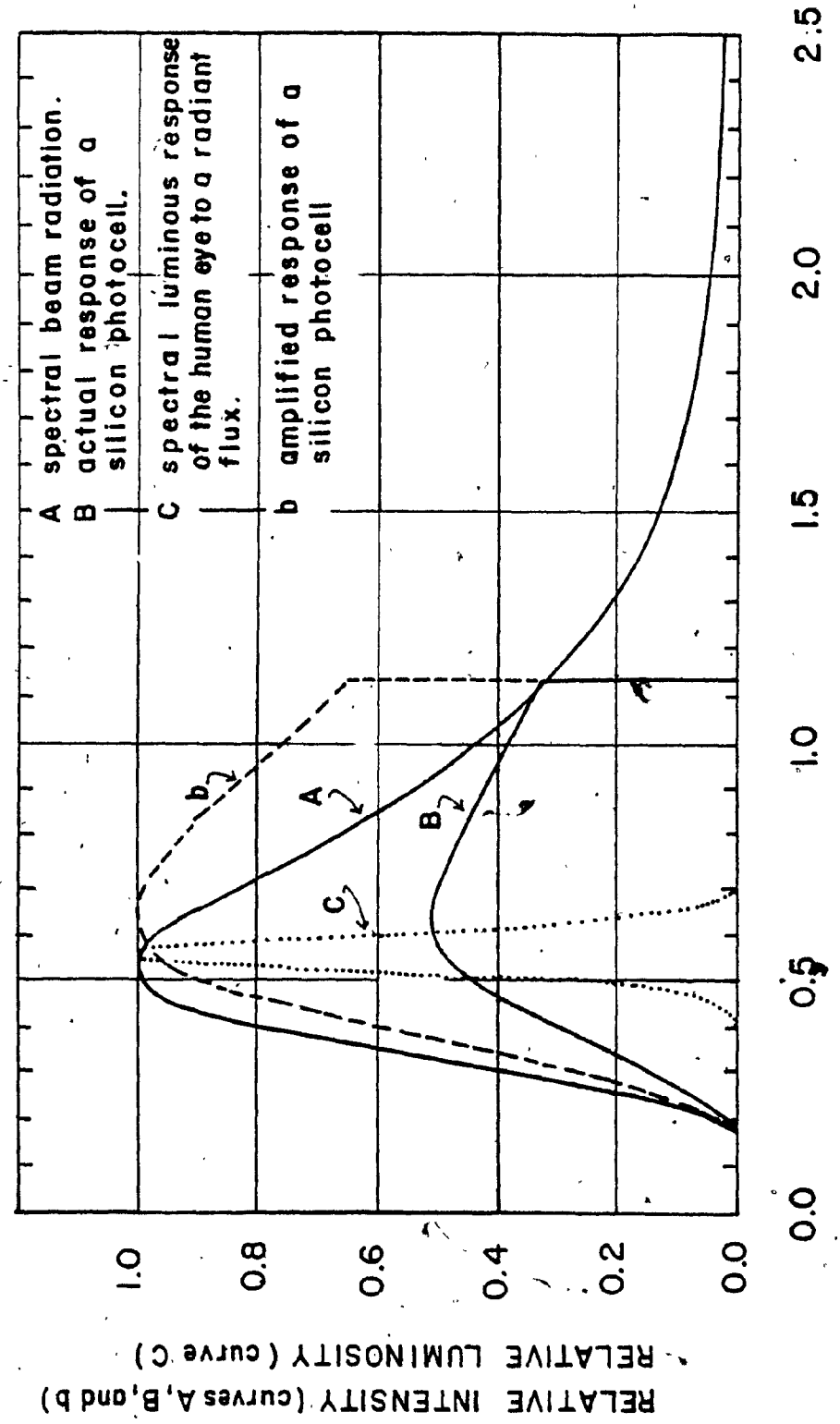

Fig. 3.12 : Actual and amplified spectral response of a silicon photocell in relation to the spectrum of solar radiation and the response of the human eye to its radiant flux.

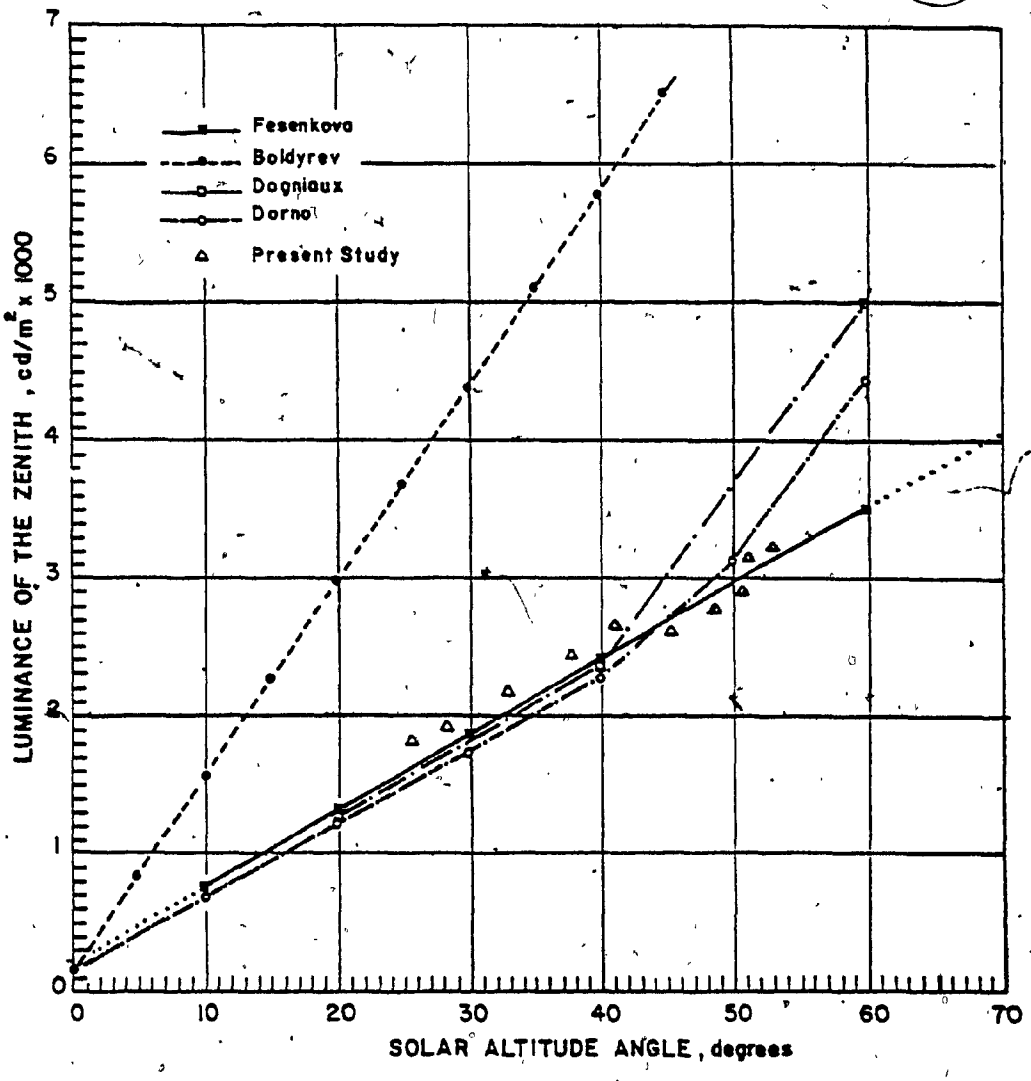

Fig. 3.13 : Preliminary experimental measurements of the zenith luminance with a clear sky in relation to previous measurements reported by Kittler [138]

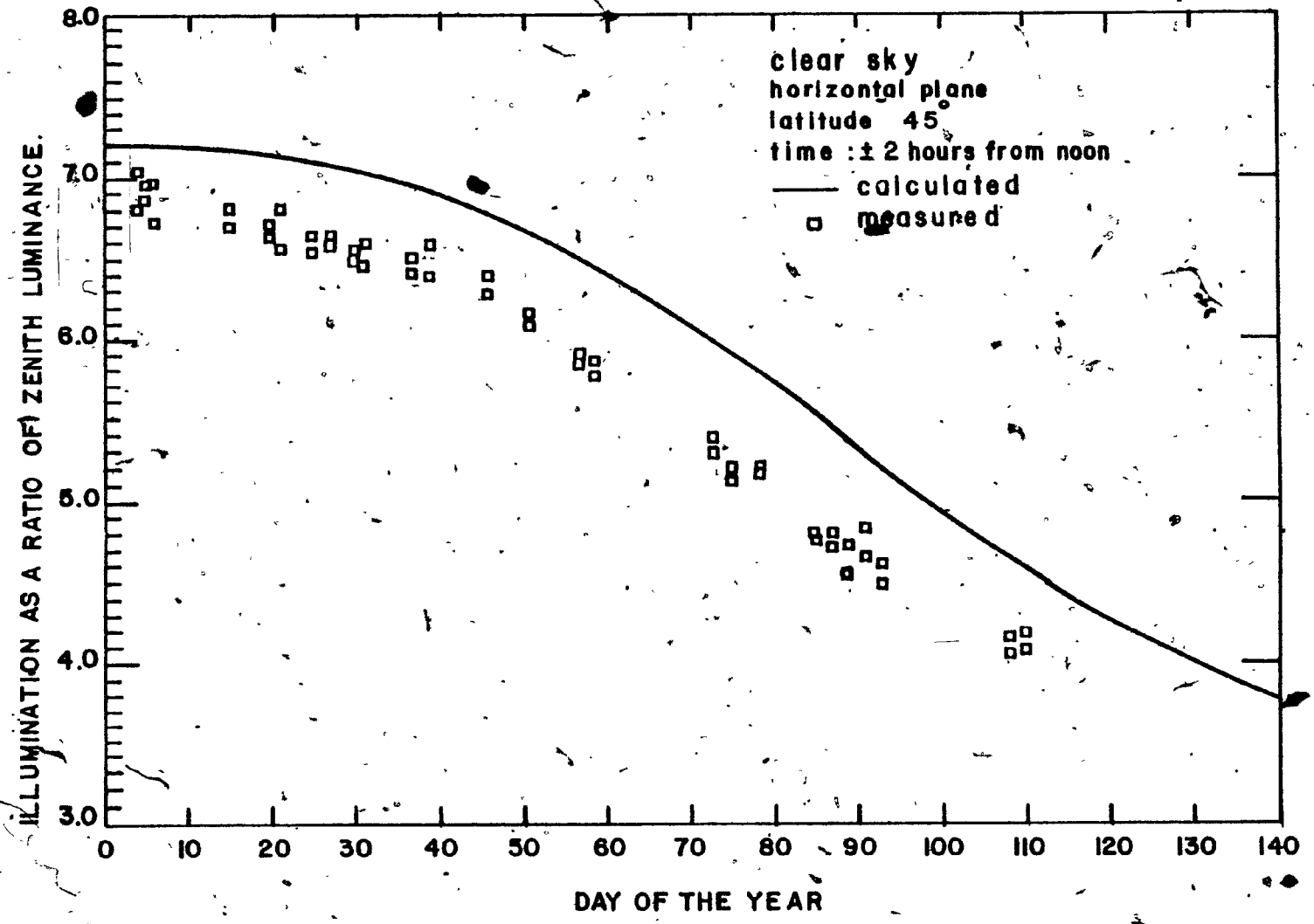

Fig. 3.14 : Comparison between calculated and experimentally determined illumination on a horizontal surface at two hours from noon.

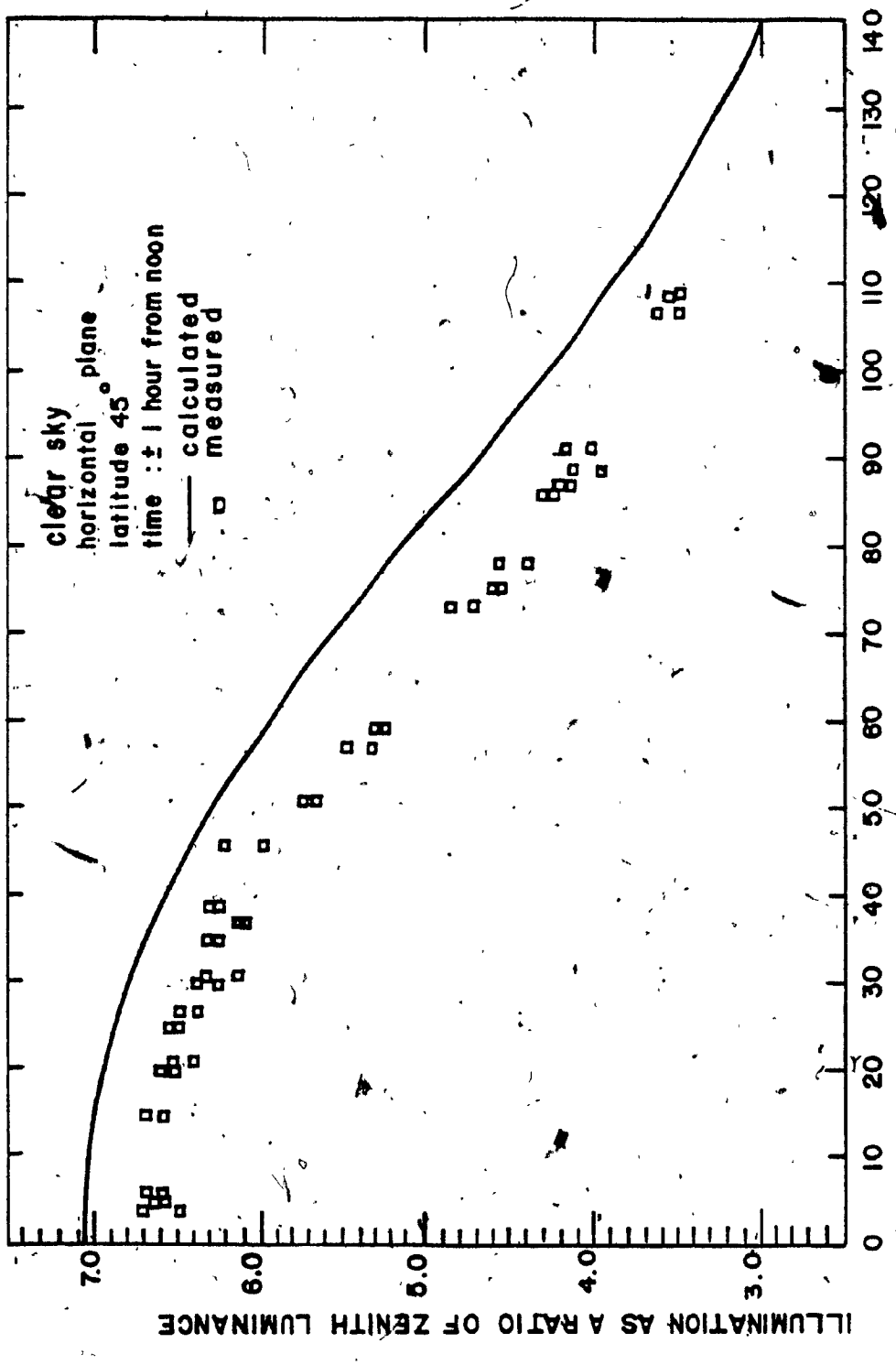

Fig. 3.15 : Comparison between calculated and experimentally determined illumination on a horizontal surface at one hour from noon.

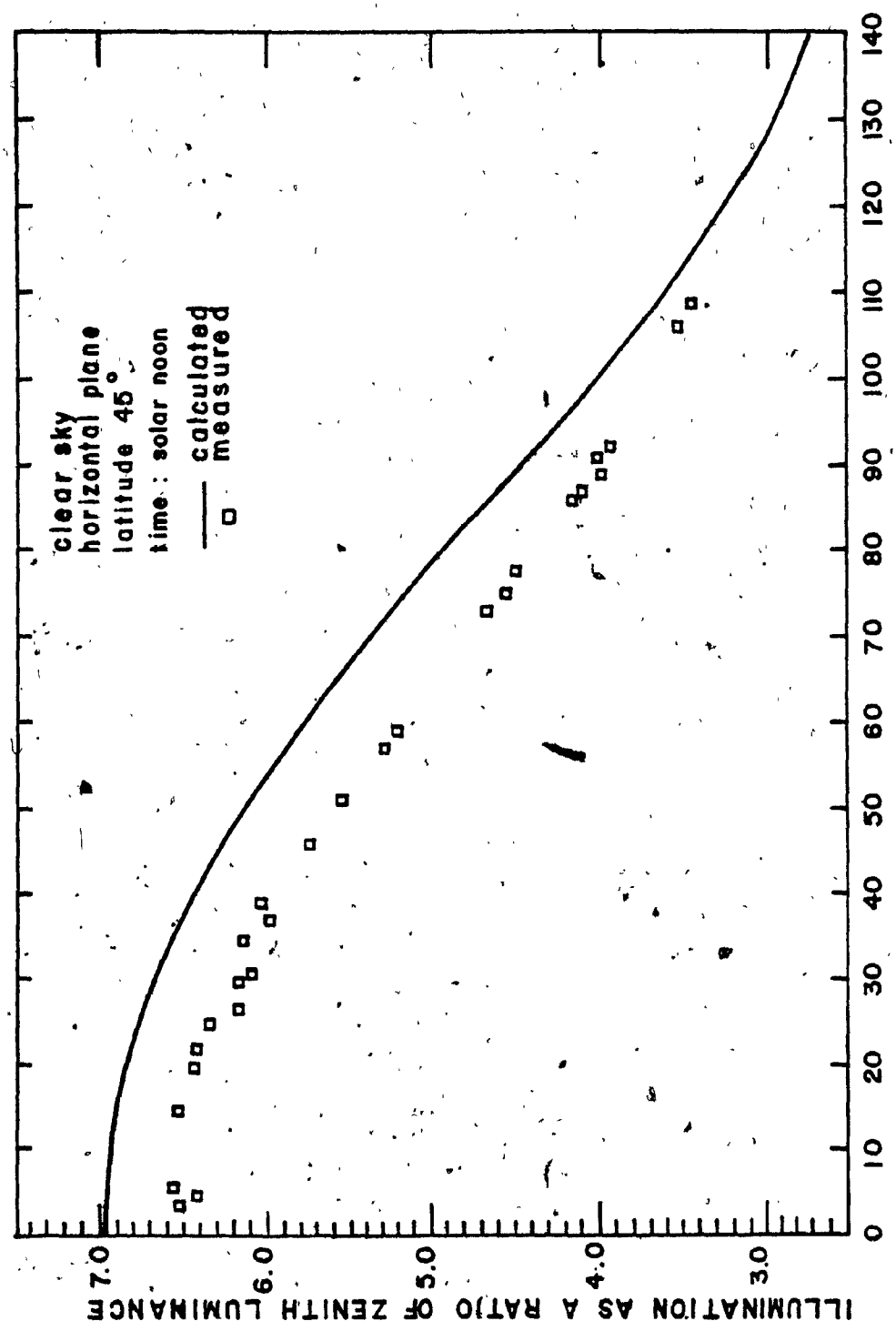

Fig. 3.16 : Comparison between calculated and experimentally determined illumination on a horizontal surface at solar noon.

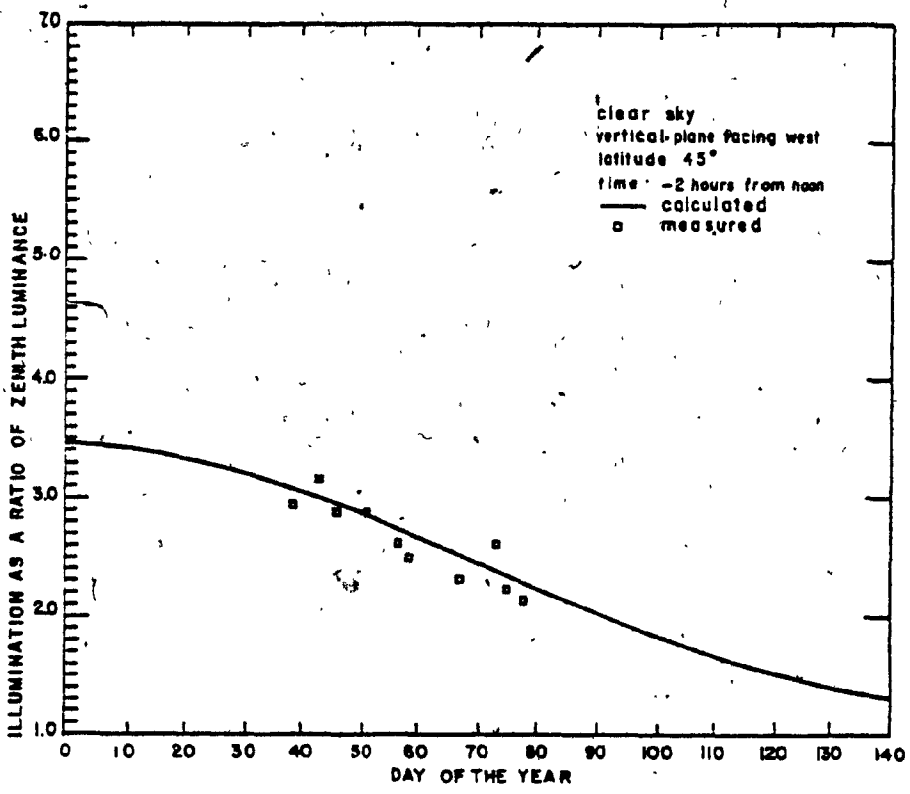

Fig. 3.17 : Comparison between calculated and experimentally determined illumination on a vertical surface facing due west at two hours before noon.

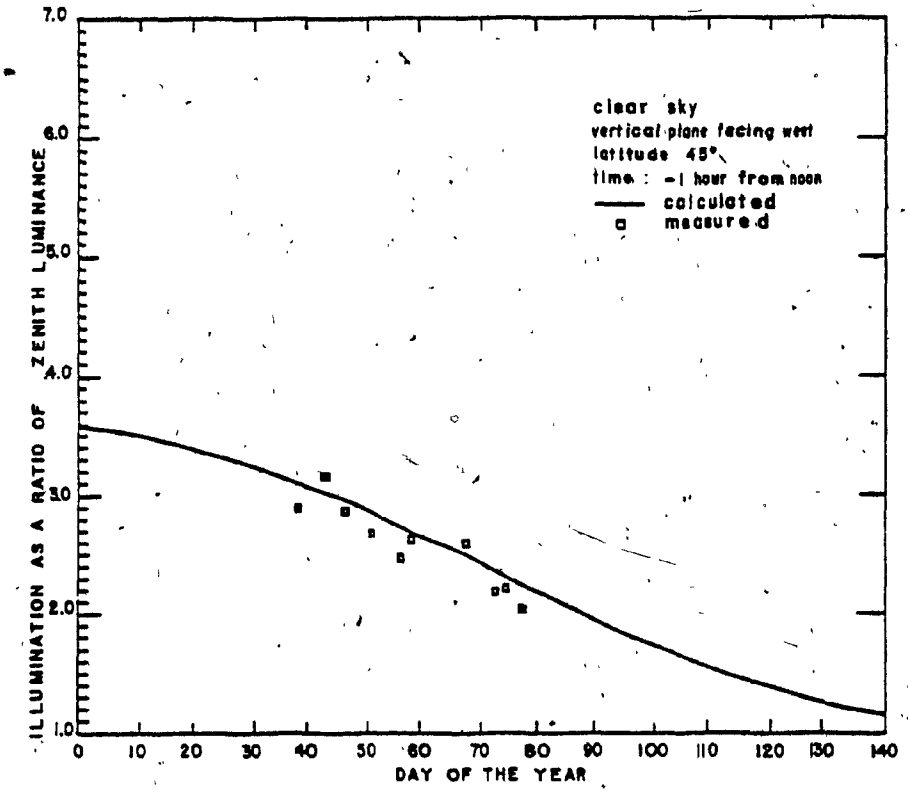

Fig. 3.18 : Comparison between calculated and experimentally determined illumination on a vertical surface facing due west at one hour before noon.

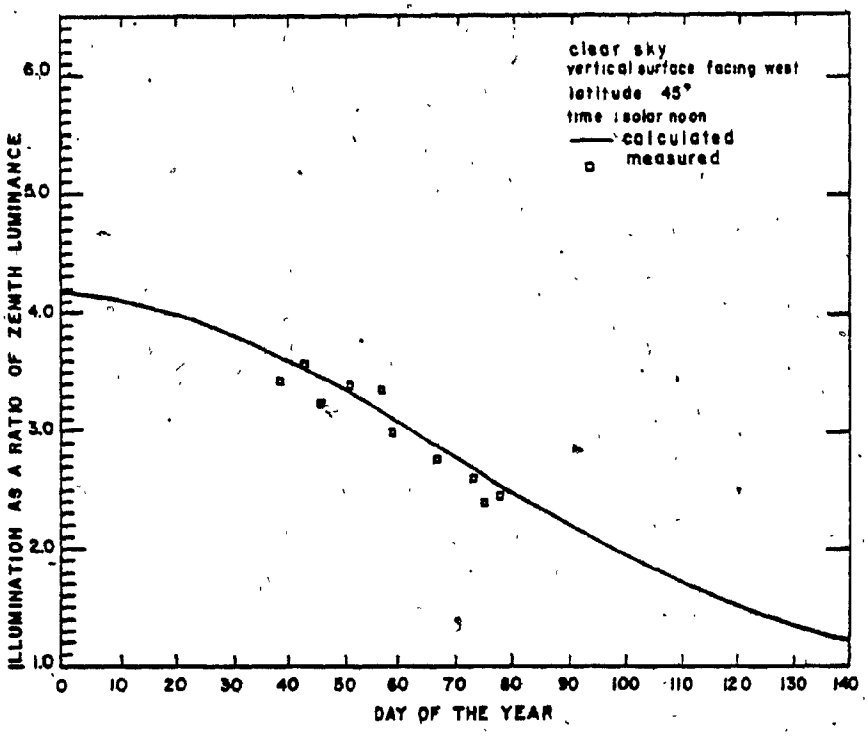

Fig. 3.19 : Comparison between calculated and experimentally determined illumination on a vertical surface facing due west at solar noon.

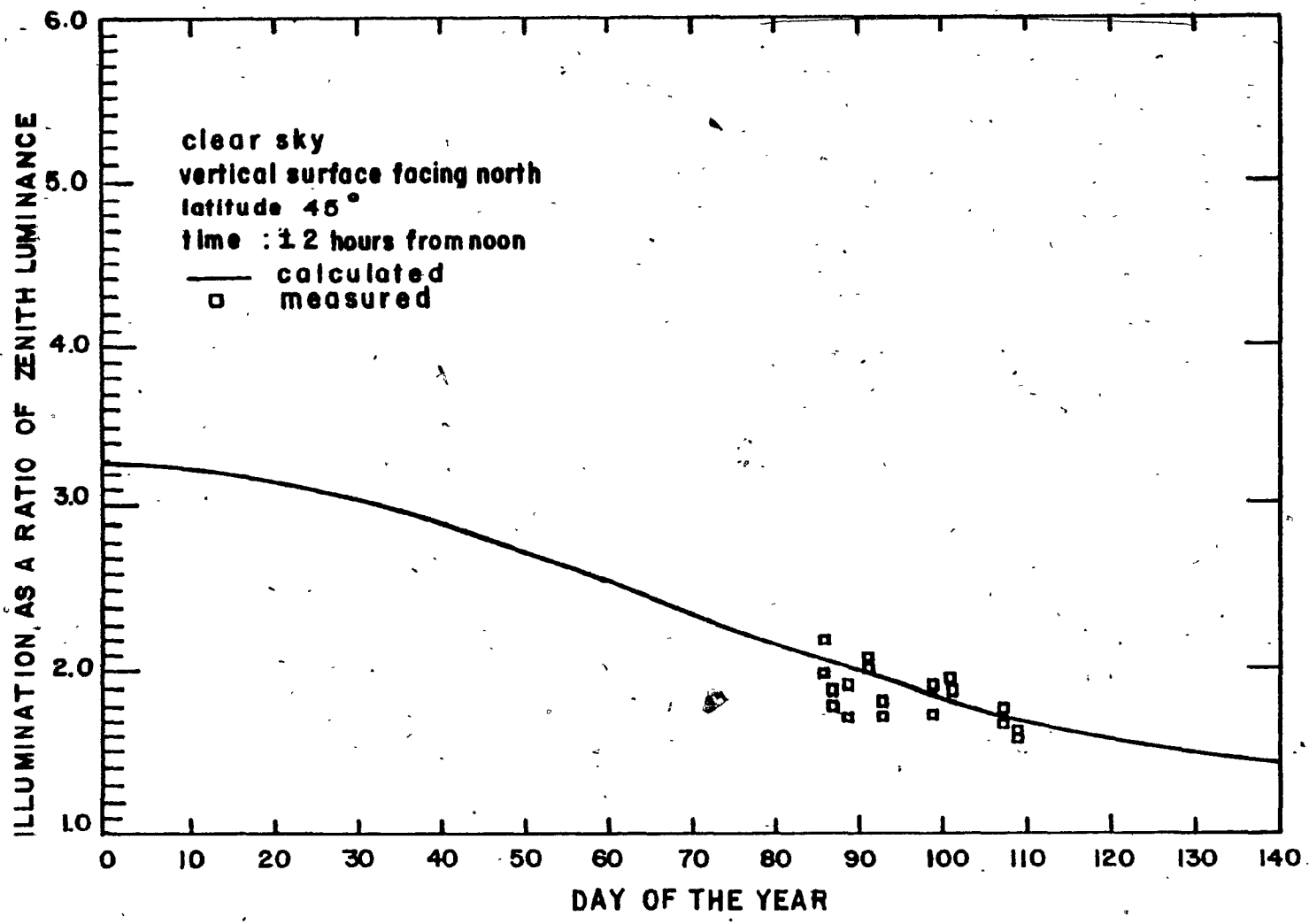

Fig. 3.20 : Comparison between calculated and experimentally determined illumination on a vertical surface facing north at two hours from noon.

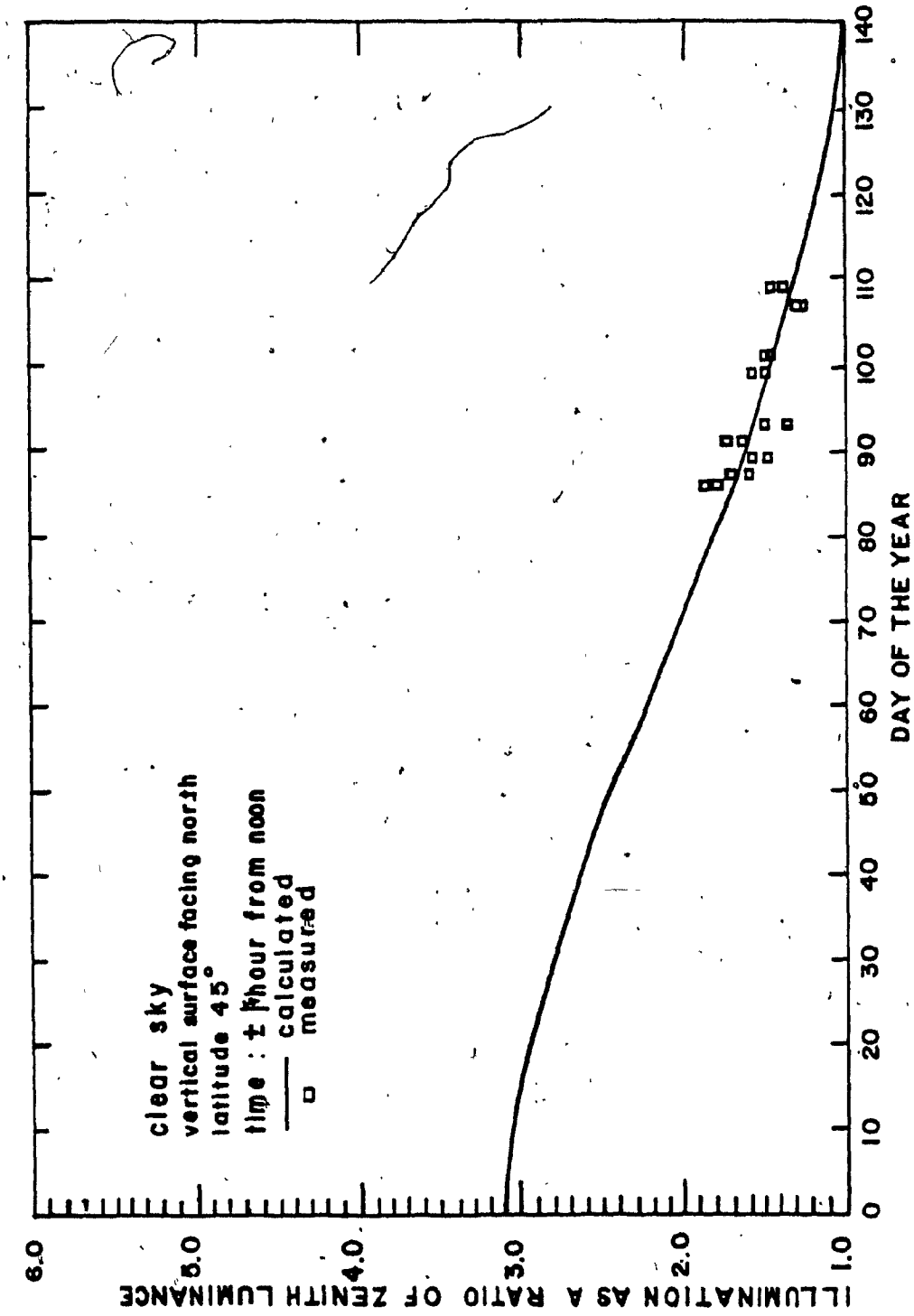

Fig. 3.21 : Comparison between calculated and experimentally determined illumination on a vertical surface facing due north at one hour before noon.

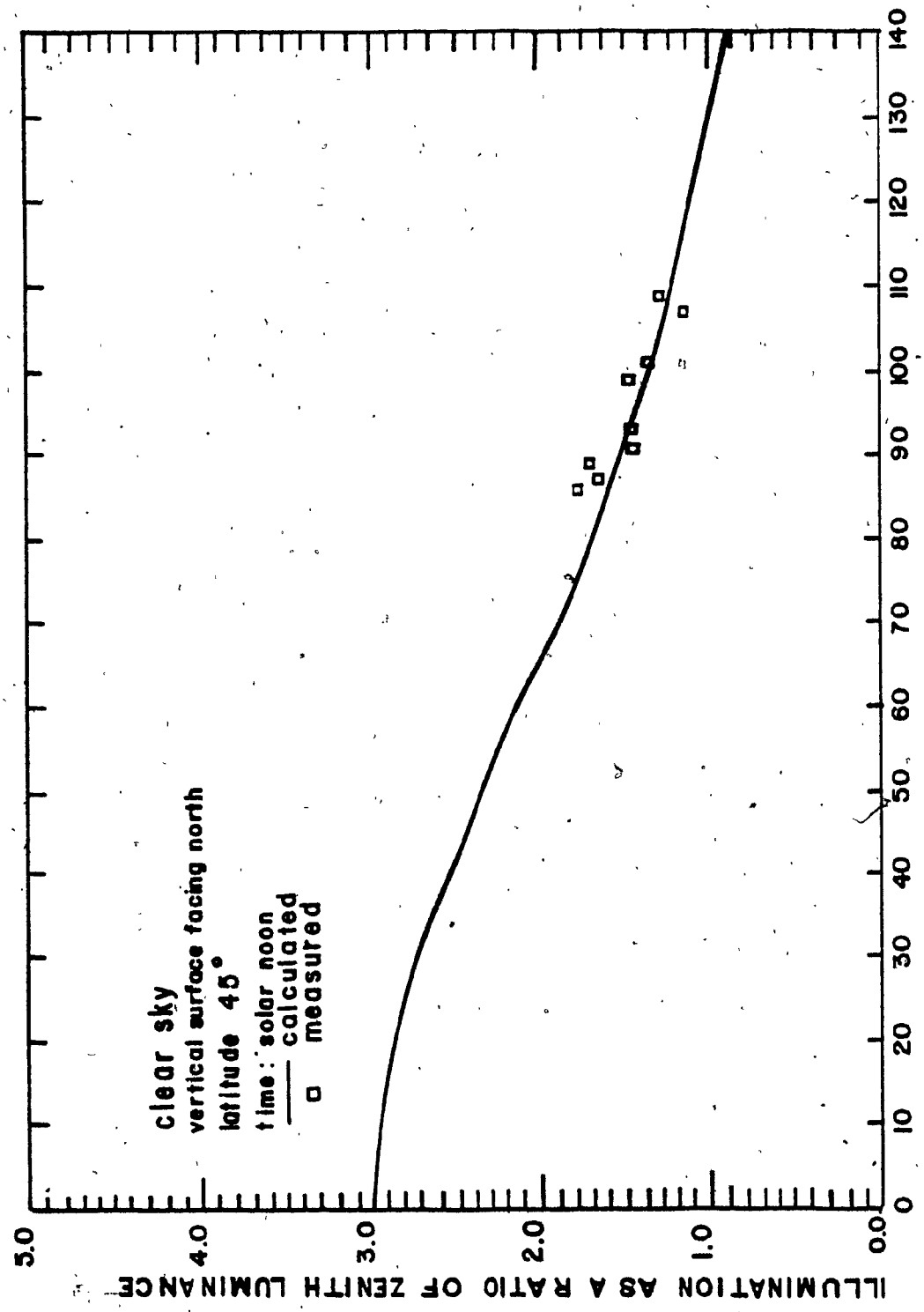

Fig. 3.22 : Comparison between calculated and experimentally determined illumination on a vertical surface facing due north at solar noon.

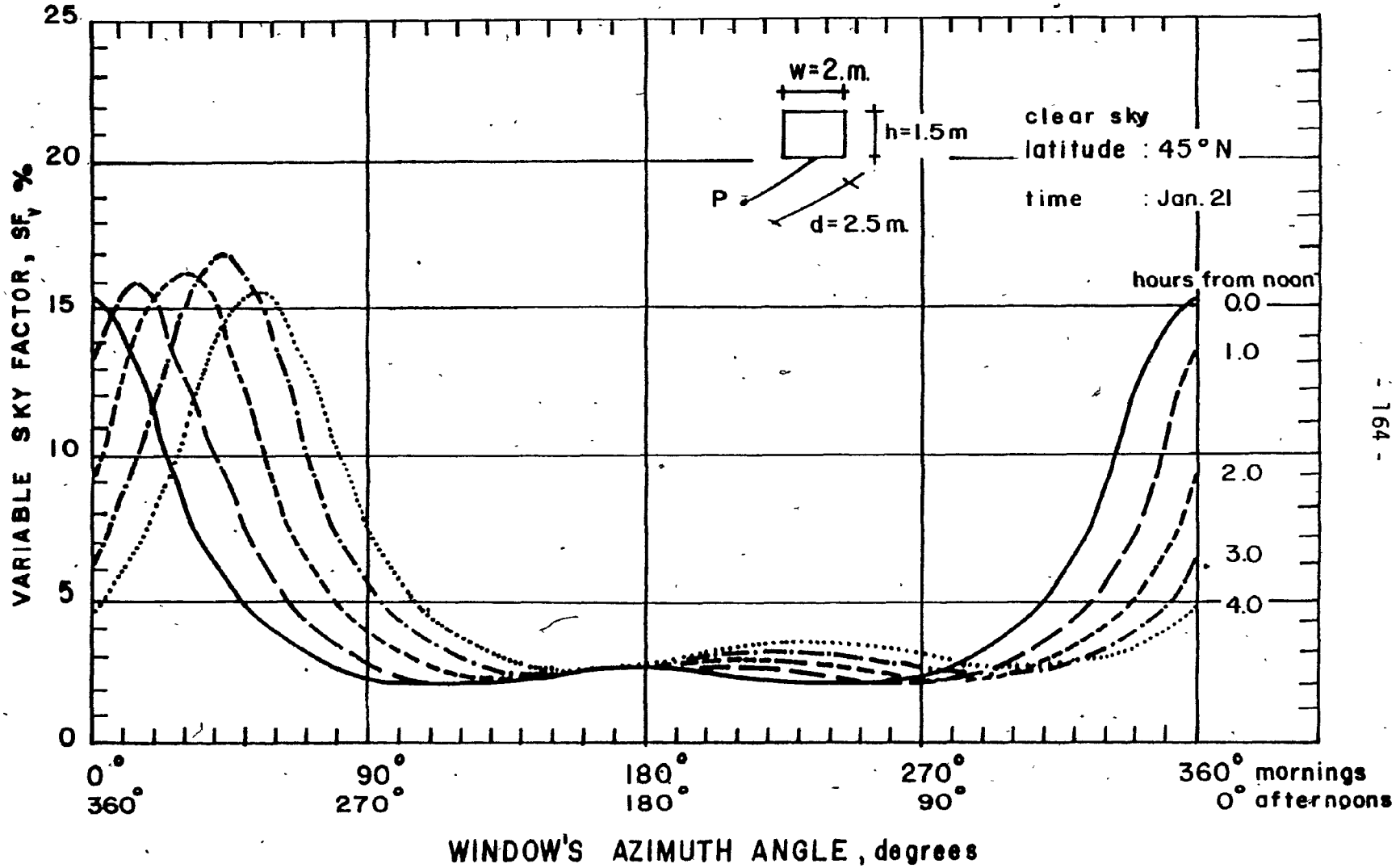

Fig. 3.23 : Variation of the variable sky factor with window azimuth angle at different times of day.

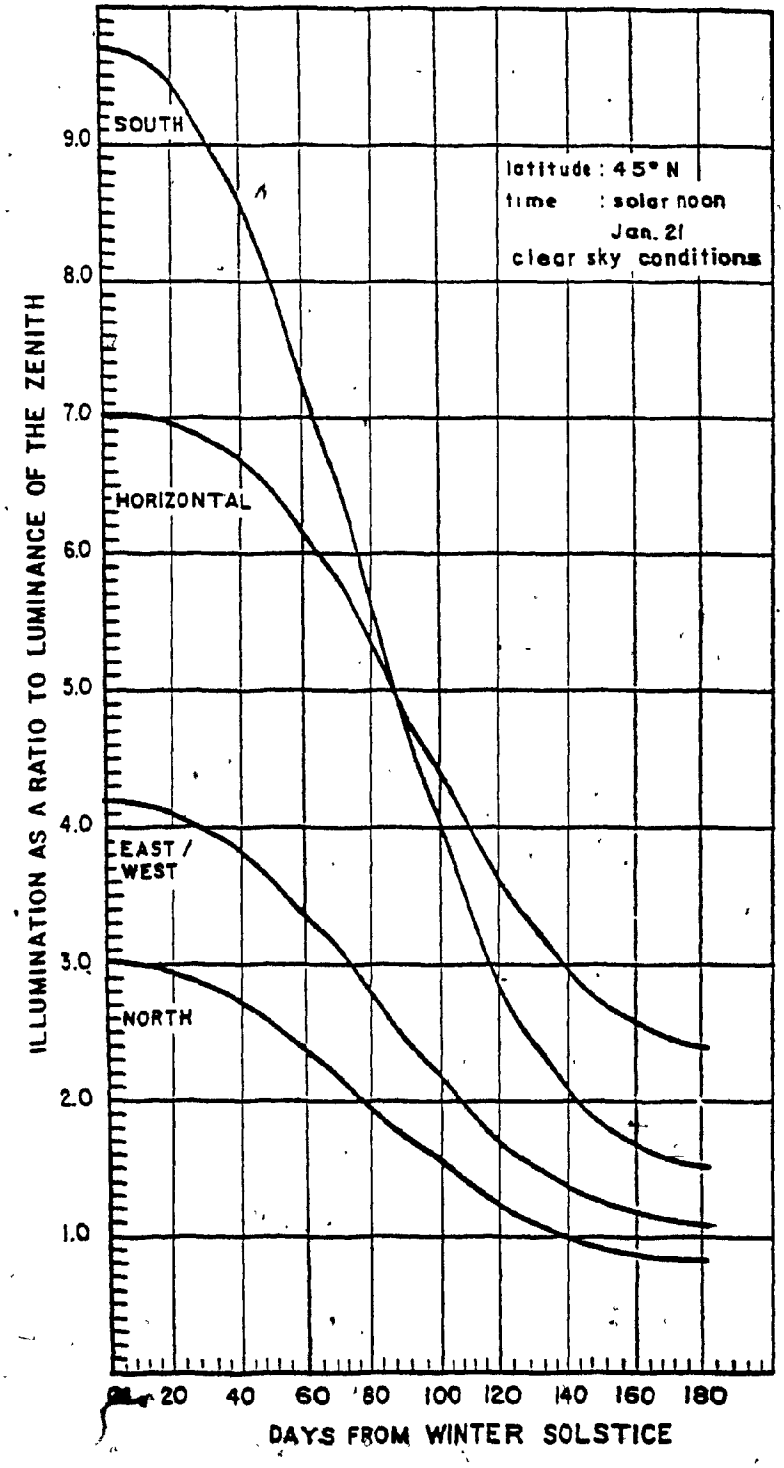

Fig. 3.24 : Variation of the illumination on horizontal and vertical surfaces with the time of year.

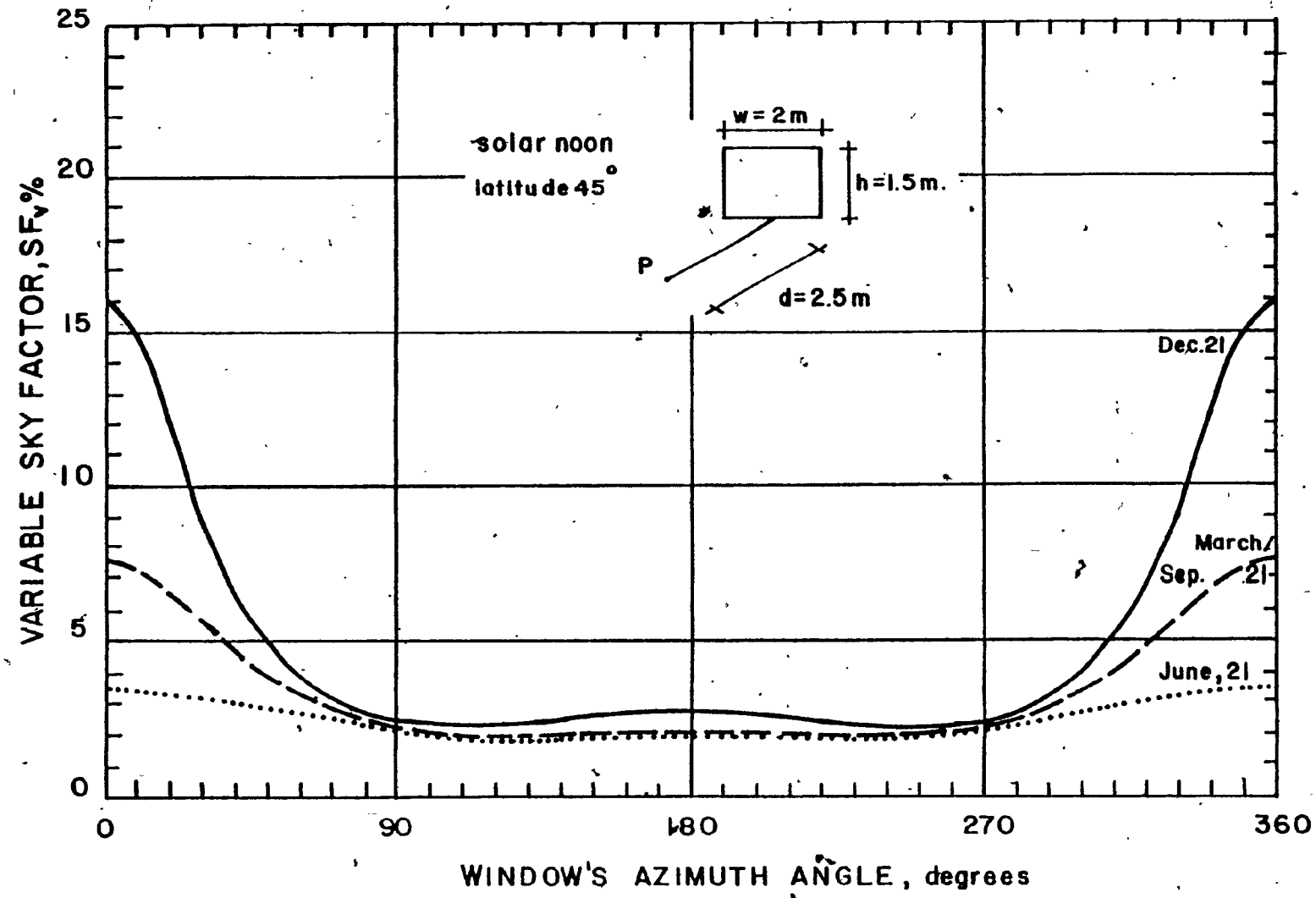

Fig. 3.25 The effect of window azimuth angle on the variable sky factor at the beginning of each season.

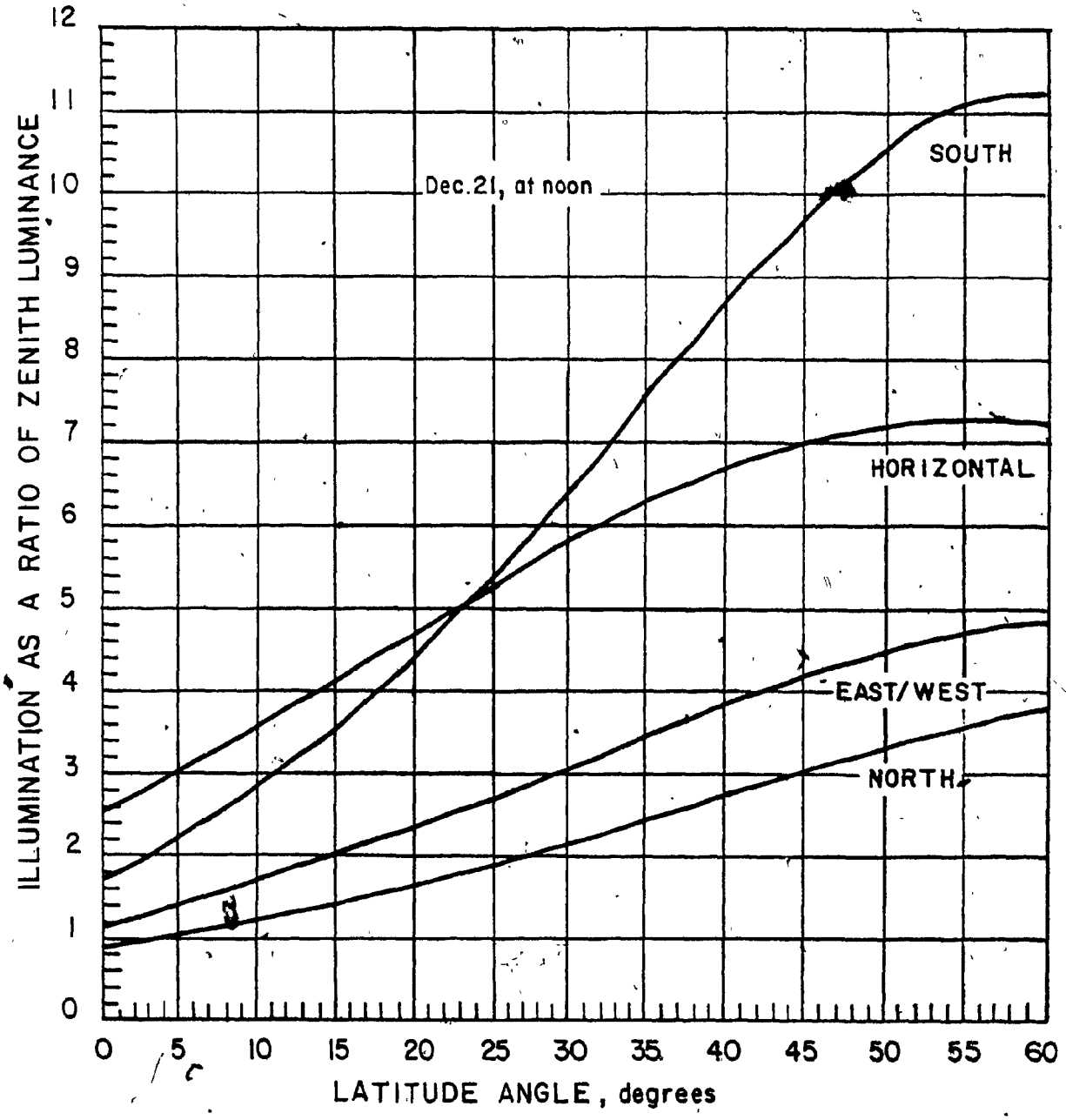

Fig. 3.26 Variation of illumination on horizontal and vertical surfaces with the latitude angle at the beginning of the winter season.

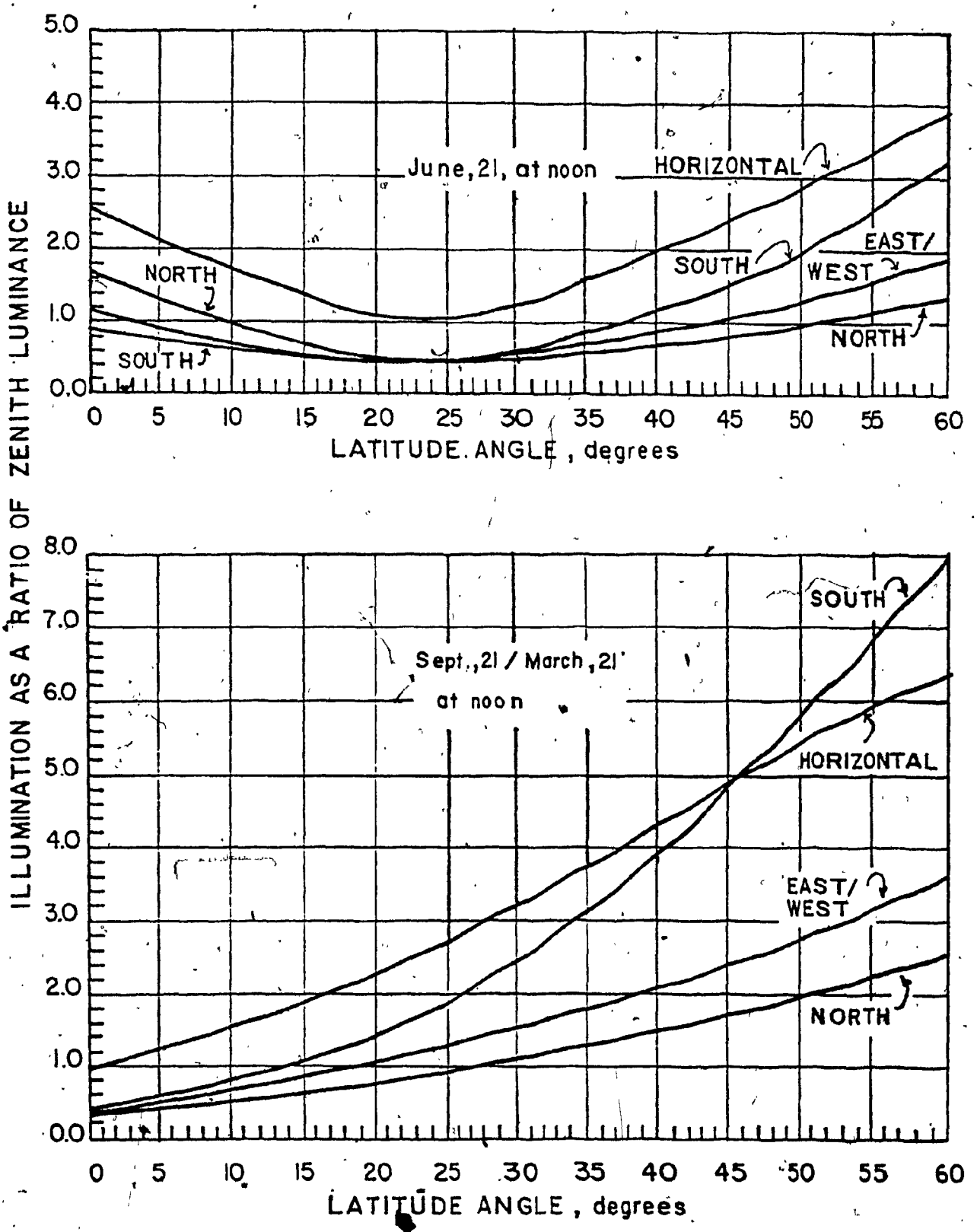

Fig. 3.27 Variation of illumination on horizontal and vertical surfaces with the latitude angle at the beginning of a) summer and b) spring and fall.

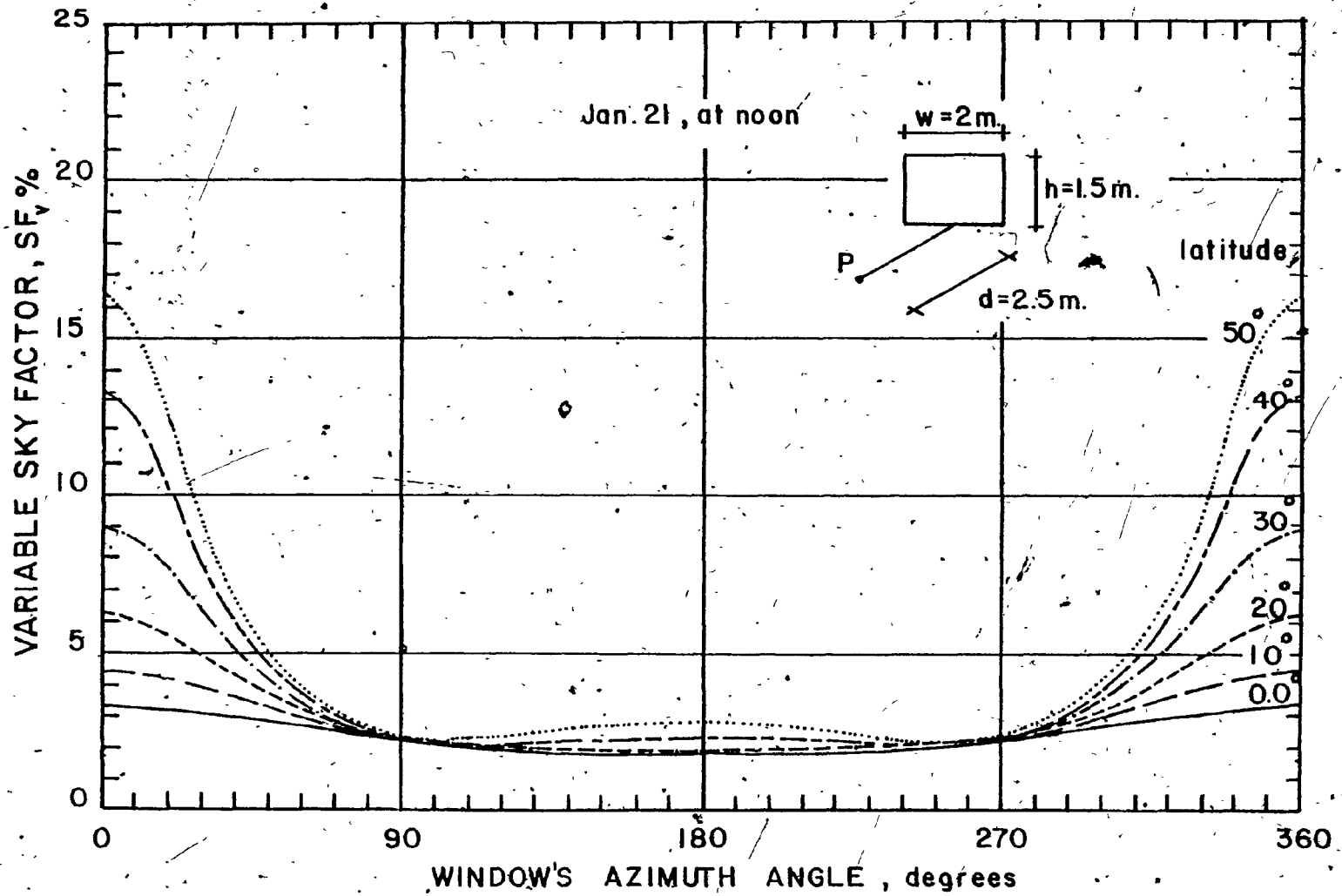

Fig. 3.28 The effect of the latitude angle on the variable sky factor on January 31 at solar noon. (clear sky).

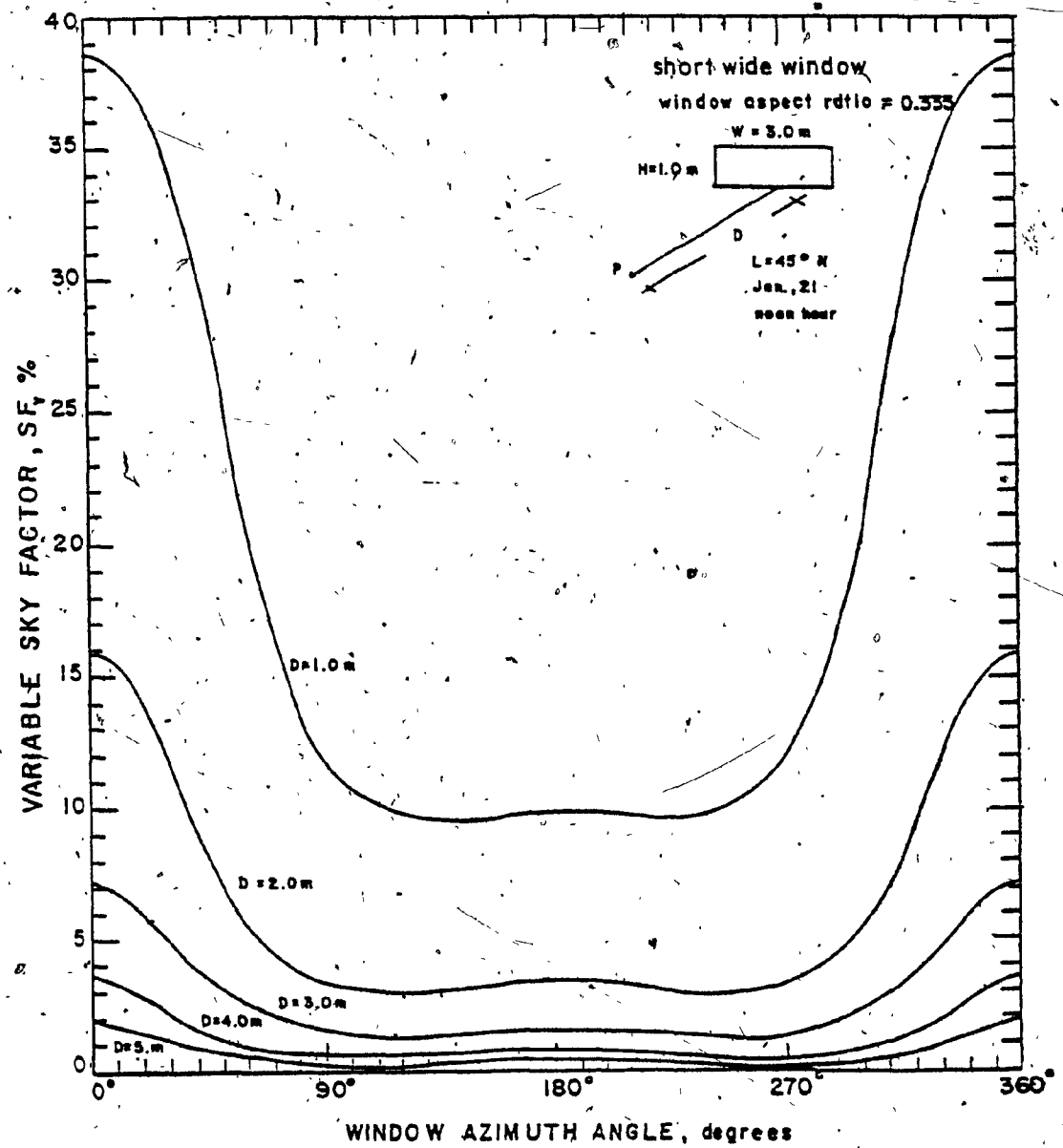

Fig. 3.29 The effect of window azimuth angle on the variable sky factor for a short wide window (aspect ratio 0.333).

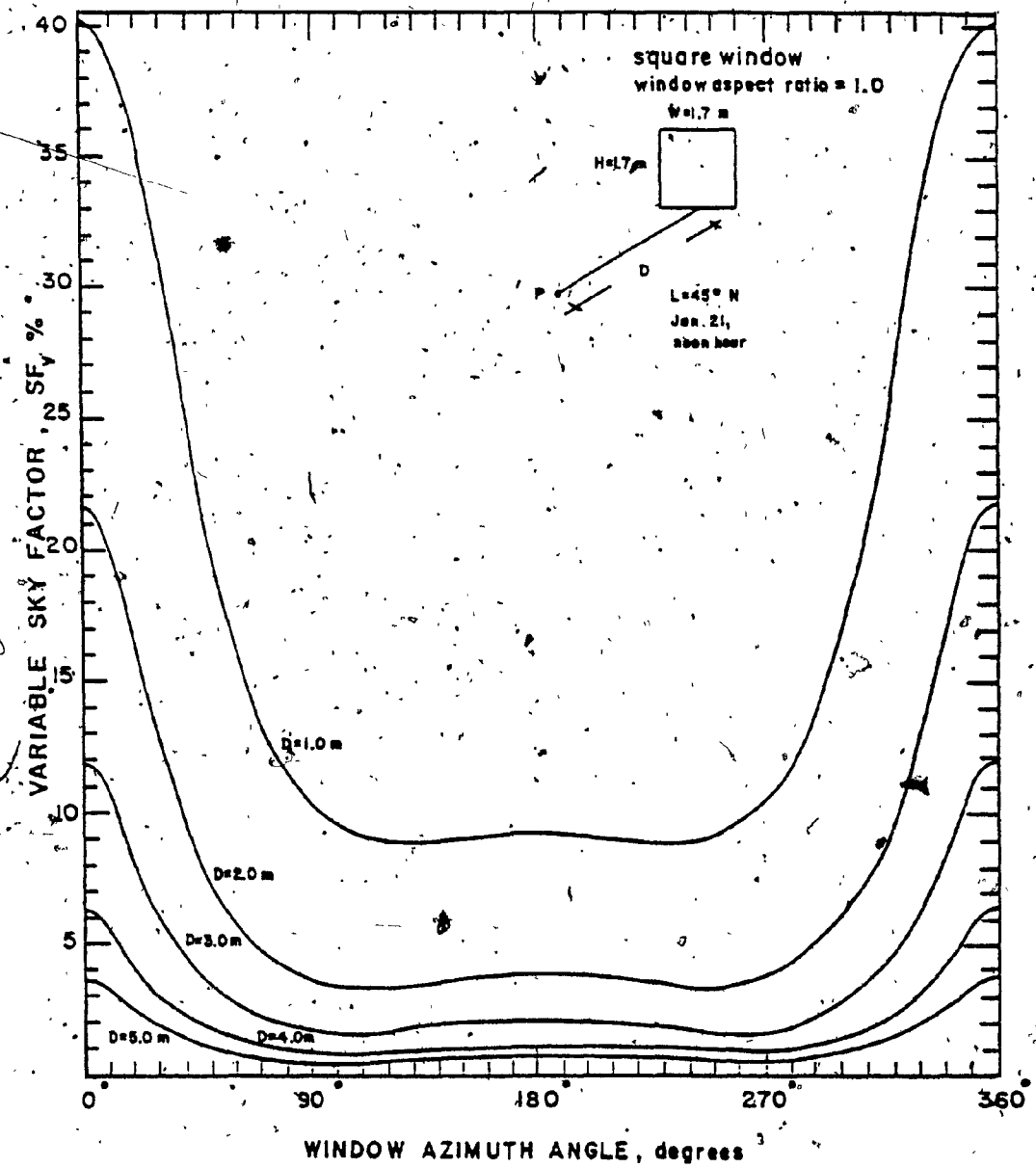

Fig. 3.30 The effect of window azimuth angle on the variable sky factor of a square window (aspect ratio 1.00).

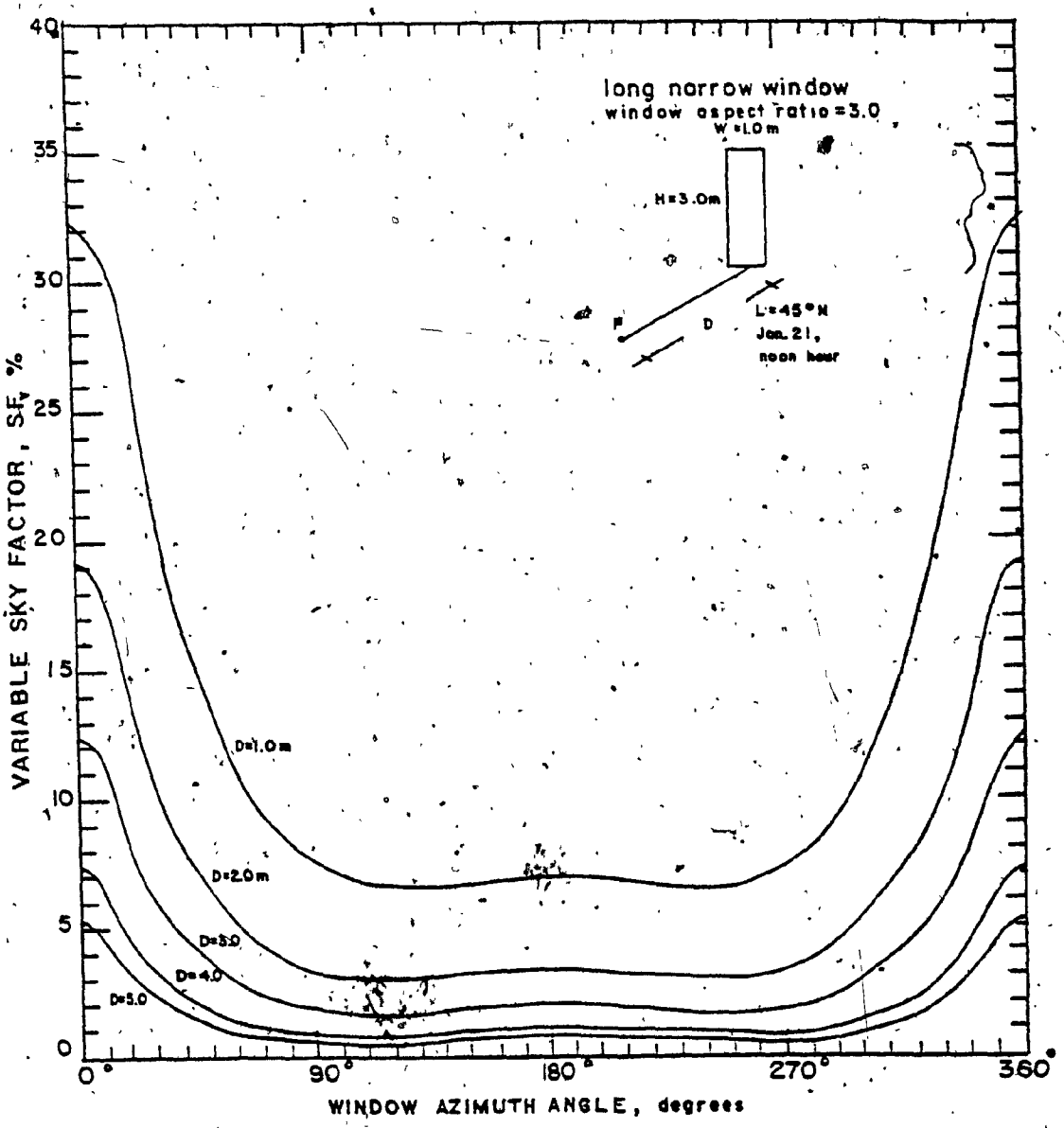

Fig. 3.31 The effect of window azimuth angle on the variable sky factor of a tall narrow window (aspect ratio 3.0).

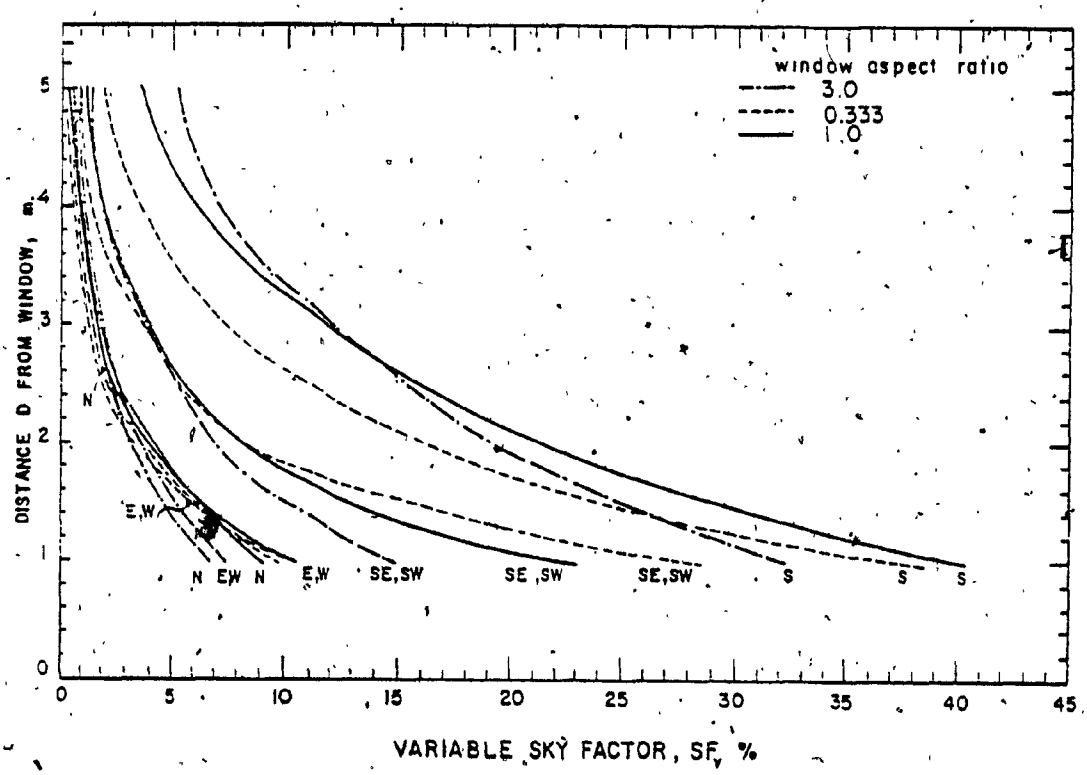

Fig. 3.32 The effect of the distance between the reference point and the window on the variable sky factor for window aspect ratio of .333, 1.0 and 3.0.

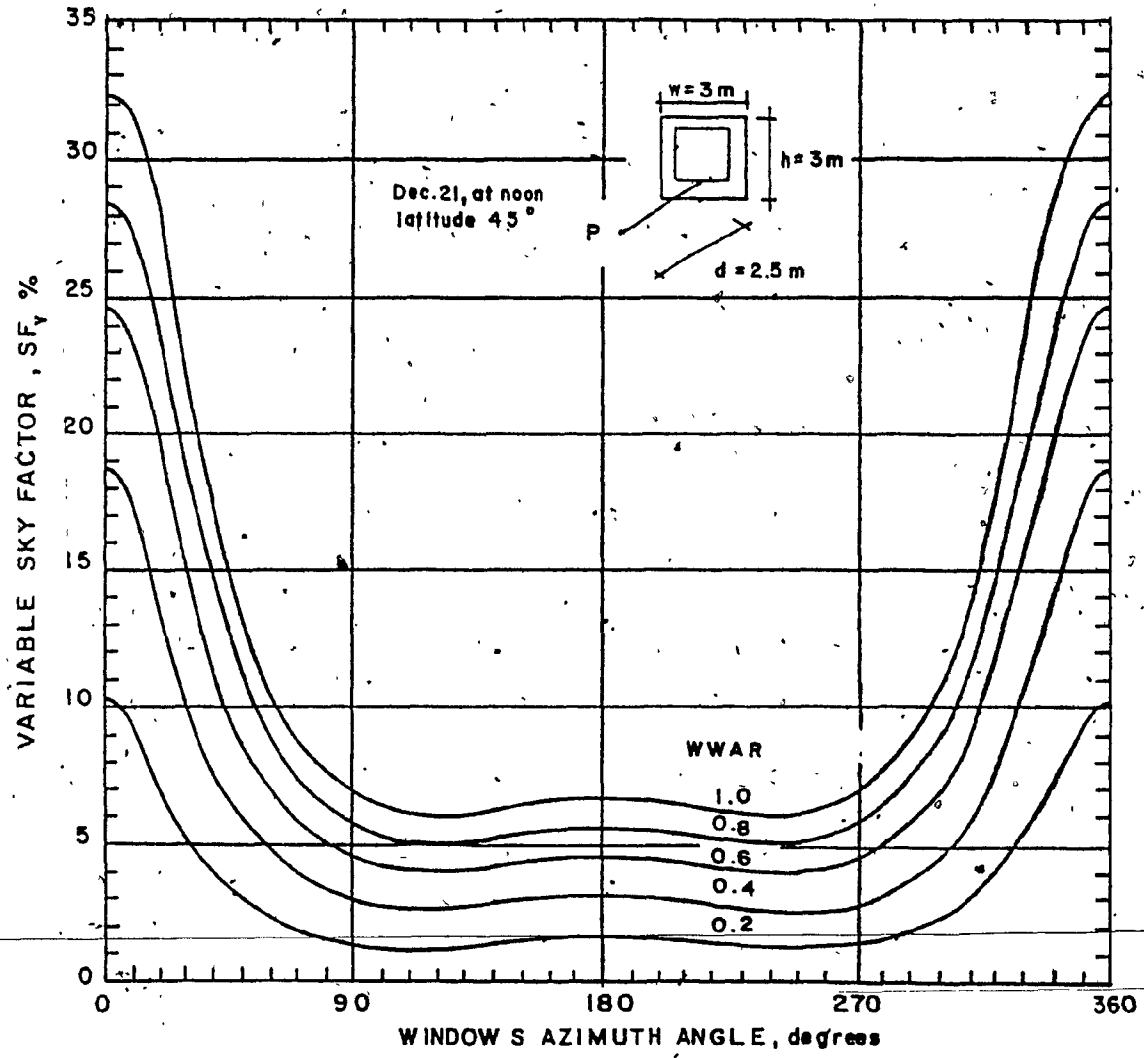

Fig. 3.33 The effect of window azimuth angle on the variable sky factor for different window-to-wall area ratios at noon on December 21.

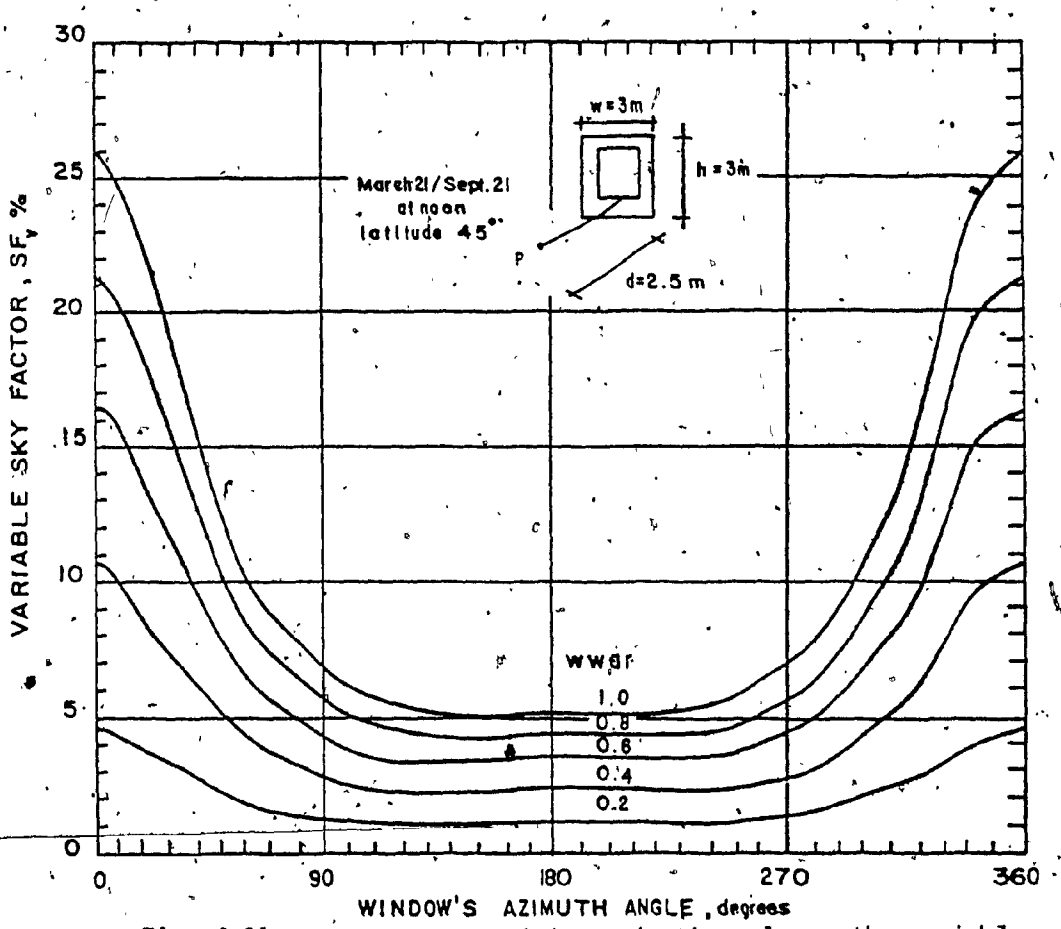

Fig. 3.34 The effect of window azimuth angle on the variable sky factor for different window-to-wall area ratios on March 21 and September 21.

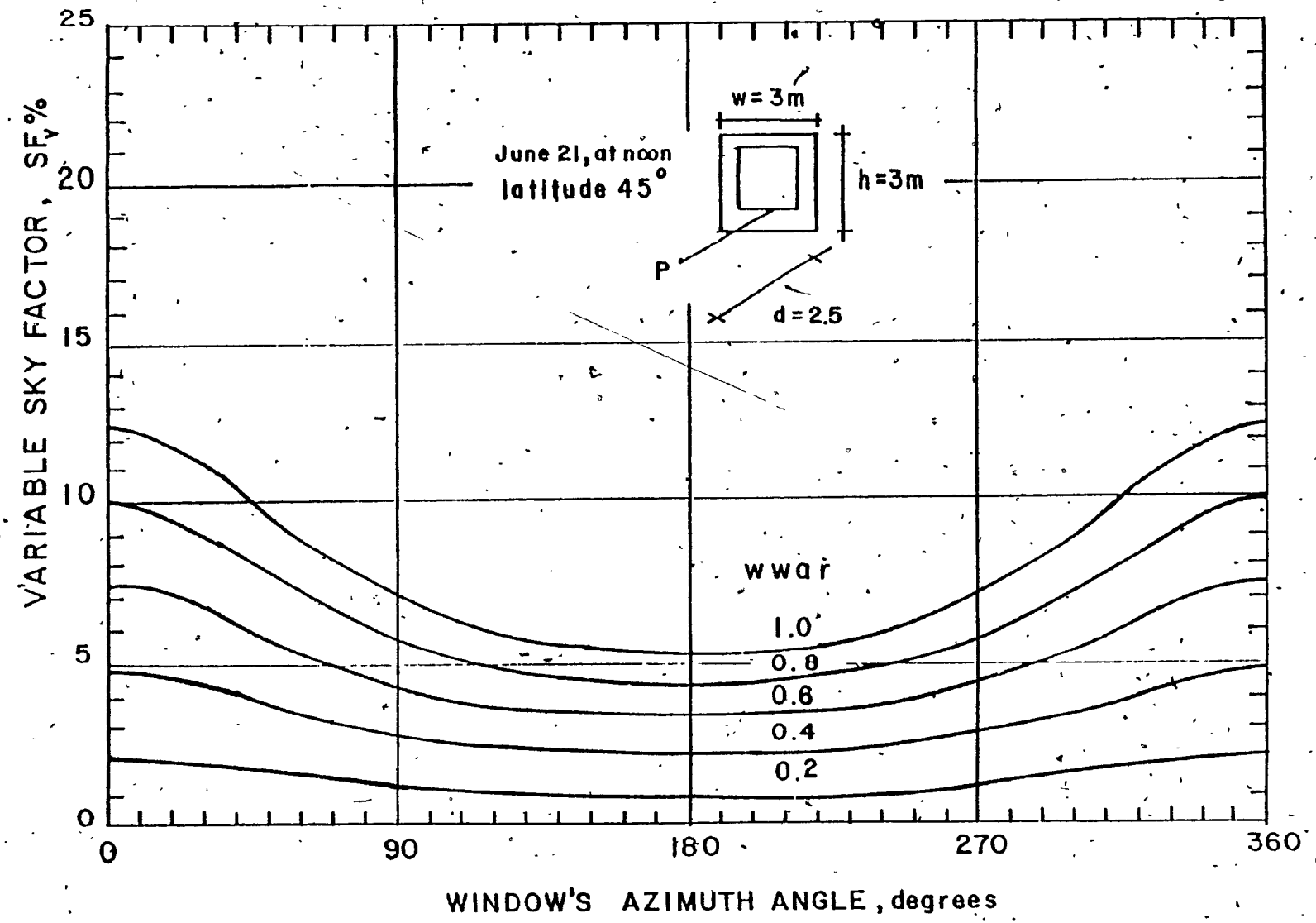

Fig. 3.35 The effect of window azimuth angle on the variable sky factor for different window-to-wall area ratios on June 21.

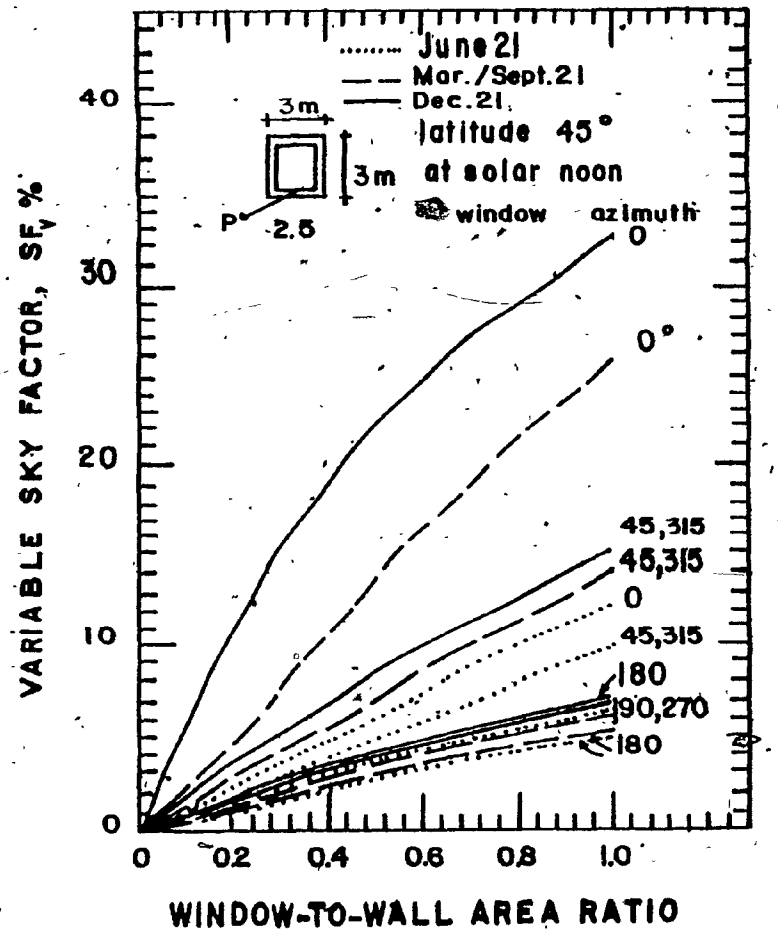

Fig. 3.36 The effect of window-to-wall area ratio on the variable sky factor at the beginning of each season for the eight main compass orientations.

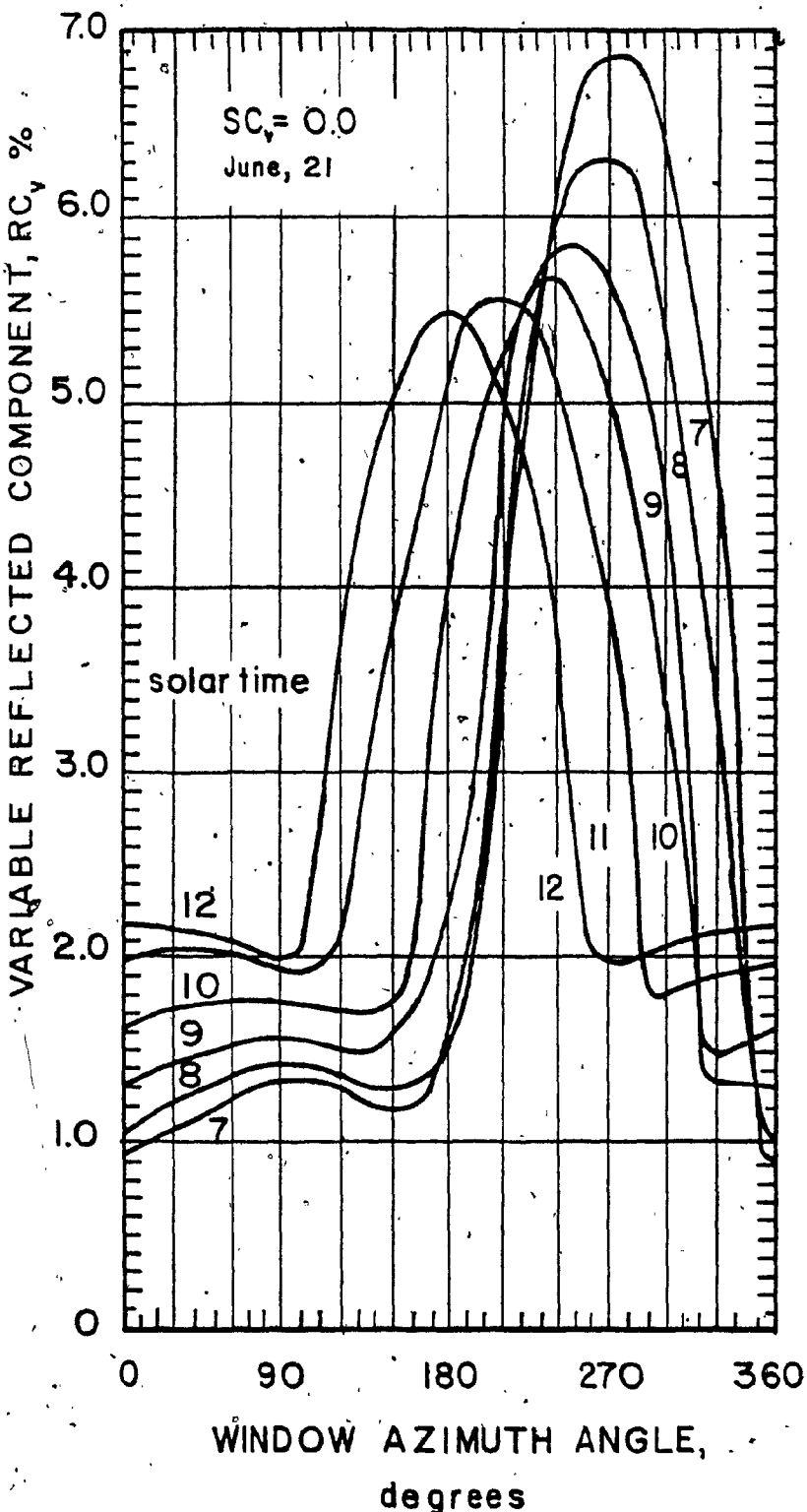

Fig. 3.37 Hourly variation of the variable reflected component RC_v, with window azimuth angle during the morning hours on June 21.

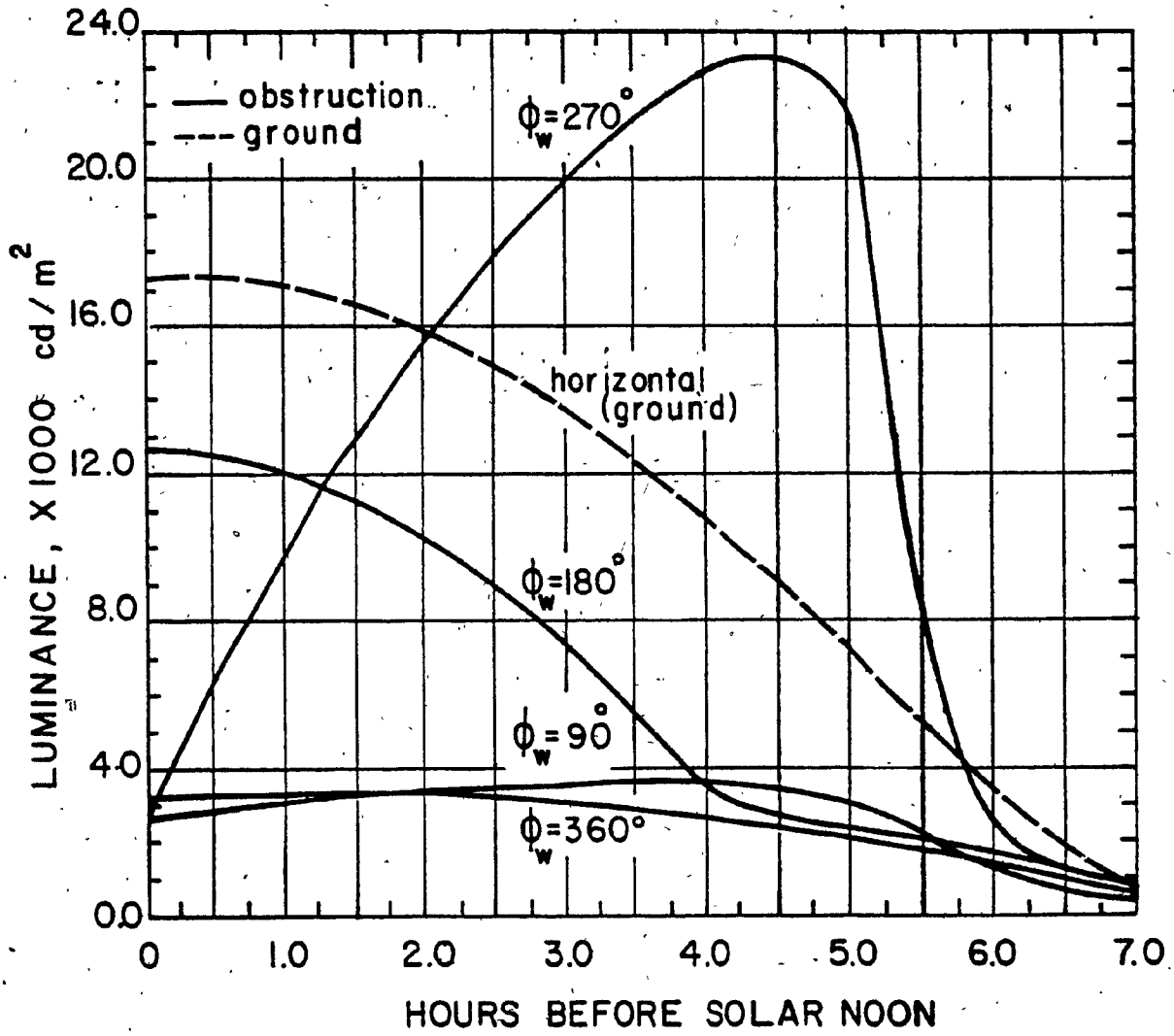

Fig. 3.38 Hourly variation of the luminance of the ground and obstruction surface for windows of azimuth angles equal to 90°, 180°, 270°, and 360°.

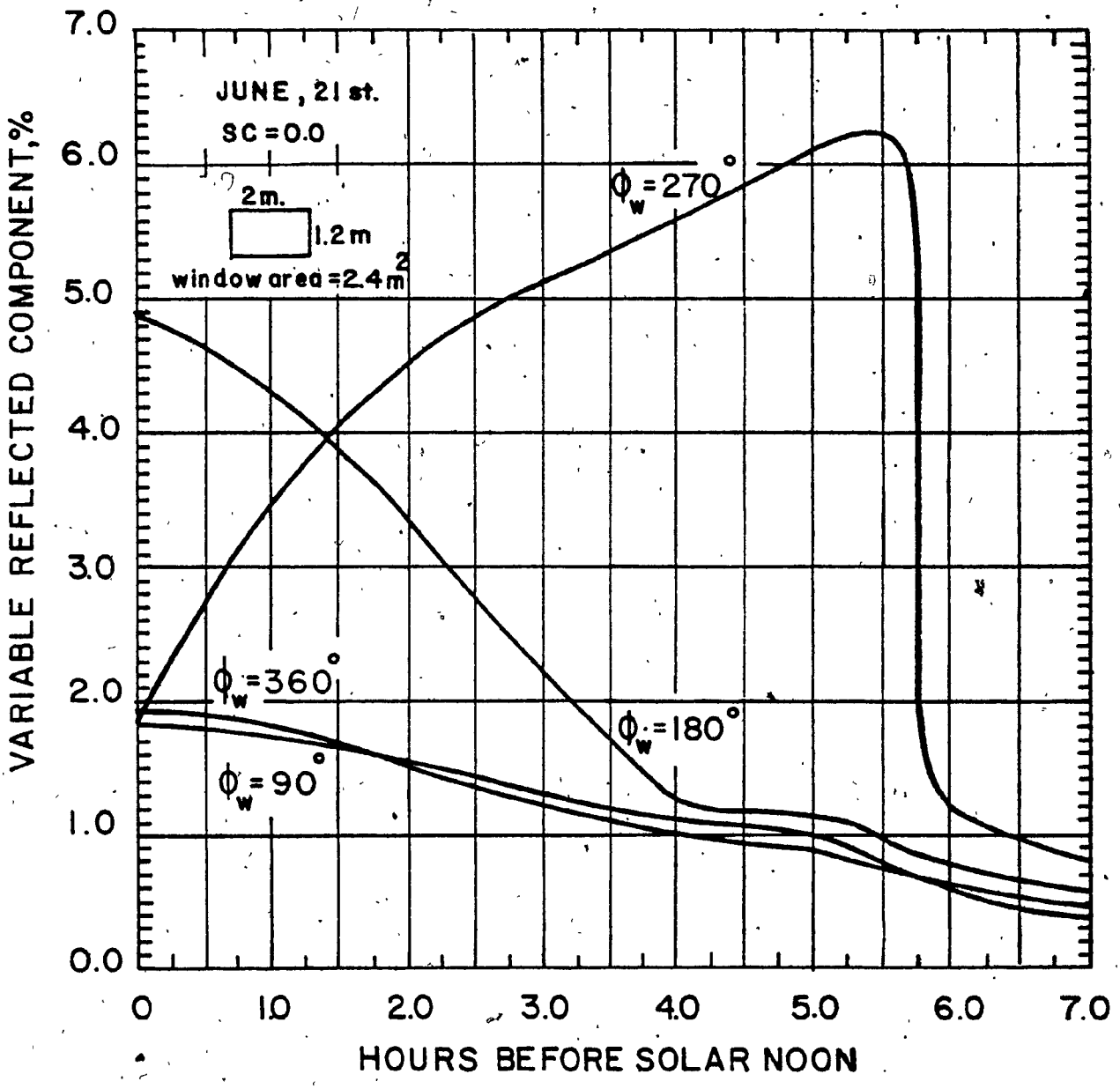

Fig. 3.39 Hourly variation of the variable reflected component for windows azimuth angles 90^{o}, 180^{o}, 270^{o}, and 360^{o}.

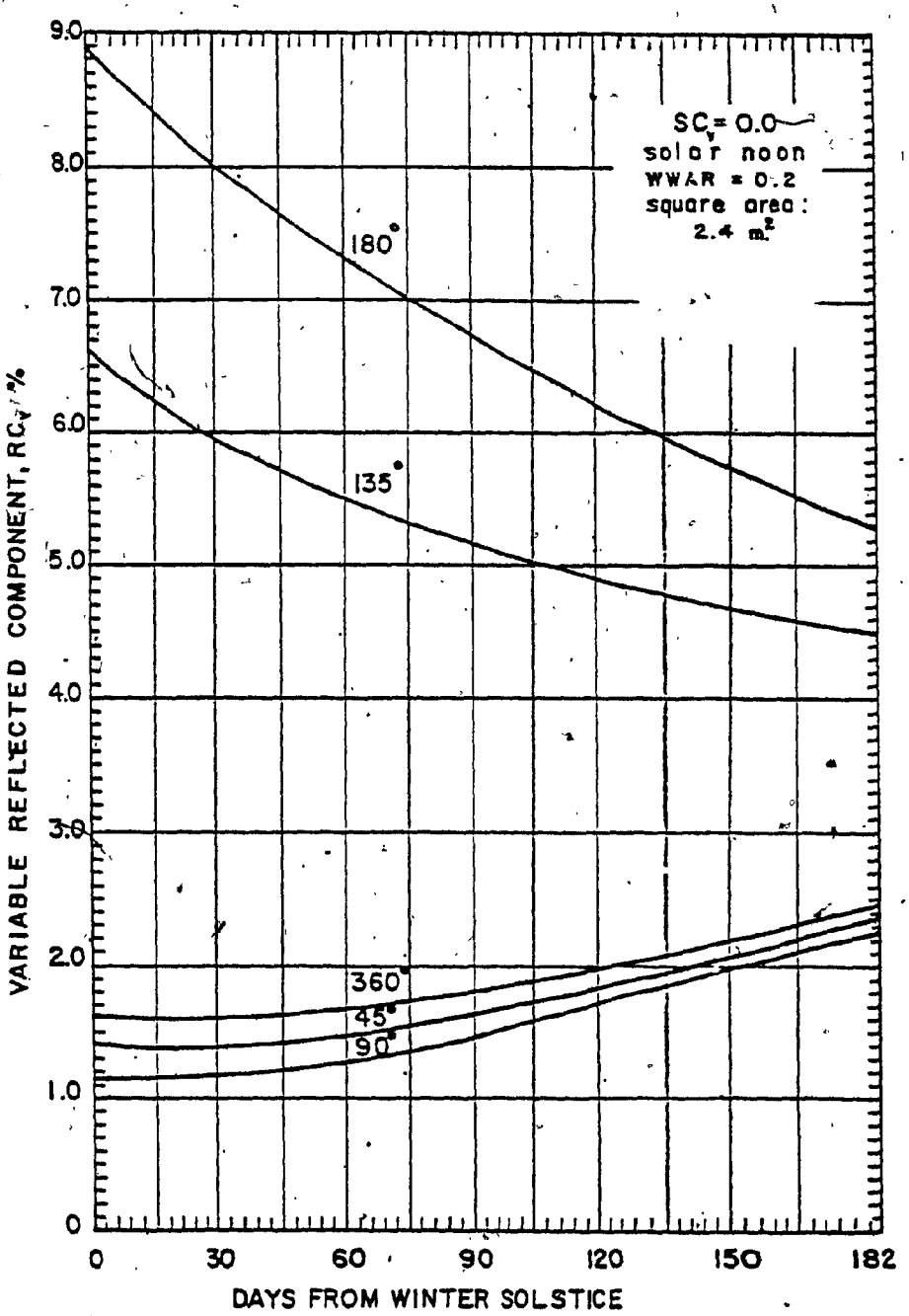

Fig. 3.40 Variation of the noon variable reflected component, with time of year.

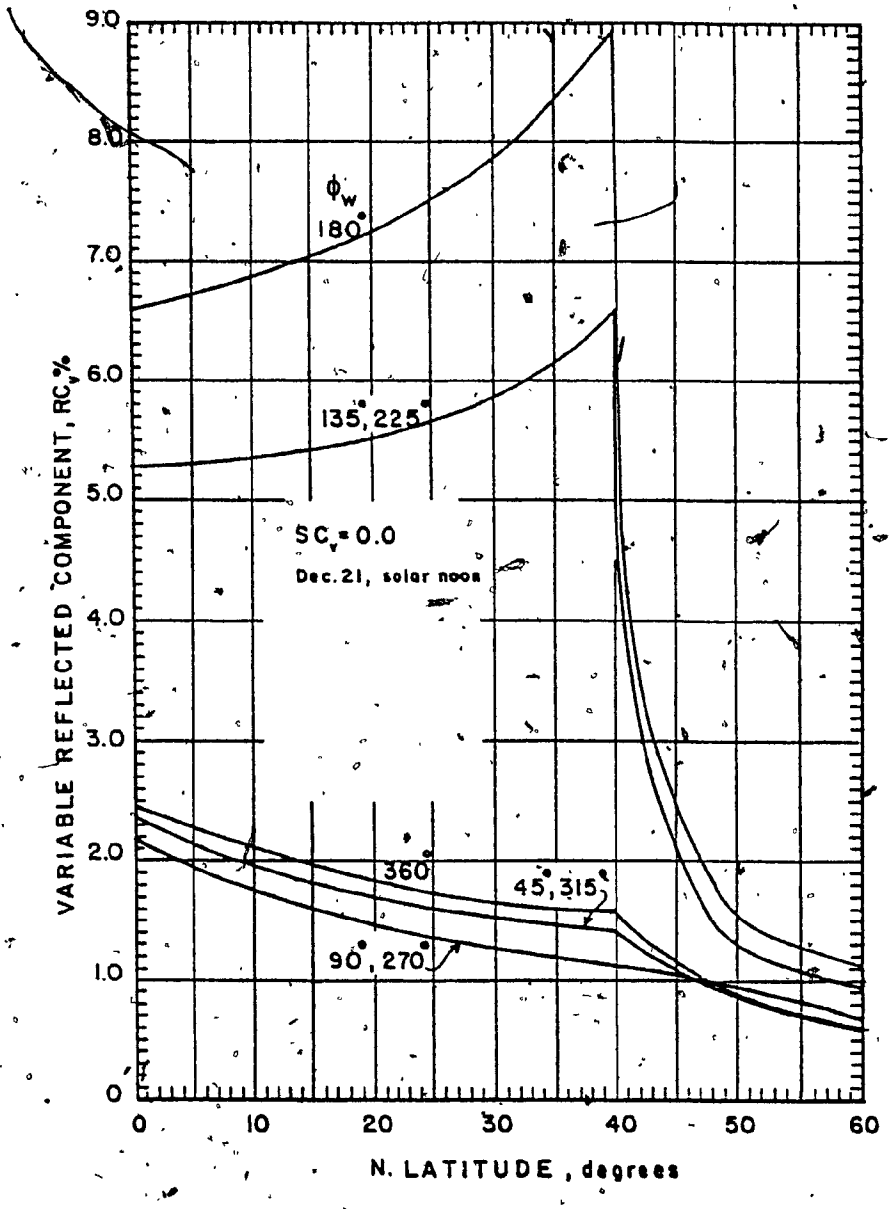

Fig. 3.41 Variation of the variable reflected component with the latitude angle at solar noon on Dec. 21.

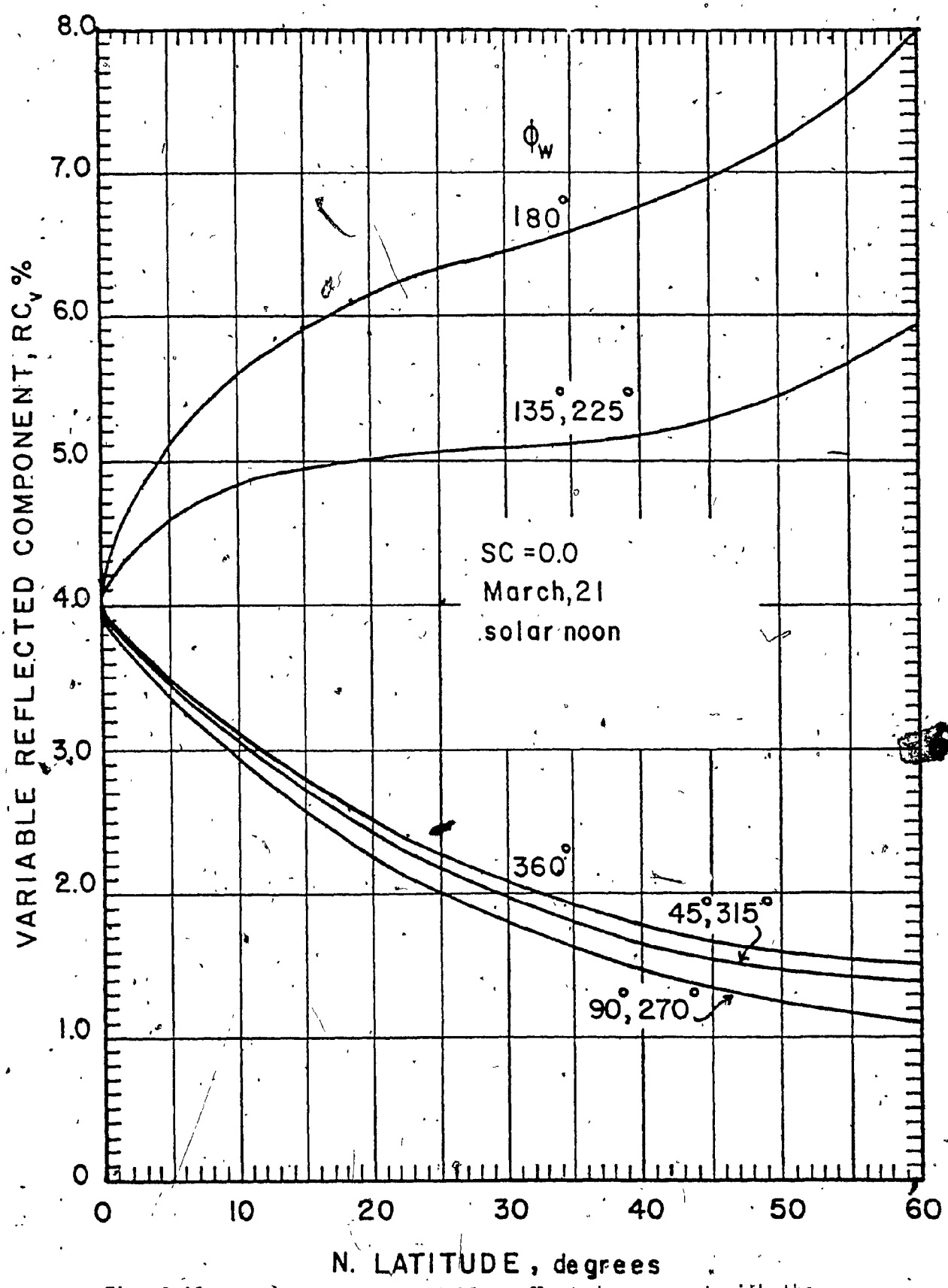

Fig. 3.42 Variation of the variable reflected component with the latitude angle at solar noon on March 21.

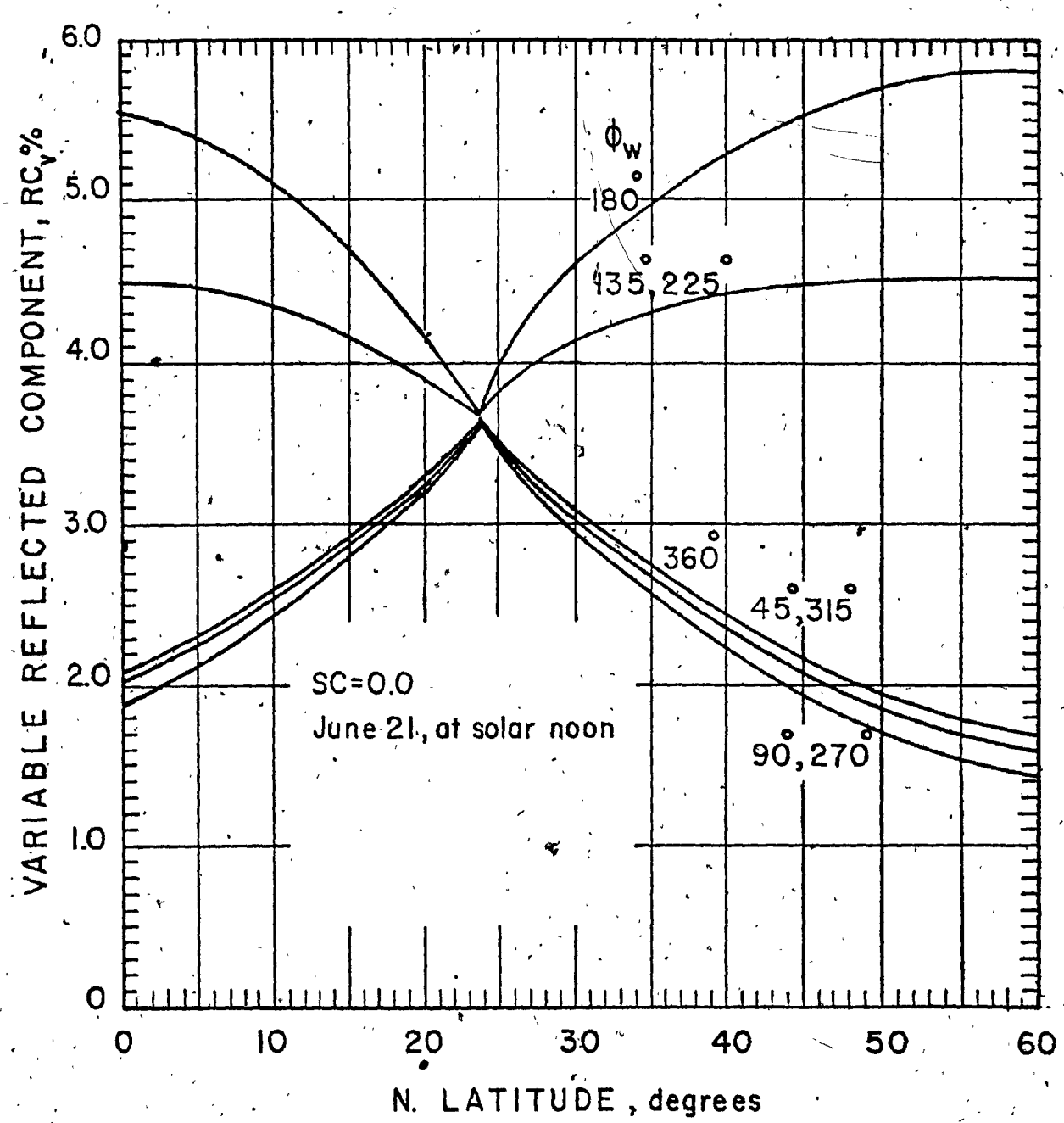

Fig. 3.43 Variation of the variable reflected component with the latitude angle at solar noon on June 21.

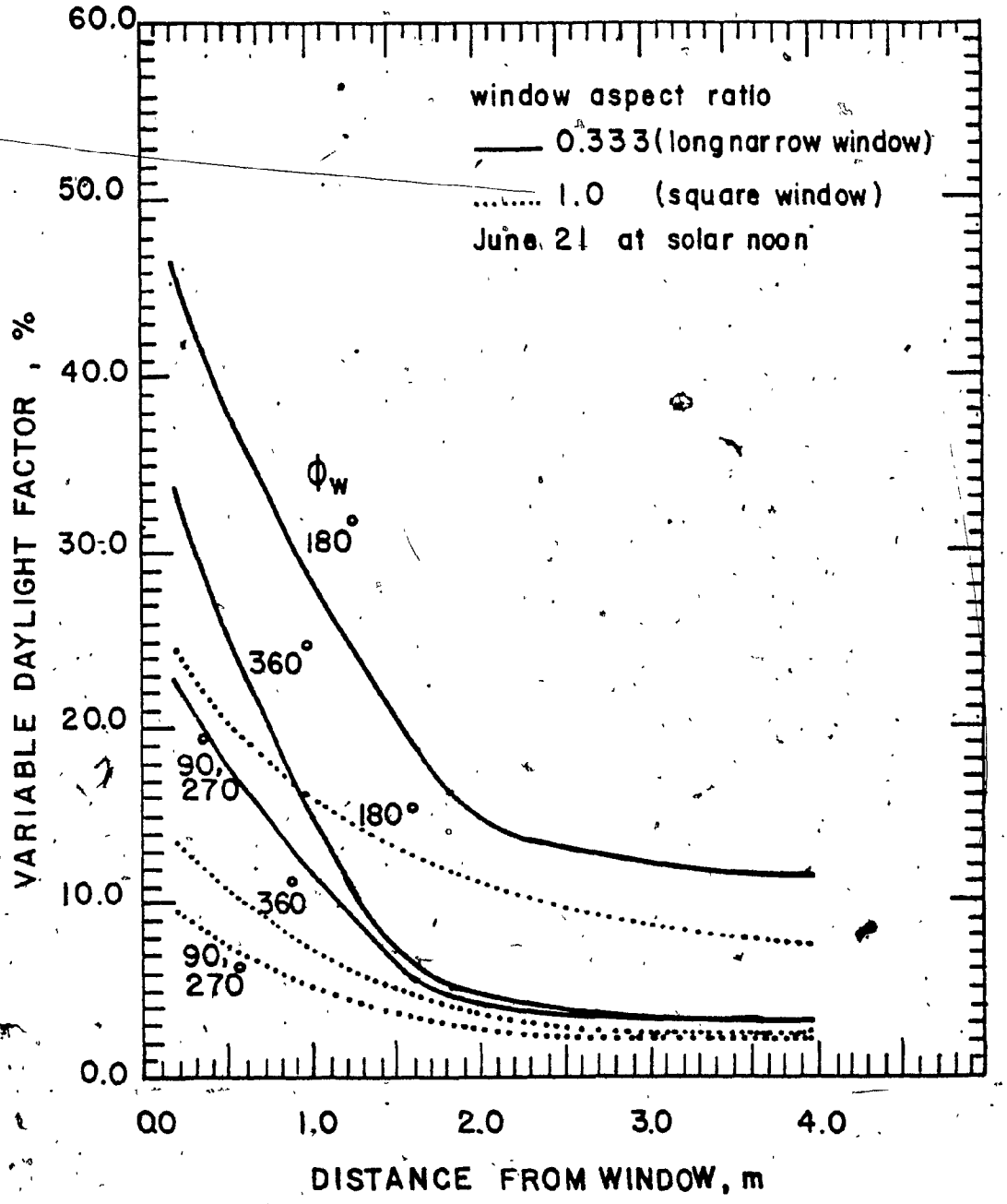

Fig. 3.44 Effect of the distance of the reference point from the window on the variable daylight factor for tall narrow and square obstructed windows.

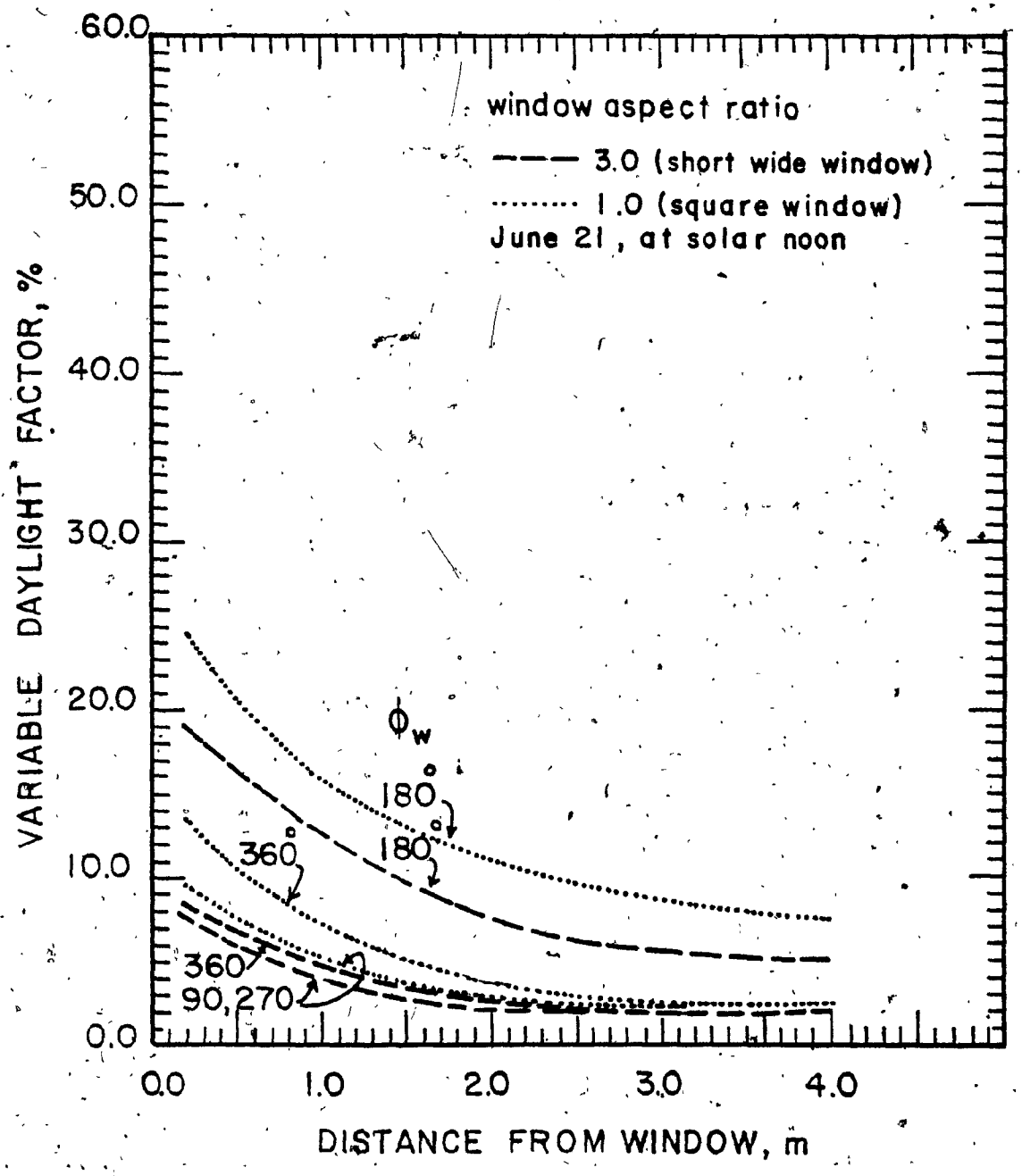

Fig. 3.45 Effect of the distance of the reference point from the window on the variable daylight factor for short wide and square obstructed windows.

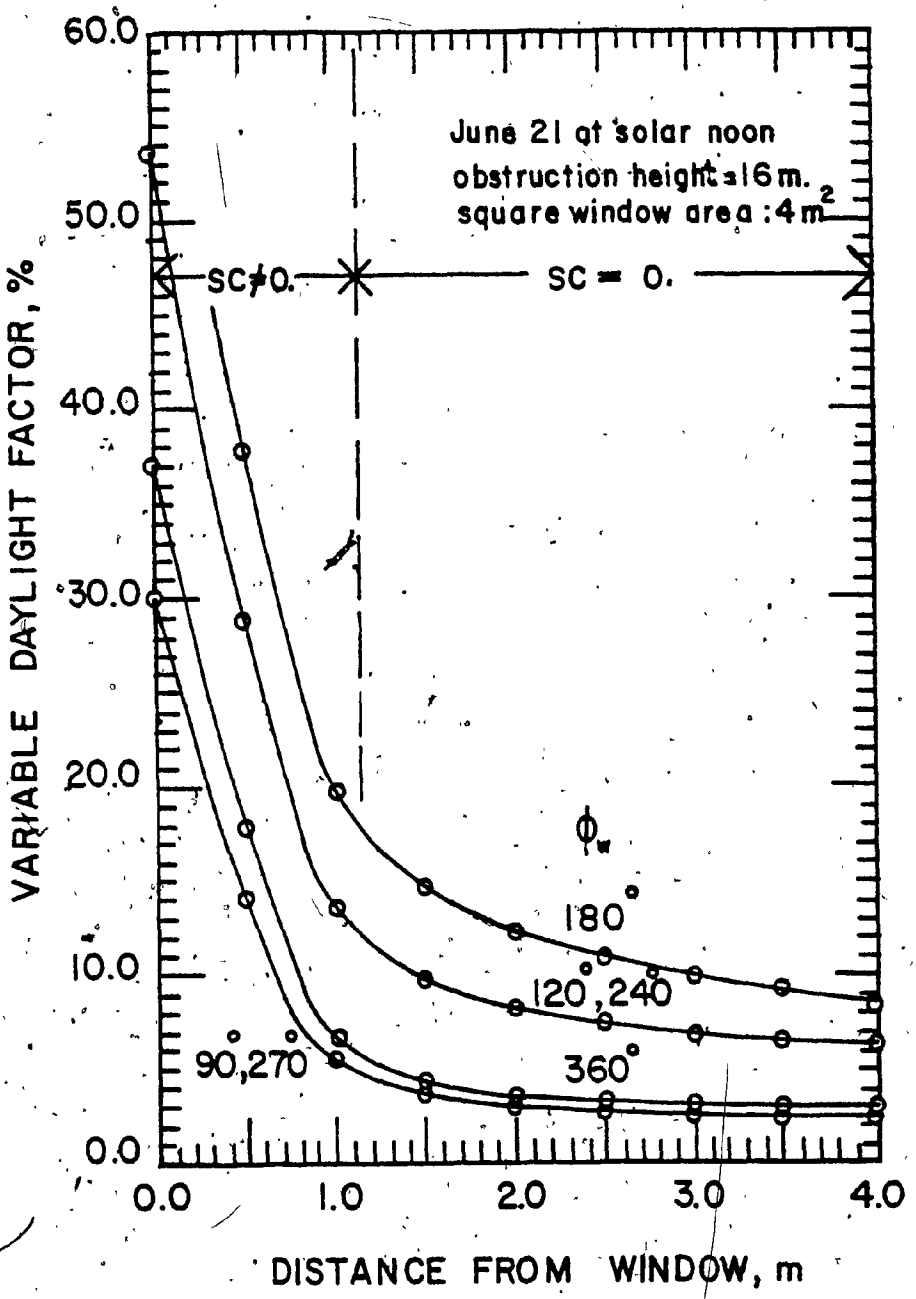

Fig. 3.46 Effect of the distance of the reference point from the window on the variable daylight factor for a fully obstructed window.

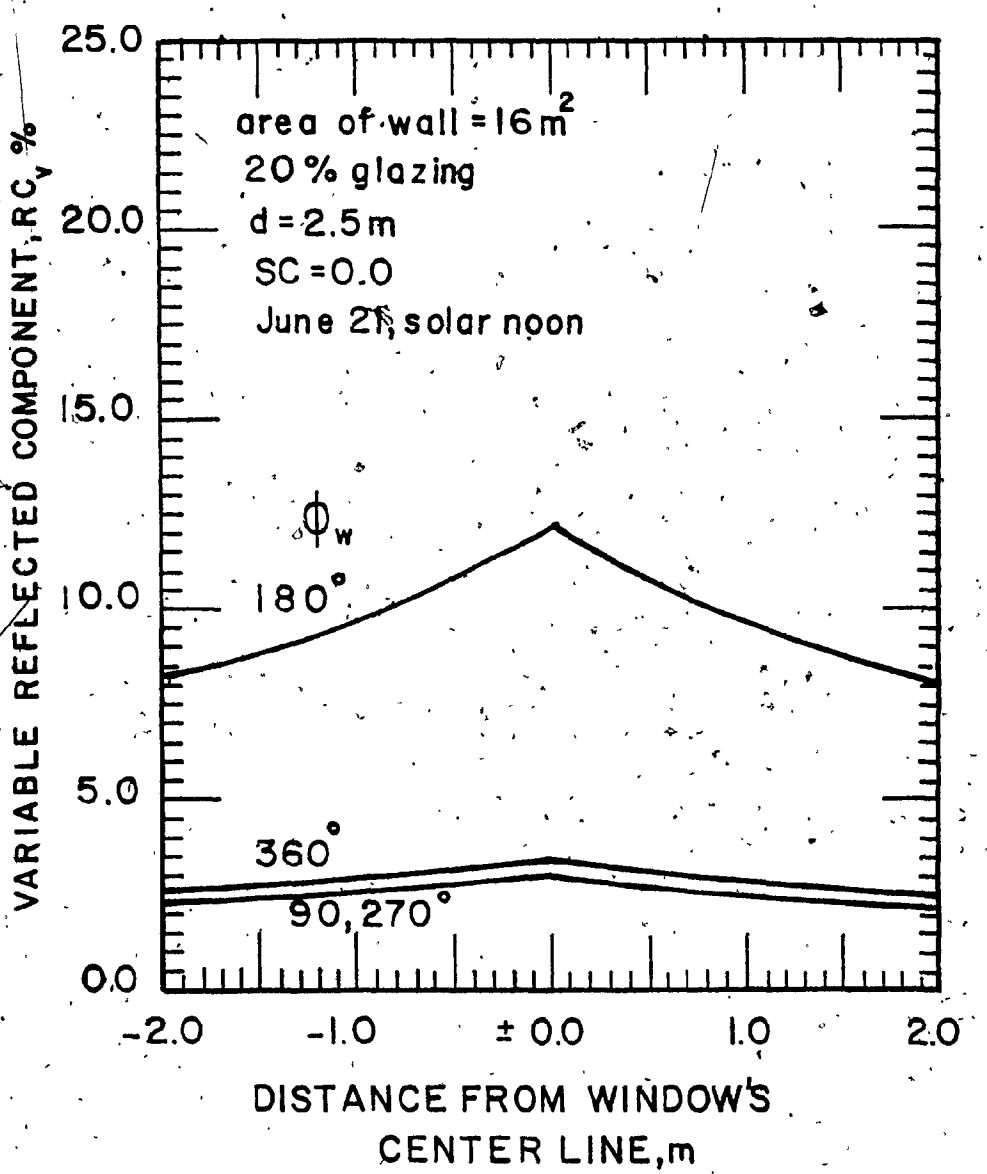

Fig. 3.47 Effect of the distance from the reference point to the perpendicular bisector of the window sill on the variable reflected component.

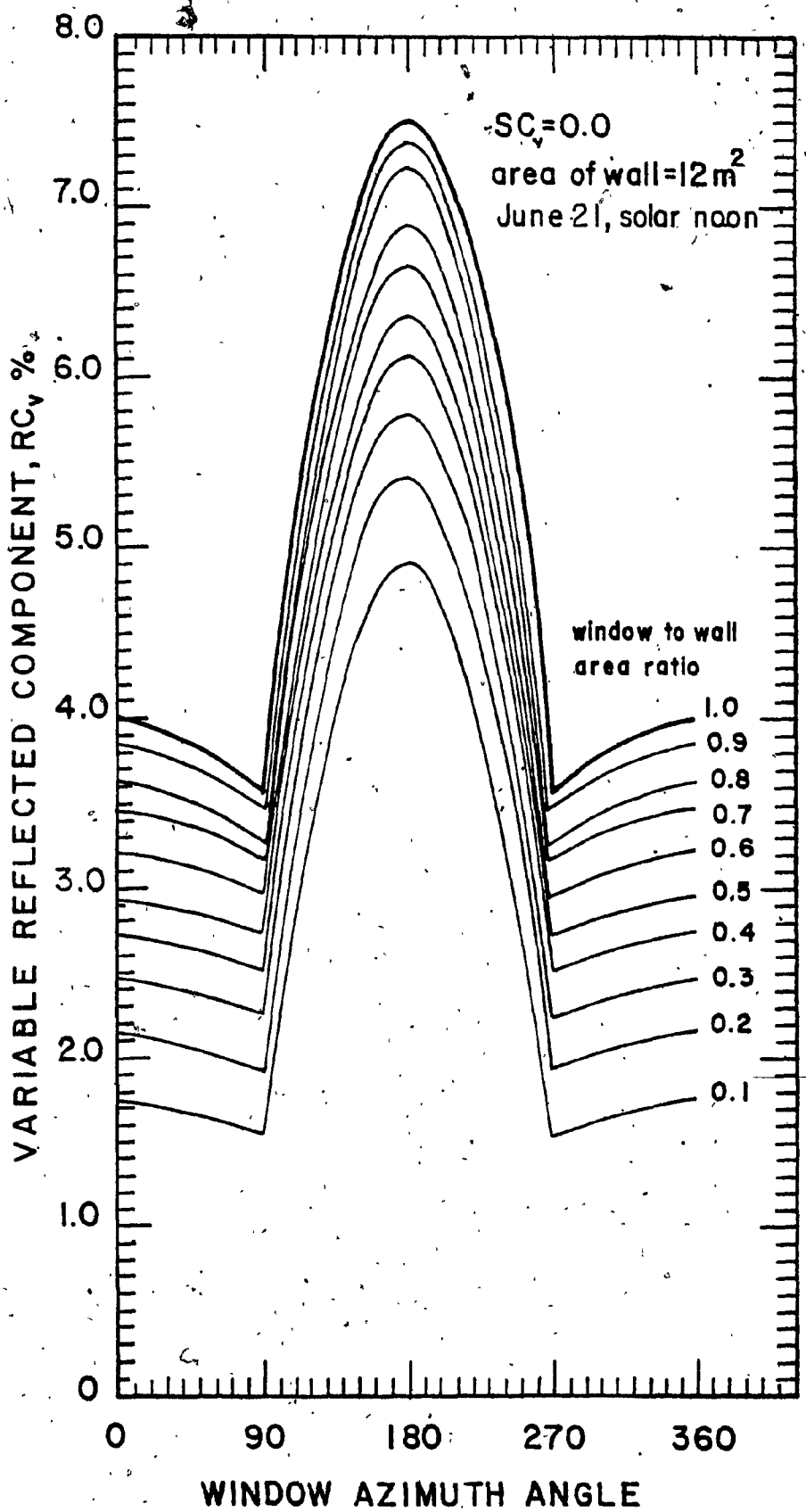

Fig. 3.48 Effect of window-to-wall area ratio on the variable reflected component for a fully obstructed window.

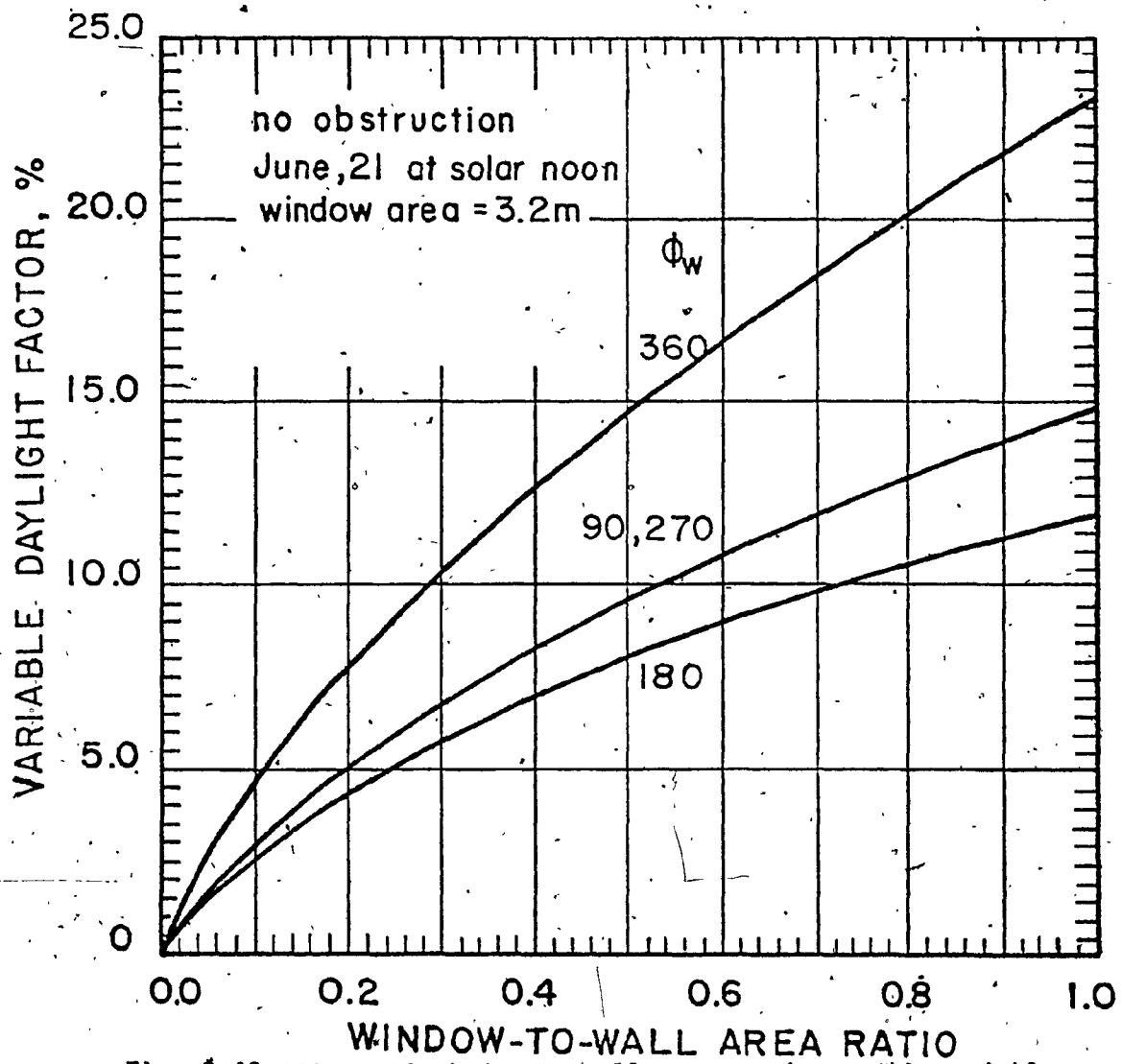

Fig. 3.49 Effect of window-to-wall area ratio on the variable daylight factor for an unobstructed window.

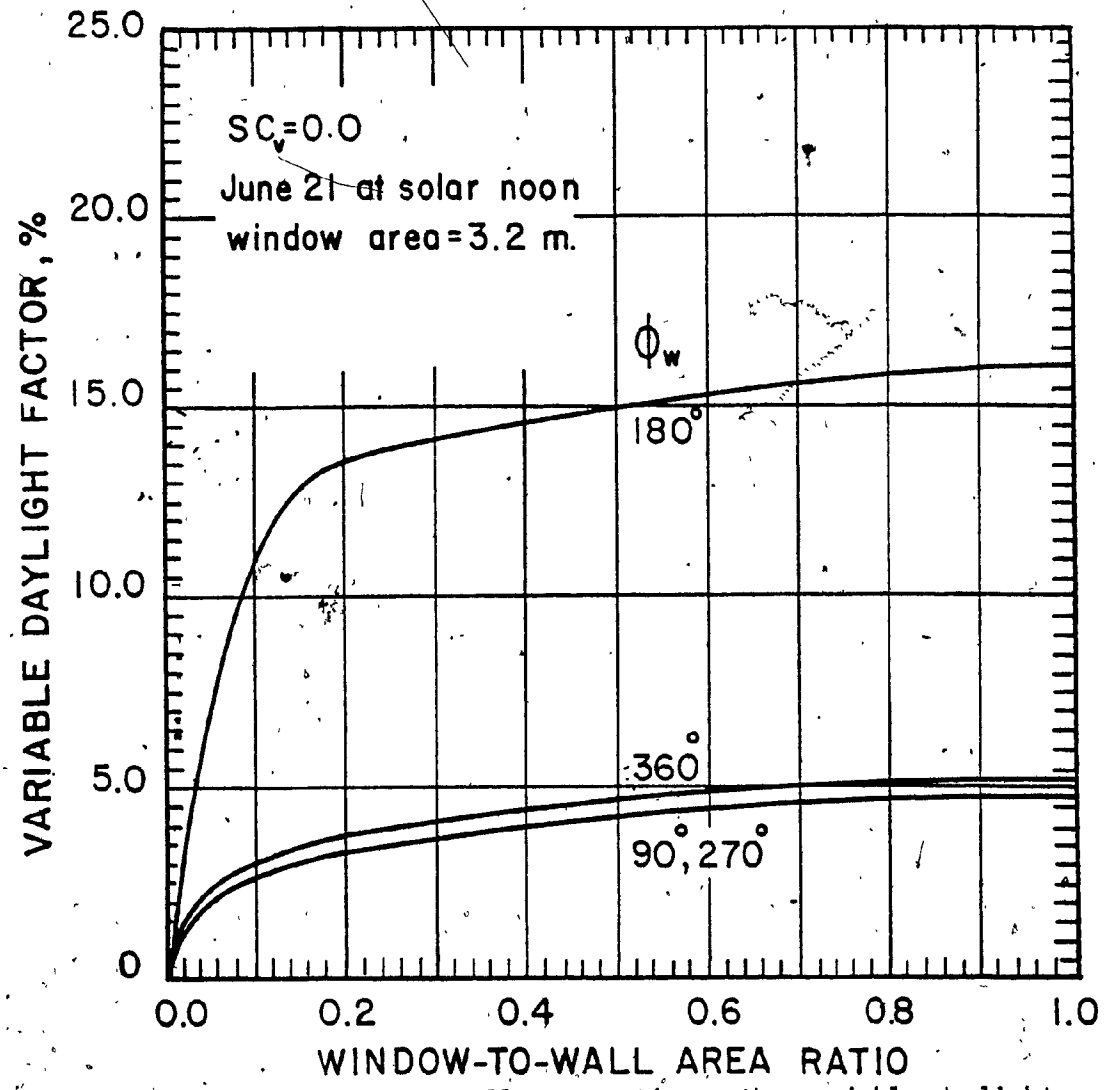

Fig. 3.50 Effect of window-to-wall area ratio on the variable daylight factor for a fully obstructed window.

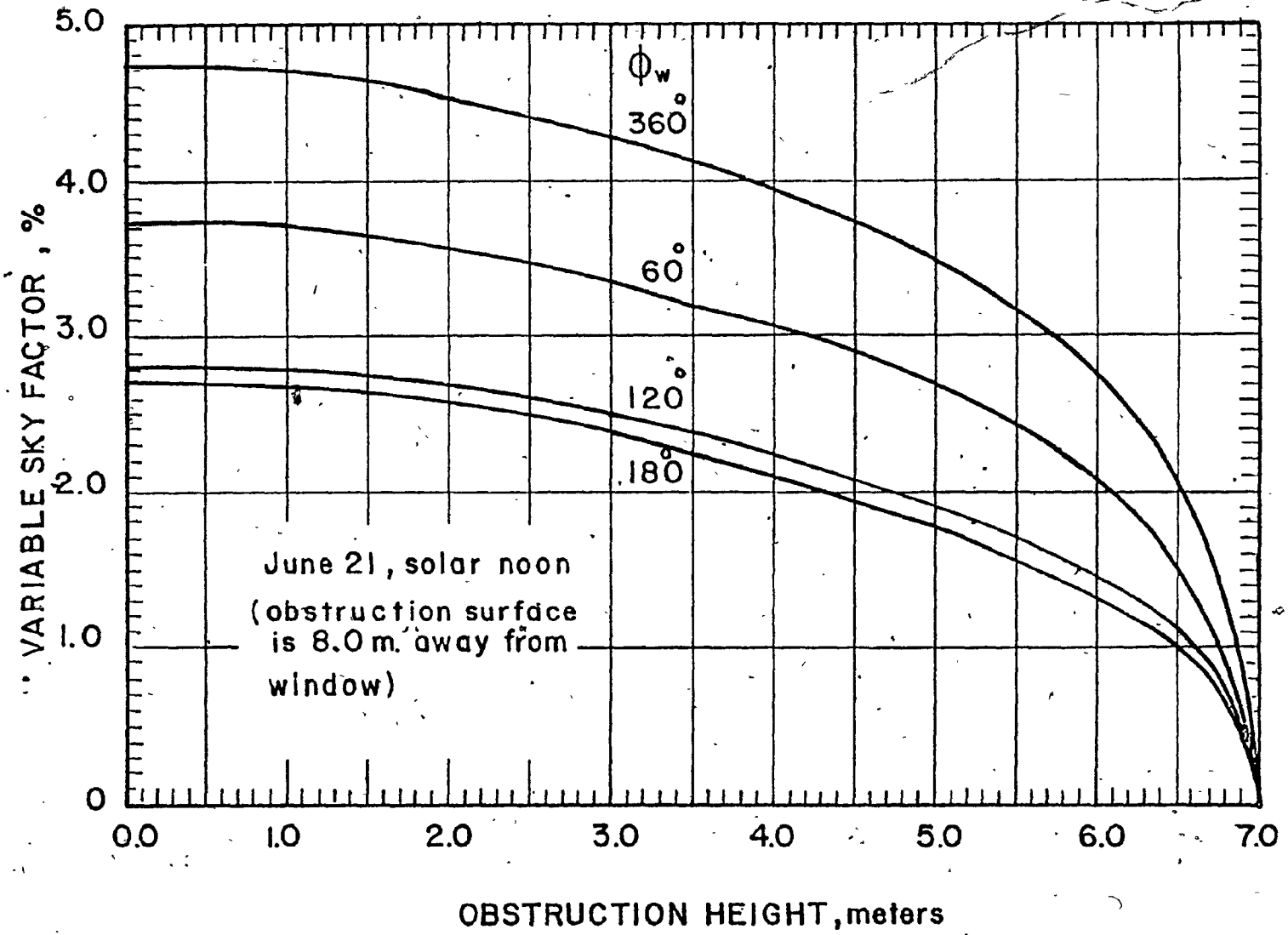

Fig. 3.51 Effect of the obstruction height on the variable sky factor.

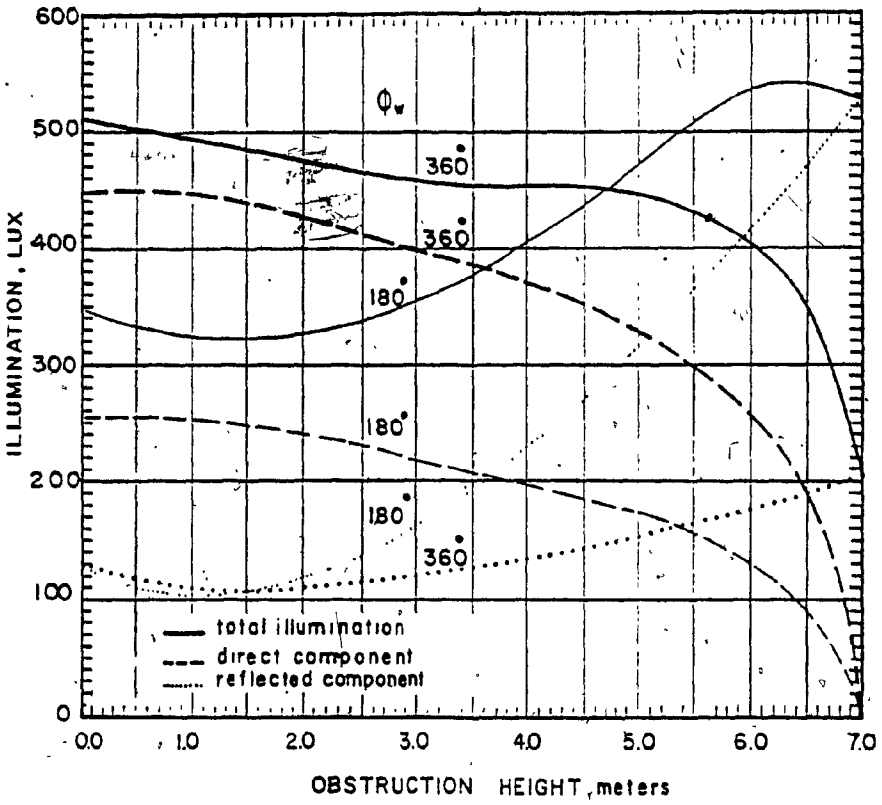

Fig. 3.52 : Effect of the obstruction height on the diffuse sky illumination received at the inside reference point.

CHAPTER IV

FIELD MEASUREMENTS OF THE NET ENERGY CONSUMPTION ASSOCIATED WITH EXTERNAL WALLS AND WINDOWS

4.1 INTRODUCTION

In the literature survey, we found no previous full scale experimental research to determine energy consumed to compensate the net loss through windows. In this chapter, a description of the first full-scale field measurements of the actual net energy consumption attributable to an external wall with an illuminated window at several orientations is presented. In this study, we examined the thermal impact of the window-to-wall area ratio on the overall energy consumption of an rotatable test chamber for three of the main compass orientations and for the three types of glazing (single, double, and triple). The net energy consumption is reduced by the energy savings when daylight is utilized in providing the required illumination.

There were three major experimental goals. The first was the prediction of the energy consumption associated with air infiltration using in site wind and temperature measurements. The second was to predict the value of the surface coefficient, and consequently the heat loss by convection and radiation at the external surface. The third goal was to measure the total energy consumed in each of the 30 cases for comparison to calculations with the finite difference and the variable daylight models presented in Chapters II and III respectively.

The infiltration heat loss is dependent upon the indoor-outdoor

temperature difference, the crack length, and an infiltration coefficient that is dependent upon the workmanship, crack thickness, and the wind speed and direction. The coefficient was obtained by using a new technique that employs surface temperatures instead of the pressure drop across the wall.

Instead of using a constant value for the outside surface coefficient, it was related to measured wind speeds and directions, using linear regression. Weather data during each experiment was recorded in addition to the temperatures of the external and internal surfaces of the window and wall, room air temperature and the heating and cooling power used.

In the following sections, a description of the test program, the design and construction of the rotatable test chamber, the measurements of the infiltration heat loss, and the dependency of the convection coefficient on wind speed and direction are presented as well as the procedure used for determining the cooling capacity of the air conditioning unit used.

4.2 THE TEST PROGRAM

The test program covered the three types of glazing: single, double, and the triple glazing. Four window-to-wall area ratios were used, namely, 0.0, 0.25, 0.50 and 0.75. The tests were limited to three main orientations, south, west, and north. The east orientation was excluded for two reasons. First, if one of the main orientations has to be excluded then it should be either the west or the east,

because on clear days they both receive the same amount of solar radiation. The only difference is the ambient temperature when that radiation is received. The second reason for exclusion of the east orientation was because of the surrounding conditions. The eastern sky was partially obstructed by neighbouring buildings while the western sky was almost unobstructed.

Ten experiments were conducted for each orientation ((3 glazing types x 3 window sizes) + a solid panel), that is a total of 30 experiments. These experiments were conducted during a period beginning at the first of January and ending at the end of April, 1980.

For each orientation, and for each window-to-wall area ratio, three panels with different types of glazing were inserted in one wall of the chamber for testing. At each orientation, three window-to-wall area ratios 0.25, 0.50, and 0.75 as well as a solid panel were examined. The test chamber was then rotated to the next orientation and the procedure was repeated.

4.3 THE EXPERIMENTAL SET-UP

4.3.1 THE TEST CHAMBER

The test chamber was constructed on the roof of the Centre for Building Studies. It was designed to test the effect of the window-to-wall area ratio on the energy consumed to maintain a constant internal temperature regardless of the external weather conditions.

The test chamber (Figs. 4.1 and 4.2) was designed to simulate a

room in a large building, with one side exposed to the outside and the other five sides adjoining rooms at a constant temperature. An external chamber was constructed around five out of the six surfaces of the inner room, only one wall of the inner room was exposed to the outside weather. On that wall, removable panels with various windows could be fitted into a metal square frame (2.50 m x 2.50 m). The external chamber was thermostatically controlled and kept at 20°C, thus simulating the effect of neighbouring rooms. Since the temperature of the inner room was also kept at 20°C, five surfaces of the inner room, could be assumed to be adiabatic and the energy consumption of the inner room was attributed to the net losses through the particular inserted external panel under investigation. Two of the panels are shown in Fig. 4.3. The test chamber was equipped with four wheels to allow for rotation to any desired orientation. When it was in the desired position, wheels were locked, and guy wires were attached to take up wind forces.

4.3.2 TEST CHAMBER CONSTRUCTION

As shown in Fig. 4.4, all external walls of the outer enclosure and the experiemental panels were of the following multi-layered construction (from the outside to the inside)

i) 9.4 mm (3/8") weather-treated and stained plywood

ii) 50 mm (2") rigid styrofoam insulation.

iii). A central cavity covered on both sides by 6.3 mm (¼") plywood sheeting and enclosing 50 x 100 mm (2"x4") studs (Fig. 4.2) placed every 600 mm (24"). In the outermost part of the cavity, was a 25 mm (1") air space and the innermost part contained 62.5 mm (2½") of fiber glass insulation and a vapour barrier. The outer plywood sheet was lined (on the cavity side) with building paper. The inner sheet formed the internal surface of the test chamber and was faced (on the cavity side) with aluminum foil with the shiny reflective side exposed so as to reduce heat loss by radiation from the thermostatically controlled cavity.

The floor of the external enclosure was supported on two 0.15 m x 0.15m wooden girders that transmitted the weight to the ground through the four wheels. Its construction was similar to that of the external walls except that the rigid insulation was situated directly beneath the plywood flooring. This change was made to allow for direct contact between the floor joists and the support girders.

The roof was tilted 20° to minimize snow accumulation and to allow rain to run off. The roof consisted of four plies of asphalt roofing; a membrane; 50 mm (2") of rigid stryofoam insulation; and a cavity similar to that of the external walls with a 6.3 mm (¼") plywood sheet; 50 x 100 mm (2"x4") rafters every 600 mm (24"); containing a water and vapour barrier; a 6.3 mm (¼") plywood sheet and finally aluminum foil facing the cavity.

From the outside in, the walls, floor, and ceiling of the inner room consisted of an aluminum foil sheet with the shiny, reflective side facing the outer chamber; a 6.3 mm (¼") plywood sheet; 50x100 mm (2"x4") studs every 600 mm (24"): containing a 25 mm (1") air space and 62.5 mm (2½") of fiber glass insulation; an air barrier; a 6.3 mm (¼") plywood sheet; 25 mm (1") of rigid styrofoam insulation; and a 6.25 (¼") plywood sheet as the internal surface. The walls were painted with a "CIL" white paint.

The frame of the opening was weather stripped and sealed. The dimensions of the opening were 2.262 x 2.262 m (7 ft. 6¾ in square). The dimensions of the panels were 2.25 x 2.25 m (7 ft. 6. in square). The ¼" difference at the sides is padded by the weather stripping tape and sealant. Every panel was raised into position in the frame by the use of a pulley with a mechanical advantage of holding the panel in front of the opening safely to allow us to insert it or to replace it (c.F. Fig. 4.3). The thermal resistance and the overall heat transfer coefficients of all components are shown in Table 4.1.

The windows tested were single, double, and triple glazed units, and all were made of clear, tempered float glass. The thickness of each pane was 6.25 mm (¼") and the air spaces were 1.25 cm (½")(c.f. Fig. 4.4). All units were factory-sealed and made by "Gloverbel Sealite Insulating Glass." The air spaces were dehydrated and hermetically sealed.

Building Component	R-value $m^2 . K°/w$	U-value $w/m^2 . K°$
External walls	3.846	0.26
External platform	3.846	0.26
Roof	3.846	0.26
Internal walls	3.334	0.30
Internal ceiling	3.334	0.30
Internal floor	2.772	0.36
Single window	0.156	6.416
Double window	0.361	2.77
Triple window	0.563	1.76

Table.4.1 Thermal resistances and overall heat transmission coefficients of the test chamber.

4.3.3 INSTRUMENTATION, EQUIPMENT, AND MEASUREMENT

The test chamber was furnished with measuring and recording instruments, and heating and cooling equipment as described in the following paragraphs.

i) Solar Radiation Measurements

Solar radiation was measured with silicon solar cell detectors (model SS-100) manufactured by "Dodge Products". These detectors had been calibrated against a reference thermopile detector by the manufacturer. The calibrated intensities ranged from 0.0 to 990 watts/ m^2 over a 48 hour period at an average ambient temperature of 33°C. The accuracy of the solar sensor was within $\pm$ 0.2 w/m^2. The output of the detector was adjusted to provide an electrical signal of 100 mv with

solar radiation of 100 mw/cm^2. The sensing element of the detector was a space grade silicon cell with an electrode grid carefully chosen to give linear output characteristic and a sensitivity of 0.1 mv per 1 w/m^2. The spectral response ranged from 0.4 to 1.1 microns with a maximum at 0.8 microns, 6 solar cells were used.

Solar cell # 1 was used to detect the intensity of the total solar radiation on the horizontal plane. It was placed horizontally outside the test chamber on the least-obstructed area of the roof.

Solar cell# 2 was used to detect diffuse radiation on the horizontal. A moveable band shaded the detector from direct beam radiation. Solar cells # 1 and # 2 are shown in fig. (4.5a).

Solar cell #3 measured the horizontal intensity at the reference point, usually 0.8m high and 2m inside the window. Solar cell #4 was placed vertically on the external surface of the tested panel and measured the total radiation impinging on the panel surface (Fig. 4.3b). With windows, solar cell #5 used to measure the total solar radiation transmitted through the glazing (Fig. 4.6a). It was placed near solar cell #4 inside the glazing facing out, in such a way that neither solar cell #4 nor solar cell #5 shaded each other on the particular test day. A smaple of the radiation measured by solar cell #4 is shown in Fig. 4.7a, 4.7b and Fig. 4.8a for a vertical surface facing south, west, and north respectively.

Solar cell #6 was placed near the internal surface of the glass and faced inwards to measure the radiation reflected from the room to the outside and is shown in Fig. (4.6a).

To simulate a room with dimmers, electric lighting was equipped with an automatic light-sensing multi-level ballast. The light sensing element of the ballast was a celenium photo cell (Radio Shack pt. 276-115). Thus, any dimming of the available daylight below the set minimum level was computed instantly by the multi-level ballast switched on one or more fluorescent bulbs. It was assumed that the nature of the activity in this room required an illumination level of 750 lux. The luminous flux (lumens) received on the work plane is always less than that emitted by the lamps due to losses in the luminaire and the room surfaces. Thus, the luminous flux must be multiplied by a coefficient of utilization which represents the portion that reaches the work plane. In actual use, and over a period of time, the components of a luminaire are likely to operate at less than its rated output. This is attributed to voltage variation, lamp depreciation, maintenance procedure, dirt accumulation and temperature variation. Thus to account for this difference the luminous flux from lamps must also be multiplied by a loss factor known as the maintenance factor. According to the calculation procedure given IES Lighting Handbook [123], the test room utilization factor and the maintenance factor for the lamps used were found to be 0.6 and 0.8 respectively. Therefore, the required installed flux was

$$\text{Installed Flux} = [750 \text{ lux} / (0.6 \times 0.8)] \times \text{Room area } (5\text{m}^2)$$
$$\simeq 18000 \text{ lumens}$$

The luminous efficiency of the fluorescent fixture and bulbs was 75 lumens per watt, thus the total power required was (18000/75) = 240

watts. Six lamps of 40 watt rating were installed.

As long as the available daylight provided an illumination about 750 lux at the reference point, the six lamps were off. The lamps were turned on or off at 125 lux intervals. The ballast responded only to illumination changes greater than 5% of the existing value.

ii) Temperature Measurements

Temperatures were measured with type T copper-constantin thermocouples. A total of 45 thermocouples were used. The temperature was measured at both external and internal surfaces of the panel and the window. On each surface 8 thermocouples were placed on the panel and nine on the window. A thermocouple was inserted at the panel-wall interface and another at the panel-window interface. Other thermocouples were used to measure room temperature (3 thermocouples, 0.2m from ceiling, mid-height, and 0.2 m from floor) outdoor air (one thermocouple) and cavity air (one themocouple). The last 4 thermocouples were used in different positions but mainly to insure that the temperature on both sides of internal walls was the same and particularly the temperature of the cavity on top of the inner room ceiling.

The thermocouples were connected to a temperature digital displayer (Doric Trendicator type 400) shown on the left hand side of Fig. 4.6b. Thermocouples were immersed in boiling water to check the boiling temperature (100°C) and in melting ice to check the melting temperature (0°C). The stability of the thermocouples was checked by obtaining continuous readings while keeping the thermocouples immersed for up to 3

hours. An ice point instrument (KAYE's Ice Point Reference) was used also to check the zero point. A mercury thermopile was also used for checking the calibration (Taylor Instuments).

iii) Wind Speed and Direction Measurements

A dual-purpose instrument for measuring wind speed and wind direction. (The Bendix Aerovane Wind Transmitter Model 120), shown in fig. 4.5b, was used. The wind speed was measured by a three-bladed impeller fastened to the armature of a tachometer magneto located in the nose of the instrument. The speed of rotation was directly proportional to the speed of the wind striking the impeller blades. Thus, the voltage generated by the magneto is proportional to wind speed. This voltage was electrically transmitted to a remotely located voltmeter which was calibrated to indicate wind speed in Km/hr (0.0656 VDC = 1 Km/hr.). It is shown on the right-hand side of Fig. 4.6b. An airfoil turned the body of the instrument into the wind. A synchro electrically transmitted the vane position to a remotely-located companion synchro (Fig. 4.6b). A rapid response synchro-to-DC converter card was used to accept 3-wire synchro input data and to convert it to a linear DC output voltage proportional to the synchro angle and displayed on the chart recorder along with the wind speed. A sample is shown in Fig. 4.8b.

iv) Heating and Cooling Equipment

Two spaces were thermostically controlled, namely, the external cavity and the inner room itself. The energy consumed for heating and

cooling the inner room was monitored as described below. The heating and cooling loads were calculated and the capacities of a heater and a cooler were chosen accordingly.

The cavity area between the inner and outer walls shown in Figs. 4.1 and 4.2 simulates the thermal environment of the rooms surrounding the test room in a real situation. The air temperature of the cavity was kept constant at 20°C by a thermostat (Honeywell-bulb pressure spring) which operated a micro switch for the cooling and heating units. The thermostat fluctuation never exceeded $\pm$ 0.5°C. Heating was provided in the cavity area by three 100 ft. long heating cables suspended in loops from the ceiling to the floor. The heating cables were used to reduce temperature variation within the cavity. We used 0.5 kw cables (model ADKS-500-C1) from Heron Cable Industries Limited. The cavity area was cooled by a window air-conditioner which delivered 1465 watts of cooling (5000 BTU/hr.). The model used was Mastercraft -5000 manufactured by "Hot Point" for "Canadian Tire Limited".

The heating of the inner room was provided by 1500 watt Mastercraft floor base heater and the cooling by an air-conditioner identical to that placed in the cavity. The temperature of the room was maintained thermostatically at 20°C with fluctuation $\pm$ 0.5°C (at the room mid-height). The temperature stratification with the height of the inner room was 3°C at the most. The maximum temperature difference across the ceiling was 2°C at the most. These figures changed slightly only right after the heater was turned on. At the other four adiabatic surfaces of the inner room, the temperature difference was zero at the

mid height and fluctuation within 1°C was found.

v) Measurements Recording

In order to calculate the energy consumed by the lights, six channels of a "Cole Parmer" 8 channel event recorder were used to register the switching of the six fluorescent lamps. The other two channels were used to record the on-off events of the heater and the air conditioner of the inner room. The output was printed on a 2" wide carbon loaded paper. A "Rustrack" current recorder (model 2107) was used to measure the variation of the current entering the air-conditioner and recorded quasi-continuously. Wind speed and direction were also recorded quasi-continuously (24 hours) on carbon loaded paper. Solar radiation measurements were recorded quasi-continuously during the day on "Rustrack" solar chart recorders. Manual readings were taken for temperature once every hour using Doric Trendicator type 400 with a channel selector.

4.4 Infiltration: Theory and Results

The interfaces between the components of the enclosure contain gaps and cracks through which an uncontrollable flow of air either infiltrates or exfiltrates from one side of the enclosure to the other. The driving force for such a flow is the pressure difference across the enclosure caused either by wind or temperature effects or both.

Air leakage gives rise to the following problems associated with either the indoor environment or deterioration of building materials:

1. Uncomfortable air draft for occupants.

2. Reduction or increase of the relative humidity inside.
3. Reduction or increase of the internal surface temperature of external walls.
4. Increased condensation on cold surfaces in winter.
5. Infiltration of odours, dust, and smoke into the building.
6. Acceleration of the spread of smoke and fire in both the horizontal and vertical directions.
7. An increase in the heating load in winter and the cooling load in summer.
8. Deterioration of the building materials of the enclosure.

4.4.1 The Relation Between Air Leakage and Air Pressure Difference

The driving force causing air leakage is the pressure difference which acts on the building enclosure. The pressure difference is induced either by the wind forces or the density difference or both. The pressure difference induced by wind forces is related to the wind speed by [10].

$$\Delta P_w = 0.601\ v^2 \qquad (4.1)$$

where

ΔP_w = pressure difference across an enclosure panel caused by the wind, P_a.

v = wind speed, m/s.

In winter, the pressure difference due to the difference in air density, resulting from the difference in the temperature between inside and outside air, produces a negative inside pressure and an inward air

flow at low levels, and a positive inside pressure with an outward flow at high levels. The reverse occurs when the inside temperature is lower than the outside. The pressure difference is zero at the neutral level and increases as the distance from the neutral level is increased. The pressure difference, ΔP_d, due to the density difference is given by [10].

$$\Delta P_d = 0.0342\ Ph\left(\frac{1}{T_o} - \frac{1}{T_i}\right) \qquad (4.2)$$

where

ΔP_d = pressure difference across the enclosure panel caused by the density difference, P_a

P = atmospheric pressure, P_a

h = distance from the neutral level, m.

T_o = outside air absolute temperature, K°

T_i = inside air absolute temperature, K°

Available data on the neutral pressure level (NPL) in various kinds of buildings are very limited. The NPL in tall buildings may vary from 0.3 to 0.7 of the total building height. For houses, the NPL is usually about mid-height [10]. Since the pressure difference caused by the difference in the air density is proportional to the distance from the neutral level, this force is relatively insignificant for single-storey houses, but in tall buildings it may be the dominant force.

4.4.2 Estimation of Air Leakage

There are two methods of estimating the air leakage in buildings. The air change method assumes a certain number of air changes per hour

for each room. The number of air changes is assumed to be dependent upon the room location, use, type of construction, and number of windows. The other method is known as the crack method. It is based on measured leakage characteristics of building components at selected pressure differences. However, no two walls are identical as built so infiltration figures are generally only estimates. As a result, heat loss or gain associated with air leakage is considered the most uncertain component of the calculated heating and cooling loads.

Based on experimental measurements of actual homes, the hourly infiltration rate in the air change method is given by [217]

$$I = A + Bv + C\Delta T \qquad (4.3)$$

where

I = infiltration rate in air changes per hour

V = wind speed (m/s)

ΔT = temperature difference between indoor and outdoor air, °C

A, B, and C are empirical constants dependent upon the characteristics of the house being measured. Their values for a typical wood frame house are: A = 0.25, B = 0.04843, and C = 0.00463.

For the crack method, the air leakage characteristics are expressed in terms of flow rate per meter of crack or per unit area. For a given pressure difference, the air leakage is the product of the air leakage characteristics and the total crack length or area.

The air flow through openings in buildings is governed by laws similar to those describing air flow through orifices and capillaries.

The flow through a capillary is directly proportional to the pressure drop across it, and the flow through an orifice is proportional to the square root of the pressure drop. The relation for the usual openings in buildings falls between these two limits. Also, the flow rate depends on the effective area of the cracks. Thus, infiltration, in terms of the volume flow rate of air, is given in the form [10]

$$V = C \ \Delta P^n$$

where,

V = volume flow rate of air, $(l/s)/m^2$

C = flow coefficient, $(l/s)\ m^2/P_a$ (accounts for crack geometry)

ΔP = Pressure difference, P_a

n = flow component, between 0.5 and 1.0 and usually near 0.65.

Because of the variations in workmanship and design of openings like windows and doors, in situ measurements are considered to have an advantage over the available mathematical formulae in predicting air leakage in buildings.

There are two techniques which are often used in field measurements. The first is to pressurize the building using the supply fans of the central air-conditioning system. When the supply fans are on, the supply air flow rate and the resultant pressure difference across the enclosure are recorded. With this technique, the air leakage flow through a typical wall area can be separated from that through the bottom and the top of the pressurized enclosure [61]. The second

technique is known as the tracer-gas technique. The rate of air change is estimated by measuring the change in the concentration of a tracer gas for which a sensitive detector exists. The most common gas used is helium (detected with a mass spectrograph).

4.4.3 Calculation of Infiltration Sensible Heat Loss

A simpler technique has been developed in the present study. The thermally - induced pressure difference across the enclosure is very small compared to the wind-induced pressure difference. Therefore, the pressure difference is assumed to be a function of wind speed only. Using temperature measurements, a simplified procedure for the calculation of the sensible heat loss associated with air infiltration was developed. The sensible heat loss due to infiltration, Q_f, can be defined as the energy required to raise the temperature of the incoming outdoor air, T_o, to the level of the indoor air temperature, T_i. Q_f as function of the crack length, L, and the indoor-outdoor temperature ΔT, can be expressed by:

$$Q_f = F\ L\ \Delta T \quad \text{watts} \qquad (4.5)$$

where F is the infiltration coefficient given by

$$F = \rho\ cp.\ B$$

where

ρ = density of the incoming outdoor air (Kg/m^3)

cp = specific heat of outdoor air ($J/Kg.K^\circ$)

B = the volume of the infiltration air per unit time per unit length of crack (m^3/s per m. of crack)

The volume of the incoming air, B, depends on the pressure difference across the external wall, crack thickness, and the workmanship involved in constructing the particular windows, walls, or roofs. The value of B for a few common types of walls and windows are given for discrete values of pressure difference (25, 50, 75, 100, and 125 P_a) by ASHRAE [10]. For our experiments, finer divisions would be required, so we determined the coefficient F experimentally as a function of wind velocity through a heat balance. To avoid solar gains, these experiments were done at night in January and February 1980. The time of operation of a calibrated heater (1500 w) was logged on an event recorder. The heat generated from lamps was constant at 40 watts. Therefore, the total heat input, Q(i) to maintain the room air at 20 $\pm$ 0.5°C during a specific hour i is

$$Q(i) = \frac{n \times 1500}{60} + 40 \quad \text{watts} \tag{4.7}$$

where n is the number of minutes within the hour i when the heater was on.

Since five surfaces of the room are maintained from both sides at 20°C (adiabatic surfaces), the hourly heat input Q(i), is just the heat loss through the external wall under test, $Q_c(i) + Q_f(i)$, where c stands for conduction and convection and f for infiltration. The test was conducted for window-to-wall area ratios of 0.25 and 0.50. For each ratio, single, double, and triple windows were examined for a total of six cases. Thus

$$Q_f(i) = Q(i) - Q_c(i) \quad \text{watts} \tag{4.8}$$

Since the variation of outdoor temperature during the 12 hours of each test was about 3°C and the indoor temperature was maintained at 20 ± 0.5°C, a steady state analysis of the heat transfer was used.

The heat loss from the external wall and window $Q_c(i)$ was evaluated from 34 equally distributed measured temperatures of the internal and external surfaces of the window and wall (Fig. 4.9) in addition to the indoor and outdoor air temperature during interval i. The hourly surface temperature used for the calculation was the average of the temperatures measured on each surface. The heat loss for the external panel was evaluated with the following expression:

$$Q_c(i) = D_g\,(T_{ig}(i) - T_{og}(i)) + D_p\,(T_{ip}(i) - T_{op}(i)) \qquad (4.9)$$

where

$$D_g = \frac{A_g}{R_g} \qquad \text{and} \qquad D_p = \frac{A_p}{R_p}$$

and

A_g, A_p = area of glass and area of panel respectively

R_g, R_p = the thermal resistance between the internal and external surfaces for the glass and panel respectively (ie. without the air films).

T_{ig}, T_{ip} = internal surface temperature for glass and panel respectively.

T_{og}, T_{op} = external surface temperature for glass and panel respectively.

Substituting in Eq. (4.5), the corresponding value for the coefficient F during interval i can be obtained as follows.

$$F_i = \frac{Q_f(i)}{L\,\Delta T(i)} = \frac{Q(i) - Q_c(i)}{L\,\Delta T(i)} \qquad (4.10)$$

The total crack length around window and panel, L, for a 0.25 window-to-wall area ratio is 13.5 meters and for a 0.50 ratio it is 15.4 meters. Since the height of the test chamber is only 2.25 meters, the thermally induced pressure difference is very small and can be neglected. Thus, the pressure difference induced by wind is the dominant force driving air leakage. The experimental points are plotted in Fig. 4.10. The pattern suggests a non-linear relationship. A polynomial regression analysis was conducted on the results and yielded a relation of the third degree relating the coefficient F to the wind speed v which is given by

$$F = 0.081 + 0.024\ v + 0.0096\ v^2 + 0.0053\ v^3 \qquad (4.11)$$

where wind speed v is measured in m/s. At these low wind speeds, typical for downtown location, the wind direction varied almost randomly during each hourly time interval. Typical outputs are shown in Appendix C.

4.5 Experimental Investigation of the Dependence of the Surface Convection Coefficient upon Wind Speed and Direction

The rate of convection heat transfer from a wall is related to the temperature difference between the external surface of the wall and the ambient air beyond the convection layer by Newton's law of cooling

$$q_c = h_c A\,(T_s - T_{amb}) \qquad (4.12)$$

where A is the area of the external surface and h_c is the convection heat transfer coefficient.

In the present study, q_c was determined as the difference between the total rate of heat transfer at the external surface, q_t, and the rate of radiation heat transfer, q_r. The rate of radiation heat transfer, q_r, also be put in a linear form:

$$q_r = h_r A (T_s - T_{amb}) \tag{4.13}$$

where h_r is the radiation heat transfer coefficient given, in Eq. (2.4) in Chapter II, by

$$h_r = \sigma\varepsilon (T_s^2 + T_{amb}^2)(T_s + T_{amb}) \tag{4.14}$$

and σ is the Stephan Poltzmann constant ($\sigma = 5.67 \times 10$ w/m^{2}K^4) and ε is the surface emissivity. Under steady state conditions, the total rate of heat transfer at the external surface is the same as the rate of conduction heat transfer through the wall and the rate of heat transfer at the internal surface. Thus, q_t can be determined experimentally by monitoring the rate of heat gained at the internal surface.

Thus if h_r is known, h_c can be found experimentally:

$$h_c = \frac{q_t - h_r A (T_s - T_{amb})}{A (T_s - T_{amb})} \tag{4.15}$$

In order to remove one complication, temperature measurements were taken during the night, without any solar heat input. Using the hourly weather data that were collected during the first four months of 1980, relations for h_c as a function of the wind speed and direction were derived.

The measurements used were

i) 36 temperature measurements for the external and internal surfaces of the wall, indoor air, and outdoor air.

ii) Wind speed and direction.

iii) Hourly heat input from the lights and heater.

Data was chosen only from nights with minimal fluctuations of the outdoor air temperature ($\pm$ 2.5°C). Since the air temperature inside was regulated to 20° $\pm$ 0.5C, and the external air temperature was almost constant, steady state heat transfer can be assumed. Since vertical and horizontal temperature gradients measured along the wall were negligible in comparison to the temperature differences from one layer to another, the heat flow was nearly unidimensional. The windowless external test wall has an overall coefficient of heat transfer (U-value) of 0.26 $w/m^2K°$. Because of the thermostats, the other five surfaces of the inner test room were adiabatic. Therefore the rate of heat loss through the external wall is equal to the heat input to the room to maintain it at 20°C. The total rate of heat transfer, q_t, was then determined for each hour as the average rate of heat delivered by the heater and lights during the hour. To minimize the possible error that can be caused by air infiltration, the room surfaces were painted and the edges of the test panel, doors and air conditioners were caulked and taped from the inside and the outside.

The hourly wind direction was chosen as the predominant direction within the hour. The measurements showed that the fluctuation in the

wind direction around the predominant direction was dependent on the wind speed and the degree of turbulence in the air. Unless there was a major shift in the wind, the fluctuation range was always less than 45°. Therefore, the wind directions were rounded to the nearest of the 8 main directions (south, south east, east, north east, etc..). Part of the turbulance occurred because the C.B.S. roof is surrounded by buildings. Even at air velocities less than 5 m/s, fluctuations in wind direction were found. The hourly wind speed was chosen as the predominant speed within the hour.

h_c was calculated and then plotted against wind speed for five of the eight primary compass points of wind directions (Fig. 4.11 and 4.15). Since the test wall always faced one of the primary compass points, the other three primary wind directions were symmetric to 3 of the five plotted.

A least-square straight line, $h_c = a + bv$ was fitted to the points for each wind direction. The coefficients obtained for each direction along with the standard error of estimate, are shown in table 4.2

Wind direction from the normal to the surface	coefficient a	coefficient b	Standard error of estimate ($w/m^2.K$)
0° (normal)	7.77	2.90	+ 0.976
+ 45°	7.50	3.26	+ 0.79
∓ 90° (parallel)	7.52	4.10	+ 0.783
∓ 135°	6.85	2.63	+ 0.572
− 180°	6.27	2.65	+ 1.089

Table 4.2 coefficients a and b for the eight primary wind directions.

A comparison between these lines and others found in the literature is shown in Fig. 4.16. The computer print out for wind speed, wind direction, heating minutes, ambient and surface temperatures, h_r, h_c, and the surface coefficient h ($h = h_r + h_c$) are shown in appendix C. Readings were taken for 142 hours. If the wind directions are ignored, the best fit to all 142 points is

$$h_c = 8.48 + 2.55\ v \qquad (4.16)$$

4.6 Cooling Capacity

On sunny days, solar gains often increased the temperature of the room above 20°C. The excess heat was removed by the air-conditoner. Since only the power input to the air conditioner was monitored, the cooling capacity of the cooler had to be determined. This was done experimentally. The cooling output can be obtained from the heat balance equation

$$Q_c = Q_{st} + Q_\ell \qquad (4.17)$$

where

Q_c = cooling output (watts)

Q_{st} = heat drawn from storage in the mass of the room

Q_ℓ = heat loss through the walls.

Therefore, the objective of this test is to determine Q_{st} and Q_ℓ experimentally in order to obtain Q_c. Both Q_{st} and Q_ℓ can be calculated if the thermal properties of the various components of the room are obtained (i.e. thermal resistances and capacities).

4.6.1 Description of the Test

The test was carried out in a well insulated, air tight test room inside the thermal environment laboratory at the Centre for Building Studies. The room had a square plan (3.05 x 3.05 m^2) and its height was 2.44 m. The thermal coefficients calculated for the components and contents of the room are shown in Table 4.3. The room was equipped with a set of fixed copper tubes used for testing heat exchangers.

The test chamber was instrumented with 31 copper - constantin thermocouples. The thermocouples (TC) were distributed as follows:

room air: dry bulb (2 TC), wet bulb	(1 TC)
ambient air near the external surfaces	(6 TC)
the external surfaces of the room	(12 TC)
copper tubes	(1 TC)
water storage	(2 TC)

The heating was provided by two base-board heaters,with a total combined output of 2.5 Kw. The cooling unit was installed on one of the walls of the test chamber and controlled from the outside. A data acquisition system (Doric 220 Digitrend) was used to record the temperature measurements every 5 minutes. In both the heating and the cooling cycles the air inside the chamber was circulated continuously to minimize stratification and maxmize the uniformity of the temperature. During this test, 2 barrels of water and a steel beam were used to introduce extra thermal storage inside the chamber. Thermocouples were

calibrated by immersing them in boiling water to check the boiling temperature (100°C) and in melting ice to check the melting temperature (0°C). An ice point instrument (KAYE's Ice Point Reference) was used also to check the zero point.

4.6.2 Determination of the Effective Thermal Properties

As a preliminary step, effective thermal resistances and capacities of the room elements were determined in a heating experiment. The two base board heaters of combined output of 2.5 Kw were put inside. The heaters output is calibrated by measuring the voltage and the current. The heaters power (in watts) is the product of the voltage and the current (amp). The temperatures of the room air, external surfaces, internal surfaces, ambient air, and storage materials inside (copper) were measured every 5 minutes. The thermal storage capacity of the room was then increased by placing a steel beam and two barrels full of water inside. The experiment was then repeated. The thermal network used to simulate measured temperatures before and after increasing the thermal storage are shown in Fig. 4.17 a and 4.17 b respectively. The 20 thermal resistances and capacities shown in table 4.3 were obtained by fitting temperatures calculated from the models to the 234 spatial average measured temperatures. The equations shown in Sec. 4.6.4 were solved by Gauss elimination using the Cyber 170-174 computer at Concordia. The program is shown in Appendix B. The initial R's and C's were calculated by ASHRAE methods and are shown in Table 4.3. For each run, measured temperatures were used to begin the calculation at time zero.

The twenty parameters were varied manually in consecutive runs in groups of 4. The variation started with the parameters which produced the most diverted calculated temperatures from the corresponding measurements. After the best fit for each of the 5 groups had been found the process was repeated 6 times until the sum of the squares of the differences between computed and experimental temperatures changed by less than 5% of the previous best fit value. The best fit temperatures are shown in Figs. 4.18 and 4.19, and the best fit parameters are shown in Table 4.3. A sensitivity test revealed no other minima within $\pm$ 35% of the initial R's and C's values.

4.6.3 Determination of the Cooling Capacity of the Air Conditioning

Once the resistances and capacities of the components of the room had been determined, the cooling capacity of the air-conditioner was determined from simulations of the temperatures observed in two similar experiments using a constant output from the air conditioner. In these simulations, the resistances and capacitance were kept constant at the best fit values from the heating experiments, and only the cooling capacity was varied to obtain a best fit. The cooling capacity of 1.432 Kw gave the best fit for both cases (Figs. 4.20 and 4.21) and was taken as the cooling capacity of the air-conditoner for the experiments in the test chamber on the roof.

4.6.4 Thermal Network Analysis

The thermal networks of the models in Figs. 4.17 a and 4.17 b can be

analyzed with the methods of Chapter II. The heat transfer rate q from point a to point b is related to the thermal resistance, R, between the two points and the temperature difference between them by

$$q = \frac{T_a - T_b}{R} \tag{4.18}$$

This has the same form as Ohm's law, $i = \frac{V_a - V_b}{R}$, so q, R and T are analogous to electrical current, resistance and voltage respectively. During these experiments, the room surrounding the test chamber had a near constant temperature of 30°± 0.5°C. The horizontal variation in air temperature around the test chamber was negligible (0.2°C), while the vertical gradient was 1.2°C, so uniform wall temperature were used in the simulation. The air inside the test chamber was thoroughly stirred with a fan to ensure uniformity of temperature and horizontal temperature gradients were unmeasurable while vertical gradient were only about 3°C per 2.44 m height. We therefore used a unidimensional thermal analysis for each wall. Because of the copper, steel and water storages, however, the overall problem is two-dimensional (Fig. 4.14 b). Similar to the procedure described in Chapter II, the implicit representation of a one-dimensional transient state heat transfer to or from a node i using the finite-difference approximation is

$$T_i + \sum_{j=1}^{2} a_{ij} T'_j = b_i \tag{4.19}$$

where

$$a_{ij} = - N_i / L_i \, R_{ij}$$

$$b_i = (T_i / L_i) + (N_i \eta_i / L_i)$$

and the parameters N_i, L_i, and η_i are given in Eq. 2.52 of Chapter II.

Applying Eq. 4.19 to each node of the system will result in a set of n equations in n unknown temperatures i.e. for the thermal network shown in fig. 4.14 a, the set contains six equations

$$
\begin{aligned}
T_1' + a_{12}\,T_2' + a_{15}\,T_5' &= (T_1/L_1) + (N_1 n_1/L_1)\\
T_2' + a_{12}\,T_1' + a_{23}\,T_3' &= (T_2/L_2)\\
T_3' + a_{23}\,T_2' + a_{34}\,T_4' &= (T_3/L_3)\\
T_4' + a_{34}\,T_3' &= (T_4/L_4) + (N_4 n_4/L_4)\\
T_5' + a_{15}\,T_1' + a_{56}\,T_6' &= (T_5/L_5)\\
T_6' + a_{56}\,T_5' &= (T_6/L_6)
\end{aligned}
\qquad (4.20)
$$

where $n_1 = 2.5$ Kw (the heater power for the heating experiment) and $n_4 = (T_{amb}/R_{4\text{-}amb})$. The initial temperatures used were the initial temperature measurements. The solution for the future temperatures was obtained by using Gauss elimination.

Further, the calculation is checked using the heat balance given by Eq. 4.17. The rate of heat stored in the system during the time interval ΔT is then obtained from

$$Q_{st} = \frac{1}{\Delta T} \sum_{i=1}^{n_k} C_i (T_i' - T_i) \qquad (4.21)$$

where n_k is the total number of nodes in the network (i.e. $n_k = 6$ for the thermal network shown in Fig. 4.14a) the rate of heat loss at the external surface

$$Q_\ell = (\bar{T}_4 - \bar{T}_{amb}) / R_{4\text{-}amb} \qquad (4.22)$$

where $\bar{T}_4$ and $\bar{T}_{amb}$ are the average temperature during each time increment for the external surface and the ambient air respectively. In any time increment $Q = Q_{st} + Q_\ell$

Node	Temperature K°	Thermal Capcity, Kw hr/K° Initial	Best fit
room air	T_1	(C_1) 0.012	0.009518
wall internal surface	T_2	(C_2) 0.092	0.0832
wall bulk	T_3	(C_3) 0.226	0.2176
wall external surface	T_4	(C_4) 0.092	0.0932
copper tube surface	T_5	(C_5) —	0.0001
copper tube bulk	T_6	(C_6) 0.0163	0.0191
steel beam surface	T_7	(C_7) —	0.0001
steel beam bulk	T_8	(C_8) 0.0168	0,0140
water barrel surface	T_9	(C_9) —	0.0001
water bulk	T_{10}	(C_{10}) 0.156	0.139
ambient air	T_{11}	—	—

a) Initial and final values of thermal capacities

Node	Thermal Resistances m.K/w Initial	Best fit
wall internal surface layer	(R_1) 1.96	2.48
wall internal surface-wall centre	(R_2) 23.3	26.92
wall centre-wall external surface	(R_3) 23.3	26.92
wall external surface layer	(R_4) 1.96	2.30
copper surface layer	(R_5) 30.8	36.61
copper bulk	(R_6) 0.009	0.005
steel surface	(R_7) 31.5	32.5
steel bulk	(R_8) 0.06	0.042
water barrel surface	(R_9) 59.3	57.8
water bulk	(R_{10}) 106.1	119.83

b) Initial and final values of thermal resistances .

Table 4.3: Initial and final values for the calculation of the room effective thermal parameters.

a) Thermal capacities, b) Thermal resistances.

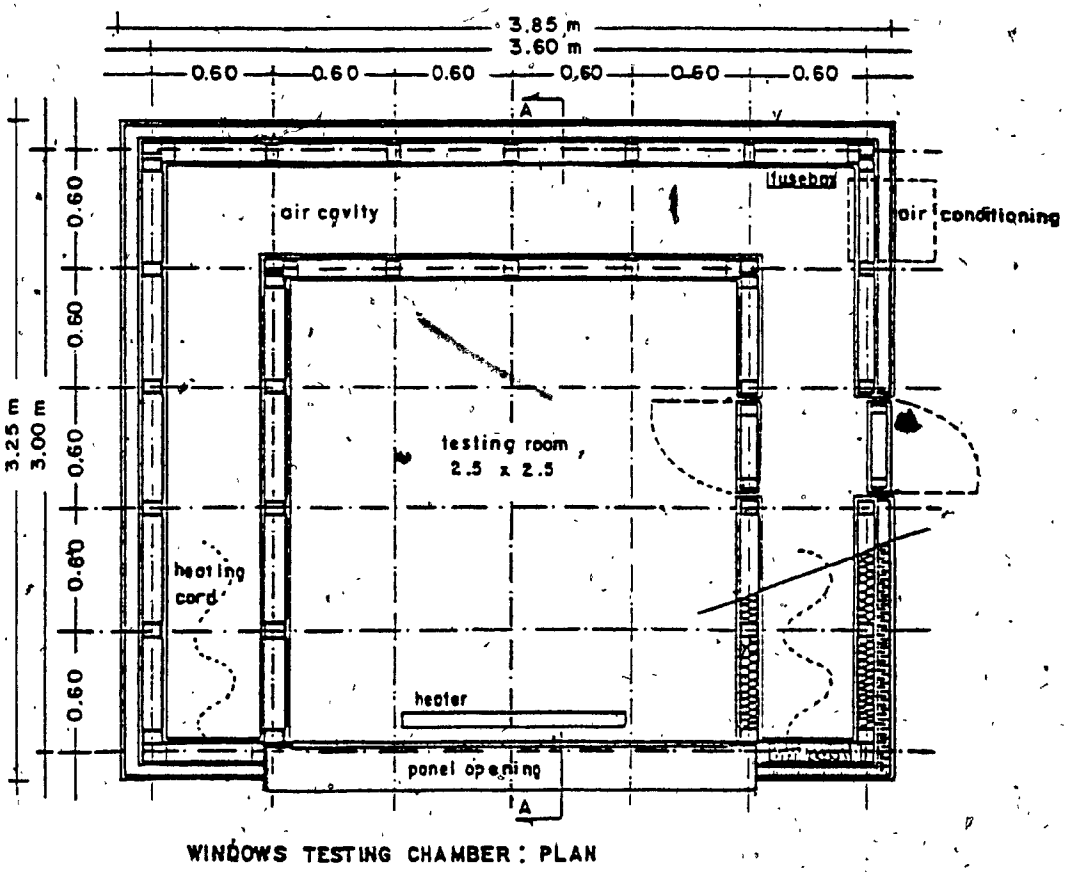

Fig. 4.1: Horizontal section through the test chamber

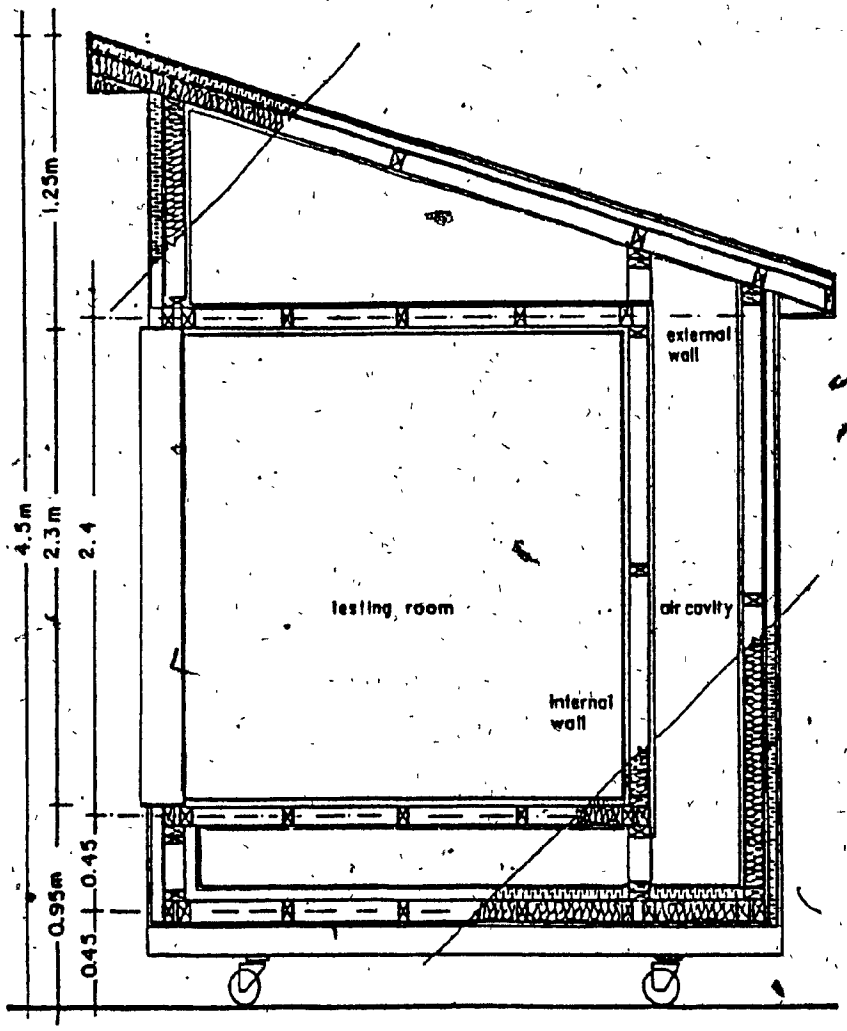

WINDOWS TESTING CHAMBER : SECTION A.A

Fig. 4.2: Vertical section through the test chamber

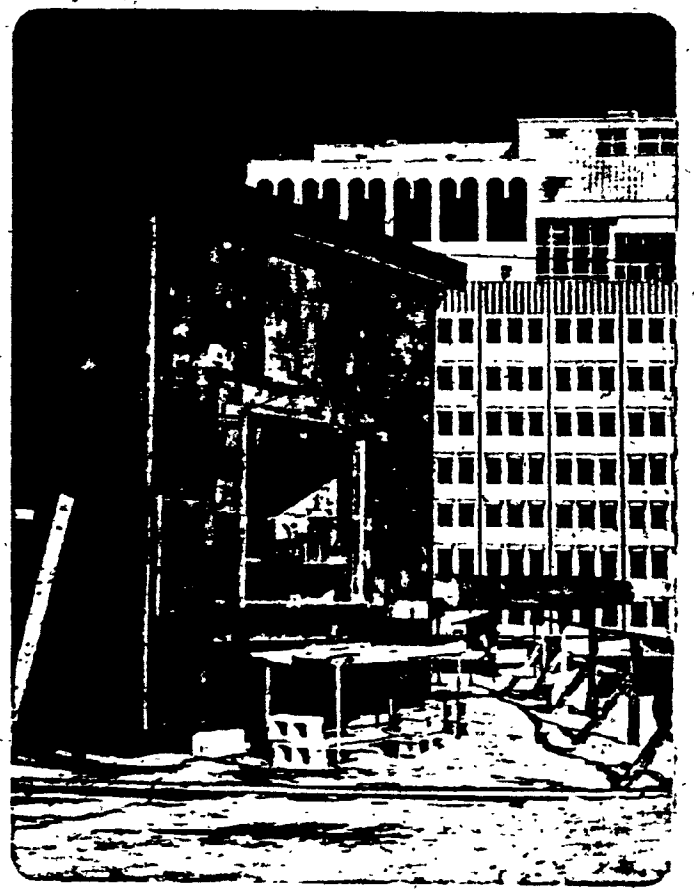

a) A panel with 0.5 window-to-wall area ratio under test

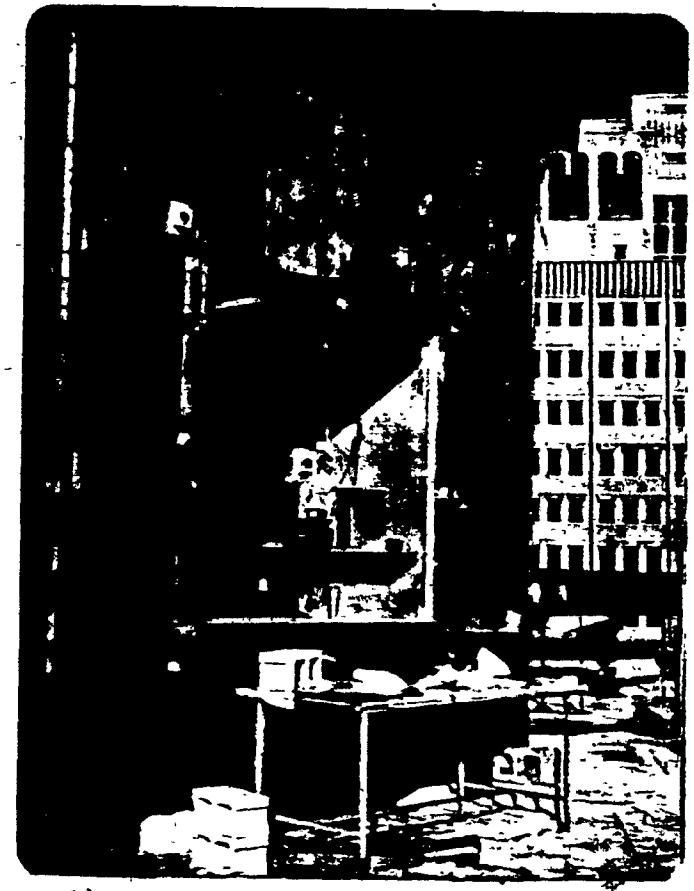

b) A panel with 0.75 window-to-wall area ratio. Vertical solar cells and thermocouples are shown

Fig. 4.3: Panels with .50 and .75 window-to-wall area under test

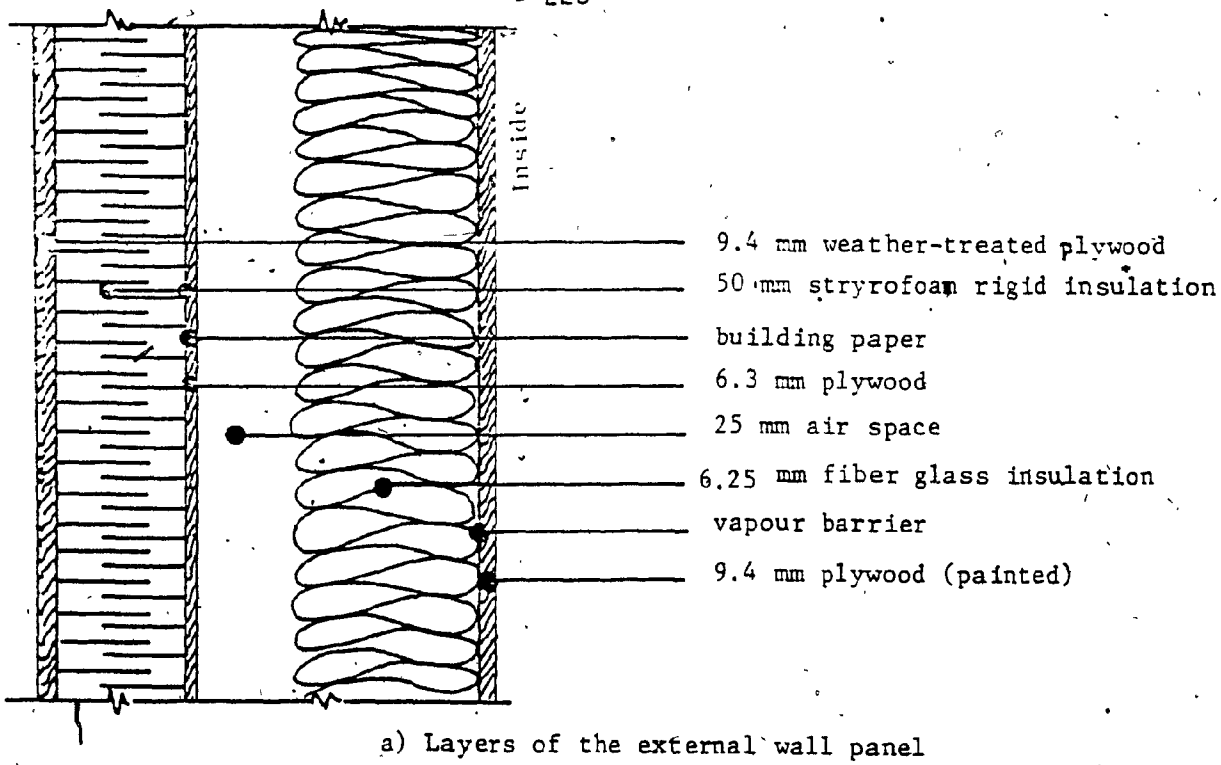

a) Layers of the external wall panel

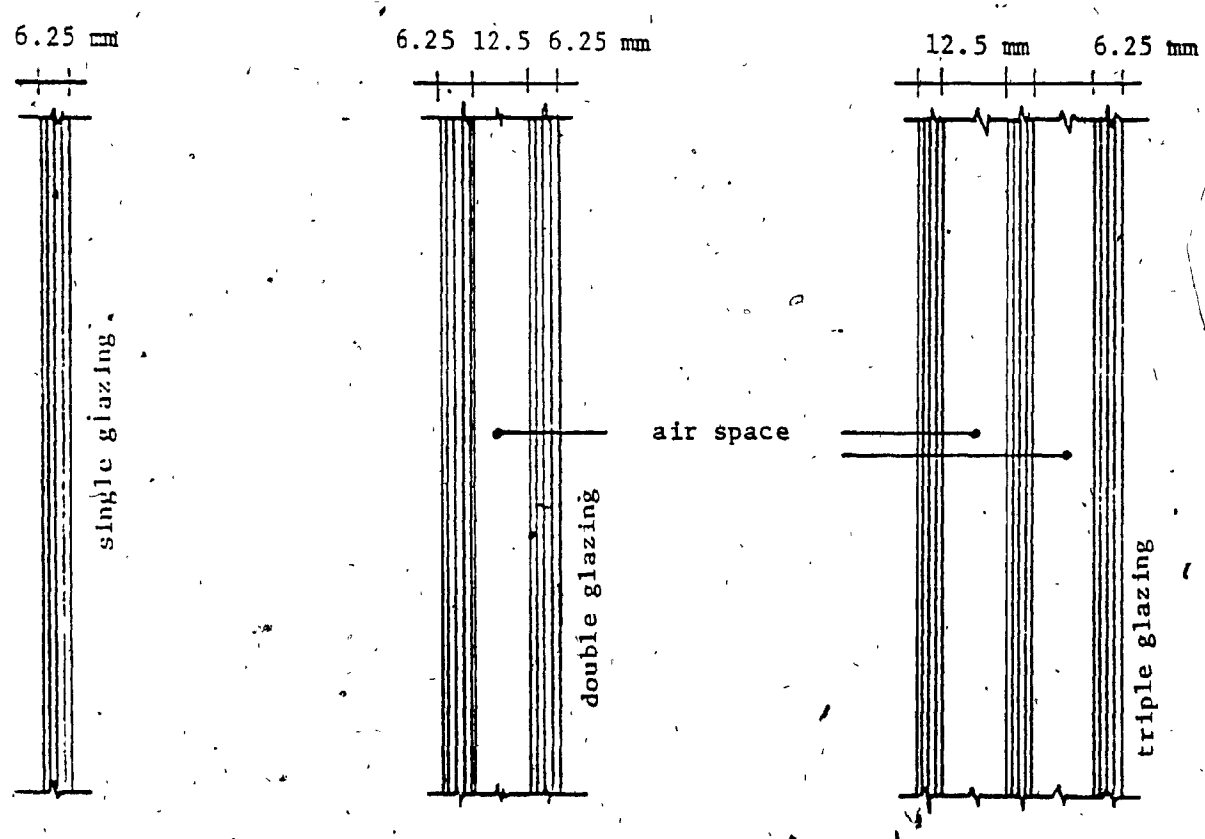

b) Layers of single, double and triple glazing used

Fig. 4.4: Vertical section through external walls and windows

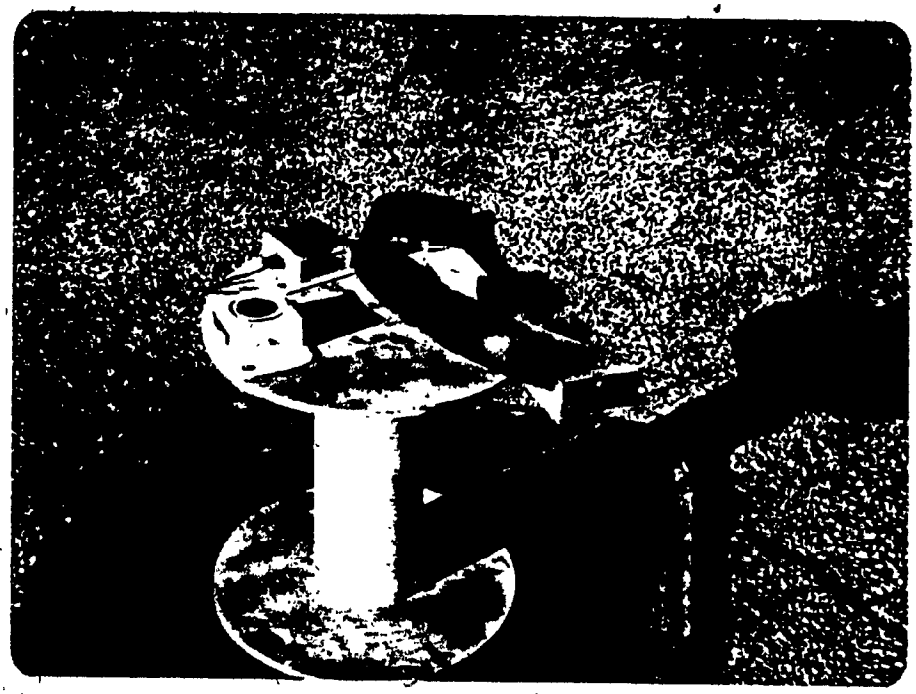

a) Solar sensors used for measuring total and diffuse solar radiation on the horizontal surface

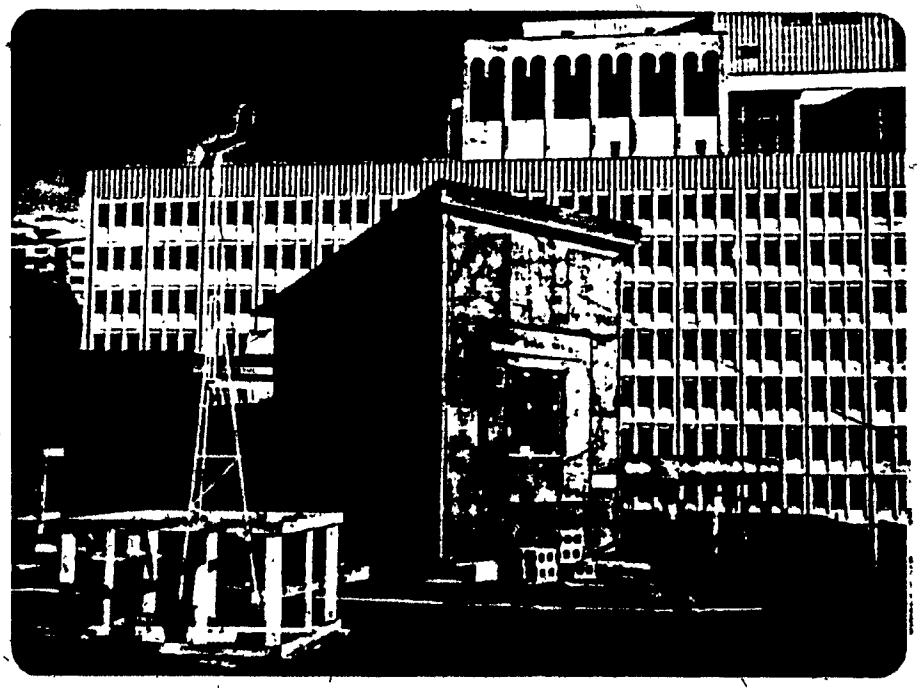

b) The Bendix Aerovane wind speed and direction instrument used for wind measurements near the test chamber

Fig. 4.5: Radiation and wind instruments.

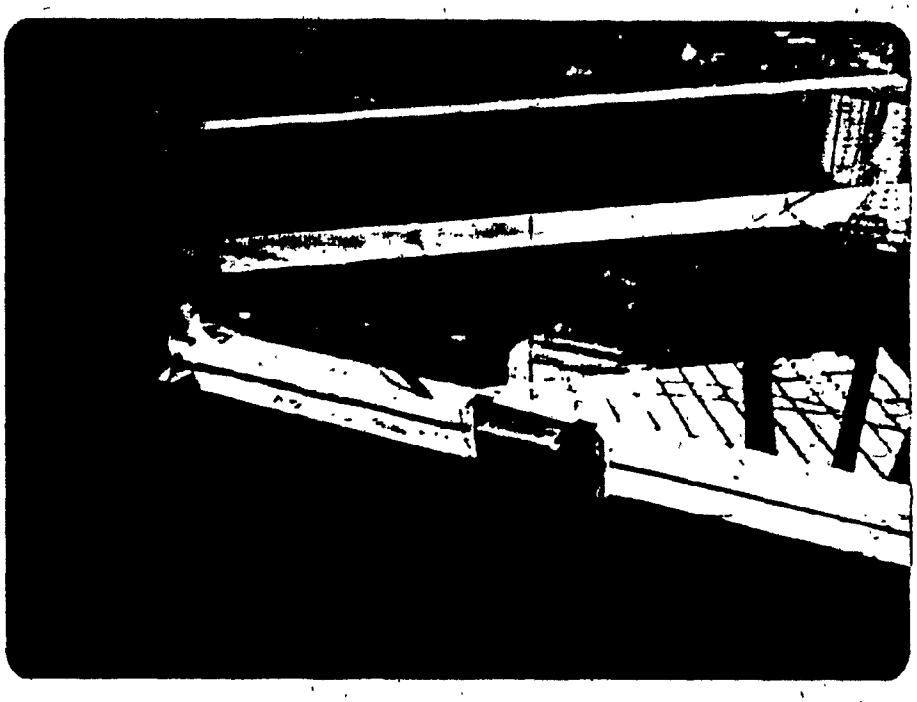

Fig. 4.6a: Solar cells #5 and #6 (back-to-back) to measure transmitted radiation and radiation reflected from the room

Fig. 4.6b: The temperature digital displayer is shown on the left-hand side, solar chart recorders and the wind speed and direction in the middle and the wind speed companion synchro on the right hand side.

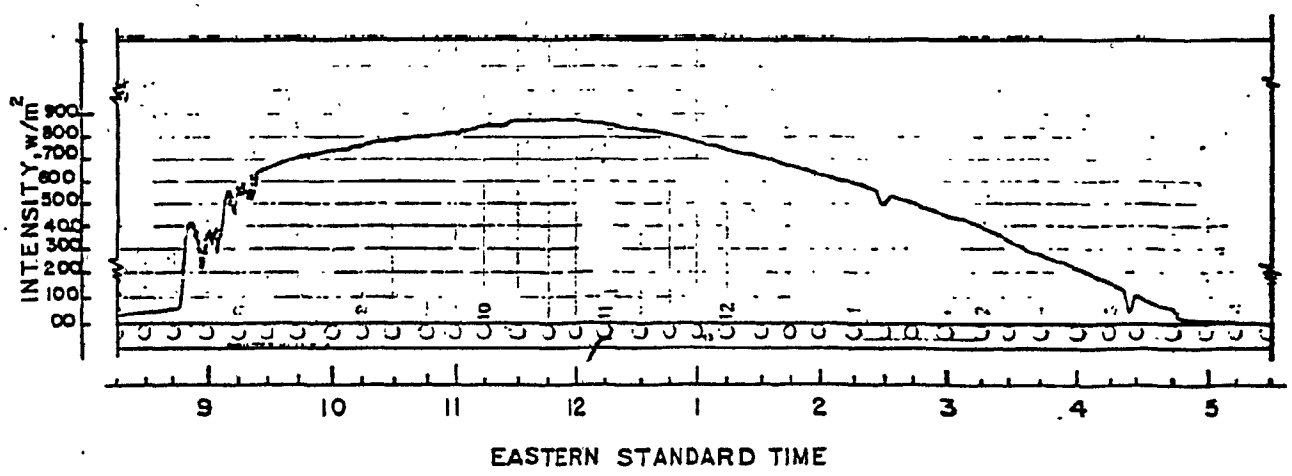

Fig. 4.7a: A sample of the measured global radiation on the external surface of the panel while it was facing due south (Jan. 20, 1980).

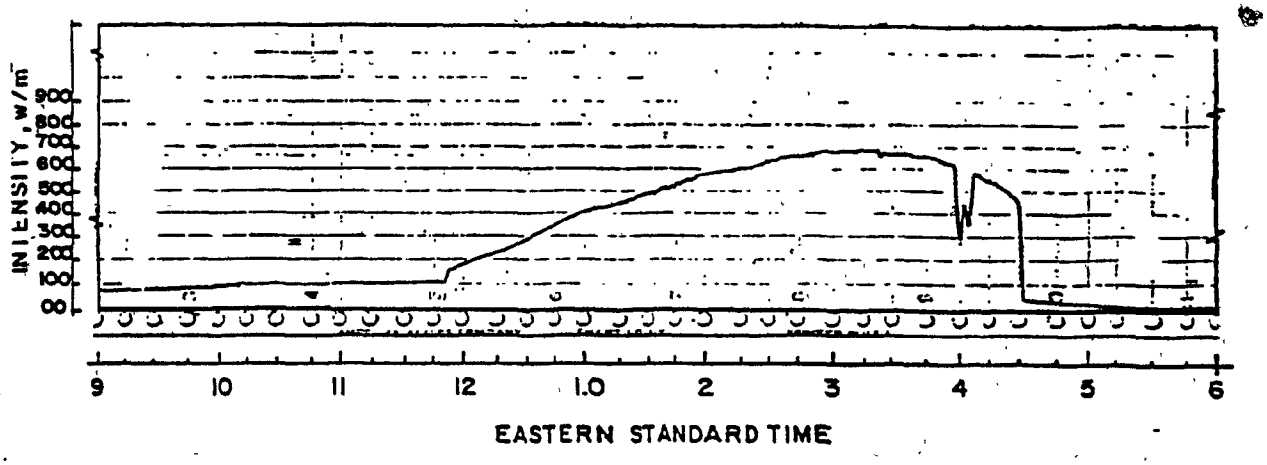

Fig. 4.7b: A sample of the measured global radiation on the external surface of the panel while it was facing due west (Feb. 8, 1980).

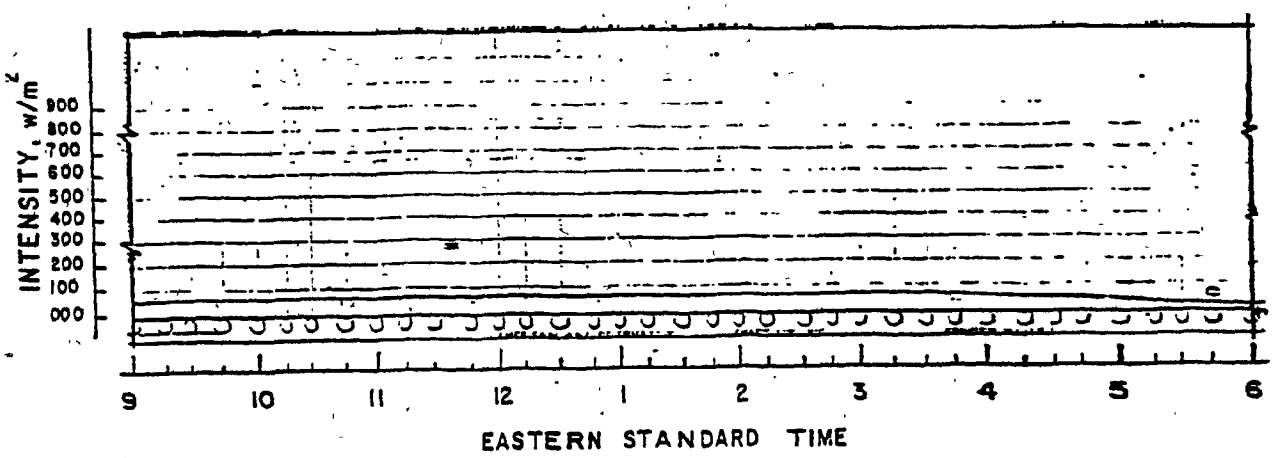

Fig. 4.8a: A sample of the measured global radiation on the external surface of the panel while it was facing due north (March 30, 1980).

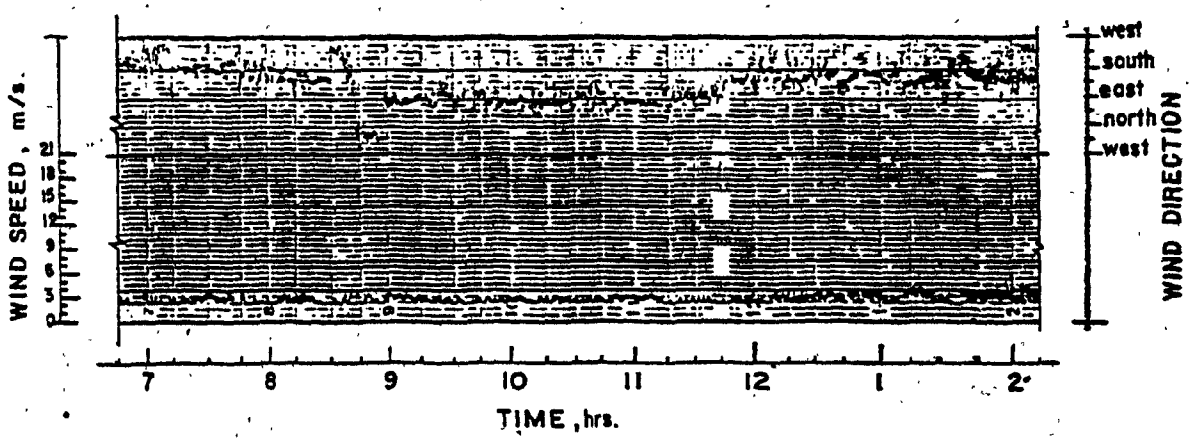

Fig. 4.8b: A sample of the measured wind speed and direction.

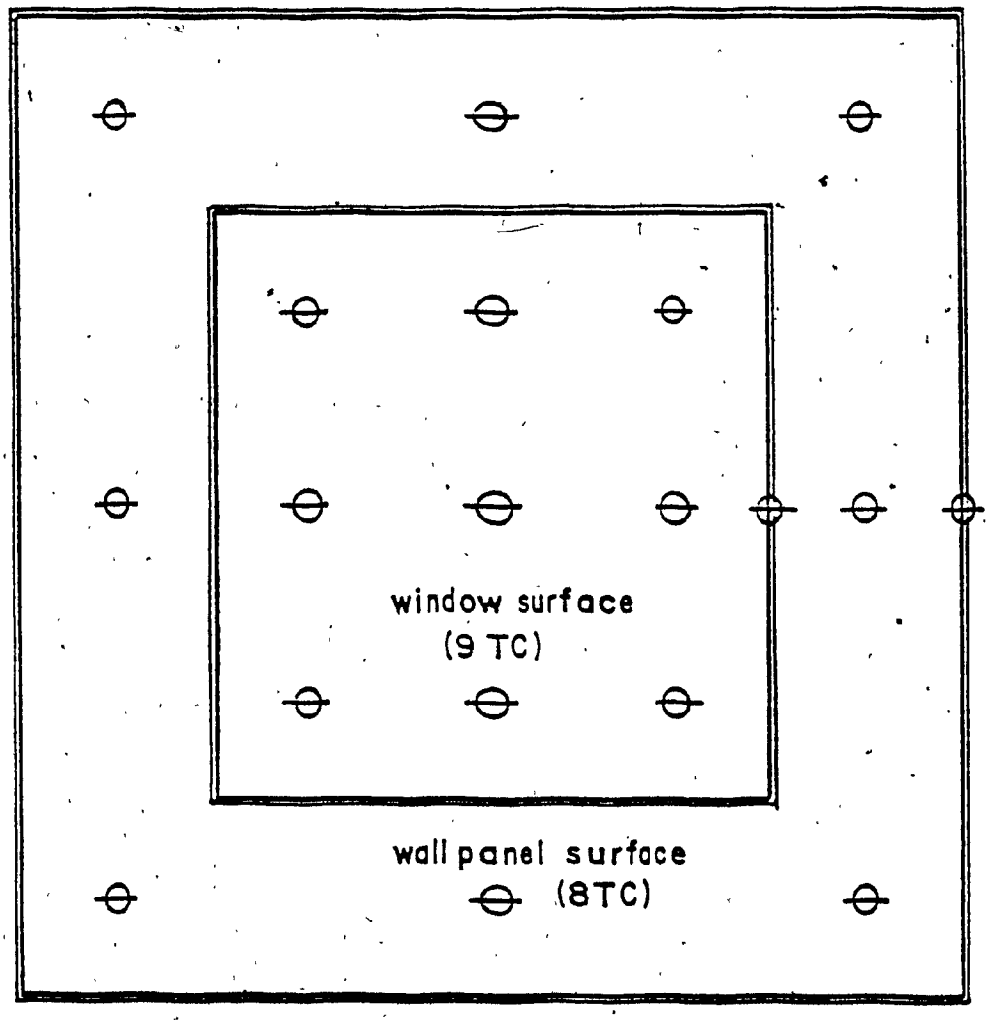

Fig. 4.9: Location of the thermocouples distributed on the external and internal surfaces of the window and the wall panel.

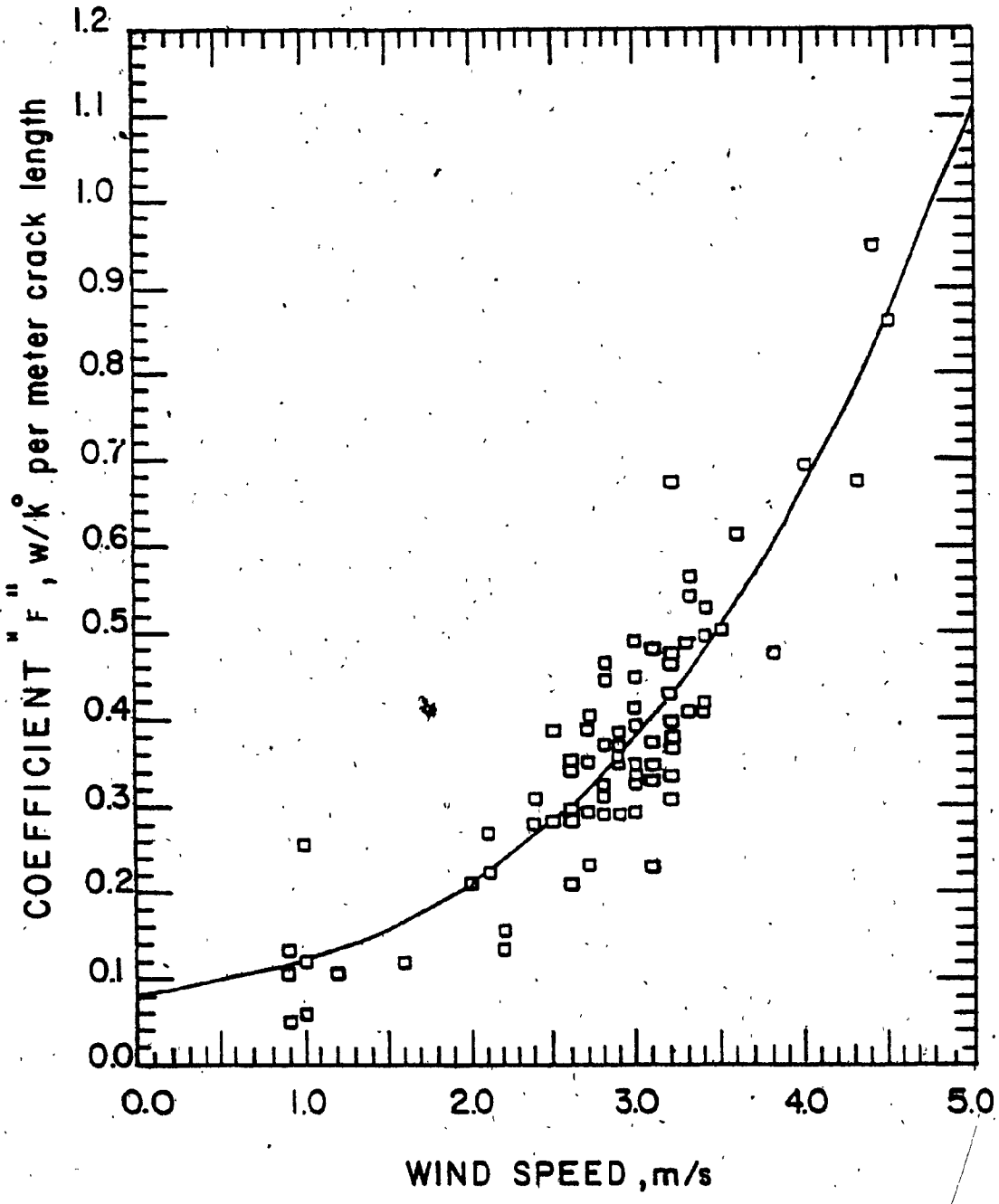

Fig. 4.10: Third degree polynomial regression of the relation between the measured values of coefficient F and wind speed.

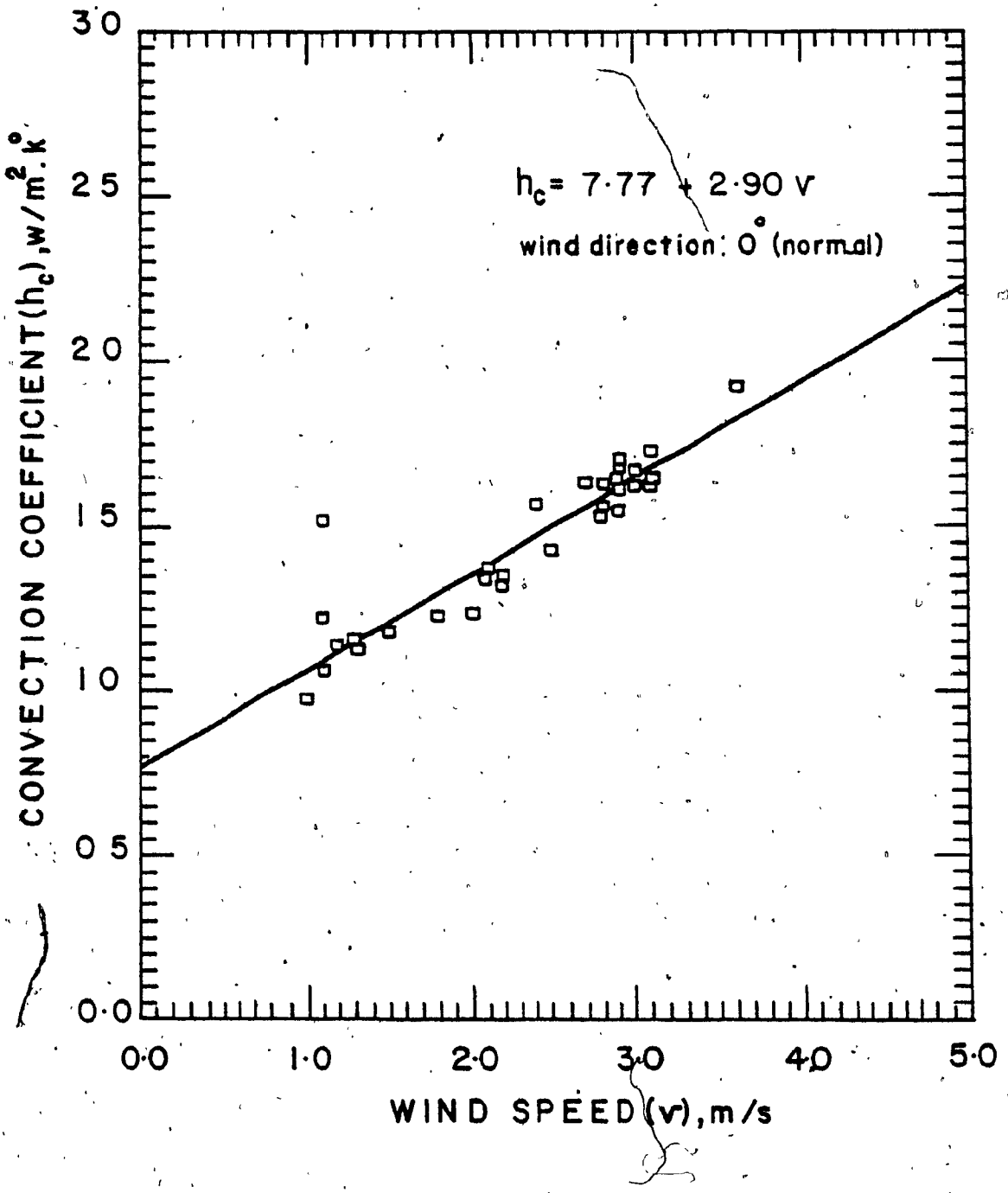

Fig. 4.11: Convection coefficient as a function of wind speed for wind direction normal to the surface.

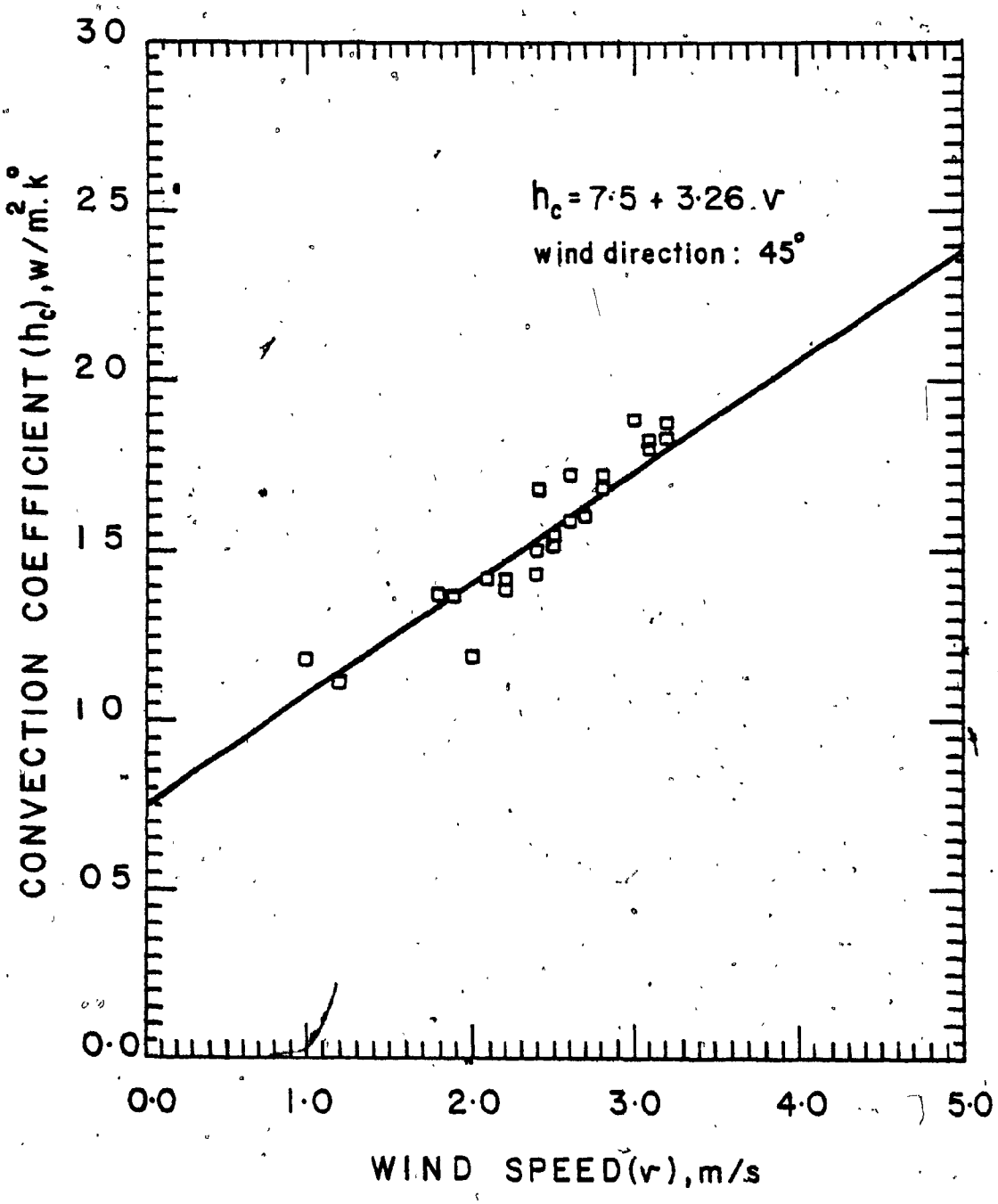

Fig. 4.12: Convection coefficient as a function of wind speed for wind direction 45° from the normal to the surface.

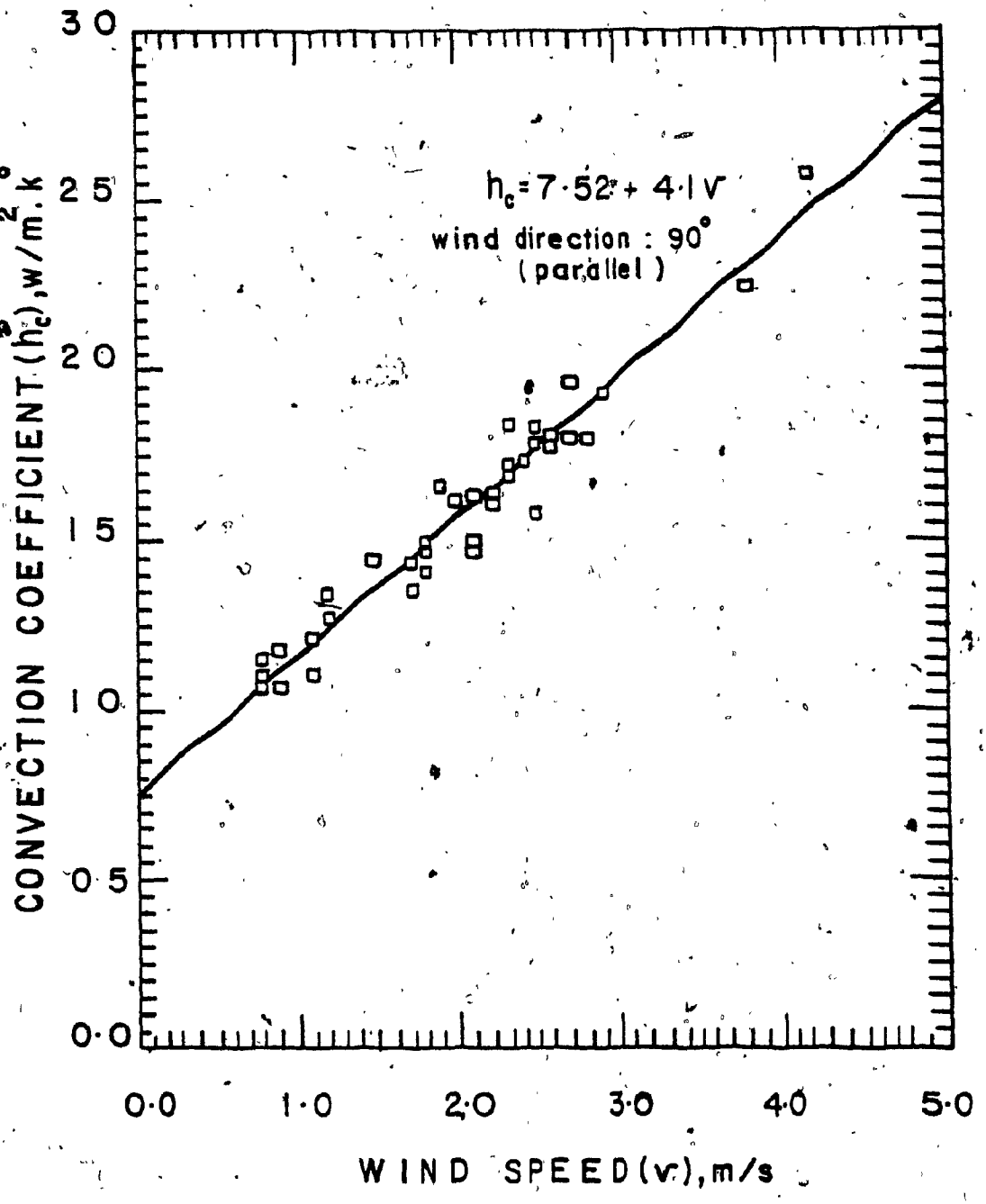

Fig. 4.13: Convection coefficient as a function of wind speed for wind direction parallel to the surface.

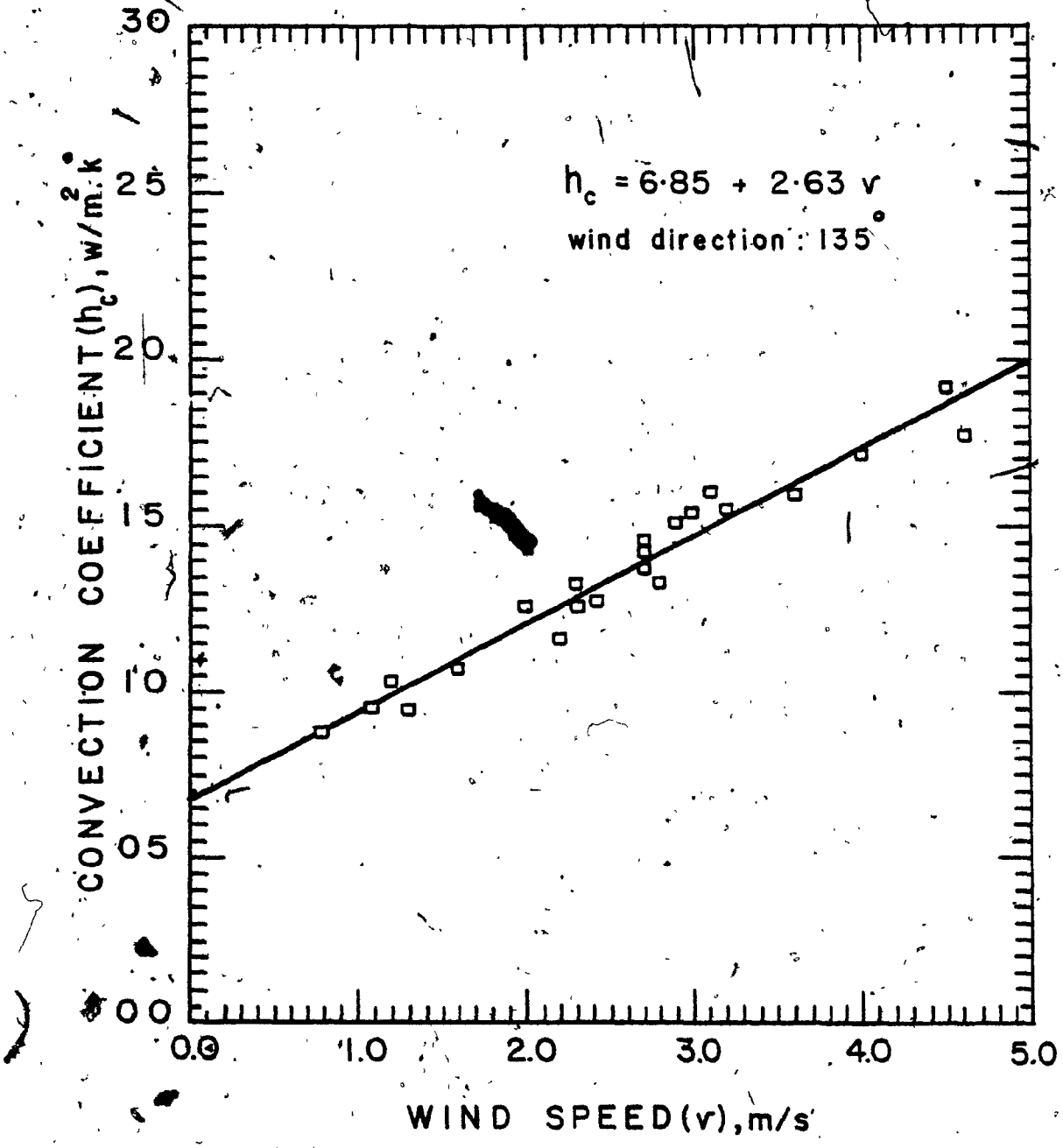

Fig. 4.14: Convection coefficient as a function of wind speed for wind direction 135° from the normal to the surface.

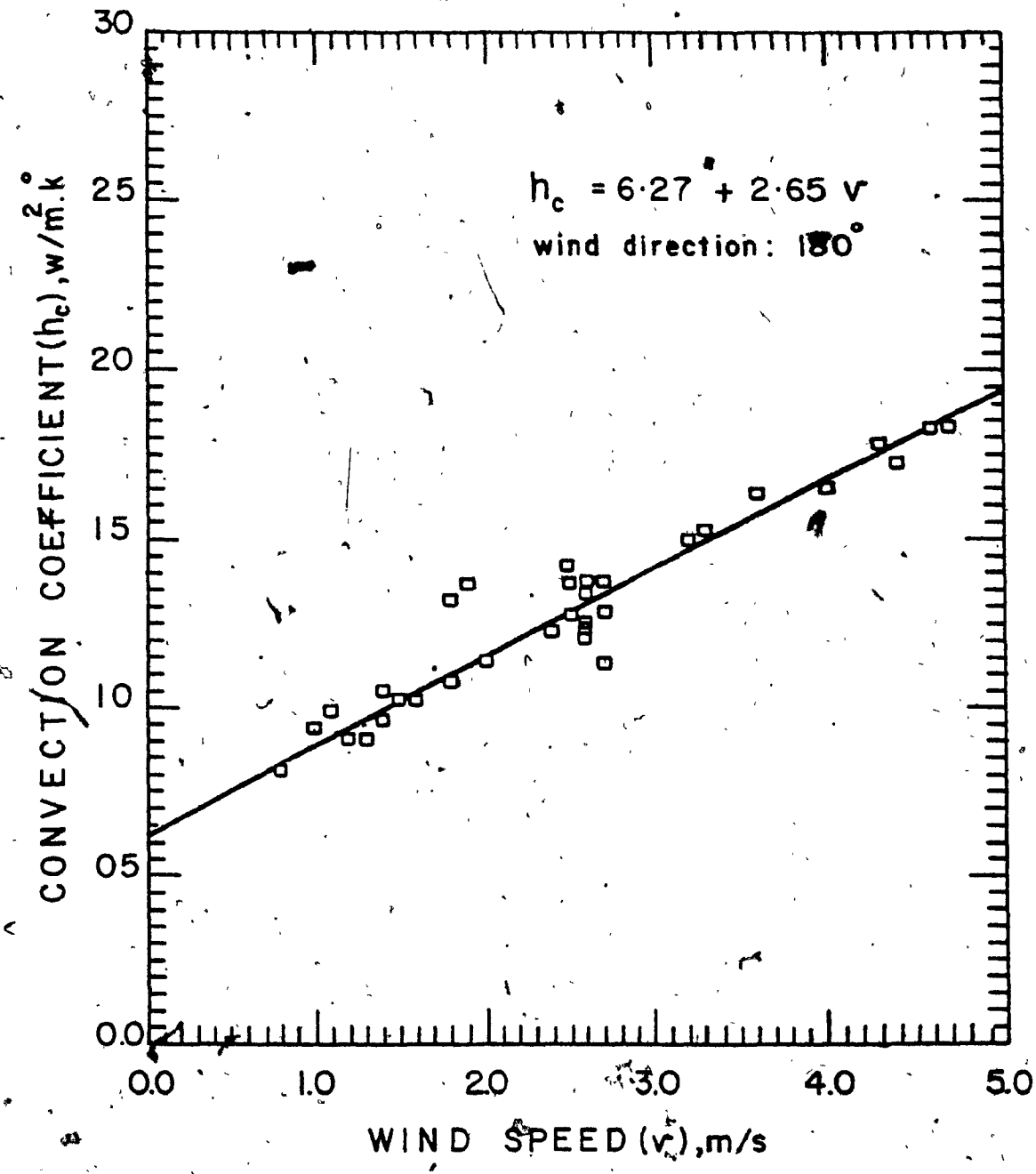

Fig. 4.15: Convection coefficient as a function of wind speed for wind direction 180° from the normal to the surface.

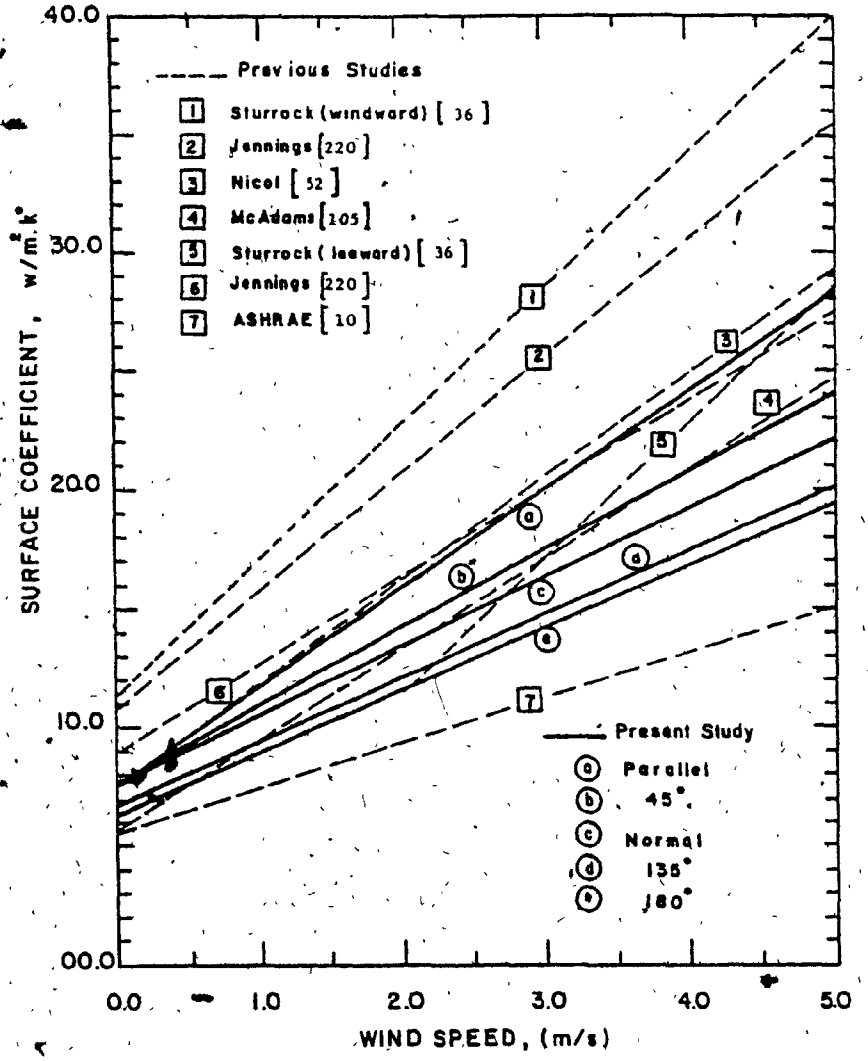

Fig. 4.16: Comparison between the results of the present study and the results of previous studies relating the convection coefficient to wind speed.

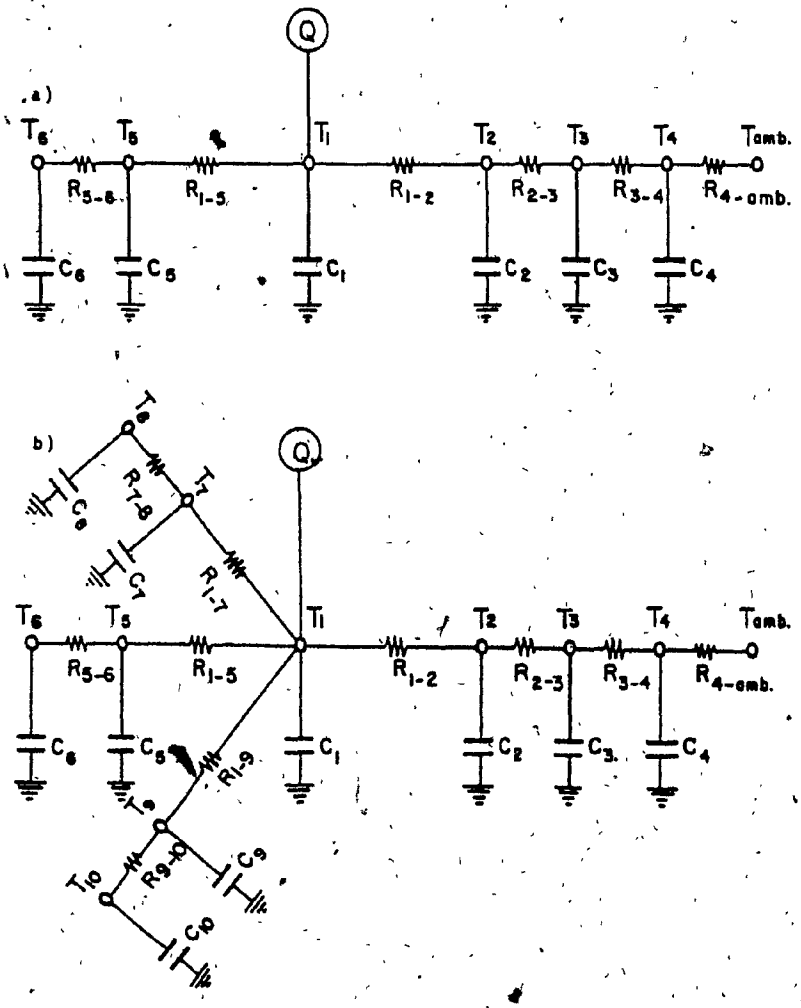

Fig. 4.17: Thermal networks showing thermal resistance and capacities of room elements:
a) before increasing the thermal capacity
b) after increasing the thermal capacity

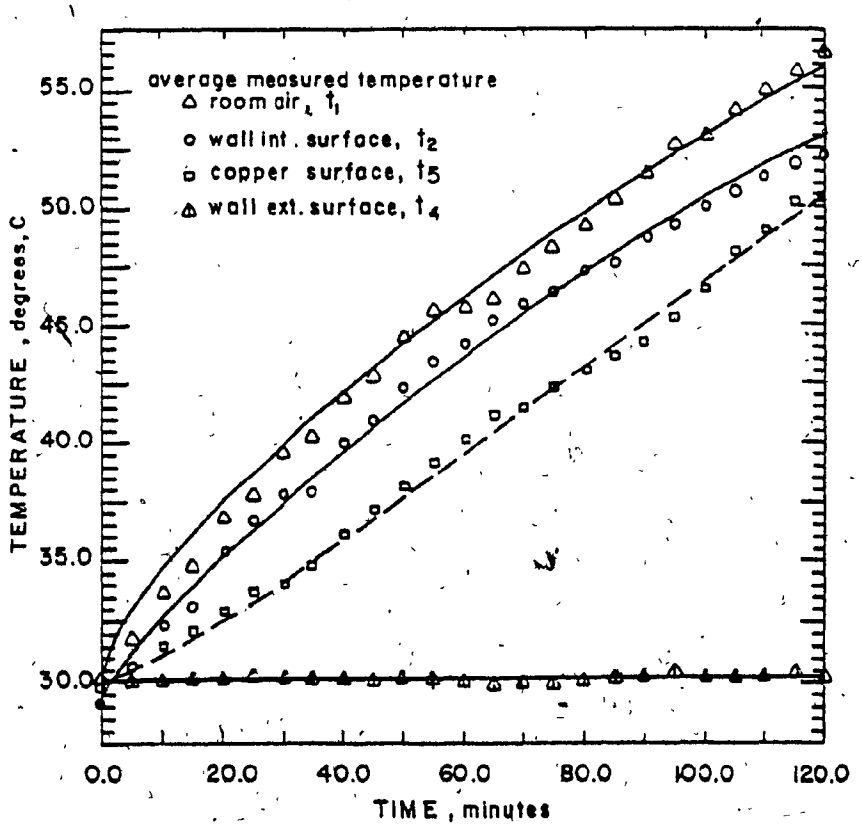

Fig.4.18 : Calculated temperatures best fitted to the average measured temperatures in the heating experiment before increasing the thermal storage capacity of the room.

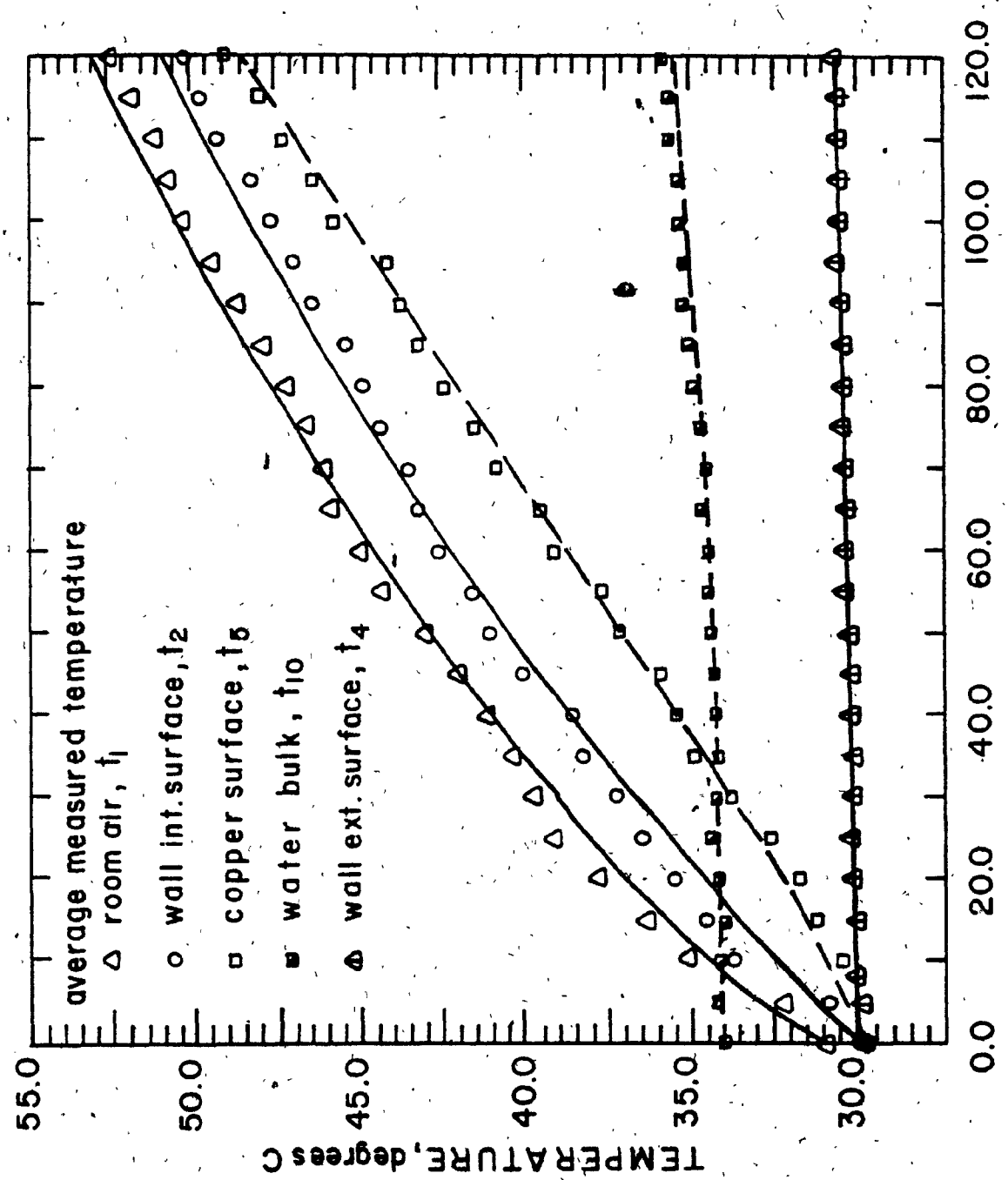

Fig. 4.19: Calculated temperatures fitted to the average measured temperatures in the heating experiment after increasing the room thermal storage.

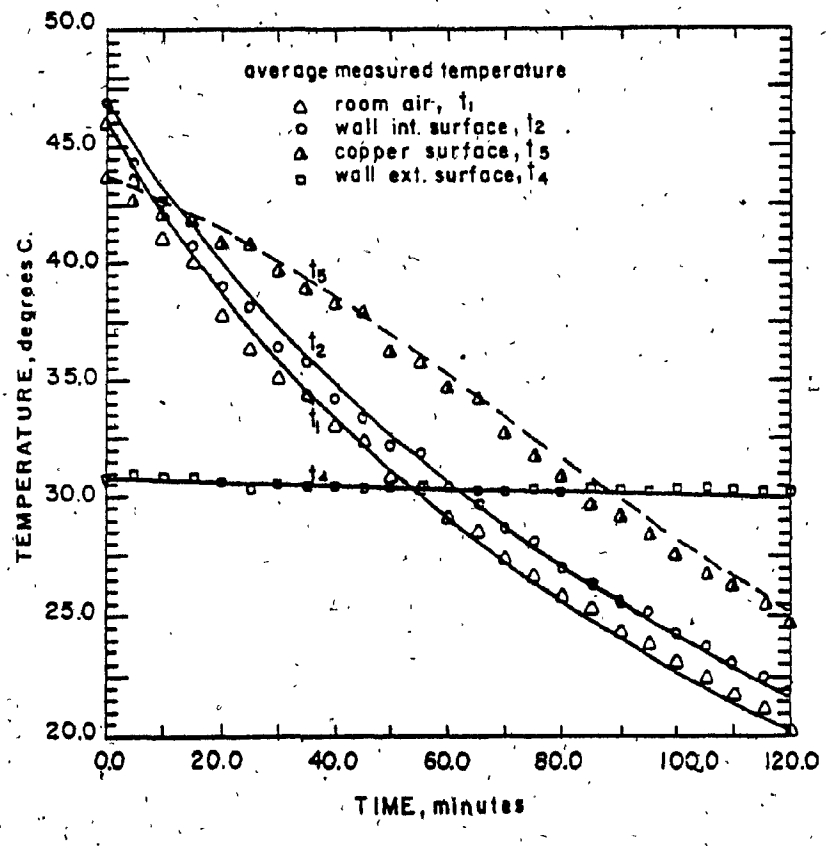

Fig. 4.20 : Calculated temperatures best fitted to the average measured temperatures in the cooling experiment before increasing the room thermal storage capacity.

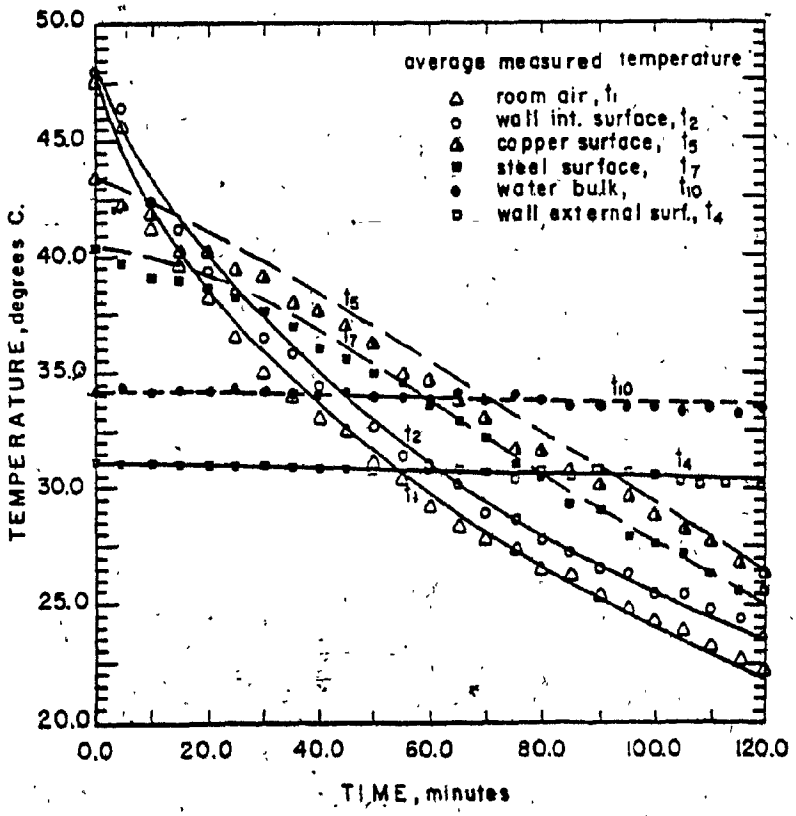

Fig.4.21 : Calculated temperatures best fitted to the average measured temperatures in the cooling experiment after increasing the thermal storage capacity of the room.

CHAPTER V

RESULTS AND DISCUSSION

5.1 INTRODUCTION

The main objective of this chapter is to discuss and to review both the calculated and the measured results obtained from this study. We focus on the following aspects: i) the basis for determining the optimal window-to-wall area ratio with respect to energy gain or loss; ii) the importance of the thermal storage capacity in the room for determining the optimum window-to-wall area ratio; iii) the comparison between the calculated and measured temperatures of windows and walls; iv) a detailed discussion of the calculated and measured net energy loss or gain from windows and walls; v) the impact of the window-to-wall area ratio, window orientation, and the type of glazing on the amount of energy savings from daylight; and vi) the net energy gain from replacement of electric lighting by daylight combined with the losses through the glazing, and the impact on choice of window-to-wall area ratios.

5.2 The Basis for the Determination of a Window-to-Wall Area Ratio for Minimal Consumption of Purchased Energy

The optimal window-to-wall area ratio is dependent on many factors, such as:

i) The particular goal of the designer: For example the designer can choose a single goal, (i.e. minimization of heat loss by conduction, minimization of heat loss associated

with air infiltration, maximization of energy savings through the use of natural daylight) or a combined goal (i.e. minimization of total energy loss, maximization of total energy gain, or maximization of the net energy gain). The present study has a combined goal which is the net energy gain or loss of both window and wall. This is the sum of the energy gain from solar radiation, the reduction in electric lighting use from utilization of daylight, the possible increase in space heating energy use because of the higher luminous efficiency of daylight, the conduction, convection, and radiation losses, and air infiltration losses on a sunny winter day. Note that in summer conditions, the luminous efficiency of daylight becomes an energy asset while solar gains increase the cooling energy requirements. Summer conditions were not studied here.

ii) The variables taken into consideration: The variables involved in this study can be classified into two groups: a) design variables, which represent the thermophysical properties, optical properties, and the geometry of the window and the wall; b) climatic variables which represent outdoor air temperature, intensity of solar radiation, wind speed, and wind direction.

iii) The architectural constraints imposed on the design by the construction materials used: These constraints have an impact on the optimal window-to-wall area ratio because of

the losses through the specific type of glazing and the specific wall construction.

iv) The impact of building codes: Despite the fact that building codes are often independent of energy calculations, structural limitations, accoustical limitations, the spacing and height allowed for neighbouring buildings, and the reflective properties of those facades can affect the optimal window-to-wall area.

v) The impact of the time span for the calculations: The time span for the energy calculation has a significant impact on the resulting optimal window-to-wall area ratio. The time span can be a "typical" winter day, a "typical" summer day, a "typical" month, a "typical" season, or a "typical" year. Depending on the designer's objective, the appropriate time span can be utilized with this model. Both the thermal and daylight models, that were presented in chapters II and III respectively, were structured to calculate hourly energy gains and losses for any given time span.

The time span for the present study was determined according to several factors. In Montreal, due to the relatively long winters, it is necessary to use heating in all buildings for about two-thirds of the year. Also, in the winter, the inside-outside air temperature difference is several times greater than the difference in the summer. Cooling is used only in some large buildings. A large portion of the

cooling load in these buildings is needed to offset the internally generated heat (lighting, equipment, and people), and humidity which are independent of the window-to-wall area ratio. The only significant portion of the cooling load that is affected by the window-to-wall area ratio, is the solar heat gain, which can be avoided partially or fully through the use of solar control devices (i.e. reflectors, shades, and shutters). One of the objectives of the case study of section 5.8 was to apply the thermal and daylight models to compare the net energy gain or loss of a wall panel or a panel with a window. Since the winter is the season in which the energy gains and losses are more apparent, the case study will be examined under winter climatic conditions. In order to test 30 different panels under similar winter conditions, during one winter season, the time span chosen for each test was 24 hours. Accordingly, the time span chosen for the simulated case study was a typical winter day (a clear January 21st).

5.3 Importance of the Thermal Storage Capacity of The Room

Thermal storage in the mass of the room was ignored in the experimental validation of the model, because of the light construction of the rotating test room. However, the storage of surplus solar heat transmitted through the window is an important factor in the determination of the appropriate window-to-wall area ratio. In the case of a non-air- conditioned room with too little thermal storage, the surplus heat gain causes thermal discomfort. With sufficient storage, and the proper number of window panes to reduce losses, the optimal window-to-

wall area ratio can be larger. In the case of an air-conditioned room, the surplus heat gain will not cause any thermal discomfort but will increase the energy consumption for cooling.

Thus, the appropriate window area, in an air-conditioned room, is that which provides enough solar heat gain to offset the heat loss by conduction and infiltration without raising room temperature. Similarly, if the internal heat gains exceed the heat losses, energy consumption for cooling increases. This situation was observed in January during the experiments with the windowless panels.

In order to utilize some of the solar heat gain with air-conditioning, thermostats with a wide dead band are required (say 19° to 23°C). Then, with neither heating or cooling between 19° and 23°C, solar heat gain is stored in the mass of the room and can be utilized after sunset. Another alternative is to pass the surplus heat from the sunlit rooms to the opposite side of the building through special ducts. For instance, the morning surplus heat gain in easterly oriented rooms is transferred to westerly oriented rooms and vice versa in the afternoons. Similarly surplus solar heat gain from southerly oriented panels with windows can be transferred to the northerly oriented rooms during sunny winter days. Thus, space heating costs can be reduced and larger window-to-wall area ratios can be used. Consequently, solar heat gain on cool sunny days can be utilized with normal thermostats.

5.4 Comparison Between Simulated and Measured Temperatures for the Rotating Test Chamber

In each experiment, the temperature variation over the external and internal surfaces of both the window and the wall panel were measured. A total of 34 thermocouples were used, half inside and half outside distributed as shown in Fig. 4.9. Since the temperatures of intermediate layers were not measured, the comparison was limited to the external and internal surfaces. For example, comparisons between the simulated and measured temperature variations in time for external and internal surfaces are shown in Figs. 5.1 to 5.6 for the three types of glazing and for window-to-wall area ratios of 0.25 and 0.75. The simulated and measured temperatures are generally in good agreement. The worst differences occur when the temperatures are changing rapidly and part of the window is shaded for double and triple glazing. Then the curve lags the experimental values in time. The most likely cause of this effect is very complex pattern of small convection eddies between the glazing panes. As shown in Fig. 5.8 the spatial distribution of surface temperatures on the window is very complex when part of the window is shaded. In the simulation, spatially uniform convection was assumed between glazing panes. In addition, the calculated temperatures are based on assumed uniform boundary conditions at the window-to-wall panel interface. During the experiments, the glazing boundary temperatures were found to vary by as much as 4°C.

As expected, in all cases, when the test wall panel was exposed to direct solar radiation, the external temperature of the wall was much

higher than the external temperature of the window. This is caused by two main factors: i) the solar absorptance of the dark wood surface of the wall is about seven times that of the glass. ii) The thermal resistance of the wall is 24 times, 10 times, and 7 times greater than the thermal resistance of single, double, and triple glazed windows respectively.

Double and triple windows show an additional thermal advantage in transient calculations when the storage of heat absorbed from the incident solar radiation is taken into account. As shown in Figs. 5.3 and 5.6, the heat absorbed caused the average temperature of the inner surface of the window to be warmer than the inside air temperature, even when the outside air temperature was 30°C lower than the room air temperature. This reverses the direction of the heat transfer by convection and radiation at the inside surface. After sunset, the stored heat replaces some of the purchased heat. As a result, the daily total solar heat gain is increased. A steady state calculation could not reveal these effects. As shown in the figures, the transient simulation agrees well with reality. The average temperatures do not reveal the whole story, however. When triple glazed windows are partially shaded, two opposite directions for the heat flow were found to exist at different parts of the internal surface for a few hours near noon. The internal surface temperature within the shaded area was found to be below room air temperature, while the rest of the internal surface was warmer than the room air. Due to large inside - outside air temperature differences during these experiments (30° to 40°C), the reversed

heat flow was observed only for triple glazing. On milder days, the same effect should be observable for double glazing as well.

5.5 A Comparison Between the Simulated and Experimental Energy Gain or Loss

The hourly simulated net energy gain or loss from each tested panel was compared to the net energy gain or loss obtained from monitoring data. Good agreement was found between the simulated and the experimental values. As an example, the ten cases examined for the south orientation are shown in figs. 5.9 to 5.18. Part of the small differences between simulated and experimental net energy gains or losses arises because inputs to the simulation were assumed constant for each hour, while the hourly experimental inputs were totals for each hour which reflect minute by minute changes.

For 0.5 window-to-wall area ratio and triple glazing the daily total heat is slightly positive (Fig. 5.14) even for a temperature reaching -14°C at night. On milder days, a net gain from double windows would have been found. Had there been no changes for the 0.75 window-to-wall area ratio, the same results would have happened. For 0.50 and 0.75 ratios and triple glazing the conduction convection and radiation losses become gains during part of the sunlit hours. The same is true for the solid panel (0.0 ratio). In some days infiltration losses are larger than conduction, convection and radiation losses. On other days, the reverse is true.

5.6 The Effect of Window-to-Wall Area Ratio, Glazing type, and Orientation on Energy Consumption

The daily net energy gain or loss from each of the thirty tested panels was obtained both from experiments and simulation. The experimental daily net flows are displayed as a function of window-to -wall area ratio for the south, west, and north orientations in Figs. 5.19, 5.20, and 5.21 respectively. On cloudy winter days, we know that the daily energy losses should increase as the window-to-wall area ratio increases. On sunny winter days, solar gains through south, east, or west windows compensate either partially or fully for the loses due to conduction, convection, radiation, and air infiltration. In five of the measured cases, the daily heat gains were positive. The daily energy gained from south and west facing double glazed windows having a 0.75 window-to-wall area ratio provided surplus energy gain. The south facing triple glazed window for both 0.50 and 0.75 area ratios showed higher surplus energy gain than the double glazed window. Similarly, due west double and triple glazed windows (Fig. 5.20) showed a surplus at the 0.75 area ratio. In winter, all north windows are net losers of energy (Fig. 5.21).

The experimental relations between window-to-wall area ratio and the net daily energy gain or loss are influenced by weather differences from one day to another. Despite the fact that all experiments were conducted under mostly sunny conditions, the intensity of solar radiation from one day to another was influenced by atmospheric conditions and the small clouds passing from time to time. Moreover, the daily

profiles of the wind speed and direction differ from one experiment to another, changing the heat losses by convection and infiltration. The ambient air temperature profiles also varied from day to day affecting all the heat losses.

To clarify the roles of window-to-wall area ratio, glazing type, and orientation in heat losses and gains, the simulation model (already verified) was used to calculate daily net losses or gains under identical weather conditions for each of the thirty experimental configurations. For simplicity, a completely clear design day with constant wind speed and direction was chosen. The profiles chosen (Jan. 21st) for outside air temperature, wind speed, wind direction, solar radiation intensity and indoor air temperature are given in Table 5.1.

The individual components, total daily solar gain, conduction and infiltration losses for south, west, and north oriented windows and panels are shown in Figs. 5.22, 5.23, and 5.24 respectively. For constant wind, and outside-inside temperature difference, the infiltration losses are proportional to the perimeter of the window and not to the area. The conduction curves are also not quite straight lines because the sideways losses are perimeter dependent.

Net daily gains were calculated for three separate cases to emphasize the inacuracies inherent in todays window design calculation methods, where infiltration losses are either ignored or not related to the net daily gains from windows.

For Case A, infiltration is ignored. For Case B all of the

Constant parameters:

Wind speed : 3m/s
Wind direction: 0.0° normal to the surface
Air temperature: (20°C) room air and (outdoor air -6°) frame

Variable parameters:

Hour	Outdoor air temperature, °C	Solar radiation W/m² South	West	North
1	-16.0	0.0	0.0	0.0
2	-16.0	0.0	0.0	0.0
3	-16.0	0.0	0.0	0.0
4	-17.0	0.0	0.0	0.0
5	-17.0	0.0	0.0	0.0
6	-16.0	0.0	0.0	0.0
7	-14.0	0.0	0.0	0.0
8	-13.0	150.0	9.0	9.0
9	-13.0	525.0	33.0	33.0
10	-10.0	750.0	49.0	49.0
11	-11.0	870.0	58.0	58.0
12	- 9.0	910.0	66.0	61.0
13	- 8.0	870.0	203.0	57.0
14	- 8.0	750.0	412.0	48.0
15	-10.0	525.0	485.0	33.0
16	-11.0	150.0	229.0	9.0
17	-11.0	0.0	0.0	0.0
18	-12.0	0.0	0.0	0.0
19	-13.0	0.0	0.0	0.0
20	-13.0	0.0	0.0	0.0
21	-14.0	0.0	0.0	0.0
22	-14.0	0.0	0.0	0.0
23	-15.0	0.0	0.0	0.0
24	-15.0	0.0	0.0	0.0

TABLE 5.1: Weather data for the typical design winter day

infiltration losses are included. For Case C, only infiltration losses beyond required ventilation were included.

For some types of glazing, with south, east or west orientations, there is a window-to-wall area ratio which gives zero net daily gains for this design day. This window-to-wall area ratio will be referred to as the energy balance ratio. For the south window in Case A, as shown in Fig. 5.25, the energy balance ratio for a single glazed window was 0.64 in this particular case. For Case B, with full infiltration, single pane windows lose energy at all window-to-wall area ratios. Similarly, for double and triple glazed south windows, the energy balance ratio shifts by 0.3 between Case A and Case B. The net daily energy gains or losses from panels with west windows are shown in Fig. 5.26. Unlike south panels on this clear January 21st, the solar heat gain provided by west panels with any of the three types of glazing was insufficient to overcome heat losses at any ratio. For Case A, the net daily gain from panels with a triple glazed window, at any ratio is less than the energy loss of a solid panel. However, this is not true for Cases B and C, which are more realistic. One must wait for longer days in February or March to achieve a net daily gain for east and west windows. For all three cases of triple glazing, the net daily losses are nearly independent of window-to-wall area ratio, between ratios of 0.25 and 0.75. For panels with double windows, the variation of losses in this range is small. On the east/west exposures, larger windows impose only a glare penalty, not an energy penalty. The daily net energy gain or loss from panels with windows facing north is shown in Fig. 5.27. As expected even with no clouds, all north windows lose

energy on the chosen "typical" design winter day (January 21st). At area ratio of 0.25, panels with triple glazed windows lose nearly as much energy as those with double glazed windows in both Case A and Case B. At area ratio of 0.75, the difference is greater but probably not enough to justify the initial cost of triple glazing even on a clear day.

To conclude, on a sunny January 21st, panels with double or triple glazed windows facing due south have not only less net daily energy loss than the solid panel but also show a surplus energy gain. Facing west, only panels with triple glazed windows show less energy loss than the solid panel. Otherwise, the solid panel has the least energy loss.

5.7 Daylight Energy Benefits

Additional energy benefits from windows can be obtained when natural daylight is utilized as the main source of illumination so that the use of electric lighting can be limited to the times when natural daylight received in the room falls below the required level of illumination. As was indicated in Chapter IV, the total number of lamps needed to provide the required illumination in the rotating test Chamber were six, each providing illumination of 125 lux (at the chosen reference point). Therefore, whenever the natural daylight illumination inside the room, at the chosen reference point, was over 750 lux, the six lamps were off, resulting in savings of 0.24 Kw.hr each hour. For illumination between 625 and 750 lux, 5 lamps were automaticaly turned off, etc.

time	25% Glazing			50% Glazing			75% Glazing		
	Single	Double	Triple	Single	Double	Triple	Single	Double	Triple
8	—	—	—	1	1	1	2	1	1
9	2	1	1	4	3	3	6	5	4
10	4	3	3	6	6	6	6	6	6
11	6	5	5	6	6	6	6	6	6
12	6	6	6	6	6	6	6	6	6
13	6	5	5	6	6	6	6	6	6
14	4	3	3	6	6	6	6	6	6
15	2	1	1	4	3	3	6	5	4
16	—	—	—	1	1	1	2	1	1

TABLE 5.2: Hourly daylight energy savings expressed in terms of the number of lamps that were turned off. (South window)

time	25% Glazing			50% Glazing			75% Glazing		
	Single	Double	Triple	Single	Double	Triple	Single	Double	Triple
8	—	—	—	1	—	—	1	1	1
9	1	1	—	2	1	1	2	2	2
10	1	1	1	2	2	2	3	3	2
11	1	1	1	3	2	2	4	3	3
12	1	1	1	3	3	2	4	4	3
13	2	1	1	4	3	3	5	5	4
14	2	2	1	4	3	3	6	6	5
15	2	2	1	4	3	3	6	5	5
16	1	1	1	3	2	2	4	3	3

TABLE 5.3: Hourly daylight energy savings expressed in terms of the number of lamps turned off (East/West window)

time	25% Glazing			50% Glazing			75% Glazing		
	Single	Double	Triple	Single	Double	Triple	Single	Double	Triple
8	—	—	—	—	—	—	1	1	1
9	1	1	—	2	1	1	2	2	2
10	1	1	1	2	2	2	3	3	2
11	1	1	1	3	2	2	4	3	3
12	1	1	1	3	3	2	4	4	3
13	1	1	1	3	2	2	4	3	3
14	1	1	1	2	2	2	3	3	3
15	1	—	—	2	1	1	2	2	2
16	—	—	—	—	—	—	1	1	1

TABLE 5.4: Hourly daylight energy savings expressed in terms of number of lamps turned off. (North windows)

For the design day used (completely clear sunny January 21st) the daylight illumination from single, double and triple glazed windows with area ratios of 0.25, 0.50, and 0.75 was calculated at hourly intervals. The illumination at the reference point from panels with south facing windows is shown in Fig. 5.28. The daylight illumination levels triggering the shutdown of each consecutive lamp is also shown. At noon, all 9 panels with windows give more illumination than six lamps. Illumination at the reference point from windows facing west and north are shown in fig. 5.29 a) and b) respectively. For the west oriented windows, the maximum illumination was received in the afternoon. Only panels with single or double glazed windows and 0.75 area ratio provided more than 750 lux at maximum illumination. all north facing panels gave less illumination than the required level throughout the design day. For south, west, and north facing windows, the number of lamps that were switched off every hour are given in Tables 5.2, 5.3, and 5.4. The corresponding lamp energy replaced by daylight as a function of window-to-wall area ratio, glazing type and orientation is shown in Fig. 5.30. Note that the effect of type of glazing may not result in a sufficient difference in the daylight illumination to turn off an additional lamp. As an example, the double and triple glazed windows at area ratio of 0.25 and 0.50, and facing south.

5.8 Thermal and Daylight Combined Effect on Window-to-Wall Area Ratio

For every type of glazing, orientation, and window-to-wall area

ratio, the daily electric lamp energy displaced was added to the corresponding net daily thermal gain or loss on a clear January 21st. The combined effect is displayed for the south, west, and north orientations in Figs. 5.31, 5.32, and 5.33 respectively.

For a south panel with single glazing on this day, a false impression of net energy gain is obtained when infiltration is ignored (Case A). Again, the extra energy gain for the triple over double glazing is small and probably does not justify the extra capital expenses. For west windows, all panels show net loss on this day. The addition of lamp energy savings keeps losses for panels with triple glazing close to those for opaque panels in both Case A and B. The impression of slight energy advantage for larger windows in Case A disappears in Case B. Here, the case for triple glazing for larger windows is still not compelling. For north windows, as expected all panels showed a net loss for a clear January 21st. At window-to-wall area ratio of 0.75, the extra losses due to air infiltration were about 10 MJ, for each of single, double, and triple glazing.

Similarly, the electric lamp energy displaced under the C.I.E. overcast sky which does not vary with time was calculated and then added to the corresponding net daily thermal gain or loss. The ambient temperature and wind profiles for January 21st, 1980 were used. Under overcast sky conditions, the thermal and daylight calculations are independent of the window orientation. The daily net energy gain or loss was calculated taking into account the electric lamp energy displaced. The net losses (shown in Fig. 5.34) were only slightly larger

than those for the north panel on the clear January 21st. For a diffuse overcast sky, more energy is received, but less illumination than for the diffuse light from a clear sky. The extra energy, that is received from a north facing panel, is nearly compensated by lower lamp energy displaced. Thus, we can simulate completely cloudy periods with the north window clear sky calculation to an acceptable accuracy. Complete seasonal calculations, however will have to be postponed until the partly cloudy sky model is well validated.

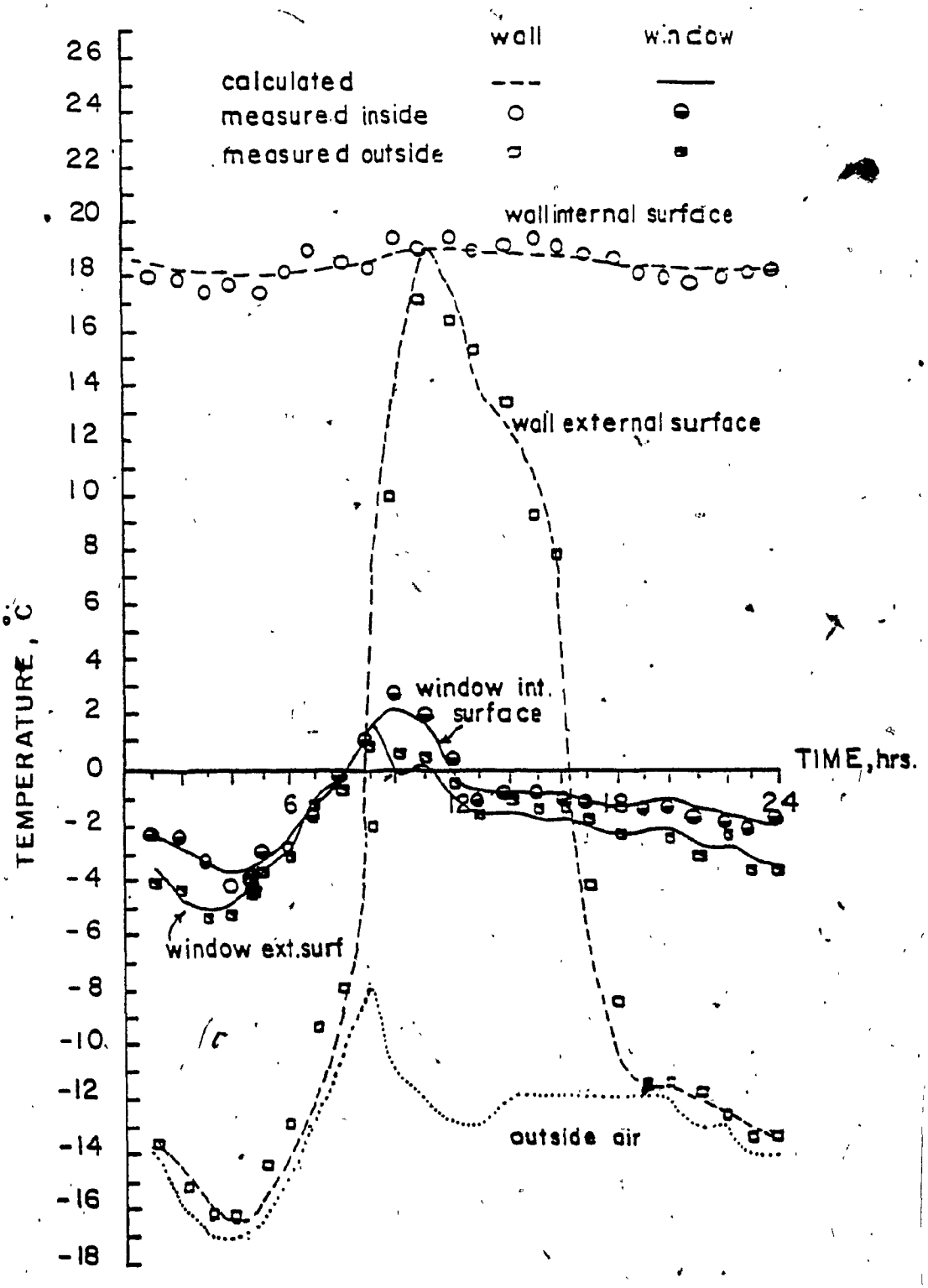

Fig. 5.1: A comparison between calculated and measured spatial average temperatures at the internal and external surfaces of the single-glazed window and the wall facing south (W.W.A.R. = 0,25)

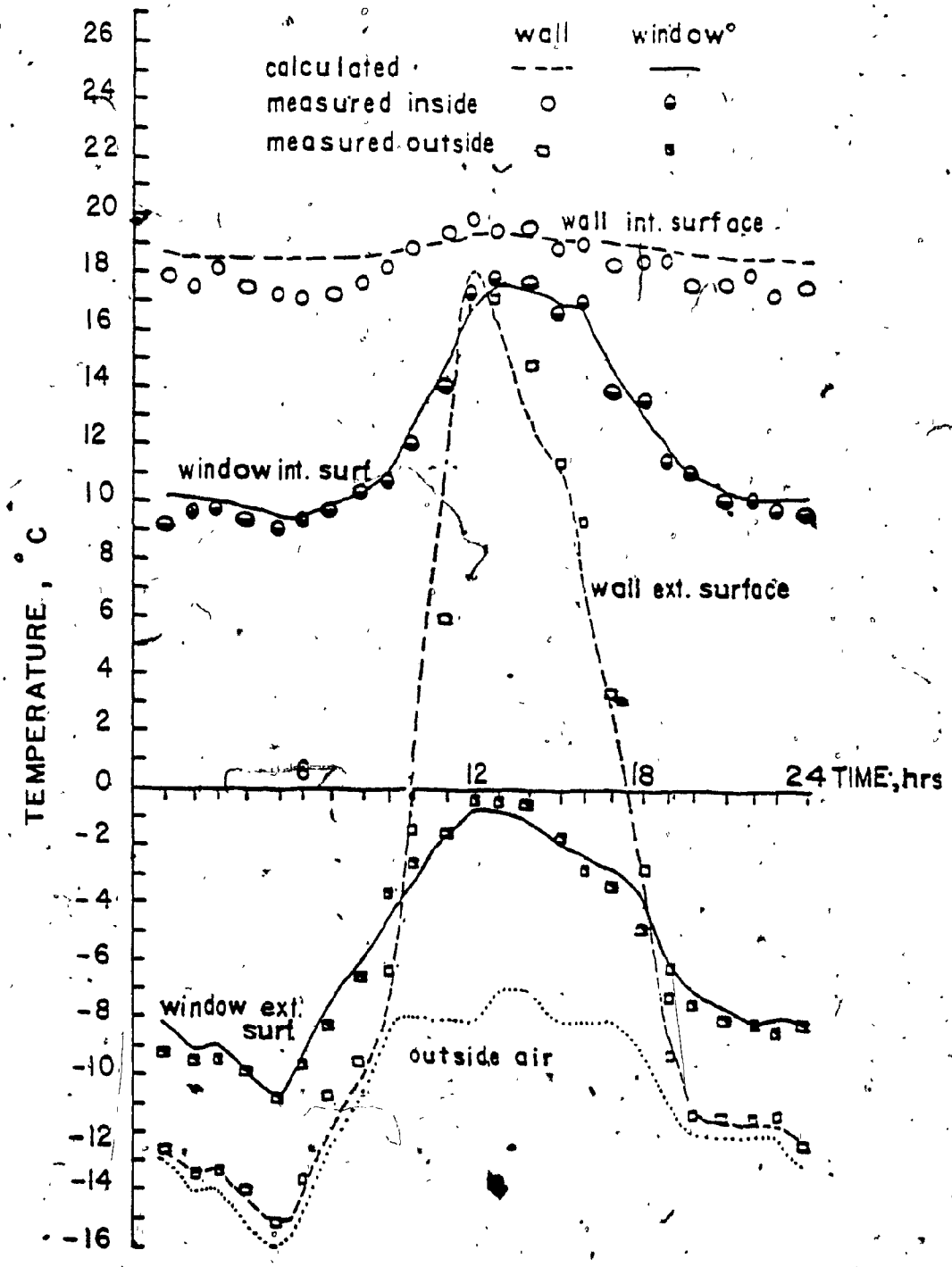

Fig. 5.2: A comparison between calculated and measured spatial average temperatures at the internal and external surfaces of the double glazed window and the wall facing south (W.W.A.R. = 0.25)

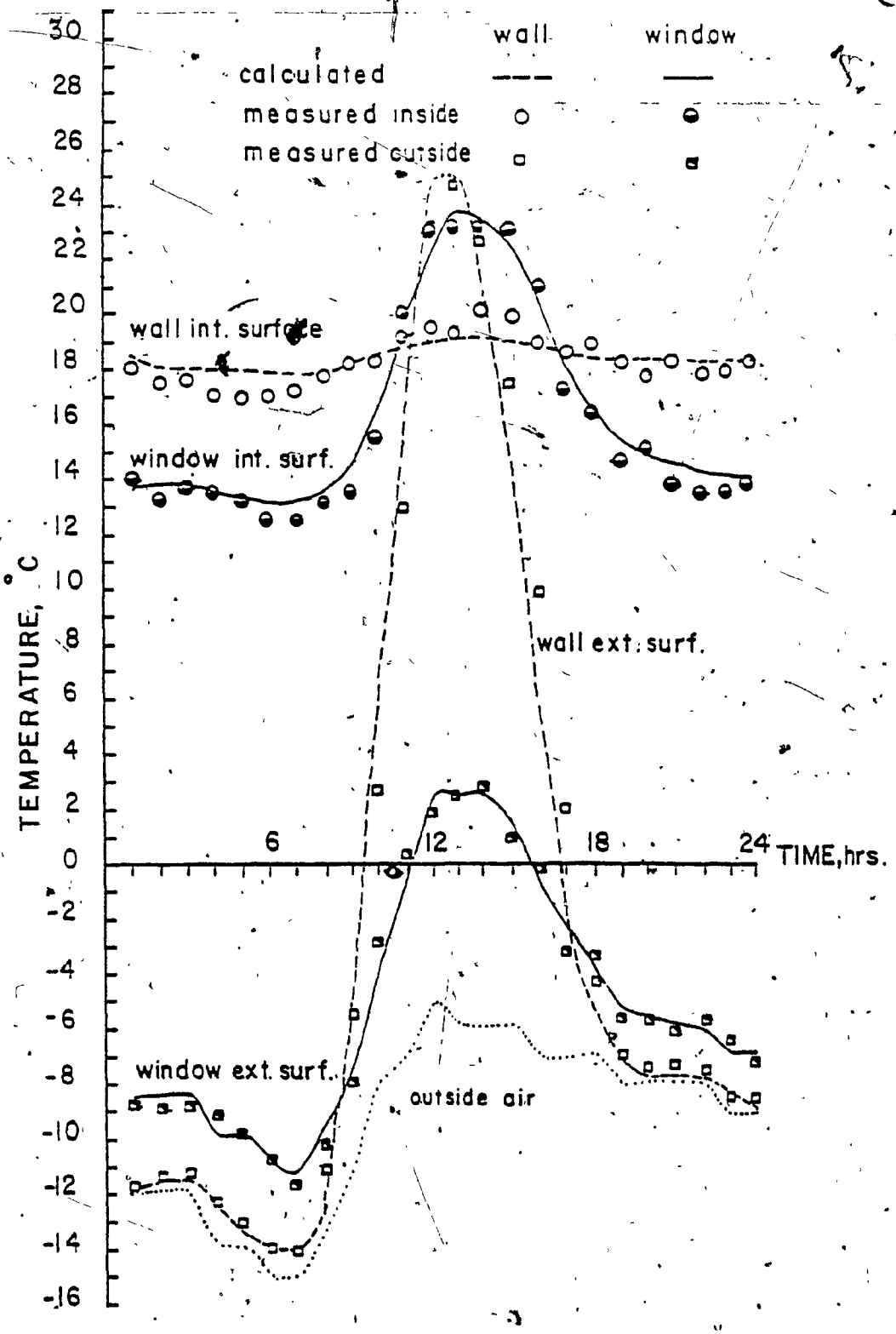

Fig. 5.3: A comparison between calculated and measured spatial average temperatures at the internal and external surfaces of the triple glazed window and the wall facing south (W.W.A.R. = 0.25)

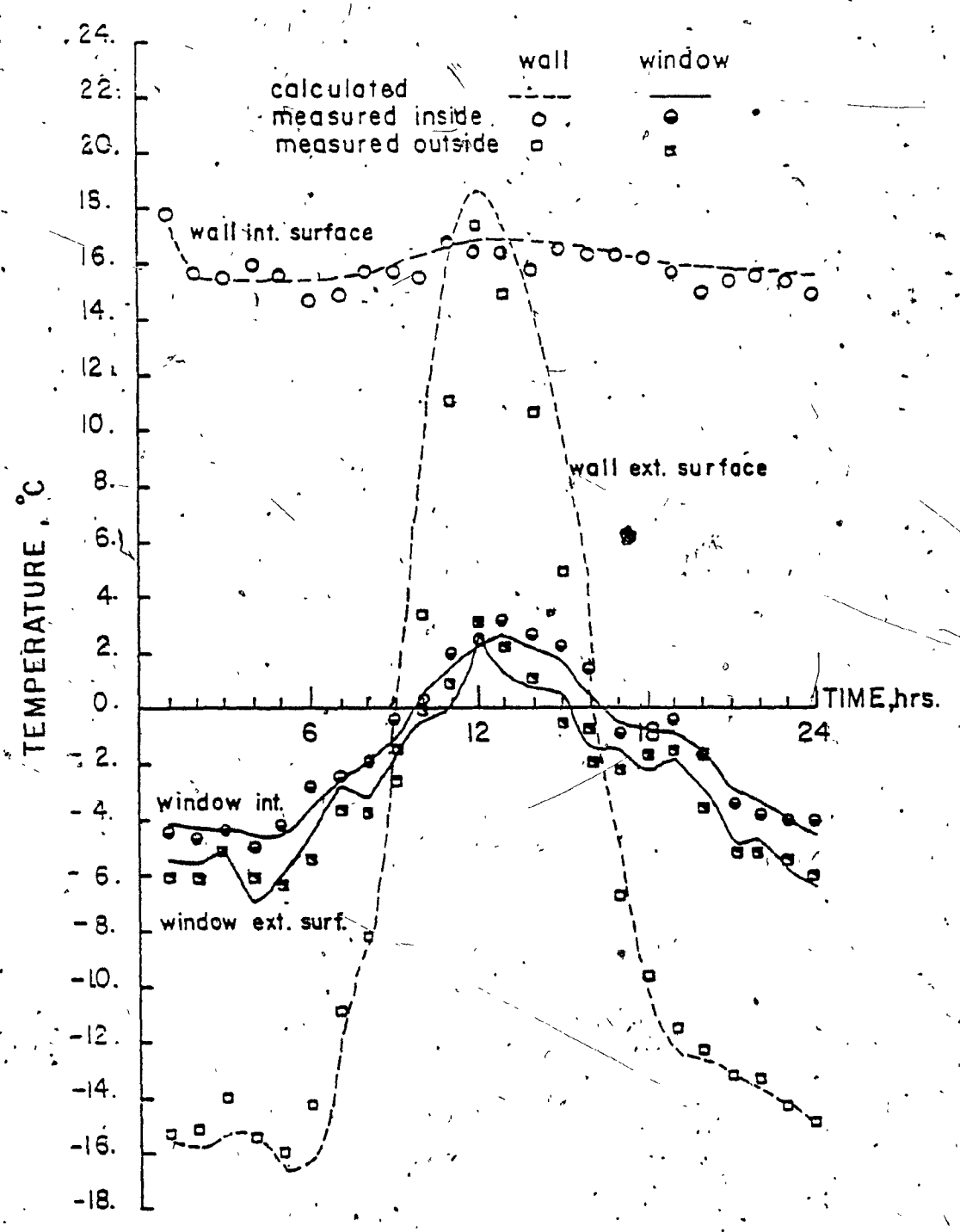

Fig. 5.4: A comparison between calculated and measured spatial average temperatures at the internal and external surfaces of the single glazed window and the wall panel facing south (W.W.A.R. = 0.75)

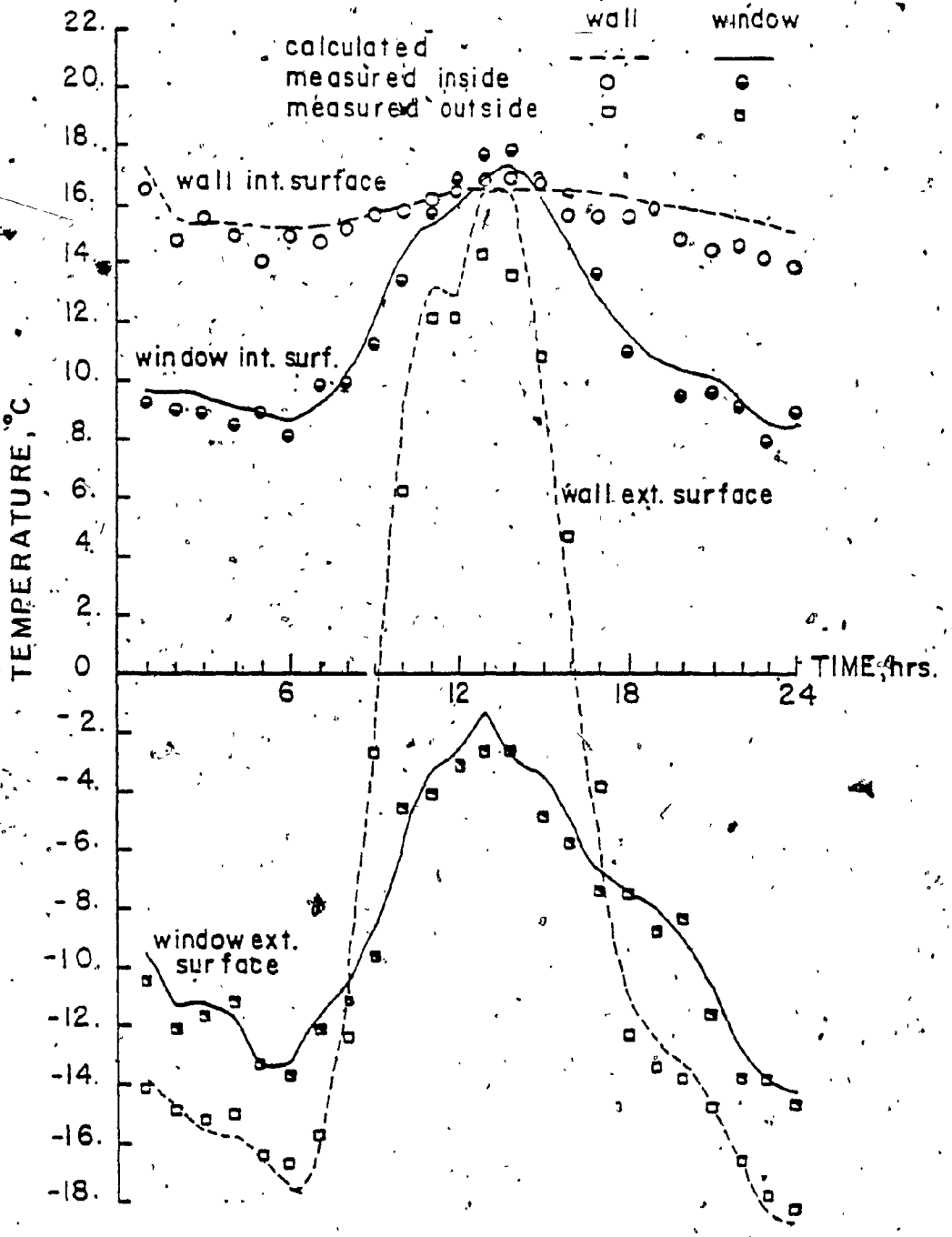

Fig. 5.5: A comparison between calculated and measured spatial average temperatures at the internal and external surfaces of the double glazed window and the wall panel facing south (W.W.A.R. = 0.75).

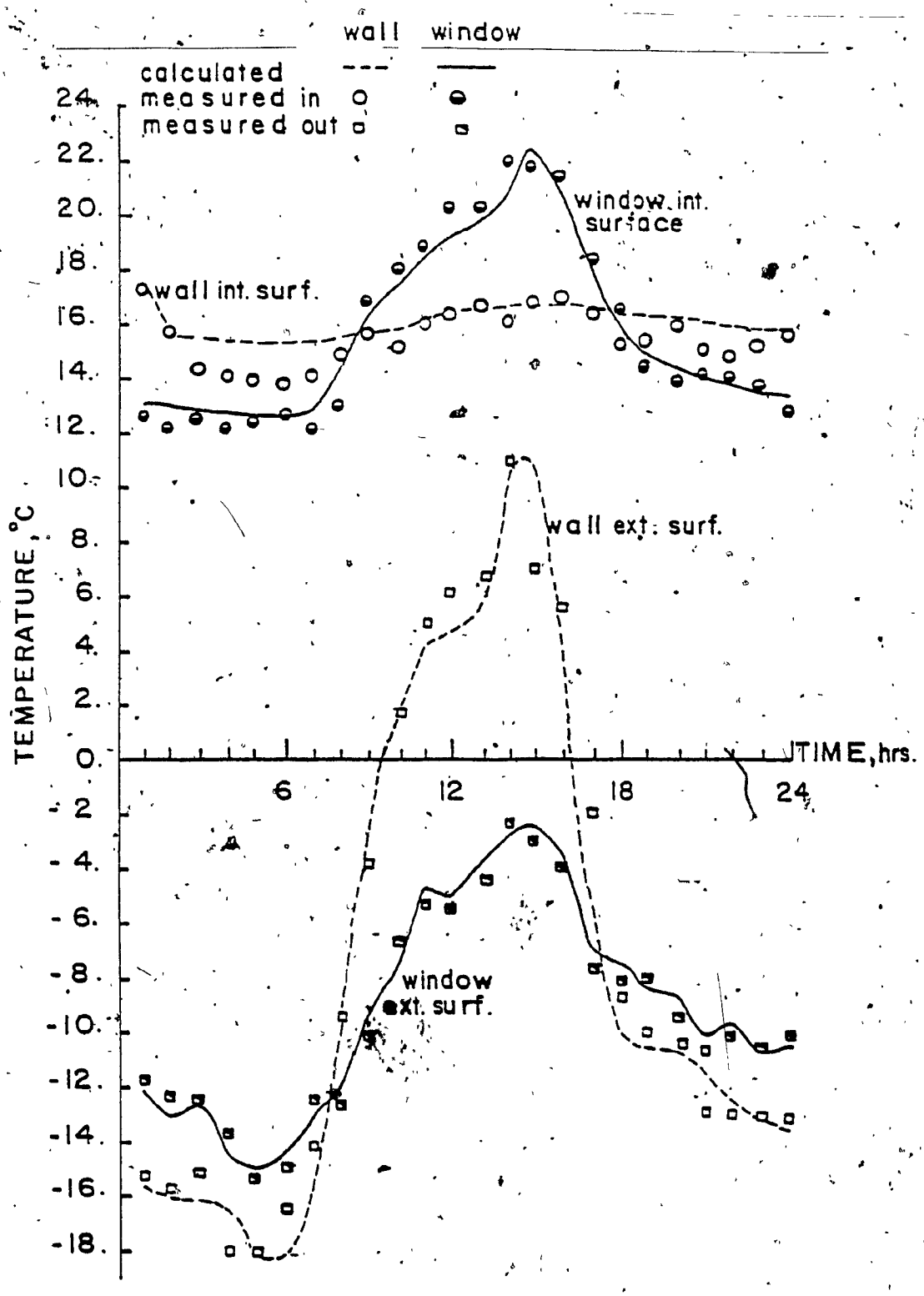

Fig. 5.6: A comparison between calculated and measured spatial average temperatures at the internal and external surfaces of the triple glazed window and the wall is facing south (W.W.A.R. = 0.75)

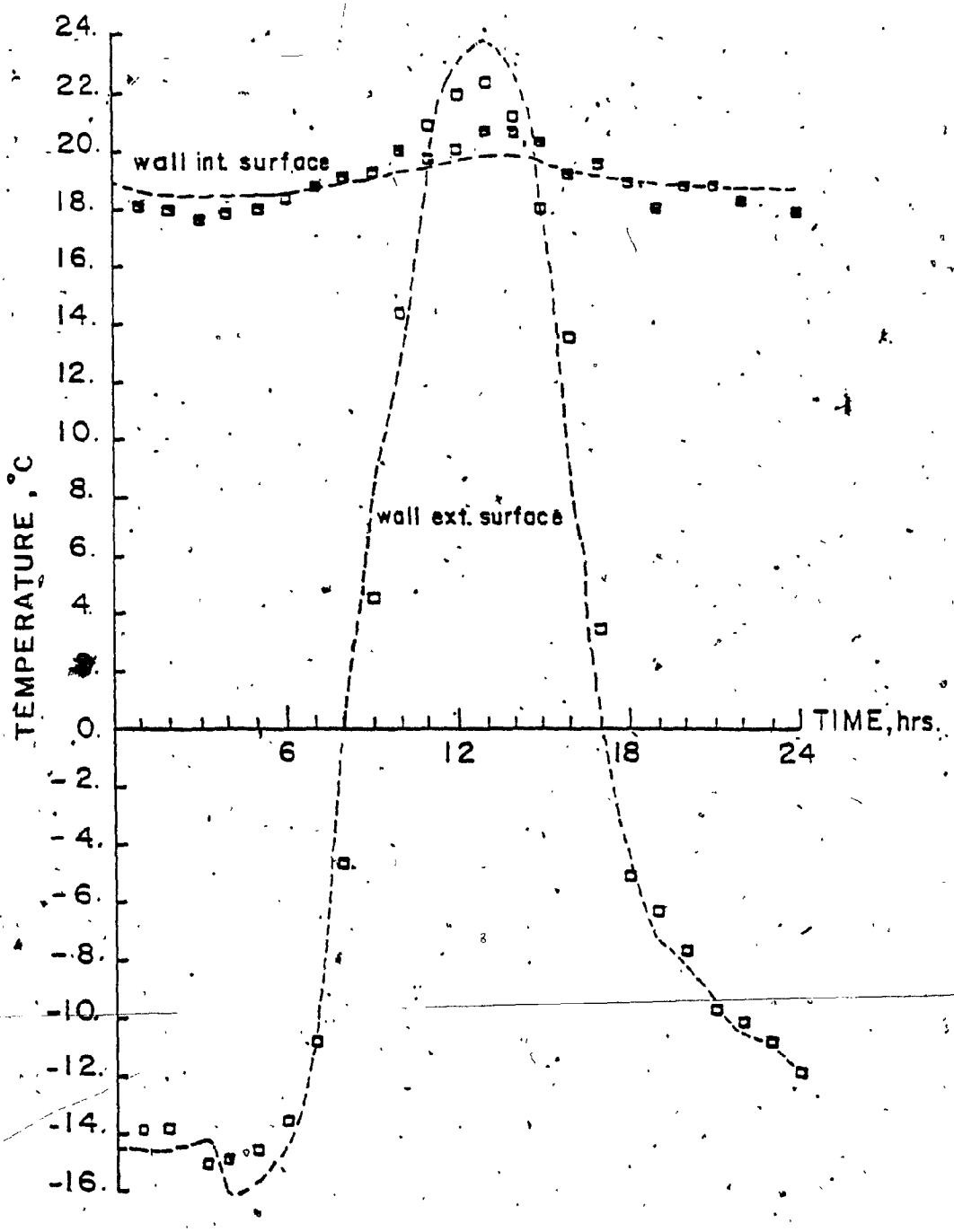

Fig. 5.7: A comparison between calculated and measured spatial average temperatures at the internal and external surfaces of a uniform (solid) wall panel facing south.

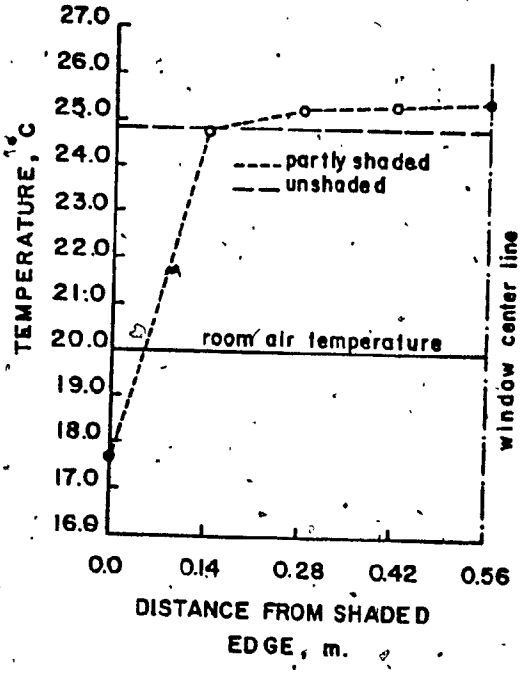

a) temperature variation on the internal surface

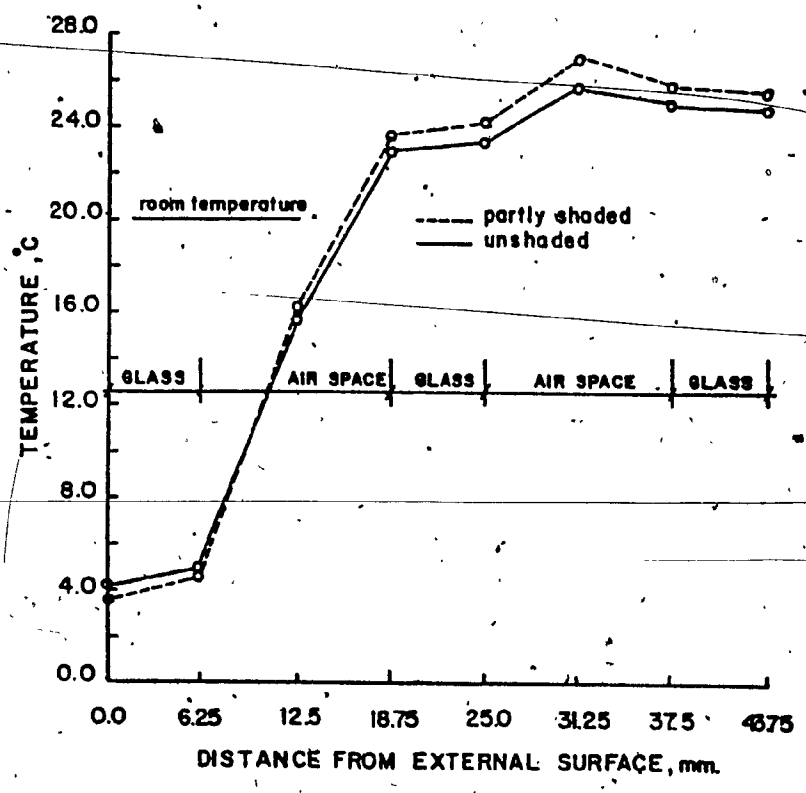

b) outside-inside temperature gradient

Fig. 5.8: The effect of shaded edges on the temperature variation on the internal surface and on the outside-inside temperature for a triple glazed window facing south at one hour after noon

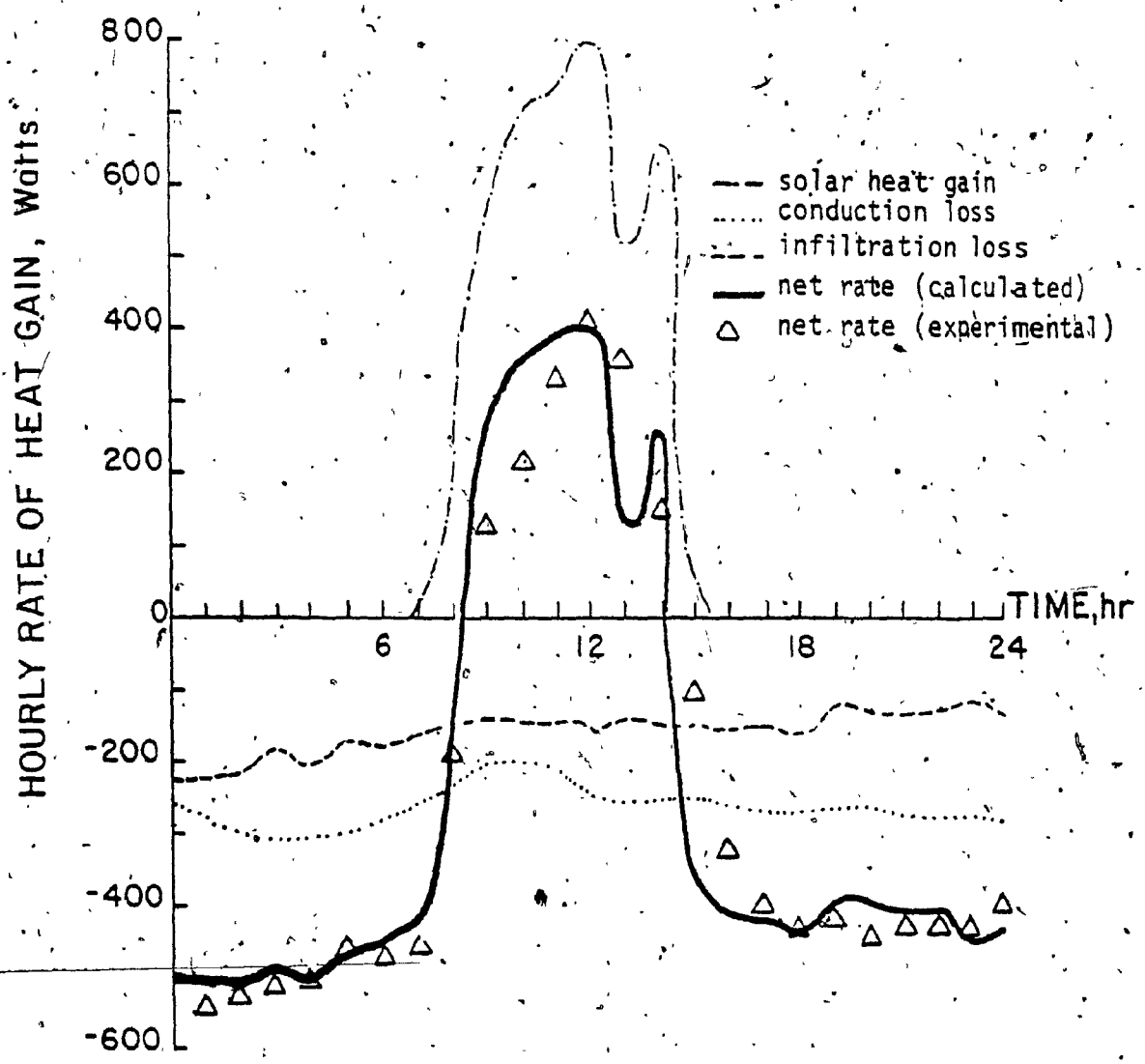

Fig. 5.9: Comparison between calculated and experimental hourly net rate of heat gain from a panel with a single glazed window facing south (W.W.A.R. = 0.25).

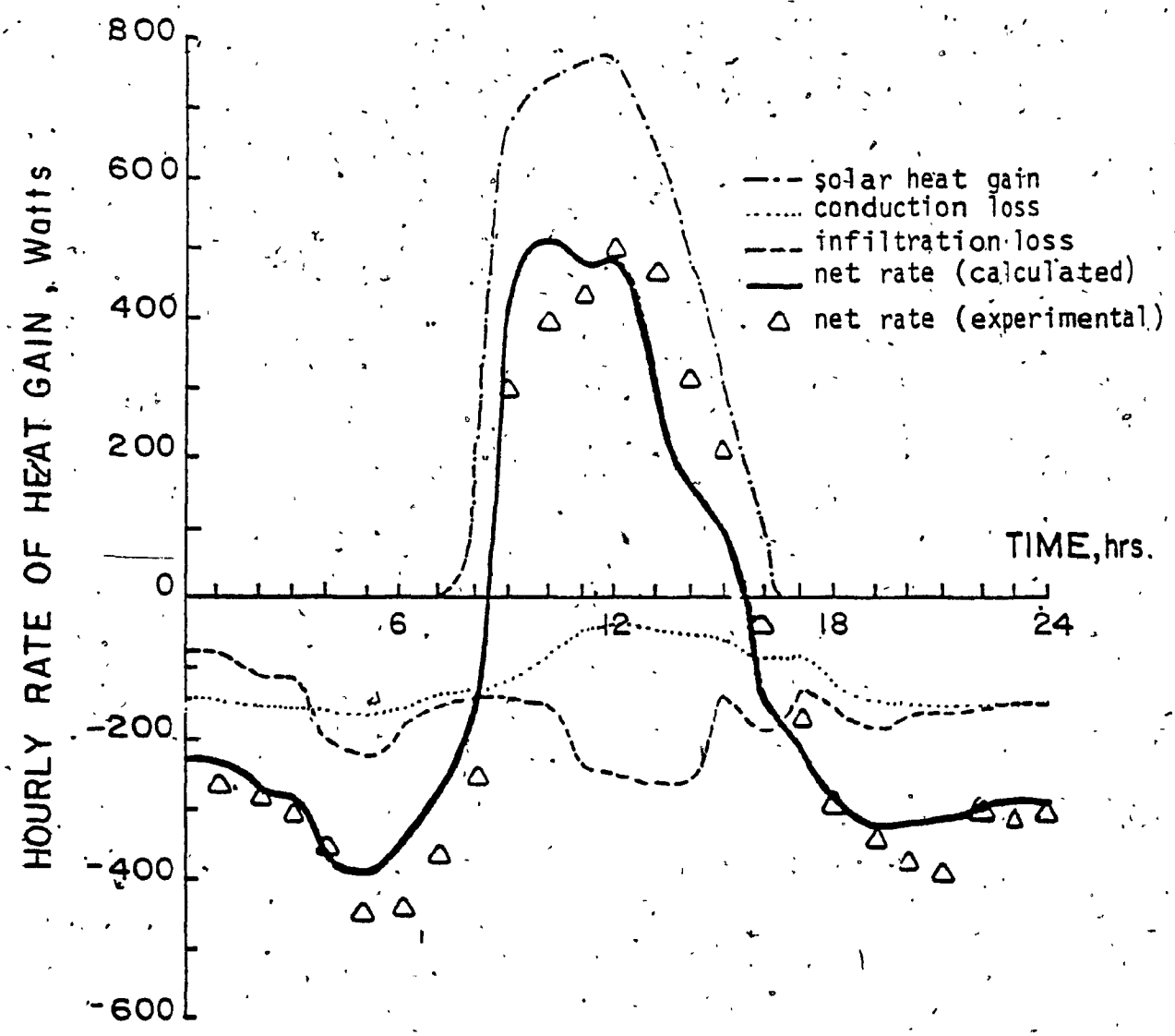

Fig. 5.10: Comparison between calculated and experimental hourly net rate of heat gain from a panel with a double glazed window facing south (W.W.A.R. = 0.25)

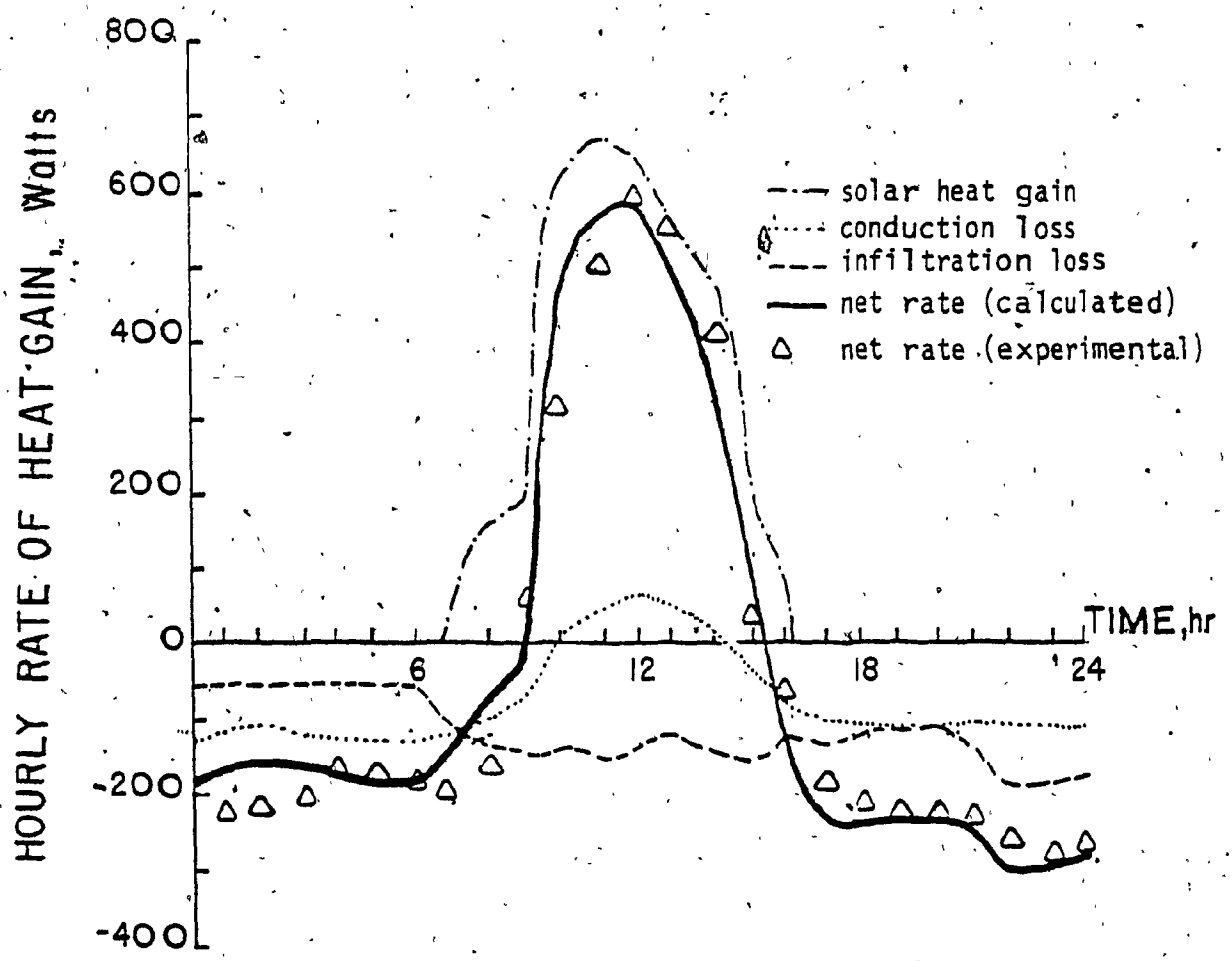

Fig. 5.11: Comparison between calculated and experimental hourly net rate of heat gain from a panel with a triple glazed window facing south (W.W.A.R. = 0.25).

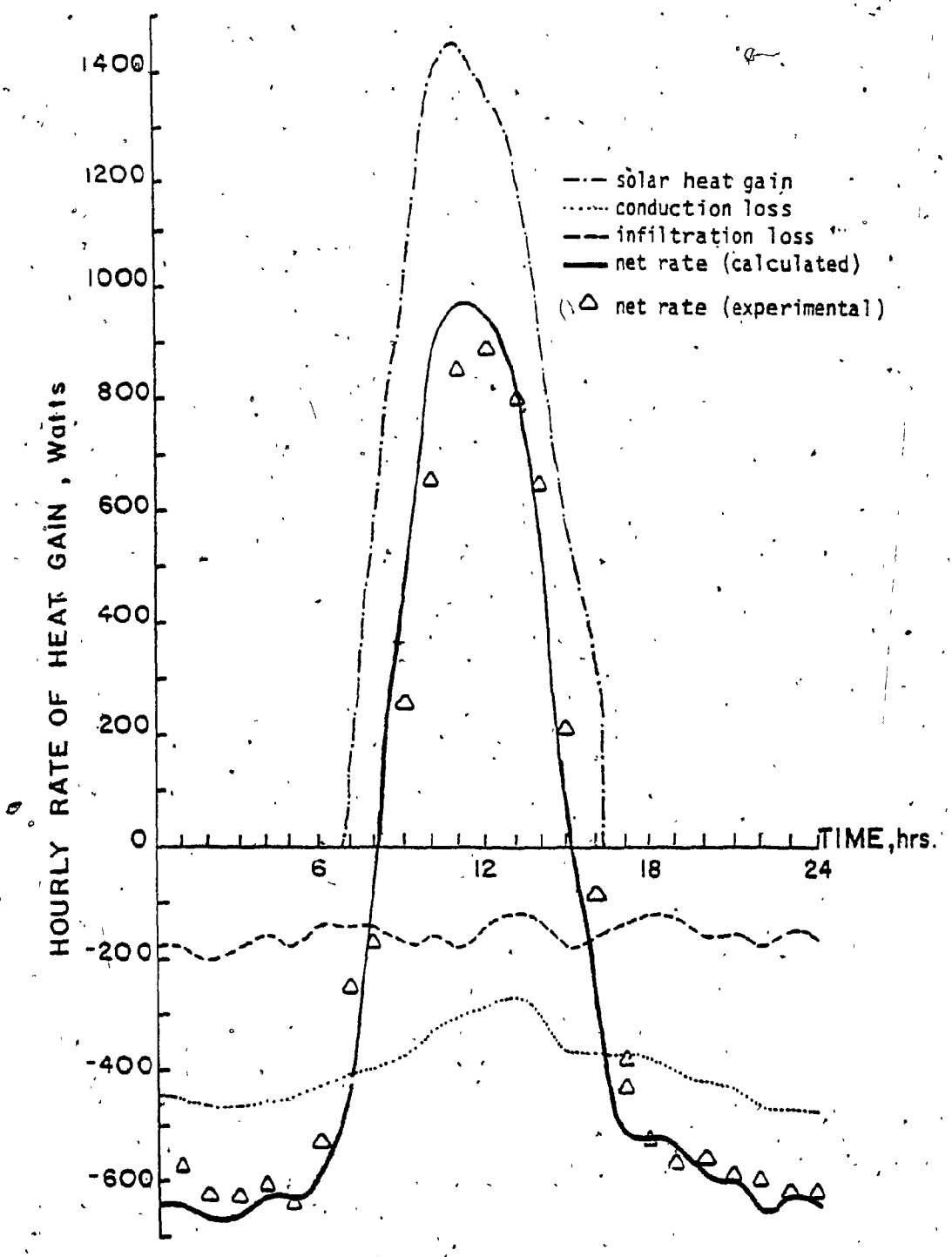

Fig. 5.12: Comparison between calculated and experimental hourly net rate of heat gain from a panel with a single glazed window facing south (W.W.A.R. = 0.50)

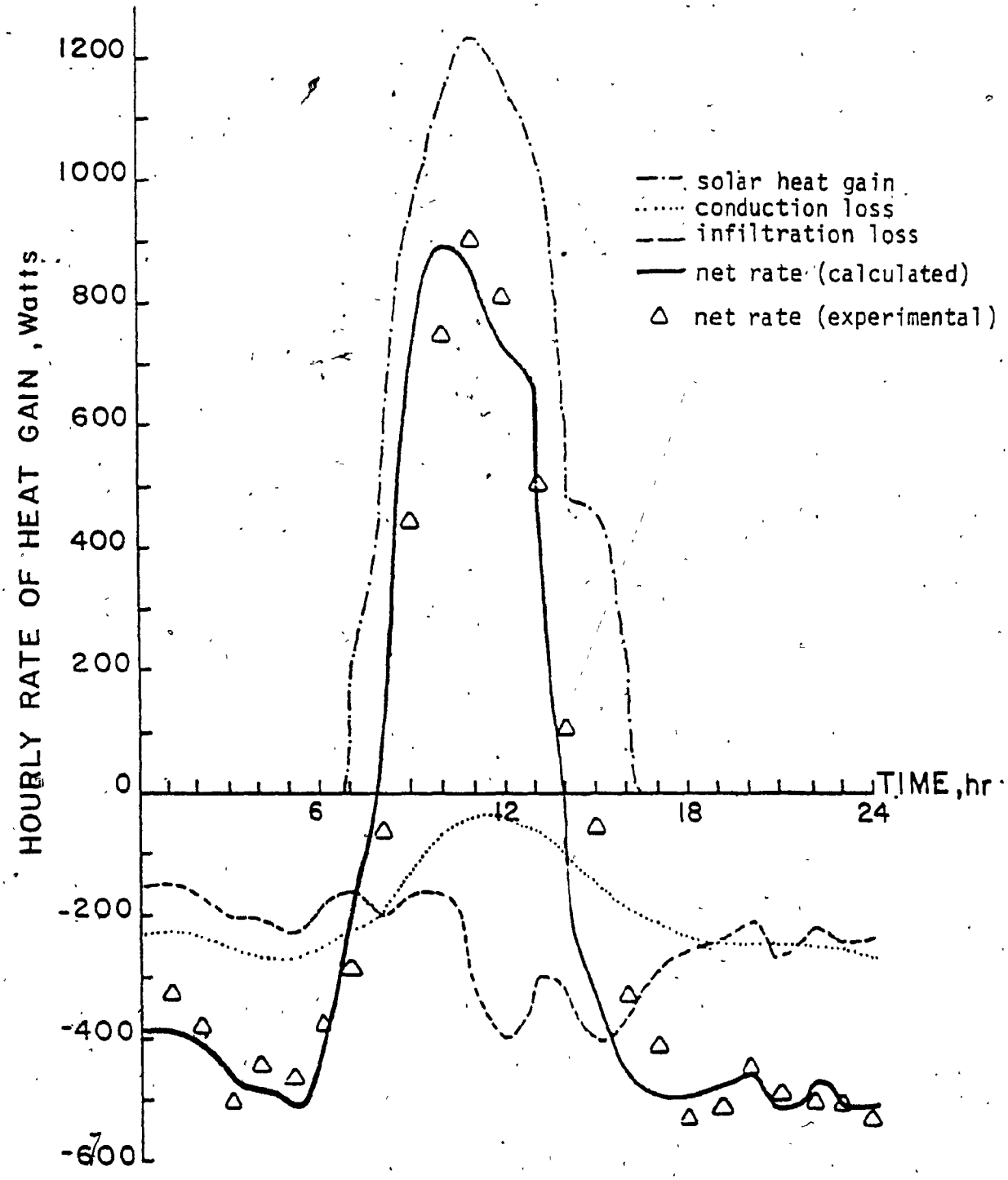

Fig. 5.13: Comparison between calculated and experimental hourly net rate of heat gain from a panel with a double glazed window facing south (W.W.A.R. = 0.50)

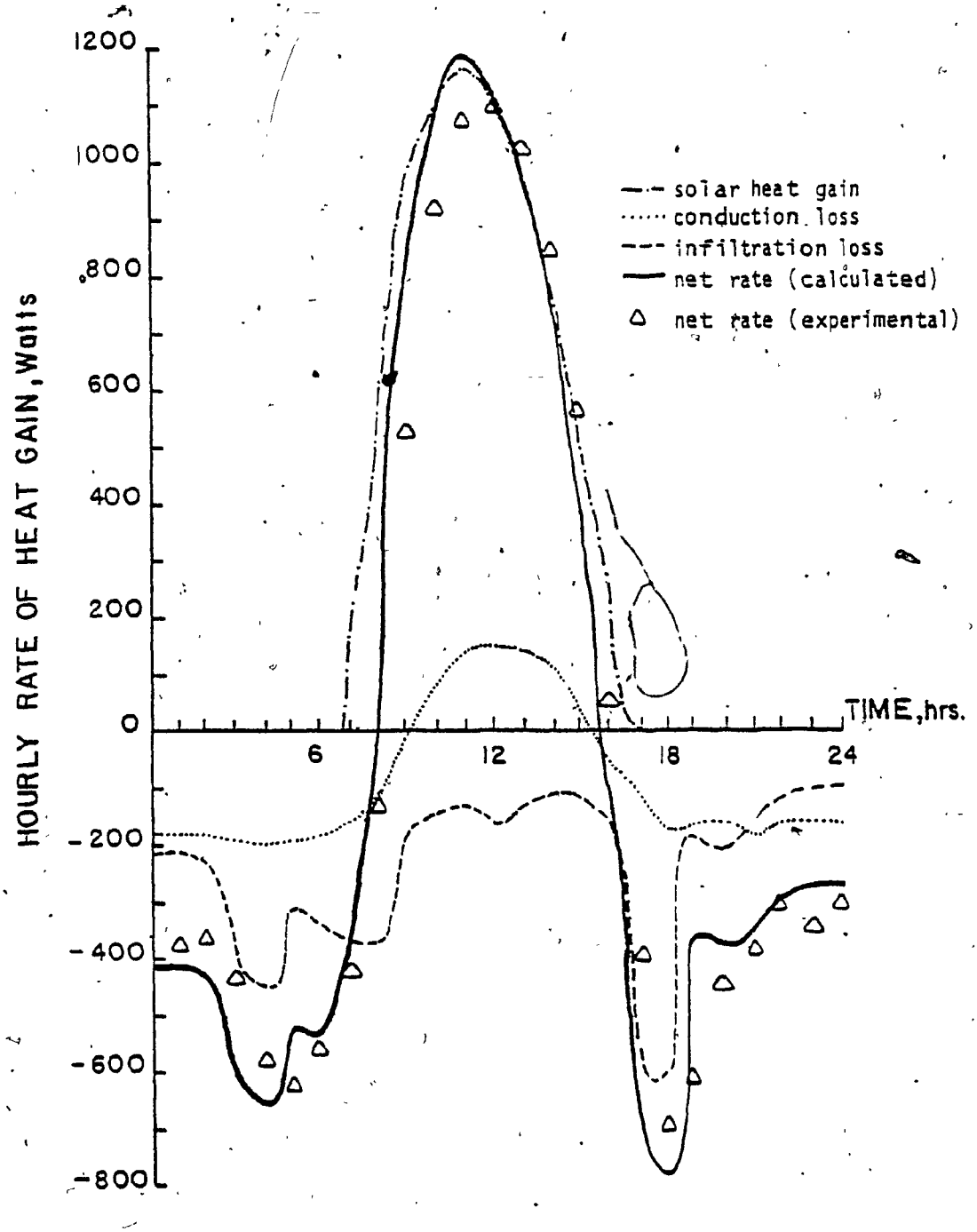

Fig. 5.14: Comparison between calculated and experimental hourly net rate of heat gain from a panel with a triple glazed window facing south (W.W.A.R. = 0.50)

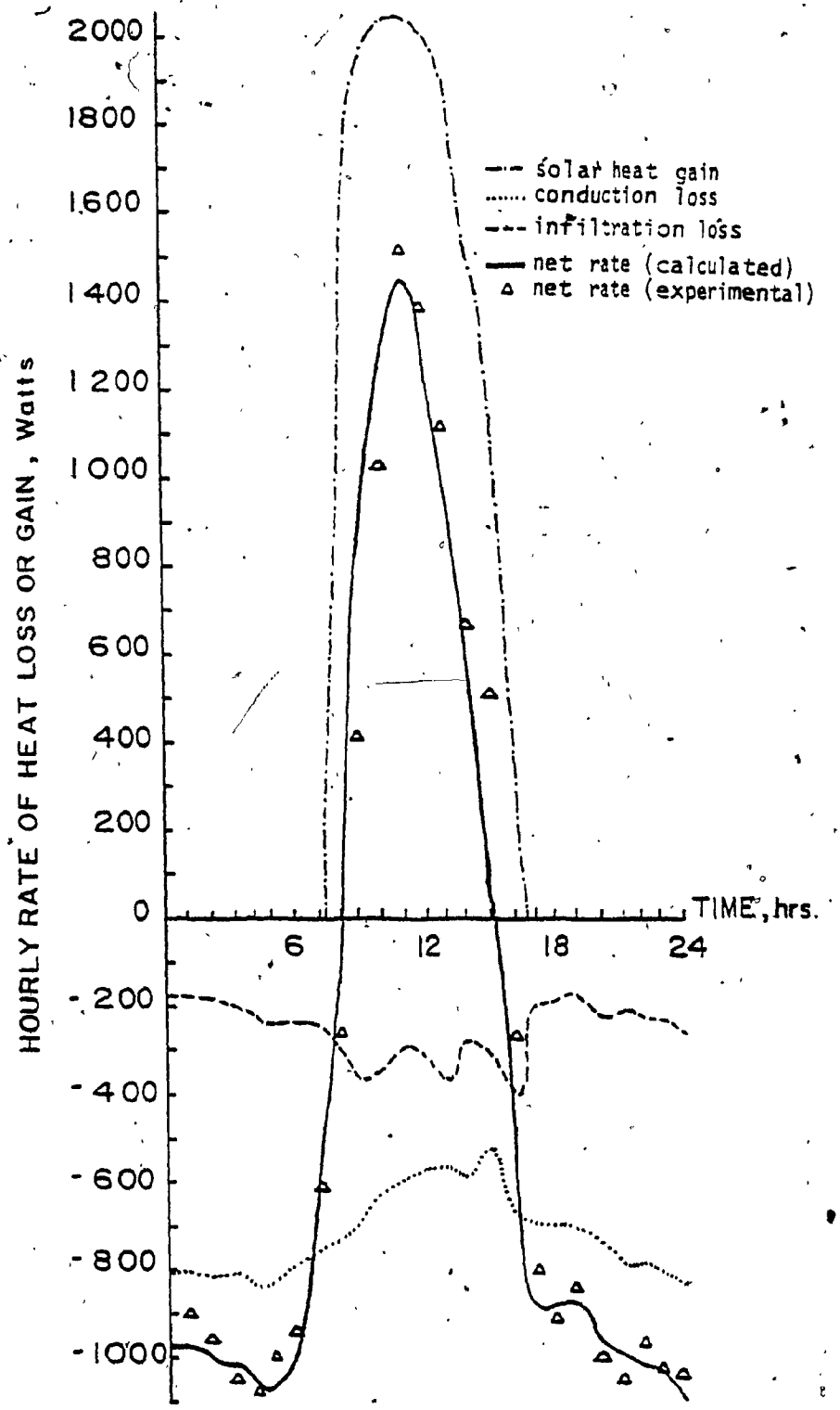

Fig. 5.15: Comparison between calculated and measured hourly net rate of heat gain from a panel with a single glazed window facing south (W.W.A.R. = 0.75)

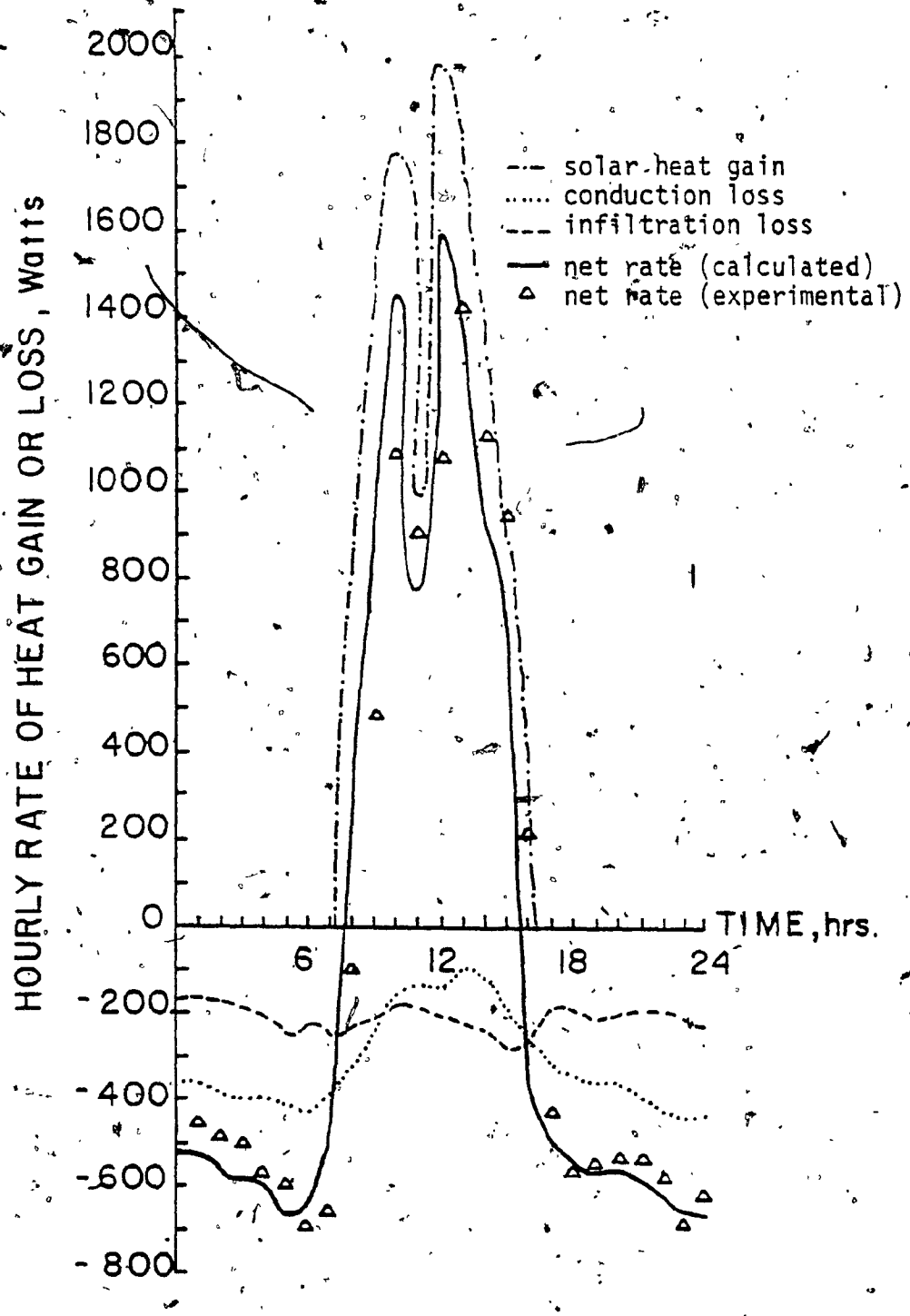

Fig. 5.16: Comparison between calculated and experimental hourly net rate of heat gain from a panel with a double glazed window facing south (W.W.A.R. = 0.75)

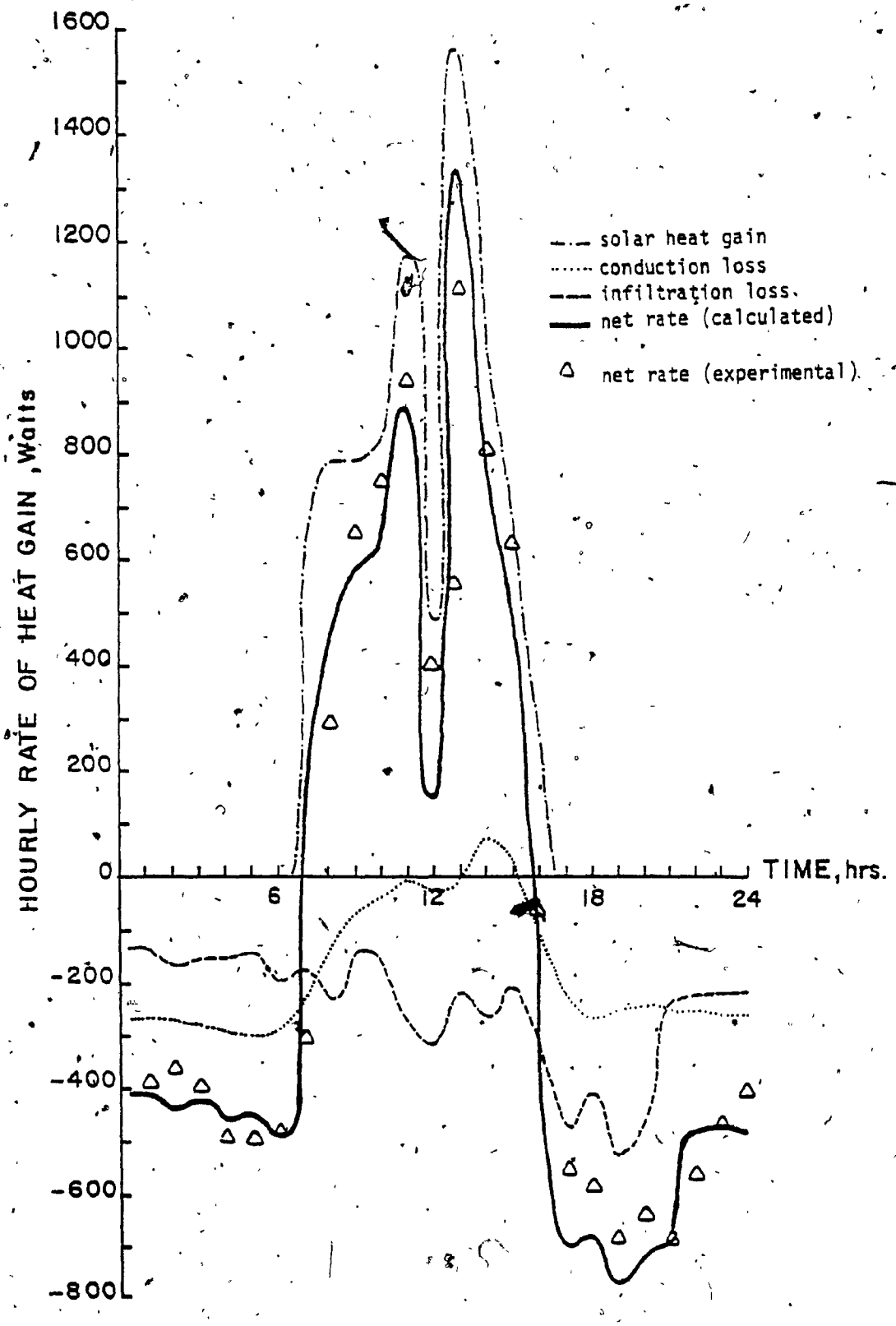

Fig. 5.17: Comparison between calculated and experimental hourly net rate of heat gain from a panel with a triple glazed window facing south (W.W.A.R. = 0.75)

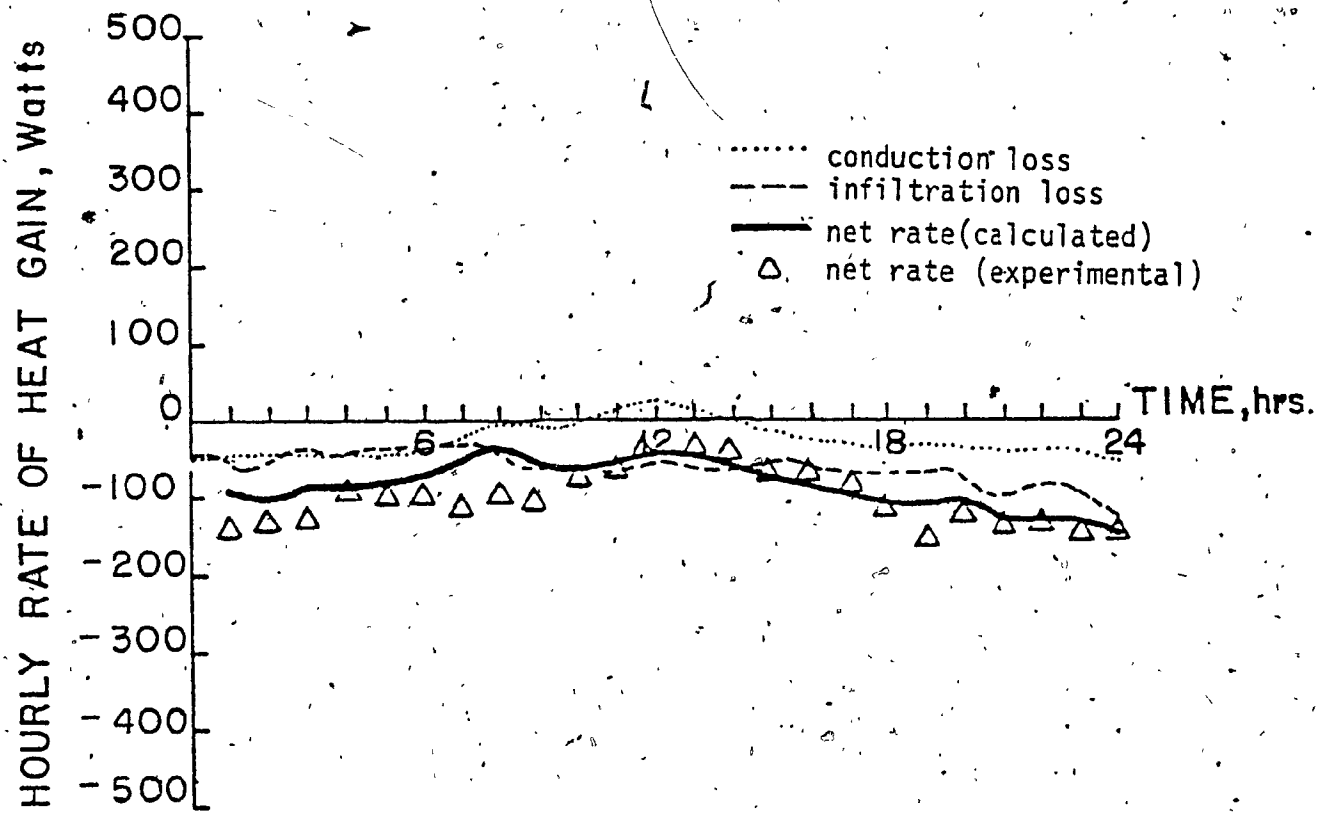

Fig. 5.18: Comparison between calculated and experimental hourly net rate of heat gain from a solid panel facing south (W.W.A.R. = 0.0)

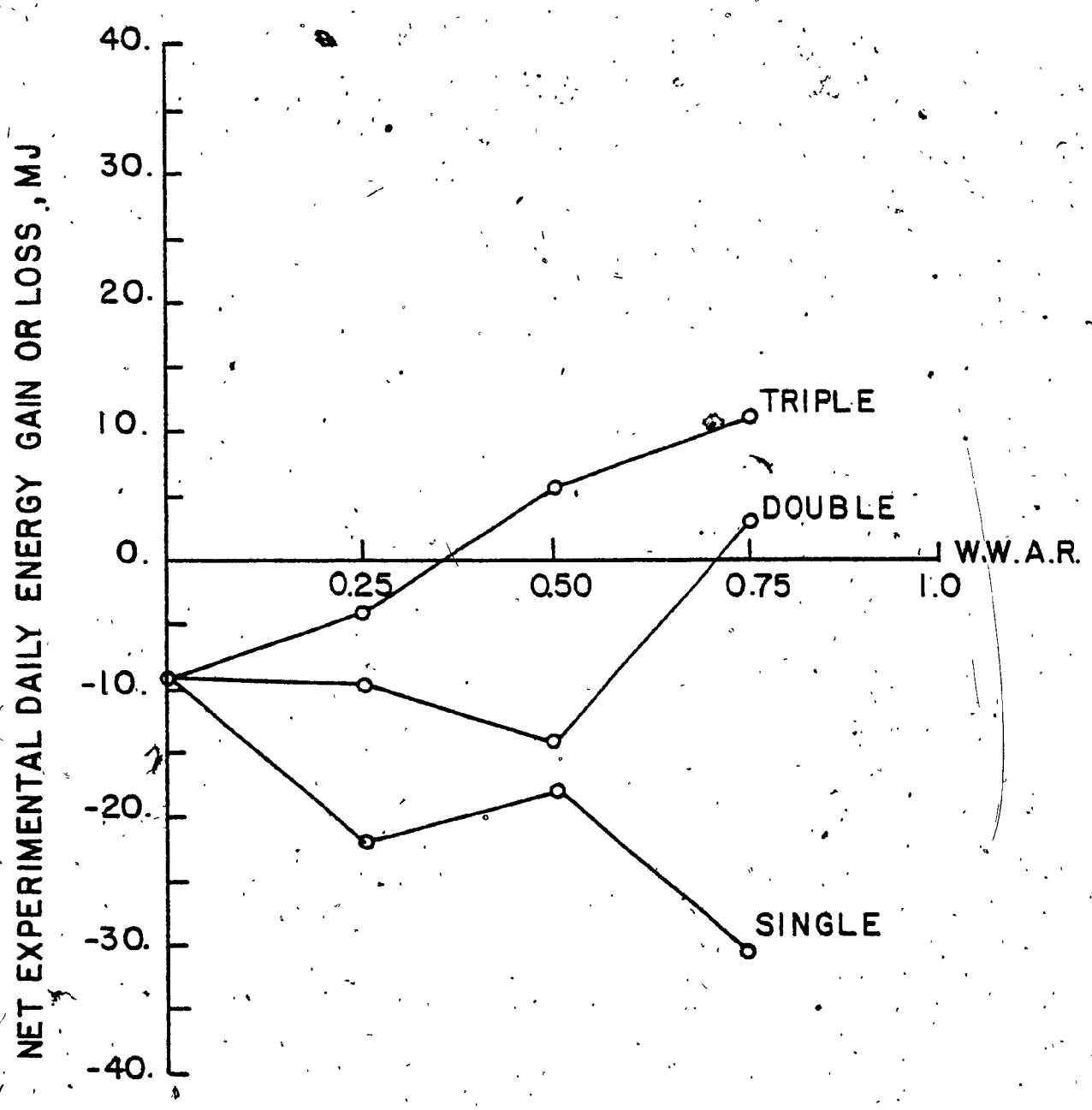

Fig. 5.19: Net experimental daily energy gain or loss from panels with single, double and triple glazed windows facing south.

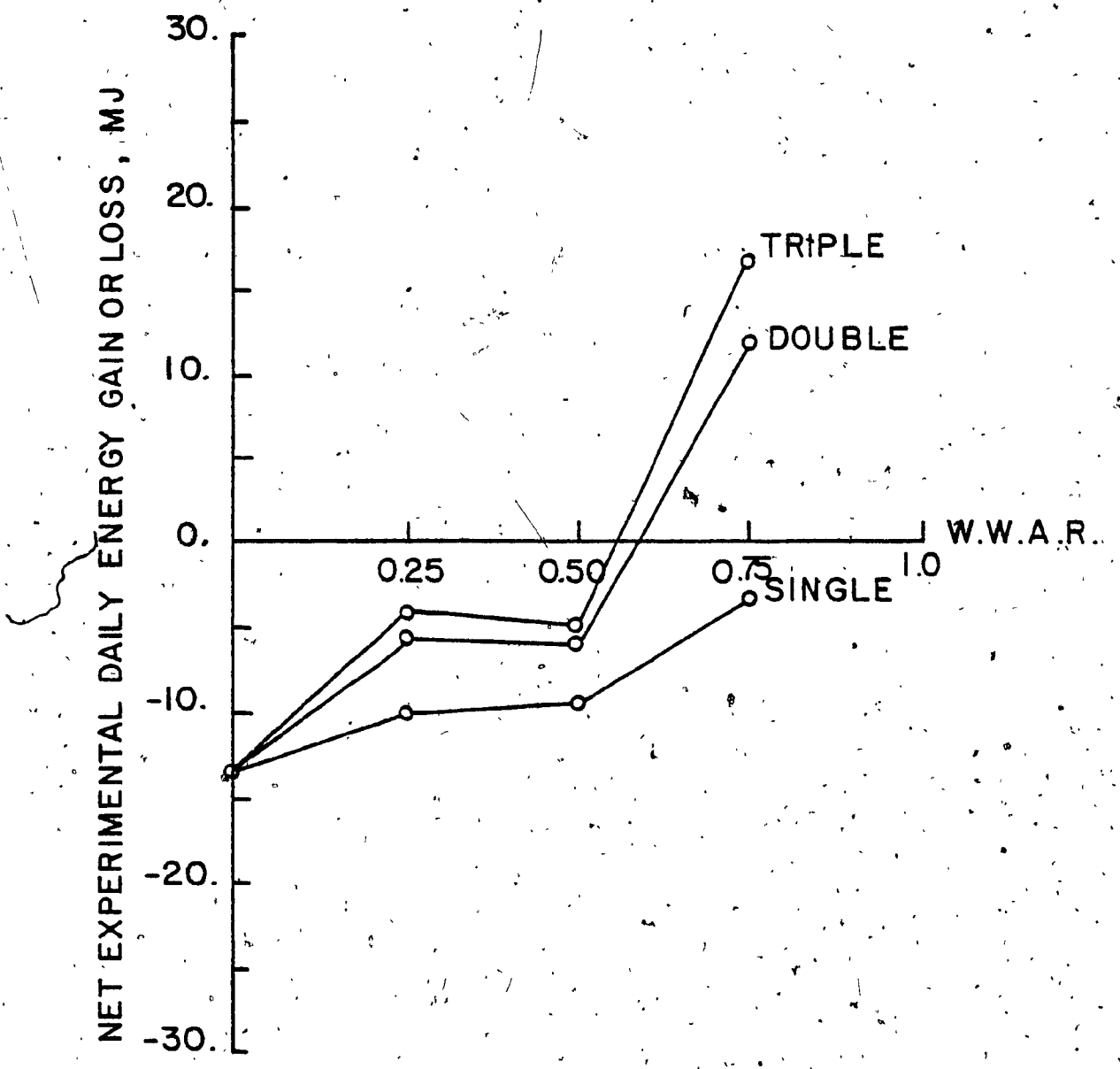

Fig. 5.20: Net experimental daily energy gain or loss from panels with single double and triple glazed windows facing west.

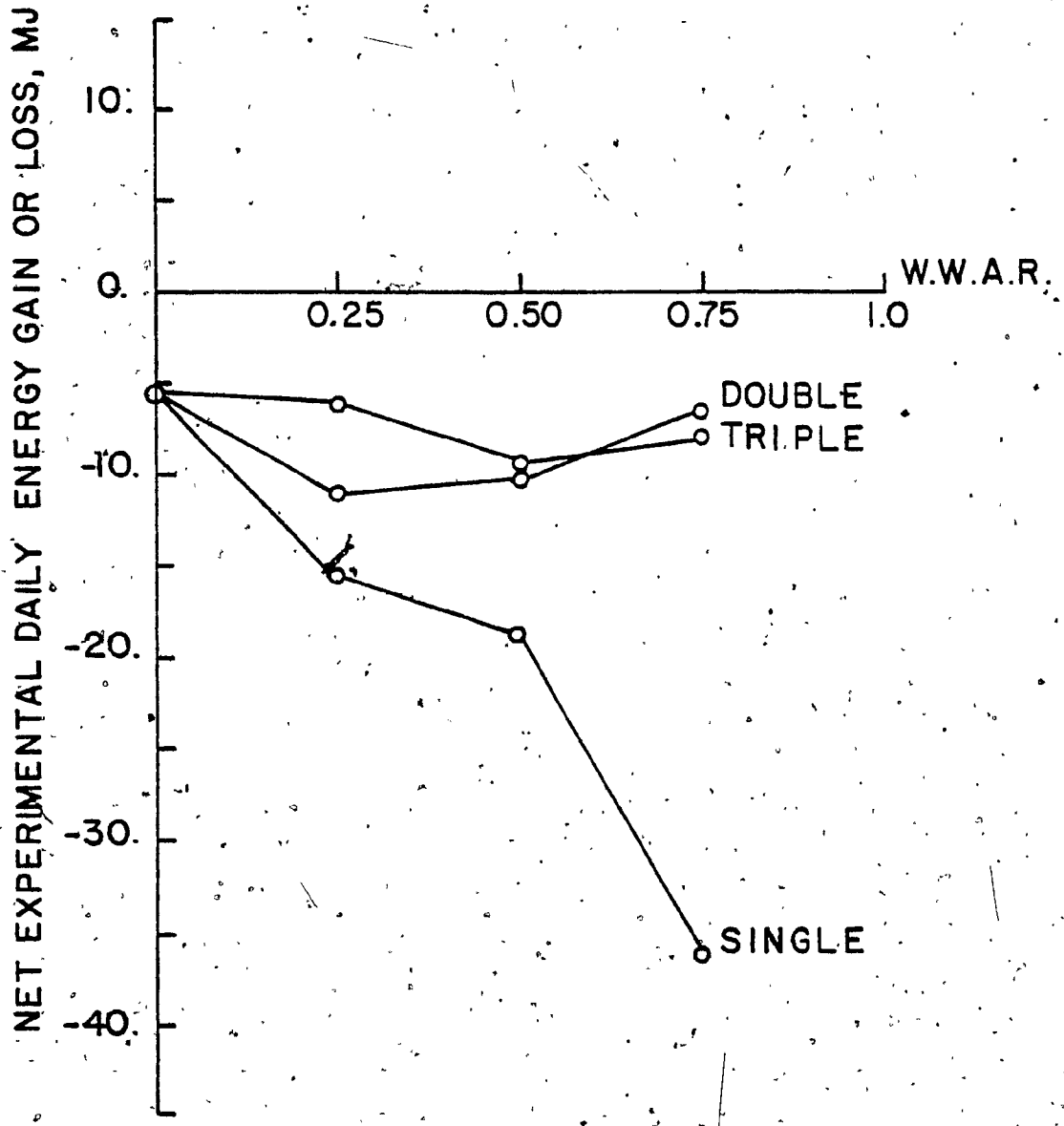

Fig. 5.21: Net experimental daily energy gain or loss from panels with single, double and triple glazed windows facing north.

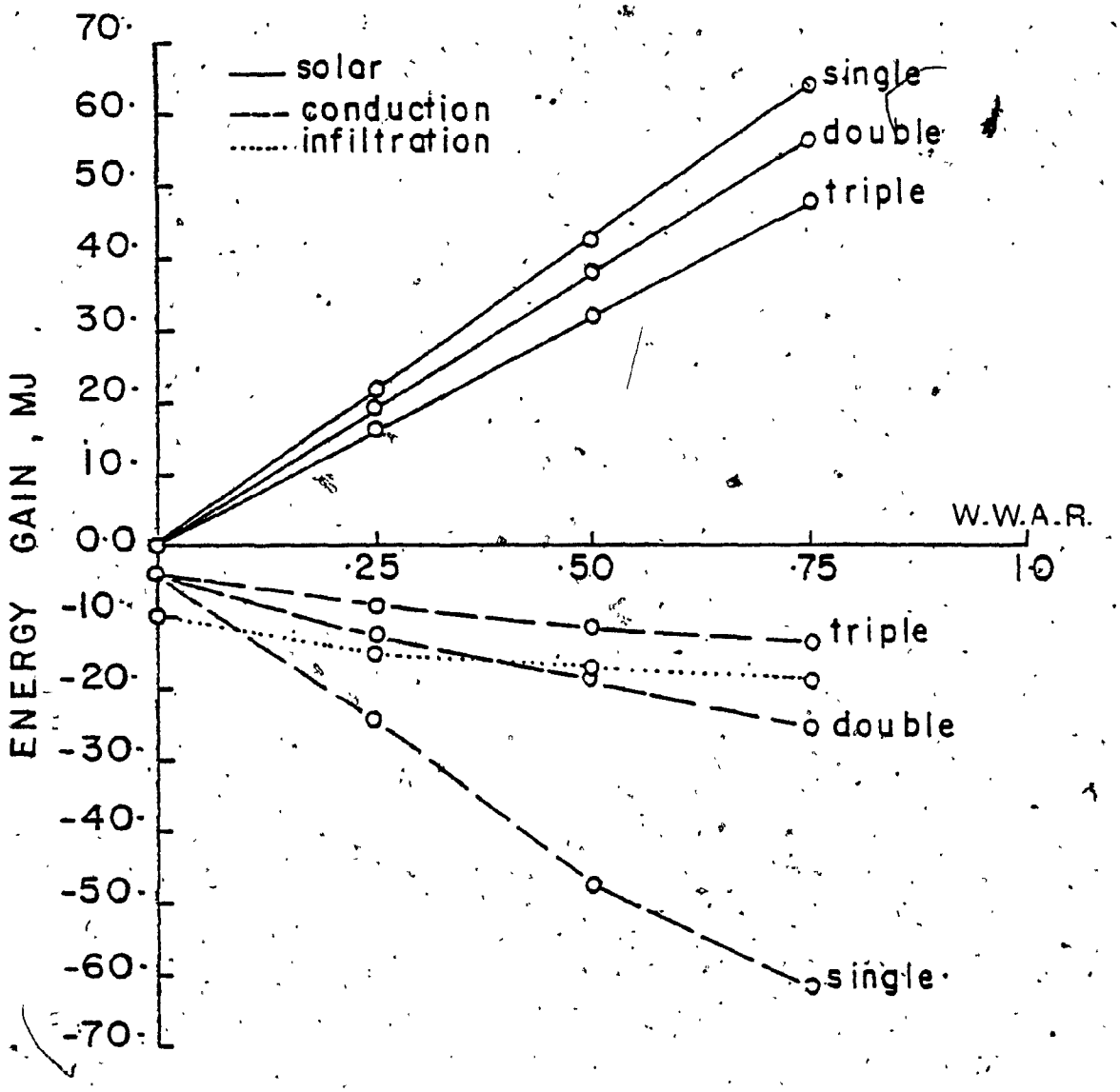

Fig. 5.22: Daily energy breakdown of the typical winter design day for panels with single, double and triple glazed windows facing south.

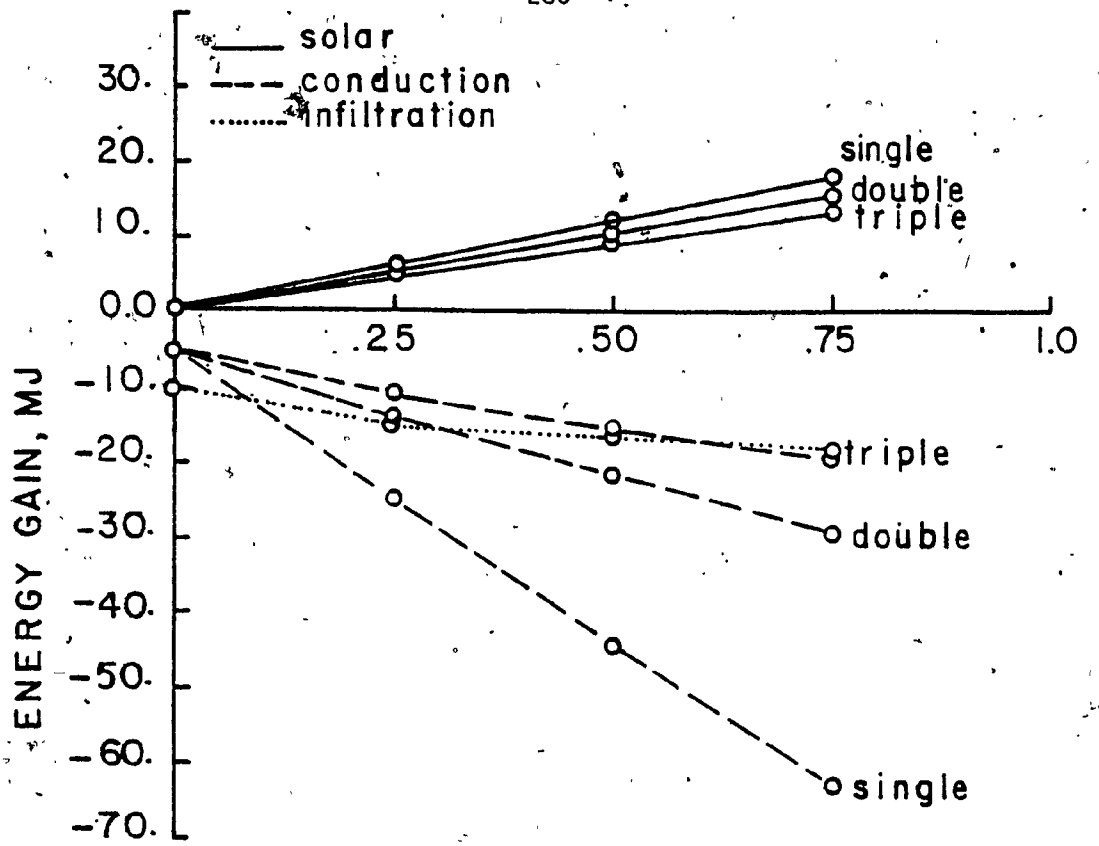

Fig. 5.23: Daily energy breakdown of the typical winter design day for panels with single, double and triple glazed window facing west.

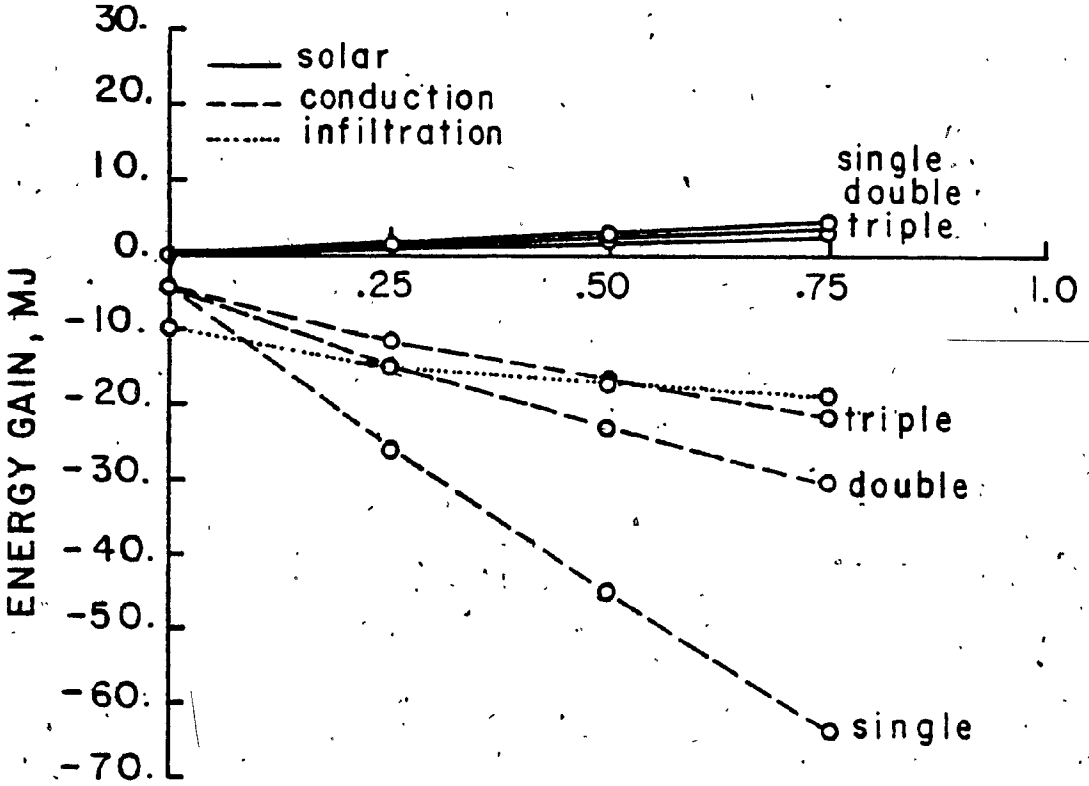

Fig. 5.24: Daily energy breakdown of the typical winter design day for panels with single, double and triple glazed windows facing north.

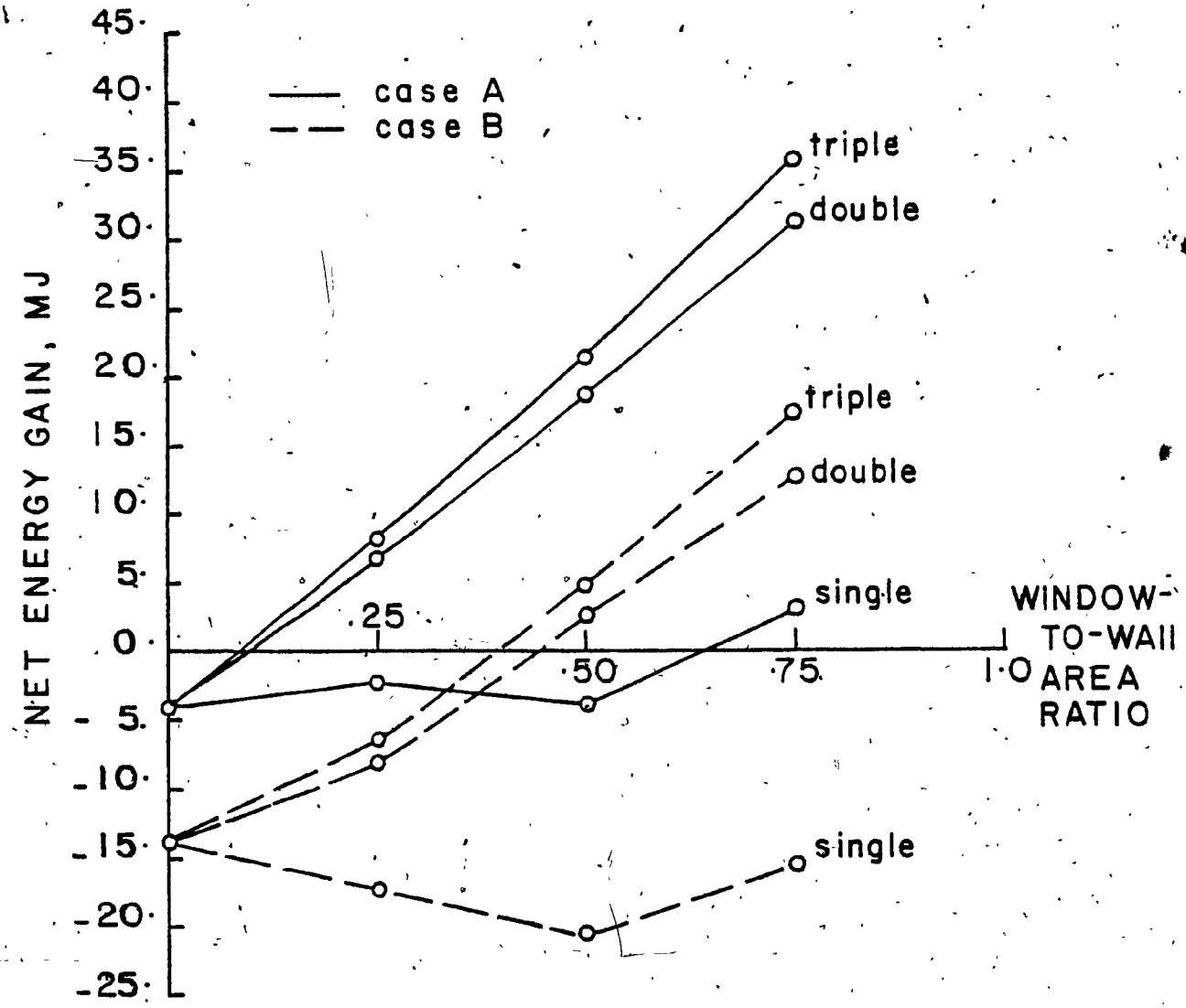

Fig. 5.25: Net daily energy gain of the typical winter design day for panels with single, double and triple glazed windows facing south and for case A and case B.

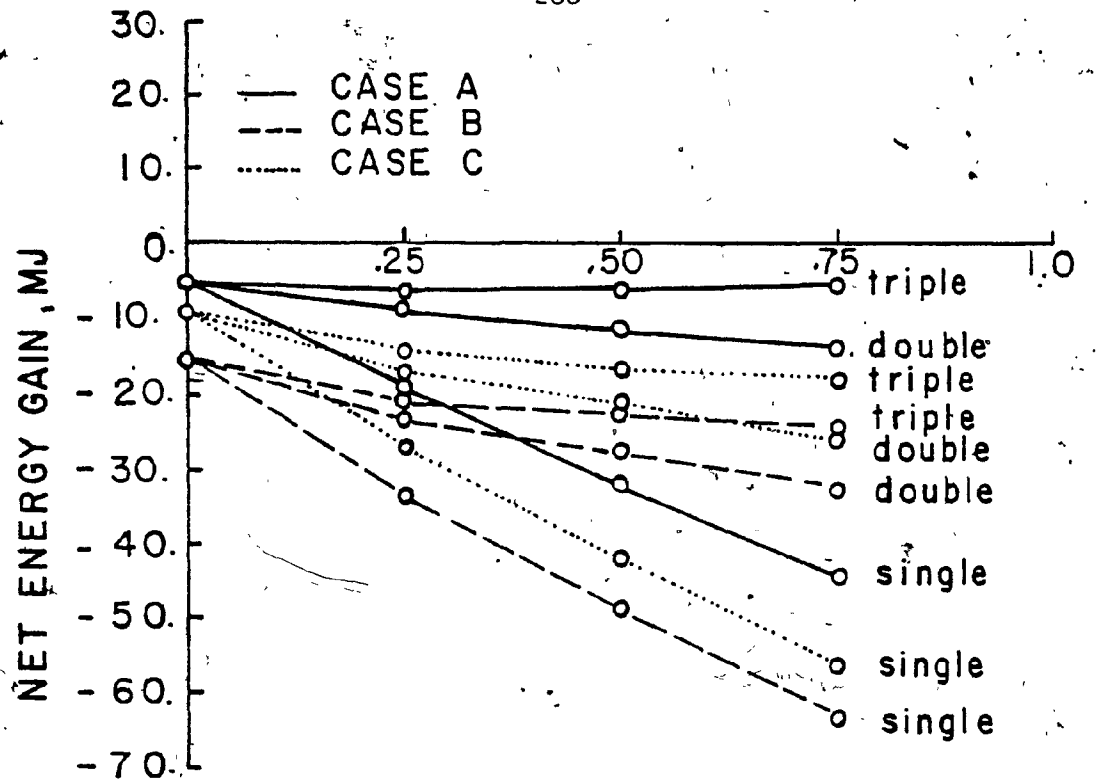

Fig. 5.26: Net daily energy gain of the typical winter design day for panels with single, double and triple glazed windows facing west and for cases A, B and C.

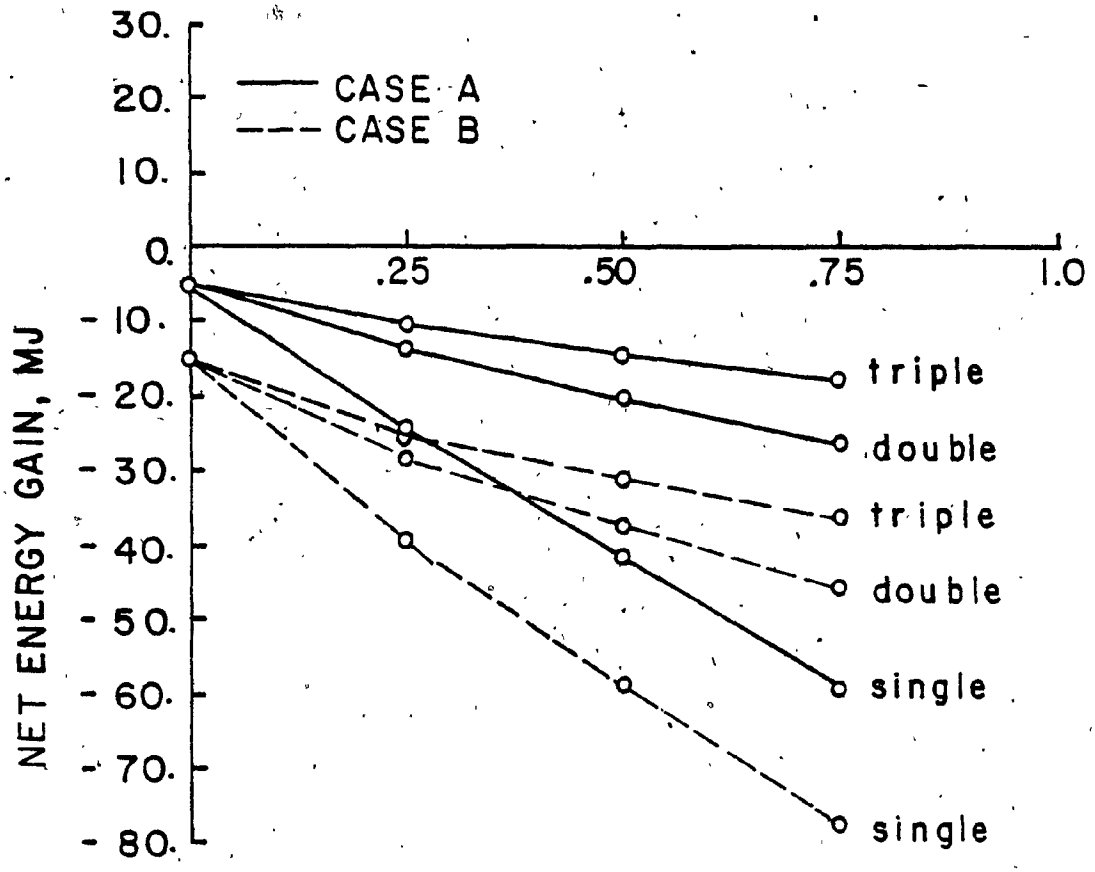

Fig. 5.27: Net daily energy gain of the typical winter design day for panels with single, double and triple glazed windows facing north and for cases A and B.

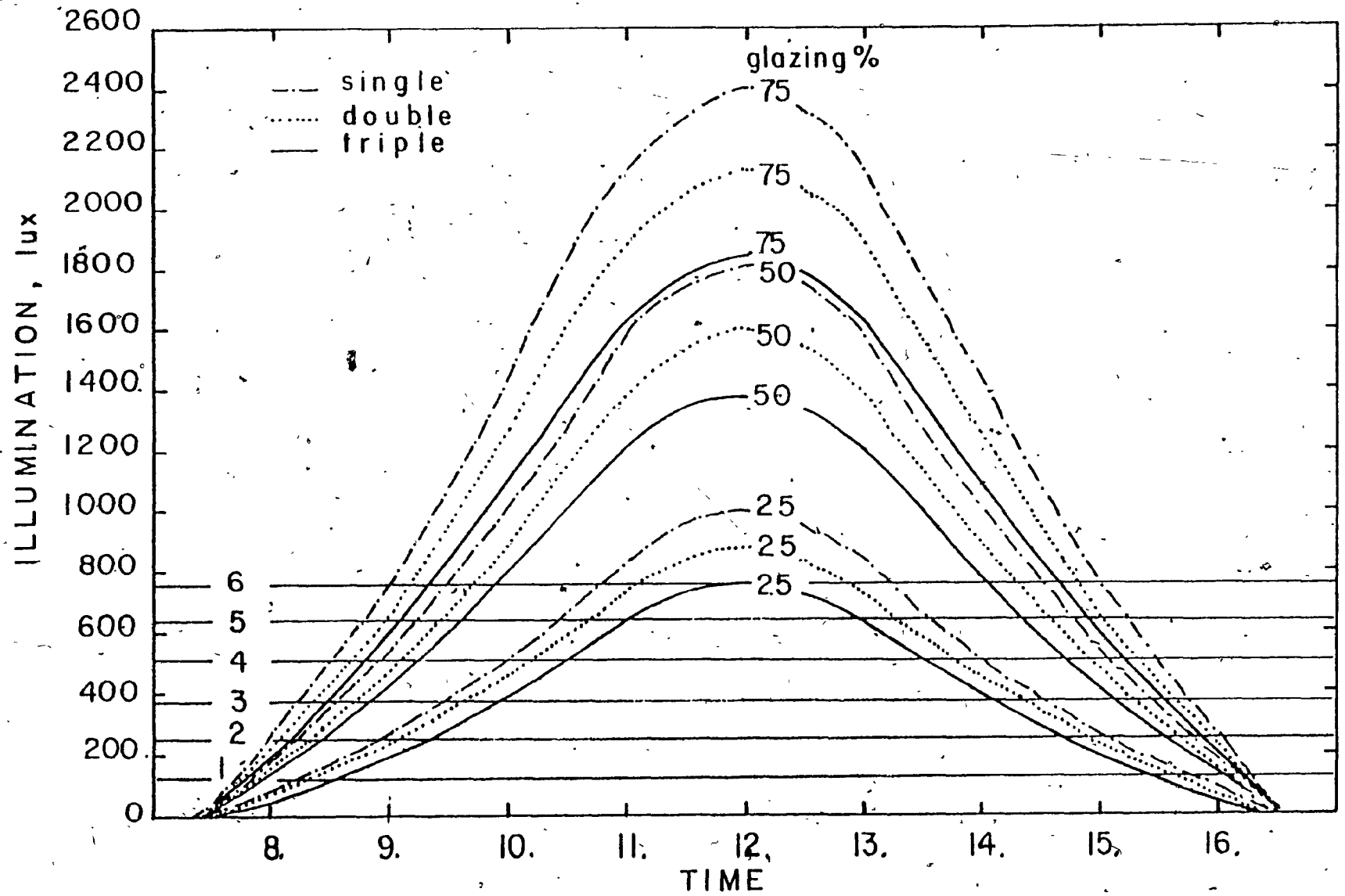

Fig. 5.28: Daylight illumination at the reference point from panels with single, double and triple glazed windows facing south.

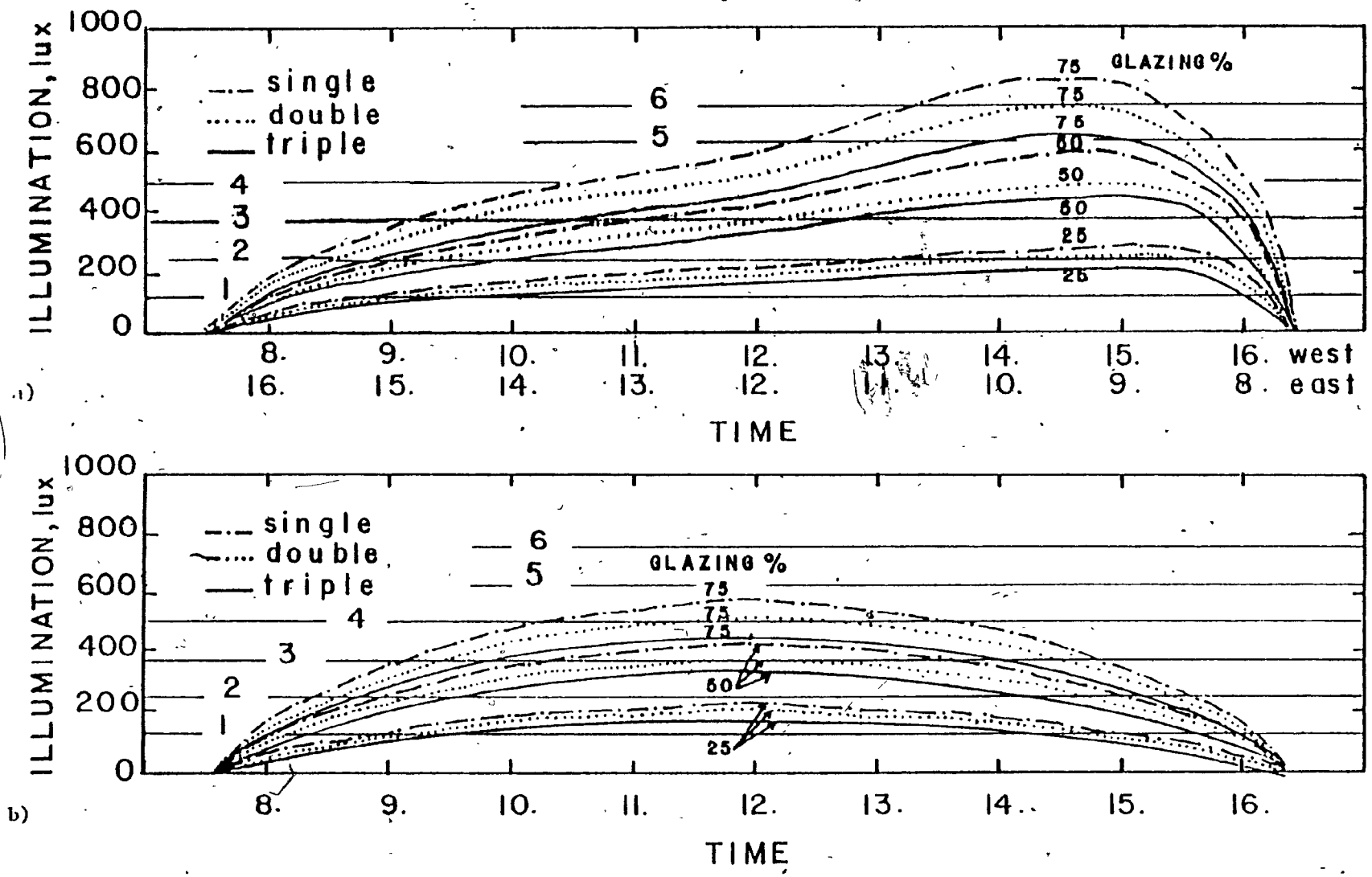

5.29: Daylight illumination at the reference point from panels with single, double and triple glazed windows facing: a) east/west, and b) north

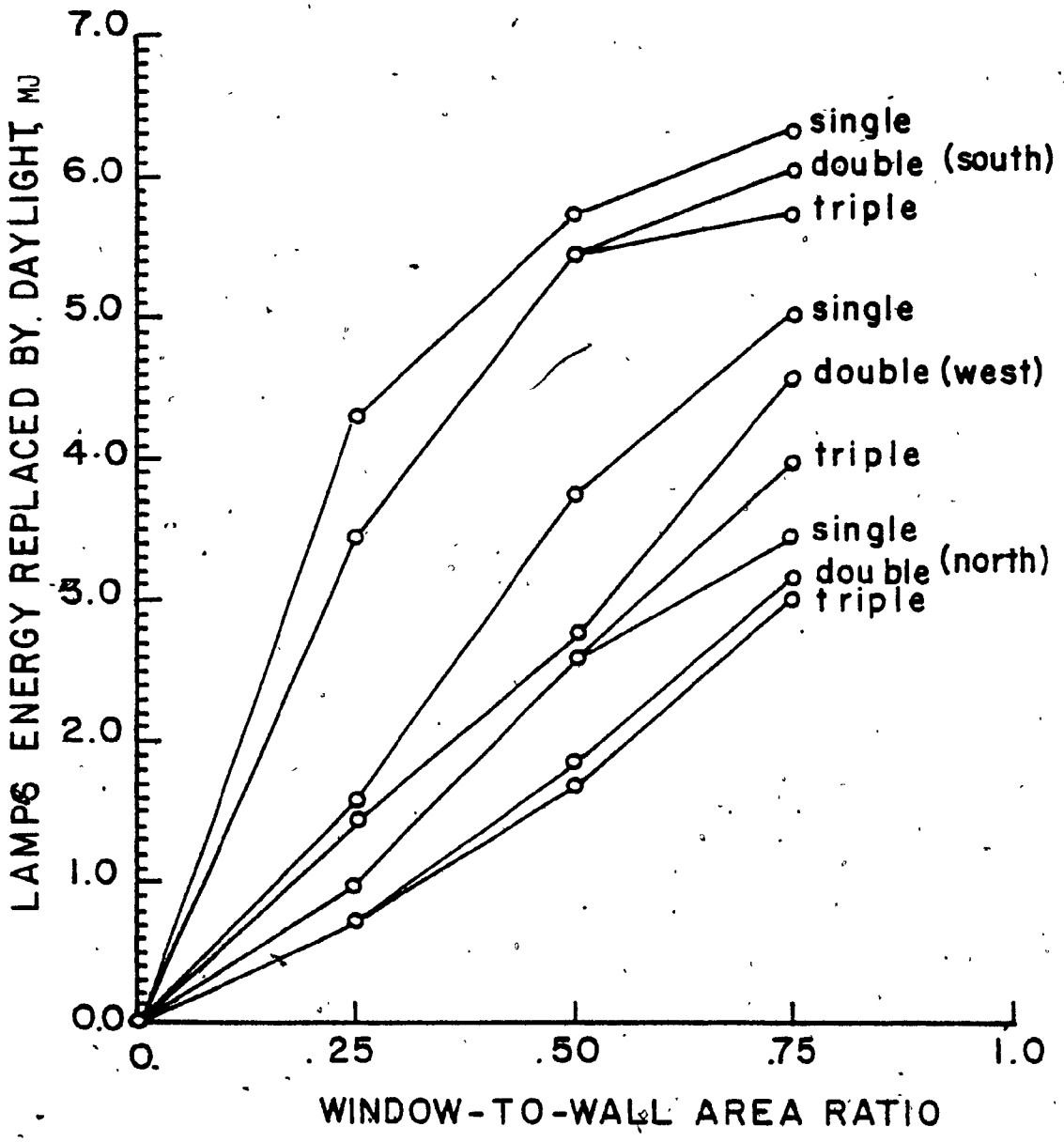

Fig. 5.30: Lamp energy replaced by daylight as a function of window to-wall area ratio, glazing type and orientation.

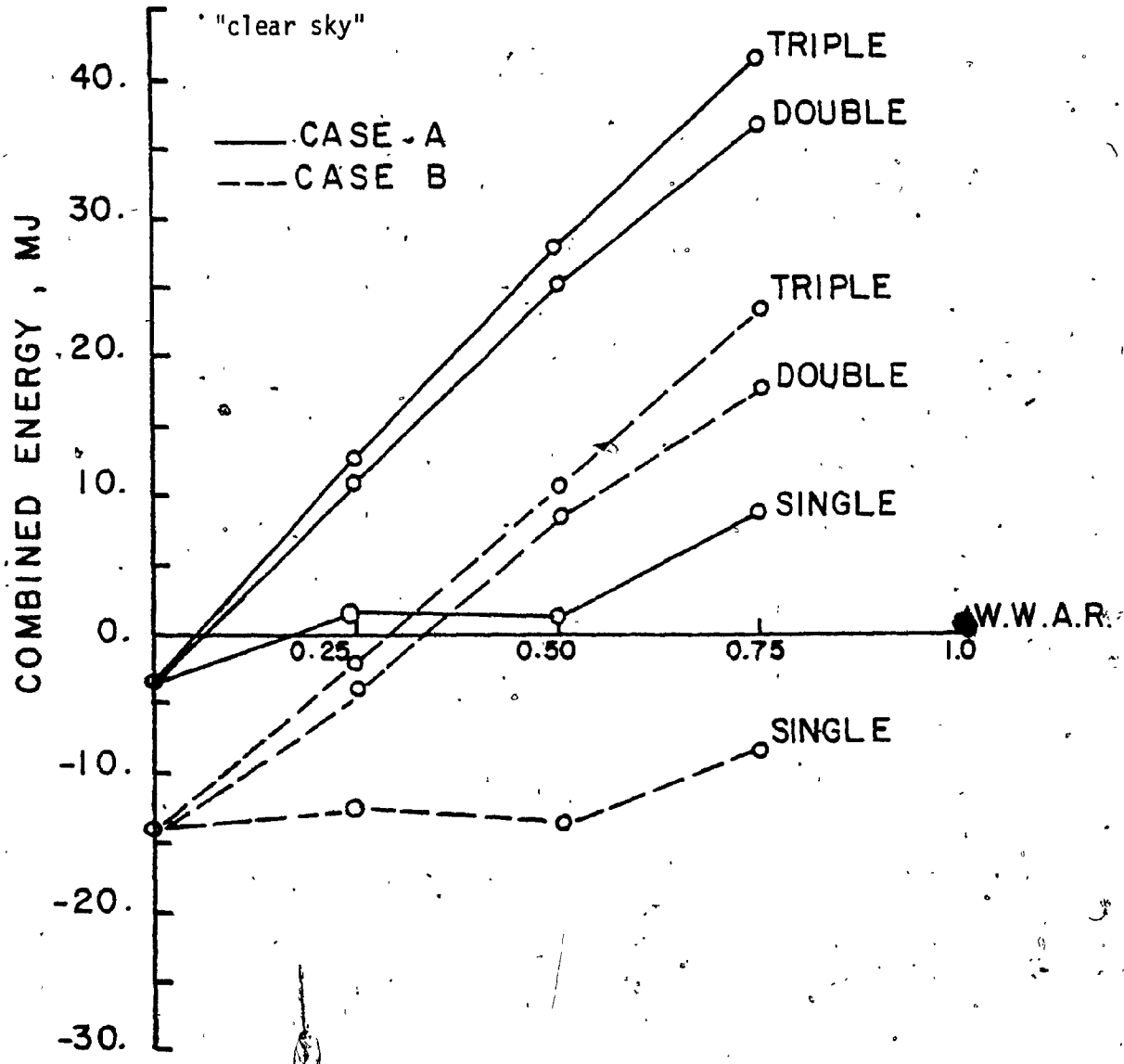

Fig. 5.31: Thermal and daylight daily combined net energy from panels with single, double and triple glazed windows facing south and for case A and case B. (clear sky)

"clear sky"

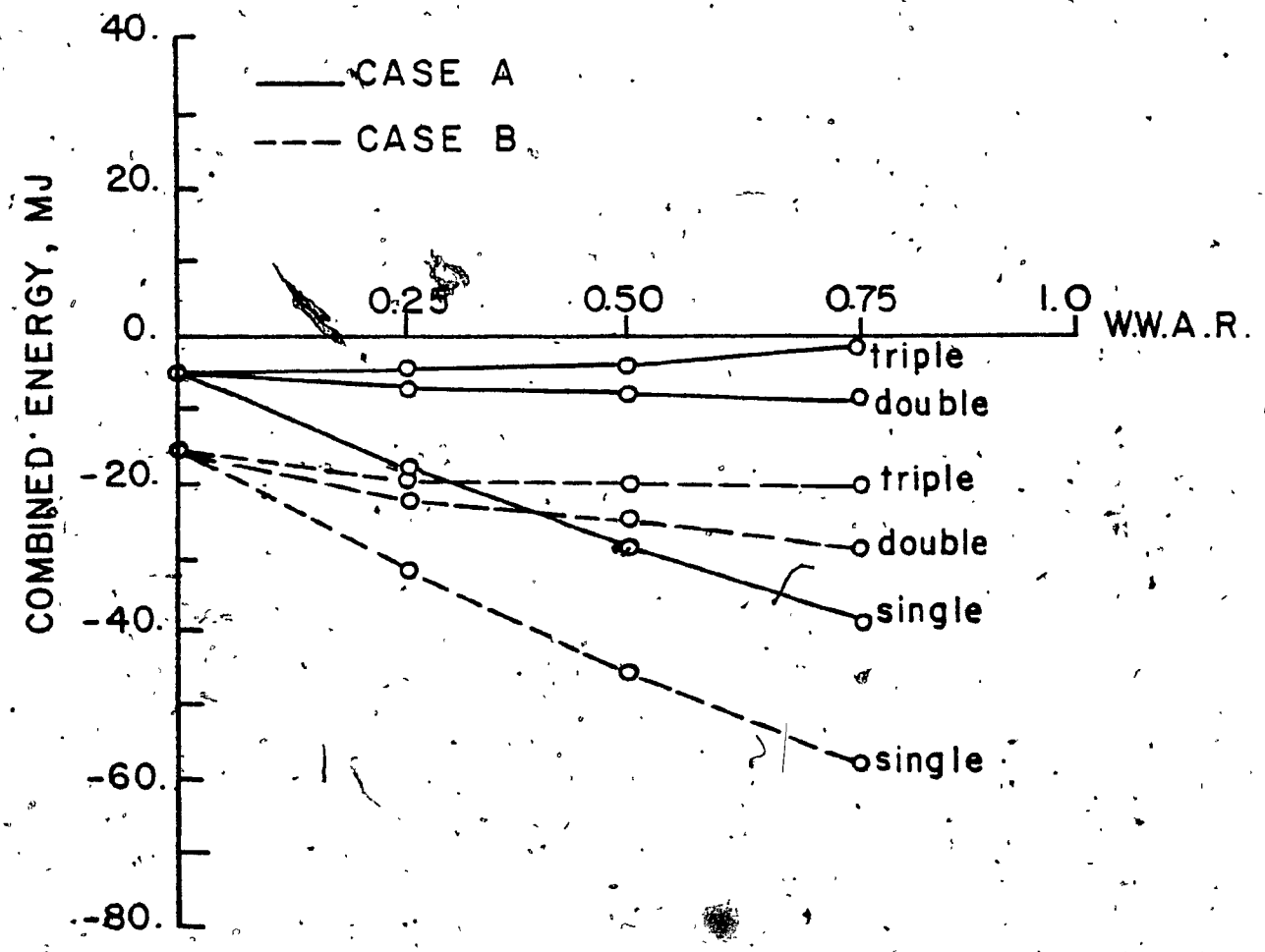

Fig. 5.32: Thermal and daylight daily combined net energy from panels with single, double and triple glazed windows facing east/west and for case A and case B. (clear sky)

"clear sky"

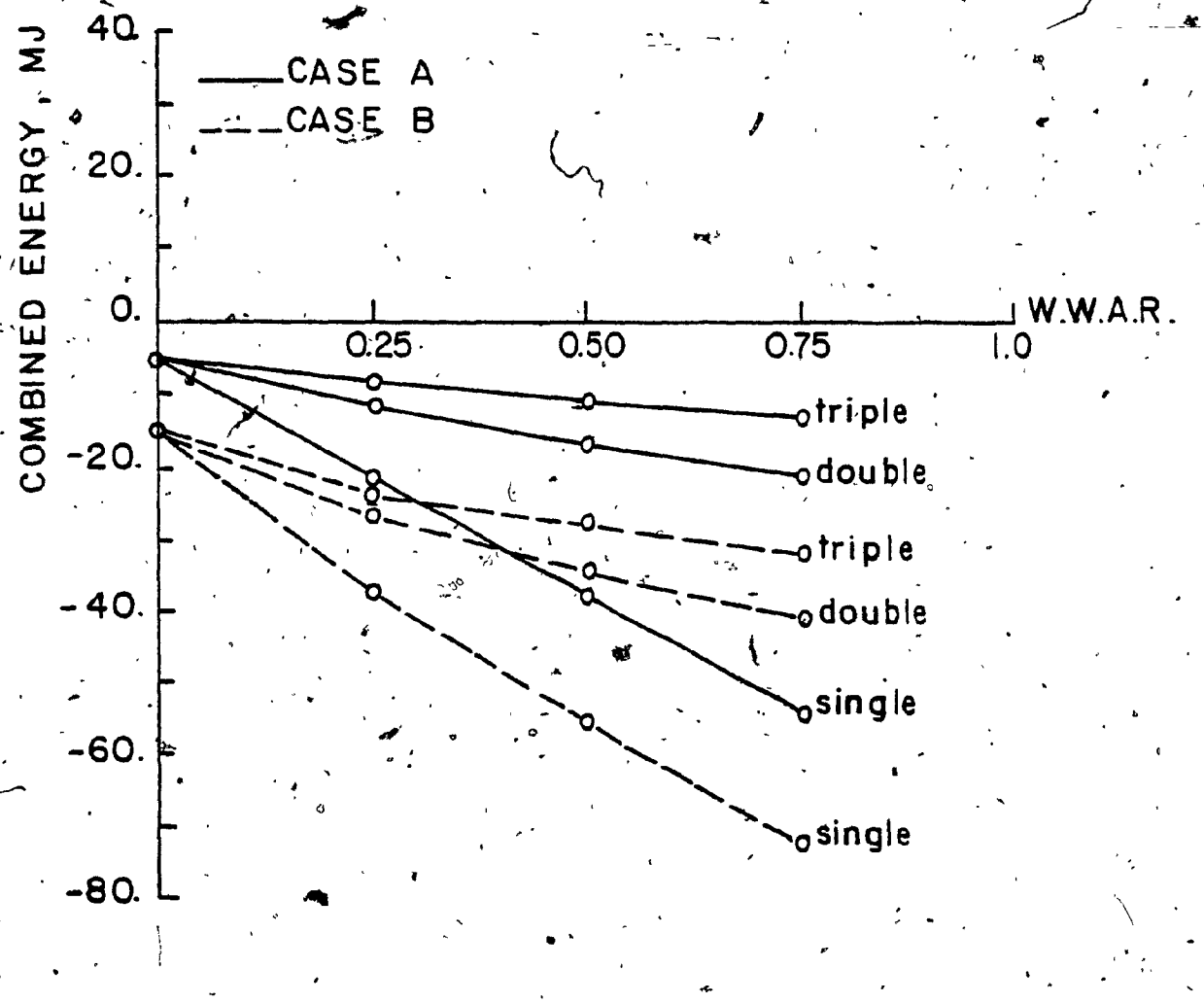

Fig. 5.33: Thermal and daylight daylight daily combined net energy from panels with single, double and triple glazed windows facing north and for cases A and B. (clear sky)

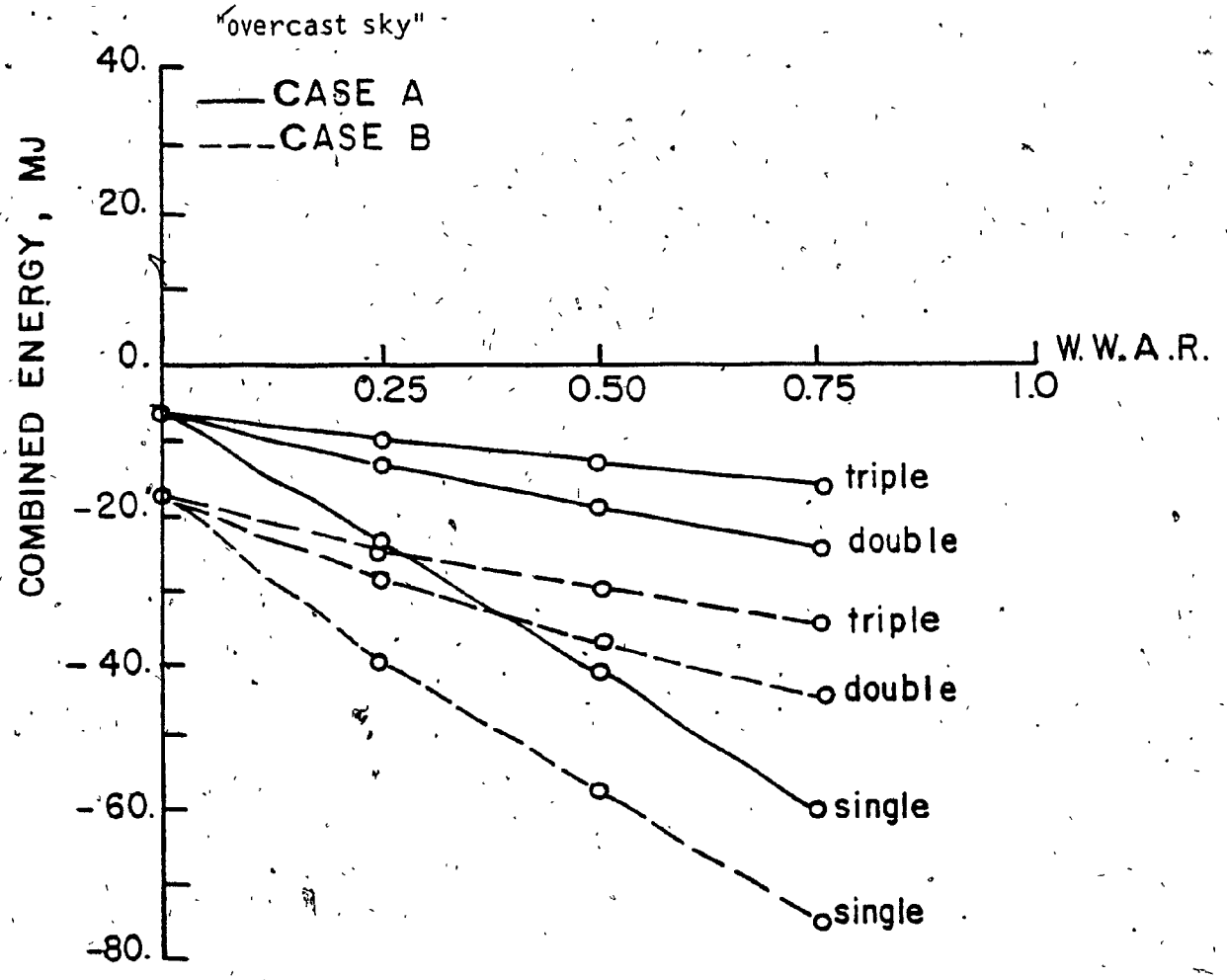

Fig. 5.34: Thermal and daylight daily combined net energy from panels with single, double and triple glazed windows facing north and for cases A and B. (overcast sky)

CHAPTER VI

CONTRIBUTIONS, CONCLUSIONS, AND RECOMMENDATION FOR FUTURE RESEARCH

6.1 CONTRIBUTIONS

Contributions in the field of the thermal and daylight performance of windows that were obtained in this study can be summarized as follows:

i) In response to the need for a more precise thermal model to analyze the energy loss and gain through windows and external walls, a transient, three-dimensional finite difference model has been developed. The implicit formulation of the finite difference method was used to ensure stable solutions with hourly inputs to correspond with Environment Canada Weather Data. Heat storage in the mass of windows and walls is accounted for. So is sideways heat flow at the window frame or between panels. While it was not required here, temperature stratification inside buildings can be handled. The convection at the external surface is calculated by the use of a variable convection coefficient to account for the variation of wind speed, wind direction, and outside air temperature with time. Also the amount by which the window is recessed changes the thermal losses.

ii) The technique of Kerr [218] and Shapiro [219] for the determination of infiltration through monitoring and simulation was extended and refined. The empirical formula obtained for air

infiltration as a function of wind speed was used in the estimation of energy losses by air infiltration in the thermal model.

iii) A practical method for the determination of the convection coefficient at the external surface as a function of wind speed and direction was developed. This method is based on full scale field measurements. A correlation between the surface convection coefficient and wind speed for eight major wind directions was determined and used in the thermal model.

iv) A multi-purpose rotating window and wall test chamber was built to simulate a typical room with one wall exposed to the outside. In the present study, the test chamber was used in full-scale field measurements of energy gains and losses through external wall panels with window-to-wall area ratios of 0.0, 0.25, 0.5, and 0.75. Single, double, and triple glazing were tested for three of the main compass orientations.

v) In response to the need for a time dependent daylight model for accurate determination of the natural daylight illumination inside a room at any given time, a time dependent version of the C.I.E. method of daylight calculation (the daylight factor) has been developed. Both the sky and reflected components of the daylight factor have been calculated as time dependent components using either the C.I.E. overcast or clear sky luminance distribution. Both of these distributions are non uniform with elevation and so represent reality much better than the uniform

sky. With the resulting variable daylight factor, we can calculate different room illuminations for different days, hours, latitudes and window orientations. Thus we obtain much better precision than previous authors. For completely clear or completely cloudy days, these daylight calculations can be combined with hour-by-hour thermal calculations for buildings in a realistic way.

A calculable daylight model for partly cloudy days has also been postulated, and partly validated. If it survives further validation, a reasonably accurate method for calculating annual energy savings through optimal use of daylight will be possible. In this model, we accounted for the non-linearity of the illumination of partly cloudy skies as a function of cloud cover by introducing a brightness factor that is dependent on the cloud cover.

vi) The variable daylight factor was combined with the transient, three dimensional finite difference thermal model to calculate net daily energy gains or losses through vertical external wall panels as a function of window-to-wall area ratio, compass orientation, and number of glazed panes. The simulations were validated with measurements on clear days using the rotating test chamber and four different wall panels for south, west, and north orientations.

The daily energy gains included solar heat gains and lamp energy displaced by daylighting. The daily energy losses included

conduction, convection, and radiation losses through the external wall panel and air infiltration losses. The criterion for lamp control was to maintain 750 lux downward on a point, at desk height, and 2 meters from the glazing. Direct beam illumination was not included in the daylight calculation except where it increased the luminance of exterior surfaces.

To compare the impact of various changes, a series of simulations for a typical design day (clear January 21st) were conducted along with a parametric study to show the impact of eight important parameters on the sky and reflected components of the variable daylight factor.

vii) Based on the thermal and daylight models, two computer codes were developed and validated.

a) The FDIMP program (a finite difference three-dimension transient model using the implicit formulation) has two versions, one for single, double, and triple windows; and the other for multi layer opaque wall panels, and panels with windows. This program calculates the temperature distribution of various layers, the rate of heat transfer, the rate of heat storage, and the rate of heat loss associated with infiltration. The rate of solar heat gain is calculated in the windows' version.

b) The DFV (the Variable Daylight Factor) program calculates the luminance distribution of the sky, the variable sky factor

and the variable reflected component for any given time interval. The program also calculates the sky diffuse illumination, direct beam illumination and the total illumination on external vertical and horizontal surfaces along with their resulting luminances.

6.2 CONCLUSIONS

6.2.1. Conclusions Concerning the Thermal Aspects of This Study

i) In the Montreal area, reducing the window-to-wall area ratio does not always lead to energy savings on a daily basis particularly if the window is facing south. On the contrary, larger windows can gain enough solar energy on a clear winter day to offset the energy losses due to conduction and air infiltration providing proper use of the energy gained was affected.

ii) During winter, the temperature at the corners of the external surface of the window are warmer than the edges and the centre. On the internal surface, the corners are the coldest part.

iii) The heat exchange at the wall panel interface with the surrounding panels and that at the window wall interface are significant (up to 35% of the total heat loss in the experiments) and should and should be taken into consideration by using a three-dimensional transient analysis instead of the most common steady state unidimensional analysis for windows and walls.

iv) The heat stored in the walls and windows showed significant effect on the time rate of heat flow particularly when they were exposed to the direct beam radiation. Therefore, it is essential to use transient heat flow equations to account for the impact of the thermal storage capacity of the panel on the time rate of heat flow.

v) The amount of the window recess within the window opening plays an important role in determining the overall rate of heat flow from inside to outside. The position of the window divides the interface surface of the window opening into three areas; an external area which is exposed to the external environment, an internal area which is exposed to the internal enviornment, and the area of the interface that is covered by the window itself. The position of the window will affect the temperature distribution over the inside and outside surfaces of the wall as well as those on the window opening. The position of the window also affects the total solar heat gain transmitted through the window since the shaded area of the window depends on the distance between the window and the external edge of the wall. The optimal window position in the case of a multilayer wall panel was found to be that position which coincides with the external layer of insulation.

vi) The glazing in the shaded area of the window is cooler than the rest of the glazing, causing an increase in the sideways heat flow within each layer.

vii) Storage of solar heat in the panes of multiple windows can cause the internal surface to be warmer than the room air. Thus, instead of being a conduit for heat loss to the outside, the window acts at times as a heat source, radiating and convecting heat both to the room and the outside. The internal surface of a partially shaded window can be subject to two opposite directions of heat flow at the same time.

viii) The direction of air leakage at the window frame has a noticeable impact on the energy balance at the edge of the wall and the window. This affects the temperature distribution over both the window and the wall. Air infiltration reduces the window edge temperature while air exfiltration increases the window edge temperature. In both cases there is heat exchange between the air leakage and the window edges. The air temperature difference between otuside and inside (T_o-T_i) which is currently used to calculate the heat losses associated with air leakage, does not take into account the heat exchange at the window frame. Due to this heat exchange, the temperature of the infiltrated air becomes warmer than the outside air and the temperature of the exfiltrated air becomes colder than the room air. In order to account for this heat exchange, the temperature difference in the case of exfiltration should be (T_o - T_{ex}) where T_{ex} is the temperature of the air after releasing a quantity of heat to the window frame and wall. In the case of infiltration, the temperature difference should be (T_{inf} - T_i),

where T_{inf} is the temperature of the air after it has gained a quantity of heat at the window frame.

6.2.2 Conclusions Concerning the Use of Daylight

i) Substantial amounts of energy can be saved by proper utilization of daylight (up to 6.4 MJ per winter day in this experiment). Whenever possible, daylight should be regarded as the main lighting source to the interior. Electric lighting should be used as a supplemental source, turned on only when natural daylight falls below the required level of illumination. Proper utilization of daylight in the summer will also reduce the cooling load associated with the heat generated from electric lamps.

ii) The C.I.E. formula for the luminance of clear sky gives good agreement to our measured values on horizontal and vertical surfaces during the first 4 months of the year.

iii) North windows were always assumed to receive the least illumination both on annual and instantaneous basis. The present study has revealed that the instantaneous least illumination is received by windows at azimuths 90° away from the sun azimuth when the C.I.E. clear sky distribution is used.

iv) With the use of the C.I.E. clear sky luminance distribution, we were able to account for the effect of latitude on the daylight factor so that identical windows at different latitude should give different daylight factors.

v) It is commonly known that windows having a window aspect ratio (width-to-height) less than 1.0 provide higher illumination at the back of the room. If the ratio is greater than 1.0, relatively less illumination is received at the back of the room but the sideways illumination gradient is reduced. This is only true if the sky is uniform, but, with the non uniform luminance distribution of the C.I.E. clear sky, this is not always true. For instance, at low sun angles the difference disappears.

vi) The luminance of an unobstructed horizontal plane is commonly used to calculate the externally reflected light from ground. This is untrue because it is often much higher than the luminance of a typical gound surrounded by buildings. Thus, it is important to realize that the ground luminance is affected by the surrounding buildings which block out part of the incoming sky diffuse radiation.

vii) The luminance of external surfaces at times was increased 8.5 times by direct beams radiation from the sun and the reflected light from other external surfaces. Thus, it is important to account for direct beam radiation in the calculation of luminances of external surfaces.

viii) If the window is fully obstructed, maximum illumination is received through a window facing away from the sun (the obstruction surface is facing the sun). This is due to the fact that luminances of external surfaces are often much higher than the sky luminance.

6.2.3 Conclusion Concerning the Combined Thermal and Daylight Aspects of this Study

i) The net energy consumption associated with windows should account for: a) thermal energy loss (due to conduction, convection, radiation, and air leakage) b) solar energy gains, c) reduction in the use of electric lighting when daylight is well utilized, and d) the consequent reduction in cooling energy.

ii) For north windows, the energy savings from daylight was insufficient to offset the thermal energy loss (on January 21st).

iii) If the rate of energy loss through a solid panel is less than the rate of heat generated from lamps in the room, the difference must be offset by cooling which consumes more energy than the window energy losses when daylight is utilized. The net daily losses of East/West triple glazed panels on a clear January 21st were found to be about equal to those of a solid panel, because of the daylighting contribution.

iv) Ignoring the infiltration losses often leads to a false impression regarding the net energy consumption associated with windows.

v) Based on the results of the case study, the energy advantages of triple glazing over double glazing for windows facing east, west, and north was found to be twice as much as that of windows facing south. For the south exposure, the reduction in the conduction losses at the expense of the reduction in the solar heat

gain by using triple glazed windows instead of double glazed windows is unjustifiable. In the case of windows facing east, west, and north the use of triple windows is justifiable. The daylight energy benefits of double glazing over triple glazing of the same type is dependent on the lighting system in the room, the required illumination level, and the illumination interval of the dimmer.

6.3 Recommendations for Further Studies

On the basis of the work presented in this study, it is recommended that the following aspects be considered for further research:

i) Further measurements are needed to relate the zenith luminance to the solar altitude and the sky conditions.

ii) Further experiments are needed to ensure the validity of the partly cloudy sky relation which accounted for the extra brightness caused by white scattered clouds.

iii) Daylight utilization was examined with respect to its energy displacement. Further research should also account for visual discomfort from side windows.

iv) Theoretical and experimental future research is needed to evaluate the convective heat transfer in the air layers within multiple windows in the presence of shading.

v) The optimal window-to-wall area ratio is dependent on the

thermal storage capacity of the room. In the present study, surplus solar heat gain is assumed to be fully utilized in the space. Further research should consider the effect of the thermal storage capacity of the room on the window-to-wall area ratio in both air-conditioned and non-air-conditioned situations.

vi) The effect of window-to-wall area ratio on energy consumption was investigated and experimentally verified for single, double, and triple glazed windows and one single wall construction. Further research should consider other common wall constructions and window types.

vii) The correlation governing infiltration loss (through the tested panel) and wind speed needs further experiments to account for differences in the air tightness from one type of construction to another, and expansion to account for air exfiltration.

viii) Further research is needed to study the proposed thermal integration between one side of the building, (that is experiencing surplus heat gain), and its opposite side (that is in the shade i.e. south-north).

REFERENCES:

[1] Griffin, C.W., Energy Conservation in Buildings: Techniques for Economical Design, The Construction Specification Institute, Inc., Washington, D.C., 1974.

[2] Suntek Research Associates, An Energy Efficient Window System, a technical report, Suntek Research Associates, Corte Madera, California, 1976.

[3] Wilson, A.G. and Sasaki, J.R., "Evaluation of Window Performance", National Bureau of Standards special publication No. 361, Vol. 1, proceedings joint RILEM-ASTM-CIB symposium on "Performance Concept on Buildings" held May 1972, Philadelphia, Pa. pp. 385-394.

[4] Hastings, S.R., "Performance Evaluation of Window Strategies", RILEM/ASTM/CIB Symposium on evaluation of the performance of external vertical surfaces of buildings, Vol. I, Otaniemi, Espoo, finland, Aug. 28 - Sept. 2, 1977, pp. 113-122.

[5] Sasaki, J.R., Thermal Performance Evaluation of Building Enclosure Elements, Technical paper No. 403 of the DBR/NRC Ottawa.

[6] Saski, J.R., "Thermal Performance of Exterior Steel-Stud Frame Walls", ASHRAE Transaction, Vol. 78, part 1, 1972, pp. 192-198.

[7] Teitsma, G.J. and Peavy, B.A., "The Thermal Performance of a Two-Bedroom Mobile Home", National Bureau of Standards report No. NBS-BSS-102 U.S. Department of Commerce, Washington, Feb. 1978.

[8] Sabine, H.J. and Lacher, M.B., "Accoustical and Thermal Performance of Exterior Residential Walls, Doors, and Windows", National Bureau of Standards publication BSS-77, U.S. Dept. of Commerce, Washington, D.C., 1975.

[9] Lowinski, J.F., "Thermal Performance of Wood Windows and Doors", ASHRAE Transactions, PH-79-6, No. 2, 1979, pp. 548-566.

[10] American Society of Heating, Refrigerating and Air-Conditioning Engineers, Handbook of Fundamentals, ASHRAE Inc., New York, 1977.

[11] Duffie, J.A., Beckman, W.A., Solar Energy Thermal Processes, John Wiley & Sons, New York, 1974.

[12] Kreith, F., Kreider, J.F., Principles of Solar Engineering, Hemispherc Publishing Corporation, Washington, 1978.

[13] Agarwal, K.N., Verma, V.V., "Thermal Characteristics of Glazing and Shading Materials", Building and Environment, Vol. 12, Pergamon Press, 1977, pp. 57-62.

[14] Lim, B.P., Conner, J., "Thermal Transmission Coefficients of Double Glazed Window Units", Architectural Science Review, June 1969, pp. 35-40.

[15] Ambrose, E.R., "Thermal Insulation and Double Glazing", paper No. 16, Handbook of Energy Conservation for Mechanical Systems in Buildings, pp. 80-83, compiled and edited by Robert W. Roose, Van Nostrand Reinhold Co., New York, 1978.

[16] Mitalas, G.P and Arseneault, J.G., "Fortran IV Program to Calculate Absorption and Transmission of Thermal Radiation by Single and Double-Glazed Windows", NBS Building Science Series No. 39, Use of Computer for Environmental Engineering Related to Buildings, U.S. Dept. of Commerce, Washington, Oct. 1977, pp. 465-476.

[17] Isfält, E., "A Computer Analysis of Window Shading Coefficients by Calculating Optical and Thermal Transmission", NBS Building Science Series No. 39, Use of Computer for Environmental Engineering Related to Buildings, U.S. Dept. of Commerce, Washington, Oct. 1977, pp. 477-486.

[18] Gupta, C.L., "Heat Transfer in Buildings - A Review", Architectural Science Review, March 1970, pp. 1-10.

[19] Kusuda, T., "Fundamentals of Building Heat Transfer", Energy Conservation in Heating, Cooling, and Ventilating Buildings, Vol. 1, edited by Hoogendoorn, C.J. and Afgan N.H., Hemisphere Publishing Corporation, Washington, 1978, pp. 321-330.

[20] Beijer, O., "Variation of Temperature in External Walls with Heat Capacity", RILEM/ASTM/CIB Symposium on Evaluation of the Performance of External Vertical Surfaces of Buildings, Vol. 1, Ontaniemi, Espoo, Finland, Aug. 28 - Sept. 2, 1977, pp. 22-31.

[21] Mitalas, G.P., "Relation Between Thermal Resistance and Heat Storage in Building Enclosures", DBR/NRC Building Research note No. 126, Ottawa, January 1978.

[22] Hassan, K., Hanna G.B., "Effect of Walls on Indoor Temperatures", Build International, July - Aug. 1972, pp. 220-226.

[23] Bystrov, V., and Galaktionov, V., "Analysis of Heat Transfer Through Walls with Vertical Air Layers and Wall Leakage", Energy Conservation in Heating, Cooling, and Ventilating Buildings, Vol. 1, edited by Hoogendoorn, C.J. and Afgan N.H., Hemisphere Publishing Corporation, Washington, 1978, pp. 125-134.

[24] Building Research Station, "Standard U-Value", digiest No. 108, HMSO, Garston, Watford, England, Aug. 1969.

[25] Loudon, A.G., "U-Value in the 1970 Guide", J.I.H.V.E., September 1968, pp. 167-174.

[26] Givoni, B., "Heat Storage in Buildings: an Overview", Energy Conservation in Heating, Cooling and Ventilating Buildings, Vol. 2, edited by Hoogendoorn, C.J. and Alfgan, N.H., Hemisphere Publishing Corporation, Washington, 1978, pp. 559-572.

[27] Rennekamp, S.J., "U-Value Testing of Windows Using a Modified Guarded Hot Box Technique", ASHRAE Transactions, PH-79-6, No. 1, 1979, pp. 527-547.

[28] Sasaki, J.R. and Wilson, A.G., "Air Leakage Values for Residential Windows", ASHRAE Transactions, Vol. 71, Part II., 1965, pp. 81-88.

[29] Trechsel, H.R., "Test Methods for Windows and Walls - The Need for a Testing Program", RILEM/ASTM/CIB Symposium on Evaluation of the Performance of External Vertical Surfaces of Buildings, Vol. I, Otaniemi, Espoo, Finland, Aug. 28 - Sept. 2 1977, pp. 374-382.

[30] Tamura, G.T. and Wilson, A.G., "Air Leakage and Pressure Measurements on Two Occupied Houses", ASHRAE Journal, Vol. 5, No. 12, Dec. 1963, pp. 65-73.

[31] Tamura, G.T., "Measurements of Air Leakage Characteristics of House Enclosures", ASHRAE Transactions, Vol. 81, Part I, 1975, pp. 202-211.

[32] Sasaki, J.R., "Measurements of Thermal Breakage Potential of Solar - Control Sealed Glazing Units", Research paper No. 617 of DBR/NRCC, Ottawa, 1974.

[33] Sasaki, J.R., "Potential for Thermal Breakage of Sealed Double - Glazing Units", Digest No. CBD - 129, DBR/NRCC, Ottawa, Sept. 1970.

[34] Sinha, N.K., "Stress State in Tempered Glass Plate and Determination of Heat Transfer Rate", Experimental Mechanics, Vol. 18, No. 1, January 1978.

[35] Solvason, K.R., "Pressures and Stresses in Sealed Double Glazing Units", Technical paper No. 423, DBR/NRCC, Ottawa, Aug. 1974.

[36] Cole, R.J., Sturrock, N.S., "The Convective Heat Exchange at the External Surface of Buildings", Building and Environment, Vol. 12, Pergamon Press, 1977, pp. 207-214.

[37] Pennington, C.W., Morrison, C., Pena, R. Jr., "Effect of Inner surface Air Velocity and Temperature Upon Heat Loss and Gain through Insulating Windows", ASHRAE Transactions, Vol. 79, Part II, 1973, pp. 111-126.

[38] Pennington, C.W., McDuffey, D.E., "Effect of Inner Surface Air Velocity and Temperature Upon Heat Gain and Loss Through Glass Fenestration," ASHRAE Transactions, Vol. 76, 1970, pp. 190-214.

[39] Eckert, E.R.G., and Carlson, W.O., "Natural Convection in an Air Layer Enclosed Between Two Vertical Plates with Different Temperatures," Int. J. of Heat Transfer, Vol. 2, Pergamon Press, 1961, pp. 106-120.

[40] Railhby, G.d., Hollands, K.G.T., Unny, T.E., "Analysis of Heat Transfer by Natural Convection Across Vertical Fluid Layer," Journal of Heat Transfer, Vol. 99, May 1977, pp. 287-293.

[41] Ozoe, H., Sayama, H., and Churchill, S.W., "Natural Convection in an Inclined Rectangular Channel at Various Aspect Ratios and Angles-Experimental Measurements," Int. J. of Heat Transfer, Vol. 18, Pergamon Press, 1975, pp. 1425-1431.

[42] Gray, W.A., and Müller, R., "Engineering Calculations in Radiative Heat Transfer, Pergamon Press, Oxford, G.B., 1974.

[43] Garden, R., "A Review of Radiant Heat Transfer in Glass," Journal of The American Ceramic Society, July 1961, pp. 305-312.

[44] Liu, B.H. and Jordan, R.C., "The Interrelationship and Characteristic Distribution of Direct, Diffuse and Total Solar Radiation," Solar Energy, Vol. 4, No. 3, 1960, pp. 1-19.

[45] Cole, R.J., "Direct Solar Radiation Data as Input into Mathematical Models Describing the Thermal Performance of Buildings - I: A Review of Existing Relationships which Predict the Direct Component of Solar Radiation," Building and Environment, Vol. 11, Pergamon Press, 1976, pp. 173-179.

[46] Kasten, F., "Measurement and Analysis of Solar Radiation Data," Energy and Buildings, Vol. 3, Elsevier Sequoia, 1981, pp. 1-29.

[47] Cole, R.J., "Direct Solar Radiation Data as Input into Mathematical Models Describing the Thermal Performance of Buildings," Building and Environment, Vol. 11, Pergamon Press, 1976, pp. 181-186.

[48] Stephenson, D.G., "Equations for Solar Heat Gain Through Windows," Solar Energy, Vol. 9, No. 2, 1965, pp. 81-86.

[49] Threlkeld, J.L., and Jordon, R.C., "Direct Solar Radiation Available on Clear Days," ASHRAE Transactions, Vol. 64, 1958, p. 45.

[50] Stephenson, D.G., "Tables for Solar Altitude, Azimuth, Intensity, and Heat Gain Factors for Latitudes from 43° to 55° North," Technical paper No. 243, DBR/NRCC, Ottawa, April 1967.

[51] Stephenson, D.G., "Solar Heat Gain Through Glass Walls," Digest No. CBD-39, DBR/NRCC, Ottawa, March, 1963.

[52] Nicol, K., "The Energy Balance of an Exterior Window Surface, Inuvik, N.W.T., Canada," Building and Environment, Vol. 12, Pergamon Press, 1977, pp. 215-219.

[53] Dave, J.V., "Validity of the Isotropic Distribution Approximation in Solar Energy Estimations," Solar Energy, Vol. 19, Pergamon Press, 1977, pp. 331-333.

[54] Viskanta, R. & Hirleman, E.D., "Solar Radiation Transmission and Heat Transfer Through Architectural Windows," Energy Conservation in Heating, Cooling and Ventilating Buildings, Vol. 2, edited by Hoogendoorn, C.J., and Afgan, N.H., Hemisphere Publishing Corporation, Washington, 1978, pp. 869-882.

[55] Kiss, L.I. and Benkö, I., "An Improved Model for Calculation of Heat Transfer due to Solar Radiation through Windows," Energy Conservation in Heating, Cooling, and Ventilating Buildings, Vol. 2, edited by Hoogendoorn, C.J., and Afgan, N.H., Hemisphere Publishing Corporation, Washington, 1978, pp. 883-896.

[56] Building Research Station, "Window Design and Solar Heat Gain," Digest No. 68, Second Series, HMSO, Garston, G.B., March, 1966.

[57] Sasaki, J.R., Wilson, A.G., "Window Air Leakage," Digest No. CBD-25, DBR/NRCC, Ottawa, January, 1962.

[58] Tamura, G.T., "Predicting Air Leakage for Building Design," Technical paper No. 437, DBR/NRCC, Ottawa, 1974.

[59] Tamura, G.T., "Measurement of Air Leakage Characteristics of House Enclosures", ASHRAE Transactions, Vol. 81, Part 1, 1975, pp. 202-211.

[60] Tamura, G.T., and Shaw, C.Y., "Studies on Exterior Wall Air Tightness and Air Infiltration of Tall Buildings", ASHRAE Transactions, Vol. 82, Part 1, 1976, pp. 122-134.

[61] Shaw, C.Y., Sander, D.M., and Tamura, G.T., "Air Leakage Measurements of the Exterior Walls of Tall Buildings", ASHRAE Transactions, Vol. 79, Part 2, 1973, pp. 40-48.

[62] Phillips, C.W., Peavy, B.A., and Kuklewicz, M.E., "Air Leadkage and Thermal Performance of a Mark III Relocatable Lewis Building", N.B.S. publication No. PB 264211, U.S. Dept. of Commerce, Washington, 1976.

[63] Gupta, C.L., "A Systematic Approach to Optimum Thermal Design," Building Science, Vol. 5, Pergamon Press, 1970, pp. 165-173.

[64] Gupta, C.L., "Thermal Design of Building Envelopes for Minimum Total Cost," Build International, Nov - Dec. 1972, pp. 363-366.

[65] Gupta, C.L., "A System Model for Environmental Design of Buildings", NBS Building Science Series No. 39, Use of Computer for Environmental Engineering Related to Buildings, U.S. Dept. of Commerce, Washington, October 1971, pp. 61-70.

[66] Radford, A.D., "Some Room/Environment Optimization Models Using Dynamic Programming", Computer Report No. CR30, Dept. of Architectural Science, University of Sydney, N.S.W., Australia, 1978.

[67] Galbreath, M. "Daylight Design," Digest No. CBD-17, Division of Building Research, National Research Council of Canada, Ottawa, May 1961.

[68] Page, J.K., "The Optimization of Building Shape to Conserve Energy," Journal of Architectural Research, Royal Institute of British Architects and the American Institute of Architects, No. 3, Sept. 1974, pp. 15-20.

[69] Kimura, K., "Optimum shape of External Shape for The Window to Minimize Annual Solar Heat Gain and to Maximize View Factor," NBS Building Science Series No. 39, Use of Computer for Environmental Engineering Related to Buildings, U.S. Dept. of Commerce, Washington, 1971, pp. 487-500.

[70] Arumi, F., "Daylighting as a Factor in Optimizing the Energy Performance of Buildings", Energy and Buildings, Vol. 1, 1977, pp. 175-192.

[71] Gupta, C.L., Spencer, J.W., and Muncey, R.W.R., "A Conceptual Survey of Computer-Oriented Thermal Calculation Methods," NBS Building Science Series No. 39, Use of Computer for Environmental Engineering Related to Buildings, U.S. Dept. of Commerce, Washington, 1971, pp. 103-110.

[72] Norman, S.F., Mutka, N.E., "Design Considerations for a Practical Heat Gain Computer Code," NBS Building Science Series No. 39, Use of Computer for Environmental Engineering Related to Buildings, U.S. Dept. of Commerce, Washington, 1971, pp. 71-85.

[73] Magnussen, J.L., "Analog Computer Simulation of an Air Conditioning System in a Commercial Building Incorporating Yearly Weather," NBS Building Science Series No. 39, Use of Computer for Environmental Engineering Related to Buildings, U.S. Dept. of Commerce, Washington, 1971, 147-158.

[74] Sheridan, N.R., "Experience with a Thermal Network Analysis Programme Applied to Heat Flow in Buildings," NBS Building Science Series No. 39, Use of Computer for Environmental Engineering Related to Buildings, U.S. Dept. of Commerce, Washington, 1971, pp. 159-170.

[75] Oegema, S.W.T.M., and Euser, P., "An Accurate Computing Method for the Analysis of the Non-Steady Thermal Behaviour of Office Buildings", NBS Building Science Series No. 39, Use of Computer for Environmental Engineering Related to Buildings, U.S. Dept. of Commerce, Washington, 1971, pp. 289-304.

[76] Fromm, J.E., "A Numerical Method for Computing the Non-linear, Time Dependent, Buoyant Circulation of Air in Rooms," NBS Building Science Series No. 39, Use of Computer for Environmental Engineering Related to Buildings, U.S. Dept. of Commerce, Washington, 1971, pp. 451-464.

[77] ASHRAE Task Group on Energy Requirements for Heating and Cooling of Buildings, "Procedure for Determining Heating and Cooling Loads for Computerizing Energy Calculations: Algorithms for Building Heat Transfer Subroutines," American Society of Heating, Refrigerating and Air-Conditioning engineers Inc., New York, 1976.

[78] Mitalas, G.P., and Arsenault, J.G., "Fortran IV Program to Calculate Z-Transfer Functions for the Calculation of Transient Heat Transfer Through Walls and Roofs", NBS Building Science Series No. 39, Use of Computer for Environmental Engineering Related to Buildings, U.S. Dept. of Commerce, Washington, 1971, pp. 633-662.

[79] Degelman, L.O., "Monte Carlo Simulation of Solar Radiation and Dry-Bulb Temperatures for Air-Conditioning Purposes," Proceeding of the Kentucky Workshop on Computer Application to Environmental Design, College of Architecture, University of Kentucky, 1970, pp. 213-223.

[80] ASHRAE STANDARD 90-75, Energy Conservation in New Building Design," American Society of Heating, Refrigerating and Air-Conditioning Engineers, 1975.

[81] Associate Committee on the National Building Code, "Commentary on Measures for Energy Conservation in New Buildings", National Research Council of Canada, Ottawa, 1978.

[82] Ayres, J.M., "Predicting Building Energy Requirements," Energy and Buildings, Vol. 1, 1977, pp. 11-18.

[83] Dickens, H.B., and Wilson, A.G., "Energy Conservation and Building Regulations", Proceedings, First Canadian Building Congress: Energy and Building, Sponsored by The Canadian Committee on Building Research of the National Research Council of Canada, Toronto, 1976, pp. 201-207.

[84] Dubin, F., "Energy Conservation Studies," Energy and Buildings, Vol. 1, 1977, pp. 31-42.

[85] Fantl, K., "Saving Energy in Housing," Building Research and Practice, Sept./Oct. 1976, pp. 284-294.

[86] Ambrose, E.R., "Architectural Aspects of Energy Conservation in HVAC," paper No. 15, Handbook of Energy Conservation for Mechanical Systems in Buildings, Compiled and edited by Robert W. Roose, Van Nostrand Reinhold Co, New York, 1978, pp. 77-79.

[87] Rudoy, W., and Duran, F., "Effect of Building Envelope Parameters On Annual Heating/Cooling Load," ASHRAE Journal, July 1975, pp. 19-25.

[88] Arens, E.A. and Williams, P.B., "The Effect of Wind On Energy Conservation in Buildings," Energy and Buildings, Vol. 1, 1977, pp. 77-84.

[89] Berman, S.M., and Silverstein, S.D., editors, "Energy Conservation and Window Systems," American Institute of Physics Conference Proceedings, No. 25, Part III, Efficient Use of Energy, AIP, New York, 1975.

[90] Collins, B.L., Ruegg, R.T., Chapman, R., Kusuda, T., "A New Look at Windows," NBS publication No. NBSIR 77-1388, U.S. Dept. of Commerce, Washington, D.C., January 1978.

[91] Gujral, P.S., "Will Less Glass Save More Energy?", paper No. 17, Handbook of Energy conservation for Mechanical Systems in Buildings, Compiled and edited by Robert W. Roose, Van Nostrand Reinhold Co., New York, 1978, pp. 84-89.

[92] Silverstein, S.D., "Effect Energy Utilization In Building: The Architectural Window," Reprint No. 7761, General Electric Company, Research and Development Report, Schenectady, New York, 1976.

[93] Kusuda, T., Bean, J.W., "Estimating the Energy Conservation Potential of Ventilation Control Through Weather Data Analysis," NBS publication No. PB 273-949, U.S. Dept. of Commerce, Washington, 1977.

[94] National Bureau of Standard, Energy Effective Windows, NBS publication No. 512 of the Proceedings of a Joint DOE (CERDA)/NBS Round Table Conference on Energy-Effective Windows, U.S. Dept. of commerce April, 1978.

[95] Shurcliff, W.A., "Thermal Shutters and Shades, Cambridge, Massachusettes, 1978.

[96] Hagman, F., "Insulating Shutters," RILEM/ASTM/CIB Symposium on Evaluation of the Performance of External Vertical Surfaces of Buildings, Vol. I, Otaniemi, Espoo, Finland, 1977, pp. 106-112.

[97] Rubin, A.I., Collins, B.L., Tibbott, R.L., "Window Blinds as a Potential Energy Saver - A Case Study," BSS No. 112, National Bureau of Standards, U.S. Dept. of Commerce, Washington, 1978.

[98] Rubin, A.I., Collins, B.L., Tibbott, R.L., "Window Usage at the National Bureau of Standards - Venetian Blinds as a Potential Energy Saver," ASHRAE Transactions, PH-79-6, No. 3, 1979, pp. 567-581.

[99] Paulsen, E., "Performance Requirements for Windows", NBS Special Publication No. 361, Vol. 1: Performance Concept in Buildings, Proceedings of the Joint RILEM/ASTM/CIB Symposium, Philadelphia, Pa., May 1972, pp. 385-394.

[100] Silverstein, S.D., "A Dual-Mode Internal Window Management Device For Energy Conservation," Energy and Building, Vol. 1977, pp. 51-56.

[101] Glen, E.M., Analytical Methods in Conduction Heat Transfer, McGraw-Hill, New York, 1971.

[102] Gebhart, B., Heat Transfer, McGraw-Hill, New York, 1961.

[103] Thomas, L.C., Fundamental of Heat Transfer, Prentice-Hall, Englewood Cliffs, New Jersey, 1980.

[104] Chapman, A.J., Heat Transfer, 3rd edition, Macmillan Publishing Co., New York, 1967.

[105] McAdams, W.C., Heat Transmission, 3rd edition, New York McGraw-Hill, 1954.

[106] Mackey, C.O., and Wright, Jr., L.T., "Periodic Heat Flow-Hometers Walker Roof," ASHRAE Transactions, Vol. 50, 1944, p. 293.

[107] Paramelee, G.V., and Aubele, W.W., "Radiation Energy Emission of Atmosphere and Ground," ASHRAE Transactions, Vol. 58, 1952, pp. 85-106.

[108] Roux, A.J.A., "Periodic Heat Flow Through Building Components - Heat Exchange at the Outside Surface," Brussels Building Resource Congress, Vol. III, No. 2, 1951, p. 82.

[109] Hoglund, B.L., Mitalas, G.P., and Stephenson, D.G., "Surface Temperatures and Heat Fluxes for Roofs," Building Science, Vol. 2, 1967, pp. 29-36.

[110] Kusuda, T., "SATG: A Useful Concept for Window Heat Gain Analysis," RILEM/ASTM/CIB Symposium on Evaluation of the Performance of External Vertical Surfaces of Buildings, Vol. 1, Otaniemi, Espoo, Finland, 1977, pp. 157-168.

[111] Mackey, C.O., "Sol-Air Temperature - A New Concept," Heating and Ventilating, Vol. 41, No. 12, 1944, p. 62.

[112] Threlkeld, J.C., "Thermal Environmental Engineering", Prentice Hall, Englewood Cliffs, N.J., 1962.

[113] Alereza, T., and Hossli, R.I., "A Simplified Method of Calculating Heat Loss and Solar Heat Gain Trhough Residential Windows During the Heating Season," ASHRAE Transactions, Vol. 85, PH-79-6, No. 4, 1979, pp. 582-606.

[114] Mitalas, G.P. and Stephenson, D.G., Room thermal Response Factor," ASHRAE Transactions, Vol. 73, paper No. 2019, 1967.

[115] Mitalas, G.P., "Transfer Function Method of Calculating Cooling Loads Heat Extraction and Space Temperature," ASHRAE Journal, Vol. 14, No. 12, 1972, pp. 54-56.

[116] Kusuda, T., "Thermal Response Factors for Multilayer Structures of Various Heat conduction Systems," ASHRAE Transactions, Vol., 75, 1969, pp. 246-271.

[117] Muncey, R.W.R., Spencer, J.W., Gupta, C.L., "Methods for Thermal Calculations Using Total Building Response Factor," NBS Building Science Series No. 39: Use of Computer For Environmental Engineering Related to Buildings, U.S. Dept. of commerce, Washington, 1971, 111-116.

[118] Kusuda, T., "Calculation of Building Thermal Response Factors (BTLRF) as Wiener Filter Coefficients," NBS Building Science Series No. 39: Use of Computer For Environmental Engineering Related to Buildings, U.s. Department of Commerce, Washington, 1971, 117-126.

[119] Kusuda, T., Tsuchiya, T., and Powell, F.J., "Prediction of Temperature by Using Equivalent Thermal Mass Response Factors," Proceedings of the 5th Symposium on Temperature, National Bureau of Standards, 1971.

[120] Kimura, K., and Ishino, H., "Air Conditioning Load Calculation by the Equivalent Mass Weighting Factors Method for the Computerized Control," Proceedings of the Japanese Architectural Society, Kyushu, Oct. 1972, pp. 249-250.

[121] Hopkinson, R.G., Petherbridge, P., Longmore, J., Daylighting, William Heinemann Ltd., London, 1966.

[122] Moon, P., Scientific Basis of Illuminating Engineering, McGraw Hill, New York, 1936. (Dover Publications, New York 1961).

[123] Kaufman, J.E., (editor), IES Lighting Handbook, 2 Vols., Illuminating Engineering Society of North america, New York, 1981.

[124] Narasimhan, V., An Introduction to Building Physics, Central Building Research Institute, Roorkee, India, 1974.

[125] Lynes, J.a., Principles of Natural Lighting, Elsevier Publishing Co., London, 1968.

[126] Boast, W.B., Illuminating Engineering, McGraw Hill Co., New York, 1953.

[127] Helms, R.N., McGovern, J.M., Lighting Design Handbook, Lum-I-Ineering Associates, Boulder, Colorado, for the U.S. Naval Material Naval and Naval Facilities Engineering Command, 1979.

[128] Moon, P., Spencer, D.E., Lighting Design, Addison-Wesley Press, Cambridge, Mass., 1948.

[129] Illuminating Engineering Society, "Recommended Practice of Daylighting," RP-S, Illuminating Engineering Society of North America, New York, 1978.

[130] Commission Internationale de l'Eclairage, CIE, "Daylight: International Recommendations for the Calculation of Natural Daylight," C.I.E. publication No. 16 (E 3.2), Paris, France, 1970.

[131] Kingsbury, H.F., Anderson, H.H., and Bizzaro, V.U., "Availability of Daylight," Illuminating Engineering, Vol. 52, No. 2, 1957.

[132] Boyd, R.A., "Daylight Availability," Illuminating Engineering, Vol. 53, No. 6, 1958.

[133] Petterbridge, P., "Natural Lighting Prediction and Design of Window Systems for Tropical Climates," Commission Internationale de l'Eclairage Compte Rendu, 1953, pp. 335-343.

[134] Bryan, H.J., "A Simplified Daylight Design Methodology, Centre for Planning and Development Research, University of California, Berkeley, 1976.

[135] Compt Rendue, Commission Internationale de l'Eclairage, CIE, "Natural Daylight Official Recommendations, the 13th session, 1955, [Quoted from ref. 121.].

[136] Compte Rendu, Commission International de l'Eclairage CIE, 7th session, 1928, (Teddington: The Commission, 1929). [Quoted from ref. 121].

[137] Commission Internationale de l'Eclairage, "Standardisation of Luminance Distribution on Clear skies," CIE Publication No. 22 (TC-4.2), Paris, France, 1973.

[138] Kittler, R., "Standardisation of Outdoor Conditions for the Calculation of Daylight Factor with Clear Skies," Commission Internationale de l'Eclairage 'CIE', 1965 Proceedings: Sunlight in Buildings, 1967, pp. 273-285.

[139] Hopkinson, R.G., "Measurements of Sky Luminance Distribution at Stockholm," Journal of Optical Society of America, Vol. 44, 1945, p. 455.

[140] Rennhackkamp, W.H.M., "Sky Luminance in Warm Climate," Compete Rendu, Commission Internationale de l'Eclairage, Washington, June 1967, p. 465.

[141] Narasimhan, V., and Saxena, B.K., "Measurements of the Luminance Distribution of the Clear Blue Sky in India," Indian Journal of Pure and Applied Physics, Vol. 5, 1967, p. 83.

[142] Nakamura, H., and Oki, M., "Measurements of Luminance Distribution Under Various Sky Conditions by Orthographic Projection Camera," C.I.E. publication No. 36 (1967 Rendu 18a session), London, 1975.

[143] Narasimhan, V., Maitreya, V.K., "Luminance Pre-Determination by Digital Analogue and Model Techniques, Indian Journal of Pure and Applied Physics, Vol. 6, 1968, p. 394.

[144] O'Brien, P.F., and Howard, J.A., "Pre-determination of Luminance by Finite Difference Equations, Illuminating Engineering Society, Vol. 54, London, 1959, p. 209.

[145] Wong, F.M., "The Daylight Factor Concept and the Lumen Method of Daylight Prediction," Architectural Science Review, June 1963, p. 67.

[146] Daylighting Committee of the IES: "Recommended Practice of Daylighting", Lighting Design and Application, Vol. 9, Feb. 1979, p. 25.

[147] Libbey - Owens - Ford Glass Co., "Lumen Method: Predicting Daylight as Interior Illumination," Libbey - Owens - Ford Glass Co., Toledo, Ohio, 1960.

[148] Biesele, R.L. Jr., Arner, W.J., Conover, E.W., "A Lumen Method of Daylighting Design,"Illuminating Engineering, March, 1953.

[149] Krochman, J., "The Calculation of Daylight Factor for Clear Sky Conditions," Commission Internationale de l'Eclairage CIE, 1965 Proceedings: Sunlight in Buildings, 1967, p. 287-301.

[150] Farrell, R., "Calculating Direct Illumination from Sky Under Clear Sky Conditions," Journal of Illuminating Engineering Society, July 1975.

[151] Saxena, B.K., and Bansal, G.D., "Sky Component Grids for Glazed Vertical Windows," Energy and Buildings, Vol. 2, 1979, pp. 45-53.

[152] Narasimhan, V., and Saxena, B.K., "Precise Values of Sky Components Due to a Clear Blue Sky for a Vertical Rectangular Apature, Indian Journal of Technology, Vol. 5, No. 10, 1967, pp. 329-331.

[153] Kojic, b., "The Graphical Method for the Determination of Interior Daylighting Under Clear Sky Conditions," Bulletin, T., Technique No. 6, de l'Academie Serbe des Sciences et des Arts, Classes des Sciences, 1963.

[154] Bryan, H.J., "A Simplified Procedure for Calculating The Effects of Daylight from Clear Skies," Journal of Illuminating Engineering Society, Vol. 9, April, 1980.

[155] Farrell, R., "The Use of the Perspective Technique in the Calculation of Illumination Levels from Clear Skies," Journal of Illuminating Engineering Society, Vol. 3, No. 1, 1974, pp. 153-156.

[156] Hopkinson, R.G., Longmore, J., and Petherbridge, P., "An Emperical Formula for the Computation of the Indirect Component of Daylight Factor," Transactions of the Illuminating Engineering Scoiety, Vol. 19, London, 1954, p. 201.

[157] Narasimhan, V., Saxena, B.K., and Maitreya, V.K., "The Internal Reflected Component of Daylight, A Finite Difference Approach to the Split Flux Method," Indian Journal of Pure and Applied Physics, Vol. 6 1968, p. 100.

[158] Narasimhan, V., Maitreya, V.K., "The Reflected Component of Daylight in Multistoryed Buildings in the Tropic Building Science, Vol. 4, 1969 - pp. 93-97.

[159] Morris, E.N., "The Calculation of the Internally Reflected Component for Partially Obstructed Windows," Building Science, Vol. 5, 1970, pp. 73-77.

[160] Griffith, J.W., Wezler, O.F., and Conover, E.W., "The Importance of Ground Reflection in Daylighting," Illuminating Engineering, Vol. 48, January, 1953.

[161] Reed, B.H., "Effect of Nearby Walks and Concrete Areas on Indoor Natural Lighting," Illuminating Engineering, Vol. 51, No. 7, July 1956.

[162] Nëeman, E., Light, W., Hopkinson, R.G., "Recommendations for the Admission and Control of Sunlight in Buildings," Building and Environment, Vol. 11, 1976, pp. 91-101.

[163] Nëeman, E., Light, W., "Availability of Sunshine," Building and Environment, Vol. 11, 1976, pp. 103-130.

[164] Nëeman, E., "Sunlight Requirements in Buildings - II: Visits of an Assessment Team and Experiments in a Controlled Room," Building and Environment, Vol. 12, 1977, pp. 147-157.

[165] Hopkinson, R.G., "Sunlight in Buildings," Proceedings of the Commission Internationale de l'Eclairage 'C.I.E.', Bouwcentrum International, Rotterdam, The Netherland, 1967.

[166] Smith, P.R., "Windows and Sunlight Penetration," Build International, Vol. 5, May 1972, p. 173.

[167] Van Deventer, E.N., "Sunlight and Shade Design," Build International, Vol. 5, July 1972.

[168] Shaviv, E., "A Method for the Design of Fixed External Sunshades," Build International, Vol. 8, 1975.

[169] Gero, J.S., Aynsley, R.M., "Shading Devices, Shadows, and Effect of Glass on Traffic," Architectural Science Review, March 1972, pp. 6-10.

[170] Nëeman, E., "Visual Aspects of Sunlight in Buildings," Lighting Research and Technology, Vol. 6, 1974, pp. 159-164.

[171] Dilaura, D.L., "On the computation of Visual Comfort Probability," Journal of the Illuminating Engineering Society, July 1976.

[172] Dilaura, D.L., "On the Computation of Equivalent Sphere Illumination," Journal of Illuminating Engineering Society, January 1975.

[173] Hastings, S.R., and Crenshaw, R., "Window Design Strategies to Conserve Energy," NBS Building Science Series No. 104, U.S. Department of Commerce, Washington, 1977.

[174] Dorsey, R.T., "The Potential for Energy Conservation in Lighting," Lighting Design and Application, Vol. 8 No. 7, 1978, pp. 25-34.

[175] Peery, R., "Daylighting and Energy Conservation," Lighting Design and Application, Vol. 4, No. 10, 1974, p. 27.

[176] Levy, A.W., "Interior Lighting Design and Energy Conservation", Digest No. CBD-192, Division of Building Research, NRCC, Ottawa, Nov. 1977.

[177] Levy, A.W., "Lighting Controls, Patterns of Lighting Consumption, and Energy Conservation," paper No. 929, Division of Building Research, NRCC, Ottawa, 1980.

[178] Khan, F.R., "Optimum Design of Glass in Buildings," Building Research, May - June 1967.

[179] Kaufman, J., "Optimizing the Use of Energy for Lighting," Lighting Design and Application, Vol. 3, No. 10, 1973.

[180] Dorsey, R.T., "Cost Benefit Analysis Applied to Lighting in the Energy Equation," Lighting Design and Application, Vol. 8, No. 7, 1975, pp. 36-38.

[181] Collins, J.B. and Crisp, V.H.C., "Energy Management and The IES Code," Current Paper, Building Research Establishment, Department of the Environment, U.K., 1977.

[182] Hopkinson, R.G. and Longmore, J., "The Permanent Supplementary Artificial Lighting of Interiors," Transactions I.E.S., London, Vol. 24, No. 3, 1959, pp. 121-142.

[183] Kendrick, J.D., "The Intergration of Artificial Light with Daylight in the Design of Australian Buildings," IES Lighting Review, Vol. 26, Australia, 1964, 115-120.

[184] Hopkinson, R.G. and Kay, J.D., The Lighting of Buildings, Faber and Faber, London, 1969.

[185] Heath, T.F., "Problems of Measurement in Environmental Aesthetics," Architectural Science Review, March 1968, pp. 17-28.

[186] Pilkington Brothers Limtied, Windows and Environment, Pilkington Environmental Advisory Service, Pilkington Brothers Limited, London, 1969.

[187] Collins, B.L., "Windows and People: a Literature Survey," NBS publication BSS-70, U.S. Department of Commerce, Washington, 1978.

[188] Collins, B.L., "Human Response to Windows," RILEM/ASTM/CIB Symposium on the Evaluation of the Performance of External Vertical Surfaces of Buildings, Vol. II, Otaniemi, Espoo, Finland, 1977, pp. 327-333.

[189] Markus, T.A., "The Function of Windows - A Reappraisal," Building Science, Vol. 2, 1967, pp. 97-121.

[190] Hopkinson, R.G., "The Psychophysics of Sunlighting," Proceedings of the CIE Conference: Sunlight in Buildings, Bouwcentrum International, Rotterdam, 1967, pp. 13-19.

[191] Hollister, F.D., "A Report On the Problems of Windowless Environments," Greater London Council, Hobbs, the Printers Ltd., London, 1968.

[192] Brown, S.W. and Hult, E.E., "New York's First Windowless Air-Conditioned School," ASHRAE Journal, Jan., 1967, pp. 47-51.

[193] Burts, E., "Windowless Classrooms: Windows Help to Promote Better Classroom Learning," National Educational Association Journal, Vol. 50, Oct. 1961, 13-14.

[194] McDonald, E.G., "Opinions Differ on Windowless Classrooms," National Educational Association Journals, Vol. 50, 1961, pp. 12-14.

[195] Keighley, E.C., "Visual Requirements and Reduced Fenestration in Offices - A Study of Multiple Apertures and Window Area," Journal of Building Science, Vol. 8, 1973, pp. 321-331.

[196] Keighley, E.C., "Visual Requirements and Reduced Fenestration in Office Buildings - A Study of Window Shape," Journal of Building Science, Vol. 8, 1973, 311-320.

[197] Néeman, E., and Hopkinson, R.G., "Critical Minimum Acceptable Window Size: A Study of Window Design and Provision of View," Lighting Research and Technology, Vol. 2, 1970, pp. 17-27.

[198] Kusuda, T., Collins, B.L., "Simplified Analysis of Thermal and Lighting Characteristics of Windows: Two Case Studies," NBS Building Science Series 109, U.S. Department of Commerce, Washington, 1978.

[199] Lim, B.P., Rao, K.R., and Mattar, A.M., Environmental Factors in the Design of Building Fenestration, Applied Science Publisher, London, 1979.

[200] Rowley, F.B., and Eckley, W.A., "Surface Coefficients as Affected by Wind Direction," ASHRAE Transactions, Vol. 38, 1932.

[201] Kind, R.J., Gladston, D. and Moizer, A.D., "Wind-Induced Heat Losses From Solar Collectors," The Fourth U.S. National Conference on Wind Engineering Research, University of Washington, Seattle, Washington, July 1981, pp. 333-338.

[202] Sriramulu, V., "Heat Transfer from Flat Places to an Air Jet", M.Sc. (Engg) Thesis, Indian Institute of Science, Bungalore, India, 1965.

[203] Sturrock, N.S., "Localised Boundary Layer Heat Transfer from External Building Surfaces," Ph.D. Thesis, University of Liverpool, 1971.

[204] Ito, N., Kimura, K., and Oka, J., "A Field Experiment Study on the Convective Heat Transfer Coefficient on Exterior Surface of a Building," ASHRAE Semi-Annual Meeting Proceedings, New Orleans, L.A., Jan. 1972.

[205] Fedorov, V.K., "An Engineering Method of Calculating Convective Heat Transfer for a Body in an Attached Gas Flow," Journal of Engineering Physics, Vol. 8, 1965, pp. 198-203.

[206] Threlkeld, J.L., "Solar Irradiation of Surfaces on Clear Days," ASHRAE Transactions, Vol. 59, 1963, p. 24.

[207] Rowley, F.B., Algren, A.B., and Blackshaw, J.L., "Effect of Air Velocity on Surface Coefficients," ASHRAE Transactions, Vol. 36, 1930, p. 123.

[208] Barakat, S.A., "Solar Heat Gain Through Windows in Canada," paper No. 944, Division Building Research, NRCC, Ottawa, Oct. 1980.

[209] Cooper, P.I., "The Absorption of Solar Radiation in Solar Stills," Solar Energy, Vol. 12, No. 3, 1969.

[210] Wolf, M., "Limitations and Possibilities for Improvement of Photovolatic Solar Energy Converters," Proceedings of IRE, Vol 48, 1960, pp. 1246-1263.

[211] Hornbeck, R.W., Numerical Methods, Quantum Publishing Inc., N.Y., 1975.

[212] Segerlind, L.J., Applied Finite Element Analysis, John Willey & Sons, New York 1976.

[213] Patankar, S.V., Numerical Heat Transfer And Fluid Flow, Hemisphere Publishing Co., Washington, 1980.

[214] Yager, A.J., A Study of La Macaza Solar House, Master Thesis, C.B.S., Concordia University, Montreal, 1980.

[215] Budde, W., Measurements of the Spectural Distribution of Solar and Global Radiation, PO-535, Physics Division, NRCC, Ottawa, July 1979.

[216] Mitalas, G.P., "Cooling Load Caused by Lights," Canadian Society for Mechanical Engineering Transactions, Vol. 2, No. 3, 1973-1974, pp. 169-174.

[217] Howell, R.H., and Sauer, H.J., Environmental Control Principles, An Educational Supplement to ASHRAE Handbook 1977 Fundamental Volume, American Society of Heating, Refrigerating and Air-Conditioning Engineers, Inc., New York, 1978.

[218] Kerr, R.G., A Study of A Solar Heated House in Quebec, Master Thesis, C.B.S., Concordia University, Montreal, 1978.

[219] Kerr, R.G., and M.M. Shapiro, "The Effect of Wind Speed and Direction on the Heat Loss of A House," Proceedings of the Second Canadian Workshop on wind Engineering, Canadian wind Engineering Association, Varennes, Quebec, Sept. 1979, pp. 102-113.

[220] Jennings, B., Environmental Engineering, Internal Text-Book Co., London, 1970.

APPENDIX A

DETERMINATION OF THE VEIW FACTOR FOR EXTERNAL AND INTERNAL SURFACES

i) View Factor for an external surface

There are three external surfaces, the building surface containing the window, the obstruction surface facing the building surface and the ground between them. The building and obstruction surfaces are assumed parallel and infinite in width. The view factor for a vertical surface, of infinite width from a reference point in the horizontal plane through the bottom of the vertical surface (Fig. A.1a) was described by Lim et al. [199]. The procedure is summarized as follows: the top horizontal (head) line of the vertical surface is projected on to the sky dome centred on the reference point forming a great semi-circle on the hemisphere. The orthogonal projection of this great semi-circle on the horizontal plane is half of an ellipse (Fig. A.1a).

The projected area of the vertical surface on the horizontal plane is the difference of the areas of the projection of half the sky dome (a semi-circle) and the semi ellipse (Fig. A.1a). The area of the semi-ellipse is $(\pi/2)$ (R x R cos a) where R and R cos a are the major and minor axes of the ellipse. The area of the semi-circle is $\pi R^2/2$. Hence the projected area of the vertical surface

$$\text{Projected area} = (\pi/2) \quad (R^2 - R^2 \cos a)$$

$$= (\pi R^2/2)\,(1 - \cos a) \qquad \text{(A.1)}$$

dividing the projected area of the vertical surface by the projected area of the hemisphere, the view factor can be obtained.

$$F_V = \pi R^2(1-\cos a)/2\pi R^2$$

$$= \tfrac{1}{2}(1-\cos a) \qquad (A.2)$$

In the case where point p is lower than the horizontal plane through the bottom of the vertical surface (Fig. A.1b), the veiw factor becomes

$$F_V = \tfrac{1}{2}(\cos b - \cos a) \qquad (A.3)$$

where b and a are the angles of elevation of the bottom and top of the vertical surface.

In the case where point p is higher than the horizontal plane through the bottom line of the vertical surface (Fig. A.2) the view factor is calculated in two steps. The first is for the upper portion of the vertical surface above the horizontal plane through the reference point using Eq. A.2. The second is for the lower portion of the vertical surface below the horizontal plane through the reference point. The sum is the view factor for the vertical surface from the reference point.

For a reference point on the ground (Fig. a.3), the view factors of the building surface and the obstruction surface are also calculated using Eq. A.2.

ii) View Factor of an Internal Surface

Internal surfaces of a room and the visible portions of external surfaces through the window are not infinite in length. Thus, they were treated differently. Portions of vertical internal surfaces below the horizontal working plane containing the reference point do not contribute directly to the illumination at the reference point. Thus,

only the portions of the surfaces of the walls above the reference plane were taken into consideration. The view factor for an internal surface (Fig. A.4) is calculated as follows. The top horizontal line of the internal vertical surface (CD) is projected as before and the orthographic projection on to the circle subtending the sphere is shown in Fig. A.4c. The bottom line AB is in the reference plane and so projects a semi circle. The projected area A'B'C'D' is the difference of two sectors, P'AB' of the semi circle and PC'D' of the semi-ellipse. For a hemisphere of a unit radius, sector PC'D' is related to sector PCD such that area PC'D' = area PCD x cos a. The area of sector PCD is given by $R^2 \delta / 2\pi$, sector PC'D' by $R^2 \delta \cos a / 2\pi$, and the area of sector PA'B' by $R^2\gamma/2\pi$. Therefore the projected area A'B'C'D' is

$$\text{Area A'B'C'D'} = (\text{sector PA'B'}) - (\text{sector PC'D'})$$

$$= (R^2\gamma/2\pi) - (R^2\delta \cos a / 2\pi)$$

$$= R^2 (\gamma - \delta \cos a)/2\pi \qquad (A.4)$$

putting R = 1, the view factor for an internal surface is

$$F_V = (\gamma - \delta \cos a)/2 \qquad (A.5)$$

where a, γ, and δ are expressed in radians and are shown in Fig. A.4. δ is related to γ by

$$\tan \delta = \tan \gamma \cdot \cos a \qquad (A.6)$$

The view factor expressed by Eq.A.5 can further be generalized to account for situations where the bottom line of the vertical surface is above the horizontal plane through point p (Fig. A.5). The vertical surface is first extended downward until it intercepts the reference plane. The view factor of the vertical surface of concern is the

difference between the view factor of the extended plane and the expansion done, thus

$$F_V = (\gamma - \varepsilon \cos a/2\pi) - (\gamma - \delta \cos b/2\pi)$$

$$= (\delta \cos b - \varepsilon \cos a)/2\pi \qquad (A.7)$$

where angles γ, δ, ε, a, and b are shown in Fig. A.5(a) and (b). Substituting for δ and ε by

$$\delta = \tan^{-1} (\tan \gamma \cos b)$$

$$\varepsilon = \tan^{-1} (\tan \gamma \cos a)$$

Eq. (A.7) becomes

$$F_V = [\tan^{-1}(\tan \cos b) . \cos b) - (\tan^{-1}(\tan h. \cos a) . \cos a)]/2\pi \qquad (A.8)$$

To calculate luminances, when the reference point is on a wall and higher than the horizontal plane through the bottom of the vertical surface of concern (similar to the case shown in Fig. 2), the view factor becomes a sum of two view factors. The first is for the portion above the reference plane and the second is for the portion below the reference plane.

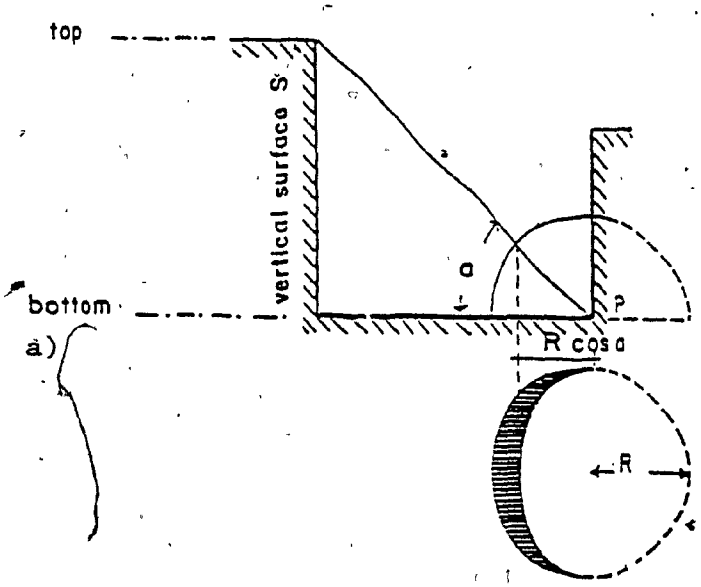

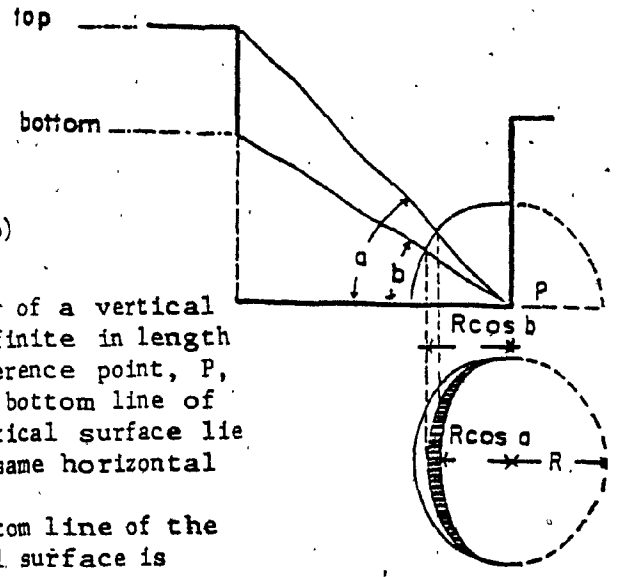

Fig. A.1:
View factor of a vertical surface infinite in length
a) the reference point, P, and the bottom line of the vertical surface lie in the same horizontal plane;
b) the bottom line of the vertical surface is above the horizontal plane of the reference point P.

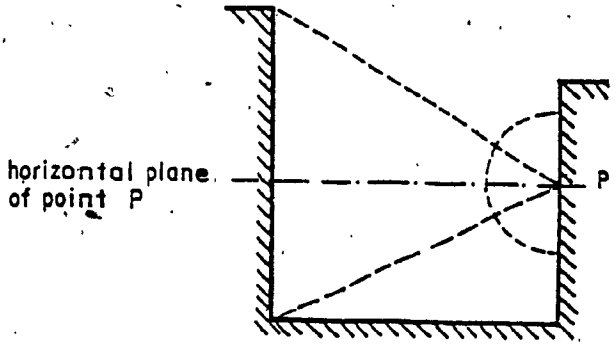

Fig. A.2: View factor of a vertical surface infinite in length from a reference point p above the horizontal plane.

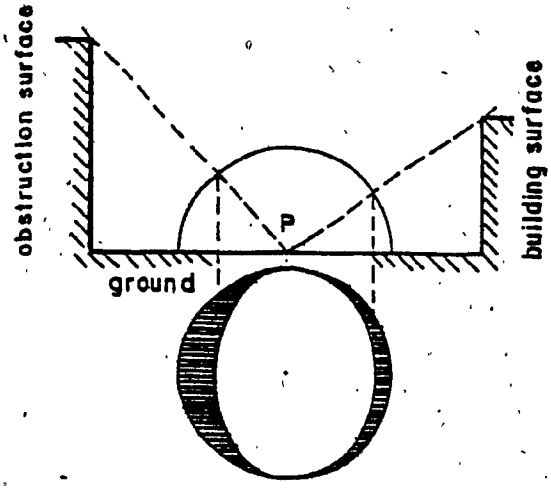

Fig. A.3: View factors of the building surface containing the window and the obstruction surface facing it from a reference point on ground.

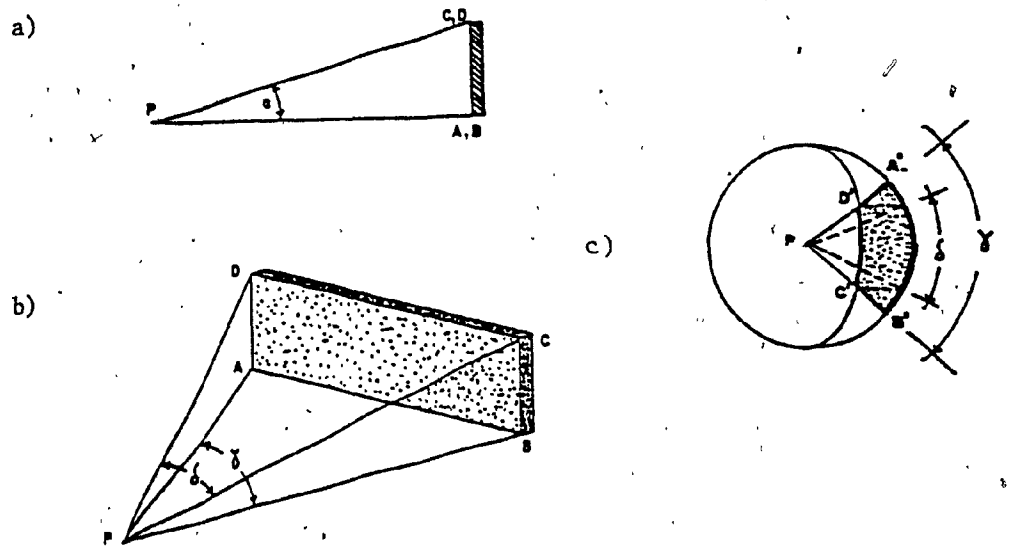

Fig. A.4: View factor of a vertical surface of a finite length having its bottom line, AB, in the same horizontal plane of the reference point P.
a) elevation angle a of the top line CD;
b) the horizontal angles γ and δ of the bottom and top lines from the reference point P;
c) orthographical projection of the vertical surface on a unit hemisphere centered at the reference point.

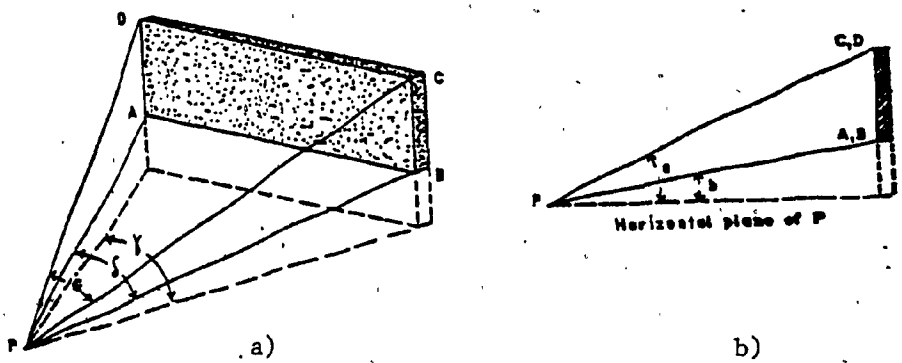

Fig. A.5: View factor of a vertical surface of a finite length having its bottom line, AB, above the horizontal plane of the reference point p.
a) the horizontal angles γ, δ and ϵ measured on the horizontal plane of P, plane PAB and plane PDC respectively.
b) vertical angles a and b for lines CD and AB.

APPENDIX B

COMPUTER PROGRAMS

```
PROGRAM FDIMP1     74/835  OPT=1                    FTN 4.8+552

      1            PROGRAM FDIMP1(INPUT,OUTPUT)
                   DIMENSION HK1(8),HH1(9),WIND(24),WD(24),TI(24),HOA(24)
                   DIMENSION ABSO(8),TD(200),TS(24),H(8),HK(8),HH(9),CC(8),POT(8)
                   DIMENSION PN(8) , PO(8),ENT(8),TO(24),Q(24),AR(200),AH(8)
      5            COMMON A(200,200),C(200),TN(200)
                C  ************************************************************
                C
                C
                C
     10         C   PROGRAM FDIMP CALCULATES THE TEMPERATURE DISTRIBUTION OF
                C   VARIOUS LAYERS OF SINGLE,DOUBLE,AND TRIPLE GLAZED WINDOWS.
                C   FDIMP USES THE IMPLICIT FORMULATION OF THE FINITE-DIFFERNCE
                C   METHOD TO ALLOW NUMERICAL APPROXIMATION TO THE PARTIAL
                C   DIFFERENTIAL EQUATION OF HEAT,CONDUCTION IN 3-DIMENSIONAL
     15         C   TRANSIENT STATE.
                C   DURING EACH TIME INCREMENT,THE TEMPERATURE DISTRIBUTION
                C   OF ONE QUARTER OF THE SYMMETRICAL WINDOW IS OBTAINED.
                C   CONSEQUENTLY,THE RATE OF HEAT LOSS OR GAIN AT THE EXTERNAL
                C   ,INTERNAL, AND THE INTERFACE SURFACES ARE CALCULATED.
     20         C   MOREOVER,THE RATE OF THE HEAT ADDITION OR EXTRACTION
                C   (NET HEAT STORAGE) IS CALCULATED ,ALSO THE TEMPERATURES
                C   DIFFERENCE AT THE EXTERNAL AND THE INTRENAL SURFACES
                C   IS CALCULATED
                C   THE DATA GIVEN BELOW IS APPLICABLE TO ORDINARY CLEAR
     25         C   DOUBLE STRNGTH FLOAT GLASS OF 1/4" THICKNESS AND THE
                C   INSULATED WINDOWS MUST HAVE 1/2" AIR SPACE.SIMPLE MODIFI-
                C   CATIONS MAY BE RQUIRED TO ALLOW FURTHER APPLICATIONS.
                C   ************************************************************
                C
     30         C
                C                    D E F I N I T I O N S
                C
                C   HOAA   =OUTSIDE SURFACE RESISTANCE (INITIAL)
                C   HOII   =INSIDE SURFACE RESISTANCE  (INITIAL)
     35         C   TO     =OUTSIDE AIR TEMPERATURE    (INITIAL)
                C   GTI    =INSIDE  AIR TEMPERATURE    (INITIAL)
                C   RG     =RESISTANCE OF A SINGLE GLASS PANE
                C   RA     =RESISTANCE OF AN AIR SPACE(INTER-PANES)
                C   TAS    =ABSOLUTE TEMP. OF OUTDOOR AIR
     40         C   QTRANS =TOTAL SOLAR HEAT GAIN PER UNIT AREA
                C   DT     =TIME INCREMENT
                C
                C
                C   SM1    =ENERGY STORAGE CAPACITY PER TIME INCREMENT
     45         C            FOR A FULL LUMP
                C   SM2    =FOR A BOUNDARY HALF LUMP
                C   SM3    =FOR A BOUNDARY QUARTER ELEMENT
                C
                C   SK1    =A COMMON DOMINATOR FOR A FULL LUMP
     50         C   SK2    =FOR A BOUNDARY HALF LUMP
                C   SK3    =FOR A BOUNDARY QUARTER LUMP
                C   SK5    =FOR ADIABATIC INTERMEDIATE FULL LUMP
                C   SK6    =FOR ADIABATIC CORNER FULL LUMP
                C   SK7    =FOR ADIABATIC BOUNDARY HALF LUMP
     55         C   P1     =VALUE OF THE COEFFICIENT 'A'REPRESENTING THE
                C            HEAT TRANSFER BETWEEN TWO FULL LUMPS IN THE.
                C            SAME LAYER.
```

PROGRAM FDIMP1 74/835 OPT=1 FTN 4.8+552

```
C       P2     =AS P1 EXCEPT ONE LUMP IS A BOUNDARY LUMP
C       P3     = AS P1 EXCEPT  BOTH LUMPS ARE BOUNDARY LUMPS
C       P4     =AS P1 EXCEPT ONE LUMP IS A CORNER QUARTER LUMP
C       P5     =AS P1 EXCEPT BOTH LUMPS ARE ADIABATIC INTERMEDIATE
C       P6     =ASP1 EXCEPT ONE IS ADIABATIC INTERMEDIATE AND THE
C               OTHER IS ADIABATIC CORNER FULL LUMP
C       P7     =AS P1 EXCEPT ONE LUMP IS ADIABATIC BOUNDARY HALF LUMP
C       P8     =AS P1 EXCEPT BOTH LUMPS ARE BOUNDARY AND ONE ISADIABATIC
C
C
C       W1     =COEFFICIENT 'A' REPRESENTING THE HEAT TRANSFER
C               BETWEEN TWO FULL LUMPS IN TWO CONSEQUETIVE LAYER
C               ,THE NODE IN CONCERN AND THE NODE BEHIND IT.
C       W2     =AS W1 EXCEPT THE NODE  IN FRONT OF IT
C       W3     =BOUNDARY NODE AND THE NODE BEHIND IT
C       W4     =BOUNDARY NODE AND THE NODE IN FRONT OF IT
C       W5     =CORNER NODE AND THE NODE BEHIND IT
C       W6     =CORNER NODE AND THE NODE IN FRONT OF IT
C       W7     =ADIABATIC INTERMED. NODE AND NODE BEHIND IT
C       W8     =ADIABATIC INTERMED. NODE AND NODE IN FRONT OF IT
C       W9     =ADIABATIC CORNER NODE AND NODE BEHIND IT
C       W10    =ADIABATIC CORNER NODE AND NODE IN FRONT OF IT
C       W11    =ADIABATIC BOUNDARY NODE AND NODE BEHIND IT
C       W12    =ADIABATIC BOUNDARY NODE AND NODE IN FRONT OF IT
C
C
C       KLM    =TOTAL NUMBER OF NODES IN ALL LAYERS UP TO LAYER(L-1)
C       IV     =THE LUMP NUMBER IN THE TWO DIMENSIONAL MATRIX'A'
C       IV1    =THE LUMP TO THE LEFT OF IV
C       IV2    =THE LUMP TO THE RIGHT OF IV
C       IU1    =THE LUMP ABOVE IV
C       IU2    =THE LUMP BELOW IV
C       IW1    =THE LUMP BEHIND IV
C       IW2     =THE LUMP IN FRONT OF LUMP IV
C
C
C       AC     =THE INVERSE OF THE CONVECTION RESISTANCE BETWEEN
C               A NODE AND THE SURROUNDING AIR
C       TC     =TEMPERATURE OF SURROUNDING AIR
C
C
C
C
C      WIND(IT)=WIND SPEED AT TIME IT
C      WD(IT)  =WIND DIRECTION AT TIME 'IT'
C      TI(IT)  =INDOOR TEMPERATURE AT TIME(IT)
C      HOA(IT) =OUTSIDE SURFACE COEFFICIENTAT TIME (IT)
C      ABSO(IT)=ABSORPTION% OF LAYER (L)
C      TD(I)   =TEMPERATURE OF NODE (I) AT TIME(IT-1)
C      TN(I)   =TEMPERATURE OF NODE (I) AT TIME(IT-1)
C      C(I)    =COEFFICIENT'C'OF NODE (I)
C      A(I,J)  =ELEMENT(I,J)OF MATRIX 'A'
C      TS(IT)  =FRAME TEMPERATURE AT TIME (IT)
C
C
C       H(L)   =INVERSE OF THE TOTAL THRMAL RESISTANCE BETWEEN
C               TWO NODES IN THE SAME LAYER
```

```
      PROGRAM FDIMP1     74/835  OPT=1                    FTN 4.8+552

  115         C       HK(L)   =SAME AS H(L) BUT FOR BOUNDARY NODES(CONVECTION)
              C       HH(L)   =INVERSE OFTHE TOTAL THERMAL RESISTANCE BETWEEN
              C                TWO NODES IN TWO CONSEQUETIVE LAYERS
              C       CC(L)   =TOTAL THERMAL STORAGE CAPACIT OF A FULL LUMP
              C       POT(L)  =AVERAGE TEMP. OF LAYER(L)AT TIME(IT-2)
  120         C       PN(L)   =AVERAGE TEMP. OF LAYER(L) AT TIME(IT)
              C       PO(L)   =AVERAGE TEMP. OF LAYER (L) AT TIME (IT-1)
              C                IN LAYER (L)
              C       ENT(L)  =ENTHALPY CHANGE OF LAYER(L)DURING THE TIME INCREMENT
              C       TO(IT)  =TEMPERATURE OUTSIDE AT TIME(IT)
  125         C       Q(IT)   =INTENSITY OF SOLAR RADIATION AT TIME(IT)
              C       AR(I)   =AREA OF LUMP(I) IN THE LAYER PLANE
              C       AH(I)   =AREA OF CONTACT AT INTERFACE BETWEEN TWO LUMPS
              C                IN THE SAME LAYER(THICKNESS DIRECTION)
              C
  130         C
              C       IHOUR   =NUMBER OF HOURS TO BE CALCULATED
              C       GR      =GLAZING RATIO
              C       NNR     =NUMBER OF NODES PER ROW
              C       NL      =NUMBER OF LAYERS IN THE SYSTEM
  135         C       NN      =NUMBER OF LUMBS PER LAYER
              C       N       =TOTAL NUMBER OF LUMPS IN THE SYSTEM
              C       BENGTH  =WIDTH OF THE WINDOW
              C       BENTEM  =HEIGHT AND WIDTH OF SQUARE LUMP
              C       A1      =AREA OF A FULL LUMP
  140         C
              C                GIVEN DATA
                    DATA(H(K),K=1,8)/.003192,.003192,.000328,.003192
                   Q ,.003192,.000328,.003192,.003192/
                    DATA(HK1(K),K=1,8)/.00547,.00547,.02188,.00547,.00547,
  145              Q.02188,.00547,.00547/
                    DATA(HH1(K),K=1,9)/2.0875,10.35,.5548,.5548,10.35,.5548
                   Q ,.5548,10.35,.5181875/
                    DATA(CC(K),K=1,8)/403.36,403.36,.9251,403.36,403.36,
                   Q .9251,403.36,403.36/
  150               DATA(AH(K),K=1,8)/.00078,.00078,.003125,.00078,.00078,
                   Q .003125,.00078,.00078/
                    DATA(ABSO(K),K=1,8)/.035,.035,.05,.03,.03,.05,.025,.025/
              C     A NON ZERO VALUE FOR MAT INSTRUCT THE PROGRAM TO PRINT
              C     MATRIX[A] AND MATRIX[C].
  155               READ*,MAT
                    READ*,(WIND(IT),IT=1,24)
                    READ*,(WD(IT),IT=1,24)
                    READ*,(TI(IT),IT=1,24)
                    READ*,(TO(IT),IT=1,24)
  160               READ*,(Q(IT),IT=1,24)
                    READ*,GR,TIME,NNR,NL,BENGTH,HOC,IHOUR,HOI
                    DT=3600.0*TIME
                    DO 9 IT=1,IHOUR
                    TS(IT)=TO(IT)+6.
  165         9     CONTINUE
                    NN=NNR**2
                    N =NN*NL
                    NS=NNR-1
                    BEN=BENGTH/2.
  170               TEM=NNR-0.5
                    BENTEM=BEN/TEM
```

```
      PROGRAM FDIMP1     74/835  OPT=1                    FTN 4.8+552

                  A1=BENTEM**2.
                  DO 10 I=1,N
                  DO 10 J=1,N
175               A(I,J)=0.00
            10    CONTINUE
                  DO 15 L=1,N
                  A(L,L)=1.00
                  C(L)=0.0
180         15    CONTINUE
                  PRINT 700
            700   FORMAT(/,25X,*I N P U T   D A T A*)
                  PRINT 701,GR
                  PRINT 702,NNR
185               PRINT 703,NL
                  PRINT 704,BENGTH,BENGTH
                  PRINT 705,IHOUR
            701   FORMAT(5X,*WINDOW-TO-WALL RATIO(GR)=*,F6.3)
            702   FORMAT(5X,*NUMBER OF NODES PER LAYER NNR =*,I2)
190         703   FORMAT(5X,*NUMBER OF LAYERS NL           =*,I2)
            704   FORMAT(5X,*WINDOW DIMENSIONS =*,F6.3,*X*,F6.3,*METERS*)
            705   FORMAT(5X,*NUMBER OF HOURS TO BE CALCULATED=*,I3)
            C
            C
195         C     INITIAL TEMPERATURE OF ALL LAYERS
            C     **********************************
            C
                  HOAA=1./17.47
                  HOII=1./HOI
200               GTO=TO(1)
                  GTI=TI(1)
                  TIO=GTI-GTO
                  RG=.006156
                  RA=.199004
205               TT1=HOAA
                  TT2=TT1+RG
                  TT3=TT2+RA
                  TT4=TT3+RG
                  TT5=TT4+RA
210               TT6=TT5+RG
                  IF(NL.EQ.8)GOTO 600
                  IF(NL.EQ.5)GOTO 601
            C
            C     SINGLE GLAZING
215         C
                  XTRANS=.86
                  RT1=HOAA+RG+HOII
                  T1=GTO+((TT1*TIO)/RT1)
                  T2=GTO+((TT2*TIO)/RT1)
220               PRINT*,T1,T2,TIO,HOAA,HOII
                  GOTO 605
            C
            C     DOUBLE GLAZING
            C
225         601   RT2=HOAA+HOII+RA+(2.*RG)
                  T1=GTO+((TT1*TIO)/RT2)
                  T2=GTO+((TT2*TIO)/RT2)
                  T4=GTO+((TT3*TIO)/RT2)
```

```
                T3=(T4+T2)/2.
230             T5=GTO+((TT4*TIO)/RT2)
                PRINT*,T1,T2,T3,T4,T5
                XTRANS=.75
                GOTO 605
              C
235           C     TRIPLE GLAZING
              C
              600   RT3=HOAA+HOII+(3.*RG)+(2.*RA)
                    T1=GTO+((TT1*TIO)/RT3)
                    T2=GTO+((TT2*TIO)/RT3)
240                 T4=GTO+((TT3*TIO)/RT3)
                    T3=(T2+T4)/2.
                    T5=GTO+((TT4*TIO)/RT3)
                    T7=GTO+((TT5*TIO)/RT3)
                    T6=(T5+T7)/2.
245                 T8=GTO+((TT6*TIO)/RT3)
                    PRINT*,T1,T2,T3,T4
                    PRINT*,T5,T6,T7,T8
                    XTRANS=.65
              C
250           C     FILLING ARRAY TD(N) WITH INITIAL TEMPERATURE
              C
              605   DO 500 I=1,25
                    TD(I)=T1
                    TD(I+25)=T2
255           500   CONTINUE
                    IF(NL.EQ.2) GOTO 707
                    DO 501 I=51,75
                    TD(I)=T3
                    TD(I+25)=T4
260                 TD(I+50)=T5
              501   CONTINUE
                    IF(NL.EQ.5)GOTO 707
                    DO 502 I=126,150
                    TD(I)=T6
265                 TD(I+25)=T7
                    TD(I+50)=T8
              502   CONTINUE
              C
              C     DETERMINATION OF COEFFICIENTS FOR MATRIX  'A'
270           C
              707   DO 5 K=1,8
                    HK(K)=HK1(K)* (BENTEM/.25)*(HOE/7.0)*
                    IF(K.EQ.1)GOTO 606
                    HH(K)=HH1(K)*(A1/.0625)
275           606   CC(K)=CC(K)*(A1/.0625)
                    AH(K)=AH(K)* (BENTEM/.25)
                    POT(K)=0.0
              5     CONTINUE
                    HH(9)=HH1(9)*(A1/.0625)*(HOI/8.291)
280                 DO 106 IT=1,IHOUR
                3   FORMAT(//,12X,*TEMPERATURE DISTRIBUTION AFTER *,I2,*HOURS*)
                    WINDY=WIND(IT)
                    WDD=WD(IT)
                    TAS=TO(IT)+273.
285                 QTRANS=Q(IT)*XTRANS
```

PROGRAM FDIMP1 74/835 OPT=1 FTN 4.8+552

```
      CALL FILM(WINDY,WDD,TAS,QTRANS,GR,XUG,HOPE,SATG,FG)
      PRINT 3,IT
      HOA(IT)=HOPE
      HH(1)=HH1(1)*(A1/.0625)*(HOA(IT)/33.4)
290   QAB=0.0
      DO 239 K=1,NL
C     IF(IT.NE.1.AND.K.NE.1)GO TO 222
      IF(K.EQ.NL) GOTO 224
      KN=K+1
295   GOTO 225
224   KN=9
C
C     CALCULATION OF PARAMETERS SM,SK,P,AND W
C     ***************************************
300   C
C     INTERNAL NODES
225   SM1=(DT/CC(K))
      SK1=1.0+(4.0 *H(K)*SM1)+(SM1*HH(K))+(SM1*HH(KN))
      P1=(-1.0*SM1*H(K))/SK1
305   W1=(-1.0*SM1*HH(K))/SK1
      W2=(-1.0*SM1*HH(KN))/SK1
C
C     BOUNDARY NODES
      SM2=(DT/CC(K)*.5)
310   SK2=1.0+(2.0*H(K)*.5*SM2)+(SM2*HH(K)*.5)+(SM2*HH(KN)*.5)+
     Q (H(K)*SM2)+(HK(K)*SM2)
      P2=((-1.0*SM2)/SK2)*H(K)*.5
      P3=((-1.0*SM2)/SK2)*H(K)
      W3=((-1.0*SM2)/SK2)*HH(K)*.5
315   W4=((-1.0*SM2)/SK2)*HH(KN)*.5
C
C     CORNER NODES
      SM3=(DT/CC(K)*.25)
      SK3=1.0+(2.0*H(K)*.5*SM3)+((SM3*HH(K)*.25)+(SM3*HH(KN)*.25))
320  Q +(SM3*HK(K))
      P4=((-1.0*SM3)/SK3)*H(K)*.5
      W5=((-1.0*SM3)/SK3)*HH(K)*.25
      W6=((-1.0*SM3)/SK3)*HH(KN)*.25
C
325   C     ADIBATIC INTERMEDIATE NODES
      SK5=1.0+(3.0*H(K)*SM1)+(SM1*HH(K))+(SM1*HH(KN))
      P5=((-1.0*SM1)/SK5)*H(K)
      W7=((-1.0*SM1)/SK5)*HH(K)
      W8=((-1.0*SM1)/SK5)*HH(KN)
330   C
C     ADIBATIC CORNER NODES
      SK6=1.0+(2.0*H(K)*SM1)+(SM1*HH(K))+(SM1*HH(KN))
      P6=((-1.0*SM1)/SK6)*H(K)
      W9=((-1.0*SM1)/SK6)*HH(K)
335   W10=((-1.0*SM1)/SK6)*HH(KN)
C
C     ADIABATIC/BOUNDARY NODES
      SK7=1.0+(SM2*(H(K)+H(K)*.5))+(SM2*HH(K)*.5)+(SM2*HH(KN)*.5)
     Q +(SM2*HK(K))
340   P7=((-1.0*SM2)/SK7)*H(K)
      P8=((-1.0*SM2)/SK7)*H(K)*.5
      W11=((-1.0*SM2)/SK7)*HH(K)*.5
```

PROGRAM FDIMP1 74/835 OPT=1 FTN 4.8+552

```
                W12=((-1.0*SM2)/SK7)*HH(KN)*.5
      C
      C     DEVELOPMENT OF THE COEFFICIENTS MATRIX'A'
      C     ****************************************
      C
      C     IDENTIFICATION OF THE SIX NODES SURROUNDING NODE IV
      C
      C     REFERENCE NODES(TYPE 1)
      C
                KLM=(K-1)*NN
                DO 20 I=2,NS
                DO 20 J=2,NS
                IV=((I-1)*NNR)+J+KLM
                IV1=IV-1
                IV2=IV+1
                IU1=((I-2)*NNR)+J+KLM
                IU2=(I*NNR)+J+KLM
                IW1=IV-NN
                IW2=IV+NN
                A(IV,IV1)=P1
                A(IV,IV2)=P1
                A(IV,IU1)=P1
                A(IV,IU2)=P1
                IF(K.EQ.1)GOTO 16
                IF(K.EQ.NL)GOTO 17
                A(IV,IW1)=W1
                A(IV,IW2)=W2
                GO TO 20
           17   A(IV,IW1)=W1
                GO TO 20
           16   A(IV,IW2)=W2
           20   CONTINUE
      C
      C     BOUNDARY NODES(TYPE 2)
      C
                DO 25 J=2,NS
                I=1
                IV=J+KLM
                IV1=IV-1
                IV2=IV+1
                IU2=(I*NNR)+J+KLM
                IW1=IV-NN
                IW2=IV+NN
                A(IV,IV1)=P2
                A(IV,IV2)=P2
                A(IV,IU2)=P3
                IF(K.EQ.1)GOTO 21
                IF(K.EQ.NL)GOTO 22
                A(IV,IW1)=W3
                A(IV,IW2)=W4
                GO TO 25
           22   A(IV,IW1)=W3
                GO TO 25
           21   A(IV,IW2)=W4
           25   CONTINUE
                DO 30 I=2,NS
                J=1
```

PROGRAM FDIMP1 74/835 OPT=1 FTN 4.8+552

```
      IV=((I-1)*NNR)+J+KLM
      IV2=IV+1
      IU1=((I-2)*NNR)+J+KLM
      IU2=(I*NNR)+J+KLM
      IW1=IV-NN
      IW2=IV+NN
      A(IV,IV2)=P3
      A(IV,IU1)=P2
      A(IV,IU2)=P2
      IF(K.EQ.1)GOTO 26
      IF(K.EQ.NL)GOTO 27
      A(IV,IW1)=W3
      A(IV,IW2)=W4
      GOTO 30
27    A(IV,IW1)=W3
      GOTO 30
26    A(IV,IW2)=W4
30    CONTINUE
C
C     ADIABATIC REFERENCE NODES(TYPE 4)
C
      DO 35 I=2,NS
      J=NNR
      IV=((I-1)*NNR)+J+KLM
      IV1=IV-1
      IU1=((I-2)*NNR)+J+KLM
      IU2=(I*NNR)+J+KLM
      IW1=IV-NN
      IW2=IV+NN
      A(IV,IV1)=P5
      A(IV,IU1)=P5
      A(IV,IU2)=P5
      IF(K.EQ.1)GOTO 31
      IF(K.EQ.NL)GOTO 32
      A(IV,IW1)=W7
      A(IV,IW2)=W8
      GOTO 35
32     A(IV,IW1)=W7
      GOTO 35
31    A(IV,IW2)=W8
35    CONTINUE
      DO 40 J=2,NS
      I=NNR
      IV=((I-1)*NNR)+J+KLM
      IV1=IV-1
      IV2=IV+1
      IU1=((I-2)*NNR)+J+KLM
      IW1=IV-NN
      IW2=IV+NN
      A(IV,IV1)=P5
      A(IV,IV2)=P5
      A(IV,IU1)=P5
      IF(K.EQ.1)GOTO 38
      IF(K.EQ.NL)GOTO 39
      A(IV,IW1)=W7
      A(IV,IW2)=W8
      GOTO 40
```

PROGRAM FDIMP1 74/835 OPT=1 FTN 4.8+552

```
                39      A(IV,IW1)=W7
                        GOTO 40
                38        A(IV,IW2)=W8
460             40      CONTINUE
                C
                C       CORNER NODES(TYPE 3)
                C
                        IV=1+KLM
465                     IV2=IV+1
                        IU2=1+NNR+KLM
                        A(IV,IV2)=P4
                        A(IV,IU2)=P4
                        IW1=IV-NN
470                     IW2=IV+NN
                        IF(K.EQ.1)GOTO41
                        IF(K.EQ.NL)GOTO42
                        A(IV,IW1)=W5
                        A(IV,IW2)=W6
475                     GOTO 43
                42      A(IV,IW1)=W5
                        GOTO 43
                41      A(IV,IW2)=W6
                C
480             C       ADIABATIC BOUNDARY NODES(TYPE 5)
                C
                43      IV=NNR+KLM
                        IV1=IV-1
                        IU2=(NNR*2)+KLM
485                     A(IV,IV1)=P8
                        A(IV,IU2)=P7
                        IW1=IV-NN
                        IW2=IV+NN
                        IF(K.EQ.1)GOTO 44
490                     IF(K.EQ.NL)GO TO 46
                        A(IV,IW1)=W11
                        A(IV,IW2)=W12
                        GOTO 47
                46      A(IV,IW1)=W11
495                     GOTO 47
                44      A(IV,IW2)=W12
                47      IV=(NS*NNR)+1+KLM
                        IV2=IV+1
                        IU1=((NNR-2)*NNR)+1+KLM
500                     A(IV,IV2)=P7
                        A(IV,IU1)=P8
                        IW1=IV-NN
                        IW2=IV+NN
                        IF(K.EQ.1)GOTO 80
505                     IF(K.EQ.NL)GOTO 81
                        A(IV,IW1)=W11
                        A(IV,IW2)=W12
                        GO TO 83
                 81     A(IV,IW1)=W11
510                     GOTO 83
                80      A(IV,IW2)=W12
                C
                C       ADIABATIC REFERENCE CORNER NODES(TYPE 6)
```

```
      C
515   83    IV=NN+KLM
            IV1=IV-1
            IU1=(NN-NNR)+KLM
            A(IV,IV1)=P6
            A(IV,IU1)=P6
520         IW1=IV-NN
            IW2=IV+NN
            IF(K.EQ.1)GOTO 84
            IF(K.EQ.NL)GOTO 85
            A(IV,IW1)=W9
525         A(IV,IW2)=W10
            GOTO 222
      85    A(IV,IW1)=W9
            GOTO 222
      84    A(IV,IW2)=W10
530   C
      C     DEVELOPMENT OF MATRIX [C]
      C     *************************
      C
      222   IF(K.EQ.1)GOTO 90
535         IF(K.EQ.NL)GO TO 91
            HC=0.0
            TC=0.0
            GOTO 95
      91    HC=HH(9)
540         TC=TL(IT)
            GOTO 95
      90    HC=HH(1)
            TC=TO(IT)
      95    A2=.5*A1
545         A3=.25*A1
            SRT=QTRANS*BENGTH**2.
            IF(IT.NE.1)GOTO 92
            SOLINT=Q(IT)
            GOTO 93
550   92    SOLINT=(Q(IT)+Q(IT-1))/2.
      93    QS=SOLINT*ABSO(K)
            QAB=QAB+(QS*BENGTH*BENGTH)
      C      REFERENCE NODES (TYPE 1)
            DO 60 I=2,NS
555         DO 60 J=2,NS
            IV=((I-1)*NNR)+J+KLM
            C(IV)=(TO(IV)/SK1)+((SM1/SK1)*(HC*TC))+((SM1*QS*A1)/SK1)
            AR(IV)=A1
      60    CONTINUE
560   C     BOUNDARY NODES (TYPE 2)
            DO 62 J=2,NS
            IV=J+KLM
            C(IV)=(TO(IV)/SK2)+((SM2/SK2)*(HK(K)*TS(IT)))+
           Q ((SM2/SK2)*(HC*TC*.5))+((SM2*QS*A2)/SK2)
565         AR(IV)=A2
      62    CONTINUE
            DO 64 I=2,NS
            IV=((I-1 )*NNR)+1+KLM
            C(IV)=(TO(IV)/SK2)+((SM2/SK2)*(HK(K)*TS(IT)))+
570        Q ((SM2/SK2)*(HC*TC*.5))+((SM2*QS*A2)/SK2)
```

```
      PROGRAM FDIMP1     74/835  OPT=1                    FTN 4.8+552

                        AR(IV)=A2
                   64   CONTINUE
                   C    ADIABATIC REFERENCE NODES(TYPE 4)
                        DO 66 I=2,NS
          575           IV=((I-1)*NNR)+NNR+KLM
                        C(IV)=(TD(IV)/SK5)+((SM1/SK5)*(HC*TC))+((SM1*QS*A1)/SK5)
                        AR(IV)=A1
                   C
                   66   CONTINUE
          580           DO 68 J=2,NS
                        IV=(NNR*NS)+J+KLM
                        C(IV)=(TD(IV)/SK5)+((SM1/SK5)*(HC*TC))+((SM1*QS*A1)/SK5)
                        AR(IV)=A1
                   68   CONTINUE
          585      C    CORNER NODES(TYPE 3)
                        C(1+KLM)=(TD(1+KLM)/SK3)+(((SM3*HK(K)*.5)/SK3)*(TS(IT)+TS(IT)))
                     Q +(SM3/SK3)*(HC*TC*.25)+((SM3*QS*A3)/SK3)
                        AR(1+KLM)=A3
                   C    ADIABATIC BOUNDARY NODES (TYPE 5)
          590           C(NNR+KLM)=(TD(NNR+KLM)/SK7)+((SM2/SK7)*(HK(K)*TS(IT)))+
                     Q ((SM2/SK7)*(HC*TC*.5))+((SM2*QS*A2)/SK7)
                        AR(NNR+KLM)=A2
                        NSR=(NS*NNR)+1
                        C(NSR+KLM)=(TD(NSR+KLM)/SK7)+((SM2/SK7)*(HK(K)*TS(IT)))
          595        Q +(SM2/SK7)*(HC*TC*.5)+((SM2*QS*A2)/SK7)
                        AR(NSR+KLM)=A2
                   C    ADIABATIC REFERENCE CORNER NODES(TYPE 6)
                        C(NN+KLM)=(TD(NN+KLM)/SK6)+((SM1/SK6)*(HC*TC))
                     Q +((SM1*QS*A1)/SK6)
          600           AR(NN+KLM)=A1
                   239  CONTINUE
                   240  FORMAT(5X,*TOTAL HEAT ABSORBED=*,F10.5)
                        IF(MAT.EQ.0)GOTO 101
                   C    PRINTING THE VALUES OF MATRIX[A]AND[B]
          605      48   FORMAT(2X,10(F8.6,2X))
                        DO 45 I=1,N
                        PRINT 48,(A(I,J),J=1,10)
                   45   CONTINUE
                        PRINT 49
          610      49   FORMAT(2X,10(1H*))
                        DO 50 I=1,N
                        PRINT 48,(A(I,J),J=11,20)
                   50   CONTINUE
                        PRINT 49
          615           DO 52 I=1,N
                        PRINT 48,(A(I,J),J=21,30)
                   52   CONTINUE
                        PRINT 49
                        PRINT 70,(C(IV),IV=1,N)
          620      70   FORMAT(8(2X,F10.4))
                   C    SOLUTION FOR THE NODES TEMPERATURES
                   C    ************************************
                   101  CALL GAUSS(N )
                        HST=0.0
          625           TBOUND=0.0
                        COUNT1=0.0
                        TBONE1=0.0
```

PROGRAM FDIMP1 74/835 OPT=1 FTN 4.8+552

```
                      TBO1=0.0
                      TBO=0.0
630                   COUNT2 =0.0
                      PO(1)=T1
                      PO(2)=T2
                      PO(3)=T3
                      PO(4)=T4
635                   PO(5)=T5
                      PO(6)=T6
                      PO(7)=T7
                      PO(8)=T8
                      DO 102 JK=1,NL
640                   PRINT 103,JK
                      IF(IT.NE.1)GOTO 127
                      POT(JK)=PO(JK)
                127   PTN=0.0
                      AREA=0.0
645                   PTO=0.0
                      NF=(JK*NN)
                      MN=(NF+1-NN)
                      DO 110 IQ=MN,NF
                      PTN=(TN(IQ)*AR(IQ))+PTN
650                   PTO=(TO(IQ)*AR(IQ))+PTO
                      AREA=AREA+AR(IQ)
                110   CONTINUE
                      PN(JK)=PTN/AREA
                      PO(JK)=PTO/AREA
655                   AWAX=(((PO(JK)-POT(JK))/2.)+POT(JK))
                      WAX=(((PN(JK)-PO(JK))/2.)+PO(JK))-AWAX
                      ENT(JK)=CC(JK)*20.25*WAX
                C     WAX IS THE TEMPERATURE CHANGE WITHIN THE TIME INCREMENT
                C     ENT(JK)IS THE HEAT STORED IN LAYER JK DURING THE TIME INCREMENT
660             C     TS IS THE TEMPERATURE AT THE GLASS -FRAME INTERFACE
                C     TSX IS THE AVERAGE TS DURING THE TIME INCREMENT
                C     AHXIS AN AREA FACTOR BETWEEN NODES AND BOUNDARY NODES
                C
                      PRINT 100,(TN(I),I=MN,NF)
665             100   FORMAT(/,5(2X,F10.5))
                103   FORMAT(//,25X,*LAYER NUMBER *,I2)
                      TSX=((TS(IT)-TS(IT-1))/2.)+TS(IT-1)
                      DO 306 J=1,NNR
                      IF(J.EQ.1)GOTO 312
670                   AHX=1.
                      GOTO 313
                312   AHX=.5
                313   I=((JK-1)*NN)+J
                      TNX=((TN(I)-TO(I))/2.)+TO(I)
675             C
                C     CALCULATION OF THE AVERAGE TEMPERATURE OF THE NODES AT
                C     INTERFACE HAVING TEMPERATURE HIGHER THAN THAT OF THE
                C     INTERFACE (TSX)
                C
680                   IF(TNX.LT.TSX) GOTO 307
                      TBOUND=TBOUND+(TN(I)*AH(JK)*AHX)
                      TBONE1=TBONE1+(TO(I)*AH(JK)*AHX)
                      COUNT1=COUNT1+(AH(JK)*AHX)
                      GOTO 306
```

```
      PROGRAM FDIMP1     74/835  OPT=1                    FTN 4.8+552

685           C      CALCULATION OF THE AVERAGE TEMPERATURE OF THE NODES AT
              C      INTERFACE HAVING TEMPERATURE LESS THAN THAT OF THE INTERFACE
              C
              307    TBO=TBO+(TN(I)*AH(JK)*AHX)
                     TBO1=TBO1+(TD(I)*AH(JK)*AHX)
690                  COUNT2=COUNT2+(AH(JK)*AHX)
              306    CONTINUE
              102    CONTINUE
                     DO 126 JK=1,NL
                     POT(JK)=PO(JK)
695           126    CONTINUE
                     IF(COUNT1.EQ.0.0)GOTO 104
                     TB1=TBOUND/COUNT1
                     TB2=TBONE1/COUNT1
                     TB=((TB1-TB2)/2.)+TB2
700                  TBDIF=(TB-TSX)
                     GOTO 505
              104    TBDIF=0.0
              505    IF(COUNT2.EQ.0.0)GOTO 506
                     TBB1=TBO/COUNT2
705                  TBB2=TBO1/COUNT2
                     TBB=((TBB1-TBB2)/2.)+TBB2
                     TBBDIF=(TSX-TBB)
                     GOTO 507
              506    TBBDIF=0.0
710           507    CONB1=COUNT1 *HOC*TBDIF*8.
                     CONB2=COUNT2 *HOC*TBBDIF*8.
                     PRINT 119,CONB1,CONB2
              119    FORMAT(/,5X,*HEAT LOSS BY CONVEC. AT BOUNDARY SURFACES*,F10.5
                    Q ,5X,F10.5)
715                  IF(IT.NE.1) GOTO 121
                     TOUT=TO(IT)
                     HOAAVE=HOA(IT)
                     PO(1)=PN(1)
                     PO(NL)=PN(NL)
720                  GOTO 122
              121    TOUTD=TO(IT-1)
                     TOUT=((TO(IT)-TOUTD)/2.)+TOUTD
                     HOAAVE=(HOA(IT)+HOA(IT-1))/2.
              122    DO 123 L=1,NL
725                  HST=HST+ENT(L)
              123    CONTINUE
                     HSTORE=(HST/3600.)*4.
                     SAMB= (((PN(1)-PO(1))/2.)+PO(1))-TOUT
                     SROOM=TI(IT)-(((PN(NL)-PO(NL))/2.)+PO(NL))
730                  CONO=SAMB*AREA*HOAAVE*4.0
                     CONI=SROOM*AREA*HOI*4.0
                     HL1=CONB1+CONO
                     HL2=CONB2+CONI-HSTORE
                     PRINT 115,CONO
735                  PRINT 116,CONI
                     PRINT 117,HSTORE
                     PRINT 118,SAMB,SROOM
                     PRINT 416,HL1
                     PRINT 417,HL2
740                  PRINT 240,QAB
                     PRINT 418,QTRANS
```

PROGRAM FDIMP1 74/835 OPT=1 FTN 4.8+552

```
      418   FORMAT(/,5X,*TOTAL HEAT GAIN=*,F10.5,/)
      416   FORMAT(/,5X,*HOURLY RATE OUTSIDE: *,F10.5)
      417   FORMAT(/,5X,*HOURLY RATE INSIDE: *,F10.5)
745   115   FORMAT(/,5X,*HEAT LOSS BY CONVECTION AT EXT. SURFACE= *
     Q ,F20.5)
      116   FORMAT(/,5X,*HEAT LOSS BY CONVECTION AT INT. SURFACE= *
     Q ,F20.5)
      117   FORMAT(/,5X,*HEAT STORED WITHIN THE PANEL =*,F20.5)
750   118   FORMAT(/,5X,*TEMP. DIFF OUT=*,F10.5,*TEMP. DIFF.IN =*,F10.5)
      C
            DO 105 I=1,N
            TD(I)=TN(I)
      105   CONTINUE
755         DO 107 I=1,N
            DO 107 J=1,N
            A(I,J) =0.0
      107   CONTINUE
            DO 108 I=1,N
760         A(I,I)=1.0
      108   CONTINUE
      106   CONTINUE
            PRINT 754
            PRINT 750
765   750   FORMAT(2X,*TIME*,1H*,8X,*WIND*,8X,1H*,5X,
     Q *SURFACE COEFFICIENTS*,5X,1H*,8X,*AIR TEMPERATURE*,7X,1H*,
     Q 6X,*INCIDENT*,6X,1H*)
            PRINT 751
      751   FORMAT(2X,*HOUR*,1H*,2X,*SPEED*,2X,*DIRECTION*,2X,1H*,
770  Q 2X,*INSIDE*,2X,*OUTSIDE*,2X,*INTERFACE*,2X,1H*,2X,
     Q *INSIDE*,2X,*OUTSIDE*,2X,*INTERFACE*,2X,1H*,2X,
     Q*TOTAL RADIATION*,3X,1H*)
            PRINT 754
      754   FORMAT(2X,109(1H*))
775         DO 752 IT=1,IHOUR
            PRINT 753,IT,WIND(IT),WD(IT),HOI, HOA(IT),HOC,TI(IT),TO(IT),
     Q TS(IT),Q(IT)
      753   FORMAT(2X,I4,1H*,F8.3,4X,F8.3,1H*,F10.6,F10.6,F10.6,1H*,
     Q F10.5,F10.5,F10.5,1H*,5X,F10.5,5X,1H*)
780   752   CONTINUE
            PRINT 754
            STOP
            END
```

SUBROUTINE FILM 74/835 OPT=1 FTN 4.8+552

```
      1           SUBROUTINE FILM(WINDY,WDD,TAS, XUG,HOPE,SATG,FG)
                C THIS SUBROUTINE CALCULATESTHE EXTERNAL SURFACE COEFFICIENT
                C (HOPE)USING THE HOURLY VALUE OF WIND SPEED(WINDY),WIND
                C DIRECTION(WDD),OUTDOOR ABSOLUTE TEMP.(TAS),AND THE THERMAL
      5         C RESISTANCE OF THE GLASS(XUG).
                  TSS=TAS+((293-TAS)*(.02994/(.02994+XUG)))
                  TSKY=TAS-20.
                  STBOL=5.67/(10.**8.)
                  HR=.92*.5*STBOL*(TSS+TSKY)*((TSS**2.)+(TSKY**2.))
     10           IF(WDD.EQ.0.0)GOTO 5
                  IF(WDD.EQ.45.)GOTO 10
                  IF(WDD.EQ.90.)GOTO 15
                  IF(WDD.EQ.135.)GOTO 20
                  HC=6.27+(2.65*WINDY)
     15           GOTO 25
                5 HC=7.77+(2.9*WINDY)
                  GOTO 25
               10 HC=7.5+(3.26*WINDY)
                  GOTO 25
     20        15 HC=7.35+(4.1*WINDY)
                  GOTO 25
               20 HC=6.85+(2.63*WINDY)
               25 HOPE=HC+HR
                  RETURN
     25           END
```

SUBROUTINE GAUSS 74/835 OPT=1 FTN 4.8+552

```
      SUBROUTINE GAUSS(N)
      COMMON A(200,200),C(200),TN(200)
C     THIS SUBROUTINE SOLVES SIMULTANEOUSLY N ALGEBRAIC EQUATIONS
C     IN N UNKNOWN TEMPERATURES.
C     A(I,J)=HEAT TRANSFER COEFFICIENT
C     TN(I) =UNKNOWN TEMPERATURE
C     C(I)  =THE CONSTANT TERM OF THE HEAT BALANCE EQ.
C
      M=N-1
   10 DO 10 I=1,M
      L=I+1
      DO 10 J=L,N
      IF(A(I,J))6,10,6
    6 DO 8 K=L,N
    8 A(J,K)=A(J,K)-A(I,K)*A(J,I)/A(I,I)
      C(J)=C(J)-C(I)*A(J,I)/A(I,I)
   10 CONTINUE
      TN(N)=C(N)/A(N,N)
      DO 30 I=1,M
   20 K=N-I
      L=K+1
      DO 20 J=L,N
   20 C(K)=C(K)-TN(J)*A(K,J)
      TN(K)=C(K)/A(K,K)
   30 CONTINUE
      RETURN
      END
```

PROGRAM FDIMP2 74/835 OPT=1 FTN 4.8+552

```
      PROGRAM FDIMP2(INPUT,OUTPUT)
      DIMENSION TD(180),HCC(5),TCC(5) , H(5), HH(6),CC(5)
      DIMENSION WIND(24),TS(24),WD(24),TI(24),HOA(24)
      DIMENSION PW(5) , PO(5),ENT(5),TO(24),Q(24)
      DIMENSION HW(5),HKW(5),HHW(6),CCI(5),AR(180),AH(5)
      COMMON A(180,180),C(180),TN(180)
C     ************************************************************
C
C     PROGRAM FDIMP2 CALCULATES THE TEMPERATURE DISTRIBUTION OF
C     VARIOUS LAYERS OF A COMPOSITE WALL WITH OR WITHOUT A WIN-
C     DOW.FDIMP USES THE IMPLICIT FORMULATION OF THE FINITE DIF-
C     FERENCE METHOD TO ALLOW NUMERICAL APPROXIMATION OF THE
C     PARTIAL DIFFERENTIAL EQUATION OF HEAT CONDUCTION IN THREE
C     DIMENSIONAL TRANSIENT STATE.AT EACH TIME INCREMENT,THE
C     RATE OF HEAT TRANSFER AT VARIOUS SURFACES AND THE HEAT
C     STORAGE IN THE VOLUME ARE CALCULATED.THE RATE OF HEAT
C     LOSS ASSOCIATED WITH AIR INFILTRATION IS ALSO CALCULATED
C     AS A FUNCTION OF WIND SPEED ,WINDOW PRIMETER,AND THE IN-
C     SIDE-OUTSIDE TEMP. DIFFERENCE.
C
C     THE DATA GIVEN BELOW IS APPLICIABLE TO A WOOD FRAME PANEL
C     .THE THERMAL PROPERTIES AND DIMENSIONS ARE GIVIN IN CHA-
C     PTER II.
C
C     ************************************************************
C           GIVEN DATA
      DATA(HW(K),K=1,5)/.00035,.0014,.000175,.00245,.00035/
      DATA(HKW(K),K=1,5)/.0046,.00276,.0023,.0073,.0046/
      DATA(HHW(K),K=1,6)/.1708,.03123,.0416,.025,.0208,.0424/
      DATA(CCI(K),K=1,5)/4.354,17.416,2.177,30.478,4.354/
      DATA(AH(K),K=1,5)/.002557,.010227,.00128,.02045,.002557/
      DATA(H(K),K=1,5)/.00286,.00142,.00143,.004139,.00286/
     DATA(HH(K),K=1,6)/1.38596,.044754,.046803,.041229,.03963,.34404/
      DATA(CC(K),K=1,5)/35.624,22.447,17.812,12.528,35.624/
C           D E F I N I T I O N S
C     INK=PANEL TYPE INDICATOR(WITH OR WITHOUT A WINDOW)
C     INDEX=POSITION OF THE WINDOW CORNER NODE
C     IHOUR=NUMBER OF HOURLY CALCULATIONS REQUIRED
C     HOC=SIDEWAYS HEAT TRANSFER COEFFICIENT
C     HOI=INTERNAL SURFACE COEFFICIENT OF H.T.
C     INTFACE=PANEL LAYER AT WHICH WINDOW IS INSTALLED
C
C     WIND(IT)=WIND SPEED AT TIME (IT)
C     WD(IT)=WIND DIRECTION AT TIME (IT)
C     TI(IT)=INSIDE AIR TEMP. AT TIME (IT)
C     TO(IT)=OUTDOOR AIR TEMPERATURE AT TIME (IT)
C     Q(IT)=INTENSITY OF INCIDENT SOLAR RADIATION AT TIME (IT)
C     H(K)=HEAT TRANSFER COEFFICIENT BETWEEN TWO NODES IN THE
C          SAME LAYER.
C     HH(K)=HEAT TRANSFER COEFFICIENT BETWEEN TWO NODES IN
C          TWO CONSECUTIVE LAYERS.
C     CC(K)=THERMAL STORAGE CAPACITY OF THE NODE VOLUME.
C     A(K)=AREA OF CONTACT BETWEEN TWO NODES IN TWO CONSECUTIVE
C          LAYERS.
C     AH(K)=AREA OF CONTACT BETWEEN TWO NODES IN THE SAME LAYER
C     HW(K)=SAME AS H(K) BUT FOR WINDOW FRAME NODES
C     HHW(K)=SAME AS HH(K) BUT FOR WINDOW FRAME NODES
```

```
PROGRAM FDIMP2    74/833  OPT=1                    FTN 4.8+552

      C     HKW(K)=SAME AS H(K) BUT FOR TWO NODES ONE SITUATED ON THE
      C           FRAME AND THE OTHER ON THE PANEL.
      C     CCI(N)=SAME AS CC(K) BUT FOR WINDOW FRAME NODES
      C     A(I,J) COEFFICIENT MATRIX OF HEAT TRANSFER
      C     C(I)=COEFFICIENT MATRIX OF THE SPECIFIED CONSTANT INPUT
      C     TD(I)=PRIVIOUS TEMPERATURE OF NODE I
      C     TN(I)=FUTURE TEMPERATURE OFV NODE I
      C     ENT(K)=RATE OF HEAT STORAGE ADDED TO THE LAYER K
      C     HOA(IT)=OUTSIDE SURFACE COEFFICIENT AT TIME IT
      C     HCC(IT)=SIDEWAY SURFACE COEFFICIENT AT TIME IT
      C     TS(IT)=INTER-PANELS AND PANEL-WINDOW INTERFACE TEMP.
      C     TCC(K)=TEMPERATURE OF LAYER K ON THE WINDOW OPENING
      C
      C
            HLOSS1=0.0
            HLOSS2=0.0
            HLOSS3=0.0
            HLOSS4=0.0
            CLC=0.0
            QINFILT=0.0
            DT=3600.0
            READ*,(WIND(IT),IT=1,24)
            READ*,(WD(IT),IT=1,24)
            READ*,(TI(IT),IT=1,24)
            READ*,(TO(IT),IT=1,24)
            READ*,(Q(IT),IT=1,24)
            READ*,INK,INDEX,IHOUR,HOC,HOI,GP,GTYPE,INTFACE
            READ*,ISTART
            HOPEOLD=33.4
            HO=10.
            IWW=6-INDEX
            WI=IWW+((.20454545-.025)/.20454545)
            IX=INDEX-1
            DO 10 I=1,180
            DO 10 J=1,180
            A(I,J)=0.00
      10    CONTINUE
            DO 15 L=1,180
            A(L,L)=1.00
            C(L)=0.0
      15    CONTINUE
      C
      C     DETERMINATION OF INITIAL TEMPERATURE OF THE LAYERS
      C     **************************************************
      C
            R1=.02994012
            R2=.65913475
            R3=1.3451104
            R4=2.456512
            R5=3.5359594
            R6=3.6565721
            DELTAT=(TI(1)-TO(1))/R6
            T1=(DELTAT*R1)+TO(1)
            T2=(DELTAT*R2)+TO(1)
            T3=(DELTAT*R3)+TO(1)
            T4=(DELTAT*R4)+TO(1)
            T5=(DELTAT*R5)+TO(1)
```

PROGRAM FDIMP2 74/835 OPT=1 FTN 4.8+552

```
      DO 2 IV=1,36
      TD(IV)=T1
    2 CONTINUE
      DO 4 IV=37,72
      TD(IV)=T2
    4 CONTINUE
      DO 5 IV=73,108
      TD(IV)=T3
    5 CONTINUE
      DO 6 IV=109,144
      TD(IV)=T4
    6 CONTINUE
      DO 7 IV=145,180
      TD(IV)=T5
    7 CONTINUE
      PRINT*,T1,T2,T3,T4,T5
C
      HH(6)=HH(6)*(HOI/8.291)
      HHW(6)=HHW(6)*(HOI/8.291)
      ICOUNT=INTFACE+1
      ICOUNT2=INTFACE-1
      HCC(INTFACE)=AH(INTFACE)*HOC
      DO 585 I=ICOUNT,5
      HCC(I)=AH(I)*HOI
  585 CONTINUE
C
C     DETERMINATION OF COEFFICIENTS FOR MATRIX  'A'
C     **********************************************
C
      TSS=T1+273.
      DO 106 IT=ISTART,IHOUR
      WINDY=WIND(IT)
      WDD=WD(IT)
      TAS=TO(IT)+273.
      QY=Q(IT)
      CALL FILM(WINDY,WDD,TAS,TSS,QY,HOPE )
      CALL INFILT(INK,INDEX,TAS,WINDY,CLCK,QINF)
      HOA(IT)=HOPE
      HH(1)=HH(1)*(HOA(IT)/HOPEOLD)
      HHW(1)=HHW(1)*(HOA(IT)/HOPEOLD)
      IF(INTFACE.EQ.1)GOTO 587
      DO 586 I=1,ICOUNT2
      HCC(I)=AH(I)*HOA(IT)
  586 CONTINUE
  587 HOPEOLD=HOA(IT)
      TS(IT)=TO(IT)+6.
      PRINT 3,IT
    3 FORMAT(//,25X,*TEMPERATURE DISTRIBUTION AFTER *,I2,*HOURS*)
      DO 9 K=1,5
      KN=K+1
C
C     INTERNAL NODES (TYPE 1)
C
      SM1=(DT/CC(K))
      SK1=1.0+(4.0 *H(K)*SM1)+(SM1*HH(K))+(SM1*HH(KN))
      P1=(-1.0*SM1*H(K))/SK1
      W1=(-1.0*SM1*HH(K))/SK1
```

```
      PROGRAM FDIMP2     74/835  OPT=1                          FTN 4.8+552

                        W2=(-1.0*SM1*HH(KN))/SK1
                        SKI1=1.+(SM1*((3.*H(K))+HKW(K)+HH(K)+HH(KN)))
                        PI1=(-1.*(SM1/SKI1))*HKW(K)
  175                   C
                        C       BOUNDARY NODES (TYPE 2)
                        C
                        SM2=(DT/CC(K)*.5)
                        SK2=1.0+(2.0*H(K)*.5*SM2)+(SM2*HH(K)*.5)+(SM2*HH(KN)*.5)+
  180                  Q (H(K)*SM2)+(AH(K)*HO*SM2)
                        P2=((-1.0*SM2)/SK2)*H(K)*.5
                        P3=((-1.0*SM2)/SK2)*H(K)
                        W3=((-1.0*SM2)/SK2)*HH(K)*.5
                        W4=((-1.0*SM2)/SK2)*HH(KN)*.5
  185                   SKI2=1.+(SM2*(H(K)+(.5*HH(K))+(.5*HH(KN))+HKW(K)))
                        PI3=((-1.*(SM2/SKI2))*HKW(K))
                        C
                        C       CORNER NODES  (TYPE 3)
                        C
  190                   SM3=(DT/CC(K)*.25)
                        SK3=1.0+(2.0*H(K)*.5*SM3)+(SM3*HH(K)*.25)+(SM3*HH(KN)*.25)
                       Q +(AH(K)*HO*.5*SM3)
                        P4=((-1.0*SM3)/SK3)*H(K)*.5
                        W5=((-1.0*SM3)/SK3)*HH(K)*.25
  195                   W6=((-1.0*SM3)/SK3)*HH(KN)*.25
                        C
                        C       ADIBATIC INTERMEDIATE NODES (TYPE 4)
                        SK5=1.0+(3.0*H(K)*SM1)+(SM1*HH(K))+(SM1*HH(KN))
                        P5=((-1.0*SM1)/SK5)*H(K)
  200                   W7=((-1.0*SM1)/SK5)*HH(K)
                        W8=((-1.0*SM1)/SK5)*HH(KN)
                        SKI5=1.+(SM1*((2.*H(K))+HH(K)+HH(KN)+HKW(K)))
                        PI5=((-1.*(SM1/SKI5))*HKW(K))
                        C
  205                   C       ADIBATIC CORNER NODES  (TYPE 6)
                        SK6=1.0+(2.0*H(K)*SM1)+(SM1*HH(K))+(SM1*HH(KN))
                        P6=((-1.0*SM1)/SK6)*H(K)
                        W9=((-1.0*SM1)/SK6)*HH(K)
                        W10=((-1.0*SM1)/SK6)*HH(KN)
  210                   C
                        C       ADIABATIC/BOUNDARY NODES (TYPE 5)
                        C
                        SK7=1.0+(SM2*(H(K)+H(K)*.5))+(SM2*HH(K)*.5)+(SM2*HH(KN)*.5)
                       Q +(AH(K)*HO*SM2)
  215                   P7=((-1.0*SM2)/SK7)*H(K)
                        P8=((-1.0*SM2)/SK7)*H(K)*.5
                        W11=((-1.0*SM2)/SK7)*HH(K)*.5
                        W12=((-1.0*SM2)/SK7)*HH(KN)*.5
                        SKI7=1.+(SM2*(H(K)+(.5*HH(K))+(.5*HH(KN))+HKW(K)))
  220                   PI7=((-1.*(SM2/SKI7))*HKW(K))
                        IF(INDEX.EQ.6.AND.INK.EQ.0)GOTO 333
                        C
                        C       WINDOW BOUNDARY NODES (TYPE 7)
                        C
  225                   SM20=(DT/CCI(K) )
                        SK20=1.+(SM20*((2.*HW(K))+HKW(K)+HHW(K)+HHW(KN)+HCC(K)))
                        P13=((-1.*SM20)/SK20)*HKW(K)
                        P11=((-1.*SM20)/SK20)*HW(K)
```

```
      PROGRAM FDIMP2    74/835  OPT=1                    FTN 4.8+552

                  W13=((-1.*SM20)/SK20)*HHW(K)
      230         W14=((-1.*SM20)/SK20)*HHW(KN)
                  C
                  C
                  C       WINDOW CORNER NODES (TYPE 9)
                  C
      235         SM30=(DT/CCI(K)*1.877778)
                  SK30=1.+(SM30*((2.*HKW(K))+(2.*HW(K))+(1.878*HHW(K)
                 Q )+(1.878*HHW(KN))+(HCC(K)*1.878)))
                  P14=((-1.*SM30)/SK30)*HW(K)
                  P15=((-1.*SM30)/SK30)*HKW(K)
      240         W15=((-1.*SM30)/SK30)*HHW(K)*1.878
                  W16=((-1.*SM30)/SK30)*HHW(KN)*1.878
                  C
                  C
                  C         ADIBATIC BOUNDARY NODES (TYPE 8)
      245         C
                  C
                  SK70=1.+(SM20*(HW(K)+HKW(K)+HHW(K)+HHW(KN)+HCC(K)))
                  P17=((-1.*SM20)/SK70)*HKW(K)
                  P18=((-1.*SM20)/SK70)*HW(K)
      250         W111=((-1.*SM20)/SK70)*HHW(K)
                  W112=((-1.*SM20)/SK70)*HHW(KN)
                  C
                  C       DEVELOPMENT OF THE COEFFICIENTS MATRIX'A'
                  C       ****************************************
      255         C
                  C
                  C       REFERENCE NODES
                  C
                  333     KLM=(K-1)*36
      260                 IF(INDEX.EQ.2)GOTO 257
                          DO 20 I=2,IX
                          DO 20 J=2,5
                          IV=((I-1)*6)+J+KLM
                          IV1=IV-1
      265                 IV2=IV+1
                          IU1=((I-2)*6)+J+KLM
                          IU2=(I*6)+J+KLM
                          IW1=IV-36
                          IW2=IV+36
      270                 A(IV,IV1)=P1
                          A(IV,IV2)=P1
                          A(IV,IU1)=P1
                          A(IV,IU2)=P1
                          IF(K.EQ.1)GOTO 16
      275                 IF(K.EQ.5)GOTO 17
                          A(IV,IW1)=W1
                          A(IV,IW2)=W2
                          GO TO 20
                  17      A(IV,IW1)=W1
      280                 GO TO 20
                  16      A(IV,IW2)=W2
                  20      CONTINUE
                          DO 805 J=INDEX,5
                          I=IX
      285                 IV=((I-1)*6)+J+KLM
```

PROGRAM FDIMP2 74/835 OPT=1 FTN 4.8+552

```
                IU2=(I*6)+J+KLM
                A(IV,IU2)=PI1
          805   CONTINUE
                IF(INDEX.EQ.6)GOTO 257
290             DO 210 I=INDEX,5
                DO 210 J=2,IX
                IV=((I-1)*6)+J+KLM
                IV1=IV-1
                IV2=IV+1
295             IU1=((I-2)*6)+J+KLM
                IU2=(I*6)+J+KLM
                IW1=IV-36
                IW2=IV+36
                A(IV,IV1)=P1
300             A(IV,IV2)=P1
                A(IV,IU1)=P1
                A(IV,IU2)=P1
                IF(K.EQ.1)GOTO 172
                IF(K.EQ.5) GOTO 173
305             A(IV,IW1)=W1
                A(IV,IW2)=W2
                GOTO 210
          173   A(IV,IW1)=W1
                GOTO210
310       172   A(IV,IW2)=W2
          210   CONTINUE
                DO 806 I=INDEX,5
                J=IX
                IV=((I-1)*6)+J+KLM
315             IV2=(IV+1)
                A(IV,IV2)=PI1
          806   CONTINUE
          257   IF(INDEX.EQ.2)GOTO 258
                PS=P3
320             GOTO 259
           258  PS=PI3
                C
                C       FOR NODES TYPE 2
                C
325       259   DO 25 J=2,5
                I=1
                IV=J+KLM
                IV1=IV-1
                IV2=IV+1
330             IU2=(I*6)+J+KLM
                IW1=IV-36
                IW2=IV+36
                A(IV,IV1)=P2
                A(IV,IV2)=P2
335             A(IV,IU2)=PS
                IF(K.EQ.1)GOTO 21
                IF(K.EQ.5)GOTO 22
                A(IV,IW1)=W3
                A(IV,IW2)=W4
340             GO TO 25
          22    A(IV,IW1)=W3
                GO TO 25
```

```
      PROGRAM FDIMP2     74/835  OPT=1                    FTN 4.8+552

           21      A(IV,IW2)=W4
           25      CONTINUE
      345          DO 30 I=2,5
                   J=1
                   IV=((I-1)*6)+J+KLM
                   IV2=IV+1
                   IU1=((I-2)*6)+J+KLM
      350          IU2=(I*6)+J+KLM
                   IW1=IV-36
                   IW2=IV+36
                   A(IV,IV2)=P5
                   A(IV,IU1)=P2
      355          A(IV,IU2)=P2
                   IF(K.EQ.1)GOTO 26
                   IF(K.EQ.5)GOTO 27
                   A(IV,IW1)=W3
                   A(IV,IW2)=W4
      360          GOTO 30
           27      A(IV,IW1)=W3
                   GOTO 30
           26      A(IV,IW2)=W4
           30      CONTINUE
      365          IF(INDEX.EQ.2)GOTO 471
                   C
                   C       FOR NODES TYPE 4
                   C
                   DO 35 I=2,IX
      370          J=6
                   IF(I.EQ.IX) GOTO 807
                   PSSS=P5
                   GOTO 808
            807    PSSS=PI5
      375  808     IV=((I-1)*6)+J+KLM
                   IV1=IV-1
                   IU1=((I-2)*6)+J+KLM
                   IU2=(I*6)+J+KLM
                   IW1=IV-36
      380          IW2=IV+36
                   A(IV,IV1)=P5
                   A(IV,IU1)=P5
                   A(IV,IU2)=PSSS
                   IF(K.EQ.1)GOTO 31
      385          IF(K.EQ.5)GOTO 32
                   A(IV,IW1)=W7
                   A(IV,IW2)=W8
                   GOTO 35
           32      A(IV,IW1)=W7
      390          GOTO 35
           31      A(IV,IW2)=W8
           35      CONTINUE
                   DO 40 J=2,IX
                   I=6
      395          IF(J.EQ.IX)GOTO 809
                   PSSS=P5
                   GOTO 810
           809     PSSS=PI5
           810     IV=((I-1)*6)+J+KLM
```

PROGRAM FDIMP2 74/835 OPT=1 FTN 4.8+552

```
      IV1=IV-1
      IV2=IV+1
      IU1=((I-2)*6)+J+KLM
      IW1=IV-36
      IW2=IV+36
      A(IV,IV1)=P5
      A(IV,IV2)=PSSS
      A(IV,IU1)=P5
      IF(K.EQ.1)GOTO 38
      IF(K.EQ.5)GOTO 39
      A(IV,IW1)=W7
      A(IV,IW2)=W8
      GOTO 40
39    A(IV,IW1)=W7
      GOTO 40
38    A(IV,IW2)=W8
40    CONTINUE
C
C     FOR CORNER NODES (TYPE 3)
C
471   IV=1+KLM
      IV2=IV+1
      IU2=7+KLM
      A(IV,IV2)=P4
      A(IV,IU2)=P4
      IW1=IV-36
      IW2=IV+36
      IF(K.EQ.1)GOTO41
      IF(K.EQ.5)GOTO42
      A(IV,IW1)=W5
      A(IV,IW2)=W6
      GOTO 43
42    A(IV,IW1)=W5
      GOTO 43
41    A(IV,IW2)=W6
C
C     ADIABATIC BOUNDARY NODES
C
43    IF(INDEX.EQ.2)GOTO 800
      PSS=P7
      GOTO 801
C     FOR NODES TYPE 5
C
800   PSS=PI7
801   IV=6+KLM
      IV1=IV-1
      IU2=12+KLM
      A(IV,IV1)=P8
      A(IV,IU2)=PSS
      IW1=IV-36
      IW2=IV+36
      IF(K.EQ.1)GOTO 44
      IF(K.EQ.5)GO TO 46
      A(IV,IW1)=W11
      A(IV,IW2)=W12
      GOTO 47
46    A(IV,IW1)=W11
```

```
      PROGRAM FDIMP2     74/833  OPT=1                    FTN 4.8+552
                        GOTO 47
                  44    A(IV,IW2)=W12
                  47    IV=31+KLM
  460                   IV2=IV+1
                        IU1=25+KLM
                        A(IV,IV2)=PSS
                        A(IV,IU1)=P8
                        IW1=IV-36
  465                   IW2=IV+36
                        IF(K.EQ.1)GOTO 80
                        IF(K.EQ.5)GOTO 81
                        A(IV,IW1)=W11
                        A(IV,IW2)=W12
  470                   GO TO 83
                   81   A(IV,IW1)=W11
                        GOTO 83
                  80    A(IV,IW2)=W12
                  83    IF(INK.NE.0)GO TO 232
  475             C
                  C     FOR ADIABATIC CORNER (TYPE 6)
                  C
                        IV=36+KLM
                        IV1=IV-1
  480                   IU1=30+KLM
                        A(IV,IV1)=P6
                        A(IV,IU1)=P6
                        IW1=IV-36
                        IW2=IV+36
  485                   IF(K.EQ.1)GOTO 84
                        IF(K.EQ.5)GOTO 85
                        A(IV,IW1)=W9
                        A(IV,IW2)=W10
                        GOTO 222
  490             85    A(IV,IW1)=W9
                        GOTO 222
                  84    A(IV,IW2)=W10
                        GOTO 222
                  C
  495             C     FOR NODES TYPE 9
                  C
                  232   IV=KLM+(IX*6)+INDEX
                        IV1=IV-1
                        IV2=IV+1
  500                   IU1=IV-6
                        IU2=IV+6
                        IW1=IV-36
                        IW2=IV+36
                        A(IV,IV1)=P15
  505                   A(IV,IV2)=P14
                        A(IV,IU1)=P14
                        A(IV,IU2)=P15
                        IF(K.EQ.1)GOTO 500
                        IF(K.EQ.5)GOTO 501
  510                   A(IV,IW1)=W15
                  500   A(IV,IW2)=W16
                        GOTO 502
                  501   A(IV,IW1)=W15
```

```
      PROGRAM FDIMP2     74/835  OPT=1                    FTN 4.8+552

            502     IF(INK.EQ.0) GOTO222
      515           IF(INDEX.EQ.6) GOTO 222
                    C
                    C       FOR NODES TYPE 8
                    C
                    IVQ=KLM+(INDEX*6)
      520           IV1=IVQ-1
                    IV2=IVQ+1
                    IU1=IVQ-6
                    IW1=IVQ-36
                    IW2=IVQ+36
      525           A(IVQ,IV1)=P18
                    A(IVQ,IU1)=P17
                    IF(K.EQ.1)GOTO 503
                    IF(K.EQ.5)GOTO 504
                    A(IVQ,IW1)=W111
      530     503   A(IVQ,IW2)=W112
                    GOTO 505
                    A(IVQ,IW1)=W111
            505     IVY=KLM+(30+INDEX)
                    IV1=IVY-1
      535           IU1=IVY-6
                    IW1=IVY-36
                    IW2=IVY+36
                    A(IVY,IV1)=P17
                    A(IVY,IU1)=P18
      540           IF(K.EQ.1)GOTO 506
                    IF(K.EQ.5)GOTO 507
                    A(IVY,IW1)=W111
            506     A(IVY,IW2)=W112
                    GOTO 508
      545     507   A(IVY,IW1)=W111
                    C
                    C       FOR NODES TYPE 7
                    C
            508     INJ=INDEX+1+KLM+(IX*6)
      550           IMJ=IVQ-1
                    DO 510 IV=INJ,IMJ
                    IV1=IV-1
                    IV2=IV+1
                    IU1=IV-6
      555           IW1=IV-36
                    IW2=IV+36
                    A(IV,IV1)=P11
                    A(IV,IV2)=P11
                    A(IV,IU1)=W13
      560           IF(K.EQ.1)GOTO 511
                    IF(K.EQ.5)GOTO 512
                    A(IV,IW1)=W13
            511     A(IV,IW2)=W14
                    GOTO 510
      565   512     A(IV,IW1)=W13
            510     CONTINUE
                    INJ=INDEX+6+KLM+(IX*6)
                    IMJ=IVY-6
                    DO 520 IV=INJ,IMJ,6
      570           IV1=IV-1
```

```
                IU1=IV-6
                IU2=IV+6
                IW1=IV-36
                IW2=IV+36
575             A(IV,IV1)=P13
                A(IV,IU1)=P11
                A(IV,IU2)=P11
                IF(K.EQ.1)GOTO 521
                IF(K.EQ.5)GOTO 522
580             A(IV,IW1)=W13
          521   A(IV,IW2)=W14
                GOTO 520
          522   A(IV,IW1)=W13
          520   CONTINUE
585       C
          222   IF(K.EQ.1)GOTO 90
                IF(K.EQ.5)GO TO 91
                HC=0.0
                TC=0.0
590             GOTO 95
          91    HC=HH(6)
                TC=TI(IT)
                GOTO 95
          90    HC=HH(1)
595             TC=TO(IT)
          C
          C     DEVELOPMENT OF MATRIX 'C'
          C     *************************
          C
600       95    DO 820 I=1,5
                IF(I.LT.INTFACE)GOTO 821
                IF(I.GT.INTFACE)GOTO 822
                TCC(I)=TS(IT)
                GOTO 820
605       821   TCC(I)=TO(IT)
                GOTO 820
          822   TCC(I)=TI(IT)
          820   CONTINUE
                A1=.04183884
610             A2=.02091942
                A3=.01045971
                A6=.00991478
                A5=.00511364
                ST=TS(IT)
615             QSS=((Q(IT)+Q(IT-1))/2.)*.65
                IF(K.NE.1)  GOTO 94
                QS=QSS
                GOTO 96
          94    QS=0.0
620       C
          C     FOR WALL PANEL NODES
          C
          96    IF(INDEX.EQ.2)GOTO 603
          C
625       C     FOR NODES TYPE 1
          C
                DO 60 I=2,IX
```

PROGRAM FDIMP2 74/835 OPT=1 FTN 4.8+552

```
                      DO 60 J=2,5
                      IV=((I-1)*6)+J+KLM
630                   C(IV)=(TD(IV)/SK1)+((SM1/SK1)*(HC*TC))+((SM1*QS*A1)/SK1)
                      AR(IV)=A1
            60        CONTINUE
                      IF(INDEX.EQ.6)GOTO 603
                      DO 601 I=INDEX,5
635                   DO 601 J=2,IX
                      IV=((I-1)*6)+J+KLM
                      C(IV)=(TD(IV)/SK1)+((SM1/SK1)*(HC*TC))+((SM1*QS*A1)/SK1)
                      AR(IV)=A1
            601       CONTINUE
640                   GOTO 603
            97        I=6
                      DO 602 J=2,IX
                      IV=((I-1)*6)+J+KLM
                      C(IV)=(TD(IV)/SK1)+((SM1/SK1)*(HC*TC))+((SM1*QS*A1)/SK1)
645                   AR(IV)=A1
            602       CONTINUE
                      C
                      C     FOR NODES TYPE 2
                      C
650         603       DO 62 J=2,5
                      IV=J+KLM
                      C(IV)=(TD(IV)/SK2) +((SM2/SK2)*(HC*TC*.5))
                     Q +((SM2*QS*A2)/SK2)+((SM2/SK2)*(AH(K)*HO*ST))
                      AR(IV)=A2
655         62        CONTINUE
                      DO 64 I=2,5
                      IV=((I-1 )*6)+1+KLM
                      C(IV)=(TD(IV)/SK2) +((SM2/SK2)*(HC*TC*.5))
                     Q +((SM2*QS*A2)/SK2)+((SM2/SK2)*(AH(K)*HO*ST))
660                   AR(IV)=A2
            64        CONTINUE
                      IF(INDEX.EQ.2)GOTO 647
                      C
                      C     FOR NODES TYPE 4
665                   C
                      DO 66 I=2,IX
                      IV=((I-1)*6)+6+KLM
                      C(IV)=(TD(IV)/SK5)+((SM1/SK5)*(HC*TC))+((SM1*QS*A1)/SK5)
                      AR(IV)=A1
670         66        CONTINUE
                      DO 68 J=2,IX
                      IV=30+J+KLM
                      C(IV)=(TD(IV)/SK5)+((SM1/SK5)*(HC*TC))+((SM1*QS*A1)/SK5)
                      AR(IV)=A1
675         68        CONTINUE
                      C
                      C     FOR NODES TYPE 3
                      C
            647       C(1+KLM)=(TD(1+KLM)/SK3)+((SM3/SK3)*(AH(K)*HO*ST*.5))
680                  Q +(SM3/SK3)*(HC*TC*.25)+((SM3*QS*A3)/SK3)
                      AR(1+KLM)=A3
                      C
                      C     FOR NODES TYPE 5
                      C
```

```
      PROGRAM FDIMP2    74/835  OPT=1                    FTN 4.8+552

685               C(6+KLM)=(TD(6+KLM)/SK7)+((SM2/SK7)*(AH(K)*HO*ST))+
                 Q ((SM2/SK7)*(HC*TC*.5))+((SM2*QS*A2)/SK7)
                  AR(6+KLM)=A2
                  C(31+KLM)=(TD(31+KLM)/SK7)+((SM2/SK7)*(AH(K)*HO*ST))
                 Q +(SM2/SK7)*(HC*TC*.5)+((SM2*QS*A2)/SK7)
690               AR(31+KLM)=A2
                  IF(INK.NE.0)GOTO 93
                C
                C     FOR NODES TYPE 6
                C
695               C(36+KLM)=(TD(36+KLM)/SK6)+((SM1/SK6)*(HC*TC))
                 Q +((SM1*QS*A1)/SK6)
                  AR(36+KLM)=A1
                  GOTO 9
                C
700             C     FOR NODES TYPE 7
                C
                C
                C     FOR WINDOW FRAME NODES(TYPE 8)
                C
705             93    IV=KLM+(IX*6)+INDEX
                  C(IV)=(TD(IV)/SK30)+((SM30/SK30)*((HC*TC*.2295)+(QS*A6)))+
                 Q (HCC(K)*TCC(K)*1.878)*(SM30/SK30)
                  AR(IV)=A6
                  IF(INDEX.EQ.6) GOTO 9
710               IVQ=KLM+(INDEX*6)
                  C(IVQ)=(TD(IVQ)/SK70)+((SM20/SK70)*((HC*TC*.1222)+(QS*A5)+
                 Q (HCC(K)*TCC(K))))
                  AR(IVQ)=A5
                  IVY=KLM+(30+INDEX)
715               C(IVY)=(TD(IVY)/SK70)+((SM20/SK70)*((HC*TC*.1222)+(QS*A5)+
                 Q (HCC(K)*TCC(K))))
                  AR(IVY)=A5
                  INJ=INDEX+1+KLM+(IX*6)
                  IMJ=IVQ-1
720               DO 700,IV=INJ,IMJ
                  C(IV)=(TD(IV)/SK20)+((SM20/SK20)*((HC*TC*.1222)+(QS*A5)+
                 Q (HCC(K)*TCC(K))))
                  AR(IV)=A5
              700 CONTINUE
725               INJ=INDEX+6+KLM+(IX*6)
                  IMJ=IVY-6
                  DO 720 IV=INJ,IMJ,6
                  C(IV)=(TD(IV)/SK20)+((SM20/SK20)*((HC*TC*.1222)+(QS*A5)+
                 Q (HCC(K)*TCC(K))))
730               AR(IV)=A5
              720 CONTINUE
                  IF(INDEX.EQ.0)GOTO 9
                  IF(INDEX.GT.5)GOTO 9
                  NX=INDEX+1
735               DO 740 I=NX,6
                  DO 740 J=NX,6
                  IV=KLM+((I-1)*6)+J
                  C(IV)=0.0
                  AR(IV)=0.0
740           740 CONTINUE
              9   CONTINUE
```

PROGRAM FDIMP2 .*74/835 OPT=1 FTN 4.8+552

```
                GOTO 101
          101   N=180
                CALL GAUSS(N )
745             DO 936 JK=1,5
                AVN=0.
                AVO=0.
                AREA=0.
                PRINT 103,JK
750             NNE=(JK*36)
                MN=(NNE-35)
                PRINT 100,(TN(I),I=MN,NNE)
                IF(NNE.EQ.36.OR.NNE.EQ.180)GOTO 937
                GOTO 936
755       937   DO 938 IQ=MN,NNE
                AVN=AVN+(TN(IQ)*AR(IQ))
                AVO=AVO+(TD(IQ)*AR(IQ))
                AREA=AREA+AR(IQ)
          938   CONTINUE
760             AVTI=((AVN/AREA)+(AVO/AREA))/2.
                PRINT 939,AVTI
          936   CONTINUE
          100   FORMAT(/,6(2X,F10.5))
           939   FORMAT(2X,*AVERAGE SURFACE TEMPERATURE =*,F10.4)
765             TBOUND=0.0
                TBO=0.0
                COUNT1=0.0
                COUNT2=0.0
                TWIN1=0.0
770             TWIN2=0.0
                TWON1=0.0
                TWON2=0.0
                TWIN3=0.0
                TWON3=0.0
775             AHB=0.0
                AHH=0.0
                AHA=0.0
          C
          C     CALCULATION OF THE RATE OF HEAT STORAGE
780       C     ***************************************
          C
                DO 102 JK=1,5
                PTN=0.0
                PTO=0.0
785             AREA=0.0
                AREAF=0.0
                PTNF=0.0
                PTOF=0.0
                NNE=(JK*36)
790             MN=(NNE-35)
                DO 110 IQ=MN,NNE
                IF(INK.EQ.0.AND.INDEX.EQ.6)GOTO 909
                 IF(AR(IQ).EQ.A5.OR.AR(IQ).EQ.A6)GOTO 900
          909   PTN=(TN(IQ)*AR(IQ))+PTN
795             PTO=(TD(IQ)*AR(IQ))+PTO
                AREA=AREA+AR(IQ)
                GOTO 110
          900   PTNF=(TN(IQ)*AR(IQ))+PTNF
```

```
      PROGRAM FDIMF2     74/835  OPT=1                    FTN 4.8+552

                  PTOF=(TD(IQ)*AR(IQ))+PTOF                                  A
      800         AREAF=AREAF+AR(IQ)
            110   CONTINUE
                  AREATOT=AREA+AREAF
                  PN(JK)=(PTN+PTNF)/AREATOT
                  PO(JK)=(PTO+PTOF)/AREATOT
      805         IF(INK.EQ.0)GOTO 910
                  ENTF=(CCI(JK)*(AREAF/.00511364)*((PTNF-PTOF)/AREAF))
                  GOTO 912
            910   ENTF=0.0
            912   ENT(JK)=(CC(JK)*(AREA/.04183884)*((PTN-PTO)/AREA))
      810       Q +ENTF
            103   FORMAT(//,25X,*LAYER NUMBER *,I2)
                  C
                  C     CALCULATION OF THE SIDEWAYS HEAT LOSS OR GAIN
                  C     ***********************************************
      815         C
                  DO 306 J=1,6
                  I=((JK-1)*36)+J
                  IF(TN(I).LT.TS(IT)) GOTO 307

      820         TBOUND=TBOUND+TN(I)
                  COUNT1=COUNT1+1.0
                  GOTO 306
            307   TBO=TBO+TN(I)
                  COUNT2=COUNT2+1.0
      825   306   CONTINUE
                  DO 312 J=INDEX,6
                  I=((JK-1)*36)+(IX*6)+J
                  IF(JK.EQ.INTFACE)GOTO 315
                  IF(JK.LT.INTFACE)GOTO 313
      830         IF(JK.GT.INTFACE)GOTO 314
            315   TWIN2=TWIN2+(TN(I)*AH(JK))
                  TWON2=TWON2+(TD(I)*AH(JK))
                  AHH=AHH+AH(JK)
                  GOTO 312
      835   313   TWIN1=TWIN1+(TN(I)*AH(JK))
                  TWON1=TWON1+(TD(I)*AH(JK))
                  AHA=AHA+AH(JK)
                  GOTO 312
            314   TWIN3=TWIN3+(TN(I)*AH(JK))
      840         TWON3=TWON3+(TD(I)*AH(JK))
                  AHB=AHB+AH(JK)
            312   CONTINUE
            102   CONTINUE
                  TSS=PN(1)+273.
      845         IF(COUNT1.EQ.0.)GOTO 1100
                  TB=TBOUND/COUNT1
                  TBDIF=(TB-TS(IT))
                  CONB1=(COUNT1/30.)*1.518*HO*TBDIF
                  GOTO 1101
      850   1100   CONB1=0.0
            1101  IF(COUNT2.EQ.0.) GOTO 1200
                  TBB=TBO/COUNT2
                  TBBDIF=(TS(IT)-TBB)
                  CONB2=(COUNT2/30.)*1.518*HO*TBBDIF
      855         GOTO 1201
```

```
PROGRAM FDIMP2    74/835  OPT=1                          FTN 4.8+552

      1200   CONB2=0.0
      1201   PRINT 119,CONB1,CONB2
      119    FORMAT(/,5X,*HEAT LOSS BY CONVEC. AT BOUNDARY SURFACES =*,
     Q F10.5,5X,F10.5)
860   C
      C      CALCULATION OF THE RATE OF SIDEWAYS HEAT LOSS OR GAIN AT
      C      THE WINDOW OPENING.
      C      ***********************************************************
      C
865    940    IF(IT.NE.1) GOTO 121
             TOUT=TO(IT)
             HOAAVE=HOA(IT)
             TSAV=TO(IT)+6.
             TW2=TWIN2/AHH
870          IF(AHA.EQ.0.0)GOTO 325
             TW1=TWIN1/AHA
             GOTO 326
      325    TW1=0.0
      326    IF(AHB.EQ.0.0)GOTO 327
875          TW3=WIN3/AHB
             GOTO 328
      327    TW3=0.0
      328    GOTO 122
      121    TOUTD=TO(IT-1)
880          TSAV=(TO(IT)+TOUTD+12.)/2.
             TOUT=((TO(IT)-TOUTD)/2.)+TOUTD
             HOAAVE=(HOA(IT)+HOA(IT-1))/2.
             IF(AHH.EQ.0.0)GOTO 343
             TW2=(((TWIN2/AHH)-(TWON2/AHH))/2.)+(TWON2/AHH)
885          GOTO 345
      343    TW2=0.
      345    IF(AHA.EQ.0.0)GOTO 340
             TW1=(((TWIN1/AHA)-(TWON1/AHA))/2.)+(TWON1/AHA)
             GOTO 341
890   340    TW1=0.0
      341    IF(AHB.EQ.0.0)GOTO 342
             TW3=(((TWIN3/AHB)-(TWON3/AHB))/2.)+(TWON3/AHB)
             GOTO 122
      342    TW3=0.0
895   122    HSTORE=((ENT(1)+ENT(2)+ENT(3)+ENT(4)+ENT(5))/3600.)*4.
             SAMB= (((PN(1)-PO(1))/2.)+PO(1))-TOUT
             TAS= (SAMB/2.) +273.
             SROOM=TI(IT)-(((PN(5)-PO(5))/2.)+PO(5))
             CONO=SAMB* (1.125**2.-((WI*.20454545)**2.0))*HOAAVE*4.
900          CONI=SROOM*(1.125**2.-((WI*.20454545)**2.0))*HOI*4.0
             IF(INK.NE.0) GOTO 533
             COW1=0.0
             COW2=0.0
             COW3=0.0
905          GOTO 545
      C      TW11=TW1+(((TOUT-TW1)*RF)/(RF+(1./HOA(IT))))
      C      TW22=TW2+(((TOUT-2.-TW2)*RF)/(RF+(1./HOC)))
      533    IF(INTFACE.EQ.1)GOTO 814
             IF(INTFACE.EQ.2)GOTO811
910          IF(INTFACE.EQ.3)GOTO 812
             IF(INTFACE.EQ.4)GOTO 813
             DEP1=.16875
```

```
                DEP2=.0125
                DEP3=0.0
      915       GOTO 815
           814  DEP1=0.0
                DEP2=.0125
                DEP3=.16875
                GOTO 815
      920  811  DEP1=.0125
                DEP2=.05
                DEP3=.11875
                GOTO 815
           812  DEP1=.0625
      925       DEP2=.00625
                DEP3=.1125
                GOTO 815
           813  DEP1=.06875
                DEP2=.10
      930       DEP3=.0125
           815  IF(INTFACE.EQ.5)GOTO 816
                COW3=(TI(IT)-( TW3))*HOI*(DEP3*WI*8.*.20454545)
                GOTO 817
           816  COW3=0.0
      935  817  IF(INTFACE.EQ.1)GOTO 818
                COW1=((TW1)-TOUT)*HOA(IT)* (DEP1*WI*.2045454S*8.)
                GOTO 819
           818  COW1=0.0.
           819  COW2=((TW2)-TSAV)*HOC*(DEP2*WI*.20454545*8.)
      940  C
           C    PRINT OF RESULTS AND INITIALIZATION OF THE FOLLOWING TIME
           C    INCREMENT.
           C    ************************************************************
           C
      945  545  PRINT 115,CONO
                PRINT 116,CONI
                PRINT 117,HSTORE
                PRINT 118,SAMB,SROOM
                PRINT415,COW1,COW2,COW3
      950       HL1= CONO+COW1+COW2+CONB2
                HL2= CONI+COW3 -HSTORE+CONB1
                PRINT 416,HL1
                PRINT 417,HL2
           416  FORMAT(/,5X,*HOURLY RATE OF H.L.TO OUTSIDE:*,F10.5)
      955  417  FORMAT(/,5X,*TOTATL RATE OF H. INPUT:*,F10.5)
           415  FORMAT(/,5X,*CONVECTION AT INTERFACE!  *,3(F10.5,5X))
           115  FORMAT(/,5X,*HEAT LOSS BY CONVECTION AT EXT. SURFACE= *
               Q ,F20.5)
           116  FORMAT(/,5X,*HEAT LOSS BY CONVECTION AT INT. SURFACE= *
      960     Q ,F20.5)
           117  FORMAT(/,5X,*HEAT STORED WITHIN THE PANEL =*,F20.5)
           118  FORMAT(/,5X,*TEMP. DIFF OUT=*,F10.5,*TEMP. DIFF.IN =*,F10.5)
                DO 105 I=1,180
                TR(I)=TN(I)
      965  105  CONTINUE
                DO 107 I=1,180
                DO 107 J=1,180
                A(I,J) =0.0
           107  CONTINUE
```

```
      PROGRAM FDIMP2     74/835  OPT=1                    FTN 4.8+552

970                 DO 108 I=1,180
                    A(I,I)=1.0
              108   CONTINUE
                    HLOSS1=HLOSS1+CONO
                    HLOSS2=HLOSS2+HL1
975                 HLOSS3=HLOSS3+HL2
                    HLOSS4=HLOSS4+COW1+COW2
                    PRINT*,CLCK,QINF
                    CLC=CLCK+CLC
                    QINFILT=QINFILT+QINF
980           106   CONTINUE
                    PRINT 953,HLOSS1,HLOSS2,HLOSS3,HLOSS4
                    PRINT* ,CLC,QINFILT
              953   FORMAT(/,5X,4(F14.5,5X))
                    PRINT 711
985           711   FORMAT(/,45X,*I N P U T  D A T A *,/)
                    PRINT 755
                    PRINT 750
              750   FORMAT(2X,*TIME*,1H*,8X,*WIND*,8X,1H*,5X,
                   Q *SURFACE COEFFICIENTS*,5X,1H*,8X,*AIR TEMPERATURE*,7X,1H*,
990                Q 6X,*INCIDENT*,6X,1H*)
                    PRINT 751
              751   FORMAT(2X,*HOUR*,1H*,2X,*SPEED*,2X,*DIRECTION*,2X,1H*,
                   Q 2X,*INSIDE*,2X,*OUTSIDE*,2X,*INTERFACE*,2X,1H*,2X,
                   Q *INSIDE*,2X,*OUTSIDE*,2X,*INTERFACE*,2X,1H*,2X,
995                Q *TOTAL RADIATION*,3X,1H*)
                    PRINT 755
              755   FORMAT(2X,109(1H*))
                    DO 752 IT=1,IHOUR
                    PRINT 753,IT,WIND(IT),WD(IT),HOI,HOA(IT),HOC,TI(IT),TO(IT),
1000                Q TS(IT),Q(IT)
              753   FORMAT(2X,I4,1H*,F10.5,F10.5,1H*,F10.6,F10.6,F10.6,1H*,
                   Q F10.5,F10.5,F10.5,1H*,5X,F10.5,5X,1H*)
              752   CONTINUE
                    PRINT 755
1005                STOP
                    END
```

SUBROUTINE FILM 74/835 OPT=1 FTN 4.8+552

```
      1           SUBROUTINE FILM(WINDY,WDD,TAS,TSS,QY,HOPE )
                  TSKY=TAS-20.
                  STBOL=5.67/(10.**8.)
                  HR=.85*.50*STBOL*(TSS+TSKY)*((TSS**2.)+(TSKY**2.))
      5           IF(WDD.EQ.0.)GOTO 5
                  IF(WDD.EQ.45.)GOTO 10
                  IF(WDD.EQ.90.)GOTO 15
                  IF(WDD.EQ.135.)GOTO 20
                  HC=6.27+(2.65*WINDY)
     10           GOTO 25
                5 HC=7.77+(2.9*WINDY)
                  GOTO 25
               10 HC=7.5+(3.26*WINDY)
                  GOTO 25
     15        15 HC=7.53+(4.1*WINDY)
                  GOTO 25
               20 HC=6.85+(2.63*WINDY)
               25 HOPE=HR+HC
                  RETURN
     20           END
```

SUBROUTINE GAUSS 74/835 OPT=1 FTN 4.8+552

```
      SUBROUTINE GAUSS(N)
      COMMON A(180,180),C(180),TN(180)
      M=N-1
      DO 10 I=1,M
      L=I+1
      DO 10 J=L,N
      IF(A(I,J))6,10,6
    6 DO 8 K=L,N
    8 A(J,K)=A(J,K)-A(I,K)*A(J,I)/A(I,I)
      C(J)=C(J)-C(I)*A(J,I)/A(I,I)
   10 CONTINUE
      TN(N)=C(N)/A(N,N)
      DO 30 I=1,M
      K=N-I
      L=K+1
      DO 20 J=L,N
   20 C(K)=C(K)-TN(J)*A(K,J)
      TN(K)=C(K)/A(K,K)
   30 CONTINUE
      RETURN
      END
```

SUBROUTINE INFILT 74/835 OPT=1 FTN 4.8+552

```
      SUBROUTINE INFILT(INK,INDEX, TAS,WINDY,CLCK,QINF)
C
C     THIS SUBROUTINE CALCULATES THE HEAT LOSS ASSOCIATED WITH
C     INFILTRATION.
C     INK IS A PARAMETER TO INDICATE  THE PANEL TYPE(WITH OR
C     WITHOUT A WINDOW.
C     INDEX IS A PARAMETER TO INDICATE TEHE POSITON OF THE WIN-
C     DOW CORNER.
C     TAS IS OUTDOOR AIR TEMP(ABSOLUTE)
C     WINDY IS THE WIND SPEED
C     CL=CRACK LENGTH
C     CK=INFILTRATION COEFFICIENT
C     CLCK (CRACK LENGTH XINFILTRATION COEFFICIENT)
C     QINF IS THE HEAT LOSS DUE TO AIR INFILTRATION
C     ************************************************************
      IF(INK.EQ.0)GOTO 5
      IF(INDEX.EQ.2)GOTO 10
      IF(INDEX.EQ.3)GOTO 15
      IF(INDEX.EQ.4)GOTO 20
      IF(INDEX.EQ.5)GOTO 25
      IF(INDEX.EQ.6)GOTO 30
   10 CL=17.
      GOTO 35
   15 CL=15.34
      GOTO 35
   20 CL=13.71
      GOTO 35
   25 CL=12.07
      GOTO 35
   30 CL=10.44
      GOTO 35
    5 CL=9.
   35 CK=.081+(.024*WINDY)+(.0096*(WINDY**2.))+(.0053*(WINDY**3.))
      CLCK=CL*CK
      QINF=(20.-(TAS-273.))*CLCK
      RETURN
      END
```

```
      PROGRAM TRANS(INPUT,OUTPUT),
C     THIS PROGRAM CALCULATES ANGLE DEPENDENT REFLECTANCE,
C     TRANSMITTANCE,AND ABSORPTANCE FOR SINGLE,DOUBLE ,ANDTRIPLE
C     GLAZING
C
C     M=NUMBER OF LAYER(PANES)
C      EK=EXTINCTION COEFFICIENT
C      RI=REFRACTIVE INDEX
C      A1=ANGLE OF INCIDENCE
C      GT=GLASS THICKNESS
C
C                    INPUT DATA
C
      READ*,EK,RI,GT,M
      PRINT 50,M
      PRINT 54
      PRINT 53
      PRINT 54
      PI=3.1415927
      CON1=(PI/180.)
      DO 200 I=5,95,5
      ROON=0.0
      ROOP=0.0
      COUNT=I-5.
      A1=(COUNT)*CON1
      IF(COUNT.EQ.0.)GOTO 5
      IF(COUNT.EQ.90.)GOTO 6
C
C     DETERMINE REFRACTION ANGLE A2
      AA2=  SIN(A1)/RI
      A2=ASIN(AA2)
      ADIFF=A1-A2
      ASUM=A1+A2
      ROON=((SIN(ADIFF))**2./(SIN(ASUM))**2.)
      ROOP=((TAN(ADIFF))**2./(TAN(ASUM))**2.)
      GOTO 7
5     ROON=(RI-1)**2./(RI+1)**2
      ROOP=ROON
      GOTO 7
6     ROON=1.
      ROOP=1.
7     TAU1=EXP(-1.*EK*GT)
C     CALCULATION OF TOTAL REFLECTION (ROO),AND TOTAL TRANSMITTANCE
C
C
C     SINGLE GLAZING
C
C     NORMAL COMPONENT OF POLARIZATION(N=1)
C     PARALLEL COMPONENT OF POLARIZATION(N=2)
C
C
      DO 100 N=1,2
      IF(N.EQ.2)GOTO 8
      ROOS=ROON
      GOTO 9
8     ROOS=ROOP
C       X=((1. ROOS)**2.)/(1.-((ROOS**2.)*(TAU1**2.)))
9     X=((1.-ROOS)*(1. ROOS))/(1.-(ROOS*ROOS*TAU1*TAU1))
      ROO=ROOS*(1.+((TAU1**2.)*X))
      TAU TAU1*X
      IF(N.EQ.2)GOTO 10
      ROOPAR1=ROO
      TAUPAR1=TAU
      GOTO 100
10    ROOPAR1=ROO
      TAUPAR1=TAU
100   CONTINUE
      IF(M.EQ.1)GOTO 20
C
C     DOUBLE GLAZING
C
      IF(COUNT.EQ.90.)GOTO 75
      ROONOR2=ROONOR1+((ROONOR1*(TAUNOR1**2.))/(1.-(ROONOR1**
     @ 2.)))
      TAUNOR2=(TAUNOR1**2.)/(1.-(ROONOR1**2.))
      ROOPAR2=ROOPAR1+((ROOPAR1*(TAUPAR1**2.))/(1.-(ROOPAR1**
     @ 2.)))
      TAUPAR2=(TAUPAR1**2.)/(1.-(ROOPAR1**2.))
      IF(M.EQ.2)GOTO 30
C
C     TRIPLE GLAZING
C
      IF(COUNT.EQ.90.)GOTO 75
      ROONOR3=ROONOR1+((ROONOR2*(TAUNOR1**2.))/(1.-(ROONOR1*
     @ ROONOR2)))
      TAUNOR3=(TAUNOR2*TAUNOR1)/(1.-(ROONOR2*ROONOR1))
      ROOPAR3=ROOPAR1+((ROOPAR2*(TAUPAR1**2.))/(1.-(ROOPAR1*
     @ ROOPAR2)))
      TAUPAR3=(TAUPAR2*TAUPAR1)/(1. (ROOPAR2*ROOPAR1))
      GOTO 40
C
C     CALCULATION OF AVERAGE REFLECTANCE(ROOAVE),AVERAGE TRANSMITTANC
C     (TAUAVE),AND AVERAGE ABSORPTANCE(ALFAVE).
C
20    ROOAVE=.5*(ROONOR1+ROOPAR1)
      TAUAVE=.5*(TAUNOR1+TAUPAR1)
      ALFAVE=1.-(ROOAVE+TAUAVE)
      GOTO 70
30    ROOAVE=.5*(ROONOR2+ROOPAR2)
      TAUAVE=.5*(TAUNOR2+TAUPAR2)
      ALFAVE=1.-(ROOAVE+TAUAVE)
      GOTO 70
40    ROOAVE=.5*(ROONOR3+ROOPAR3)
      TAUAVE=.5*(TAUNOR3+TAUPAR3)
      ALFAVE=1.-(ROOAVE+TAUAVE)
      GOTO 70
75    ROOAVE=1.
      TAUAVE=0.0
      ALFAVE=0.0
C
C     PRINT OUTPUT
C
70    PRINT 54
50    FORMAT(20X,*NUMBER OF LAYERS=*,I2)
53    FORMAT(2X,1H*,*ANGLE OF INCIDENCE*,1H*,*REFLECTANCE*,1H*
     @ ,*TRANSMITTANCE*,1H*,*ABSORPTANCE*,1H*)
54     FORMAT(2X,50(1H*))
      PRINT 55,COUNT,ROOAVE,TAUAVE,ALFAVE
55    FORMAT(2X,1H*,7X,F5.2,6X,1H*,4X,F8.6,1H*,3X,F8.6,2X,1H*
     @ ,3X,F8.6,1H*)
200   CONTINUE
      PRINT 54
      STOP
      END
```

PROGRAM DFV 74/835 OPT=1 FTN 4.8+552

```
      PROGRAM  DFV (INPUT,OUTPUT)
      DIMENSION PLUM(9,36)
      COMMON  EHE(9,36),DELTAS(9)
      COMMON W1,W2,W3,D,DSS,DIS,PDS,HP,H1,H2,H3,Y,HH,W,OH,ZLZ
     EQUIVALENCE (EHE(1,1),PLUM(1,1))
C     ************************************************************
C
C
C     THIS PROGRAM CALCULATES DAYLIGHT LEVELS AT A GIVEN REFERENCE
C     POINT INSIDE THE ROOM.IT IS A TIME DEPENDENT VERSION OF THE
C     CIE DAYLIGHT FACTOR METHOD.THE LUMINANCE DISTRIBUTION OF
C     THE CLEAR SKY THAT WAS DEVELOPED BY KITTLER IS UTILIZED.
C
C     THE GIVEN DATA ARE AS FOLLOWS:
C
C      OH=HEIGHT OF OBSTRUCTION
C      BH=HEIGHT OF BUILDING
C      DIS=DISTANCE OF OBST. SURF. FROM BUILDING
C      OBREF=OBSTRUCTION REFLECTANCE
C      BREF=BUILDING REFLECTANCE
C      GREF=GROUND REFLECTANCE
C      W1=WINDOW R.S.EDGE TO R.S.WALL DISTANCE
C      W2=WINDOW WIDTH
C      W3=WINDOW L.S.EDGE TO L.S.WALL DISTANCE
C      DSS=DISTANCE OF REF POINT FROM WINDOW
C      PDS=DISTANCE OF THE REF.POINT FROM R.S.WALL
C      HP=REF.POINT HEIGHT ABOVE FLOOR
C      H1=DISTANCE BETWEEN WINDOW HEAD AND CEILING
C     H2=WINDOW HEIGHT
C     H3=DISTANCE BETWEEN WINDOW SILL AND FLOOR
C     AT=LATITUDE ANGLE(INITIAL VALUE)
C     Y =EXTERNAL WALL THICKNESS
C     WA=AREA OF EXTERNAL WALL
C     HII=GLAZING % INCREMENT REQUIRED
C     GLASST=AVERAGE TRANSMISSION OF GLASS
C     LWAZ=INCREMENT REQUIRED FOR WINDOW AZIMUTH ANGLE
C     AVREF=AVERAGE REFLECTANCE OF INTERIOR SURFACES
C     NBU=NUMBER OF VARIOUS LATITUDES TO BE EXAMINED
C     NBS=NUMBER OF HOURS NEED TO BE EXAMINED PER HALF DAY
C     N =DAY OF YEAR TO BE EXAMINED
C     LL2=MAXIMUM GLAZING % TO BE EXAMINED
C     ATMAX=LATITUDE ANGLE INCREMENT
C     HH=ROOM HEIGHT
C     D =ROOM DEPTH
C     W =ROOM WIDTH
C     OB=OBSTRUCTION ANGLE
C     DEC=DECLINATION ANGLE
C     AZS=SUN AZIMUTH ANGLE
C     V=INCREMENT IN THE ALTITUDE ANGLE(SKY RINGS)
C     U=INCREMENT IN THE AZIMUTH ANGLE(SKY ELEMENTS)
C     VX=ALTITUDE ANGLE FOR THE CENTER OF THE SKY RING
C     UX=AZIMUTH ANGLE FOR THE SKY RING CENTER
C     ZENP=ZENITH-ELEMENT ANGULAR DISTANCE
C     ALTP=ALTITUDE ANGLE OF A CENTER POINT OF AN ELEMENT
C     AZP=AZIMUTH ANGLE OF A CENTER POINT OF AN ELEMENT
C     COSAM=COSINE OF THE ANGULAR DISTANCE BETWEEN THE ELEMENT
C           AND THE SUN.
```

```
      C     POINTSN=ANGULAR DISTANCE BETWEENTHE ELEMENT AND THE SUN
      C     EQU=COEFFICINT(ALPHA)OF THE SKY ELEMENT
      C     PLUM=LUMINANCE OF THE SKY ELEMENT AS A RATIO OF ZENITH LUMIN.
      C     DELATS(I)=AREA OF ELEMENT IN THE I TH. RING
      C     EH=ILLUMINATION ON HORIZONTAL UNOBSTRUCTED PLANE
      C     ZLZ=LUMINANCE OF THE ZENITH
      C     EAST=ILLUMINATION ON EAST VERTICAL SURFACE
      C     WEST=ILLUMINATION ON WEST VERTICAL SURFACE
      C     HNORTH=ILLUMINATION ON NORTH VERTICAL SURFACE
      C     SOUTH=ILLUMINATION ON SOUTH VERTICAL SURFACE
      C     WAZ=WINDOW AZIMUTH ANGLE
      C     LWAZ=WINDOW AZIMUTH INCREMENT
      C     EHP=SKY ILLUMINATION AT THE REFERNCE POINT
      C     SKYFACT=SKY FACTOR
      C     OBL1=DIRECT ILUMINATION ON OBSTRUCTION(BEAM+DIFFUSE)
      C     BFL1=DIRECT ILLUMINATION ON BUILDING (BEAM+DIFFUSE)
      C     GLUM1=DIRECT ILLUMINATION ON GROUND (BEAM+DIFFUSE)
      C     OBL=TOTAL ILLUMINATION ON OBSTRUCTION(REFLEC. INC.)
      C     GLUM=TOTAL ILLUMINATION ON GROUND (REFLECTION INCL.)
      C     ECIE=LUMINANCE DUE TO SKY AND EXTERNALLY REFLECTED LIGHT
      C          AT A REFERENCE POINT OF INTERNAL SURFACE
      C     CIEL=CEILING LUMINANCE
      C     RSWL=LUMINANCE OF RIGHT SIDE WALL
      C     RLSWL=LUMINANCE OF LEFT SIDE WALL
      C     BWL=LUMINANCE OF BACK WALL
      C     EREF=REFLECTED ILLUMINATION AT THE ROOM REF. POINT
      C     TOTE=TOTAL ILLUMINATION AT THE ROOM REF. POINT
      C     DF=VARIABLE DAYLIGHT FACTOR
      C     ************************************************************
      C
      C     INPUT DATA
      C
            READ*,IK
            DO 176 IJK=1,IK
            READ*,OH,BH,DIS,OBREF,BREF,GREF
            READ*,W1,W2,W3,D,DSS,PDS
            READ*,HP,H1,H2,H3,AT,ROO
            READ*,Y,WA,HII,GLASST,LWAZ,AVREF
            READ*,NBU,NBS,N,LL2,ATMAX
            HH=H1+H2+H3
            W=W1+W2+W3
            PI=3.1415927
            CONVERT=PI/180.
            INCONV=180./PI
      C
      C     DETERMINATION OF THE VIEW FACTORS,LATITUDES,DECLINATION
      C     ANGLE,POSITION OF THE SUN,ANDTHE ALPHA COEFFICIENT FOR
      C     EACH SKY ELEMENT.
      C
            CALL RATIO(RAB,RAR,RAL,RAC,RABW)
            DO 44 NB=1,NBU
            ATMAX=AT+ATMAX
            PRINT19,ATMAX
         19 FORMAT(5X,*LATITUDE ANGLE =*,F10.5)
            ATITUDE=(ATMAX)*CONVERT
            CALL DECLIN(N,DECL)
            DEC=DECL*CONVERT
```

```
PROGRAM DFV        74/835  OPT=1                    FTN 4.8+552

      115               CALL COEF(N,AM,ASC)
                        AZSOLD=0.0
                        DO 3 NF=1,NBS
                        HU= (NF*15.0)-15.0
                        HOUR=HU*CONVERT
      120               VSUN=COS(ATITUDE)*COS(DEC)*COS(HOUR)
                      A +(SIN(ATITUDE)*SIN(DEC))
                        ALTSUN=ASIN(VSUN)
                        USUN=(COS(DEC)*SIN(HOUR))/COS(ALTSUN)
                        AZSUN=ASIN(USUN)
      125               ALTS=ALTSUN*(INCONV)
                        AZS=AZSUN*(180./PI)
                        IF(AZS.GE.AZSOLD)GOTO 873
                        AZS=(90.-AZS)+90.
                  873   PRINT 10,ALTS
      130               PRINT 11,AZS
                        AZSOLD=AZS
                        ZLZ=(55.943*ALTS)+164
                  10    FORMAT(2X,*SUN ALTITUDE ANGLE =*,F10.5,* DEGREES*)
                  11    FORMAT(2X,*SUN AZIMUTH ANGLE  =*,F10.5,* DEGREES*)
      135               ZENSUN  =((PI/2.0)-ALTSUN)*R00
                        EEH=0.0
                        V=0.0
                        DO 150 KLM=1,2
                        IF(KLM.EQ.2)GOTO 155
      140               KK=1
                        KKK=1
                        GOTO 156
                  155   KK=9
                        KKK=36
      145         156   DO 100 I=KK,9
                        V=V+10.0
                        U=0.0
                        DO 100 J=KKK,36
                        U=U+10.
      150               IF(KLM.EQ.2) GOTO 157
                        VX=V-5.0
                        UX=U-5.0
                        GOTO 158
                  157   VX=V
      155               UX=U
                  158   ALTP=((VX)/360.0)*2.0*PI
                        AZP=((UX)/360.0)*2.0*PI
                        ZENP   =((PI/2.0)-ALTP)
                        ALPHA=(AZP-AZSUN)
      160               COGAM=(COS(ZENSUN)*COS(ZENP))+(SIN(ZENSUN)*SIN(ZENP)*COS(ALPHA))
                        POINTSN=ACOS(COGAM)
                        AA=1.0/COS(ZENP)
                        A=  EXP(-.32*AA)
                        B= 10.0*EXP(-3.0*POINTSN)
      165               BB=.45*(COS(POINTSN)**2.0)
                        BBC= (10.0*(EXP( -3.0*ZENSUN)))
                        CC=.45*(COS(ZENSUN)**2.0)
                        EQU=((1.0-A)*(0.91+B+BB))/(.27385*(.91+BBC+CC))
                        IF(KLM.EQ.2)GOTO 159
      170               PLUM(I,J)=EQU
                        GOTO 100
```

PROGRAM DFV 74/835 OPT=1 FTN 4.8+552

```
                  159   ZLUM=EQU
                  100   CONTINUE
                  150   CONTINUE
      175               IF(LU.EQ.0)GOTO 103
                        DO 83 J=1,36
                        PRINT 92,(J,(PLUM(I,J),I=1,9))
                  83    CONTINUE
                  103   PLUMEN=0.0
      180               DO 80 J=1,36
                        PLUMEN =PLUM(9,J)+PLUMEN
                  80    CONTINUE
                        LUM=PLUMEN / 36.0
                        TM=0.0
      185         C
                  C     DETERMINATION OF SKY ELEMENTS AREAS
                  C
                        DO 90 I=1,9
                        TM=TM+10.0
      190               B1=ROO*COS(TM*(PI/180.0))
                        B2=ROO*COS((PI/180.0)*(TM-10))
                        SQ1=SQRT((ROO**2.0)-(B1**2.0))
                        AREA1=2.0*PI*ROO*(ROO-SQ1)
                        SQ2=SQRT((ROO**2.0)-(B2**2.0))
      195               AREA2=2.0*PI*ROO*(ROO-SQ2)
                        ARDIF=AREA2-AREA1
                        DELTAS(I)=ARDIF/36.0

                  90    CONTINUE
      200         C
                  C     DETERMINATION OF SKY ILLUMINATION ON VERTICAL
                  C     SURFACES FACING SOUTH,NORTH,EAST,AND WEST.
                  C
                        HNOR=0.0
      205               HNT=0.0
                        EAST=0.0
                        WEST=0.0
                        HNORTH=0.0
                        DO 200 J=1,36
      210               DO 201 I=1,9
                        DPLUM=PLUM(I,J)
                        CALL AREA( I,J,DPLUM )
                        SIR=(I*10.0)-5.0
                        EEH=EEH+EHE(I,J)*(SIN(SIR*(PI/180.)))
      215         201   CONTINUE
                        EH=EEH*ZLZ
                        IF(LU.EQ.0)GOTO 200
                        PRINT 92,(J,(EHE(I,J),I=1,9))
                  92    FORMAT(2X,I2,2X,9(F7.4,3X))
      220         200   CONTINUE
                        IF(LU.EQ.0)GOTO 280
                  999   DO 210 I=1,9
                        TIR=(I*10.0)-5.0
                        TRR=COS(TIR*(PI/180.))
      225               DO 202 J=1,18
                        Z1=(.5*PI)-((J*10.-5.)*(PI/180.))
                        EAST=EAST+EHE(I,J)*TRR*COS(Z1)
                  202   CONTINUE
```

PROGRAM DFV 74/835 OPT=1 FTN 4.8+552

```
                DO 203 J=19,36
230             Z2=(1.5*PI)-((J*10.-5.)*(PI/180.))
                WEST=WEST+EHE(I,J)*TRR*COS(Z2)
          203   CONTINUE
                DO 204 J=10,27
                Z3=(PI)-((J*10.-5.)*(PI/180.))
235             HNORTH=HNORTH+EHE(I,J)*TRR*COS(Z3)
          204   CONTINUE
                DO 220 J=1,9
                HNOR=HNOR+EHE(I,J)*TRR*(COS((J*10.-5.)*(PI/180.)))
          220   CONTINUE
240             DO 222 J=28,36
                HNT=HNT+EHE(I,J)*TRR*(COS((J*10.-5.)*(PI/180.)))
          222   CONTINUE
          210   CONTINUE
                SOUTH=HNOR+HNT
245             PRINT 205,HU,EAST
                PRINT 206,HU,WEST
                PRINT 207,HU,HNORTH
                PRINT 208,HU,SOUTH
          205   FORMAT(/,2X,*HOUR ANGLE =*,F7.2,2X,*EASTERN HEM. ILL.=*,F20.10)
250       206   FORMAT(/,2X,*HOUR ANGLE =*,F7.2,2X,*WESTERN HEM. ILL.=*,F20.10)
          207   FORMAT(/,2X,*HOUR ANGLE =*,F7.2,2X,*NORTHERN H.  ILL.=*,F20.10)
          208   FORMAT(/,2X,*HOUR ANGLE =*,F7.2,2X,*SOUTHERN H.  ILL.=*,F20.10)
          280   PRINT 125,EH
          125   FORMAT(///,5X,*ILLUMINATION ON HORIZONTAL PLANE=*,F20.8)
255       130   FORMAT(/,5X,*(*,I2,*,*,I2,*)*,10X,*COS(ZENP=0.0)*)
          127   FORMAT(2X,110(1H*))
          126    FORMAT(2X,*WAZ*,2X,1H*,*SKYFACT*,1H*,3X,*EHP*,2X,1H*,
                Q 3X,*DHOR*,3X,1H*,2X,*EHG*,2X,1H*,4X,*DBF*,3X,1H*,2X,
                Q *EHB*,2X,1H*,4X,*DOB*,3X,1H*,7X,*EHO*,2X,1H*,4X,*OBL*,5X
260             Q ,1H*,4X,*GLUM*,4X,1H*)
                DO 410 L=1,LL2
                PRINT 127
                PRINT 126
                PRINT 127
265             HI=L*HII
          C     DETERMINATION OFTHE WINDOW DIMENSIONS
                CALL WINDOW(WA,HI,HH,W,H1,H2,H3,W1,W2,W3)
                KPP=3
                WAZ=0.0
270             KWAZ=360/LWAZ
                IF(OH.EQ.0.0)GOTO 13
                OB=ATAN((OH-HP)/(DIS+DSS+YY)*(180./PI)
                GOTO 14
          13    OB=0.0
275       14    F=ATAN(((H2+H3)-HP)/(Y+DSS))*(180./PI)
                DO 400 K=1,KWAZ
                WAZ=WAZ+LWAZ
                IF(F.GT.OB) GOTO 393
          C
280       C     DETERMINATION OF THE SKY ILLUMINATION AND THE SKY FACTOR
          C     AT THE REFERENCE POINT
          C
                EHP=0.00
                SKYFACT=0.00
285       C
```

PROGRAM DFV 74/835 OPT=1 FTN 4.8+552

```
      C     CALCULATION OF DIRECT BEAM ILLUMINATION.
      C
            GOTO 394
      393   CALL CONFIG(KPP, WAZ, EHP)
      290   SKYFACT=(EHP/EH)*100.
      394   CALL DIRECT(AM,ASC,DEC,HOUR,WAZ,AZSUN,ALTS,ATITUDE,
     Q OH,H3,DIS,BWL,DHOR,DBF,DOB)
      C
      C     CALCULATION OF THE LUMINANCE OF THE EXTERNAL SURFACES
      295   C
            CALL LUMIN(WAZ,ZLZ,OH,DIS,BH,EHO,EHB,EHG,C,B,OBS,OBB)
            OBL1=(EHO+DOB)*OBREF
            BFL1=(EHB+DBF)*BREF
            GLUM1=(EHG+DHOR)*GREF
      300   TOB=(EHO+DOB)+((C/180.)*GLUM1*COS(.5*OBS*(PI/180.)))
     Q +((B/180.)*BFL1)
            THOR=(EHG+DHOR)+((OBS/180.)*OBL1*SIN(.5*OBS*(PI/180.)))
     Q +((OBB/180.)*BFL1*SIN(.5*OBB*(PI/180.)))
            OBL=TOB*OBREF
      305   GLUM=THOR*GREF
      C
      C     CALCULATION OF THE LUMINANCE OF INTERNAL SURFACES,THE REF-
      C     LECTED COMPONENT,THE TOTAL ILLUMINATION,AND THE DAYLIGHT
      C     FACTOR.
      310   C
            DO 408 ISURFAC=1,4
            CALL WALL(ISURFAC,WAZ,SKY,OBF,GROF)
            ECIE=((OBF*OBL*GLASST)+(GROF*GLUM*GLASST)+(SKY*GLASST)
     Q )*AVREF
      315   IF(ISURFAC.EQ.1)GOTO 501
            IF(ISURFAC.EQ.2)GOTO 502
            IF(ISURFAC.EQ.3)GOTO 503
            CIEL=ECIE
            GOTO 408
      320   501   RSWL=ECIE
            GOTO 408
            502   RLSWL=ECIE
            GOTO408
            503   BWL=ECIE
      325   408   CONTINUE
            IF(LU.EQ.0)GOTO 120
            PRINT 506,CIEL,RSWL,RLSWL,BWL
            506   FORMAT(2X,4(F10.2,2X))
            120   PRINT 122,WAZ,SKYFACT,EHP,DHOR,EHG,DBF,EHB,DOB,EHO,OBL,GLUM
      330   122   FORMAT(2X,F5.1,1H*,F7.2,1H*,F8.2,1H*,F10.2,1H*,F7.2,1H*,F10.2
     Q ,1H*,F8.2,1H*,F9.2,1H*,F12.2,1H*,F12.2,1H*,F12.2,1H*)
            EREF=(CIEL*RAC)+(RSWL*RAR)+(RLSWL*RAL)
     Q +(BWL*RABW)+(OBL*RAB*GLASST)
            TOTE=EREF+(EHP*GLASST)
      335   DF=(TOTE/EH)*100.
            PRINT 409,CIEL,RSWL,RLSWL,BWL,EREF,TOTE,DF
            409   FORMAT(2X,7(F8.2,2X),/)
            400   CONTINUE
            410   CONTINUE
      340   3     CONTINUE
            PRINT 127
            44    CONTINUE
```

PROGRAM DFV 74/835 OPT=1 FTN 4.8+552

```
      176   CONTINUE
            STOP
345         END
```

```
SUBROUTINE AREA      74/835  OPT=1                          FTN 4.8+552

1                    SUBROUTINE AREA(I,J,DPLUM )
                     COMMON  EHE(9,36),DELTAS(9)
                C    THIS SUBROUTINE CALCULATES ILLUMINATION DUE TO EACH SKY
                C    ELEMENT.
5                    PI=3.14159265927
                     EHE(I,J)=(DPLUM* DELTAS(I))
                     RETURN
                     END
```

SUBROUTINE DECLIN 74/835 OPT=1 FTN 4.8+552

```
1               SUBROUTINE DECLIN(N,DECL)
          C     THIS SUBROUTINE CALCULATES THE DECLINATION ANGLE OF THE
          C     SUN FOR, A GIVIN DAY N.
                PI=3.1415927
5               C=SIN(2.*PI*(284+N)/365.0)
                DECL=23.45*C
                PRINT 63,N
          63    FORMAT(/,2X,*DAY OF THE YEAR =*,I3)
                PRINT 61,DECL
10        61    FORMAT(/,2X,*ANGLE OF DECLINATION =*,F20.10)
                RETURN
                END
```

```
SUBROUTINE CONFIG     74/835  OPT=1                    FTN 4.8+552

      SUBROUTINE CONFIG(KPP,  WAZ ,EHP)
      COMMON EHE(9,36),DELTAS(9)
      COMMON W1,W2,W3,D,DSS,DIS,PDS,HP,H1,H2,H3,Y,HH,W,OH,ZLZ
C     THIS SUBROUTINE CALCULATES THE THE ILLUMINATION AT THE
C     REFERENCE POINT(EHP) DUE TO SKY PATCH VISIBLE THROUGH
C     THE WINDOW CONFIGURATION.KPP IS THE RELEVANT POSITION OF
C     POINT WITH RESPECT TO THE WINDOW ,AND WAZ IS THE AZIMUTH
C     ANGLE OF THE WINDOW.
C
C
C     ANGA=WINDOW HORIZONTAL ANGLE
C     ANGE=WINDOW VERTICAL ANGLE
C     VW1=VERTICAL ANGLE OF THE LOWEST VISIBLE SKY RING ABOVE
C         OBSTRUCTION
C     VW2=VERTICAL ANGLE OF THE HIGHEST VISIBLE SKY RING BELOW
C         THE WINDOW HEAD.
C     UW1=THE AZIMUTH ANGLE OF THE VISIBLE ELEMENTS AT THE
C        EXTREME RIGHT SIDE OF THE WINDOW
C     UW2=THE AZIMUTH ANGLE OF THE VISIBLE ELEMENTS AT THE
C       EXTREME LEFT SIDE OF THE WINDOW
C      B =OBSTRUCTION ANGLE
C      F =WINDOW VERTICAL ANGLE
C
C
      S=W1+W2
      G=Y
      DS=DSS
      PI=3.1415927
C     CALCULATION OF WINDOW VERTICAL ANGLES VW1,VW2
      IF(OH.EQ.0.0)GOTO 17
      OB=ATAN((OH-HP)/(DIS+DS+Y))*(180./PI)
      GOTO 16
   17 OB=0.0
   16 F=ATAN(((H2+H3)-HP)/(G+DS))*(180./PI)
      IF(F.LE.OB)GOTO 100
      ANGE=F-OB
      VW1=OB
      VW2=VW1+ANGE
      IF(KPP.EQ.1) GO TO 35
      IF(KPP.EQ.2) GO TO 35
      IF(KPP.EQ.3) GO TO 45
   35 BA=ATAN((Y/DS)/S)*(180./PI)
      CA=ATAN(W1/DS)*(180./PI)
      ANGA=(90.)-BA-CA
      GOTO 60
   45 BA=ATAN((Y+DS)/(.5*W2))*(180./PI)
      ANGA=2.*((90.)-BA)
   60 IF(KPP.EQ.2) GOTO 61
      UW1=270.+WAZ+BA
      GOTO 62
   61 UW1=270.+WAZ-BA
   62 UW2=UW1+ANGA
      IVW1=VW1
      IF(IVW1.EQ.0)GO TO 6
      II=IVW1
      GOTO 8
    6 II=1
```

SUBROUTINE CONFIG 74/835 OPT=1 FTN 4.8+552

```
      8     IVW2=VW2
            JUW1=UW1
60          JUW2=UW2
            EEHP=0.0
            KJ=(JUW2-JUW1)
      C     CALCULATION OF TOTAL SKY ILLUMINATION
      C     RECEIVED AT THE REFERENCE POINT
65          DO 80 I=II,IVW2
            IM=(I/10)+1
            DO 80 J=1,KJ
            JJJ=JUW1+J
            IF(JJJ.LT.360)GOTO 20
70          IF(JJJ.GE.360.AND.JJJ.LT.720)GOTO 23
            IF(JJJ.EQ.720)GOTO 24
            JX=((JJJ-720)/10)+1
            GO TO 22
      23    JX=((JJJ-360)/10)+1
75          GOTO 22
      24    JX=(JJJ-360)/10
            GOTO 22
      20    JX=(JJJ/10)+1
      22    EEHP=EEHP+(EHE(IM,JX)*(SIN((IM*10.-5.)*(PI/180.)))/100.)
80    80    CONTINUE
            EHP=EEHP*ZLZ
            GOTO 101
      100   EHP=0.0
      101   RETURN
85          END
```

```
SUBROUTINE DIRECT     74/835  OPT=1                    RTN 4.8+552

      1               SUBROUTINE DIRECT(AM,ASC,DEC,HOUR,WAZ,AZSUN,ALTS,ATITUDE,
                     Q OH,H3,DIS,BH,DHOR,DBF,DOB)
                C      THIS SUBROUTINE CALCULATES THE DIRECT ILLUMINATION ON THE
                C      GROUND(DHOR),ON THE BUILDING SURFACE(DBF),AND ON THE
      5         C      OBSTRUCTION(DOB).
                C
                C
                C      EXRAD=EXTRA TERRESTRIAL RADIATION
                C      TH=COSINE OF THE INCIDENT ANGLE OF BEAM RADIATION
     10         C      S=TILT ANGLE OF THE SURFACE
                C      CANN=SUN-WINDOW AZIMUTH ANGLE DIFFERENCE
                C      TERAD=TERRESTRIAL RADIATION
                C      DIERC=DIRECT BEAM ILLUMINATION ON THE SURFACE
                C      DHOR=DIRECT BEAM ILLUMINATION ON THE GROUND
     15         C      DBF=DIRECT BEAM ILLUMINATION ON BUILDING
                C      DOB=DIRECT BEAM ILLUMINATION ON OBSTRUCTION
                C
                C
                       PI=3.1415927
     20                S=(PI/2.)
                       EXRAD=1353.*(1.+(.035*COS(2.*PI*(N-4)/366)))
                       DO 40 I=1,3
                       IF(I.EQ.1)GOTO 10
                       IF(I.EQ.2)GOTO 15
     25                TH=SIN(ALTS*(PI/180.))
                       S=0.0
                       GAM=WAZ*(PI/180.)
                       GOTO 20
                10     GAM=WAZ*(PI/180.)
     30                GOTO 20
                15     GGAM=(WAZ+180.)
                       IF(GGAM.GT.360) GOTO 22
                       GAM=GGAM*(PI/180.)
                       GOTO 20
     35          22    GAM=(GGAM-360.)*(PI/180.)
                 20    TH=(SIN(DEC)*SIN(ATITUDE)*COS(S))
                     Q -(SIN(DEC)*COS(ATITUDE)*SIN(S)*COS(GAM))
                     Q +(COS(DEC)*COS(ATITUDE)*COS(S)*COS(HOUR))
                     Q +(COS(DEC)*SIN(ATITUDE)*SIN(S)*COS(GAM)*COS(HOUR))
     40              Q +(COS(DEC)*SIN(S)*SIN(GAM)*SIN(HOUR))
                       CAN=((AZSUN-GAM)*(180./PI))**2.
                       CANN=SQRT(CAN)
                       THET=ACOS(TH)
                       IF(CANN.EQ.360.) GOTO 2
     45                CAD=360.-CANN
                       GOTO 3
                 2     CAD=0.0
                 3     IF(CANN.LE.CAD) GOTO26
                      ZDIFF=CAD
     50                GOTO 27
                26     ZDIFF=CANN
                27     IF(ZDIFF.GE.90.AND.I.NE.3)GOTO 30
                       AE=EXP(AM/(SIN(ALTS*(PI/180.))))
                       TERAD=ASC/AE
     55          C
                       DIREC=SQRT(((TERAD*TH*100.)**2.))
                       GOTO 32
```

```
SUBROUTINE DIRECT     74/835  OPT=1                    FTN 4.8+552

            30      DIREC =0.0
            32      IF(I.EQ.1) GOTO 41
60                  IF(I.EQ.2) GOTO 42
                    DHOR=DIREC
                    GOTO 40
            41     BANG=ATAN((.5*OH)/DIS)*(180./PI)
                    IF(ALTS.LT.BANG)GOTO 48
65                  DBF=DIREC
                    GOTO 40
            48      DBF=0.0
                    GOTO 40
            42       BANG=ATAN((.5*BH)/DIS)*(180./PI)
70                  IF(ALTS.LT.BANG)GOTO 49
                    DOB=DIREC
                    GOTO 40
            49      DOB=0.0
                    GOTO 40
75          40      CONTINUE
                    RETURN
                    END
```

```
SUBROUTINE LUMIN      74/835  OPT=1                    FTN 4.8+552

      1               SUBROUTINE LUMIN(WAZ,ZLZ,OH,DIS,BH,EHO,EHB,EHG,C,B,OBS,OBB)
                      COMMON EHE(9,36)
                C     THIS SUBROUTINE CALCULATES OBSTRUCTION AND GROUND LUMINANCES
                C     EHO IS THE LUMINANCE OF OBSTRUCTION DUE TO SKY;EHB IS THE
      5         C     LUMINANCE OF BUILDING DUE TO SKY;AND EHG IS THE LUMINANCE
                C     OF THE GROUND DUE TO SKY.
                C     OBS IS THE VERTICAL ANGLE OF OBSTRUCTION FROM A REFERENCE
                C     POINT ON THE GROUND. OBB IS THE VERTICAL ANGLE OF THE
                C     BUILDING FROM THE SAME REF. POINT ON GROUND.
     10         C
                C     WAZ=WINDOW AZIMUTH ANGLE
                C     ZLZ=ZENITH LUMINANCE
                C     OH=OBSTRUCTION HEIGHT
                C     DIS=DISTANCE BETWEEN OBSTRUCTION AND BUILDING
     15         C     BH=BUILDING HEIGHT
                C
                C     OAZ=AZIMUTH ANGLE OF OBSTRUCTION
                C     JOZ=AZIMUTH OF THE ELEMENTS ON THE EXTREME RIGHT SIDE OF
                C          THE OBSTRUCTION.
     20         C     IS=FIRST RING OF ELEMENTS ABOVE BUILDING AS VIEWED FROM
                C        OBSTRUCTION.
                C     SKB=AZIMUTH OF THE ELEMENTS ON THE EXTREME RIGHT SIDE OF
                C          THE BUILDING.
                C     ISK=FIRST RING OF ELEMENTS ABOVE OFSTRUCTION AS VIEWED
     25         C        FROM BUILDING.
                      PI=3.1415927
                      DEG=180./PI
                C
                C     CALCULATION OF ANGLE C FACING GROUND,B FACING BUILDING AND A
     30         C     FACING SKY(AT OBSTRUCTION MID HEIGHT).
                C
                      C=ATAN(DIS/(.5*OH))*DEG
                      B1=(90.-C)
                      B2=ATAN((BH-(.5*OH))/DIS)*DEG
     35               B=B1+B2
                      A=(90-B2)
                C
                C     CALCULATION
                C     OF OBSTRUCTION LUMINANCE DUE TO SKY( EHO )
     40         C
                      EEHO=0.0
                      OAZ=WAZ+180.
                      JOZ=(OAZ-90)/10
                      IS=B2/10
     45               DO 202 IA=IS,9
                      DO 202 J=1,18
                      JNZ=JOZ+J
                      IF(JNZ.GT.36) GOTO 201
                      GOTO 199
     50         201   JNZ= JNZ-36
                199   TIR=(IA*10.)-5.
                      TRR=COS(TIR*(PI/180.))
                      TRS=COS((OAZ-(JNZ*10.-5.))*(PI/180.))
                      EEHO=EEHO+(EHE(IA,JNZ)*TRR*TRS)
     55         202   CONTINUE
                      EHO=EEHO*ZLZ
                C
```

```
      SUBROUTINE LUMIN     74/835  OPT=1                    FTN 4.8+552

                C     CALCULATION OF BUILDING FACADE LUMINANCE DUE TO SKY(EHB)
                C
           60         EEHB=0.0
                      JWAZ=(270+WAZ)/10
                      SKB=ATAN((OH-(.5*BH))/DIS)*DEG
                      ISK=SKB/10
                      IF(ISK.GT.0)GOTO 207
           65         ISK=1
                207   DO 203 IE=ISK,9
                      DO 203 J=1,18
                      JW=JWAZ+J
                      IF(JW.GT.36.AND.JW.LT.72)GOTO 204
           70         IF(JW.EQ.72)GOTO 209
                      IF(JW.GT.72)GOTO 213
                      JWJ=JW
                      GOTO 205
                204   JWJ= JW-36
           75         GOTO 205
                209   JWJ= JW-36
                      GOTO 205
                213   JWJ= JW-72
                205   TIR=(IE*10.)-5.
           80         TRR=COS(TIR*(PI/180.))
                      WAZD=(((JW*10.)-5.)-JWAZ*10.)
                      IF(WAZD.GT.90.)GOTO 258
                      WAZDIF=90.-WAZD
                      GOTO 259
           85   258   WAZDIF=180.-WAZD
                259   TRS=COS(WAZDIF*(PI/180.))
                      EEHB=EEHB+(EHE(IE,JWJ)*TRR*TRS)
                203   CONTINUE
                      EHB=EEHB*ZLZ
           90   C
                C     CALCULATION OF GROUND LUMINANCE DUE TO SKY( EHG )
                C
                      OBS=ATAN(OH/(.5*DIS))*DEG
                      OBB=ATAN(BH/(.5*DIS))*DEG
           95         IF(WAZ.GE.270) GOTO333
                      NM=(90+WAZ)/10
                      GOTO 323
                333   NM=((90+WAZ)-360)/10
                323   IF(WAZ.GT.90.)GOTO 313
          100         IF(WAZ.EQ.90.) GO TO 314
                      KM=(270+WAZ)/10
                      GOTO 303
                313   KM=(270+WAZ-360)/10
                      GOTO 303
          105   314   KM=1
                303   EEHG1=0.0
                      EEHG2=0.0
                      IOBS=OBB/10
                C
          110   C     CALCULATION OF ILLUMINATION ON GROUND FROM ONE HALF OF THE
                C     SKY.
                C
                      DO 979 IY=IOBS,9
                      DO 979 J=1,18
```

```
      SUBROUTINE LUMIN      74/835  OPT=1                    FTN 4.8+552

115                   NMN=NM+J
                      IF(NMN.LT.36)GOTO 343
                      IF(NMN.EQ.36) GOTO 344
                      JZ= NMN-36
                      GOTO 353
120             344   JZ= NMN
                      GOTO 353
                343   JZ= NMN
                353   SIR=SIN(((IY*10.)-5.)*(PI/180.))
                      EEHG1=EEHG1+(EHE(IY,JZ)*SIR)
125             979   CONTINUE
                      IOBR=OBS/10
                C
                C     CALCULATION OF ILLUMINATION ON THE GROUND FROM THE OTHER
                C     HALF OF THE SKY.
130             C
                      DO 879 IC=IOBR,9
                      DO 879 J=1,18
                      KMN=KM+18-J
                      IF(KMN.LT.36)GOTO 363
135                   IF(KMN.EQ.36)GOTO364
                      JZ= KMN-36
                      GOTO 373
                364   JZ=KMN
                      GOTO 373
140             363   JZ=KMN
                373   SIR=SIN(((IC*10.)-5.)*(PI/180.))
                      EEHG2=EEHG2+ (EHE(IC,JZ)*SIR)
                879   CONTINUE
                      EEHG=EEHG1+EEHG2
145                   EHG=EEHG*ZLZ
                      RETURN
                      END
```

```
SUBROUTINE WALL      74/835  OPT=1                    FTN 4.8+552

      1               SUBROUTINE WALL(ISURFAC, WAZ,SKY,OBF,GROF)
                      COMMON EHE(9,36),DELTAS(9)
                      COMMON W1,W2,W3,D,DSS,DIS,PDS,HP,H1,H2,H3,Y,HH,W,OH,ZLZ
                      PI=3.1415927
      5               DEG=180./PI
                C
                C     CALCULATION OF HORIZONTAL ANGLES SUBTENDED FROM REF.POINT
                C     ON A GIVIN SURFACE (UW1 AND UW2)
                C
     10               IF(ISURFAC.EQ.1) GOTO 5
                      IF(ISURFAC.EQ.2)GOTO 6
                      IF(ISURFAC.EQ.3)GOTO 7
                      IF(ISURFAC.EQ.4)GOTO 7
                C
     15         C     HORIZONTAL ANGLES FOR RIGHT SIDE WALL
                C
                5     WAZZ=WAZ+90.
                      DS=.5*D
                      DSY=DS+Y
     20               HPS=H3+((HH-H3)*.5)
                      PDS=0.0
                      HTR=ATAN((W2+W3)/DSY)
                      AR=ATAN(W1/DSY)
                      HRL=HTR-AR
     25               BRL=AR+(.5*HRL)
                      UW1=(WAZ+((AR)*DEG))
                      UW2=WAZ+(HTR*DEG)
                      GOTO 25
                C
     30         C     HORIZONTAL ANGLES FOR LEFT SIDE WALL
                C
                6     DS=.5*D
                      DSY=DS+Y
                      HPS=H3+(.5*(HH-H3))
     35               PDS=W

                      IF(WAZ.LE.90.)GOTO 18
                      WAZZ=WAZ-90.
                      GOTO 19
     40         18    WAZZ=(360.+WAZ)-90.
                19    HTL=ATAN((W2+W1)/DSY)
                      AL=ATAN(W3/DSY)
                      HRL=HTL-AL
                      BRL=AL+(.5*HRL)
     45               IF(WAZ.LE.90.)GOTO 17
                      UW1=WAZ-(HTL*DEG)
                      UW2=WAZ-(AL*DEG)
                      GOTO 25
                17    UW1=WAZ+360.-(HTL*DEG)
     50               UW2=WAZ+360.-(AL*DEG)
                      GOTO 25
                7     WAZZ=WAZ
                C
                C     HORIZONTAL ANGLES FOR BACK WALL
     55         C
                      IF(ISURFAC.EQ.4) GOTO 42
                      DS=D
```

```
      SUBROUTINE WALL      74/835  OPT=1                    FTN 4.8+552

                           DSY=DS+Y
                           HPS=H3+(.5*(HH-H3))
     60                    PDS=.5*W
                           GOTO 43
                     C
                     C     HORIZONTAL ANGLES FOR CEILING
                     C
     65              42    DS=.5*D
                           DSY=DS+Y
                           HPS=HH
                           PDS=.5*W
                     43    WW=W2+W3
     70                    IF(PDS.GT.W3.AND.PDS.LT.WW) GOTO 80
                           IF(PDS.GE.WW) GOTO 70
                           HTB=ATAN((WW-PDS)/DSY)
                           AB=ATAN((W3-PDS)/DSY)
                           HRL=HTB-AB
     75                    BRL=AB+(.5*HRL)
                           UW1=WAZ+((AB)*DEG)
                           UW2=WAZ+(HTB*DEG)
                           GOTO 25
                     80    HTB=ATAN((WW-PDS)/DSY)
     80                    AB=ATAN((PDS-W3)/DSY)
                           HRL=HTB+AB
                           WWW=W3+(.5*W2)
                           IF(PDS.GE.WWW) GOTO 81
                           BRL=ATAN((WWW-PDS)/DSY)
     85                    GOTO 24
                     81    BRL=ATAN((PDS-WWW)/DSY)
                     24    UW1=WAZ-((AB)*DEG)
                           UW2=WAZ+(HTB*DEG)
                           GOTO 25
     90              70    HTB=ATAN((PDS-W1)/DSY)
                           AB=ATAN((PDS-(W1+W2))/DSY)
                           HRL=HTB-AB
                           BRL=AB+(.5*HRL)
                           UW1=WAZ-(HTB*DEG)
     95                    UW2=WAZ-(AB*DEG)
                     C
                     C     CALCULATION OF VERTICAL ANGLES AND VIEW FACTORS (VW1 AND VW2)
                     C
                     25    WTOPL=H3+H2
    100                    IF(HPS.LT.WTOPL) GOTO 20
                     C     FOR REF. POINT ON INTERNAL SURFACES HIGHER THAN THE
                     C     WINDOW HEAD(HPS IS GREATER THAN WTOPL).
                     C
                           H31=H3-(HH-HPS)
    105                    WOB=ATAN(H31/(DS*COS(BRL)))
                           DNOB=ATAN(HPS/((DSY+DIS)*COS(BRL)))
                           OB=DNOB-WOB
                           DNHORIZ=ATAN((H31+H2)/(DS*COS(BRL)))
                           GRO=DNHORIZ-DNOB
    110                    X1=ATAN(TAN(HRL)*COS(WOB))
                           X2=ATAN(TAN(HRL)*COS(DNOB))
                           X3=ATAN(TAN(HRL)*COS(DNHORIZ))
                           SKYF=0.0
                           OBF=(X1-(X2*COS(OB)))/(2.*PI)
```

SUBROUTINE WALL 74/835 OPT=1 FTN 4.8+552

```
      GROF=(X2-(X3*COS(GRO)))/(PI*2.)
      VW1=0.0
      VW2=0.0
      GOTO60
   20 IF(OH.NE.0.0) GOTO 40
C     IN THE CASE OF OBSTRUCTION AND HPS IS LESS THAN WTOPL
C
      SKY=ATAN((WTOPL-HPS)/(DSY*COS(BRL)))
      GRO=ATAN((HPS-H3)/(DSY*COS(BRL)))
      X1=ATAN(TAN(HRL)*COS(SKY))
      X2=ATAN(TAN(HRL)*COS(GRO))
      SKYF=(HRL-(X1*COS(SKY)))/(2.*PI)
      OBF=0.0
      GROF=(HRL-(X2*COS(GRO)))/(2.*PI)
      VW1=0.0
      VW2=SKY*DEG
      GOTO 60
   40 IF(OH.LT.HPS) GOTO 50
C
C     IN THE CASE OF OBSTRUCTION AND OBSTRUCTION HEIGHT IS
C     GREATER THAN THE HEIGHT OF REF. POINT:HPS.GT.WTOPL
C
      UPHORIZ=ATAN((WTOPL-HPS)/(DSY*COS(BRL)))
      UPOB=ATAN((OH-HPS)/((DSY+DIS)*COS(BRL)))
      SKY=(UPHORIZ-UPOB)
      DNHORIZ=ATAN((HPS-H3)/(DSY*COS(BRL)))
      DNOB=ATAN(HPS/((DSY+DIS)*COS(BRL)))
      GRO=DNHORIZ-DNOB
      OB=UPOB+DNOB
      X1=ATAN(TAN(HRL)*COS(UPHORIZ))
      X2=ATAN(TAN(HRL)*COS(UPOB))
      X3=ATAN(TAN(HRL)*COS(DNOB))
      X4=ATAN(TAN(HRL)*COS(DNHORIZ))
      IF(UPHORIZ.LE.UPOB)GOTO 39
      SKYF=(X2-(X1*COS(SKY)))/(2.*PI)
      GOTO 44
   39 SKYF=0.0
   44 UPOBF=(HRL-(X2*COS(UPOB)))/(2.*PI)
      DNOBF=(HRL-(X3*COS(DNOB)))/(2.*PI)
      OBF=UPOBF+DNOBF
      GROF=(X3-(X4*COS(GRO)))/(2.*PI)
      VW1=UPOB*DEG
      VW2=UPHORIZ*DEG
      GOTO 60
   50 SKY=ATAN((WTOPL-HPS)/(DSY*COS(BRL)))
      DNHORIZ=ATAN((HPS-H3)/(DSY*COS(BRL)))
      DNOB=ATAN(HPS/((DSY+DIS)*COS(BRL)))
      GRO1=ATAN((HPS-OH)/((DSY+DIS)*COS(BRL)))
      GRO2=DNHORIZ-DNOB
      OB=DNOB-GRO1
      GRO=GRO1+GRO2
      X1=ATAN(TAN(HRL)*COS(SKY))
      X2=ATAN(TAN(HRL)*COS(GRO1))
      X3=ATAN(TAN(HRL)*COS(DNOB))
      X4=ATAN(TAN(HRL)*COS(DNHORIZ))
      SKYF=(HRL-(X1*COS(SKY)))/(2.*PI)
      OBF=(X2-(X3*COS(OB)))/(2.*PI)
```

```
      SUBROUTINE WALL      74/835 OPT=1                    FTN 4.8+552

                  GROF1=(HRL-(X2*COS(GRO1)))/(2.*PI)
                  GROF2=(X3-(X4*COS(GRO2)))/(PI*2.)
                  GROF=GROF1+GROF2
      175         VW1=0.0
                  VW2=SKY*DEG
            60    IF(SKYF.LE.0.0) GOTO 84
            C
            C     CALCULATION OF THE SKY ILLUMINATION ON THE INTERNAL SURFACES
      180   C     OF CONCERN(EEHP) AFTER UW1,UW2,VW1,AND VW2 HAVE BEEN
            C     DETERMINED.
            C
                  IVW1=VW1
                  IF(IVW1.EQ.0)GOTO 9
      185         II=IVW1
                  GOTO 8
            9     II=1
            8     IVW2=VW2
                  JUW1=UW1
      190         JUW2=UW2
                  EEHP=0.0
                  KJ=(JUW2-JUW1)
                  DO 82 I=II,IVW2
                  IM=(I/10)+1
      195         DO 82 J=1,KJ
                  JJJ=JUW1+J
                  IF(JJJ.LT.360)GOTO 21
                  IF(JJJ.GE.360.AND.JJJ.LT.720)GOTO 23
                  IF(JJJ.EQ.720) GOTO 26
      200         JX=((JJJ-720)/10)+1
                  GOTO 22
            23    JX=((JJJ-360)/10)+1
                  GOTO 22
            26    JX=(JJJ-360)/10
      205         GOTO22
            21    JX=(JJJ/10)+1
            22    EEHP=EEHP+(EHE(IM,JX)*(SIN((IM*10.-5.)*(PI/180.)))/100.)
            82    CONTINUE
                  SKY=EEHP*ZLZ
      210         GOTO 85
            84    SKY=0.0
            85    RETURN
                  END
```

```
SUBROUTINE RATIO      74/835  OPT=1                    FTN 4.8+552

      1               SUBROUTINE RATIO(RAB,RAR,RAL,RAC,RABW)
                      DIMENSION H(11),V(8),R(12)
                      COMMON EHE(9,36),DELTAS(9)
                      COMMON W1,W2,W3,D,DSS,DIS,PDS,HP,H1,H2,H3,Y,HH,W,OH,ZLZ
      5         C
                C     THIS SUBROUTINE CALCULATES THE VIEW FACTORS ,AT THE ROOM
                C     REFERENCE POINT ,FOR ALL SURFACES.
                C
                C     H(I)=THE HORIZONTAL ANGLE SUBTENDED TOWARDS SURFACE I.
     10         C     V(I)=THE VERTICAL ANGLE SUBTENDED TOWARDS SURFACE I.
                C     R(I)=THE VIEW FACTOR OF SURFACE I.
                C     EHE(I,J)=ILLUMINATION FROM SKY ELEMENT I,J.
                C     DELTAS(I)=AREA OF SKY ELEMENT IN THE I.TH. RING.
                C
     15               PI=3.1415927
                      PI2=PI*2.0
                C
                C     CALCULATION OF VERTICAL ANGLES V(I)
                C
     20               DS=DSS
                      IF(OH.EQ.0.0)GOTO 30
                      V(1)=ATAN((OH-H3)/(DS+Y+DIS))
                      GOTO 31
                30    V(1)=0.0
     25         31    EXSKY=ATAN(H2/(DS+Y))
                      V(2)=EXSKY-V(1)
                      V(4)=ATAN((HH-H3)/(DS ))
                      V(5)=V(4)
                      V(3)=V(4)-EXSKY
     30               V(6)=ATAN((HH-H3)/(D-DS))
                      V(7)=ATAN((HH-H3)/PDS)
                      V(8)=ATAN((HH-H3)/(W-PDS))
                C
                C     CALCULATION OF THE HORIZONTAL ANGLES
     35         C
                      H(1)=2.0*ATAN((.5*W2)/(DS+Y))
                      H(2)=H(1)
                      H(3)=H(1)
                      RLEFT=ATAN((W1+(.5*W2))/DS)
     40               RIGHT=ATAN((W3+(.5*W2))/DS)
                      H(6)=ATAN((W-PDS)/(D-DS))
                      H(9)=ATAN(PDS/(D-DS))
                      H(4)=RLEFT-(.5*H(1))
                      H(5)=RIGHT-(.5*H(1))
     45               H(7)=ATAN(DS/PDS)
                      H(10)=ATAN((D-DS)/PDS)
                      H(8)=ATAN(DS/(W-PDS))
                      H(11)=ATAN((D-DS)/(W-PDS))
                C
     50         C     CALCULATION OF THE VIEW FACTORS R(I)
                C
                      R(1)=(H(1)-(ATAN(TAN(H(1))*COS(V(1)))*COS(V(1))))/PI2
                      HMOD1=ATAN(TAN(H(1))*COS(V(1)))
                      HMOD2=ATAN(TAN(H(1))*COS(EXSKY))
     55               HMOD3=ATAN(TAN(H(1))*COS(V(4)))
                      R(3)=((HMOD2-(HMOD3*COS(V(3))))/PI2)
                      FRONT=(H(1)-((HMOD3)*COS(V(4))))/PI2
```

```
      SUBROUTINE RATIO      74/835  OPT=1                    FTN 4.8+552

                        R(2)=FRONT-(R(3)+R(1))
                        R(4)=(H(4)-(ATAN(TAN(H(4))*COS(V(4)))*COS(V(4))))/PI2
     60                 R(5)=(H(5)-(ATAN(TAN(H(5))*COS(V(5)))*COS(V(5))))/PI2
                        R(6)=(H(6)-(ATAN(TAN(H(6))*COS(V(6)))*COS(V(6))))/PI2
                        R(10)=(H(9)-(ATAN(TAN(H(9))*COS(V(6)))*COS(V(6))))/PI2
                        R(7)=(H(7)-(ATAN(TAN(H(7))*COS(V(7)))*COS(V(7))))/PI2
                        R(11)=(H(10)-(ATAN(TAN(H(10))*COS(V(7)))*COS(V(7))))/PI2
     65                 R(8)=(H(8)-(ATAN(TAN(H(8))*COS(V(8)))*COS(V(8))))/PI2
                        R(12)=(H(11)-(ATAN(TAN(H(11))*COS(V(8)))*COS(V(8))))/PI2
                        TOPH=(.5*PI)-V(7)
                        TOPHH=(.5*PI)-V(8)
                        TOPV1=ATAN((D-DS)/(HH-H3))
     70                 TOPV2=ATAN((DS)/(HH-H3))
                        TOP1=(TOPH-(ATAN(TAN(TOPH)*COS(TOPV1))*COS(TOPV1)))/PI2
                        TOP2=(TOPH-(ATAN(TAN(TOPH)*COS(TOPV2))*COS(TOPV2)))/PI2
                        TOP3=(TOPHH-(ATAN(TAN(TOPHH)*COS(TOPV1))*COS(TOPV1)))/PI2
                        TOP4=(TOPHH-(ATAN(TAN(TOPHH)*COS(TOPV2))*COS(TOPV2)))/PI2
     75                 R(9)=TOP1+TOP2+TOP3+TOP4
                        SUM=R(1)+R(2)+R(3)+R(4)+R(5)+R(6)+R(7)+R(8)+R(9)
                      Q +R(10)+R(11)+R(12)
                        RAB=R(1)
                        IF(PDS.EQ.0.0) GOTO 2
     80                 RAR=R(7)+R(11)
                        GOTO 3
                  2     RAR=0.0
                  3     IF(PDS.EQ.W)GOTO 4
                        RAL=R(6)+R(10)
     85                 GOTO 5
                  4     RAL=0.0
                  5     IF(DSS.EQ.D)GOTO 6
                        RABW=R(8)+R(12)
                        GOTO 7
     90           6     RABW=0.0
                  7     RAC=R(9)
                        RETURN
                        END
```

SUBROUTINE COEF 74/835 OPT=1 FTN 4.8+552

```
      SUBROUTINE COEF(N,AM,ASC)
      DIMENSION DAY(13),AMASS(13),AS(13)
C
C     THIS SUBROUTINE INTERPOLATES THE VALUES OF AM AND ASC
C     FOR ANY GIVEN DAY N FROM THE VALUES OF THE 21 ST. OF EACH
C     MONTH.
C     DAY(I)=21 ST OF EACH MONTH
C     AMSS(I)=AIR DENSITY ON THE 21 ST OF THE MONTH I
C     AS(I)=INTENSITY OF NORMAL SOLAR RADIATION
C
      DATA(DAY(I),I=1,13)/21.,52.,80.,111.,141.,172.,202.,233.,
     Q 264.,294.,325.,355.,386./
      DATA(AMASS(I),I=1,13)/.142,.144,.156,.18,.196,.205
     Q ,.207,.201,.177,.16,.149,.142,.142/
      DATA(AS(I),I=1,13)/1230.,1215.,1186.,1136.,1104.,1088.,
     Q 1085.,1107.,1151.,1192.,1221.,1233.,1230./
      IF(N.GE.DAY(1))GOTO 18
      NS=N+365
      GOTO 20
   18 NS=N
   20 DO 10 J=1,12
      IF(DAY(J).LE.NS.AND.DAY(J+1).GT.NS) GOTO 15
      GOTO 10
   15 AM=AMASS(J)-(((AMASS(J)-AMASS(J+1))/(DAY(J+1)-DAY(J)))*
     Q (NS-DAY(J)))
      ASC=AS(J)-(((AS(J)-AS(J+1))/(DAY(J+1)-DAY(J)))*
     Q (NS-DAY(J)))
   10 CONTINUE
      RETURN
      END
```

SUBROUTINE WINDOW 74/835 OPT=1 FTN 4.8+552

```
      SUBROUTINE WINDOW(WA,HI,HH,W,H1,H2,H3,W1,W2,W3)
      WAREA=WA*HI
      H2=SQRT(WAREA)
      W2=H2
      H1=(HH-H2)/2.
      H3=H1
      W1=(W-W2)/2.
      W3=W1
      RETURN
      END
```

APPENDIX C

SAMPLES OF THE COMPUTER OUTPUTS

TEMPERATURE DISTRIBUTION AFTER 8HOURS

LAYER NUMBER 1

-3.10873	-.74887	-.72938	-.72924	-.72924
-.74887	-.08508	-.07415	-.07398	-.07397
-.72939	-.07415	-.06347	-.06329	-.06329
-.72934	-.07398	-.06329	-.06312	-.06312
-.72934	-.07397	-.06329	-.06312	-.06312

LAYER NUMBER 2

-1.27290	.19929	.21903	.21929	.21929
.19929	.87955	.89074	.89092	.89092
.21903	.89074	.90168	.90186	.90186
.21929	.89092	.90186	.90204	.90204
.21929	.89092	.90186	.90204	.90204

HEAT LOSS BY CONVEC. AT BOUNDARY SURFACES .97916 0.00000

HEAT LOSS BY CONVECTION AT EXT. SURFACE= 200.59100

HEAT LOSS BY CONVECTION AT INT. SURFACE= 208.10319

HEAT STORED WITHIN THE PANEL = 6.51971

TEMP. DIFF OUT= 9.49271TEMP. DIFF. IN = 19.83201

HOURLY RATE OUTSIDE: 201.57016

HOURLY RATE INSIDE: 201.58748
TOTAL HEAT ABSORBED= 8.85937

TOTAL HEAT GAIN= 172.00000

(Single Glazing)

TEMPERATURE DISTRIBUTION AFTER 8HOURS

LAYER NUMBER 1

-10.14397	-10.20550	-10.20690	-10.20688	-10.20687
-10.20550	-9.43599	-9.41007	-9.40919	-9.40916
-10.20690	-9.41007	-9.38263	-9.38167	-9.38163
-10.20688	-9.40919	-9.38167	-9.38070	-9.38067
-10.20687	-9.40916	-9.38163	-9.38067	-9.38063

LAYER NUMBER 2

-9.77240	-9.77984	-9.80110	-9.80107	-9.80106
-9.77984	-8.96057	-8.93273	-8.93198	-8.93195
-9.80110	-8.93273	-8.90353	-8.90249	-8.90246
-9.80107	-8.93198	-8.90249	-8.90146	-8.90142
-9.80106	-8.93195	-8.90246	-8.90142	-8.90139

LAYER NUMBER 3

-2.61438	-1.81731	-1.81059	-1.81039	-1.81039
-1.81731	.20468	.25413	.25371	.25376
-1.81059	.25413	.30399	.30370	.30376
-1.81039	.25371	.30370	.30342	.30348
-1.81038	.25376	.30376	.30348	.30354

LAYER NUMBER 4

6.96544	7.95183	7.96402	7.96440	7.96442
7.95183	9.38407	9.44643	9.44855	9.44862
7.96402	9.44643	9.51210	9.51439	9.51447
7.96440	9.44855	9.51439	9.51668	9.51676
7.96442	9.44862	9.51447	9.51676	9.51684

LAYER NUMBER 5

7.11324	8.10025	8.11427	8.11465	8.11466
8.10025	9.89346	9.94466	9.94674	9.94681
8.11427	9.94466	10.00911	10.01136	10.01143
8.11465	9.94674	10.01136	10.01361	10.01369
8.11466	9.94681	10.01143	10.01369	10.01377

HEAT LOSS BY CONVEC AT BOUNDARY SURFACES 8.59058 .37190

HEAT LOSS BY CONVECTION AT EXT SURFACE= 102.93704

HEAT LOSS BY CONVECTION AT INT SURFACE= 110.54112

HEAT STORED WITHIN THE PANEL = .39665

TEMP DIFF OUT= 4.8137 TEMP DIFF IN = 10.53445

HOURLY RATE OUTSIDE 111.48764

HOURLY RATE INSIDE 110.54112
TOTAL HEAT ABSORBED= 8.59058

TOTAL HEAT GAIN= 93.99706

(Double Glazing)

A Sample from FDIMP1

TEMPERATURE DISTRIBUTION AFTER 7HOURS

LAYER NUMBER 1

	-11		-11 81963	-11	81979
	-11		-11	-11	
	-11		-11	-11	
	-11		-11	-11	
	-11		-11	-11	

LAYER NUMBER 2

	-11		-11	-11	
	-11		-11	-11	
	-11		-11	-11	
	-11		-11	-11	
	-11		-11	-11	

LAYER NUMBER 3

	-6		-6 92971	-6	92962
	-4		-4 93001	-4	97931
	-4		-4 93210	-4	82355
	-4		-4 82440	-4	81161
	-4		-4 81248	-4	81074

LAYER NUMBER 4

	-2		-2 01274	-2	01504
			1 13796	1	14103
	1		1 38773	1	38902
	1		1 40610	1	40743
	1		1 40743	1	40876

LAYER NUMBER 5

	-1		-1 75603	-1	75788
	1		1 49518	1	46625
	1		1 71468	1	71597
	1		1 73314	1	73448
	1		1 73448	1	73581

LAYER NUMBER 6

	7		7 73904	7	73915
	7		7 48304	7	48391
	7		7 70350	7	70456
	7		7 71882	7	71991
	7		7 71991	7	72099

LAYER NUMBER 7

	10		10 16409	10	16419
	13		13 37034	13	37098
	13		13 55204	13	55280
	13		13 56376	13	56457
	13		13 56457	13	56537

LAYER NUMBER 8

	10		10	10	
	13		13	13	
	13		13	13	
	13		13	13	
	13		13	13	

HEAT LOSS BY CONVECTION AT EXT SURFACE= 73 53253

HEAT LOSS BY CONVECTION AT INT SURFACE= 72 44610

HEAT STORED WITHIN THE PANEL = -5 39399

TEMP DIFF ACROSS PANEL DIRECTION IN = 6 50404

HOURLY RATE OUTSIDE 69 88515

HOURLY RATE INSIDE 78 64678
TOTAL HEAT ABSORBED= 68 03939

TOTAL HEAT GAIN= 32 50902

(Triple Glazing)

A Sample from FDIMP1.

TEMPERATURE DISTRIBUTION AFTER 7HOURS

LAYER NUMBER 1

-11.01497	-10.49861	-10.49377	-10.49431	-10.49440	-10.49441
-10.49861	-10.32308	-10.32136	-10.32742	-10.32796	-10.32799
-10.49377	-10.32136	-10.33129	-10.47990	-10.48501	-10.48517
-10.49431	-10.32742	-10.47990	-10.91792	-10.92609	-10.92608
-10.49440	-10.32796	-10.48501	-10.92609	0.00000	0.00000
-10.49441	-10.32799	-10.48517	-10.92608	0.00000	0.00000

LAYER NUMBER 2

-7.46363	-6.27704	-6.25380	-6.25758	-6.25819	-6.25824
-6.27704	-5.74764	-5.73914	-5.78020	-5.78391	-5.78415
-6.25380	-5.73914	-5.80942	-6.72461	-6.75829	-6.75936
-6.25758	-5.78020	-6.72461	-10.93884	-10.92771	-10.92756
-6.25819	-5.78391	-6.75829	-10.82771	0.00000	0.00000
-6.25824	-5.78415	-6.75936	-10.82756	0.00000	0.00000

LAYER NUMBER 3

-.74788	.34431	.37765	.37051	.36936	.36925
.34431	.91223	.92335	.84768	.84069	.84024
.37765	.92335	.78967	-.61638	-.67604	-.67796
.37051	.84768	-.61638	-10.39915	-10.25769	-10.25708
.36936	.84069	-.67604	-10.25769	0.00000	0.00000
.36925	.84024	-.67796	-10.25708	0.00000	0.00000

LAYER NUMBER 4

9.72216	10.25529	10.28517	10.27643	10.27503	10.27490
10.25529	10.56433	10.57110	10.47733	10.46871	10.46816
10.28517	10.57110	10.39875	8.60585	8.53557	8.53381
10.27643	10.47733	8.60383	-9.67088	-9.50286	-9.50176
10.27503	10.46871	8.53557	-9.50286	0.00000	0.00000
10.27490	10.46816	8.53381	-9.50176	0.00000	0.00000

LAYER NUMBER 5

18.35003	18.43832	18.44322	18.44163	18.44137	18.44135
18.43832	18.49274	18.49381	18.47690	18.47537	18.47527
18.44322	18.49381	18.46259	18.12620	18.11589	18.11556
18.44163	18.47690	18.12620	6.12449	6.39177	6.39300
18.44137	18.47537	18.11589	6.39177	0.00000	0.00000
18.44135	18.47527	18.11556	6.39300	0.00000	0.00000

HEAT LOSS BY CONVECTION AT EXT. SURFACE= 37.78134

HEAT LOSS BY CONVECTION AT INT. SURFACE= 64.68550

HEAT STORED WITHIN THE PANEL = 5.76840

TEMP. DIFF OUT= .63187TEMP. DIFF. IN = 2.12208

CONVECTION AT INTERFACE: 11.95793 7.10648

HOURLY RATE OF H.L. TO OUTSIDE: 56.84579

TOTATL RATE OF H. INPUT: 58.91709

(Wall panel with 25 % glazing)

A Sample from FDIMP2

TEMPERATURE DISTRIBUTION AFTER [illegible] HOURS

LAYER NUMBER 1

-17.[illegible]	-18.37531	[illegible]	-18.37531	-18.37490	-19.[illegible]
[illegible]	[illegible]	[illegible]	[illegible]	[illegible]	[illegible]
[illegible]	[illegible]	0.00000	0.00000	0.00000	0.00000
[illegible]	[illegible]	0.00000	0.00000	0.00000	0.00000
[illegible]	[illegible]	0.00000	0.00000	0.00000	0.00000
[illegible]	[illegible]	0.00000	0.00000	0.00000	0.00000

LAYER NUMBER 2

-11.[illegible]	-14.62813	-14.71677	-14.72040	-14.71848	-14.67961
-14.62813	-19.73272	-19.63961	-18.63785	-19.63774	-19.63598
-14.71677	-19.63961	0.00000	0.00000	0.00000	0.00000
-14.72040	-18.63785	0.00000	0.00000	0.00000	0.00000
-14.71848	-18.63774	0.00000	0.00000	0.00000	0.00000
-14.67961	-18.63598	0.00000	0.00000	0.00000	0.00000

LAYER NUMBER 3

-2.48234	-7.66076	-7.82621	-7.84312	-7.82942	-7.76908
-7.66076	-18.14112	-17.[illegible]	-17.89940	-17.87717	-17.87330
-7.82621	-17.90041	0.00000	0.00000	0.00000	0.00000
-7.84312	-17.87940	0.00000	0.00000	0.00000	0.00000
-7.82942	-17.87717	0.00000	0.00000	0.00000	0.00000
-7.76908	-17.87330	0.00000	0.00000	0.00000	0.00000

LAYER NUMBER 4

7.82313	2.93692	2.75779	2.74944	2.75443	2.86406
2.93692	-17.12064	-16.84032	-16.83844	-16.83220	-16.83413
2.75779	-16.84032	0.00000	0.00000	0.00000	0.00000
2.74944	-16.83844	0.00000	0.00000	0.00000	0.00000
2.75443	-16.83820	0.00000	0.00000	0.00000	0.00000
2.86406	-16.83413	0.00000	0.00000	0.00000	0.00000

LAYER NUMBER 5

18.04749	17.10327	17.07821	17.07779	17.07867	17.09327
[illegible]	[illegible]	[illegible]	[illegible]	[illegible]	[illegible]
17.07821	2.53980	0.00000	0.00000	0.00000	0.00000
17.07779	2.54052	0.00000	0.00000	0.00000	0.00000
17.07867	2.54042	0.00000	0.00000	0.00000	0.00000
17.09327	2.54233	0.00000	0.00000	0.00000	0.00000

HEAT LOSS BY CONVECTION AT EXT SURFACE= 9.13726

HEAT LOSS BY CONVECTION AT INT. SURFACE= 49.71993

HEAT STORED WITHIN THE PANEL = - 88820

TEMP DIFF OUT= .53212 TEMP DIFF IN = 5.54925

CONVECTION AT INTERFACE 21.47427 13.13537

HOURLY RATE OF H L. TO OUTSIDE 45.74689

TOTATL RATE OF H INPUT 59.69813

(Wall panel with 75% glazing)
A Sample from FDIMP2

Variation of the convection coefficient with wind speed and direction.

The hourly weather data, temperature measurements, and heating time used in determining the value of the convection coefficient.

	WIND SPEED	WIND DIRECTN	AMBIENT TEMP	SURF. TEMP	[illegible]	HEAT LOSS	[illegible] COEFF	[illegible] COEFF	RESISTANCE	R/[illegible] RATIO
1	.800	135.000	-13.000	-12.[illegible]	[illegible]	[illegible]	[illegible]	[illegible]	[illegible]	.102
2	1.700	90.000	-13.000	-12.[illegible]	[illegible]	[illegible]	[illegible]	[illegible]	15.193	.118
3	1.200	45.000	-15.000	-14.200	2.[illegible]	70.000	11.297	1.566	12.863	.109
4	.900	90.000	-15.000	-14.250	1.700	81.000	10.686	1.767	12.253	.147
5	.300	90.000	-17.000	-16.300	1.500	80.000	10.30[illegible]	1.529	12.329	.142
6	.800	90.000	-17.000	-16.200	1.700	82.500	11.506	1.529	13.034	.133
7	1.100	135.000	-15.000	-14.200	1.300	65.000	9.613	1.587	11.185	.163
8	1.600	135.000	-15.000	-14.350	2.100	92.500	10.692	1.565	12.258	.146
9	1.900	90.000	-15.000	-14.100	4.200	145.000	16.603	1.565	18.171	.094
10	2.200	90.000	-16.000	-15.150	4.500	152.500	16.[illegible]	1.549	17.[illegible]	.076
11	2.700	90.000	-16.000	-15.150	6.200	195.000	19.[illegible]	1.549	[illegible]	.079
12	2.900	90.000	-16.000	-15.100	6.900	212.500	19.467	1.549	21.016	.080
13	2.500	90.000	-16.000	-15.050	5.800	185.000	17.[illegible]	1.550	19.366	.087
14	2.400	90.000	-15.000	-14.100	5.300	172.500	17.834	1.568	19.402	.088
15	2.600	90.000	-15.000	-14.100	5.700	182.500	17.661	1.568	19.229	.087
16	2.300	90.000	-15.000	-14.150	4.300	160.000	17.219	1.567	18.786	.0[illegible]1
17	2.700	90.000	-14.000	-13.200	5.500	177.500	18.073	1.586	19.659	.088
18	2.400	45.000	-13.000	-12.160	4.400	150.000	15.022	1.606	16.627	.107
19	2.200	45.000	-13.000	-12.250	3.600	130.000	14.131	1.605	15.736	.114
20	2.000	90.000	-11.000	-10.150	3.800	135.000	16.134	1.644	17.778	.102
21	2.100	0.000	-11.000	-10.200	3.400	125.000	13.880	1.644	15.524	.118
22	1.600	0.000	-12.000	-11.160	2.900	112.500	12.226	1.625	13.851	.133
23	1.300	0.000	-12.000	-11.150	2.100	72.500	10.500	1.625	12.125	.155
24	1.300	0.000	-12.000	-11.120	2.600	105.000	11.832	1.625	13.457	.137
25	1.700	45.000	-13.000	-12.150	3.400	125.000	13.812	1.606	15.418	.116
26	2.600	0.000	-13.000	-12.150	5.500	177.500	16.207	1.606	17.813	.099
27	2.900	0.000	-12.000	-11.150	5.700	182.500	16.670	1.625	18.295	.097
28	3.000	0.000	-12.000	-11.200	5.700	182.500	16.258	1.624	17.882	.100
29	2.900	0.000	-11.000	-10.200	5.300	172.500	16.126	1.644	17.770	.102
30	3.100	0.000	-11.000	-10.200	6.000	190.000	17.353	1.644	18.997	.095
31	3.100	0.000	-11.000	-10.300	5.500	177.500	16.541	1.643	18.184	.099
32	2.800	45.000	-9.000	-8.250	4.300	160.000	17.116	1.683	[illegible].778	.093
33	2.900	0.000	-9.000	-8.300	4.600	155.000	15.518	1.682	17.200	.108
34	2.600	0.000	-9.000	-8.300	4.400	150.000	15.637	1.682	17.319	.108
35	3.000	0.000	-9.000	-8.350	4.800	160.000	16.625	1.682	18.307	.101
36	2.900	0.000	-7.000	-6.250	4.600	155.000	16.039	1.723	17.762	.107
37	3.100	0.000	-6.000	-5.150	5.[illegible]	172.500	15.[illegible]	1.744	18.051	.107
38	2.600	0.000	-7.000	-6.250	4.300	147.500	15.393	1.723	17.116	.112
39	3.000	45.000	-7.000	-6.400	4.500	152.500	17.908	1.721	19.629	.096
40	3.100	45.000	-7.000	-6.350	4.800	160.000	16.976	1.722	18.698	.0[illegible]
41	2.[illegible]	90.000	-9.000	-8.400	3.900	137.500	17.703	1.[illegible]	19.3[illegible]	.0[illegible]
42	2.300	90.000	-9.000	-8.250	4.400	150.000	15.329	1.[illegible]	[illegible]	.0[illegible]
43	1.700	90.000	-9.000	-8.250	2.700	107.500	14.567	1.683	16.249	.11[illegible]
44	1.100	180.000	-8.000	-7.100	1.200	70.000	6.689	1.704	8.393	.255
45	2.000	180.000	-9.000	-8.100	3.000	115.000	11.545	1.684	13.229	.11[illegible]

Cont.

46*	1.200*	180.000*	-9.000*	-8.400*	1.100*	67.500*	9.136*	1.681*	10.817*	.154*
47*	1.300*	90.000*	-9.000*	-8.400*	2.000*	90.000*	14.328*	1.681*	16.189*	.116*
48*	1.800*	90.000*	-9.000*	-8.300*	2.700*	107.500*	14.946*	1.652*	16.628*	.113*
49*	2.800*	45.000*	-8.000*	-7.200*	4.800*	160.000*	16.675*	1.703*	18.379*	.102*
50*	2.700*	0.000*	-7.000*	-6.100*	4.300*	160.000*	16.333*	1.724*	18.057*	.106*
51*	2.900*	0.000*	-7.000*	-6.100*	5.300*	172.500*	16.913*	1.724*	18.643*	.102*
52*	2.600*	45.000*	-7.000*	-6.200*	4.200*	145.000*	16.005*	1.723*	17.729*	.102*
53*	1.100*	0.000*	-7.000*	-6.250*	2.200*	95.000*	15.227*	1.723*	16.955*	.113*
54*	.700*	90.000*	-6.000*	-5.400*	1.100*	67.500*	11.682*	1.741*	13.424*	.149*
55*	.800*	90.000*	-8.000*	-7.100*	1.800*	85.000*	10.921*	1.704*	12.625*	.156*
56*	.800*	180.000*	-8.000*	-7.250*	1.000*	65.000*	8.180*	1.703*	9.883*	.208*
57*	1.000*	180.000*	-8.000*	-7.250*	1.100*	67.500*	8.120*	1.703*	9.822*	.210*
58*	1.200*	0.000*	-8.000*	-7.250*	1.700*	82.500*	11.216*	1.703*	12.919*	.132*
59*	1.300*	90.000*	-7.000*	-6.100*	3.200*	120.000*	14.657*	1.724*	16.422*	.117*
60*	2.100*	90.000*	-7.000*	-6.250*	3.300*	122.500*	16.289*	1.723*	18.012*	.106*
61*	2.600*	180.000*	-7.000*	-6.100*	4.100*	142.500*	13.486*	1.724*	15.210*	.128*
62*	3.200*	180.000*	-5.000*	-4.400*	4.300*	147.500*	14.987*	1.762*	16.749*	.113*
63*	3.300*	180.000*	-6.000*	-5.350*	4.900*	162.500*	15.295*	1.742*	17.037*	.114*
64*	3.600*	180.000*	-6.000*	-5.250*	6.200*	195.000*	16.417*	1.743*	18.157*	.106*
65*	4.300*	180.000*	-6.000*	-5.200*	3.700*	262.500*	17.850*	1.743*	19.604*	.098*
66*	4.400*	180.000*	-6.000*	-5.300*	8.800*	260.000*	17.262*	1.742*	19.004*	.101*
67*	4.700*	180.000*	-6.000*	-5.400*	9.800*	285.000*	18.483*	1.741*	20.225*	.094*
68*	4.600*	180.000*	-7.000*	-6.100*	10.900*	312.500*	18.343*	1.724*	20.068*	.094*
69*	4.000*	180.000*	-7.000*	-6.300*	7.500*	227.500*	16.581*	1.722*	18.303*	.104*
70*	3.200*	45.000*	-8.000*	-7.300*	5.500*	177.500*	17.848*	1.702*	19.550*	.095*
71*	2.100*	45.000*	-8.000*	-7.250*	3.100*	117.500*	14.435*	1.703*	16.167*	.119*
72*	1.800*	45.000*	-8.000*	-7.250*	2.800*	105.000*	13.610*	1.703*	15.302*	.125*
73*	1.200*	90.000*	-11.000*	-10.150*	2.300*	102.500*	13.569*	1.644*	15.214*	[illegible]
74*	2.200*	90.000*	-11.000*	-10.150*	4.100*	142.500*	16.134*	1.644*	17.779*	[illegible]
75*	1.800*	90.000*	-11.000*	-10.150*	3.200*	120.000*	14.176*	1.644*	15.820*	[illegible]
76*	1.300*	0.000*	-11.000*	-10.200*	2.100*	72.500*	11.550*	1.644*	13.194*	[illegible]
77*	1.000*	0.000*	-12.000*	-11.170*	1.700*	82.500*	9.794*	1.625*	11.418*	[illegible]
78*	1.100*	90.000*	-12.000*	-11.150*	2.200*	95.000*	12.017*	1.625*	13.642*	.135*
79*	1.200*	90.000*	-13.000*	-12.200*	2.300*	97.500*	12.735*	1.605*	14.340*	.12[illegible]*
80*	1.400*	180.000*	-13.000*	-12.130*	2.300*	97.500*	[illegible]	1.608*	[illegible]	[illegible]
81*	1.300*	180.000*	-13.000*	-12.150*	2.400*	100.000*	[illegible]	1.606*	11.[illegible]	.127*
82*	1.[illegible]	180.000*	-13.[illegible]	-12.1[illegible]	2.[illegible]	[illegible]	[illegible]	1.608*	11.[illegible]	[illegible]
83*	1.[illegible]	180.000*	-13.[illegible]	-12.1[illegible]	[illegible]	[illegible]	[illegible]	1.606*	11.[illegible]	[illegible]
84*	1.30[illegible]	180.[illegible]	-15.[illegible]	-14.1[illegible]	[illegible]	[illegible]	[illegible]	[illegible]	12.[illegible]	.143*
85*	2.300*	90.[illegible]	-16.[illegible]	-15.[illegible]	4.[illegible]	[illegible]	17.[illegible]	1.547*	18.647*	.0[illegible]
86*	2.[illegible]	135.[illegible]	-16.[illegible]	-15.400*	[illegible]	[illegible]	12.774*	1.545*	14.[illegible]	[illegible]
87*	3.000*	135.[illegible]	-16.[illegible]	-15.[illegible]	[illegible]	[illegible]	15.[illegible]	1.547*	17.068*	[illegible]
88*	3.100*	45.00[illegible]	-15.[illegible]	-14.2[illegible]	[illegible]	[illegible]	[illegible]	1.5[illegible]	17.7[illegible]	.0[illegible]
89*	2.900*	135.[illegible]	-15.[illegible]	-14.[illegible]	[illegible]	[illegible]	[illegible]	1.5[illegible]	15.[illegible]	[illegible]
90*	3.200*	135.[illegible]	-15.[illegible]	-14.[illegible]	[illegible]	[illegible]	[illegible]	[illegible]	17.0[illegible]	[illegible]
91*	3.100*	135.[illegible]	-14.[illegible]	-13.[illegible]	[illegible]	[illegible]	[illegible]	[illegible]	[illegible]	[illegible]
92*	2.700*	135.[illegible]	-13.000*	-12.[illegible]	[illegible]	[illegible]	[illegible]	[illegible]	[illegible]	[illegible]
93*	1.200*	135.[illegible]	-13.000*	-12.[illegible]	[illegible]	[illegible]	[illegible]	[illegible]	[illegible]	[illegible]
94*	1.300*	135.000*	-13.000*	-12.300*	1.700*	[illegible]	9.942*	1.604*	11.[illegible]	.[illegible]
95*	2.600*	180.000*	-12.000*	-11.1[illegible]	[illegible]	150.000*	12.[illegible]	1.625*	13.[illegible]	.133*
96*	2.500*	180.000*	-12.000*	-11.[illegible]	[illegible]	[illegible]	[illegible]	[illegible]	[illegible]	[illegible]

Cont.

97%	2.500%	180.000%	-12.000%	-11.150%	4.300%	147.000%	13.071%	1.6[illegible]%	18.296%	.119%
98%	2.700%	180.000%	-12.000%	-11.150%	4.800%	155.000%	12.787%	1.[illegible]%	14.[illegible]%	.122%
99%	2.600%	180.000%	-[illegible]%	-[illegible]%	4.200%	[illegible]%	12.[illegible]%	[illegible]%	[illegible]%	.103%
.00%	2.[illegible]%	[illegible]%	-[illegible]%	-[illegible]%	[illegible]%	[illegible]%	-[illegible]%	[illegible]%	[illegible]%	.[illegible]%
01%	2.500%	180.000%	-10.000%	-9.150%	3.800%	135.000%	12.700%	[illegible]%	[illegible]%	.[illegible]%
02%	2.400%	180.000%	-10.000%	-9.[illegible]%	3.700%	132.500%	12.879%	[illegible]%	[illegible]%	.134%
.03%	2.700%	180.000%	-8.000%	-7.150%	4.000%	137.500%	10.[illegible]%	1.[illegible]%	[illegible]%	.[illegible]%
.04%	2.700%	180.000%	-8.000%	-7.[illegible]%	[illegible]%	[illegible]%	[illegible]%	[illegible]%	[illegible]%	.[illegible]%
.05%	2.600%	180.000%	-8.000%	-7.[illegible]%	3.400%	122.000%	12.[illegible]%	[illegible]%	15.352%	.140%
.06%	2.700%	135.000%	-8.000%	-7.250%	4.100%	142.500%	14.079%	1.[illegible]%	15.301%	.117%
.07%	2.800%	135.000%	-7.000%	-6.250%	4.000%	140.000%	13.419%	1.[illegible]%	15.[illegible]%	.126%
.08%	2.700%	135.000%	-7.000%	-6.[illegible]%	3.700%	132.500%	13.734%	1.[illegible]%	15.[illegible]%	.[illegible]%
.09%	2.300%	135.000%	-8.000%	-7.250%	3.200%	120.000%	13.223%	1.[illegible]%	14.926%	.129%
.10%	2.500%	0.000%	-8.000%	-7.150%	4.000%	140.000%	14.[illegible]%	1.[illegible]%	15.[illegible]%	.120%
111%	2.200%	0.000%	-8.000%	-7.250%	3.100%	117.500%	13.548%	1.[illegible]%	15.[illegible]%	.[illegible]%
112%	2.100%	0.000%	-7.000%	-6.250%	2.900%	112.500%	13.656%	1.[illegible]%	15.378%	.[illegible]%
113%	2.400%	45.000%	-7.000%	-6.200%	3.900%	150.000%	14.35[illegible]%	1.[illegible]%	16.[illegible]%	.[illegible]%
114%	2.200%	45.000%	-7.000%	-6.150%	3.400%	125.000%	13.967%	1.[illegible]%	15.[illegible]%	.[illegible]%
115%	2.500%	45.000%	-7.000%	-6.[illegible]%	4.300%	147.500%	15.[illegible]%	1.[illegible]%	17.[illegible]%	.111%
116%	2.400%	45.000%	-6.000%	-7.150%	4.300%	147.500%	16.937%	1.[illegible]%	18.[illegible]%	.[illegible]%
117%	2.300%	45.000%	-6.000%	-7.150%	4.200%	145.000%	15.384%	1.[illegible]%	17.[illegible]%	.111%
.18%	2.700%	45.000%	-6.000%	-7.150%	4.700%	157.500%	16.[illegible]%	1.[illegible]%	17.869%	.[illegible]%
.19%	1.000%	45.000%	-11.000%	-10.250%	1.800%	85.000%	11.9[illegible]%	1.[illegible]%	13.[illegible]%	.[illegible]%
.20%	1.100%	0.000%	-11.000%	-10.200%	1.800%	85.000%	10.[illegible]%	1.[illegible]%	12.305%	.154%
.21%	2.000%	135.000%	-11.000%	-10.250%	2.900%	112.500%	12.[illegible]%	1.[illegible]%	14.[illegible]%	.[illegible]%
.22%	1.000%	45.000%	-12.000%	-11.200%	3.000%	115.000%	11.[illegible]%	[illegible]%	[illegible]%	.[illegible]%
.23%	2.000%	0.000%	-13.000%	-12.150%	3.300%	122.500%	12.[illegible]%	1.[illegible]%	15.[illegible]%	.[illegible]%
.24%	2.200%	135.000%	-12.000%	-11.150%	3.400%	125.000%	11.[illegible]%	1.[illegible]%	13.[illegible]%	.[illegible]%
.25%	2.500%	90.000%	-13.000%	-12.200%	4.600%	155.000%	15.8[illegible]%	1.[illegible]%	17.[illegible]%	.[illegible]%
.26%	2.300%	135.000%	-13.000%	-12.100%	4.000%	140.000%	12.[illegible]%	1.[illegible]%	14.[illegible]%	.[illegible]%
.27%	2.000%	45.000%	-10.000%	-9.050%	5.300%	122.500%	17.[illegible]%	1.[illegible]%	18.[illegible]%	.[illegible]%
.28%	2.100%	90.000%	-9.000%	-8.100%	3.700%	132.500%	14.641%	1.[illegible]%	16.[illegible]%	.115%
.29%	1.100%	90.000%	-8.000%	-7.[illegible]%	2.000%	90.000%	11.078%	1.[illegible]%	12.[illegible]%	.[illegible]%
.30%	2.300%	90.000%	-8.000%	-7.300%	3.800%	135.000%	18.523%	1.[illegible]%	20.[illegible]%	.[illegible]%
.31%	2.[illegible]%	90.000%	-7.000%	-6.250%	4.700%	167.500%	18.027%	1.[illegible]%	19.[illegible]%	.[illegible]%
.32%	2.100%	90.000%	-7.000%	-6.250%	3.100%	117.500%	14.972%	1.[illegible]%	16.[illegible]%	.115%
.33%	1.[illegible]%	180.000%	-8.000%	-7.300%	2.600%	105.000%	13.384%	1.[illegible]%	13.[illegible]%	.[illegible]%
.34%	1.800%	180.000%	-8.000%	-7.350%	2.400%	100.000%	14.435%	1.[illegible]%	16.[illegible]%	.[illegible]%
.35%	2.200%	0.000%	-9.000%	-8.300%	3.000%	115.000%	13.348%	1.[illegible]%	15.[illegible]%	.[illegible]%
.36%	2.400%	0.000%	-9.000%	-8.200%	4.000%	140.000%	13.[illegible]%	1.[illegible]%	17.[illegible]%	.107%
.37%	3.800%	0.000%	-9.000%	-8.200%	7.400%	225.000%	19.158%	1.[illegible]%	23.841%	.068%
.38%	4.200%	90.000%	-9.000%	-8.150%	10.900%	312.500%	25.857%	1.[illegible]%	27.541%	.083%
.39%	4.[illegible]%	135.000%	-10.000%	-9.140%	11.400%	325.000%	19.297%	1.[illegible]%	20.761%	.[illegible]%
.40%	4.[illegible]%	135.000%	-11.000%	-10.100%	12.100%	342.500%	17.819%	1.[illegible]%	19.[illegible]%	.[illegible]%
.41%	4.000%	135.000%	-11.000%	-10.100%	9.300%	272.500%	17.160%	1.[illegible]%	18.[illegible]%	.[illegible]%
.42%	3.[illegible]%	135.000%	-12.000%	-11.100%	7.000%	205.000%	15.7[illegible]%	1.[illegible]%	17.[illegible]%	.[illegible]%

E INFERIEURE

NUMBER OF LAYERS= 1

ANGLE OF INCIDENCE	REFLECTANCE	TRANSMITTANCE	ABSORPTANCE
0.00	.079329	.872008	.0486638
5.00	.079331	.872006	.0486638
10.00	.079352	.871985	.0486638
15.00	.079451	.871887	.0486638
20.00	.079730	.871608	.0486620
25.00	.080361	.870978	.0486618
30.00	.081615	.869727	.0486588
35.00	.083912	.867435	.0486538
40.00	.087903	.863453	.0486458
45.00	.094599	.856771	.0486308
50.00	.105575	.845811	.0486068
55.00	.123290	.828143	.0485678
60.00	.151577	.799922	.0485018
65.00	.196308	.755301	.0483908
70.00	.266117	.685687	.0481968
75.00	.372419	.579750	.0478318
80.00	.526884	.426070	.0470468
85.00	.734071	.221220	.0447108
90.00	1.000000	0.000000	0.0000008

A sample of the results of the program Trans used to calculate angle dependent reflectance, transmittance and absorptance for single, double, and triple glazing. Angle of incidence is ranging from 0.0° to 90°.

```
LATITUDE ANGLE          =45.0
DAY OF THE YEAR = 21
ANGLE OF DECLINATION =       -20.1380138896
SUN ALTITUDE ANGLE =  24.73364 DEGREES
SUN AZIMUTH ANGLE  =   0.00000 DEGREES
ILLUMINATION ON HORIZONTAL PLANE=10561.33

*****************************************
WINDOW AZIMUTH ANGLE:  180.00
*****************************************

DIRECT BEAM ILLUMINATION
BUILDING SURFACE:      0.000
OBSTRUCTION SURFACE: 79482.744
GROUND             : 36830.583

SKY DIFFUSE ILLUMINATION
BUILDING SURFACE:  4304.659
OBSTRUCTION SURFACE:  9793.700
GROUND             :  4578.299

LUMINANCE OF EXTERNAL SURFACES
OBSTRUCTION SURFACE: 27826.098
GROUND             :  8826.157

LUMINANCE OF INTERNAL SURFACES
CEILING            :   304.035
R. SIDE WALL       :   306.549
L. SIDE WALL       :   306.549
BACK WALL          :   113.476

ILLUMINATION AT THE REFERENCE POINT(LUX)
DIRECT SKY ILLUMINATION     75.030LUX
REFLECTED ILLUMINATION   398.686LUX
TOTAL ILLUMINATION   462.462LUX
VARIABLE SKY FACTOR       .710%
VARIABLE DAYLIGHT FACTOR     4.379%
WINDOW AZIMUTH ANGLE:  360.00
*****************************************
```

(A sample of the hourly calculation output of the DFV program)

The luminance distribution of a clear cloudless sky was calculated for sun altitude angles of 20°, 30°, ... 90°. The results are presented here. Luminance of a sky element is displayed as a function of the element altitude angle, element azimuth angle, and the sun altitude angle. Luminance is expressed as a ratio of the zenith luminance.

SUN ALTITUDE ANGLE =20.0 DEGREES

SKY ELEMENT ALTITUDE ANGLE

AZIMUTH	5	15	25	35	45	55	65	75	85
10	16.6635	17.6868	13.2960	7.3514	4.2873	2.7068	1.8504	1.3665	1.0888
20	13.5656	12.4471	9.4794	6.1715	3.9051	2.5728	1.8023	1.3508	1.0858
30	10.2131	8.6754	6.6752	4.8017	3.3388	2.3474	1.7155	1.3211	1.0799
40	7.6575	6.2405	4.8381	3.6936	2.7738	2.0865	1.6046	1.2806	1.0715
50	5.8813	4.6730	3.6408	2.8862	2.2953	1.8331	1.4845	1.2331	1.0611
60	4.6788	3.6526	2.8524	2.3167	1.9199	1.6098	1.3670	1.1822	1.0490
70	3.8757	2.9831	2.3286	1.9196	1.6368	1.4248	1.2597	1.1314	1.0359
80	3.3544	2.5480	1.9818	1.6458	1.4290	1.2778	1.1665	1.0830	1.0223
90	3.0405	2.2783	1.7593	1.4619	1.2809	1.1651	1.0889	1.0390	1.0087
100	2.8856	2.1314	1.6281	1.3453	1.1798	1.0819	1.0265	1.0002	.9955
110	2.8548	2.0783	1.5659	1.2800	1.1158	1.0234	.9782	.9672	.9832
120	2.9186	2.0959	1.5557	1.2536	1.0805	.9849	.9421	.9398	.9719
130	3.0486	2.1635	1.5825	1.2554	1.0665	.9620	.9164	.9179	.9620
140	3.2162	2.2607	1.6323	1.2754	1.0672	.9505	.8989	.9008	.9536
150	3.3931	2.3678	1.6917	1.3046	1.0764	.9467	.8877	.8881	.9468
160	3.5528	2.4666	1.7484	1.3348	1.0887	.9471	.8811	.8792	.9416
170	3.6730	2.5419	1.7925	1.3590	1.0996	.9490	.8775	.8736	.9381
180	3.7374	2.5824	1.8165	1.3723	1.1059	.9505	.8760	.8708	.9364
190	3.7374	2.5824	1.8165	1.3723	1.1059	.9505	.8760	.8708	.9364
200	3.6730	2.5419	1.7925	1.3590	1.0996	.9490	.8775	.8736	.9381
210	3.5528	2.4666	1.7484	1.3348	1.0887	.9471	.8811	.8792	.9416
220	3.3931	2.3678	1.6917	1.3046	1.0764	.9467	.8877	.8881	.9468
230	3.2162	2.2607	1.6323	1.2754	1.0672	.9505	.8989	.9008	.9536
240	3.0486	2.1635	1.5825	1.2554	1.0665	.9620	.9164	.9179	.9620
250	2.9186	2.0959	1.5557	1.2536	1.0805	.9849	.9421	.9398	.9719
260	2.8548	2.0783	1.5659	1.2800	1.1158	1.0234	.9782	.9672	.9832
270	2.8856	2.1314	1.6281	1.3453	1.1798	1.0819	1.0265	1.0002	.9955
280	3.0405	2.2783	1.7593	1.4619	1.2809	1.1651	1.0889	1.0390	1.0087
290	3.3544	2.5480	1.9818	1.6458	1.4290	1.2778	1.1665	1.0830	1.0223
300	3.8757	2.9831	2.3286	1.9196	1.6368	1.4248	1.2597	1.4314	1.0359
310	4.6788	3.6526	2.8524	2.3167	1.9199	1.6098	1.3670	1.1822	1.0490
320	5.8813	4.6730	3.6408	2.8862	2.2953	1.8331	1.4845	1.2331	1.0611
330	7.6575	6.2405	4.8381	3.6936	2.7738	2.0865	1.6046	1.2806	1.0715
340	10.2131	8.6754	6.6752	4.8017	3.3388	2.3474	1.7155	1.3211	1.0799
350	13.5656	12.4471	9.4794	6.1715	3.9051	2.5728	1.8023	1.3508	1.0858
360	16.6635	17.6868	13.2960	7.3514	4.2873	2.7068	1.8504	1.3665	1.0888

SUN ALTITUDE ANGLE =30.0 DEGREES

SKY ELEMENT ALTITUDE ANGLE

AZIMUTH	5	15	25	35	45	55	65	75	85
10	9.5808	10.1974	11.1999	9.0757	5.2702	3.2011	2.0905	1.4717	1.1164
20	8.5089	8.4539	8.1150	6.7036	4.5634	2.9813	2.0187	1.4498	1.1124
30	7.0235	6.4879	5.7886	4.8570	3.6787	2.6348	1.8922	1.4087	1.1046
40	5.6480	4.9368	4.2364	3.5973	2.9141	2.2631	1.7359	1.3533	1.0934
50	4.5591	3.8287	3.2089	2.7477	2.3266	1.9259	1.5725	1.2890	1.0794
60	3.7553	3.0604	2.5227	2.1708	1.8934	1.6446	1.4177	1.2212	1.0633
70	3.1856	2.5337	2.0601	1.7753	1.5785	1.4201	1.2800	1.1540	1.0458
80	2.7990	2.1786	1.7477	1.5027	1.3511	1.2456	1.1624	1.0907	1.0277
90	2.5359	1.9486	1.5403	1.3161	1.1882	1.1123	1.0651	1.0332	1.0096
100	2.4273	1.8131	1.4094	1.1917	1.0734	1.0124	.9865	.9825	.9920
110	2.3897	1.7502	1.3358	1.1134	.9951	.9390	.9242	.9390	.9755
120	2.4222	1.7424	1.3051	1.0696	.9443	.8866	.8760	.9026	.9605
130	2.5044	1.7740	1.3054	1.0510	.9142	.8505	.8396	.8728	.9472
140	2.6157	1.8300	1.3257	1.0494	.8988	.8269	.8129	.8491	.9359
150	2.7354	1.8959	1.3562	1.0580	.8931	.8123	.7939	.8311	.9267
160	2.8446	1.9586	1.3879	1.0704	.8929	.8039	.7812	.8181	.9198
170	2.9273	2.0071	1.4135	1.0817	.8947	.7996	.7734	.8097	.9151
180	2.9717	2.0335	1.4277	1.0882	.8963	.7978	.7697	.8055	.9127
190	2.9717	2.0335	1.4277	1.0882	.8963	.7978	.7697	.8055	.9127
200	2.9273	2.0071	1.4135	1.0817	.8947	.7996	.7734	.8097	.9151
210	2.8446	1.9586	1.3879	1.0704	.8929	.8039	.7812	.8181	.9198
220	2.7354	1.8959	1.3562	1.0580	.8931	.8123	.7939	.8311	.9267
230	2.6157	1.8300	1.3257	1.0494	.8988	.8269	.8129	.8491	.9359
240	2.5044	1.7740	1.3054	1.0510	.9142	.8505	.8396	.8728	.9472
250	2.4222	1.7424	1.3051	1.0696	.9443	.8866	.8760	.9026	.9605
260	2.3897	1.7502	1.3358	1.1134	.9951	.9390	.9242	.9390	.9755
270	2.4273	1.8131	1.4094	1.1917	1.0734	1.0124	.9865	.9825	.9920
280	2.5359	1.9486	1.5403	1.3161	1.1882	1.1123	1.0651	1.0332	1.0096
290	2.7990	2.1786	1.7477	1.5027	1.3511	1.2456	1.1624	1.0907	1.0277
300	3.1856	2.5337	2.0601	1.7753	1.5785	1.4201	1.2800	1.1540	1.0458
310	3.7553	3.0604	2.5227	2.1708	1.8934	1.6446	1.4177	1.2212	1.0633
320	4.5591	3.8287	3.2089	2.7477	2.3266	1.9259	1.5725	1.2890	1.0794
330	5.6480	4.9368	4.2364	3.5973	2.9141	2.2631	1.7359	1.3533	1.0934
340	7.0235	6.4879	5.7886	4.8570	3.6787	2.6348	1.8922	1.4087	1.1046
350	8.5089	8.4539	8.1150	6.7036	4.5634	2.9813	2.0187	1.4498	1.1124
360	9.5808	10.1974	11.1999	9.0757	5.2702	3.2011	2.0905	1.4717	1.1164

E INFERIEURE

SUN ALTITUDE ANGLE =40.0 DEGREES

SKY ELEMENT ALTITUDE ANGLE

AZIMUTH	5	15	25	35	45	55	65	75	85
10	5.4310	5.5716	6.1100	7.2831	6.2469	3.7529	2.3542	1.5824	1.1440
20	5.0598	5.0256	5.2049	5.5004	4.8376	3.3702	2.2455	1.5524	1.1389
30	4.4709	4.2377	4.1166	4.0591	3.6462	2.8430	2.0616	1.4968	1.1289
40	3.8394	3.4746	3.2092	3.0498	2.7862	2.3449	1.8462	1.4231	1.1147
50	3.2730	2.8455	2.5318	2.3539	2.1781	1.9330	1.6329	1.3393	1.0970
60	2.8124	2.3638	2.0442	1.8722	1.7477	1.6103	1.4400	1.2526	1.0767
70	2.4611	2.0091	1.6975	1.5358	1.4409	1.3630	1.2746	1.1686	1.0548
80	2.2084	1.7558	1.4529	1.2991	1.2206	1.1753	1.1371	1.0907	1.0322
90	2.0404	1.5822	1.2829	1.1326	1.0617	1.0334	1.0252	1.0209	1.0097
100	1.9439	1.4715	1.1686	1.0167	.9472	.9265	.9354	.9599	.9879
110	1.9060	1.4103	1.0965	.9381	.8657	.8466	.8642	.9078	.9676
120	1.9144	1.3874	1.0563	.8874	.8088	.7875	.8085	.8643	.9490
130	1.9560	1.3925	1.0395	.8573	.7702	.7445	.7656	.8286	.9327
140	2.0178	1.4157	1.0388	.8419	.7454	.7139	.7331	.8001	.9188
150	2.0867	1.4478	1.0475	.8361	.7302	.6928	.7094	.7782	.9076
160	2.1507	1.4802	1.0596	.8358	.7217	.6790	.6928	.7624	.8990
170	2.1996	1.5061	1.0706	.8375	.7174	.6707	.6824	.7520	.8933
180	2.2260	1.5204	1.0770	.8390	.7156	.6669	.6773	.7470	.8904
190	2.2260	1.5204	1.0770	.8390	.7156	.6669	.6773	.7470	.8904
200	2.1996	1.5061	1.0706	.8375	.7174	.6707	.6824	.7520	.8933
210	2.1507	1.4802	1.0596	.8358	.7217	.6790	.6928	.7624	.8990
220	2.0867	1.4478	1.0475	.8361	.7302	.6928	.7094	.7782	.9076
230	2.0178	1.4157	1.0388	.8419	.7454	.7139	.7331	.8001	.9188
240	1.9560	1.3925	1.0395	.8573	.7702	.7445	.7656	.8286	.9327
250	1.9144	1.3874	1.0563	.8874	.8088	.7875	.8085	.8643	.9490
260	1.9060	1.4103	1.0965	.9381	.8657	.8466	.8642	.9078	.9676
270	1.9439	1.4715	1.1686	1.0167	.9472	.9265	.9354	.9599	.9879
280	2.0404	1.5822	1.2829	1.1326	1.0617	1.0334	1.0252	1.0209	1.0097
290	2.2084	1.7558	1.4529	1.2991	1.2206	1.1753	1.1371	1.0907	1.0322
300	2.4611	2.0091	1.6975	1.5358	1.4409	1.3630	1.2746	1.1686	1.0548
310	2.8124	2.3638	2.0442	1.8722	1.7477	1.6103	1.4400	1.2526	1.0767
320	3.2730	2.8455	2.5318	2.3539	2.1781	1.9330	1.6329	1.3393	1.0970
330	3.8394	3.4746	3.2092	3.0498	2.7862	2.3449	1.8462	1.4231	1.1147
340	4.4709	4.2377	4.1166	4.0591	3.6462	2.8430	2.0616	1.4968	1.1289
350	5.0598	5.0256	5.2049	5.5004	4.8376	3.3702	2.2455	1.5524	1.1389
360	5.4310	5.5716	6.1100	7.2831	6.2469	3.7529	2.3542	1.5824	1.1440

SUN ALTITUDE ANGLE =50.0 DEGREES

SKY ELEMENT ALTITUDE ANGLE

AZIMUTH	5	15	25	35	45	55	65	75	85
10	3.0646	3.0059	3.1734	3.7545	4.7780	4.2791	2.6347	1.6986	1.1719
20	2.9389	2.8360	2.9218	3.3092	3.8042	3.5111	2.4581	1.6571	1.1655
30	2.7227	2.5565	2.5377	2.7258	2.9368	2.7841	2.1863	1.5817	1.1532
40	2.4658	2.2423	2.1413	2.2002	2.2884	2.2185	1.8985	1.4846	1.1356
50	2.2104	1.9462	1.7946	1.7823	1.8166	1.7933	1.6361	1.3778	1.1139
60	1.9828	1.6932	1.5147	1.4655	1.4741	1.4758	1.4130	1.2709	1.0892
70	1.7952	1.4899	1.2980	1.2294	1.2244	1.2384	1.2298	1.1701	1.0627
80	1.6509	1.3338	1.1344	1.0547	1.0412	1.0601	1.0821	1.0790	1.0355
90	1.5484	1.2191	1.0135	.9261	.9060	.9256	.9640	.9989	1.0086
100	1.4837	1.1396	.9265	.8321	.8060	.8238	.8703	.9300	.9828
110	1.4515	1.0892	.8664	.7644	.7322	.7466	.7963	.8718	.9588
120	1.4457	1.0620	.8271	.7168	.6781	.6884	.7383	.8234	.9371
130	1.4596	1.0524	.8038	.6844	.6391	.6447	.6932	.7840	.9180
140	1.4859	1.0550	.7919	.6633	.6115	.6125	.6588	.7526	.9019
150	1.5177	1.0644	.7877	.6504	.5927	.5894	.6333	.7285	.8889
160	1.5482	1.0762	.7877	.6431	.5803	.5735	.6152	.7110	.8790
170	1.5720	1.0863	.7894	.6394	.5730	.5636	.6037	.6996	.8724
180	1.5849	1.0921	.7907	.6379	.5696	.5588	.5981	.6940	.8691
190	1.5849	1.0921	.7907	.6379	.5696	.5588	.5981	.6940	.8691
200	1.5720	1.0863	.7894	.6394	.5730	.5636	.6037	.6996	.8724
210	1.5482	1.0762	.7877	.6431	.5803	.5735	.6152	.7110	.8790
220	1.5177	1.0644	.7877	.6504	.5927	.5894	.6333	.7285	.8889
230	1.4859	1.0550	.7919	.6633	.6115	.6125	.6588	.7526	.9019
240	1.4596	1.0524	.8038	.6844	.6391	.6447	.6932	.7840	.9180
250	1.4457	1.0620	.8271	.7168	.6781	.6884	.7383	.8234	.9371
260	1.4515	1.0892	.8664	.7644	.7322	.7466	.7963	.8718	.9588
270	1.4837	1.1396	.9265	.8321	.8060	.8238	.8703	.9300	.9828
280	1.5484	1.2191	1.0135	.9261	.9060	.9256	.9640	.9989	1.0086
290	1.6509	1.3338	1.1344	1.0547	1.0412	1.0601	1.0821	1.0790	1.0355
300	1.7952	1.4899	1.2980	1.2294	1.2244	1.2384	1.2298	1.1701	1.0627
310	1.9828	1.6932	1.5147	1.4655	1.4741	1.4758	1.4130	1.2709	1.0892
320	2.2104	1.9462	1.7946	1.7823	1.8166	1.7933	1.6361	1.3778	1.1139
330	2.4658	2.2423	2.1413	2.2002	2.2884	2.2185	1.8985	1.4846	1.1356
340	2.7227	2.5565	2.5377	2.7258	2.9368	2.7841	2.1863	1.5817	1.1532
350	2.9389	2.8360	2.9218	3.3092	3.8042	3.5111	2.4581	1.6571	1.1655
360	3.0646	3.0059	3.1734	3.7545	4.7780	4.2791	2.6347	1.6986	1.1719

SUN ALTITUDE ANGLE =60.0 DEGREES

SKY ELEMENT ALTITUDE ANGLE

AZIMUTH	5	15	25	35	45	55	65	75	85
10	1.7275	1.6158	1.6301	1.8540	2.3249	3.1191	2.8910	1.8151	1.1996
20	1.6875	1.5651	1.5616	1.7474	2.1282	2.6427	2.5327	1.7537	1.1917
30	1.6152	1.4752	1.4436	1.5734	1.8422	2.1586	2.1369	1.6478	1.1765
40	1.5229	1.3633	1.3026	1.3787	1.5569	1.7641	1.7965	1.5195	1.1551
50	1.4235	1.2459	1.1608	1.1945	1.3101	1.4564	1.5196	1.3867	1.1289
60	1.3276	1.1349	1.0316	1.0349	1.1093	1.2193	1.2985	1.2605	1.0994
70	1.2424	1.0371	.9207	.9032	.9504	1.0369	1.1230	1.1464	1.0681
80	1.1719	.9556	.8296	.7976	.8263	.8964	.9839	1.0464	1.0363
90	1.1178	.8908	.7569	.7143	.7300	.7879	.8737	.9606	1.0053
100	1.0799	.8417	.7005	.6496	.6555	.7039	.7865	.8881	.9758
110	1.0568	.8066	.6580	.6000	.5981	.6389	.7175	.8275	.9485
120	1.0464	.7833	.6271	.5626	.5543	.5887	.6632	.7777	.9241
130	1.0458	.7696	.6055	.5350	.5211	.5502	.6207	.7373	.9028
140	1.0519	.7629	.5911	.5151	.4964	.5210	.5881	.7053	.8848
150	1.0616	.7609	.5821	.5012	.4786	.4996	.5636	.6807	.8704
160	1.0719	.7615	.5768	.4920	.4663	.4845	.5462	.6628	.8595
170	1.0803	.7630	.5741	.4865	.4586	.4749	.5350	.6512	.8522
180	1.0849	.7641	.5729	.4839	.4549	.4702	.5296	.6455	.8486
190	1.0849	.7641	.5729	.4839	.4549	.4702	.5296	.6455	.8486
200	1.0803	.7630	.5741	.4865	.4586	.4749	.5350	.6512	.8522
210	1.0719	.7615	.5768	.4920	.4663	.4845	.5462	.6628	.8595
220	1.0616	.7609	.5821	.5012	.4786	.4996	.5636	.6807	.8704
230	1.0519	.7629	.5911	.5151	.4964	.5210	.5881	.7053	.8848
240	1.0458	.7696	.6055	.5350	.5211	.5502	.6207	.7373	.9028
250	1.0464	.7833	.6271	.5626	.5543	.5887	.6632	.7777	.9241
260	1.0568	.8066	.6580	.6000	.5981	.6389	.7175	.8275	.9485
270	1.0799	.8417	.7005	.6496	.6555	.7039	.7865	.8881	.9758
280	1.1178	.8908	.7569	.7143	.7300	.7879	.8737	.9606	1.0053
290	1.1719	.9556	.8296	.7976	.8263	.8964	.9839	1.0464	1.0363
300	1.2424	1.0371	.9207	.9032	.9504	1.0369	1.1230	1.1464	1.0681
310	1.3276	1.1349	1.0316	1.0349	1.1093	1.2193	1.2985	1.2605	1.0994
320	1.4235	1.2459	1.1608	1.1945	1.3101	1.4564	1.5196	1.3867	1.1289
330	1.5229	1.3633	1.3026	1.3787	1.5569	1.7641	1.7965	1.5195	1.1551
340	1.6152	1.4752	1.4436	1.5734	1.8422	2.1586	2.1369	1.6478	1.1765
350	1.6875	1.5651	1.5616	1.7474	2.1282	2.6427	2.5327	1.7537	1.1917
360	1.7275	1.6158	1.6301	1.8540	2.3249	3.1191	2.8910	1.8151	1.1996

SUN ALTITUDE ANGLE =70.0 DEGREES

SKY ELEMENT ALTITUDE ANGLE

AZIMUTH	5	15	25	35	45	55	65	75	85
10	.9761	.8695	.8363	.9084	1.0934	1.4341	2.0102	1.9169	1.2254
20	.9650	.8560	.8192	.8843	1.0551	1.3626	1.8217	1.7951	1.2155
30	.9444	.8309	.7878	.8407	.9879	1.2460	1.5920	1.6285	1.1965
40	.9167	.7974	.7485	.7849	.9055	1.1142	1.3811	1.4625	1.1702
50	.8849	.7592	.7003	.7242	.8196	.9866	1.2010	1.3120	1.1386
60	.8521	.7199	.6534	.6642	.7380	.8725	1.0511	1.1806	1.1037
70	.8208	.6821	.6088	.6086	.6649	.7745	.9279	1.0679	1.0675
80	.7928	.6477	.5686	.5592	.6018	.6925	.8271	.9724	1.0315
90	.7693	.6179	.5335	.5167	.5485	.6248	.7449	.8920	.9969
100	.7509	.5931	.5040	.4810	.5043	.5694	.6782	.8249	.9645
110	.7375	.5733	.4797	.4516	.4682	.5246	.6243	.7692	.9351
120	.7287	.5581	.4603	.4279	.4391	.4886	.5809	.7234	.9089
130	.7238	.5470	.4453	.4091	.4159	.4601	.5465	.6863	.8863
140	.7219	.5393	.4339	.3946	.3979	.4379	.5196	.6569	.8674
150	.7219	.5342	.4257	.3838	.3844	.4211	.4991	.6343	.8523
160	.7229	.5311	.4201	.3762	.3747	.4091	.4845	.6178	.8409
170	.7241	.5294	.4166	.3713	.3685	.4013	.4750	.6071	.8334
180	.7248	.5287	.4149	.3689	.3655	.3975	.4703	.6018	.8296
190	.7248	.5287	.4149	.3689	.3655	.3975	.4703	.6018	.8296
200	.7241	.5294	.4166	.3713	.3685	.4013	.4750	.6071	.8334
210	.7229	.5311	.4201	.3762	.3747	.4091	.4845	.6178	.8409
220	.7219	.5342	.4257	.3838	.3844	.4211	.4991	.6343	.8523
230	.7219	.5393	.4339	.3946	.3979	.4379	.5196	.6569	.8674
240	.7238	.5470	.4453	.4091	.4159	.4601	.5465	.6863	.8863
250	.7287	.5581	.4603	.4279	.4391	.4886	.5809	.7234	.9089
260	.7375	.5733	.4797	.4516	.4682	.5246	.6243	.7692	.9351
270	.7509	.5931	.5040	.4810	.5043	.5694	.6782	.8249	.9645
280	.7693	.6179	.5335	.5167	.5485	.6248	.7449	.8920	.9969
290	.7928	.6477	.5686	.5592	.6018	.6925	.8271	.9724	1.0315
300	.8208	.6821	.6088	.6086	.6649	.7745	.9279	1.0679	1.0675
310	.8521	.7199	.6534	.6642	.7380	.8725	1.0511	1.1806	1.1037
320	.8849	.7592	.7003	.7242	.8196	.9866	1.2010	1.3120	1.1386
330	.9167	.7974	.7485	.7849	.9055	1.1142	1.3811	1.4625	1.1702
340	.9444	.8309	.7878	.8407	.9879	1.2460	1.5920	1.6285	1.1965
350	.9650	.8560	.8192	.8843	1.0551	1.3626	1.8217	1.7951	1.2155
360	.9761	.8695	.8363	.9084	1.0934	1.4341	2.0102	1.9169	1.2254

INFERIEURE

SUN ALTITUDE ANGLE =80.0 DEGREES

SKY CLEMENT ALTITUDE ANGLE

AZIMUTH	5	15	25	35	45	55	65	75	85
10	.5564	.4712	.4315	.4468	.5133	.6453	.8777	1.2760	1.2472
20	.5542	.4685	.4283	.4425	.5072	.6357	.8605	1.2307	1.2311
30	.5501	.4634	.4221	.4344	.4957	.6178	.8291	1.1601	1.2024
40	.5444	.4563	.4135	.4232	.4798	.5936	.7884	1.0818	1.1658
50	.5375	.4476	.4030	.4096	.4610	.5654	.7430	1.0049	1.1253
60	.5298	.4380	.3914	.3948	.4407	.5356	.6967	.9334	1.0840
70	.5220	.4280	.3793	.3794	.4199	.5058	.6521	.8690	1.0437
80	.5143	.4180	.3672	.3643	.3997	.4774	.6109	.8119	1.0057
90	.5072	.4086	.3558	.3499	.3807	.4512	.5736	.7619	.9706
100	.5009	.3999	.3452	.3366	.3635	.4277	.5408	.7188	.9388
110	.4955	.3922	.3357	.3248	.3481	.4070	.5124	.6819	.9106
120	.4912	.3855	.3274	.3144	.3348	.3892	.4883	.6508	.8859
130	.4877	.3800	.3203	.3056	.3235	.3743	.4682	.6251	.8649
140	.4851	.3755	.3146	.2984	.3143	.3621	.4518	.6042	.8475
150	.4833	.3721	.3100	.2927	.3070	.3526	.4391	.5880	.8337
160	.4821	.3696	.3067	.2885	.3016	.3455	.4297	.5760	.8234
170	.4813	.3680	.3045	.2857	.2981	.3409	.4236	.5682	.8165
180	.4810	.3672	.3034	.2843	.2963	.3386	.4205	.5643	.8131
190	.4810	.3672	.3034	.2843	.2963	.3386	.4205	.5643	.8131
200	.4813	.3680	.3045	.2857	.2981	.3409	.4236	.5682	.8165
210	.4821	.3696	.3067	.2885	.3016	.3455	.4297	.5760	.8234
220	.4833	.3721	.3100	.2927	.3070	.3526	.4391	.5880	.8337
230	.4851	.3755	.3146	.2984	.3143	.3621	.4518	.6042	.8475
240	.4877	.3800	.3203	.3056	.3235	.3743	.4682	.6251	.8649
250	.4912	.3855	.3274	.3144	.3348	.3892	.4883	.6508	.8859
260	.4955	.3922	.3357	.3248	.3481	.4070	.5124	.6819	.9106
270	.5009	.3999	.3452	.3366	.3635	.4277	.5408	.7188	.9388
280	.5072	.4086	.3558	.3499	.3807	.4512	.5736	.7619	.9706
290	.5143	.4180	.3672	.3643	.3997	.4774	.6109	.8119	1.0057
300	.5220	.4280	.3793	.3794	.4199	.5058	.6521	.8690	1.0437
310	.5298	.4380	.3914	.3948	.4407	.5356	.6967	.9334	1.0840
320	.5375	.4476	.4030	.4096	.4610	.5654	.7430	1.0049	1.1253
330	.5444	.4563	.4135	.4232	.4798	.5936	.7884	1.0818	1.1658
340	.5501	.4634	.4221	.4344	.4957	.6178	.8291	1.1601	1.2024
350	.5542	.4685	.4283	.4425	.5072	.6357	.8605	1.2307	1.2311
360	.5564	.4712	.4315	.4468	.5133	.6453	.8777	1.2760	1.2472

SUN ALTITUDE ANGLE =90.0 DEGREES

SKY ELEMENT ALTITUDE ANGLE

AZIMUTH	5	15	25	35	45	55	65	75	85
10	.3227	.2594	.2258	.2226	.2437	.2923	.3806	.5339	.7995
20	.3227	.2594	.2258	.2226	.2437	.2923	.3806	.5339	.7995
30	.3227	.2594	.2258	.2226	.2437	.2923	.3806	.5339	.7995
40	.3227	.2594	.2258	.2226	.2437	.2923	.3806	.5339	.7995
50	.3227	.2594	.2258	.2226	.2437	.2923	.3806	.5339	.7995
60	.3227	.2594	.2258	.2226	.2437	.2923	.3806	.5339	.7995
70	.3227	.2594	.2258	.2226	.2437	.2923	.3806	.5339	.7995
80	.3227	.2594	.2258	.2226	.2437	.2923	.3806	.5339	.7995
90	.3227	.2594	.2258	.2226	.2437	.2923	.3806	.5339	.7995
100	.3227	.2594	.2258	.2226	.2437	.2923	.3806	.5339	.7995
110	.3227	.2594	.2258	.2226	.2437	.2923	.3806	.5339	.7995
120	.3227	.2594	.2258	.2226	.2437	.2923	.3806	.5339	.7995
130	.3227	.2594	.2258	.2226	.2437	.2923	.3806	.5339	.7995
140	.3227	.2594	.2258	.2226	.2437	.2923	.3806	.5339	.7995
150	.3227	.2594	.2258	.2226	.2437	.2923	.3806	.5339	.7995
160	.3227	.2594	.2258	.2226	.2437	.2923	.3806	.5339	.7995
170	.3227	.2594	.2258	.2226	.2437	.2923	.3806	.5339	.7995
180	.3227	.2594	.2258	.2226	.2437	.2923	.3806	.5339	.7995
190	.3227	.2594	.2258	.2226	.2437	.2923	.3806	.5339	.7995
200	.3227	.2594	.2258	.2226	.2437	.2923	.3806	.5339	.7995
210	.3227	.2594	.2258	.2226	.2437	.2923	.3806	.5339	.7995
220	.3227	.2594	.2258	.2226	.2437	.2923	.3806	.5339	.7995
230	.3227	.2594	.2258	.2226	.2437	.2923	.3806	.5339	.7995
240	.3227	.2594	.2258	.2226	.2437	.2923	.3806	.5339	.7995
250	.3227	.2594	.2258	.2226	.2437	.2923	.3806	.5339	.7995
260	.3227	.2594	.2258	.2226	.2437	.2923	.3806	.5339	.7995
270	.3227	.2594	.2258	.2226	.2437	.2923	.3806	.5339	.7995
280	.3227	.2594	.2258	.2226	.2437	.2923	.3806	.5339	.7995
290	.3227	.2594	.2258	.2226	.2437	.2923	.3806	.5339	.7995
300	.3227	.2594	.2258	.2226	.2437	.2923	.3806	.5339	.7995
310	.3227	.2594	.2258	.2226	.2437	.2923	.3806	.5339	.7995
320	.3227	.2594	.2258	.2226	.2437	.2923	.3806	.5339	.7995
330	.3227	.2594	.2258	.2226	.2437	.2923	.3806	.5339	.7995
340	.3227	.2594	.2258	.2226	.2437	.2923	.3806	.5339	.7995
350	.3227	.2594	.2258	.2226	.2437	.2923	.3806	.5339	.7995
360	.3227	.2594	.2258	.2226	.2437	.2923	.3806	.5339	.7995

The luminance distribution of the clear cloudless sky was used to determine incoming illumination from each sky element (luminance of the element x Area of the element) the results are shown for sun altitude angles of 20°, 30°, ... and 90°.

INFERIEURE

SUN ALTITUDE ANGLE =20.0 DEGREES

SKY ELEMENT ALTITUDE ANGLE

AZIMUTH	5	15	25	35	45	55	65	75	85
10	.5050	.5198	.3666	.1832	.0922	.0472	.0238	.0108	.0029
20	.4111	.3658	.2614	.1538	.0840	.0449	.0232	.0106	.0029
30	.3095	.2549	.1841	.1197	.0718	.0410	.0221	.0104	.0029
40	.2321	.1834	.1334	.0920	.0597	.0364	.0206	.0101	.0028
50	.1782	.1373	.1004	.0719	.0494	.0320	.0191	.0097	.0028
60	.1418	.1073	.0786	.0577	.0413	.0281	.0176	.0093	.0028
70	.1175	.0877	.0642	.0478	.0352	.0249	.0162	.0089	.0027
80	.1017	.0749	.0546	.0410	.0307	.0223	.0150	.0085	.0027
90	.0921	.0670	.0485	.0364	.0276	.0203	.0140	.0082	.0027
100	.0875	.0626	.0449	.0335	.0254	.0189	.0132	.0079	.0026
110	.0865	.0611	.0432	.0319	.0240	.0179	.0126	.0076	.0026
120	.0885	.0616	.0429	.0312	.0232	.0172	.0121	.0074	.0026
130	.0924	.0636	.0436	.0313	.0229	.0168	.0118	.0072	.0026
140	.0975	.0664	.0450	.0318	.0230	.0166	.0116	.0071	.0025
150	.1028	.0696	.0466	.0325	.0232	.0165	.0114	.0070	.0025
160	.1077	.0725	.0482	.0333	.0234	.0165	.0113	.0069	.0025
170	.1113	.0747	.0494	.0339	.0237	.0166	.0113	.0069	.0025
180	.1133	.0759	.0501	.0342	.0238	.0166	.0113	.0069	.0025
190	.1133	.0759	.0501	.0342	.0238	.0166	.0113	.0069	.0025
200	.1113	.0747	.0494	.0339	.0237	.0166	.0113	.0069	.0025
210	.1077	.0725	.0482	.0333	.0234	.0165	.0113	.0069	.0025
220	.1028	.0696	.0466	.0325	.0232	.0165	.0114	.0070	.0025
230	.0975	.0664	.0450	.0318	.0230	.0166	.0116	.0071	.0025
240	.0924	.0636	.0436	.0313	.0229	.0168	.0118	.0072	.0026
250	.0885	.0616	.0429	.0312	.0232	.0172	.0121	.0074	.0026
260	.0865	.0611	.0432	.0319	.0240	.0179	.0126	.0076	.0026
270	.0875	.0626	.0449	.0335	.0254	.0189	.0132	.0079	.0026
280	.0921	.0670	.0485	.0364	.0276	.0203	.0140	.0082	.0027
290	.1017	.0749	.0546	.0410	.0307	.0223	.0150	.0085	.0027
300	.1175	.0877	.0642	.0478	.0352	.0249	.0162	.0089	.0027
310	.1418	.1073	.0786	.0577	.0413	.0281	.0176	.0093	.0028
320	.1782	.1373	.1004	.0719	.0494	.0320	.0191	.0097	.0028
330	.2321	.1834	.1334	.0920	.0597	.0364	.0206	.0101	.0028
340	.3095	.2549	.1841	.1197	.0718	.0410	.0221	.0104	.0029
350	.4111	.3658	.2614	.1538	.0840	.0449	.0232	.0106	.0029
360	.5050	.5198	.3666	.1832	.0922	.0472	.0238	.0108	.0029

SUN ALTITUDE ANGLE =30.0 DEGREES

SKY ELEMENT ALTITUDE ANGLE

AZIMUTH	5	15	25	35	45	55	65	75	85
10	.2904	.2997	.3088	.2262	.1134	.0559	.0269	.0116	.0030
20	.2579	.2484	.2238	.1671	.0982	.0520	.0260	.0114	.0029
30	.2129	.1907	.1596	.1210	.0791	.0460	.0243	.0111	.0029
40	.1712	.1451	.1168	.0896	.0627	.0395	.0223	.0107	.0029
50	.1382	.1125	.0885	.0685	.0501	.0336	.0202	.0101	.0029
60	.1138	.0899	.0696	.0541	.0407	.0287	.0182	.0096	.0028
70	.0965	.0745	.0568	.0442	.0340	.0248	.0165	.0091	.0028
80	.0848	.0640	.0482	.0374	.0291	.0217	.0149	.0086	.0027
90	.0775	.0573	.0425	.0328	.0256	.0194	.0137	.0081	.0027
100	.0736	.0533	.0389	.0297	.0231	.0177	.0127	.0077	.0026
110	.0724	.0514	.0368	.0277	.0214	.0164	.0119	.0074	.0026
120	.0734	.0512	.0360	.0267	.0203	.0155	.0113	.0071	.0025
130	.0759	.0521	.0360	.0262	.0197	.0148	.0108	.0069	.0025
140	.0793	.0538	.0366	.0262	.0193	.0144	.0105	.0067	.0025
150	.0829	.0557	.0374	.0264	.0192	.0142	.0102	.0065	.0025
160	.0862	.0576	.0383	.0267	.0192	.0140	.0100	.0064	.0024
170	.0887	.0590	.0390	.0270	.0192	.0140	.0099	.0064	.0024
180	.0901	.0598	.0394	.0271	.0193	.0139	.0099	.0063	.0024
190	.0901	.0598	.0394	.0271	.0193	.0139	.0099	.0063	.0024
200	.0887	.0590	.0390	.0270	.0192	.0140	.0099	.0064	.0024
210	.0862	.0576	.0383	.0267	.0192	.0140	.0100	.0064	.0024
220	.0829	.0557	.0374	.0264	.0192	.0142	.0102	.0065	.0025
230	.0793	.0538	.0366	.0262	.0193	.0144	.0105	.0067	.0025
240	.0759	.0521	.0360	.0262	.0197	.0148	.0108	.0069	.0025
250	.0734	.0512	.0360	.0267	.0203	.0155	.0113	.0071	.0025
260	.0724	.0514	.0368	.0277	.0214	.0164	.0119	.0074	.0026
270	.0736	.0533	.0389	.0297	.0231	.0177	.0127	.0077	.0026
280	.0775	.0573	.0425	.0328	.0256	.0194	.0137	.0081	.0027
290	.0848	.0640	.0482	.0374	.0291	.0217	.0149	.0086	.0027
300	.0965	.0745	.0568	.0442	.0340	.0248	.0165	.0091	.0028
310	.1138	.0899	.0696	.0541	.0407	.0287	.0182	.0096	.0028
320	.1382	.1125	.0885	.0685	.0501	.0336	.0202	.0101	.0029
330	.1712	.1451	.1168	.0896	.0627	.0395	.0223	.0107	.0029
340	.2129	.1907	.1596	.1210	.0791	.0460	.0243	.0111	.0029
350	.2579	.2484	.2238	.1671	.0982	.0520	.0260	.0114	.0029
360	.2904	.2997	.3088	.2262	.1134	.0559	.0269	.0116	.0030

SUN ALTITUDE ANGLE =40.0 DEGREES

SKY ELEMENT ALTITUDE ANGLE

AZIMUTH	5	15	25	35	45	55	65	75	85
10	.1646	.1637	.1685	.1815	.1344	.0655	.0303	.0125	.0030
20	.1533	.1477	.1435	.1371	.1041	.0588	.0289	.0122	.0030
30	.1355	.1245	.1135	.1012	.0784	.0496	.0265	.0118	.0030
40	.1164	.1021	.0885	.0760	.0599	.0409	.0237	.0112	.0030
50	.0992	.0836	.0698	.0587	.0469	.0337	.0210	.0105	.0029
60	.0852	.0695	.0564	.0467	.0376	.0281	.0185	.0099	.0029
70	.0746	.0590	.0468	.0383	.0310	.0238	.0164	.0092	.0028
80	.0669	.0516	.0401	.0324	.0263	.0205	.0146	.0086	.0027
90	.0618	.0465	.0354	.0282	.0228	.0180	.0132	.0080	.0027
100	.0589	.0432	.0322	.0253	.0204	.0162	.0120	.0076	.0026
110	.0578	.0414	.0302	.0234	.0186	.0148	.0111	.0071	.0026
120	.0580	.0408	.0291	.0221	.0174	.0137	.0104	.0068	.0025
130	.0593	.0409	.0287	.0214	.0166	.0130	.0098	.0065	.0025
140	.0612	.0416	.0286	.0210	.0160	.0125	.0094	.0063	.0024
150	.0632	.0425	.0289	.0208	.0157	.0121	.0091	.0061	.0024
160	.0652	.0435	.0292	.0208	.0155	.0118	.0089	.0060	.0024
170	.0667	.0443	.0295	.0209	.0154	.0117	.0088	.0059	.0024
180	.0675	.0447	.0297	.0209	.0154	.0116	.0087	.0059	.0024
190	.0675	.0447	.0297	.0209	.0154	.0116	.0087	.0059	.0024
200	.0667	.0443	.0295	.0209	.0154	.0117	.0088	.0059	.0024
210	.0652	.0435	.0292	.0208	.0155	.0118	.0089	.0060	.0024
220	.0632	.0425	.0289	.0208	.0157	.0121	.0091	.0061	.0024
230	.0612	.0416	.0286	.0210	.0160	.0125	.0094	.0063	.0024
240	.0593	.0409	.0287	.0214	.0166	.0130	.0098	.0065	.0025
250	.0580	.0408	.0291	.0221	.0174	.0137	.0104	.0068	.0025
260	.0578	.0414	.0302	.0234	.0186	.0148	.0111	.0071	.0026
270	.0589	.0432	.0322	.0253	.0204	.0162	.0120	.0076	.0026
280	.0618	.0465	.0354	.0282	.0228	.0180	.0132	.0080	.0027
290	.0669	.0516	.0401	.0324	.0263	.0205	.0146	.0086	.0027
300	.0746	.0590	.0468	.0383	.0310	.0238	.0164	.0092	.0028
310	.0852	.0695	.0564	.0467	.0376	.0281	.0185	.0099	.0029
320	.0992	.0836	.0698	.0587	.0469	.0337	.0210	.0105	.0029
330	.1164	.1021	.0885	.0760	.0599	.0409	.0237	.0112	.0030
340	.1355	.1245	.1135	.1012	.0784	.0496	.0265	.0118	.0030
350	.1533	.1477	.1435	.1371	.1041	.0588	.0289	.0122	.0030
360	.1646	.1637	.1685	.1815	.1344	.0655	.0303	.0125	.0030

SUN ALTITUDE ANGLE =50.0 DEGREES

SKY ELEMENT ALTITUDE ANGLE

AZIMUTH	5	15	25	35	45	55	65	75	85
10	.0929	.0883	.0875	.0936	.1028	.0747	.0339	.0134	.0031
20	.0891	.0833	.0806	.0825	.0818	.0613	.0316	.0130	.0031
30	.0825	.0751	.0700	.0679	.0632	.0486	.0281	.0125	.0031
40	.0747	.0659	.0590	.0548	.0492	.0387	.0244	.0117	.0030
50	.0670	.0572	.0495	.0444	.0391	.0313	.0210	.0108	.0030
60	.0601	.0498	.0418	.0365	.0317	.0258	.0182	.0100	.0029
70	.0544	.0438	.0358	.0306	.0263	.0216	.0158	.0092	.0028
80	.0500	.0392	.0313	.0263	.0224	.0185	.0139	.0085	.0027
90	.0469	.0358	.0279	.0231	.0195	.0162	.0124	.0079	.0027
100	.0450	.0335	.0255	.0207	.0173	.0144	.0112	.0073	.0026
110	.0440	.0320	.0239	.0190	.0158	.0130	.0102	.0069	.0025
120	.0438	.0312	.0228	.0179	.0146	.0120	.0095	.0065	.0025
130	.0442	.0309	.0222	.0171	.0137	.0113	.0089	.0062	.0024
140	.0450	.0310	.0218	.0165	.0132	.0107	.0085	.0059	.0024
150	.0460	.0313	.0217	.0162	.0127	.0103	.0081	.0057	.0024
160	.0469	.0316	.0217	.0160	.0125	.0100	.0079	.0056	.0023
170	.0476	.0319	.0218	.0159	.0123	.0098	.0078	.0055	.0023
180	.0480	.0321	.0218	.0159	.0123	.0098	.0077	.0055	.0023
190	.0480	.0321	.0218	.0159	.0123	.0098	.0077	.0055	.0023
200	.0476	.0319	.0218	.0159	.0123	.0098	.0078	.0055	.0023
210	.0469	.0316	.0217	.0160	.0125	.0100	.0079	.0056	.0023
220	.0460	.0313	.0217	.0162	.0127	.0103	.0081	.0057	.0024
230	.0450	.0310	.0218	.0165	.0132	.0107	.0085	.0059	.0024
240	.0442	.0309	.0222	.0171	.0137	.0113	.0089	.0062	.0024
250	.0438	.0312	.0228	.0179	.0146	.0120	.0095	.0065	.0025
260	.0440	.0320	.0239	.0190	.0158	.0130	.0102	.0069	.0025
270	.0450	.0335	.0255	.0207	.0173	.0144	.0112	.0073	.0026
280	.0469	.0358	.0279	.0231	.0195	.0162	.0124	.0079	.0027
290	.0500	.0392	.0313	.0263	.0224	.0185	.0139	.0085	.0027
300	.0544	.0438	.0358	.0306	.0263	.0216	.0158	.0092	.0028
310	.0601	.0498	.0418	.0365	.0317	.0258	.0182	.0100	.0029
320	.0670	.0572	.0495	.0444	.0391	.0313	.0210	.0108	.0030
330	.0747	.0659	.0590	.0548	.0492	.0387	.0244	.0117	.0030
340	.0825	.0751	.0700	.0679	.0632	.0486	.0281	.0125	.0031
350	.0891	.0833	.0806	.0825	.0818	.0613	.0316	.0130	.0031
360	.0929	.0883	.0875	.0936	.1028	.0747	.0339	.0134	.0031

INFERIEURE

SUN ALTITUDE ANGLE =60.0 DEGREES

SKY ELEMENT ALTITUDE ANGLE

AZIMUTH	5	15	25	35	45	55	65	75	85
10	.0524	.0475	.0449	.0462	.0500	.0544	.0372	.0143	.0032
20	.0511	.0460	.0431	.0435	.0458	.0461	.0326	.0138	.0032
30	.0490	.0434	.0398	.0392	.0396	.0377	.0275	.0130	.0031
40	.0462	.0401	.0359	.0344	.0335	.0308	.0231	.0120	.0031
50	.0431	.0366	.0320	.0298	.0282	.0254	.0195	.0109	.0030
60	.0402	.0334	.0284	.0258	.0239	.0213	.0167	.0099	.0029
70	.0377	.0305	.0254	.0225	.0204	.0181	.0144	.0090	.0028
80	.0355	.0281	.0229	.0199	.0178	.0156	.0127	.0082	.0027
90	.0339	.0262	.0209	.0178	.0157	.0137	.0112	.0076	.0027
100	.0327	.0247	.0193	.0162	.0141	.0123	.0101	.0070	.0026
110	.0320	.0237	.0181	.0150	.0129	.0111	.0092	.0065	.0025
120	.0317	.0230	.0173	.0140	.0119	.0103	.0085	.0061	.0025
130	.0317	.0226	.0167	.0133	.0112	.0096	.0080	.0058	.0024
140	.0319	.0224	.0163	.0128	.0107	.0091	.0076	.0056	.0023
150	.0322	.0224	.0160	.0125	.0103	.0087	.0072	.0054	.0023
160	.0325	.0224	.0159	.0123	.0100	.0085	.0070	.0052	.0023
170	.0327	.0224	.0158	.0121	.0099	.0083	.0069	.0051	.0023
180	.0329	.0225	.0158	.0121	.0098	.0082	.0068	.0051	.0022
190	.0329	.0225	.0158	.0121	.0098	.0082	.0068	.0051	.0022
200	.0327	.0224	.0158	.0121	.0099	.0083	.0069	.0051	.0023
210	.0325	.0224	.0159	.0123	.0100	.0085	.0070	.0052	.0023
220	.0322	.0224	.0160	.0125	.0103	.0087	.0072	.0054	.0023
230	.0319	.0224	.0163	.0128	.0107	.0091	.0076	.0056	.0023
240	.0317	.0226	.0167	.0133	.0112	.0096	.0080	.0058	.0024
250	.0317	.0230	.0173	.0140	.0119	.0103	.0085	.0061	.0025
260	.0320	.0237	.0181	.0150	.0129	.0111	.0092	.0065	.0025
270	.0327	.0247	.0193	.0162	.0141	.0123	.0101	.0070	.0026
280	.0339	.0262	.0209	.0178	.0157	.0137	.0112	.0076	.0027
290	.0355	.0281	.0229	.0199	.0178	.0156	.0127	.0082	.0027
300	.0377	.0305	.0254	.0225	.0204	.0181	.0144	.0090	.0028
310	.0402	.0334	.0284	.0258	.0239	.0213	.0167	.0099	.0029
320	.0431	.0366	.0320	.0298	.0282	.0254	.0195	.0109	.0030
330	.0462	.0401	.0359	.0344	.0335	.0308	.0231	.0120	.0031
340	.0490	.0434	.0398	.0392	.0396	.0377	.0275	.0130	.0031
350	.0511	.0460	.0431	.0435	.0458	.0461	.0326	.0138	.0032
360	.0524	.0475	.0449	.0462	.0500	.0544	.0372	.0143	.0032

SUN ALTITUDE ANGLE =70.0 DEGREES

SKY ELEMENT ALTITUDE ANGLE

AZIMUTH	5	15	25	35	45	55	65	75	85
10	.0296	.0256	.0231	.0226	.0235	.0250	.0258	.0151	.0032
20	.0292	.0252	.0226	.0220	.0227	.0238	.0234	.0141	.0032
30	.0286	.0244	.0217	.0210	.0213	.0217	.0205	.0128	.0032
40	.0278	.0234	.0206	.0196	.0195	.0194	.0178	.0115	.0031
50	.0268	.0223	.0193	.0180	.0176	.0172	.0154	.0103	.0030
60	.0258	.0212	.0180	.0166	.0159	.0152	.0135	.0093	.0029
70	.0249	.0200	.0168	.0152	.0143	.0135	.0119	.0084	.0028
80	.0240	.0190	.0157	.0139	.0129	.0121	.0106	.0077	.0027
90	.0233	.0182	.0147	.0129	.0118	.0109	.0096	.0070	.0026
100	.0228	.0174	.0139	.0120	.0108	.0099	.0087	.0065	.0026
110	.0224	.0168	.0132	.0113	.0101	.0092	.0080	.0061	.0025
120	.0221	.0164	.0127	.0107	.0094	.0085	.0075	.0057	.0024
130	.0219	.0161	.0123	.0102	.0089	.0080	.0070	.0054	.0024
140	.0219	.0158	.0120	.0098	.0086	.0076	.0067	.0052	.0023
150	.0219	.0157	.0117	.0096	.0083	.0073	.0064	.0050	.0023
160	.0219	.0156	.0116	.0094	.0081	.0071	.0062	.0049	.0022
170	.0219	.0156	.0115	.0093	.0079	.0070	.0061	.0048	.0022
180	.0220	.0155	.0114	.0092	.0079	.0069	.0060	.0047	.0022
190	.0220	.0155	.0114	.0092	.0079	.0069	.0060	.0047	.0022
200	.0219	.0156	.0115	.0093	.0079	.0070	.0061	.0048	.0022
210	.0219	.0156	.0116	.0094	.0081	.0071	.0062	.0049	.0022
220	.0219	.0157	.0117	.0096	.0083	.0073	.0064	.0050	.0023
230	.0219	.0158	.0120	.0098	.0086	.0076	.0067	.0052	.0023
240	.0219	.0161	.0123	.0102	.0089	.0080	.0070	.0054	.0024
250	.0221	.0164	.0127	.0107	.0094	.0085	.0075	.0057	.0024
260	.0224	.0168	.0132	.0113	.0101	.0092	.0080	.0061	.0025
270	.0228	.0174	.0139	.0120	.0108	.0099	.0087	.0065	.0026
280	.0233	.0182	.0147	.0129	.0118	.0109	.0096	.0070	.0026
290	.0240	.0190	.0157	.0139	.0129	.0121	.0106	.0077	.0027
300	.0249	.0200	.0168	.0152	.0143	.0135	.0119	.0084	.0028
310	.0258	.0212	.0180	.0166	.0159	.0152	.0135	.0093	.0029
320	.0268	.0223	.0193	.0180	.0176	.0172	.0154	.0103	.0030
330	.0278	.0234	.0206	.0196	.0195	.0194	.0178	.0115	.0031
340	.0286	.0244	.0217	.0210	.0213	.0217	.0205	.0128	.0032
350	.0292	.0252	.0226	.0220	.0227	.0238	.0234	.0141	.0032
360	.0296	.0256	.0231	.0226	.0235	.0250	.0258	.0151	.0032

SUN ALTITUDE ANGLE =80.0 DEGREES

SKY ELEMENT ALTITUDE ANGLE

AZIMUTH	5	15	25	35	45	55	65	75	85
10	.0169	.0138	.0119	.0111	.0110	.0113	.0113	.0100	.0036
20	.0168	.0138	.0118	.0110	.0109	.0111	.0111	.0097	.0033
30	.0167	.0136	.0116	.0108	.0107	.0108	.0107	.0091	.0032
40	.0165	.0134	.0114	.0105	.0103	.0104	.0101	.0085	.0031
50	.0163	.0132	.0111	.0102	.0099	.0099	.0096	.0079	.0030
60	.0161	.0129	.0108	.0098	.0095	.0093	.0090	.0073	.0029
70	.0158	.0126	.0105	.0095	.0090	.0088	.0084	.0068	.0028
80	.0156	.0123	.0101	.0091	.0086	.0083	.0079	.0064	.0027
90	.0154	.0120	.0098	.0087	.0082	.0079	.0074	.0060	.0026
100	.0152	.0118	.0095	.0084	.0078	.0075	.0070	.0057	.0025
110	.0150	.0115	.0093	.0081	.0075	.0071	.0066	.0054	.0024
120	.0149	.0113	.0090	.0078	.0072	.0068	.0063	.0051	.0023
130	.0148	.0112	.0088	.0076	.0070	.0065	.0060	.0049	.0023
140	.0147	.0110	.0087	.0074	.0068	.0063	.0058	.0048	.0022
150	.0146	.0109	.0085	.0073	.0066	.0062	.0056	.0046	.0022
160	.0146	.0109	.0085	.0072	.0065	.0060	.0055	.0045	.0022
170	.0146	.0108	.0084	.0071	.0064	.0059	.0054	.0045	.0022
180	.0146	.0108	.0084	.0071	.0064	.0059	.0054	.0044	.0022
190	.0146	.0108	.0084	.0071	.0064	.0059	.0054	.0044	.0022
200	.0146	.0108	.0084	.0071	.0064	.0059	.0054	.0045	.0022
210	.0146	.0109	.0085	.0072	.0065	.0060	.0055	.0045	.0022
220	.0146	.0109	.0085	.0073	.0066	.0062	.0056	.0046	.0022
230	.0147	.0110	.0087	.0074	.0068	.0063	.0058	.0048	.0022
240	.0148	.0112	.0088	.0076	.0070	.0065	.0060	.0049	.0023
250	.0149	.0113	.0090	.0078	.0072	.0068	.0063	.0051	.0023
260	.0150	.0115	.0093	.0081	.0075	.0071	.0066	.0054	.0024
270	.0152	.0118	.0095	.0084	.0078	.0075	.0070	.0057	.0025
280	.0154	.0120	.0098	.0087	.0082	.0079	.0074	.0060	.0026
290	.0156	.0123	.0101	.0091	.0086	.0083	.0079	.0064	.0027
300	.0158	.0126	.0105	.0095	.0090	.0088	.0084	.0068	.0028
310	.0161	.0129	.0108	.0098	.0095	.0093	.0090	.0073	.0029
320	.0163	.0132	.0111	.0102	.0099	.0099	.0096	.0079	.0030
330	.0165	.0134	.0114	.0105	.0103	.0104	.0101	.0085	.0031
340	.0167	.0136	.0116	.0108	.0107	.0108	.0107	.0091	.0032
350	.0168	.0138	.0118	.0110	.0109	.0111	.0111	.0097	.0033
360	.0169	.0138	.0119	.0111	.0110	.0113	.0113	.0100	.0033

SUN ALTITUDE ANGLE =90.0 DEGREES

SKY ELEMENT ALTITUDE ANGLE

AZIMUTH	5	15	25	35	45	55	65	75	85
10	.0098	.0076	.0062	.0055	.0052	.0051	.0049	.0042	.0021
20	.0098	.0076	.0062	.0055	.0052	.0051	.0049	.0042	.0021
30	.0098	.0076	.0062	.0055	.0052	.0051	.0049	.0042	.0021
40	.0098	.0076	.0062	.0055	.0052	.0051	.0049	.0042	.0021
50	.0098	.0076	.0062	.0055	.0052	.0051	.0049	.0042	.0021
60	.0098	.0076	.0062	.0055	.0052	.0051	.0049	.0042	.0021
70	.0098	.0076	.0062	.0055	.0052	.0051	.0049	.0042	.0021
80	.0098	.0076	.0062	.0055	.0052	.0051	.0049	.0042	.0021
90	.0098	.0076	.0062	.0055	.0052	.0051	.0049	.0042	.0021
100	.0098	.0076	.0062	.0055	.0052	.0051	.0049	.0042	.0021
110	.0098	.0076	.0062	.0055	.0052	.0051	.0049	.0042	.0021
120	.0098	.0076	.0062	.0055	.0052	.0051	.0049	.0042	.0021
130	.0098	.0076	.0062	.0055	.0052	.0051	.0049	.0042	.0021
140	.0098	.0076	.0062	.0055	.0052	.0051	.0049	.0042	.0021
150	.0098	.0076	.0062	.0055	.0052	.0051	.0049	.0042	.0021
160	.0098	.0076	.0062	.0055	.0052	.0051	.0049	.0042	.0021
170	.0098	.0076	.0062	.0055	.0052	.0051	.0049	.0042	.0021
180	.0098	.0076	.0062	.0055	.0052	.0051	.0049	.0042	.0021
190	.0098	.0076	.0062	.0055	.0052	.0051	.0049	.0042	.0021
200	.0098	.0076	.0062	.0055	.0052	.0051	.0049	.0042	.0021
210	.0098	.0076	.0062	.0055	.0052	.0051	.0049	.0042	.0021
220	.0098	.0076	.0062	.0055	.0052	.0051	.0049	.0042	.0021
230	.0098	.0076	.0062	.0055	.0052	.0051	.0049	.0042	.0021
240	.0098	.0076	.0062	.0055	.0052	.0051	.0049	.0042	.0021
250	.0098	.0076	.0062	.0055	.0052	.0051	.0049	.0042	.0021
260	.0098	.0076	.0062	.0055	.0052	.0051	.0049	.0042	.0021
270	.0098	.0076	.0062	.0055	.0052	.0051	.0049	.0042	.0021
280	.0098	.0076	.0062	.0055	.0052	.0051	.0049	.0042	.0021
290	.0098	.0076	.0062	.0055	.0052	.0051	.0049	.0042	.0021
300	.0098	.0076	.0062	.0055	.0052	.0051	.0049	.0042	.0021
310	.0098	.0076	.0062	.0055	.0052	.0051	.0049	.0042	.0021
320	.0098	.0076	.0062	.0055	.0052	.0051	.0049	.0042	.0021
330	.0098	.0076	.0062	.0055	.0052	.0051	.0049	.0042	.0021
340	.0098	.0076	.0062	.0055	.0052	.0051	.0049	.0042	.0021
350	.0098	.0076	.0062	.0055	.0052	.0051	.0049	.0042	.0021
360	.0098	.0076	.0062	.0055	.0052	.0051	.0049	.0042	.0021